Cementation in modern and ancient reefs

Goldsmith, Ian Robert

The Florida Reef Tract.

Cementation in Modern and Ancient Reefs.

Ian Robert Goldsmith, B.Sc.

A thesis submitted to the University of Durham for the degree of
Doctor of Philosophy.

Department of Geological Sciences. June 1987.

Cementation in Modern and Ancient Reefs.

A thorough description of the petrography of Holocene reef rock from Florida and Belize provides the basis for the investigation of several major controls thought to be involved in the cementation process. The study has highlighted the importance of the interaction of cementation with other reef formation processes, namely construction, destruction and sedimentation. The geochemistry of the cements, in particular the carbon isotopic composition, indicates that there is no input of organic carbon to the inorganic carbonate. Furthermore, there does not appear to be any direct biogenic input; the cements were precipitated at or near to equilibrium with seawater of normal marine composition.

However, one particular phase of peloidal cements is associated with organic matter. This is thought to be playing a promotional, but simply mediatory role in the precipitation. The results of molecular biomarker analyses are consistent with a predominantly algal input to the organic phase. The nature of the inorganic-organic interaction is also discussed.

The development of models to describe the cementation patterns in carbonate framestones has been successful. Many of the features of the real system have been recreated through the use of simple mathematical descriptions of the geometry of the porosity and the nature of fluid flow through porous media. The results indicate that the most important control on the distribution of cements in modern reefs is the flux of water through the pore systems. This is in turn dependent on the local permeability and the energy of the environment.

Finally, the spatial and temporal distribution of cements in a Triassic reef has been investigated, concentrating on the reef scale variations. In this specific example, the precipitation of marine cements was pervasive and laterally extensive, with individual cement zones being correlatable both within and between facies. The stable carbon and oxygen isotopic compositions of most of the cements do not reflect a primary signature, but the results indicate precipitation in the marine environment followed by some diagenetic re-equilibration during shallow burial. The marine cementation was the most important diagenetic event affecting the porosity of the reef formation, reducing it from primary levels of up to 50% to less than 5%.

Declaration.

The content of this thesis is the original work of the author (with the exception of the codes used in Chapter 5) and has not previously been submitted for a degree at this or any other university. Other people's work is acknowledged by reference.

Ian Robert Goldsmith,
Department of Geological Sciences,
University of Durham.

Copyright.

Acknowledgements.

I would like to thank my two supervisors, Drs. Maurice Tucker (University of Durham) and Andy Fleet (B.P.) for their advice and guidance during the course of this research, and the preparation of this thesis. Financial assistance was provided by the Natural Environment Research Council and the British Petroleum Company Plc., and is gratefully acknowledged. I am indebted to Gene Shinn (United States Geological Survey), Robert Ginsburg (University of Miami), and Robin Lighty (University of Texas), for the provision of most of the samples from the Recent reefs of Florida and Belize. Their advice on the collection of further material is much appreciated. I would also wish to thank Francesc Calvet (University of Barcelona), for his hospitality and help during fieldwork in Spain. Technical facilities were provided by the University of Durham, Department of Geological Sciences (X.R.D., probe and thin section preparation), Department of Chemistry (n.m.r.), the British Petroleum Company Plc. (stable isotopes, I.C.P., porosity permeability measurements, n.m.r.). Technical assistance was provided by Ron Hardy and Paul Laverick (Durham), John Rouse and Marg Cox (B.P.), and many others, thanks are extended to all. I am very grateful to Dr. Andrew Peckett (Durham), and all those at B.P. who performed various analyses. Thanks are particularly due to Nick Shackleton and Mike Hall (University of Cambridge), for the isotope analyses without which Chapter 3 would not have been possible, and to Jan van de Leeuw (University of Delft) for the pyrolysis work. Many individuals lent their assistance in the completion of the molecular biomarker studies. I am particularly grateful to Geoff Eglinton for allowing access to the facilities at Bristol University, and to Anne Gowar and Simon Brassell for their help.

I would like to thank Peter King (B.P.) who provided, and spent much time modifying, the codes used for the modelling described in Chapter 5. Thanks are also due to Ron Lambert and George Randall for the preparation of nearly 800 thin sections, Gerry Dresser and Alan Carr for photography, Karen Gittins for draughtmanship, and Dave Asbery for all the odds and sods.

Diversion from duty was due to the 'boys', Dave, Kevin, Neville, Alick, Abdul; and Sally. Thank you to Grace for her many words of wisdom and several thousand cups of coffee. Thanks to my wife Jane for humouring my mental aberrations during the gestation of this monologue, and for her continuous support. Finally, I would like to thank my mother, to whom I dedicate this thesis, for her encouragement over the years.

CONTENTS.

CHAPTER 1

A review of Processes and Research Objectives.

CHAPTER 1

A review of processes and the research objectives of this thesis.

1.1 Introduction.

The first chapter of this thesis serves to introduce the topic of cementation in modern and ancient reefs. The succeeding chapters discuss the various processes involved in the precipitation of cements within reef frameworks.

This introduction sets the background from which several research objectives have been defined in Section 1.14. The definition of the term 'cement' is given in Section 1.2 and this is followed by an introduction to the interaction of cementation with other reef processes (Section 1.3). The field areas are briefly mentioned in Section 1.4, and a history of the research on this topic is presented in Section 1.5. Section 1.6 outlines the basic prerequisites for cementation to occur and Section 1.7 describes the chemical principles on which the processes controlling cementation can be discussed.

Sections 1.8 to 1.11 discuss previous work with reference to four major questions:

i) What factors prevent precipitation from supersaturated seawater?

ii) What factors control the cement mineralogy?

iii) What factors control the cement morphology?

iv) What factors control the spatial and temporal distribution of the cements?

Facies specific controls are mentioned in Section 1.12, and Section 1.13 compares the cementation processes in modern and ancient reefs. This introductory chapter is concluded in Section 1.15 with a brief outline of the processes considered in the other chapters of the thesis.

1.2 Cementation in the Marine Environment.

Many carbonate grains in shallow tropical waters can be seen to be encrusted both internally and externally by crystals of calcium carbonate . In some cases the encrustation is so great as to actually bind together individual grains and hence the term 'cementation'. However, the term 'cement' as used in this thesis is not restricted to describing a precipitate which binds grains together. It is simply defined as a crystalline in situ precipitate. Bathurst (1975) similarly defined the term as follows: "Cements include all passively precipitated space filling carbonate crystals which grow attached to a free surface".

1.3 Cementation and Other Reef Building Processes.

Reefs are sites and products of a dynamic interplay of four main processes (Schroeder & Zankl, 1974) :

1) Construction – by frame building and binding organisms.
2) Destruction – by biogenic and mechanical processes.
3) Sedimentation.
4) Cementation.

The emphasis of this analysis should be on the dynamic aspect of reef formation; reefs are not just an accumulation of frame builders, binders, users and internal sediments. Each process yields several products, i.e. frame builders produce skeletal material but also inter- and intra-skeletal voids. Similarly, destructive processes produce altered voids and re-sedimented particles. These four major processes therefore interact in a highly complex and variable manner as envisaged on Figure 1.1. There are, however, some constraints on the system which produce a general sequence; these are mainly ecological requirements, for example, a secondary framebuilder requires a primary substrate. Boring organisms may cause microenvironmental changes which produce a change in cement composition, or allow internal sediment to fill further pores due to their increased connectivity. The relative intensities of the above processes are an important consideration; this in turn depends on environmental parameters such as energy conditions, oxicity, light penetration and turbidity.

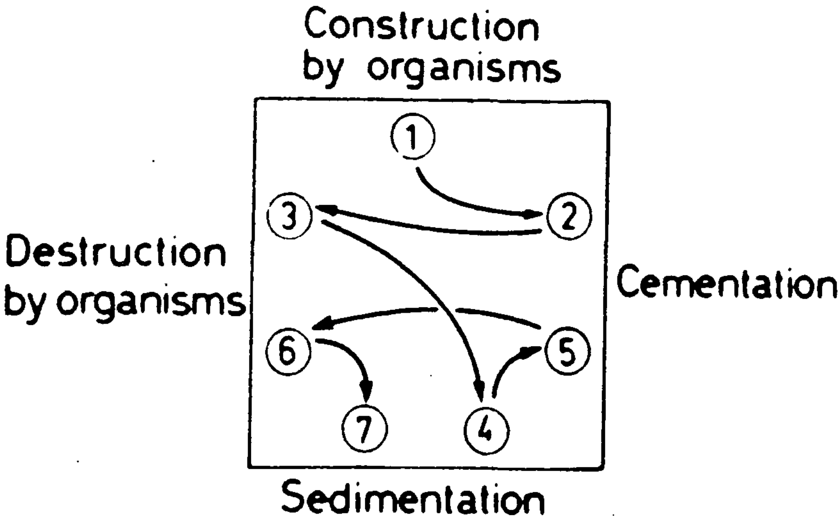

Figure 1.1 The interaction of the four major reef building processes. The sequence naturally has to start with a construction phase, but can then continue with a wide variety of events. The emphasis is on the interaction in both space and time. (After Schroeder & Zankl, 1974).

1.4 Field Areas.

Samples from three principal field areas have been studied during this project. The Holocene reefs of Florida and Belize provide an ideal starting point to study the initial genesis of the various cement phases and the processes controlling their precipitation.

The second field area is in the Northern Limestone Alps near Innsbruck, Austria. Samples come from a Triassic reef buildup which has undergone several major phases of diagenesis in marine, meteoric and burial environments. The emphasis in the study of this material has been to describe the spatial and temporal distribution of the cements on the reef scale.

The final study area was a patch reef from the Upper Miocene of Northern Spain, near Barcelona. These samples have been used to illustrate the effect of diagenesis in the the meteoric environment on the porosity and permeability of reefs. A brief description of each field area follows; full details can be found in Chapters 2, 5 and 6.

1.4.1 Florida.

The majority of the Holocene material has come from cores taken by Gene Shinn of the United States Geological Survey through several reefs of the South Eastern Florida carbonate shelf (Figure 1.2). Reef growth was initiated approximately 8,000 years b.p., when the sea level rose above the Pleistocene substrate. Some of the reefs were killed approximately 4,000 years ago at the time when the Flandrian transgression flooded the present day Florida bay leading to the efflux of turbid waters on to the shelf. However, most of the reefs are still growing today. Some of the cores penetrate the underlying Pleistocene reef rock (Section 2.18). These full cores are augmented by short cores and several hundred hand specimens collected from the surface of many of the shelf edge reefs. Further detailed description of the reefs and associated sediments can be found in Shinn et al. (1977) and Robbin (1984). Full core descriptions are given in Chapter 2. (Section 2.4, 2.10 & 2.15).

1.4.2 Belize.

All of this material, also Holocene in age, has been collected by Robert Ginsburg of the University of Miami, from the fore-reef and reef wall of reefs of the Belize reef tract (Figure 1.3). Most of the hand specimens were collected from a submersible (James & Ginsburg, 1979) and come from an atoll, Glovers reef, which is situated some 15 kilometers east of the main shelf-edge barrier reef. The samples were collected at depths of up to 100 meters.

1.4.3 Alpine Triassic.

These samples come from the Middle Triassic Wetterstein Limestone platform near Innsbruck. The upper part of the platform is dominated by a massive reef buildup, the Hafelekar Reef Complex. The location and stratigraphy are given in Figure 1.4. This Hafelekar reef has been studied previously by Bradner & Resch (1981), and a full description of the reef palaeoecology and a summary of the diagenesis is given therein.

Hand specimens were collected from all the major reef areas, including fore-reef, reef flat, reef core and back-reef facies. These samples have been studied in an attempt to correlate the cementation history across the reef. Detailed description and petrography are given in Chapter 6.

1.4.4 Miocene of Northern Spain.

This final field area was in the Upper Miocene strata, near Barcelona, Spain. A location map is shown in Figure 1.5. One specific patch reef, previously described by Permanyer & Esteban (1973) formed the major part of this study. This reef is very well exposed in a disused quarry and shows all the characteristic stages of development as identified by James (1979). The reef therefore shows a good variation in depositional character on to which the diagenetic effects are superimposed. Seventy hand specimens were collected in a regular fashion from the major units exposed on the quarry faces. The porosity and permeability of these samples were measured, with the intention of using that data to constrain mathematical models of the hydrology on the reef scale. (Section 5.7). The emphasis has been to characterise the porosity and permeability variations on the basis of both the original depositional character and the diagenetic overprint.

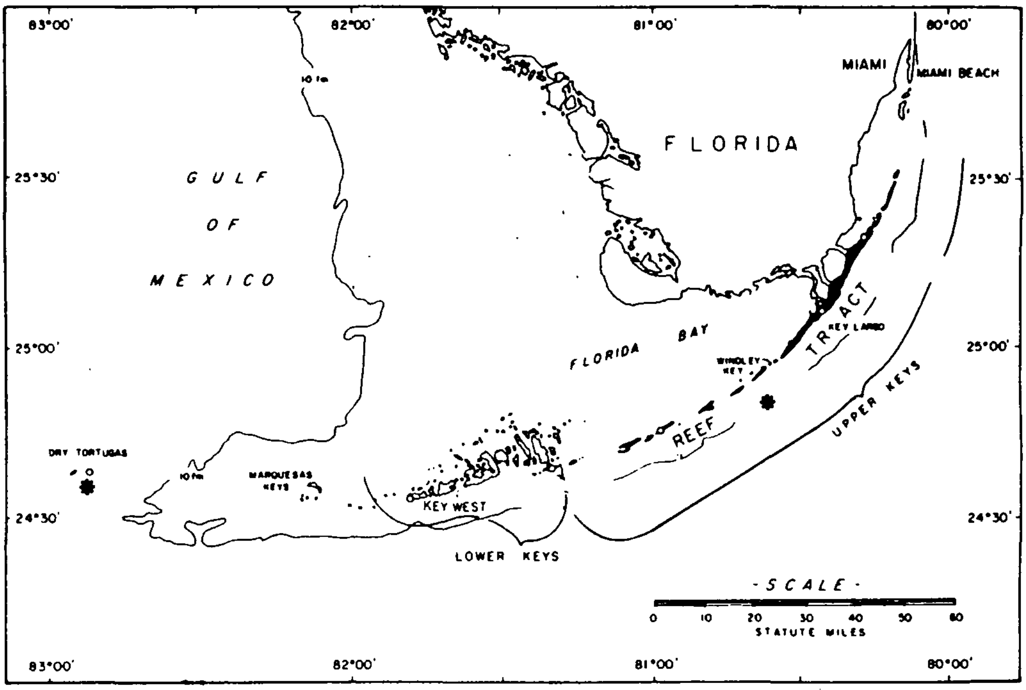

Figure 1.2 Main features of the Florida Keys and the Florida Reef Tract. Samples were collected from two areas, marked with an '*', namely Alligator Reef and Dry Tortugas. (Map from Mülter, 1977.

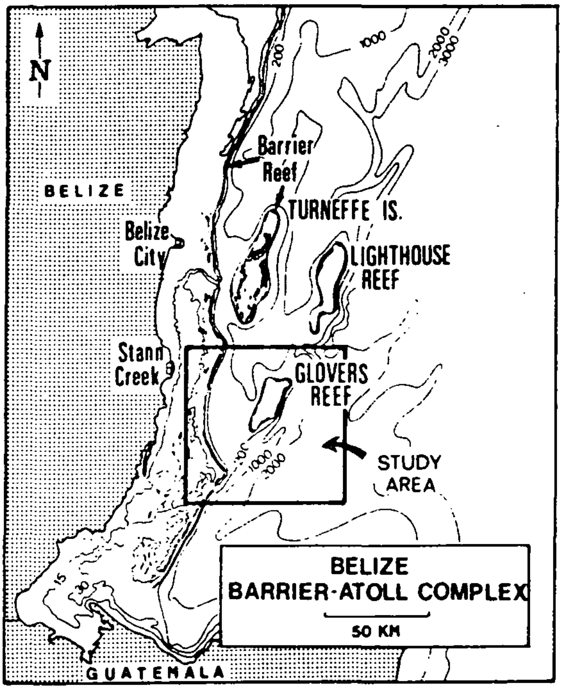

Figure 1.3 Map of the Belize continental Margin, showing the main features of the Belize Reef Tract. The material studied comes from the east side of Glovers reef. (From James & Ginsburg, 1979).

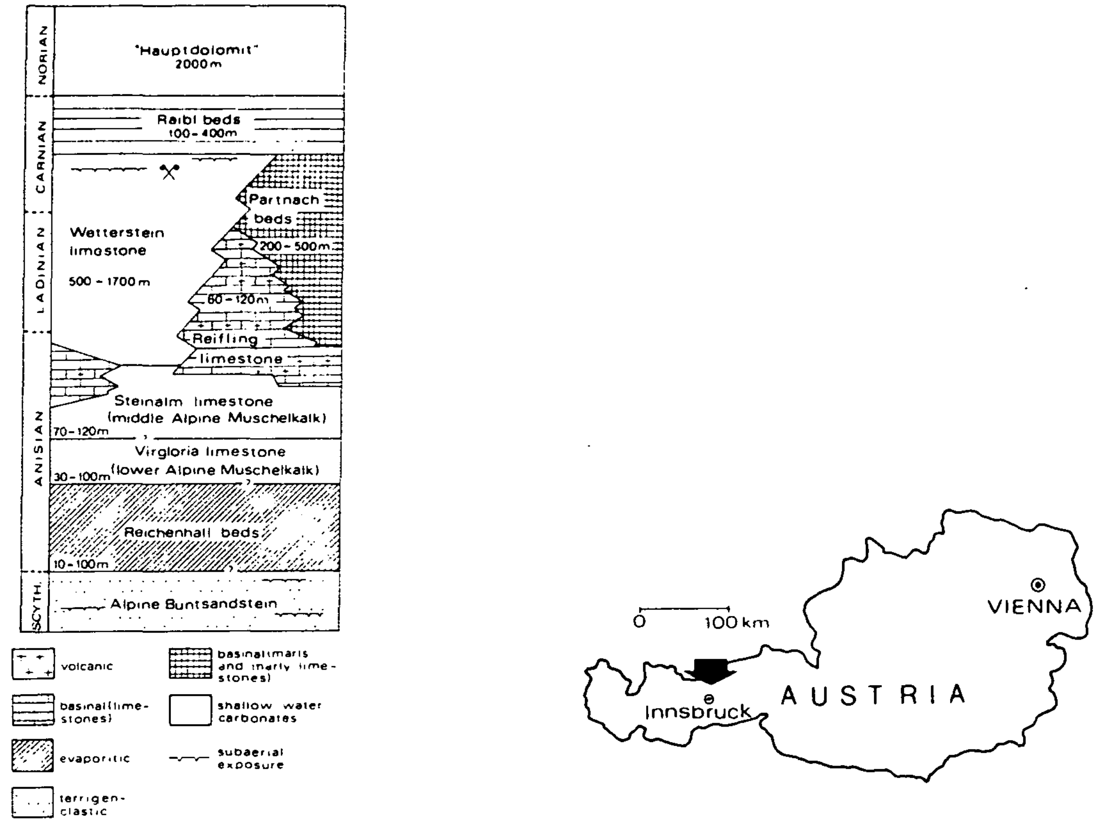

Figure 1.4 Location and stratigraphic position of the Wetterstein Limestone. The Triassic Hafelekar Reef Complex is situated in the Nordkette Range, to the north of Innsbruck. (From Bradner & Resch, 1981).

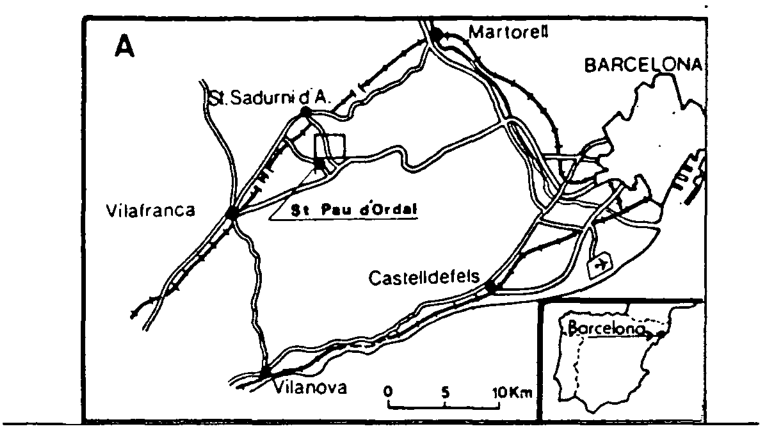

Figure 1.5 Location of the Miocene Sant Pau D'Ordal patch reef, Barcelona, Spain. (From Alvarez et al., 1977).

1.5 Previous Research on Cementation in Modern and Ancient Reefs.

It was only in the late 1960's that it was first realised that the cement crystals observed in ancient reef cavities were also present in living reefs and were therefore precipitated in the submarine environment. (Ginsburg et al., 1967; Ginsburg & Schroeder, 1969). Since that time there have been a multitude of reports in which observations of submarine cements have been documented from living reefs worldwide. Early descriptions of these cements can be found from reefs of Jamaica (Macintyre et al., 1968; Land & Goreau, 1970), from Panama (Macintyre, 1977), from the Red Sea (Amiel et al., 1971; Friedman et al., 1974), and from Mexico (Hoskin, 1971). Further descriptions can be found from reefs of the Great Barrier Reef (Marshall & Davies, 1981; Marshall, 1983a, 1983b), Brazil (Jindrich, 1983), Bermuda (Ginsburg et al., 1971; Schroeder, 1972a) and Belize (James & Ginsburg, 1979). Although a wide variety of cement morphologies is observed, there are essentially only two $CaCO_3$ mineralogies that precipitate from modern shallow seawater: aragonite and magnesium-enriched calcite. The most common areas to be cemented are the intra-skeletal cavities of the reef building and dwelling organisms. Here the chemical microenvironment is suitable for the precipitation and growth of crystals and the turbulence is low. Inter-skeletal voids are also cemented, but this is generally less common as even slight turbulence and mechanical abrasion will destroy the fragile early crystals. Much of the present literature concerning the controls on the precipitation of cements in reefs and associated sediments is summarised in Bathurst (1980), and James & Choquette (1983), who both also discuss diagenetic zones other than the modern submarine environment.

1.6 Prerequisites for Cementation.

From all the literature available on cementation in the marine environment, a number of basic prerequisites can be identified. The cementation process will not occur unless the following conditions are satisfied :

i) There is a suitable stable substrate. From a thermodynamic point of view, homogeneous nucleation, or nucleation direct from the solution without a substrate, is energetically unfavourable. Therefore, a substrate is necessary so as to allow heterogeneous nucleation to occur.

ii) There is a lack of mechanical abrasion. The delicate early crystals can be destroyed easily by mechanical abrasion. As mentioned above, therefore, the most common areas for cementation to occur are within intra-skeletal cavities. Grainstone sediments are rarely cemented to the same extent as framestone porosity in adjacent areas. Hardgrounds, notably, form several centimetres below the sediment water interface (Dravis, 1979), in a zone where there is little or no physical movement of the grains.

iii) The seawater is supersaturated. It is now accepted that aragonite and high magnesium calcite are precipitated from water of normal marine composition (Ginsburg & Schroeder, 1973). Clearly, however, for precipitation to occur, the water must be supersaturated with respect to the mineral in question. This is indeed the case for shallow water in the tropical belt (Pytkowicz, 1965; Broecker & Takahashi, 1966; Alexandersson, 1972).

iv) Water exchange is possible. A simple calculation of the molarity of the supersaturated seawater with respect to calcium and bicarbonate ions indicates that many thousand pore volumes of pore water have to pass through a pore in order to fill it with cement (Bathurst, 1975). As only that calcium carbonate above the saturation level will be removed from the solution, and as that process is likely to be quite ineffecient, this figure can probably be raised to the order of 100,000 pore volumes. Clearly, therefore, cementation will only occur in areas where there is an active pumping mechanism to force the large volumes of water through any body of sediment. Reefs are an excellent example of an area where there is likely to be a suitable hydrodynamic regime. The modern reefs of Florida have substantial relief over the sea floor and typically grow in the highest energy conditions located along the shallow shelf margin. Wave energy, tidal pumping and currents all contribute to the flow through reef porosity.

v) The pore waters must be oxygenated.

In small enclosed pores, available oxygen may be rapidly depleted by the decay of organic matter. Whilst this decay may well contribute to the precipitation of calcium carbonate, Zankl & Mülter (1977) found that pore waters from cemented areas were apparently higher in oxygen content than those from areas with no evidence of cementation.

vi) Some considerable time must pass. This is not as obvious as it may seem at first. Even in the high energy shelf edge conditions, the cementation process will be very slow. The total percentage of cement in any reef accumulation will be dependent on the rate of growth of the reef. The latter does depend on the rate of change of sea level, although it is known that reefs can accrete laterally when sea level is constant. (Hubbard et al., 1986). As the rate of growth increases, the total volume of reef formed in a fixed period of time will also increase, but the rate of precipitation of cement will remain constant. Hence, cementation may appear to be less pronounced at times of rapid reef growth.

1.7 Chemical Principles and the Supersaturation State.

1.7.1 Introduction.

The inorganic carbonate system interacts extensively with an organic and biogenic carbon cycle as indicated on Figure 1.6. Input from the organic cycle to the precipitated cements is generally quite rare, particularly in the reef environment where the turbulence and oxygenated conditions mean that any organic matter is rapidly destroyed by the many microorganisms. When direct input of organically derived carbonate does occur, it is usually easy to identify as the product will have a 'light' carbon isotopic composition. The question of organic and biogenic input to the cements of modern reefs is discussed further in Chapter 3.

1.7.2 Dissolved carbonate equilibria.

A thorough understanding of the process of the precipitation of the cements from seawater ought to be based on a knowledge of the thermodynamic and kinetic principles involved. This topic is dealt with in a rigorous fashion by Stumm & Morgan, (1970), but a brief outline of the principles is described below.

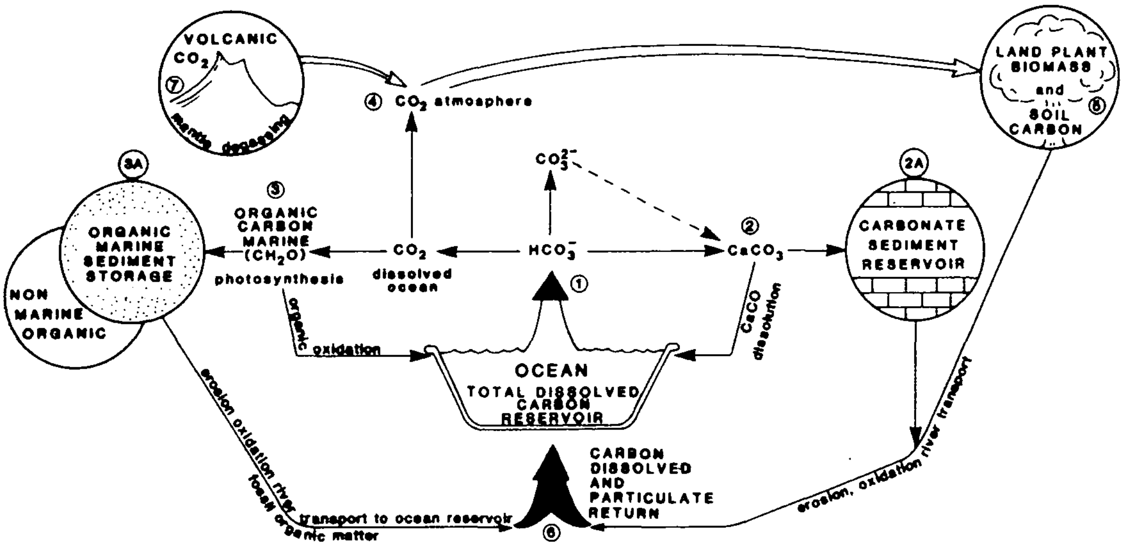

THE TERRESTRIAL CARBON SYSTEM MAJOR RESERVOIR AND FLUXES

Figure 1.6 The interaction of the inorganic and organic / biogenic cycles. (From Arthur & Anderson, 1983).

The starting point is a model system involving carbonate species dissolved in pure water. Initially, it is assumed that there is no gas phase, or in other words, the system is closed to the atmosphere.

Six chemical species are then involved, (Stumm & Morgan, 1970) these are CO_2, H_2CO_3, HCO_3^-, CO_3^{2-}, H^+, and OH^-. The chemical equilibrium ought therefore to be described by a minimum of six equations. In fact, the total dissolved CO_2, whether as CO_2 (aq) or in its hydrated form as H_2CO_3, can be defined as $H_2CO_3^*$. The number of species is therefore reduced to five and a complete description of the system can be made using the following five chemical equilibria :

$$H_2O + CO_2 \rightleftharpoons H_2CO_3 \qquad K \qquad 1.1$$

$$H_2CO_3 \rightleftharpoons HCO_3^- + H^+ \qquad K_1 \qquad 1.2$$

$$HCO_3^- \rightleftharpoons CO_3^{2-} + H^+ \qquad K_2 \qquad 1.3$$

$$H_2O \rightleftharpoons OH^- + H^+ \qquad K_w \qquad 1.4$$

$$H_2CO_3^* \rightleftharpoons HCO_3^- + H^+ \qquad K_{H_2CO_3} \qquad 1.5$$

The equilibrium constants (K) define the position of each reaction at thermodynamic equilibrium. For equation 1.2, for example :

$$K_1 = \frac{[HCO_3^-{}_{(aq)}]_{(eq)} \times [H^+{}_{aq}]_{(eq)}}{[H_2CO_{3(aq)}]_{(eq)}}$$

where $[....]_{(eq)}$ means the concentration of the species inside the square brackets, at equilibrium. If this model aqueous system is now opened to the atmosphere, an extra equilibrium relationship between the gas and solution phases has to be considered:

$$CO_{2(g)} \rightleftharpoons CO_{2(aq)} \qquad 1.6$$

The next stage involves the addition of metal ions to the system; in this case calcium carbonate precipitates are being studied, and extra equilibria can be defined to represent the interaction of the calcium ions with the other aqueous species:

$$CaCO_{3(s)} \rightleftharpoons Ca^{2+} + CO_3^{2-} \qquad K_{So} \qquad 1.7$$

$$CaCO_{3(s)} + H^+ \rightleftharpoons Ca^{2+} + HCO_3^- \qquad 1.8$$

$$CaCO_{3(s)} + H_2CO_3^* \rightleftharpoons Ca^{2+} + 2HCO_3^- \qquad 1.9$$

$$CaCO_{3(s)} + H_2O + CO_{2(g)} \rightleftharpoons Ca^{2+} + 2HCO_3^- \qquad 1.10$$

$$CaCO_{3(s)} + 2H^+ \rightleftharpoons Ca^{2+} + CO_{2(g)} + H_2O \qquad 1.11$$

$$CaCO_{3(s)} + 2H^+ \rightleftharpoons Ca^{2+} + H_2CO_3^* \qquad 1.12$$

Equation (1.7) is the standard solubility relationship for calcium carbonate. The equilibria described in equations (1.8) to (1.12) simply indicate that the solubility of calcium carbonate can be characterised by different experimental variables. For example, the solubility equilibrium for calcium carbonate can be defined from a knowledge of pCO_2, $[Ca^{2+}]$, and $[H^+]$ - equation (1.11), or from pCO_2, $[Ca^{2+}]$, and $[HCO_3^-]$ - equation (1.10). These parameters are easier to determine analytically than is the concentration of CO_3^{2-}, a figure which would have to be known in order to make calculations on the basis of equation

(1.7) alone. The above equilibria, (equations (1.1) to (1.12)), accurately and completely describe a model aqueous calcium carbonate system in contact with a gaseous phase. In a real system, however, there are a number of complicating factors which have to be considered:

i) Seawater.

In seawater, the activities of the various species described above are generally less than the measured concentrations. This is due to the formation of complexes or ion pairs with the other ions in the sea water. Effectively, not all of the analytically determined concentrations of the various ions are available for reactions. This is a vital consideration to take into account when making calculations involving carbonate equilibria in natural waters.

ii) Kinetic Considerations.

All of the ionised equilibria in the carbonate system are attained very quickly, in fractions of a second. Somewhat slower is the attainment of the equilibrium in the hydration of CO_2:

$$CO_{2(aq)} + H_2O \rightleftharpoons H_2CO_3 \qquad 1.13$$

This can, therefore, lead to many situations where the water is out of equilibrium with the atmosphere. Hence, it can be seen that although the thermodynamics provides information about the equilibrium position of any reaction, in order to gain a quantitative understanding of the products, it is essential to consider the kinetics of the system also.

1.7.3 The supersaturation state.

This factor is quantifiable using the parameter Ω, calculated as follows:

$$\Omega = \frac{a\,Ca^{2+} \times a\,CO_3^{2-}}{K_{So}} \qquad 1.14$$

Note that it is activities (a) of the ions that is being considered, this represents the real available or effective concentrations as described in Section 1.7.2. K_{So} is the standard solubility product as defined in equation (1.7). The value of Ω is calculated relative to the solubility product of the mineral concerned; in this case relative to aragonite or high-magnesium calcite. The solution is supersaturated when $\Omega > 1$. There is very little data available on the supersaturation state of waters around the Florida shelf or Bahaman platform. What there is, however, indicates that the sediment pore waters are up to 300% supersaturated with respect to both aragonite and high magnesian calcite (Morse et al., 1985). There are problems, already alluded to above, in the interpretation of these data, as it is not clear whether the observed saturation states represent a metastable equilibrium between the sediment and the pore waters or whether they are dominated by the kinetics of the system. It is not certain that the pore waters are in contact with the sediments for a long enough period of time in order for the saturation state to reach a steady state value.

However, it does appear that the waters are supersaturated with respect to all the carbonate phases of interest. This supersaturation state is thermodynamically metastable and precipitation should therefore occur. Although homogeneous nucleation is unfavourable, heterogeneous nucleation should be energetically possible and yet the supersaturation state still prevails. The reasons for this are discussed in greater detail in the following section.

1.8 Factors Preventing Precipitation from Supersaturated Seawater.

1.8.1 Nucleation energies.

Formation of a precipitate is a combination of two processes; nucleation and crystal growth. Distinction between the two can be made from an understanding of the energetics of crystallisation. A large excess of energy is required to create a new surface; this is related to the interfacial free energy and it is this which forms a barrier to nucleation, (Figure 1.7). For crystals larger than a few microns, the interfacial free energy is negligible in relation to the bulk free energy and can therefore be ignored. The energy of formation of a crystal varies as a function of the number of atoms in the nucleus as in Figure 1.7, and is also dependent on the supersaturation state. Increasing Ω causes a decrease in the energy required to form a crystal.

The interesting point about Figure 1.7 is that crystallisation initially requires an increase in free energy due to the creation of a new surface. This process is the nucleation phase. The maximum point on the curves (ΔG^*), is a position of equilibrium, where the solution is saturated with respect to crystals of a critical size (n). Only when they reach this size, and overcome the energy barrier ΔG^*, can the process of growth take over. Further increase in size is accompanied by a decrease in free energy and is therefore thermodynamically favoured. A rigorous theory can be found in Berner, (1980).

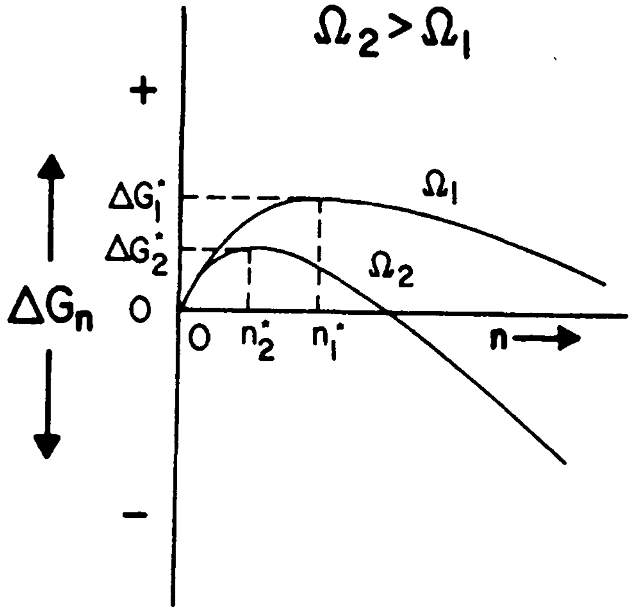

Figure 1.7 Plot of free energy of formation of a single crystal as a function of the number (n) of atoms, ions or molecules in the crystal. There is an energy barrier ΔG^* to the nucleation which corresponds to a critical size nucleus (n^*). Once the nucleus is larger than n^*, the process of crystal growth takes over from nucleation. Note that the free energy barrier is lower at higher supersaturation states. (From Berner, 1980).

Homogenous nucleation requires the subcritical size nuclei to attain the extra energy (ΔG^*), in order to grow. The kinetics of such a process in natural systems are such that it is most unlikely that homogenous nucleation would occur (Wollast, 1971). However, there are an abundance of stable nuclei on which heterogeneous nucleation could occur. In this process, the seed crystals provide a substantial amount of the excess energy required for growth to occur. As there is no need to create an entirely new surface, the energy barrier is therefore much reduced, though not necessarily zero. In the ideal situation, where the seed and potential precipitate are of the same mineralogy, the nucleation energy is minimal and the crystallisation process is then essentially pure growth. It should therefore proceed easily under natural conditions, until the concentrations are reduced below saturation levels. Nevertheless, the supersaturation state prevails, and there must therefore be some other processes inhibiting the precipitation.

1.8.2 Physical barriers.

It has been suggested that there may exist a coating of mucilagenous organic material covering all suitable substrates and thereby physically preventing contact of the calcium and carbonate ions with a potential substrate surface (Berner et al., 1978). The nature of this material, if it exists, is poorly known, though there have been reports of fulvic or humic acid type substances (Berner et. al., 1978). As mentioned above, the highly turbulent and oxygenated nature of the environment means that any organic matter is unlikely to remain intact for any substantial period. In order to act effectively, a coating which is deposited from the water would have to have a substantial thickness, perhaps 500Å ($500\times10^{-10} metres$). The surface area of carbonate sediments is very high, up to $5 m^2 g^{-1}$, (Walter & Morse, 1984b; Appendix 5), this therefore implies a large volume of organic matter:

$$500 \times 10^{-10}\ [m] \times 5\ [m^2 g^{-1}] = 2.5 \times 10^{-7}\ [m^3 g^{-1}] = 0.25\ cm^3 g^{-1}$$

If the likely range of density for the organic matter is 1 to 2 gcm^{-3}, then this implies a range of 25 to 50% by weight organic matter. It is clearly unlikely that the average organic content of modern reefal sediments would be as high as 50%, and as the total extractable organic matter from a 8000 year old reef rock (Chapter 4) is less than 0.1%, it seeems unlikely that this process would be effective.

1.8.3 Biogenic inhibition.

One might expect the calcareous organisms to have their own protection against external precipitation on their shell or skeletal material. This protection would most likely be some sort of membrane, and because it would be biogenically secreted it might be effective at a normal membrane thickness of perhaps 50 to 100Å. This would then imply a more reasonable level of organic matter in the sediment. However, as mentioned in Section 1.8.2, this organic coating will not survive for long periods of time after the death of the organism. Indeed, precipitation of cements in coral skeletons has been observed to occur within millimetres of the living surface (Hubbard, 1972), indicating that any inhibitory effect is particularly short lived. There are also many very important biogenic and organic effects which serve to catalyse or promote the precipitation of these cements. This topic is discussed in Section 4.3.

1.8.4 Inorganic inhibition.

A number of inorganic ions have an inhibitory effect and can retard and even prevent the precipitation and growth of calcite and aragonite (Reeder, 1983).

i) Magnesium ions. Both dissolution and precipitation kinetics are inhibited by magnesium ions, as shown by experiments involving the flow of solutions over calcium carbonate (Weyl, 1967). Berner (1975), found that magnesium had no effect on the precipitation kinetics of aragonite but had a very marked retarding effect on the precipitation of calcite. Magnesium ions are known to fit easily into the lattice of calcite but are not incorporated into the aragonite lattice. As the magnesium ion is smaller than the calcium ion, it has a higher surface charge and so attracts a larger hydration sphere than calcium. The reason for the inhibitory effect is thought to be related to the higher energy required to dehydrate the magnesium ions as they are incorporated into the calcite crystals. As magnesium ions do not fit into the aragonite lattice, they do not have any effect on its precipitation kinetics.

ii) Phosphate ions. Orthophosphate in solution has also been found to inhibit seeded growth of calcite. The results indicate that ions are adsorbed on to the crystal surface and inhibit precipitation simply by blocking active nucleation and growth sites (Berner & Morse, 1974; Reddy, 1977).

1.9 The Factors Controlling Cement Mineralogy.

1.9.1 Thermodynamic control.

Many experiments have been undertaken using simple solutions and seawater to try and determine which cement mineralogy is the most stable under natural conditions. The system is complex, with many interacting inhibitory effects (Section 1.8). In particular, the kinetic inhibition of the precipitation of calcite by magnesium ions means that the precipitation of aragonite may be kinetically favoured though not necessarily thermodynamically preferable.

The most recent work (Walter & Morse, 1984a), suggests that aragonite is thermodynamically equivalent to a calcite with approximately 12 mole% magnesium as magnesium carbonate. Hence, a magnesium calcite with more than 12 mole% magnesium will be less stable than aragonite. This lowered stability in the solid state leads therefore to an increased solubility. Although the experimental figures do vary (Morse, 1974; Plummer & Mackenzie, 1974; Walter, 1983; Walter & Morse, 1984a), it is clear that the solubility of calcite will increase as the magnesium content increases and so at some point, a magnesium calcite phase will become less stable than an aragonite one. This effect is related to increased lattice strain (Chave et al., 1962), due to the incorporation of the smaller magnesium ions into the calcium and carbonate layers. As the process of crystal growth is a balance between dissolution and precipitation reactions, the growth rate of calcite will become progressively more inhibited as the magnesium content increases, leading to a kinetic advantage for the precipitation of aragonite. Again it should be emphasised that it is important to analyse the thermodynamic state of the system, but it is equally important to realize that the thermodynamics do not tell us anything about the rates of various reactions. It is this information about the kinetics which is essential to the understanding of the products.

1.9.2 Organic and biogenic controls.

There are several references in the literature concerning both intra- and extra-cellular skeletal production, which describe the interaction of high molecular weight complex organic molecules with the precipitation of the inorganic phases. (Hayes & Goreau, 1977; Degens, 1979; Simkiss, 1986). These papers describe the association of proteinaceous carrier molecules with glycoprotein based mineralising matrices. These matrices are thought to be capable of chelating Ca^{2+} and CO_3^{2-} ions in specific stereochemical geometries such that a particular cement mineralogy is preferred. Hence ions held in a 9-fold coordination geometry will nucleate aragonite and ions held in a 6-fold coordination geometry will nucleate calcite (Degens, 1976).

A second form of control which is apparently exerted by some organisms is through their ability to exclude certain ions from their intra-cellular spaces. Hence, the ability of corals to nucleate only aragonite seeds, rests in their capacity to exclude magnesium ions from the site of intra-cellular skeletogenesis (Degens, 1976).

As discussed in previous sections concerning the effect of organic matter on the precipitation of cements, the effects are only likely to occur over relatively short periods of time after the death of the organisms. Nevertheless, there exists the possibility that the controls discussed above may have a significant effect on the mineralogy of nuclei on which further growth of cements may occur by purely inorganic processes. This leads to the concept of the physical control of substrate mineralogy on the mineralogy of the growing cements.

1.9.3 Substrate control.

It is often apparent that cements of a particular mineralogy are preferentially precipitated on to a surface of the same mineralogy (Alexandersson, 1972; Ginsburg & Schroeder, 1973; Bathurst, 1980). This phenomenon is by no means exclusive and exceptions certainly do occur, (Ginsburg et al., 1971). Interlamination of cements of different mineralogies also occurs (Bathurst, 1980). The reason for this common preference is due to energetic considerations (Section 1.8.1). The closer the similarity of the substrate and cement in terms of their structure at the atomic level, the lower will be the activation energy barrier to the creation of a nucleation centre. This concept is taken to its extreme in cases where cement crystals are seen to grow in optical and therefore lattice continuity with their substrates.

1.9.4 Other physical controls.

A further physical effect that can potentially determine the mineralogy of the precipitated cement is the rate of supply of CO_3^{2-} ions, (Given & Wilkinson, 1985). They suggest that high rates of supply produce aragonite, whereas lower rates of supply may lead to the precipitation of magnesian calcite. This therefore explains a common observation that magnesian calcite follows aragonite in individual pores. At first, fluid flow through a cavity is high, and therefore the rate of supply of CO_3^{2-} ions is also high and so aragonite precipitates. As the pore throats become progressively more restricted by the precipitation of the cement, the fluid flow decreases to a point where the supply rates decrease far enough for the precipitation of magnesian calcite to be preferred.

1.10 The Factors Controlling Cement Morphology.

1.10.1 Surface charge effects.

Lahann (1978) suggested that surface charge effects may be able to control calcite crystal morphology. The surfaces of calcite crystals at seawater pH will have a net positive charge simply due to the fact that there is an excess of cations to anions for the calcium carbonate system. The Ca^{2+}/HCO_3^- ratio in seawater is about 4 and if magnesium ions are included then the cation to anion ratio rises to about 26 (Turekian, 1969). This theory is confirmed by the experiments of Somasundaran & Agar (1967), which showed that for $pH < 8$, calcite rhombs acquire a net positive charge. The crystallographic orientation of the anions and cations allows differences in the surface potential to be developed on different faces. For calcite in particular, it appears that the highest charge density will be on the c-axis faces. Crystal growth will be dependent on the rate of supply of the ions in lowest concentration (Doremus, 1958; Lahann, 1978), in this case the carbonate or bicarbonate anions. The c-axis faces, having the highest positive charge, will attract the largest number of anions and therefore the growth of the crystal will be fastest in a direction parallel to the c-axis. This hypothesis accounts for the observation that most submarine cements are acicular with the c-axis being the longest dimension. The above argument is for calcite, and although less is known about the kinetics of aragonite precipitation, by analogy, this also explains the acicular nature of marine aragonite precipitates. There are, however, several examples of cements which are undoubtedly precipitated in a marine environment, but are not acicular in morphology. Microcrystalline aragonite has been observed from the Great Barrier Reef (Marshall, 1983a), and is present in grapestones (Illing, 1954). Microcrystalline high magnesium calcite precipitates are ubiquitous. In these cases the microcrystalline morphology can be explained by considering relative rates of nucleation versus rate of crystal growth. In the acicular cements, crystal growth occurs on an individual or a few nucleation centres; so the rate of growth is rapid compared to the rate of nucleation. In contrast, in the precipitation of microcrystalline cements, nucleation rates are very high compared to the rate of crystal growth. Hence, many nuclei form and then do not have the chance to grow to any substantial size, leading to the development of a fine grained texture.

1.10.2 Substrate control on morphology.

In some coral skeletons, microcrystalline aragonite occurs in pores where there is plenty of room for the crystal to grow larger. This is probably due to an effect on the nucleation rates as mentioned above. This effect may be attributable to the involvement of a Ca^{2+} binding organic secretion from the corals which may enhance the nucleation rate. Further discussion on the possible role of organic matter is given in Chapter 4. Constantz (1986), has shown that the micro-architecture of coral skeletons affects the dissolution susceptibility of the aragonite and it may also therefore affect the morphology of the cements precipitated.

1.10.3 Magnesium poisoning.

Lahann (1978) and Folk (1974) have discussed the effects of magnesium poisoning the calcite lattice and enhancing growth in the c-axis direction essentially by inhibiting growth on the other faces. The magnesium ion, being smaller than the calcium ion, causes a distortion of the lattice whenever it is incorporated into the growing layers. This distortion results in further growth around the incorporated magnesium ion being difficult. The calcium and carbonate ions are formed in layers perpendicular to the c-axis, and according to Folk (1974), the incorporation of a magnesium ion into a position at the edge of a growing crystal causes more distortion (due to a lower coordination number), than if it was incorporated into the middle of a continuous layer of calcium ions. Therefore, growth in directions other than parallel to the c-axis is inhibited, and acicular crystals are formed.

1.11 The Factors Controlling the Spatial and Temporal Distribution of the Cements.

1.11.1 Spatial distribution.

Many studies have shown evidence that the cementation patterns are extremely inhomogenous on a variety of scales. On the whole shelf and regional scales, there does seem to be a correlation between higher energy and greater cementation. Hence, the shelf edge environments tend to show more evidence of cementation than do the shelf interior facies, (Marshall, 1985). Similarly, the seaward edge of reefs is commonly cemented to a greater extent than the shoreward edge, (James & Ginsburg, 1979). However, on the smaller scales of the core, hand specimen, and thin-section, the degree of cementation is extremely irregular. This inhomogeneity is obvious right down to the scale of individual pores, where widely differing volumes of cement are observed within adjacent pores.

It appears that there is a whole hierarchy of scales on which this irregularity of cementation occurs and this variety is probably due to the complex nature of the pore systems in reef rock. There exist many different types of connected and non-connected pores in the reef framework; this variety is greatly enlarged by the activity of boring organisms, which serve to increase the connectivity of the pores, and the effects of sedimentation which tend to block pores. The cementation process itself also has an effect on the pore network, a sort of negative feedback. This complexity of interaction is that which was discussed previously (Section 1.3). The emphasis again has to be not only on the static, spatial interaction of these processes but on the dynamic aspect, the interaction over time. This concept leads to an understanding of the way in which cement generations of different mineralogies can be seen to be superimposed in some pores. If there is an area in which aragonite is being deposited and this area becomes open to a different or evolving chemical environment, perhaps through the action of some boring organism, then in the new environment it may be preferable for a magnesian calcite to precipitate. So, although it may be difficult to understand the reasons for a sudden change in cement mineralogy from the frame of reference of an individual pore, the controlling factors become more obvious from a dynamic point of view. In order to explain this irregularity, the concept of the 'microenvironment' has been developed Schroeder, (1972a).

Hence, it is suggested that where different volumes or even different morphologies of cement are present in adjacent pores, that the microenvironments in the pores are actually different. These microenvironments are considered to be under both chemical and permeability control.

1.11.2 Chemical microenvironments.

There are several examples in the literature where it is suggested that adjacent pores have different pore water chemistries. This is particularly the case when micro-organisms are thought to be involved (Schroeder, 1972b). This concept appears to create something of a paradox. In order to fill a pore with cement, it is necessary to pass through many thousands of pore volumes of water (Section 1.6). This therefore implies a highly 'open' and permeable pore system. However, the concept of a chemically varying microenvironment implies that the system is at least partially closed.

1.11.3 Permeability control.

The complexity of the biogenically formed skeletons leads to an equally complex pore system which can be modified by other processes (Section 1.11.1). This produces a great variability in the pore scale permeability and a widely ranging pore water flux throughout the reef framework, from pores which are highly turbulent to those which are essentially stagnant. This aspect of microenvironmental permeability has received very little attention in the literature and is followed up in a quantitative manner in Chapter 5.

1.11.4 Temporal distribution.

All of the previous discussion has been concerned with the controls on the precipitation of cements in the initial submarine environment. The temporal distribution of cements within any particular reef is entirely dependent on the temporal variation in the fluids occupying and flowing through the formation. These in turn are dependent on the diagenetic zones through which the reef passes. There are two further zones in which large volumes of cement are precipitated, the meteoric (phreatic and vadose) and the burial environments. Some description of meteoric cements is given in the petrographic description of samples collected from cores which penetrated the Pleistocene substrates of the Florida Holocene reefs. Prior to the Flandrian transgression, these substrates were exposed and therefore subject to the effects of meteoric waters. The basic physico-chemical controls on the precipitation of these cements are assumed to have been similar to those discussed above.

On a shorter timescale, however, there may be some evolution of the pore water passing through a formation as it interacts with the solid phases present. Although there is unlikely to have been any evolution of the pore waters passing through the modern reefs of Florida, progressive evolution of pore waters has been recognised in some ancient formations (Dickson & Coleman, 1980), and this aspect is investigated in the study of a Triassic buildup presented in Chapter 6. If the rate of evolution of the chemistry of the pore waters is fast relative to the speed of movement through the formation then this can lead to an interesting and complex temporal control on the spatial distribution of the diagenetic products (Pingitore, 1982).

1.12 Facies Specificity and Regional Cement Distribution.

There are only a limited number of studies of the larger scale and regional distribution of cements within reef systems. Those that do exist indicate that cementation is essentially restricted to the seaward margins of shelf edge reefs and that reefs shorewards of the shelf edge tend to show very few signs of lithification (James & Ginsburg, 1979; Marshall, 1985). James et al. (1976) suggested a facies and fabric specificity in the diagenetic products within cavities of the Belize Barrier reefs. Most of these observations can be explained on the basis of more fundamental controls. Hence, grainstones can be cemented to a greater extent than adjacent framestones due to their greater permeability and the concomitant greater flux of water. Conversely, in areas of very high energy, such as shelf edge reefs, although there is evidence of cementation in the reef framestone facies, the interstitial and cavity filling grainstones are commonly not cemented. This observation is probably best explained by the fact that the environment is so turbulent that the grainstones are constantly in motion and the mechanical abrasion destroys any cement crystals before they have chance to develop.

1.13 Ancient Reefs.

All of this introduction has been concerned with the controls on the precipitation of cements in modern reefs and therefore during only the very earliest stages of the diagenetic history. Much of the thesis is devoted to examining this aspect of cementation in reefs and associated facies; the initial controlling factors, the products, and their spatial distribution.

Chapter 6, however, presents a study of the diagenetic history of a Triassic reef buildup. The emphasis in this chapter is not on understanding the controls on the initial precipitation, but to concentrate on the nature of the products and their spatial and temporal distribution. Although it is assumed that many of the basic physico-chemical controls on the cementation process were the same in the ancient seas, it is clear that the sea water chemistry may have been different in the past and hence, may lead to differences in the chemistry and the mineralogy of the precipitated cements.

According to Sandberg (1983), aragonite was probably the most stable phase during the Triassic, so the original cement mineralogies may have been similar to those precipitating in modern reefs. However, the detailed geochemistry may have been different in the past and many diagenetic alterations might be expected to have occurred since the Triassic. In conclusion, there is little point in trying to compare the specific products of the modern and ancient environments. However, it is useful to study the diagenetic history and the distribution of the products observed in the ancient examples with the knowledge and understanding of the factors controlling the initial diagenetic events in the depositional environment.

1.14 Research Objectives.

From the previous discussion of the past literature concerning the controls on the precipitation of cements in modern and ancient reefs, it is apparent that there are a number of areas which deserve further study. This thesis is, therefore, dedicated to gaining an understanding of the following processes:

i) The degree of biogenic control on the precipitation of cements.

ii) The role of organic matter, whether direct or indirect, on the precipitation of cements.

iii) The factors controlling the distribution of cements on all scales.

iv) The nature of the timing and distribution of cementation in ancient reefs.

1.15 Chapter Outlines.

Chapter 2 describes the petrography of modern reef material from Florida and Belize in terms of the reef constituents and the relationships of the cements to them. This leads to the development of an idea of the relative intensities of the major reef forming processes as described in Section 1.3. The distribution of these exclusively marine cements is described on a range of scales, from the thin-section to the regional level.

Chapter 3 discusses the problem of the possible control of biogenic effects on the cementation process. It clarifies the role of reef building and dwelling organisms in the precipitation of cements.

Chapter 4 considers the possible involvement of organic matter in the precipitation of cements. The topic is discussed from several points of view; whether the organic matter contributes directly to the inorganic carbonate of the cements, or whether it simply acts in a mediatory fashion. A rigorous analysis is made of the organic matter associated with one particular cement phase from the Holocene of Florida.

Chapter 5 is a study of the hydrodynamics of the cementation process and uses mathematical modelling to investigate the degree of control exerted by the permeability of the reef rock on the pattens of cementation. Poroperm data from samples of the Miocene patch reef described in Section 1.4.3 are used to investigate the possibility of modelling the flow characteristics on a reef scale. The porosity and permeability data are described in terms of both the depositional facies and the diagenetic overprint.

Chapter 6 is a study of the diagenetic history of a Triassic reef. The detailed geochemistry of the cements is used to try and determine the environment of precipitation and to describe the diagenetic events which have occurred since the original deposition. Correlation of the cement phases across the whole reef body leads to an understanding of the timing of the cementation process on the reef scale.

Chapter 7 concludes the thesis with a discussion of the major controls on the cementation process and attempts to provide a conceptual model to account for the geochemistry and distribution of cements on a variety of scales. The implications for the development of carbonate petroleum reservoirs within reefs and associated facies is briefly discussed.

CHAPTER 2

Petrography of Recent and Pleistocene Reef Rock from Florida and Belize.

CHAPTER 2

Petrography of Recent and Pleistocene Reef Rock from Florida and Belize.

2.1 Introduction.

This chapter describes the petrography of Holocene reef rock from Florida and Belize. It is introduced with a general description of the regional and local settings of the Florida reefs and this is followed by a detailed description of one particular reef, 'Alligator reef' from which most of the material studied was collected. The components of the limestones are described separately, with emphasis on the cements and the porosity in which they are precipitated. The intensity of the various reef forming processes and the degree of interaction between them has been evaluated, again concentrating on the interaction of the cementation processes. The distribution of the cements is discussed on a variety of scales, fromthat of the thin section to the reef as a whole. A similar full description is given of the Dry Tortugas reef materials, highlighting the differences between them and the Alligator reef samples. A further section describes the reef rock of Belize, again comparing the characteristics with those of the Florida reefs.

The chapter concludes with a discussion of the controls on the cementation processes in the various reef settings. A provisional model to account for the distribution of the cements is presented, setting the background to the next three chapters, in which the processes controlling cementation are investigated in more detail.

2.2 The Holocene Reefs of Florida.

2.2.1 Regional setting.

The Holocene features of the South Florida carbonate shelf are the latest development in a long history of shallow water carbonate deposition in the area. The carbonate producing region is extremely large, being bounded by Cuba in the south, by the deep Atlantic ocean to the east, the Gulf of Mexico to the west and clastic sediments to the north (Figure 2.1).

Three major areas of shallow water sediments exist today: the S. Florida Platform, the Great and Little Bahama Banks and the Cay Sal Bank (Figure 2.1). These are separated by channels of bathyal depth (1–4000 metres), namely the Straits of Florida, Providence Channel, Nicholas Channel, Tongue of the Ocean and Exuma sound. Water depths on the positive features are generally less than 15 metres and only a very small proportion of the region is land, all of which has very low relief.

According to Applin (1944; 1951), the area has been one of predominantly shallow water carbonate deposition since the Jurassic and there exists up to 11 kilometres of sediments above pre-Jurassic basement. Ball (1967) suggested that the presently observed topography is the result of exaggerated structural relief created by post Early Cretaceous faulting (Sheridan et al., 1981). An alternative hypothesis is that the deep water basins originated as grabens in the rift stage of the Atlantic and have remained as negative features ever since (Mullins, 1977). For fuller details of the geological history of the area see Enos & Perkins (1977) and for a discussion of the origin of the Bahama Platform see Schlager et al. (1985).

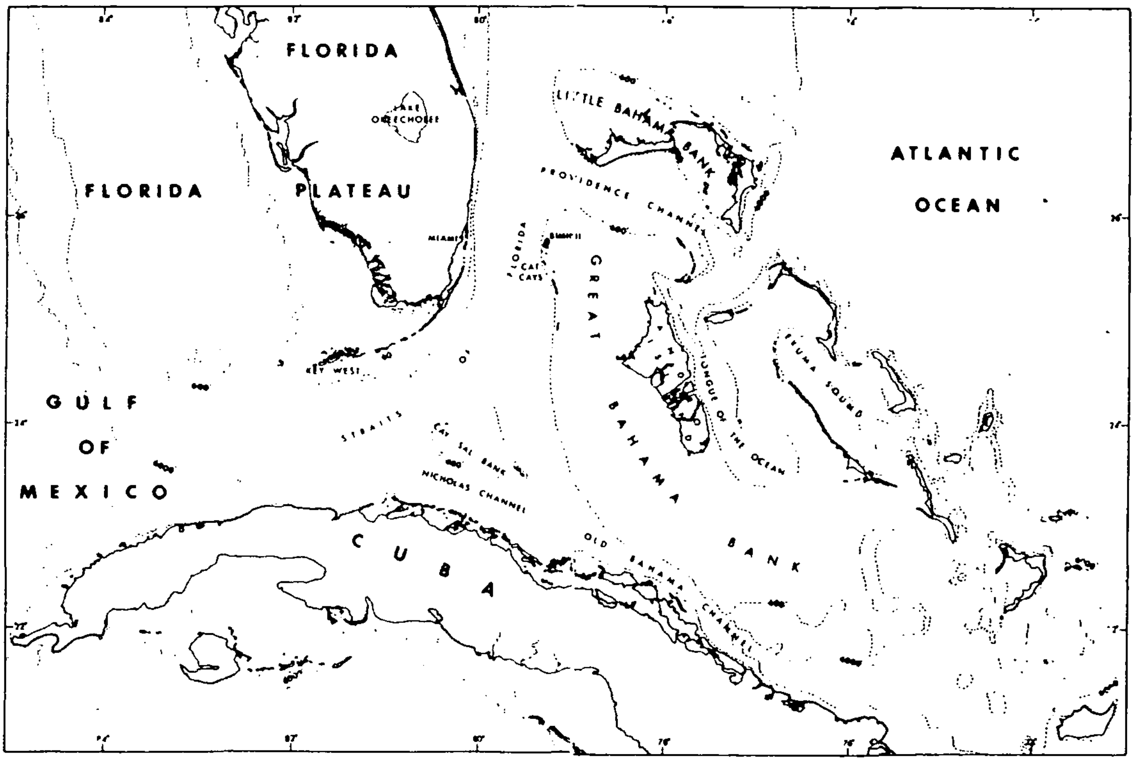

Figure 2.1 Regional location map of the Florida-Bahamas carbonate province. (From Enos & Perkins, 1977).

2.2.2 Florida local setting.

The area is an example of a rimmed shelf (Ginsburg & James, 1974) and is characterised by the development of reefs and sandbodies along the shelf margin. The shelf is between 6 and 35 km. wide and is approximately 300 km. long, forming an arcuate strip parallel to the Florida Keys (Figure 2.2). Carbonate sediments are also accumulating in Florida Bay, west of the Florida Keys. Holocene sediment thicknesses on the Florida shelf are generally less than 1 metre except along the lower Florida Keys to Dry Tortugas, and at the shelf edge where reef development is significantly thicker. The topography seaward of the shelf edge is complex and characterised by a number of recognisable terraces and slopes (Enos & Perkins, 1977). The shallow shelf break is at less than 20 metres water depth and is not the most prominent of the slopes. The material studied in this thesis was collected exclusively from the shallow shelf shorewards of the shelf break and principally from reefs of the shelf edge itself.

2.2.3 Shallow shelf edge reefs.

The reefs growing on the shallow shelf form what is commonly known as 'The Florida Reef Tract'. Two types of reef are developed on the reef tract: *Acropora palmata* reefs situated along the shelf margin, and patch reefs, composed principally of head corals like *Montastrea annularis*, located several kilometres shorewards of the shelf break. The shelf edge reefs are mostly related to the antecedent Pleistocene topography; cores through several reefs indicate that they are recent accumulations on Pleistocene shelf edge reefs. Thus the shelf edge in the Holocene is in much the same position as it was in the Pleistocene. The patch reefs are restricted in development to sites in the lee of the outer shelf edge reefs where the waters are generally calmer. The *Acropora* dominated reefs are not restricted to the shelf edge; they do occur up to 1 km. shorewards of the shelf break, in places where there is a large gap in the outer reef chain.

Present day flourishing reefs are restricted in their development to areas off the Upper Florida Keys (Figure 2.2). However, their occurrence is not haphazard; they are absent seaward of the gaps in the Florida Keys which serve as channels to distribute Florida Bay sediments and waters deleterious to active reef growth.

The shelf break acts as a focus point for wave energy so that water circulation is at its most vigorous and the zone is highly turbulent. Much coarse sediment accumulates in back-reef areas and this can become emergent at low tides. Little Molasses island is an example of a sandy bar in the back-reef zone of Molasses reef and it is up to 1 metre above sea level. Skeletal debris occurs behind the reefs, concentrated there during storms and hurricanes. Each succesive storm is capable of affecting the morphology of these debris piles quite considerably (Mülter, 1977).

In order for cementation to occur, large volumes of water have to pass through the pores (Bathurst, 1975), hence shelf edge reefs are commonly lithified to a greater degree than reefs shorewards of the shelf break. For this reason, collection of samples for this study was concentrated on shelf edge sites. The majority of the material comes from two areas, the first in the Upper Keys (Alligator Reef) and the second from Dry Tortugas, 150 km. west of Key West (Figures 2.3 and 2.7)

2.2.4.1 Alligator reef.

Alligator reef is an *Acropora* dominated reef which is now dead. It was killed by the efflux of turbid waters from Florida Bay about 4000 years b.p., at a time when the Flandrian transgression was starting to flood the Bay. It is situated seaward of a gap between Upper and Lower Matecumbe Keys (Figure 2.3) and is formed principally from the frame building corals, *Acropora palmata* and *Acropora cervicornis*. The detailed morphology of the reef is only poorly known, though the shoreward edge terminates in an abrupt ledge (Figure 2.4). The reef is no more than 4 metres thick and is in 6 metres of water (mean sea level). Seven cores drilled through the reef by Gene Shinn of the United States Geological Survey have been studied in detail. The cores are in two transects positioned approximately as shown in Figure 2.5. Logs with major constituents are shown in Figure 2.6 from which it can be seen that recovery of the cores was far from complete. Shinn, (pers. comm.) suggests from observations of the material reaching the surface in the drilling fluids that most of the unrecovered sections consisted of unconsolidated reef debris. Some of the sections may have beens caverns however, as the core barrel was observed to drop suddenly at some points. The depths of sampling points are only approximate due to some uncertainty about the exact positions of the recovered core pieces. All of the cores penetrate reef framework facies and there is no indication of any lateral migration of the facies with time. The core samples (approximately 100 individual specimens) were augmented by a similar number of hand specimens collected by diving to the reef flat surface. The latter material consists mainly of rounded fragments of the branching corals.

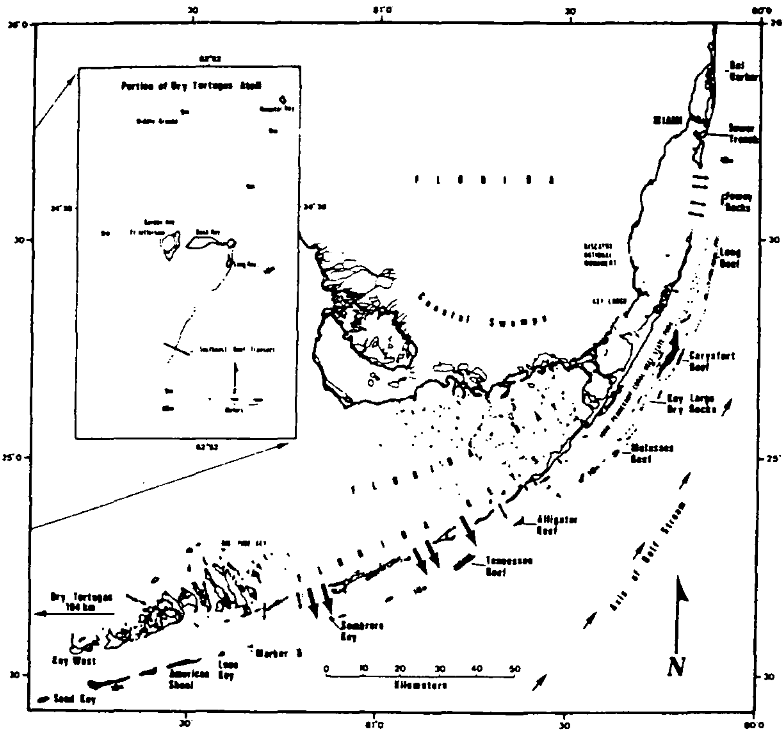

Figure 2.2 Map of the Florida Keys, showing location of major reef growth. (From Shinn et al., 1977).

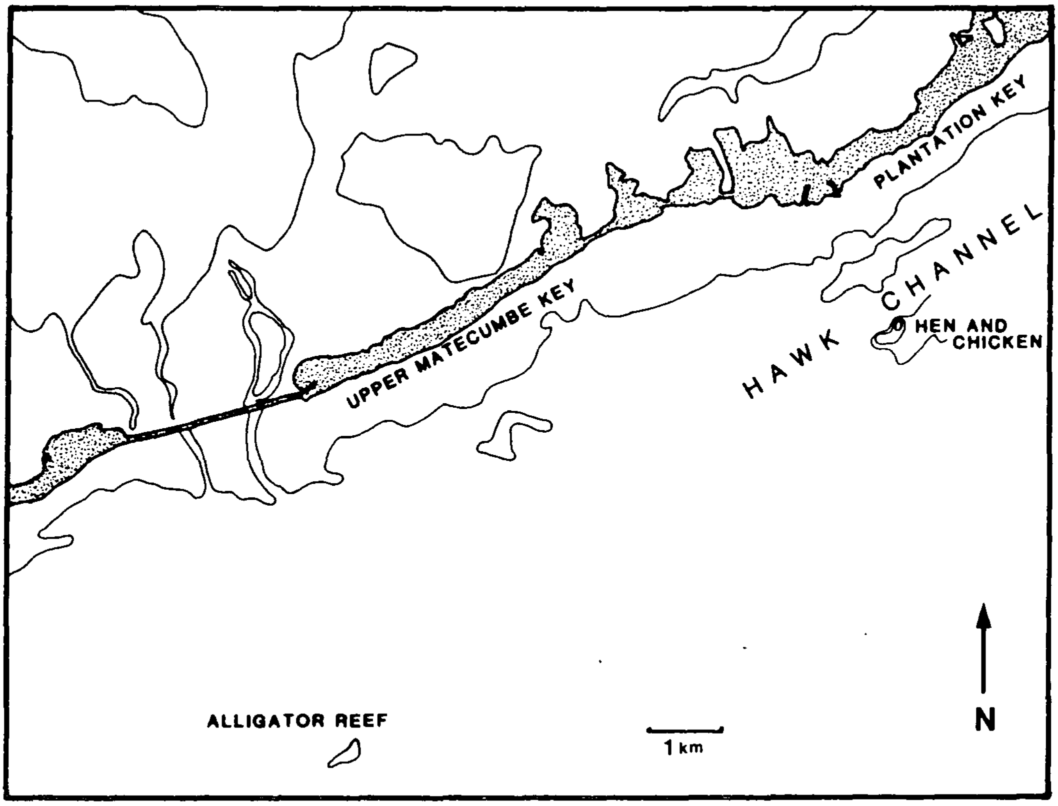

Figure 2.3 Location map showing Alligator Reef, situated seawards of a gap between Upper and Lower Matecumbe Keys.

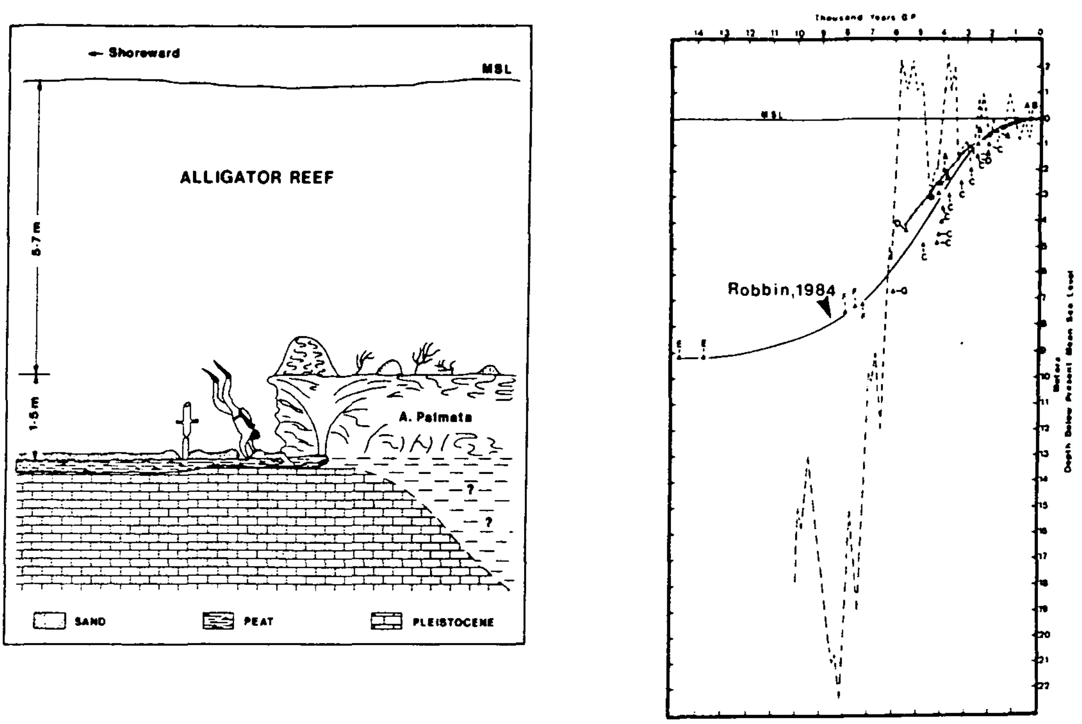

Figure 2.4 Schematic diagram of the shoreward part of Alligator reef, showing the abrupt ledge and the Pleistocene substrate. Also shown is the sea-level curve derived for the area from carbon dating studies on this reef. (From Robbin, 1984).

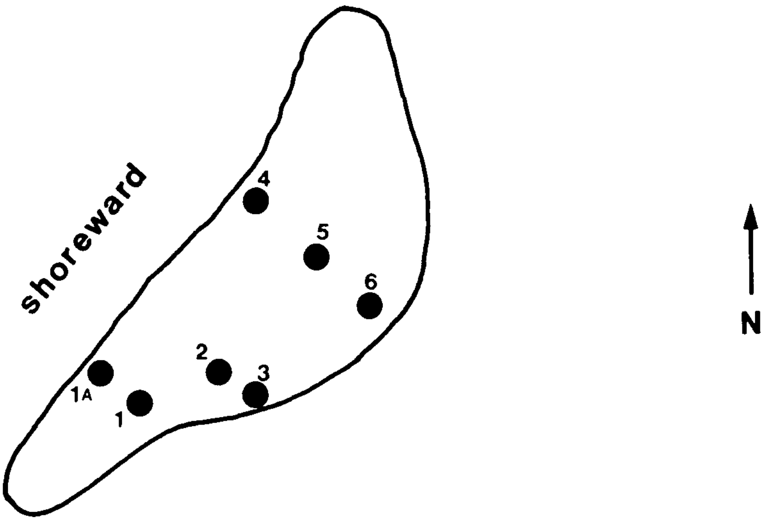

Figure 2.5 Location of the cores through Alligator reef.

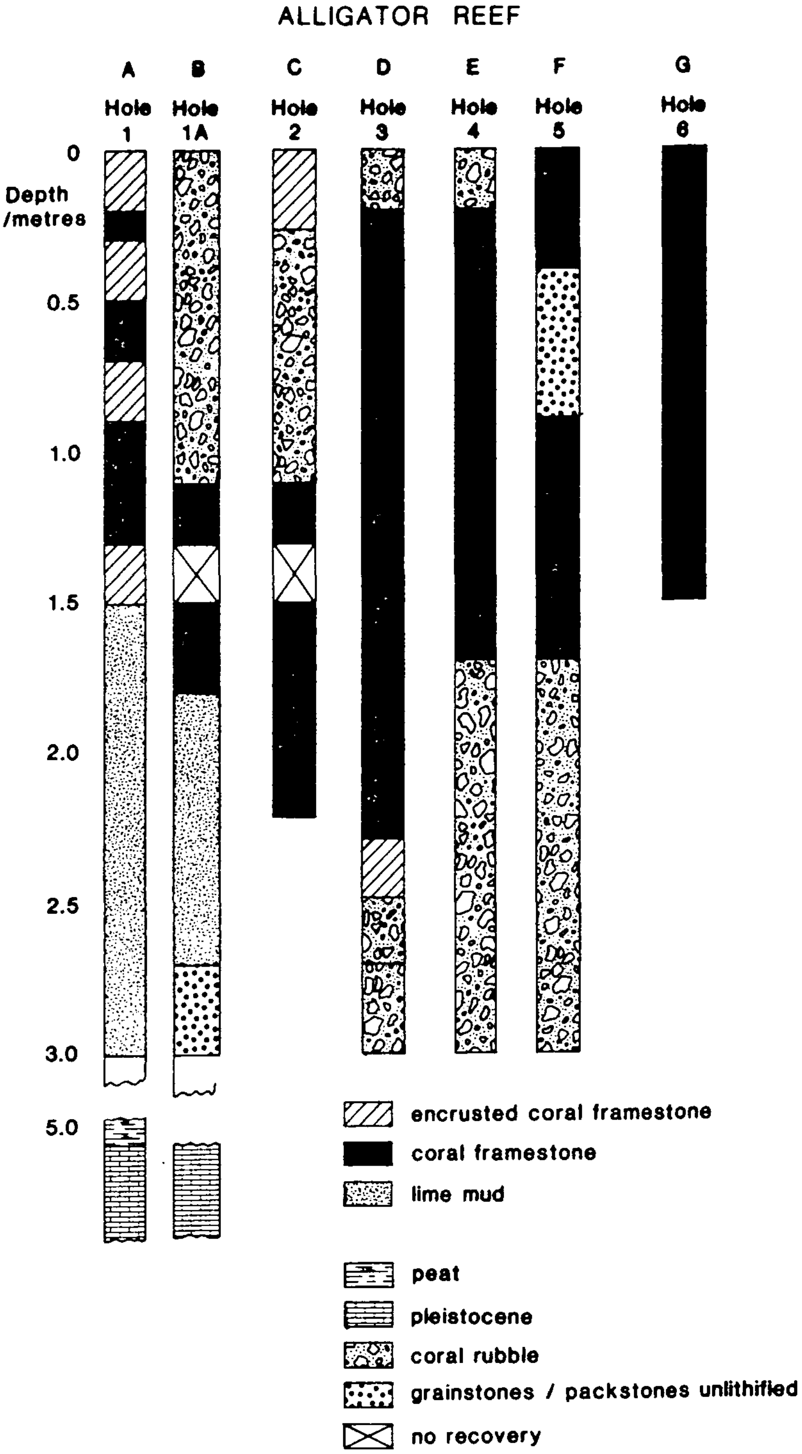

Figure 2.6 Logs of cores through Alligator Reef. Recovery from the cores was less than 70%, and so the depths of thin section sampling points (Appendix 1) are only approximate. Recovery was low from the lime mud and coral rubble lithologies.

2.2.4.2 Dry Tortugas reefs.

Dry Tortugas (Figure 2.7) is an isolated cluster of carbonate sand shoals and reefs with some emergent islands. The complex rises to the surface from a shallow limestone platform of 20 to 30 metres in depth which is probably a drowned Pleistocene surface (Jindrich 1983). The Holocene reefs have developed to a much greater extent than those of the Upper Florida Keys, reaching a maximum thickness of 13 metres. This is thought to be due to the fact that much of the accumulation has not built up in the traditional sense of reef growth but rather by accretion of reef debris thrown up and over the reef front during storms.

Five cores were drilled in a transect north west to south east across South East Reef, Dry Tortugas, near Fort Jefferson (Figure 2.8). According to Shinn et al. (1977), South East Reef is thought to have been built up on the rim of a Pleistocene atoll. Two other cores have also been studied which were taken on Pulaski Reef and Loggerhead Key (Figure 2.4). Three of the cores penetrated the Pleistocene reef substrate which is described in Section 2.18. The major discovery from the initial investigation of the cores, which were also drilled by the U.S. Geological Survey, was that the framework building coral, *Acropora palmata*, is absent from the reef, which is instead built mostly of the head corals, *Montastrea* and *Diploria*.

Logs for all seven cores are shown in Figure 2.9. As the recovery was very low, sampling depths are again only approximate. The low recovery tends to confirm that there is a lack of corals in growth position and that a large proportion of the reef is uncemented debris.

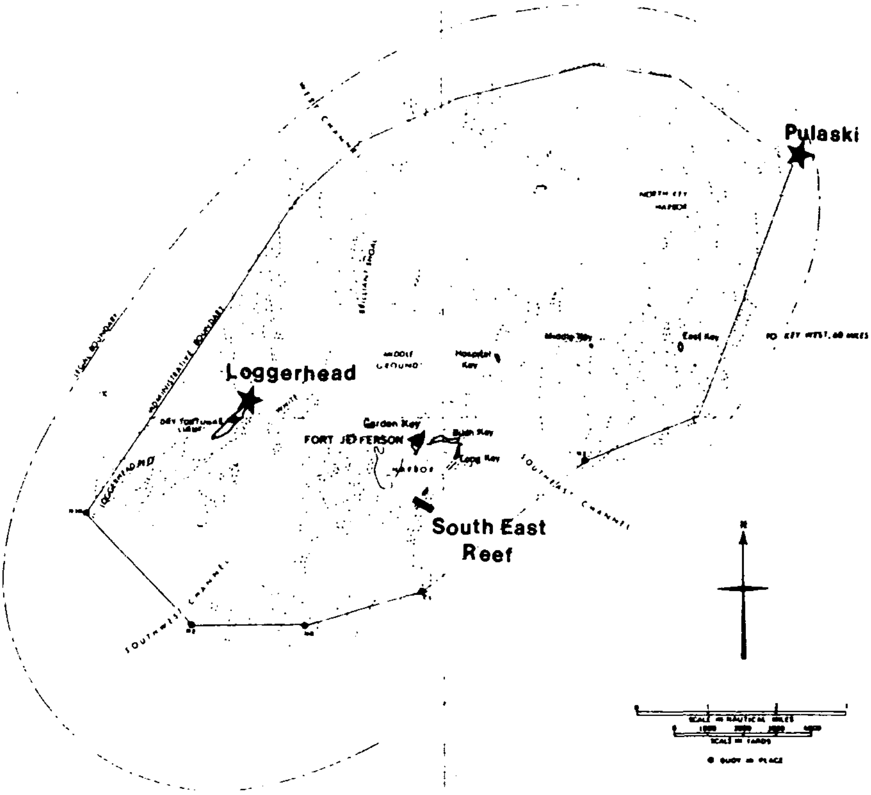

Figure 2.7 Location map of Dry Tortugas showing the transect through South East Reef and the Pulaski and Loggerhead core positions.

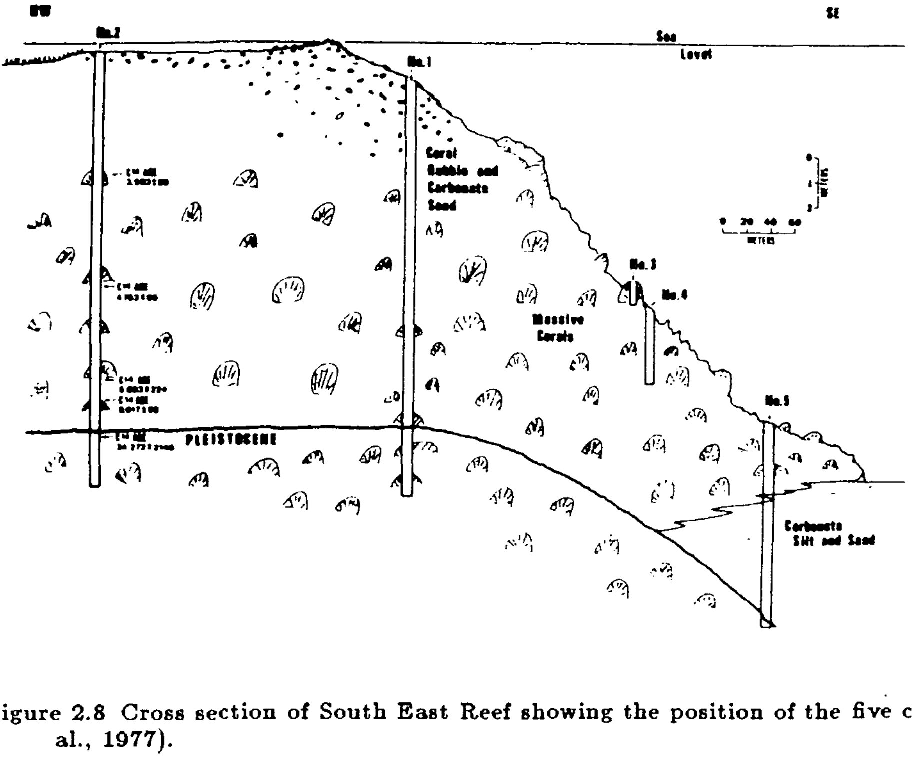

Figure 2.8 Cross section of South East Reef showing the position of the five cores. (From Shinn et al., 1977).

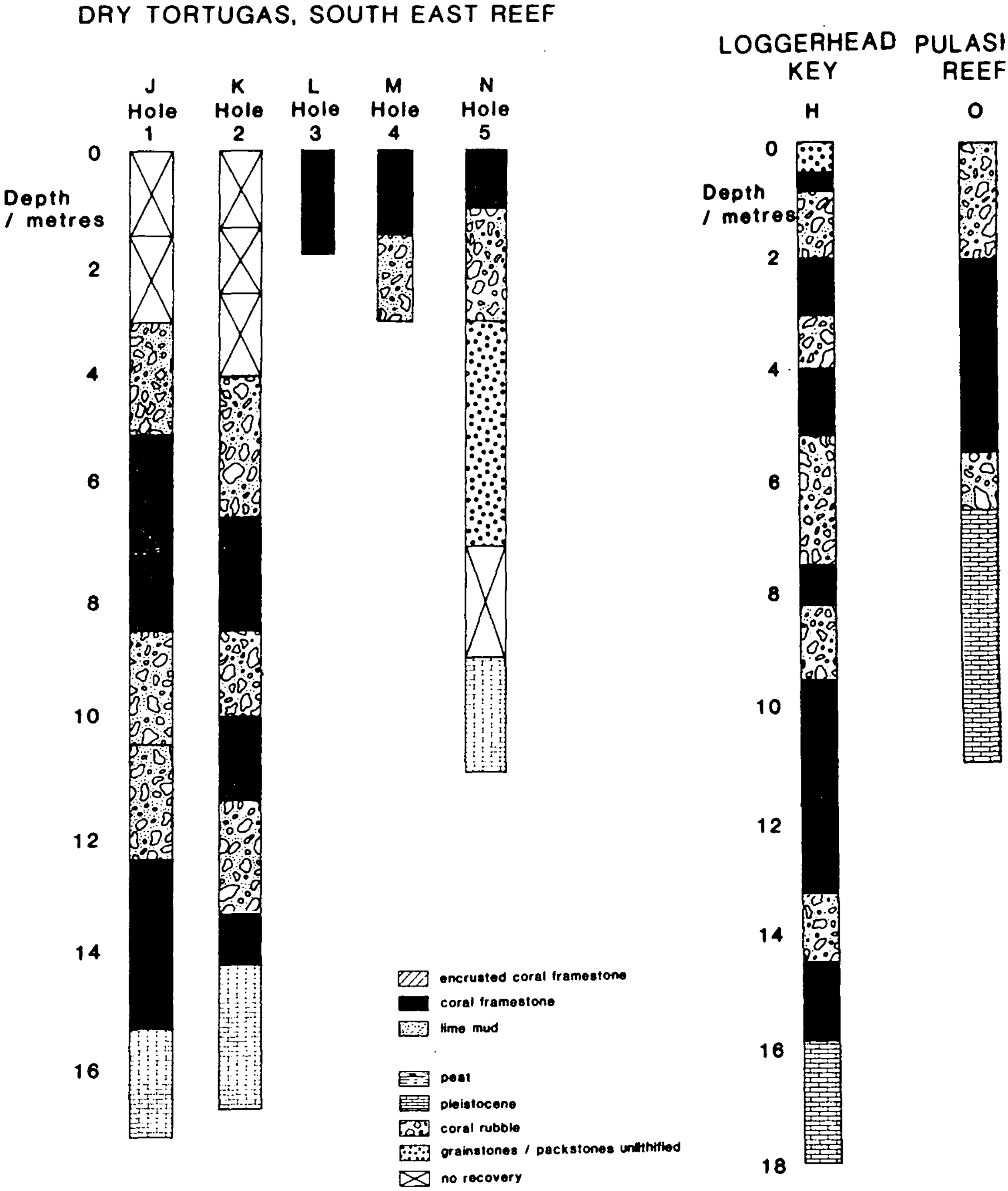

Figure 2.9 Logs of cores through South East, Pulaski and Loggerhead Reefs. Recovery was low and thin section positions are again approximate.

2.3 Sea Level Rise and Reef Growth.

Sea level in the Florida area is presently rising at less than 0.3 metres 1,000 years^{-1} (Enos & Perkins, 1977), but the rate of sea level rise has varied during the Holocene. The sea level curve for the local area which was derived using data from Alligator reef is shown in Figure 2.4 (Robbin, 1984). Alligator reef was in an active growth phase between 7,500 and 4,000 years b.p., during which period, the sea level rise was quite rapid, (1.3 metres 1,000 years $^{-1}$) Growth of the reef averaged 0.8 metres 1,000 years^{-1}, equivalent in order to that of many Holocene reefs (Shinn et al., 1977). By comparison, ^{14}C-dating indicates that Dry Tortugas South East reef has accumulated at a much faster rate of between 2–4 metres 1,000 years^{-1} (Shinn et al., 1977). This latter reef, although not necessarily grown in the classical sense, has reached sea level and is a good example of a 'catch up' reef as defined by Davies & Hopley (1983), this occurred more readily as the rate of sea level rise slowed over the last three to four thousand years. Alligator reef grew in much more of a 'keep up' sense until it was killed by the adverse change in environment. As sea level has risen only 1 to 2 metres since the death of Alligator reef, the reef is still near to the present mean sea level. This fact has important implications for the distribution of cements in the reef, and is discussed in Section 2.8.6.

2.4 Alligator Reef Petrology.

2.4.1 Hand specimen appearance.

The samples collected from the reef flat are mostly coral framestone, with smaller amounts of coralline algal bindstone material. Coral species are principally *Acropora palmata* with rare small fragments of *Montastrea annularis*. It can be quite difficult to identify the coral species due to the multiple generations of boring and sediment filling (Figure 2.10). Fuller description of the encrusting and boring organisms and the internal sediments is given in Sections 2.5.2 and 2.5.4. The internal sediments are generally very poorly lithified and sand sized sediments disaggregate on drying indicating that there is little or no intergranular precipitation of cements. In many samples the bored cavities are unfilled, giving the reef rock an extremely vuggy appearance (Figure 2.11). This macroporosity ranges from 5–50% of the total rock. The surfaces of the samples are invariably encrusted by a variety of organisms (Figure 2.12 and Section 2.5.2). These can be locally important secondary framebuilders, particularly in the case of the coralline red algae (Figure 2.11). Often surfaces are predominantly green in colour due to the presence of non calcifying green algae (Figure 2.13), often the last organism to grow over the dead encrusting community.

Hand specimen samples can also include large pieces of molluscs, which are also invariably bored and encrusted (Figure 2.14). Slabbed cut surfaces of the samples are generally white to pale grey in colour and further illustrate the intensity of the boring, encrusting and cavity filling processes.

Figure 2.10 Typical hand specimen from Alligator reef (sliced), originally a large branch of *Acropora palmata*, now difficult to recognise due to multiple bioerosional and sedimentation events. Surface encrustation of coralline red algae and *Homotrema rubrum* evident at upper left.

Specimens in all the photographs are either hand specimens (H.S.), or else from core samples. The latter are referred to using the codes as given in the point counting tables in the Appendices.

2.4.2 Core description.

The seven cores taken on Alligator reef all pass through reef core material. The total porosity is surprisingly constant for all cores at approximately 30%. (See Appendix 1). The total rock (excluding porosity) consists on average of 60% coral framestone, the remainder being secondary framebuilding coralline algal boundstone, internal sediments and cements. The average composition of the whole rock (including porosity), is:

i) 42% framestone,
ii) 9% bindstone,
iii) 29% porosity,
iv) 13% internal sediments,
v) 7% cements.

A few samples are in fact grainstones; these are rather friable but have been lithified enough to be preserved in the cores (Figure 2.21). The porosity in the core samples (29%) is split on average at about 27% micro porosity and 2% macro or boring porosity. Hence, in these core samples, the macroporosity is lower than in the hand specimens, indicating a lesser role for macroboring organisms. The macroboring porosity can however reach similar levels to that at the surface in individual specimens (Figure 2.15).

1cm.

Figure 2.11 Vuggy appearance of hand specimen due to multiple borings by lithophagid bivalves the sponge *Clione sp.* and polychaete worms. (H.S.)

1cm.

Figure 2.12 Surface of sliced hand specimen showing encrustation by serpulids, *Homotrema*, bryozoans and an attached mollusc. (H.S.)

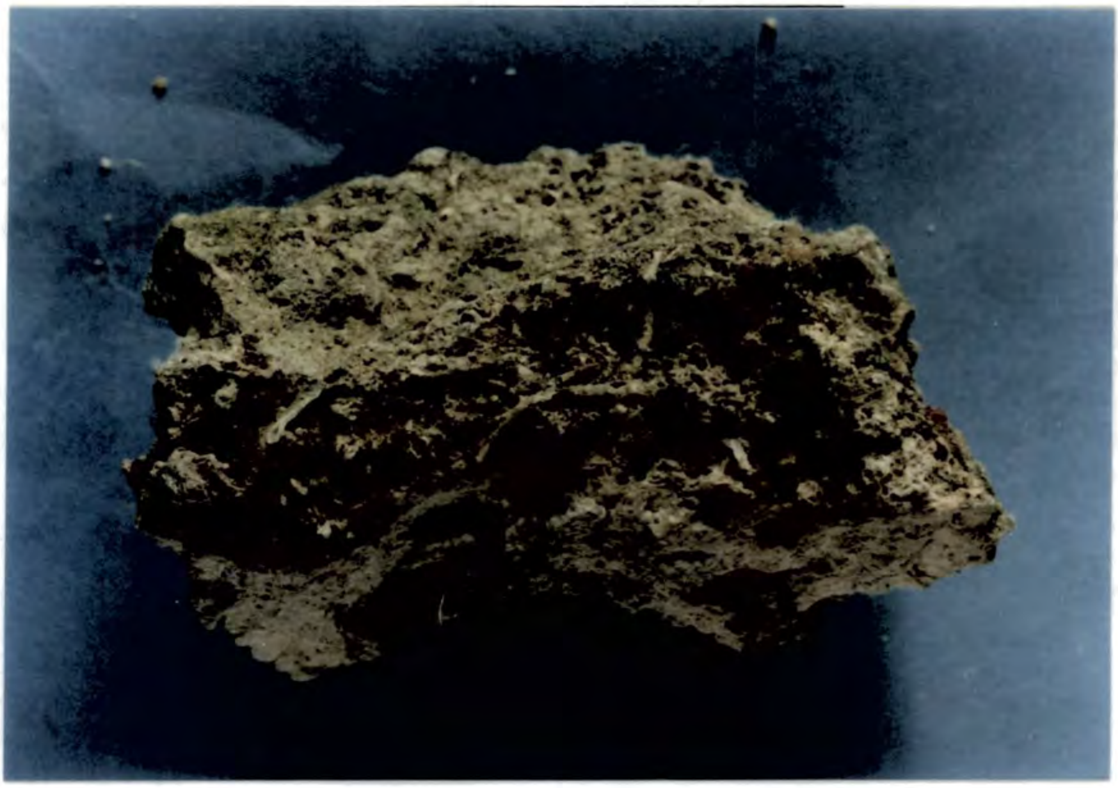

Figure 2.13 Green surface of encrusted hand specimen due to the presence of non-calcifying green (blue green ?) algae.

Figure 2.14 Sliced conch shell (*Strombus gigas*), heavily bored by sponges, creating a vesicular texure, with encrustation by *Homotrema* and serpulids.

1cm.

Figure 2.15a Large scale bioerosional porosity in core specimen from Alligator reef, with small amount of geopetal internal sediment in the lower boring.

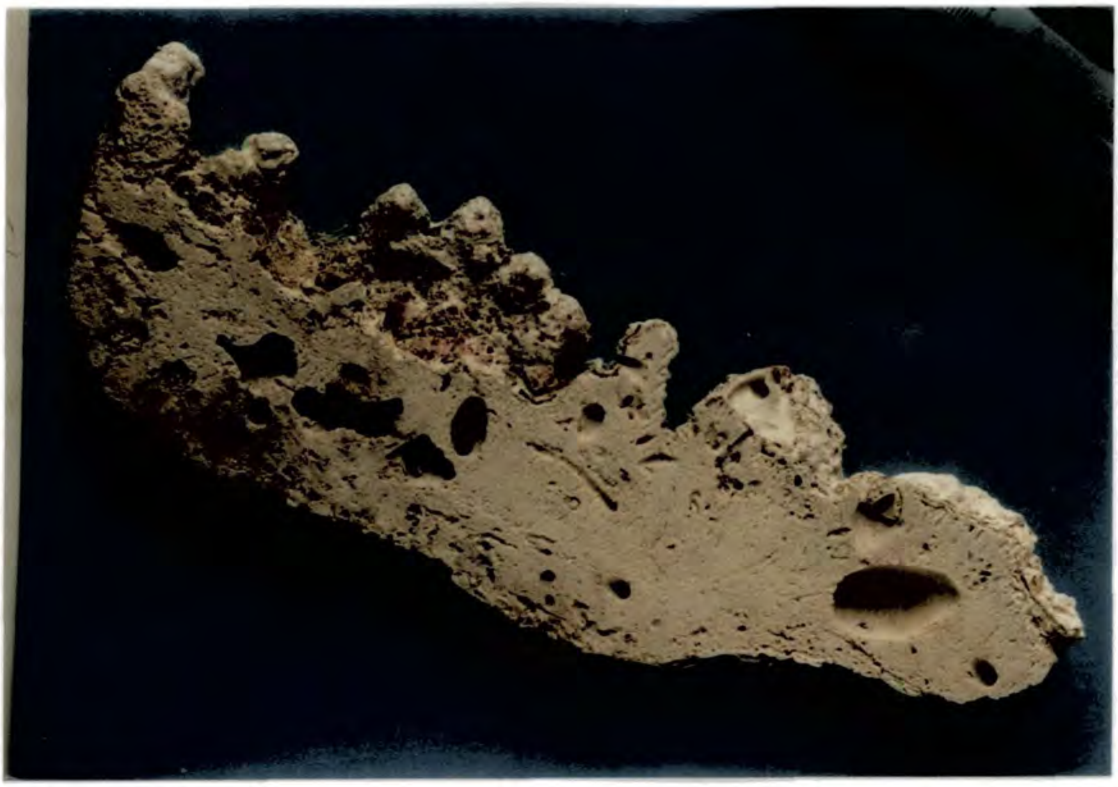

1cm.

Figure 2.15b Hand specimen from Alligator reef showing a variety of borings, including those made by bivalves, sponges and polychaete worms.

2.5 Detailed Components of Alligator Reef Cores.

This section describes the composition of the limestones in terms of the major components present. Point counting of 90 thin sections has given a quantitative idea of the relative amounts of each component. The data are presented in Appendix 1.

2.5.1 Framebuilding organisms.

The predominant group of framebuilding organisms is the scleractinian corals, forming on average about 60% of the rock (excluding porosity). The majority of this is the *Acropora* species, mostly *Acropora palmata* (Figure 2.16). Smaller amounts of the head corals *Montastrea sp.*, particularly *Montastrea annularis* occur, with rare examples of *Siderastrea sp.* and *Diploria sp.*.

The other major framebuilders which play a secondary role and form 10% or so of the total framework are the coralline algae (*Goniolithon, Porolithon* and *Lithothamnion*). The hydrozoan *Millepora* is also present. Most of these organisms are usually restricted to an encrusting role, but the volumes are such that they are important framebuilding contributors. Almost all exposed surfaces can be seen to be encrusted by these organisms (Figure 2.12). The balance (to 100%) is provided by cements (10%) and internal sediments (20%).

2.5.2 Encrusting and Binding organisms.

As well as the coralline red algae mentioned above, several other encrusting organisms are commonly observed forming lamellar coatings over exposed surfaces. These include cheilostome bryozoans (Cuffey & Kissling, 1973), and the encrusting foraminifer, *Homotrema rubrum* (Figure 2.17).

Other organisms which can be found attached to, but not necessarily forming extensive crusts on the coral framestones, include serpulids and bivalves. The total encrusting volume can reach 25 % of the total rock in hand specimen, but is generally less than 10%.

These encrusting organisms can have a significant effect on the binding of the substrates on which they are growing. Because they tend to form lamellae and have generally quite low porosity, they therefore reduce the permeability of the substrates. This is discussed further in Section 2.8.2.

2.5.3 Reef dwelling organisms.

Many mollusc species form the majority of the preserved reef dwelling communities; bivalves and gastropods are the most important. Rarer fragments of echinoids can also be found. The most commonly observed species are the lithophagid bivalves, which play a very important role in the destructive processes of boring and sediment production.

2.5.4 Boring organisms.

Lithophagid bivalves excavate most of the boring porosity (Figures 2.15 & 2.16), and often the shells can be found in place. Other boring organisms are the sponge *Clione lampa* which produces a vesicular texture (Figure 2.11), and large volumes of serrated sand sized fragments (Figure 2.18). Polychaete worms excavate long smooth walled tubes (Figure 2.15). Most of the skeletal fragments are covered in microborings (? fungal), typically 5μm. in diameter and several hundred μm. in length. These are illustrated in Figure 2.19. This boring activity can create up to 50 % of the total porosity in hand specimen.

2.5.5 Internal sediments.

The texture and abundance of internal sediments varies enormously. Point counting shows that sediments can form up to 25% of the total rock, although the average is lower at approximately 13%. Of this average, about half is mudstone, the remainder being pack- or wackestone, with rarer grainstone cavity fills. The major identifiable components of the sediments are fragments of the various corals, commonly exhibiting the scalloped edges typical of the clionid excavations. Fragments of coralline algae, molluscs, *Halimeda*, echinoids and other reef dwelling organisms are also present. The wackestone sediments alone can account for up to 25 % of the total rock; packstones are usually rather less abundant and the grainstones limited to very local derivation and often being exclusively formed of the sponge chippings.

A substantial variation in texture and abundance is apparent even in single hand specimens or small core pieces. Due to the mixed mineralogies of the reef building and dwelling organisms, the internal sediments are also a mixture of aragonite and high magnesium calcite (See XRD data in Appendix 3). Geopetal structures are commonly observed (Figure 2.16), as are multiple generations of sediments, distinguishable through their slightly varying textures and colours (Figure 2.20). Most internal sediments are poorly or un-lithified, suggesting that there is only a limited amount of cement precipitation. There is a very major problem in trying to distinguish between mechanically deposited sediments and inorganically precipitated cements when the grain size is below that resolvable by the light microscope. Loreau (1982) was apparently able to distinguish very fine grained skeletal fragments from cement crystals using the scanning electron microscope, but nevertheless, the problem of determining the relative proportions of cement and micrite in a featureless mudstone internal sediment is quite acute. A further detailed discussion of this problem and indeed the problem of defining micrite can be found in Section 2.7.4.

This heterogeneity in the texture, abundance and sequences of internal sediments indicates the complex spatial and temporal variation in the types of porosity and the interconnectivity or permeability of the pore structures. The temporal variation is particularly interesting as it is this aspect which produces the multiple generations of sediments due to the opening up of new cavities to new sources of sediment.

Figure 2.16 Core through *Acropora palmata* with small boring containing geopetal sediment. *Acropora palmata* forms the majority of the reef framework of Alligator Reef.

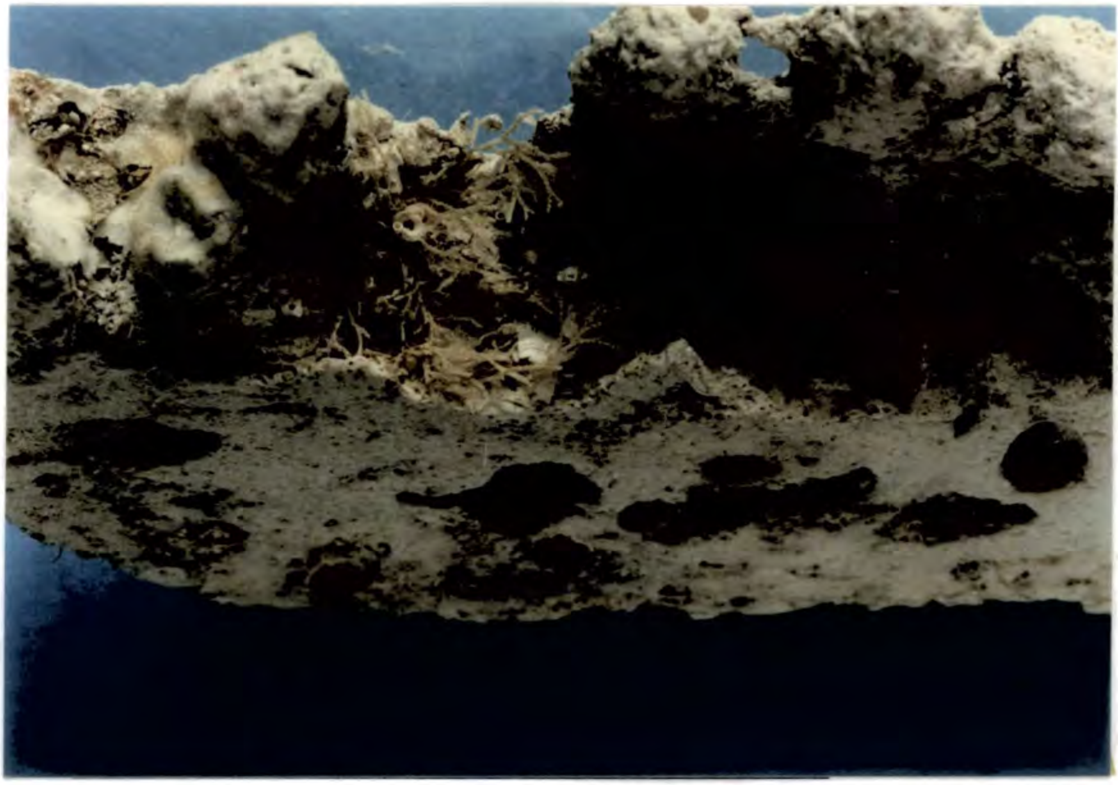

Figure 2.17 Further examples of the common encrusting organisms, including bryozoans, *Homotrema* and serpulids.

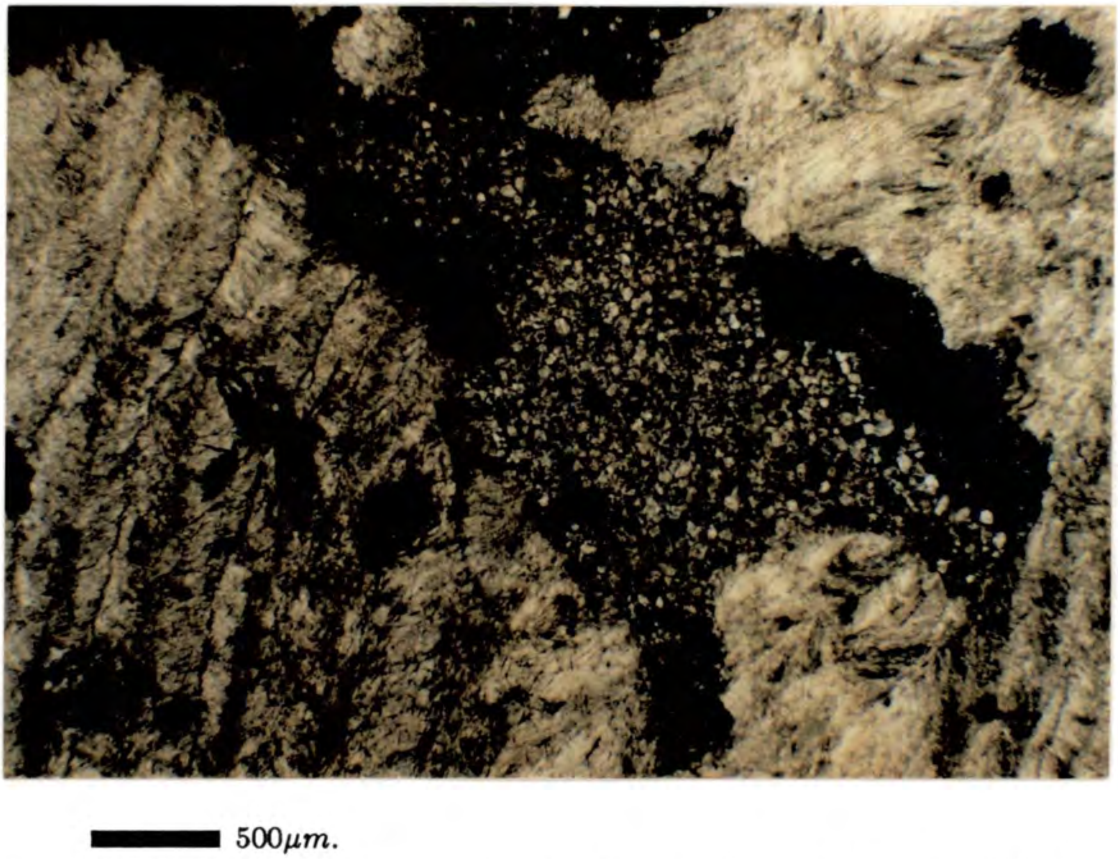

Figure 2.18 Scalloped edges of coral and sand sized fragments typical of the boring sponge, *Clione sp.*. Photomicrograph, xpolars. (H.S. Alligator Reef)

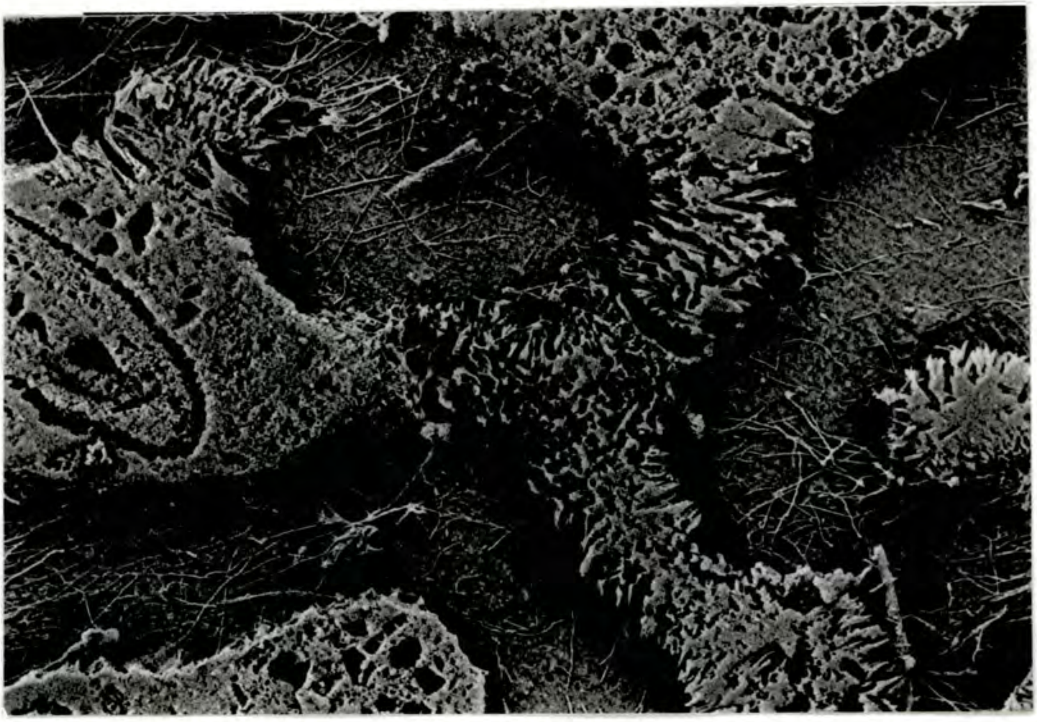

100μm.

Figure 2.19 Photos showing microborings in coral skeleta, probably fungal in origin. Upper SEM photo shows a cast of the coral made by resin impregnation followed by dissolution of the $CaCO_3$ with dilute HCl. The impression of acicular cement crystals can be seen in the centre of the picture. Lower photo in ppl. . (H.S. Alligator Reef)

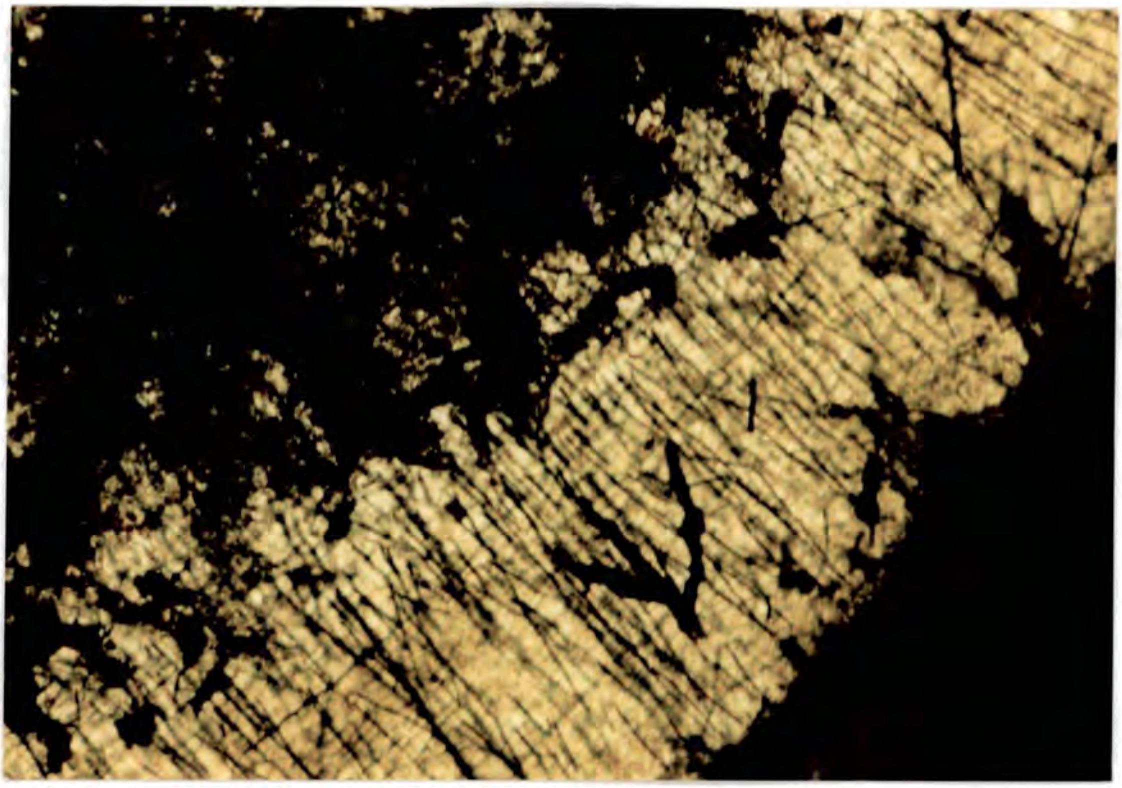

100μm.

Figure 2.19 .

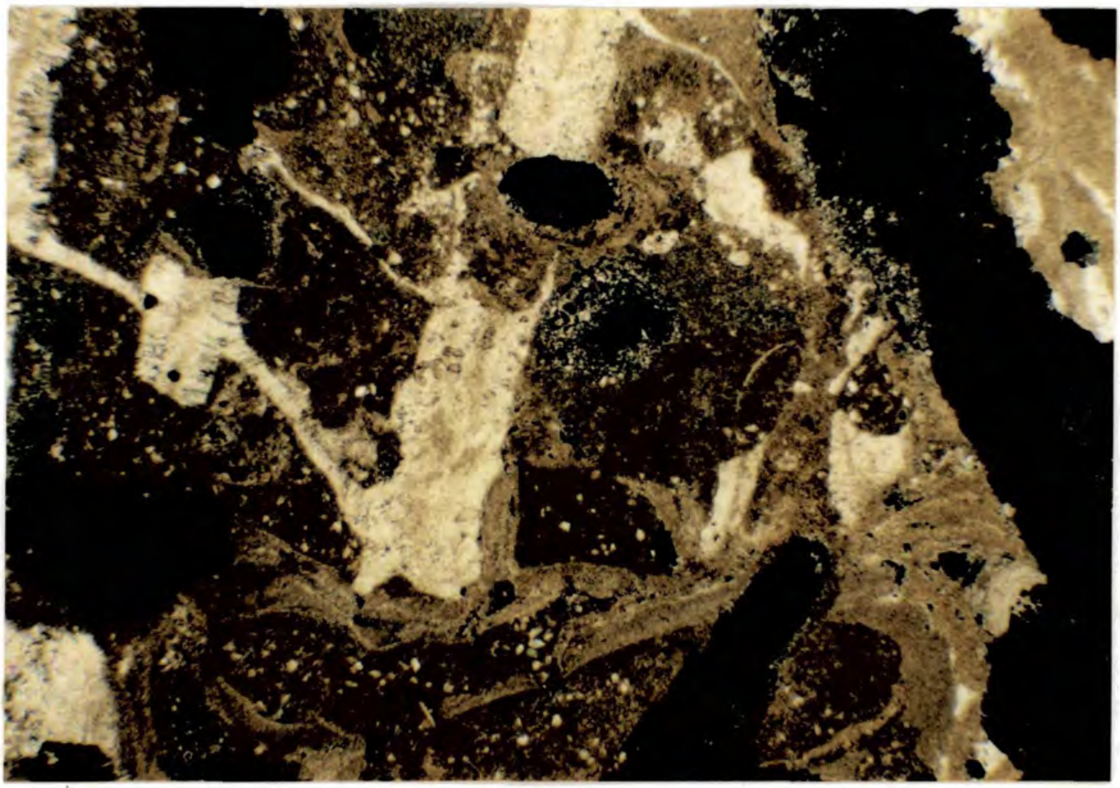

500μm.

Figure 2.20 Original coral framestone, now almost unrecognisable due to multiple sequence of boring, sedimentation and encrustation. Photomicrograph, xpolars. (F3L)

2.6 Porosity Types.

The many types of depositional porosity are modified by the involvement of the various destructive processes, the effects of deposition of internal sediments and the precipitation of cements. The types of porosity have been classified by Choquette & Pray (1970), and are described in relation to the Alligator reef limestones in the following section.

2.6.1 Cavernous porosity.

The massive growth habits of modern reef corals, particularly *Acropora palmata* create substantial cavernous porosity which is very obvious when diving on flourishing reefs of the Florida Reef Tract. Whilst no such caverns are evident at the surface of Alligator reef, there is evidence that this large scale porosity can be preserved in the shallow sub-surface (Section 2.2.4.1). In all of the Alligator reef cores studied, the recovery is 70% on average, the remainder being both unlithified sediments and some cavernous porosity.

2.6.2 Vuggy porosity.

The range of the sizes of large scale pores is so wide that it is difficult to conceive of a useful classification based on size. The term 'cavernous' as used above, is intended to describe porosity on the basis of size as originally defined (Choquette & Pray, 1970); that into which a man could fit ! The term 'vug' is intended to describe any porosity of indeterminate or multiple origin in a size range of 1 metre to a few centimetres. There are many examples of macro-porosity which is too large to have been formed by a single boring, does not appear to be obviously growth framework in origin, and is too small to be called cavernous. These pores are likely to have been created by repeated boring and mechanical destruction events and are called vugs (Figure 2.21).

2.6.3 Bioerosional porosity.

The destructive activity of many boring and rasping organisms makes a very significant contribution to the overall porosity of reef rock and can substantially increase the permeability also. The evidence of boring is not always preserved; the grazing Parrot fish and echinoids are known to consume large quantities of skeletal material and produce a significant proportion of the sand and silt sized fractions of the sediments and yet there is no real evidence of their activities in hand specimens. Those bioerosional pores which can be recognised and identified, range in size from several cm. to only a few microns. Boring bivalves produce abundant cavities 5mm. to 5cm. in diameter with the shells often preserved within them (Figure 2.22). The sponge *Clione sp.* produces abundant vesicular networks of pores 1–5mm. in size. Smaller borings are made by polychaete worms (cylindrical pores up to 3 or 4 cm. in length and 1–2 mm. in diameter), and micropores (1–10 μm. diameter), by endolithic algae and fungi.

It is very difficult to make a quantitative estimate of the contribution to the porosity of an entire reef unit which is made by the caverns, vugs and larger bioerosional pores. At the surface of a flourishing reef, visual estimates would suggest figures of as much as 70 %, but of course much of this would become filled by sediments as the reef surface is buried. It may be possible that up to

10% of the total porosity of a unit of reef at a depth of three metres may be of this type. Unfortunately the coring technique does not allow a more accurate estimate to be made; however, it is undoubtedly a contribution which should not be ignored when discussing the porosity and permeability of modern reefs.

2.6.4 Intraskeletal porosity.

This averages approximately 50% of the total rock, as measured by 100−(framestone + encrusting material), and is defined as the first generation porosity as created by the growth of the organisms. It is modified in an infinite number of interacting events including the bioerosion described above, the deposition of internal sediments and the precipitation of cements. The extent of this alteration can be so pronounced that there is little or no preserved primary skeletal material nor intraskeletal porosity (Figure 2.20).

The primary intraskeletal porosity can reach 80% in some species (e.g. *Diploria*, Figure 2.23), but in other species, particularly the coralline algae, it can be as low as 5%. Pore sizes range from 15–25μm. in the coralline algae (Figure 2.24), to 25μm.–1 mm. in coral skeletons, 1–5mm. in gastropod chambers and worm tubes, to 1–2 cm. in bivalve chambers.

It is important to note that the intraskeletal porosity is not all necessarily 'effective'; the build up of successive chambers in many coral skeleta and the arrangement of the septa and thecae are such that a significant proportion of the porosity as observed in thin section is not in fact interconnected and is therefore sealed from the environment. Comparison of the measurements of porosity of identical samples by point counting of thin sections and by pore-assymetry techniques reveals that effective porosity can be substantially overestimated by point counting (Appendix 6). This non effective porosity has a significant effect on the distribution of cements on the thin section scale and is discussed further in Chapter 5.

2.6.5 Inter-particle porosity.

Inter-particle porosity again spans a very wide range of sizes from the centimetre scale in coarse rudstones to the sub-micron scale in mudstone cavity fills. In the reef material studied in thin section, there is very little small scale porosity (< 2%), this occurs between particles in grainstone skeletal sediments. In the reef as a whole the contribution of interparticle porosity will be more significant, particularly in reef flat and back-reef areas where a lot of coarse skeletal debris collects. It is interesting that these grainstones are very poorly cemented, considering that their permeability will be at the highest end of the range for reef facies. This is primarily due to the fact that the skeletal particles are constantly in motion, and there is no stable substrate on which growth of cements can occur (Section 1.6).

2.6.6 Shelter or growth framework porosity.

This porosity varies in size from 1mm.–2cm. and is created by the growth of lamellar encrusting organisms over irregularities in the substrate (Figure 2.25), or indeed by the irregular growth of the organisms themselves. Shelter porosity is typically created when disarticulated bivalve shells settle convex up.

2.6.7 Intercrystalline porosity.

This porosity varies according to the size of the crystals, from a few microns in microcrystalline cements to up to $10\mu m$. between acicular cement crystals (Figure 2.26).

1cm.

Figure 2.21 Large, multiple origin vuggy porosity in hand specimen from Alligator Reef, some cavities containing white, muddy internal sediments. Macro-porosity of this type can form up to 50% of the porosity at the surface of the reef. (H. S.)

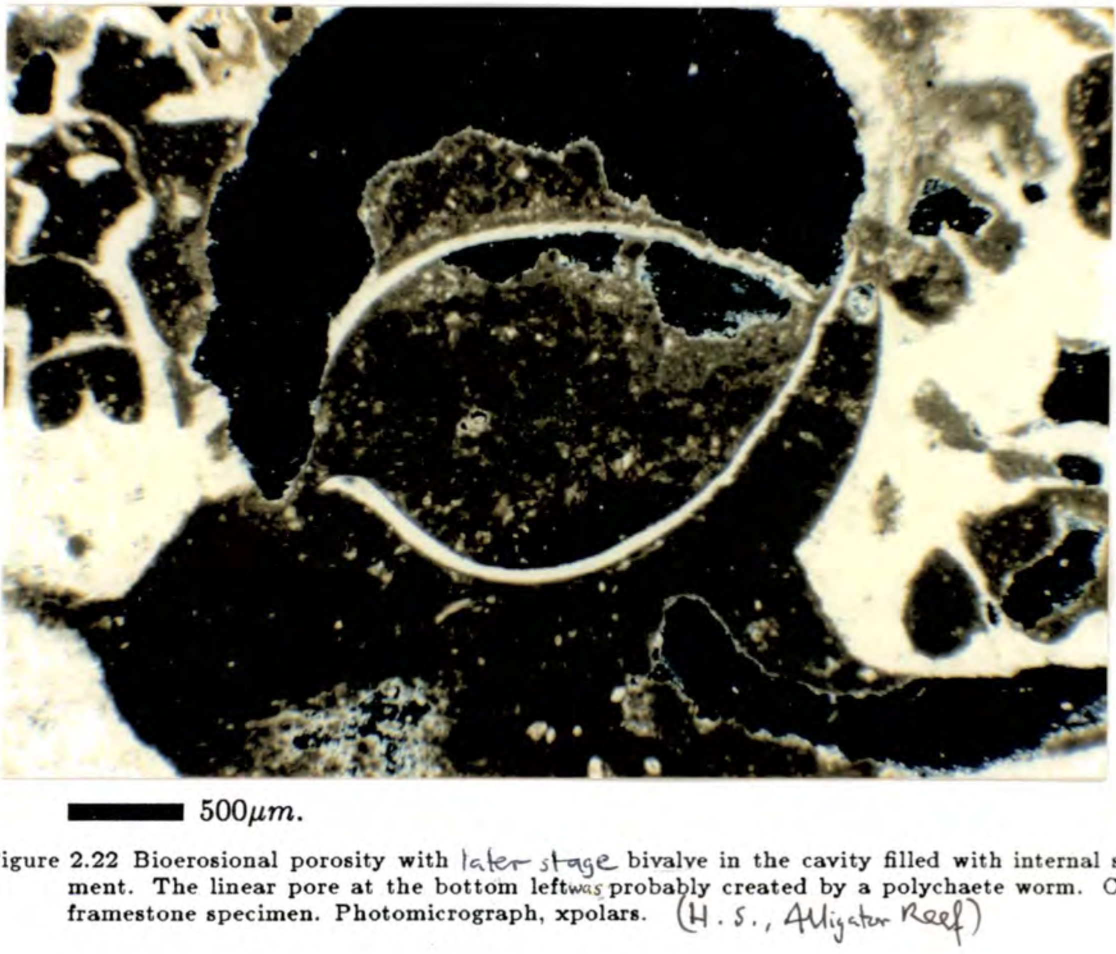

500μm.

Figure 2.22 Bioerosional porosity with later stage bivalve in the cavity filled with internal sediment. The linear pore at the bottom left was probably created by a polychaete worm. Coral framestone specimen. Photomicrograph, xpolars. (H. S., Alligator Reef)

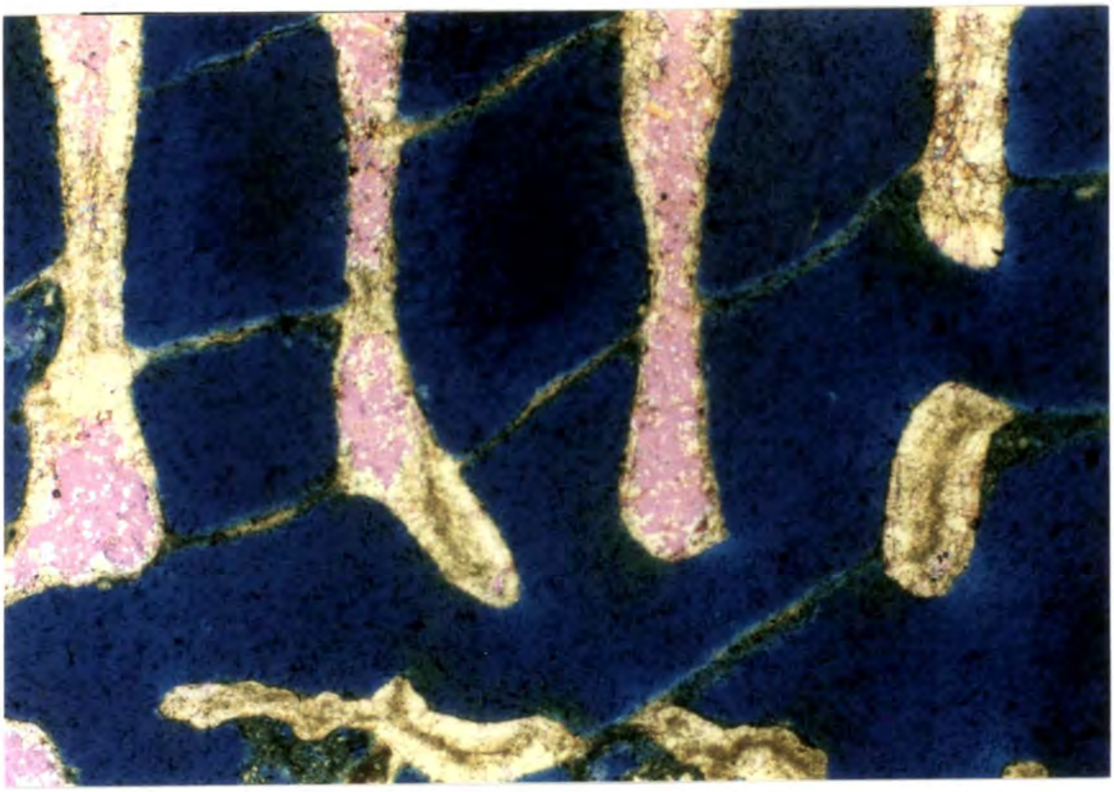

500μm.

Figure 2.23 Primary intra-skeletal porosity of the coral ***Diploria sp.***, reaching a maximum of 80% in some specimens. Porosity in blue in the photo, pink colouration due to 'plucking' during thin section preparation. Photomicrograph, xpolars, with sensitive tint plate. (Alligator Reef H.S.)

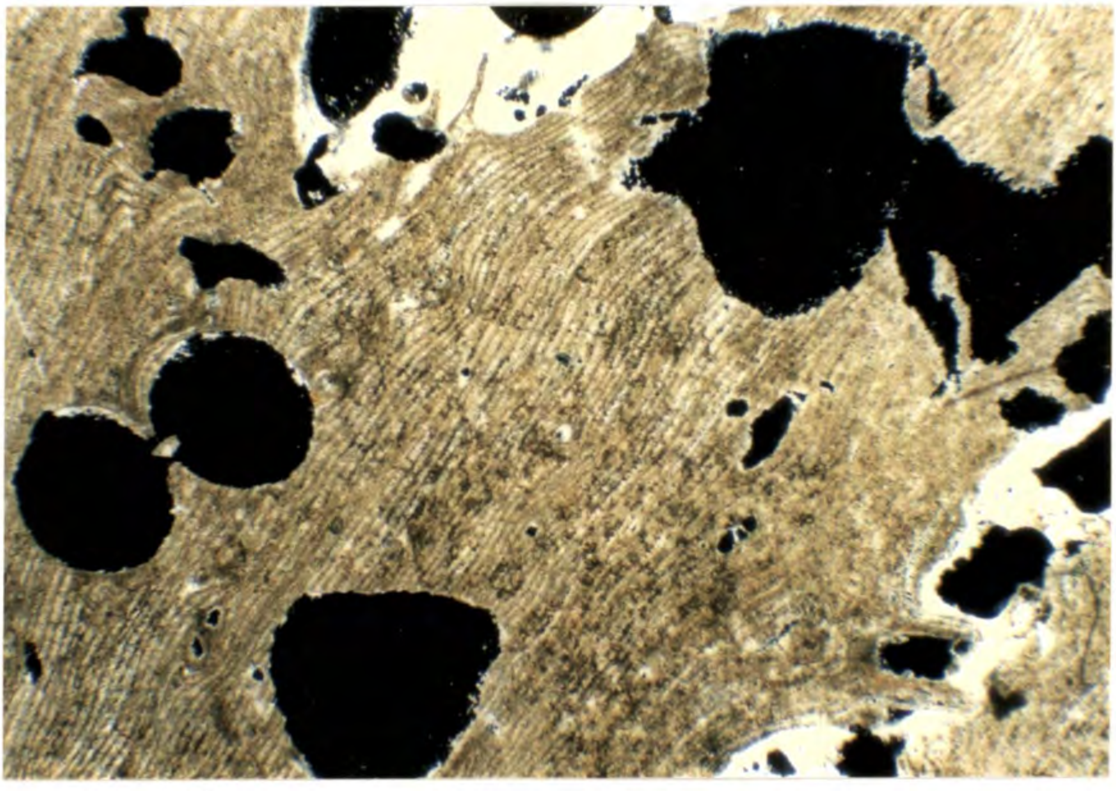

250μm.

Figure 2.24 Intraskeletal pores in coralline algae, showing a wide range of porosity sizes, from 1–2mm. bivalve and worm borings (15-25μm) Photomicrograph, xpolars. (CS)

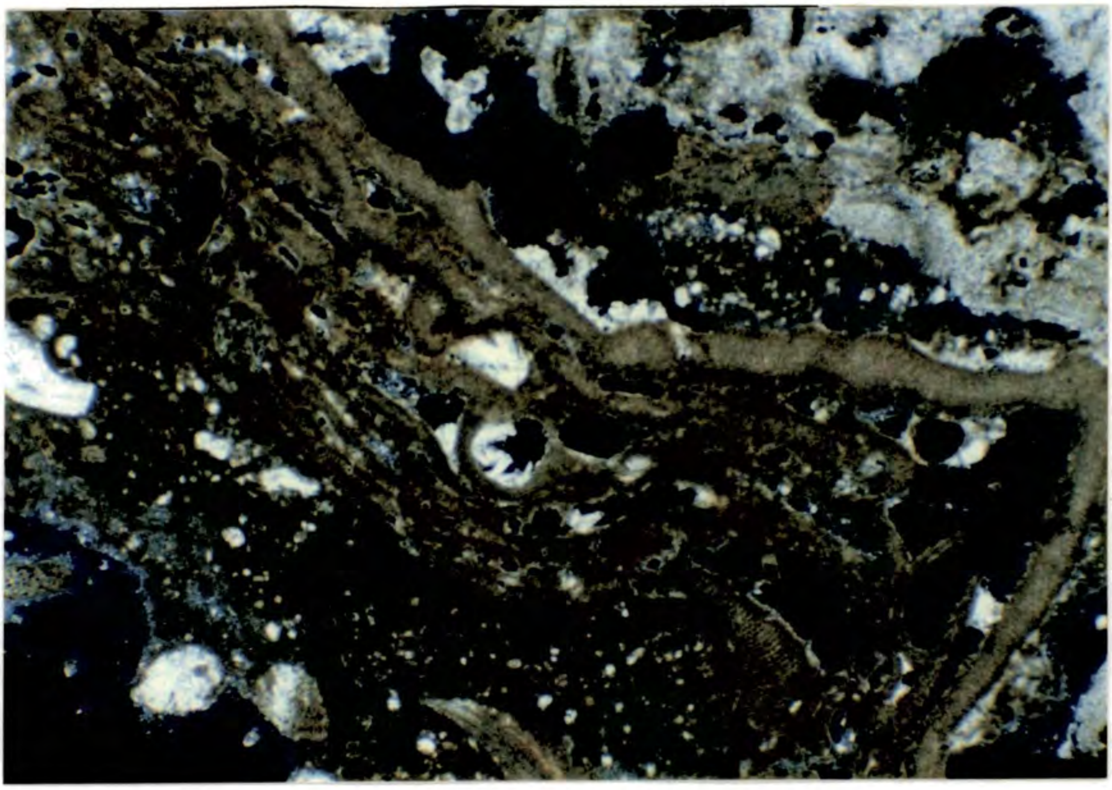

Figure 2.25 Shelter or growth framework porosity, created by the irregular growth of coralline algal laminae. Some pores have spherulitic aragonite cements precipitated within them. Photomicrograph, xpolars. (C9u)

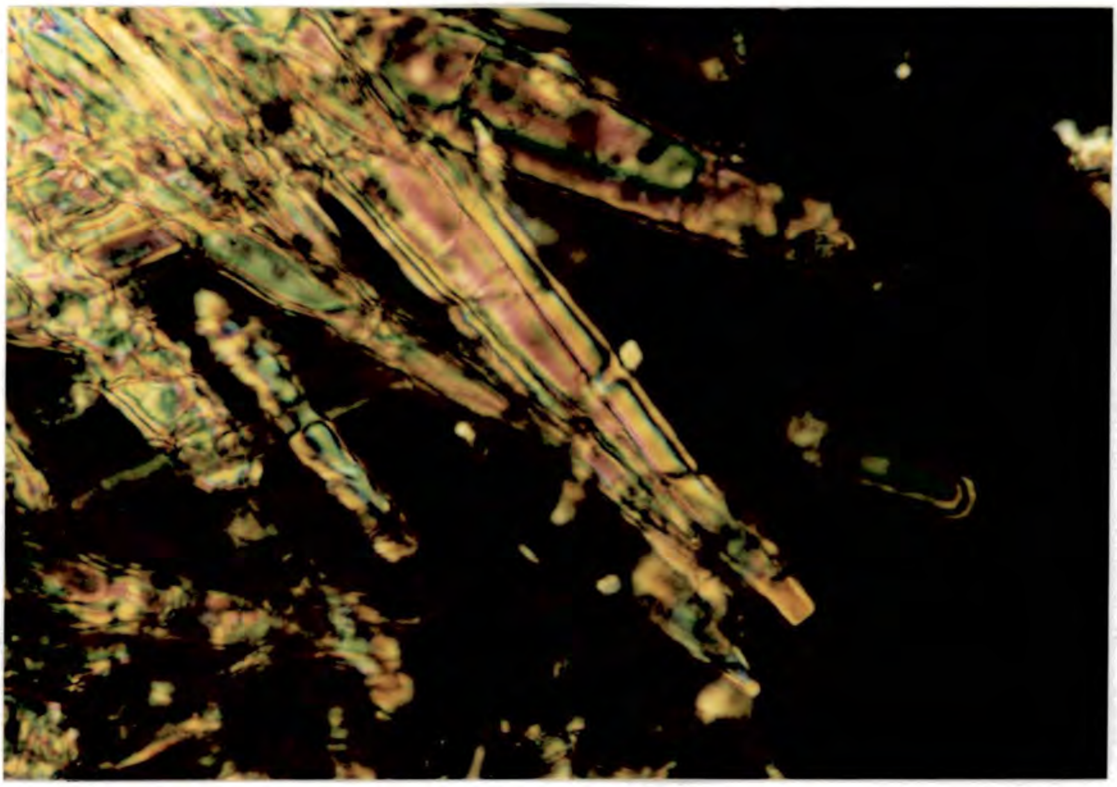

Figure 2.26 Inter-crystalline porosity between acicular aragonite crystals. Photomicrograph, xpolars. (D8)

2.7 Cementation of Alligator Reef.

2.7.1 Introduction.

The precipitation of cements in modern reefs has been the subject of a large number of studies and publications (Bricker, 1971; Schneidermann & Harris, 1985; Schroeder & Purser, 1986). Despite all of the research, many of the aspects of the geochemistry and particularly of the distribution of cements are still poorly understood. The following sections describe the petrography of the cements occurring in Alligator reef and the distribution of those cements on a variety of scales. Of fundamental importance to the understanding of the process of cementation, is the realisation that it is in continuous dynamic interaction with the other reef forming processes whose nature and products have been described in the preceding sections. A full analysis of the above mentioned interactions is presented in Section 2.17. The total abundance of cements is extraordinarily inhomogeneous on a variety of scales, but on average (on the thin section scale), cements form approximately 7% of the total rock. This total excludes microcrystalline magnesium calcite cements (Section 2.7.4), because of the difficulty in distinguishing them from micrite internal sediments. Although this average figure is rather low, it must be emphasised that the cements should be considered relative to the porosity available at the time of precipitation. The range of cement abundance varies from 0–25% of the total rock, but this reflects a range of 0–85% of the available porosity. The average as a percentage of the available porosity is 18%. The term 'cement' is used under the definition given in Section 1.2 as an in situ precipitate. Only two mineralogies of cement are known to occur within the pores of all the Holocene reef material studied: aragonite and magnesium calcite. These are described in detail in the following section.

Identification of the mineralogy has been achieved through the use of the electron microprobe, X-ray diffraction, and staining methods (See Appendix 3).

2.7.2 Aragonite cements.

Aragonite cements form in four distinct morphologies:

(i) Acicular crystals.
(ii) Spherulites.
(iii) Botryoids.
(iv) Microcrystalline.

i) Acicular. The acicular cements form on a wide variety of substrates, often in optical continuity with them. The crystals generally grow with the c-axis normal or sub-normal to the substrate, and exhibit straight extinction. Individual crystals are typically 100μm. long and 10μm. wide but the size does vary and ranges from 4–25μm. by 10–400μm.. The crystals are commonly twinned (Figure 2.27) and have either pointed or chisel shaped terminations (Figure 2.28). The acicular crystals form isopachous coatings on various substrates; these coatings vary in thickness and can be pore filling (Figure 2.29), though only rarely show compromise boundaries. They are most commonly observed in the intraskeletal cavities of *Acropora palmata* and *Montastrea annularis* (Figure 2.30), but are also present as linings on shell fragments. On the latter substrates, the crystals commonly form a more ordered or regular fringe of 50–250μm. in thickness (Figure 2.31), which can be precipitated in optical continuity with the substrate. Fibrous cements also occur in the cavities of serpulid worm tubes, where the generally larger crystals are pore filling (Figure 2.32). This fibrous or acicular growth habit is by far the most common, forming at least 90% of the total volume of aragonite cements.

ii) Spherulites are a second morphology of cement which is commonly observed (though of low total volume), and are similar to those described by Schroeder (1972a). Individual spherulites are formed of an array of crystals 5–10μm. wide and up to 400μm. long. These crystals radiate from a single point to form sectors of a sphere with opening angles of usually less than 90 degrees, but with rare examples of up to 180 degrees (Figure 2.33). This morphology is defined as distinct from other fan shaped growths of the fibrous aragonite described above, the latter forming simply due to growth on substrate convexities (Figure 2.34). The spherulitic cements are most frequently observed in the growth framework cavities of coralline red algae and in borings through these organisms, but they also occur in the intra-skeletal cavities of various coral species.

iii) Botryoids. The fabric of the spherulitic cements grades into a cement morphology which is similar to the botryoids described by James & Ginsburg (1979), albeit on a much smaller scale. These are rare and are formed of much smaller crystals than the spherulites described above, with the individual crystals being unresolvable under the optical microscope (Figure 2.35). These botryoids can reach 1600μm. in size and are restricted to occurrences within intra-skeletal cavities of corals. They have rarely been observed in internal sediments, where they have probably become detached and carried through into other cavities with the sediments (Figure 2.36). Both spherulites and botryoids generally occur as individuals, showing sweeping extinction, but are locally developed as interfering masses (Figure 2.37).

iv) Microcrystalline. Another rare morphology of aragonite cement is a microcrystalline precipitate, restricted to occurrences in coral skeleta, with submicron sized crystals which can form bridges across pores (Figure 2.38).

A final morphology of blocky aragonite crystals, which has been described separately in the literature (Marshall, 1983a; James & Ginsburg, 1979), is attributed in this study to be a fortuitous cross section through the above acicular aragonite crystals. The crystals are equant in shape, 10–15μm. in size, and exhibit straight extinction. They are exceedingly rare and are almost certainly tranverse sections (perpendicular to the c-axis) through aragonite needles.

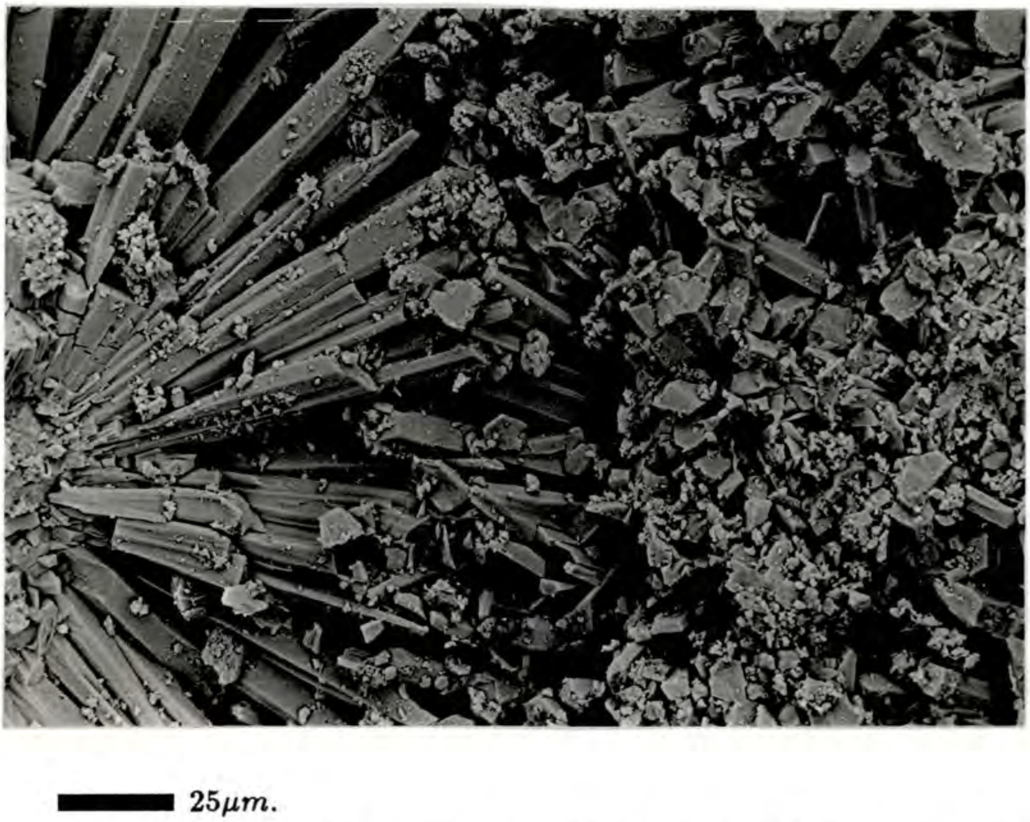

Figure 2.27 SEM photo of acicular aragonite crystals, some twinning evident, crystals growing with their c-axes normal to the substrate. (H.S. Alligator Reef)

▬ $5\mu m$.

Figure 2.28 Aragonite cement crystals within the same species of coral, exhibiting both pointed and chisel-shaped terminations. (H.S. Alligator Reef.)

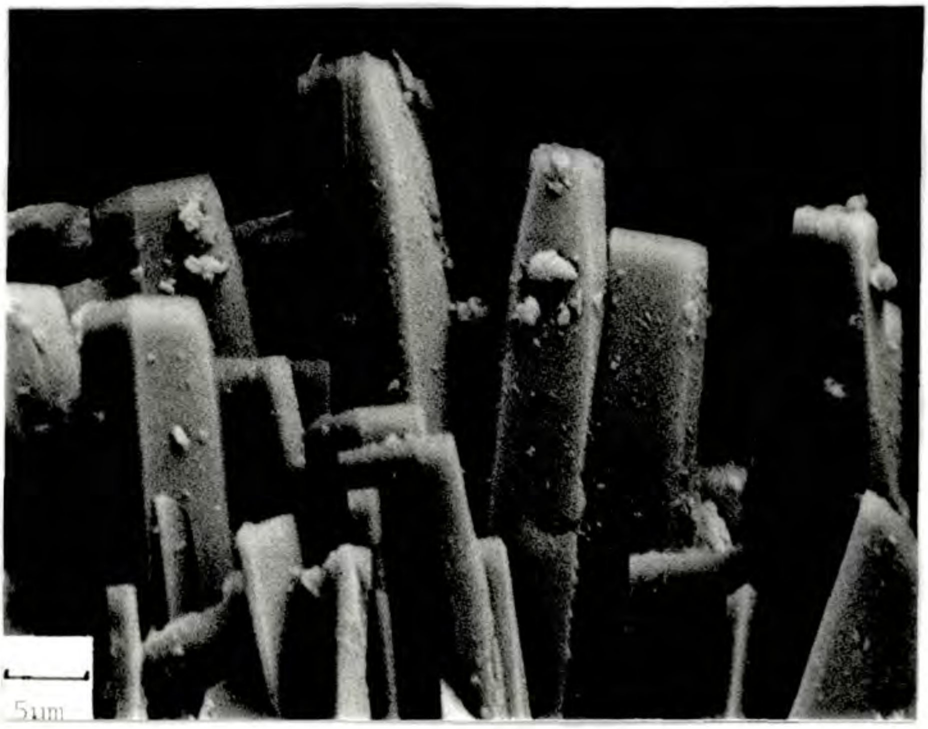

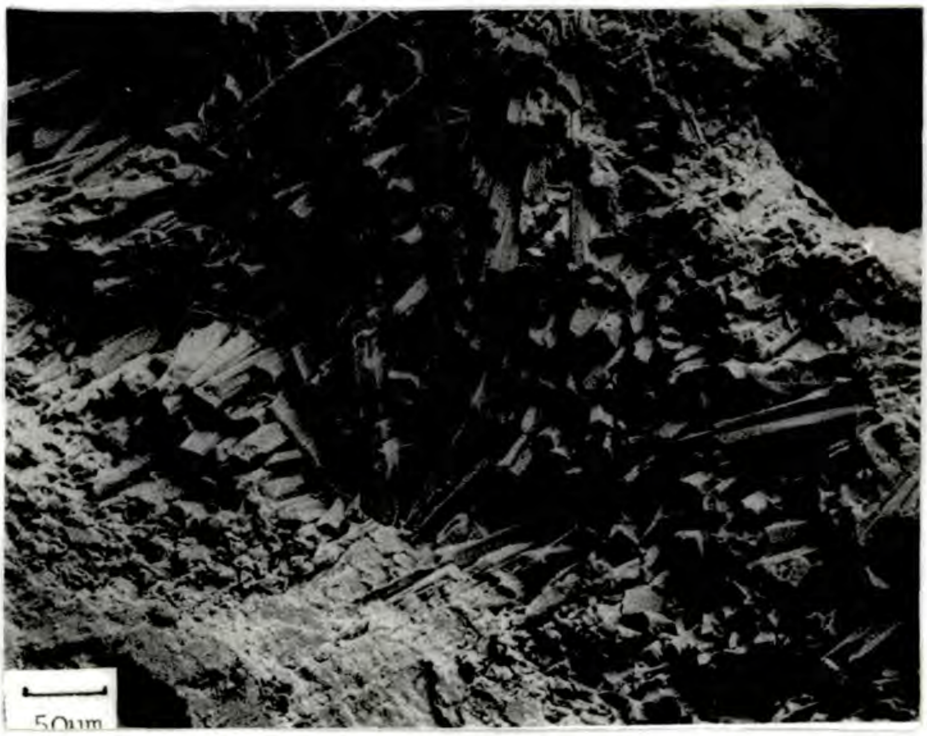

▬ 50μm.

Figure 2.29 Substantial development of acicular aragonite within intra-skeletal porosity of a coral skeleton. C-axes again normal or sub-normal to the substrate, with irregular intergrowth of crystals from opposite sides of the pore. (H.S. Alligator Reef)

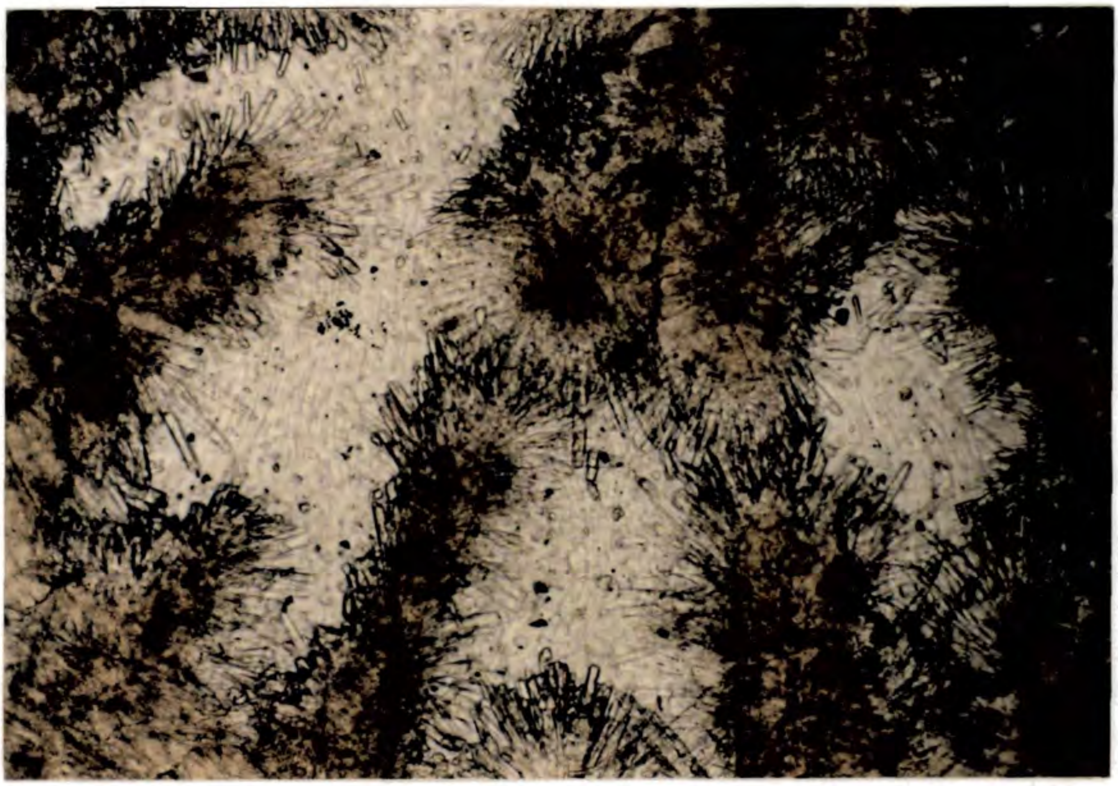

Figure 2.30 Acicular aragonite within cavities of *Montastrea sp.*. Photomicrograph, ppl. above, xpolars below. (D8)

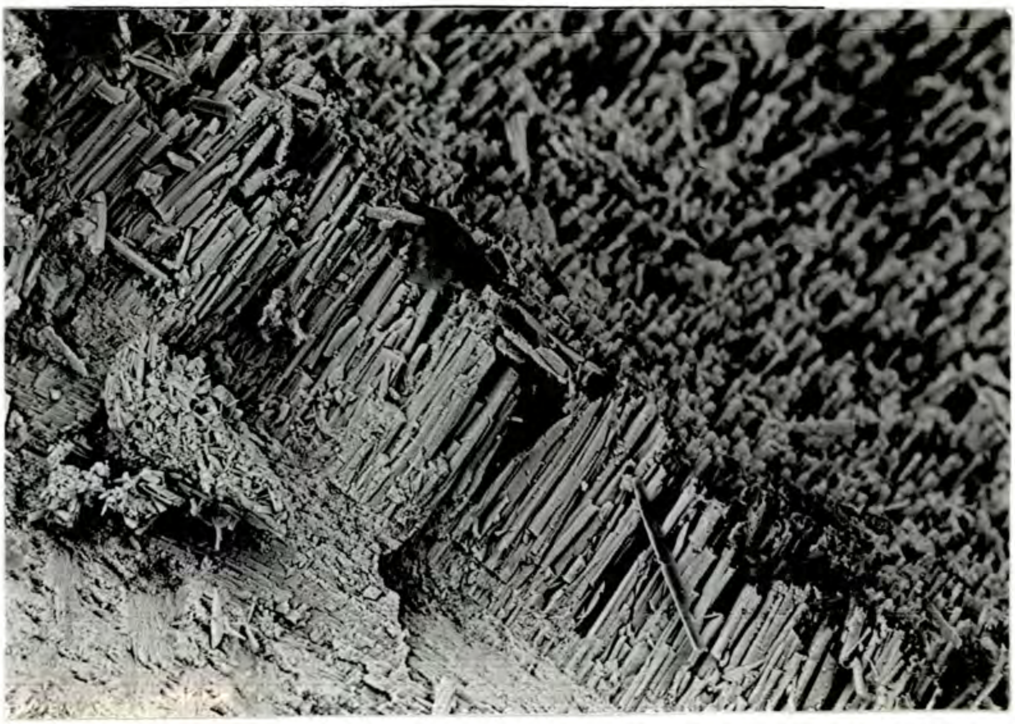

Figure 2.31 Ordered fringe of aragonite fibres precipitated on a shell fragment. The regular orientation may be due to some substrate control, and this is supported by the fact that crystals often grow in continuity with the substrate. (H.S, Alligator Reef)

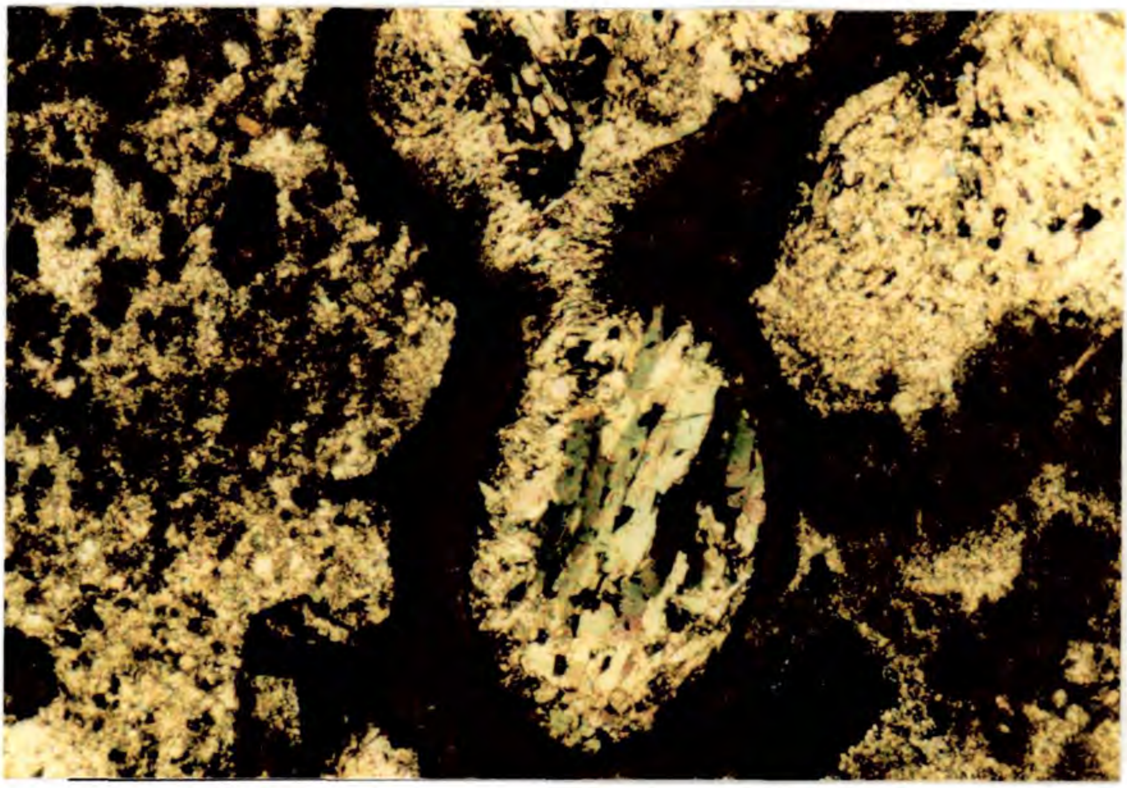

Figure 2.32 Large aragonite crystals filling the intra-skeletal cavity of a serpulid worm tube. Photomicrograph, xpolars. (C4)

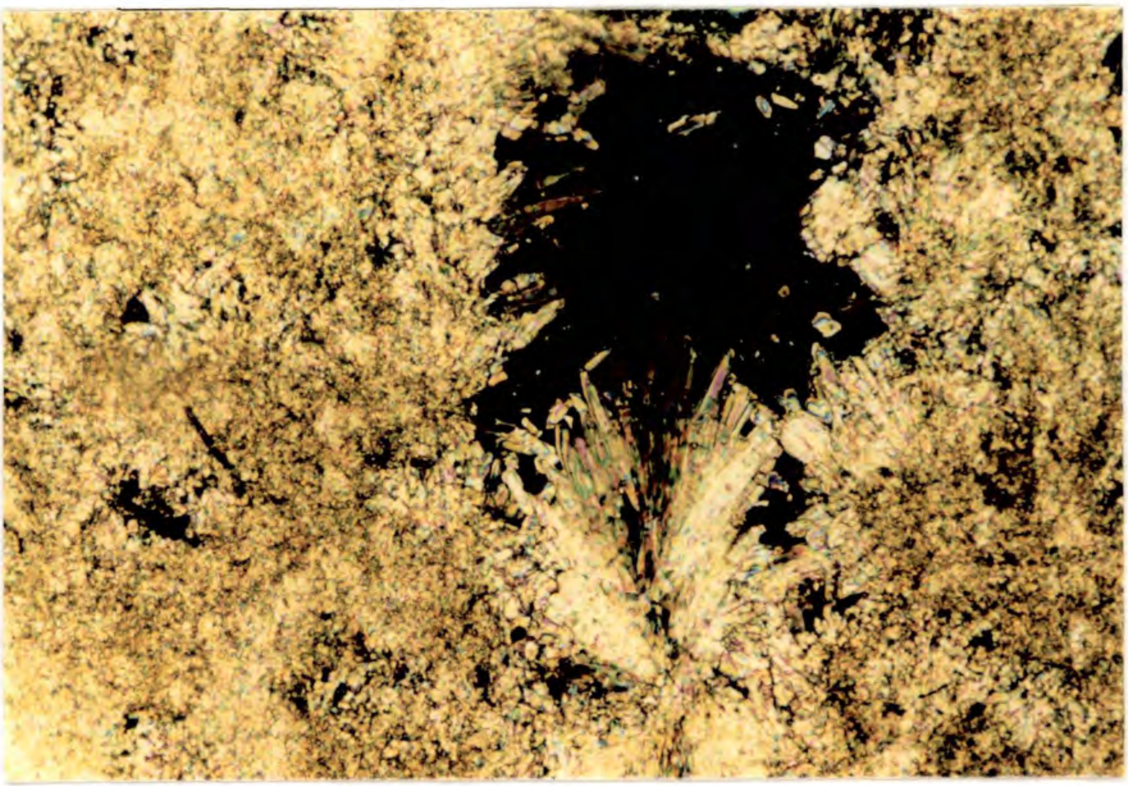

Figure 2.33 Spherulitic aragonite formed of similar acicular crystals to those described above. All the crystals radiate out from a single nucleation point, to create sectors of a cone. Photomicrograph, xpolars. (C8)

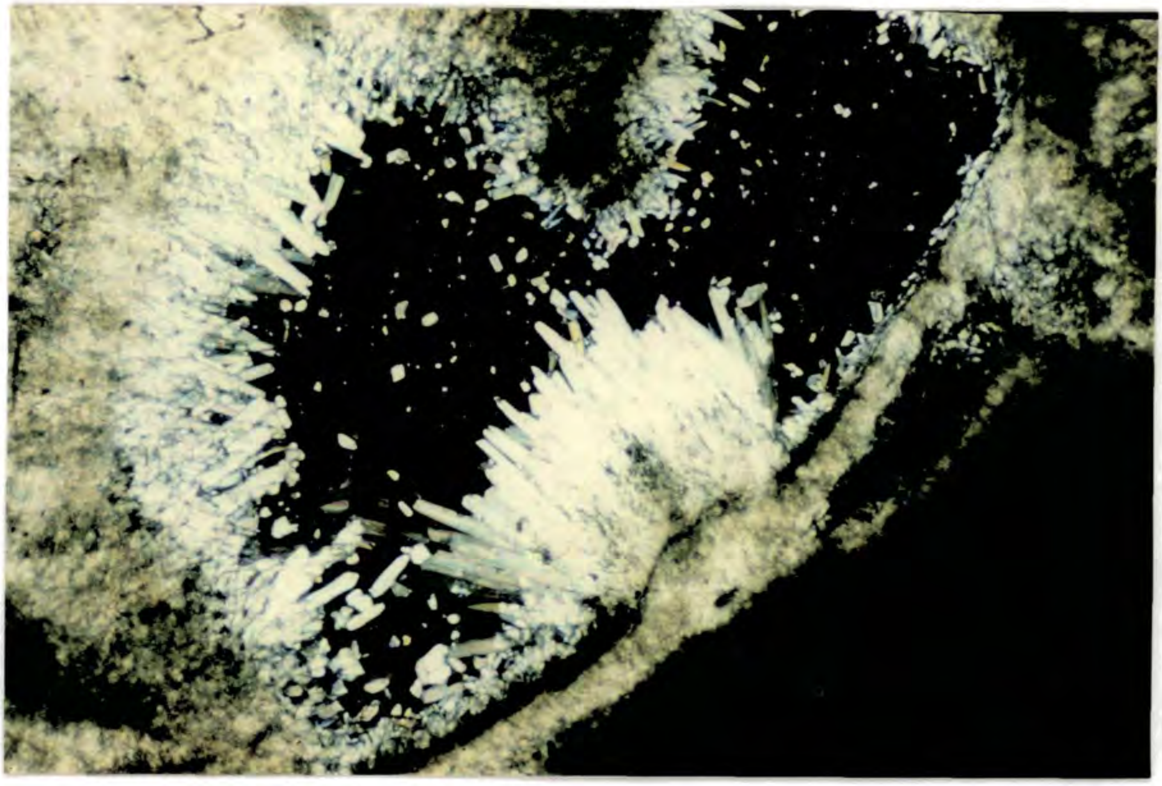

Figure 2.34 Fan shaped aragonite cement, similar to the above, but the shape is simply created by growth on a substrate convexity, and is therefore not a spherulite. Photomicrograph, xpolars. (B5)

Figure 2.35 Botryoidal aragonite in the intra-skeletal porosity of a coral skeleton. Individual crystals cannot be resolved in the optical microscope. Photomicrograph, xpolars. (D8)

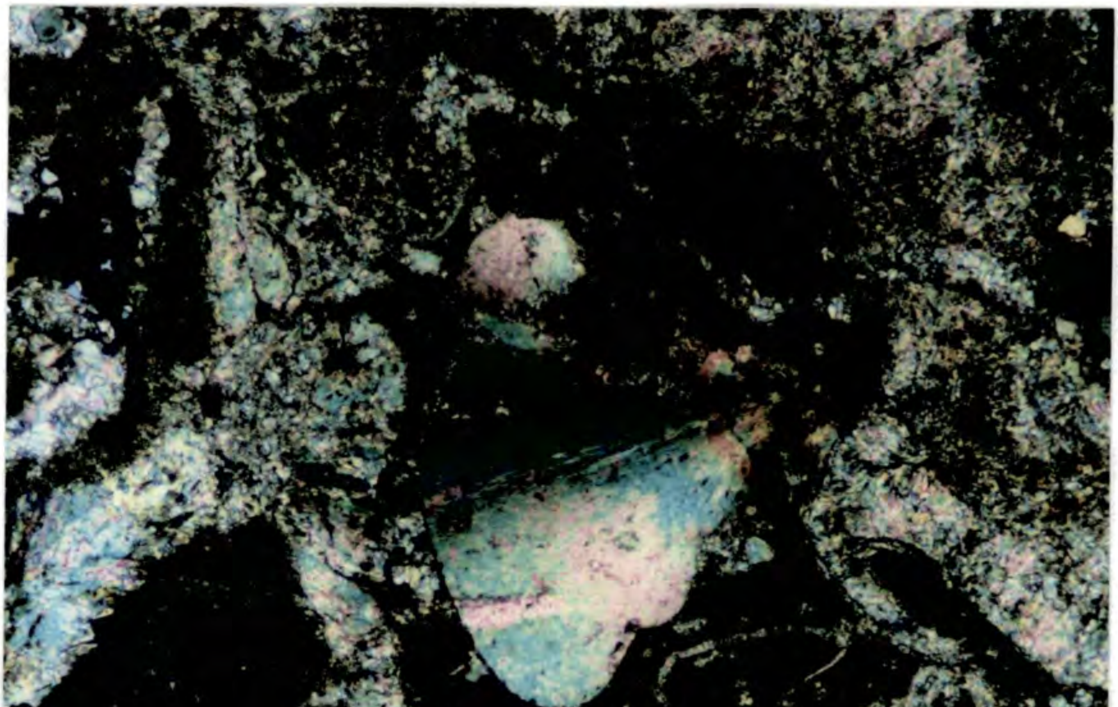

Figure 2.36 Another example of the botryoidal cement, in this case it has become detached from the substrate and carried into the pore with some internal sediment. Photomicrograph, xpolars. (C94)

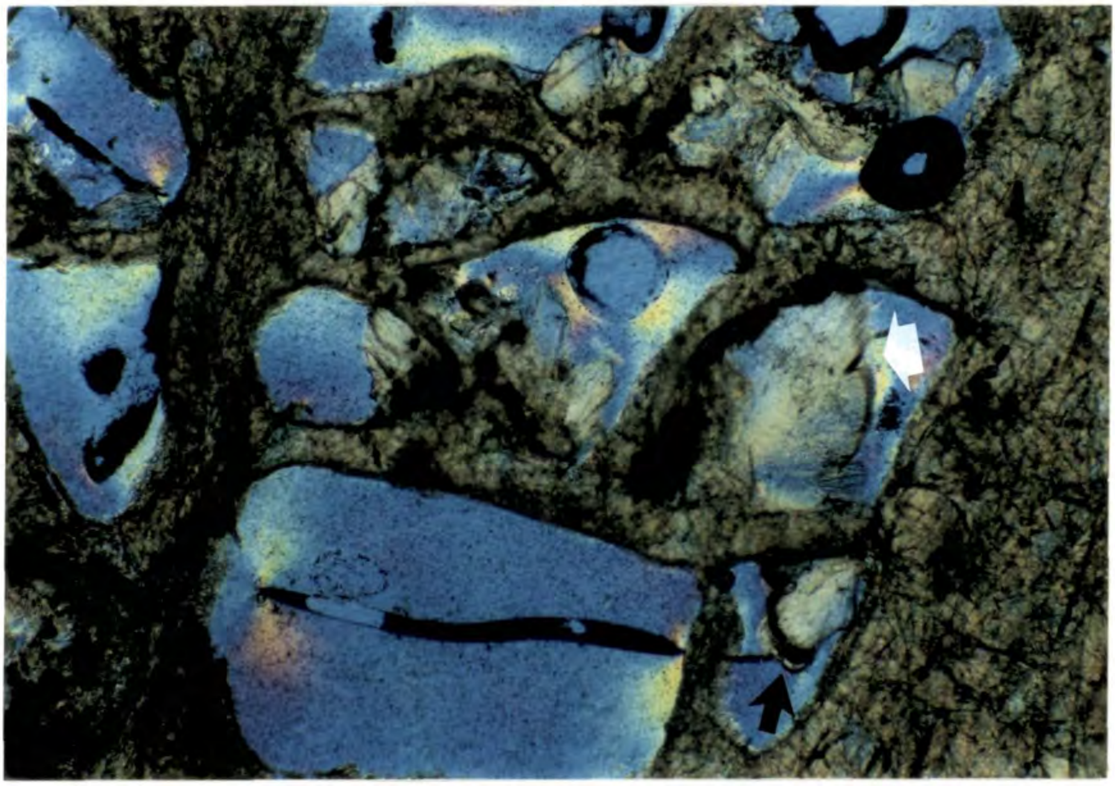

Figure 2.37 Botryoidal cements growing as coalescing masses, again within coral pores. Photomicrograph, xpolars. (B3)

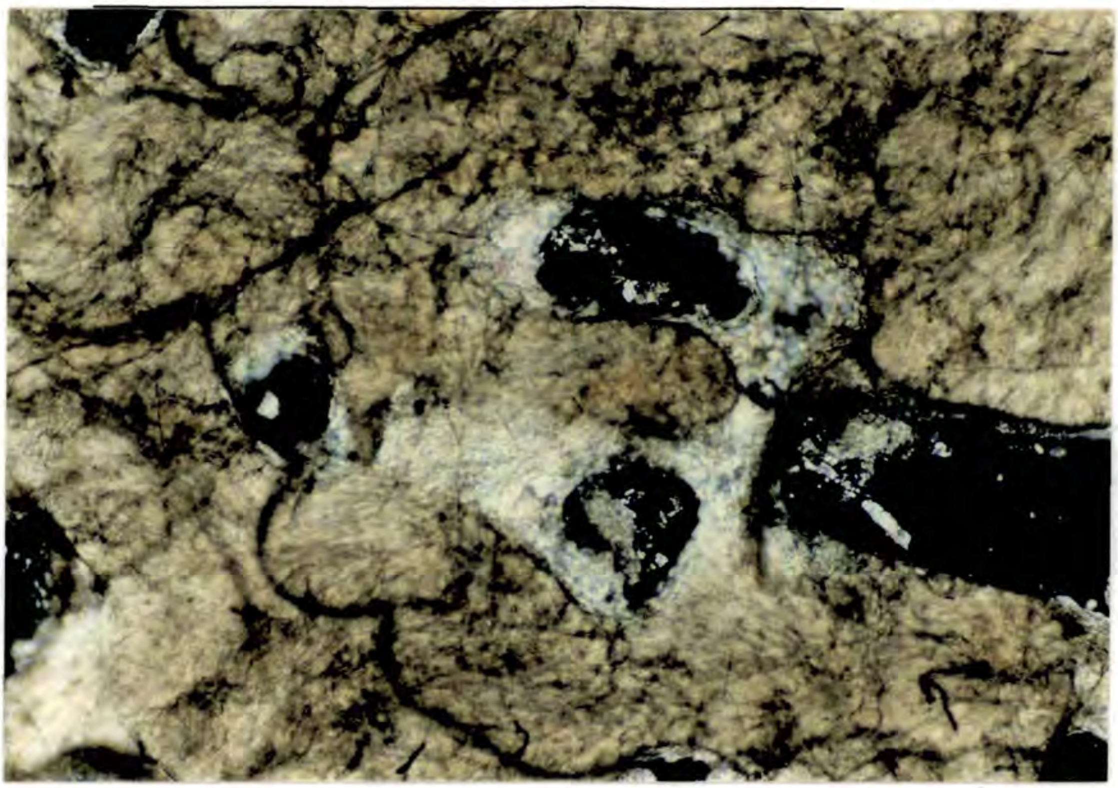

100μm.

Figure 2.38 Rare occurrence of microcrystalline aragonite forming a bridge across the cavities within a coral. Photomicrograph, xpolars. (E4)

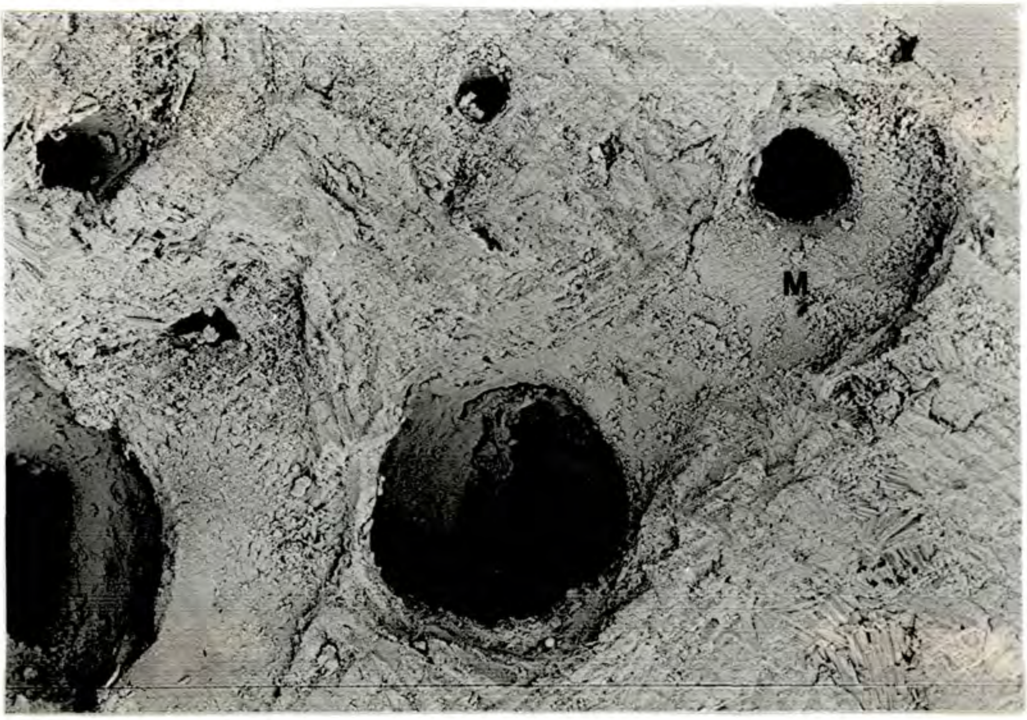

100μm.

Figure 2.38 Similar to above example, in SEM view. Some acicular aragonite also visible at lower right. Microcrystalline cement marked with an 'm'. (E4)

2.7.3 Calcite cements.

The calcite cements observed in the Holocene reefs are always associated with magnesium, having a typical composition of 12–16 mole% $MgCO_3$. The cement forms in three distinct morphologies; peloidal, fibrous and microcrystalline. Whilst in many published descriptions of the diagenetic products within reefs, magnesium calcite cements are considered to be the most abundant (Schroeder & Purser, 1986), this is certainly not the case for the reefs of Florida, where they are present in equal or lesser volumes than the aragonite cements. Some confusion exists with respect to the nature of micrites and may have led to the overestimation of the volumes of Mg-calcite cements in the past or indeed to an underestimation of the volumes in this study. The problems are discussed in detail in the next Section (2.7.4).

Fibrous fringes of Mg-calcite often described from other reefs (James et al., 1976; Marshall, 1983a, 1983b), are particularly rare in the Holocene Alligator samples, limited in fact, to a few individual occurrences. This morphology has been observed lining borings within internal sediments (Figure 2.39), and in one example only, within the intra-skeletal cavities of Halimeda plates (Figure 2.40). In these examples it occurs as a more ordered habit than the aragonite cements and forms an isopachous fringe consisting of short stubby crystals less than $30\mu m.$ long, with rhombic terminations. This is probably analogous to the bladed spar described by James & Ginsburg (1979).

Magnesium calcite microcrystalline cements forming aggregates of small rhombs up to $10\mu m.$ in size, occur either as isolated crystals on the surfaces of skeletal fragments (Figure 2.41), or as a rind of cemented crystallites. Identification is generally only possible under the scanning electron microscope, as in transmitted light the crystals vary in appearance from clear to opaque and can be easily confused with physically deposited micrites. In some grainstone samples, magnesium calcite microcrystalline cements are developed as ‘bridges’ between the grains (Figure 2.42), and can then be easily identified as a cement phase in transmitted light.

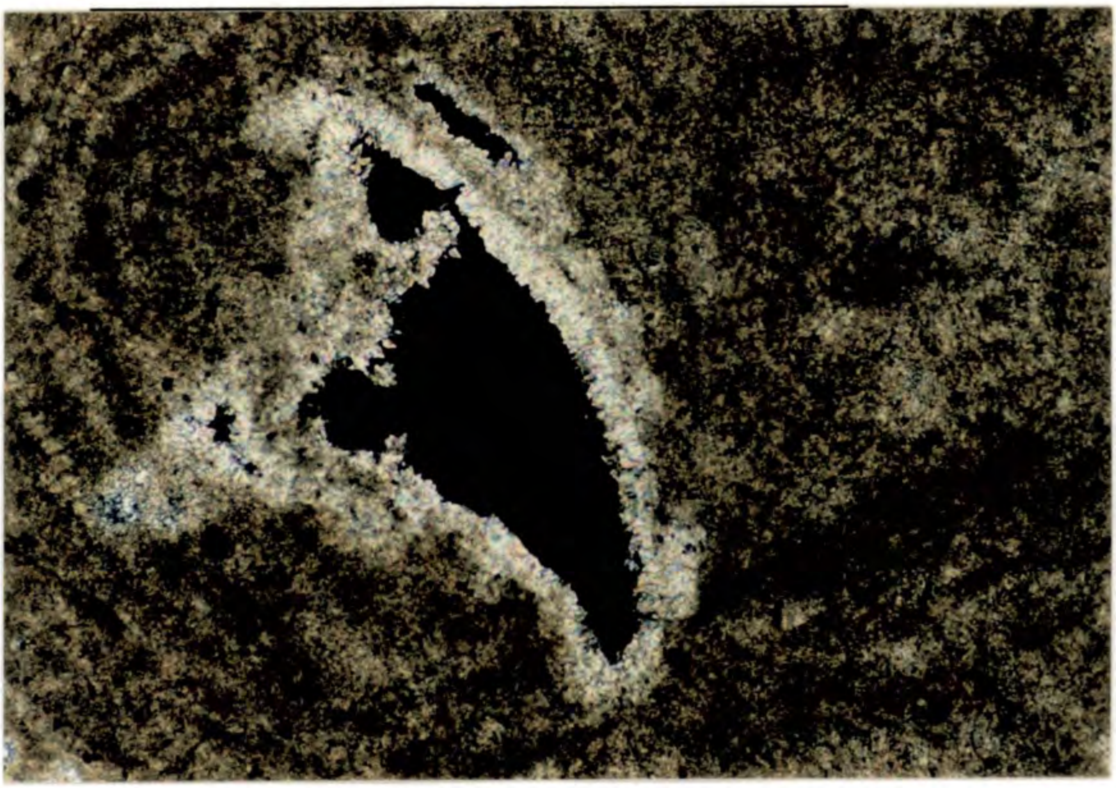

50μm.

Figure 2.39 Rare fringes of microcrystalline Mg-calcite found in the Florida reefs. Generally occurs precipitated in cavities within internal sediments, and the crystals form an ordered fringe of less than 30μm. in thickness. Upper photo with xpolars, lower photo in ppl. shows the Mg-calcite mineralogy through staining with Titan yellow. (D16)

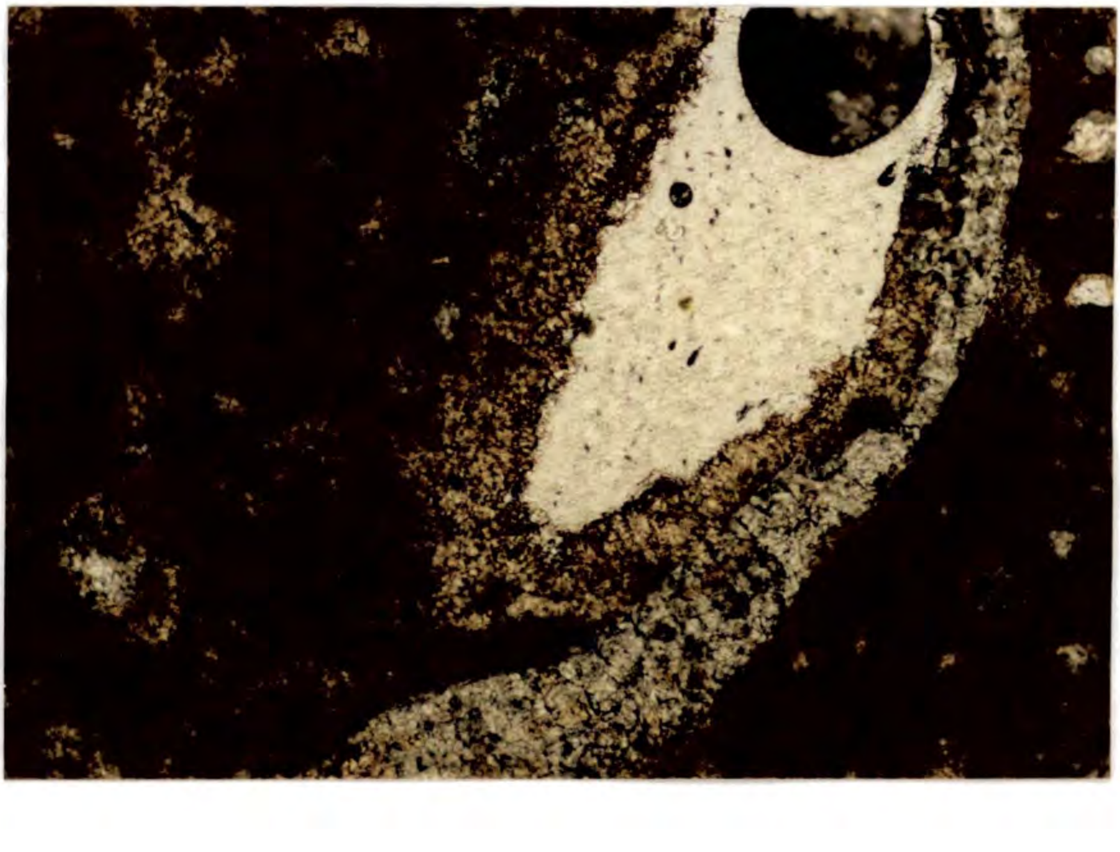

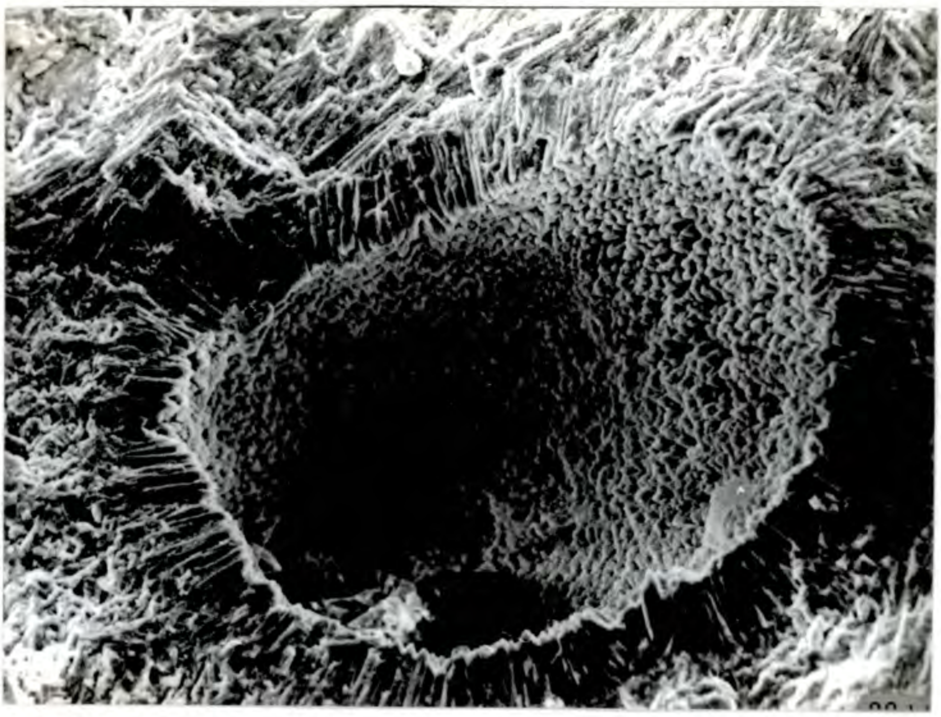

Figure 2.39 Short stubby growth of Mg-calcite as isopachous fringe in coral pore. (D16)

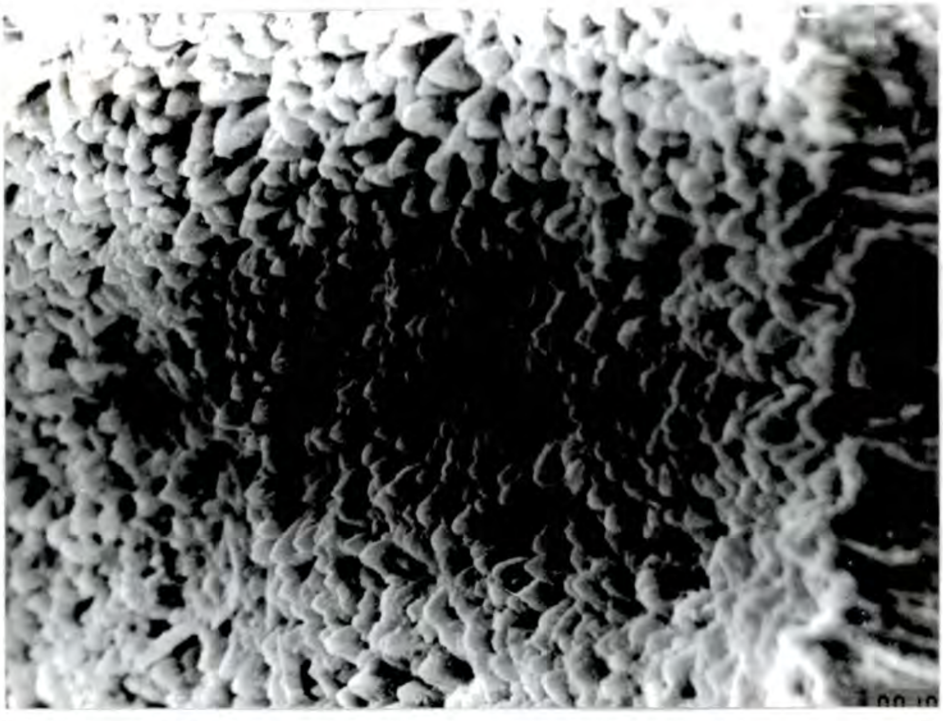

Figure 2.39 Detail of the above.

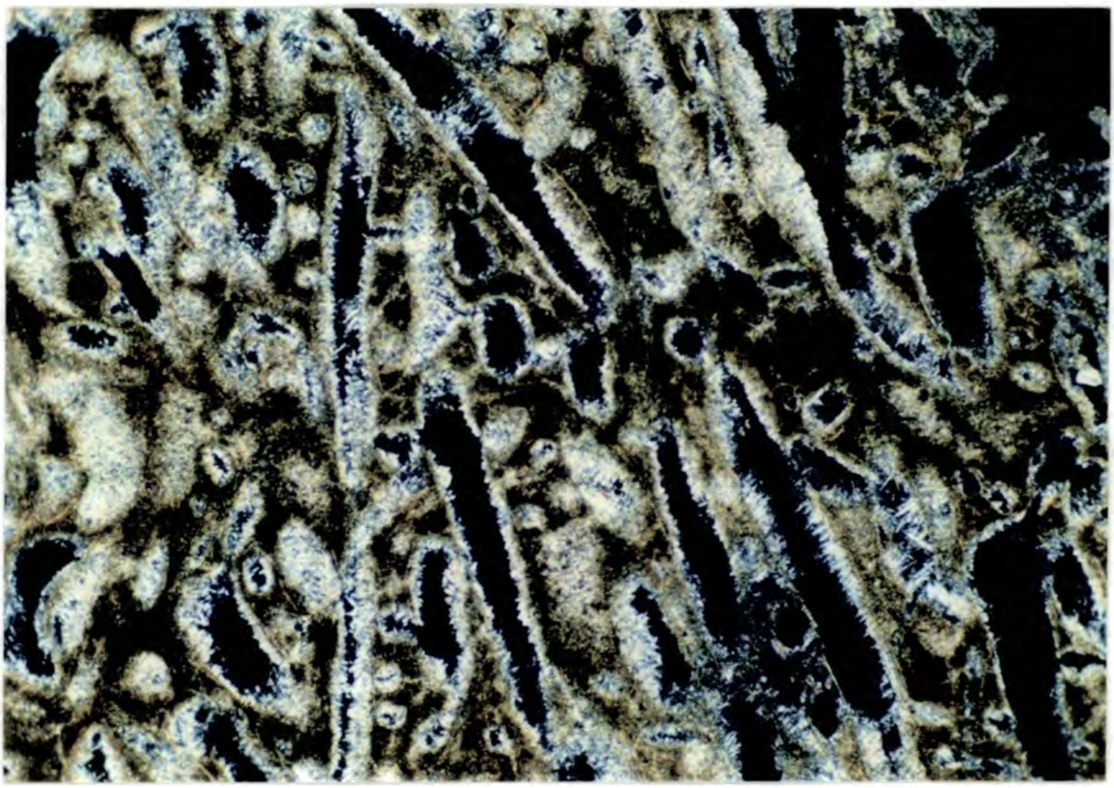

Figure 2.40 Mg-calcite cement crystals growing in *Halimeda* fragment. Photomicrograph, xpolars.
(F 18 L)

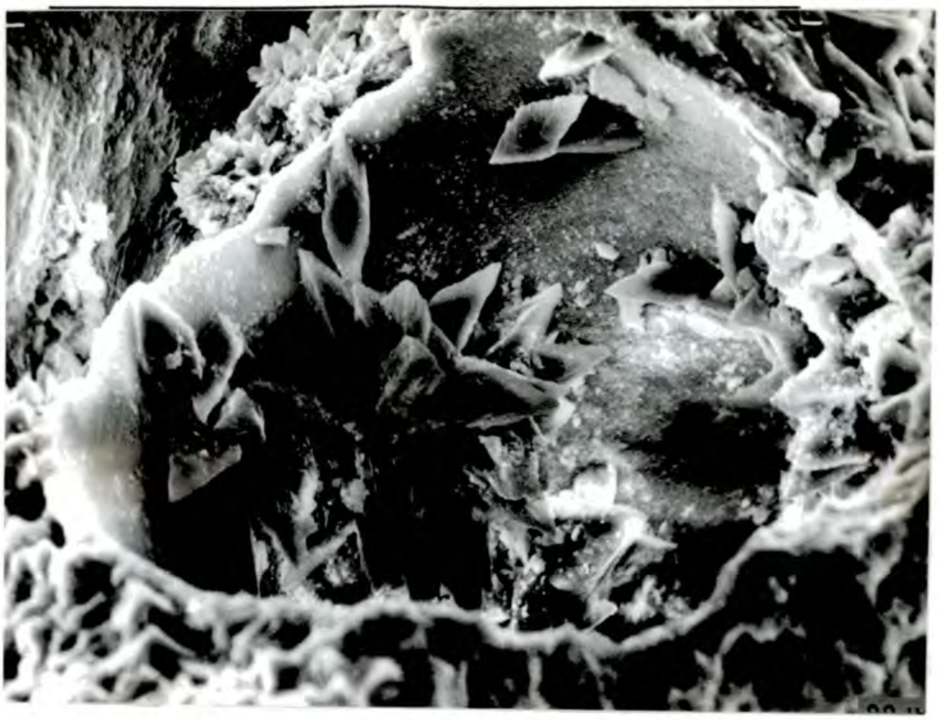

$\blacksquare$ 10μm.

Figure 2.41 Mg-calcite also forms as small rhombic crystals, either as isolated growths on skeletal fragments (above), or as clusters covering the surface (below). (H.S. Alligator Reef)

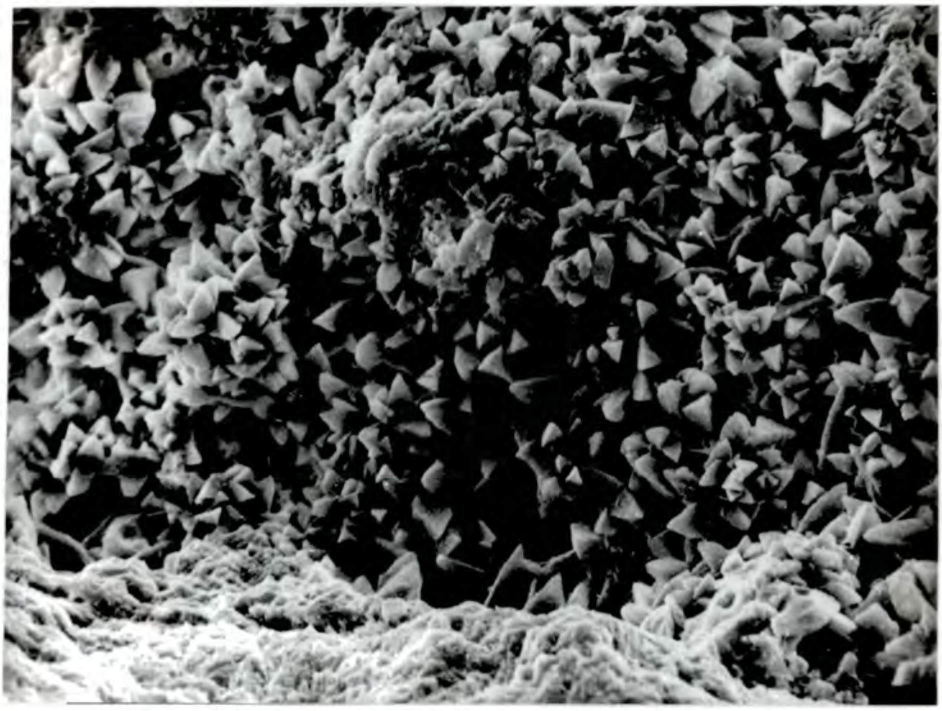

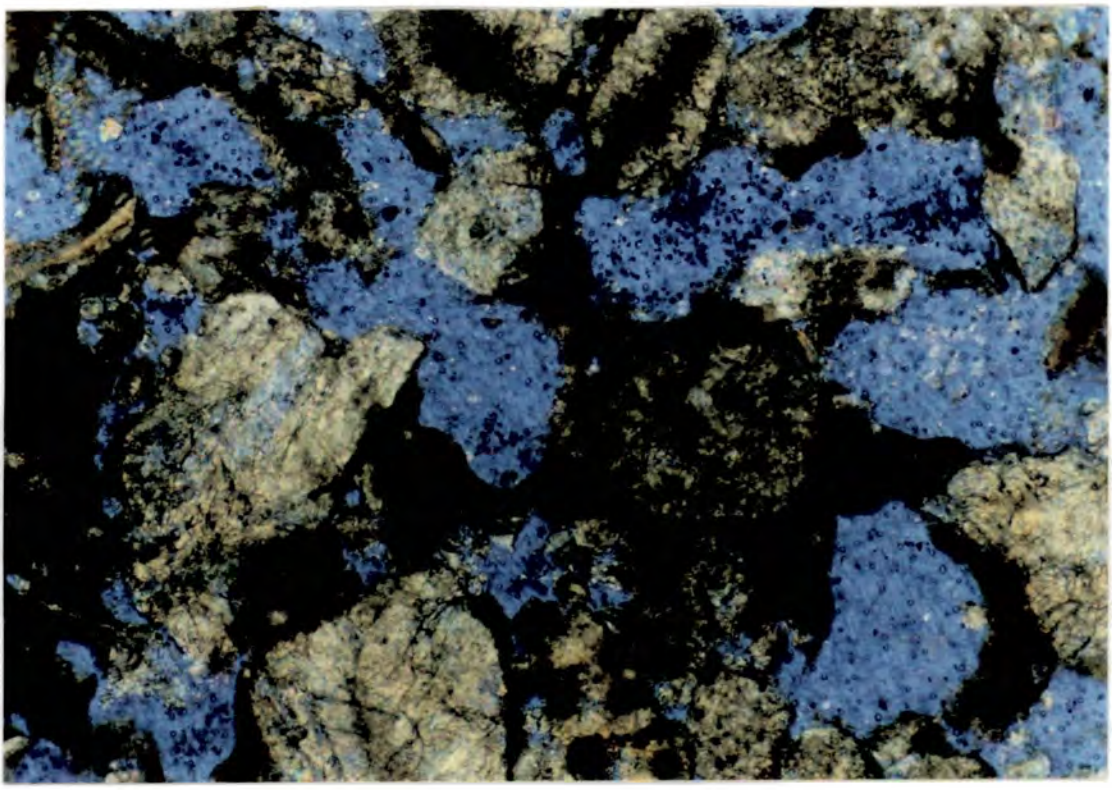

Figure 2.42 Microcrystalline Mg-calcite cement forming bridges between skeletal fragments in a grainstone. Photomicrograph, xpolars. (D6)

2.7.4 Micritic magnesium calcite cements.

The problem of the identification of micrite cements precipitated within micrite internal sediments is one which has vexed sedimentologists for a long time (Folk, 1959; Bathurst, 1975; Friedman, 1985). Indeed the preceding sentence illustrates much of the misunderstanding and misrepresentation of the term 'micrite'. Folk introduced the term in 1959 and later noted that it was a shortened version of microcrystalline calcite ooze (Folk 1962), representing a clay-sized matrix. Its description as a matrix implies mechanically deposited material, as distinct from precipitated cements (Bathurst, 1975), and so leads to a definition of micrite given by Friedman (1985) as "lithified, mechanically deposited lime mud" (Friedman & Sanders, 1978).

The problems arise when the mechanically deposited matrix and precipitated microcrystalline cements become indistinguishable, as is frequently the case in lithified packstone to mudstone internal sediments. Friedman's assessment of the fact that much of the micrite observed in reef rock pores is not mechanically deposited, but is in fact precipitated cement, is argued from the basis that the energy conditions are too high within reefs to allow clay sized material to settle and that no other deposits of lime mud are observed in his study areas (Friedman 1985). However, whilst the high energy environment may prevent lime mud accumulating by itself in shelf edge settings, this does not preclude the possibility that micrites (= mechanically deposited clay sized material), may accumulate within the pore systems of reef rock. Although the shelf edge reefs are undoubtedly in a very high energy environment, large areas within the reef framework will be well protected and may even be almost stagnant. In these low energy environments, clay-sized material could easily and certainly does settle out and accumulate in the pores of the reef rock.

The waters surrounding the Florida reefs are generally extraordinarily clear, indicating a lack of clay-sized material suspended in the water column, but this is only the case during calm weather. The situation is markedly different after storms and hurricanes, when the water can remain turbid for several days. In addition, particularly in the Florida area, there is a substantial source of clay-sized material (the sediments of Florida Bay), and this material is distributed across the shelf and into the basin of the Straits of Florida through the many gaps in the Florida Keys. There is, therefore, an adequate supply of clay-sized material and suitable mechanisms for entrapment of this material in the reef rocks of the shelf edge.

The range of textures created within these problematic cements/micrites varies enormously, throughout the range of descriptions defined by Dunham (1962), from packstones through to mudstones. These internal sediments are created when various amounts and sizes of skeletal debris are deposited along with the micrites. The range simply reflects a decreasing amount of recognisable (though not necessarily identifiable), skeletal material (Figure 2.43).

In all of the above sediments, it would be extremely difficult to determine how much of, or indeed, whether any of the micrite was truly micrite, or was precipitated microcrystalline cement. A somewhat tenuous deduction that all of the micrite was in fact cement could be made in the case where no aragonite is present. As most of the skeletal particles in modern reefs are of aragonite mineralogy, it would be impossible for a physically deposited material to consist of exclusively Mg-calcite, implying therefore that the observed sample was a precipitated cement. Although several mudstone internal sediments have been analysed by XRD (Appendix 3), they have all been found to contain both minerals and, therefore, are either micrites (sensu stricto) or micrites with an indeterminate proportion of cement.

In the samples from Alligator reef, these problematic cavity fills are almost exclusively unlithified or very friable, indicating that only a very small proportion of precipitated cement is present, and clasts of cemented micrite have not been observed. Whilst borings through micrites have been observed, indicating lithification of the first phase of internal sedimentation in these cases (Figure 2.20), examination of such occurrences in hand specimen again shows that the lithification is slight.

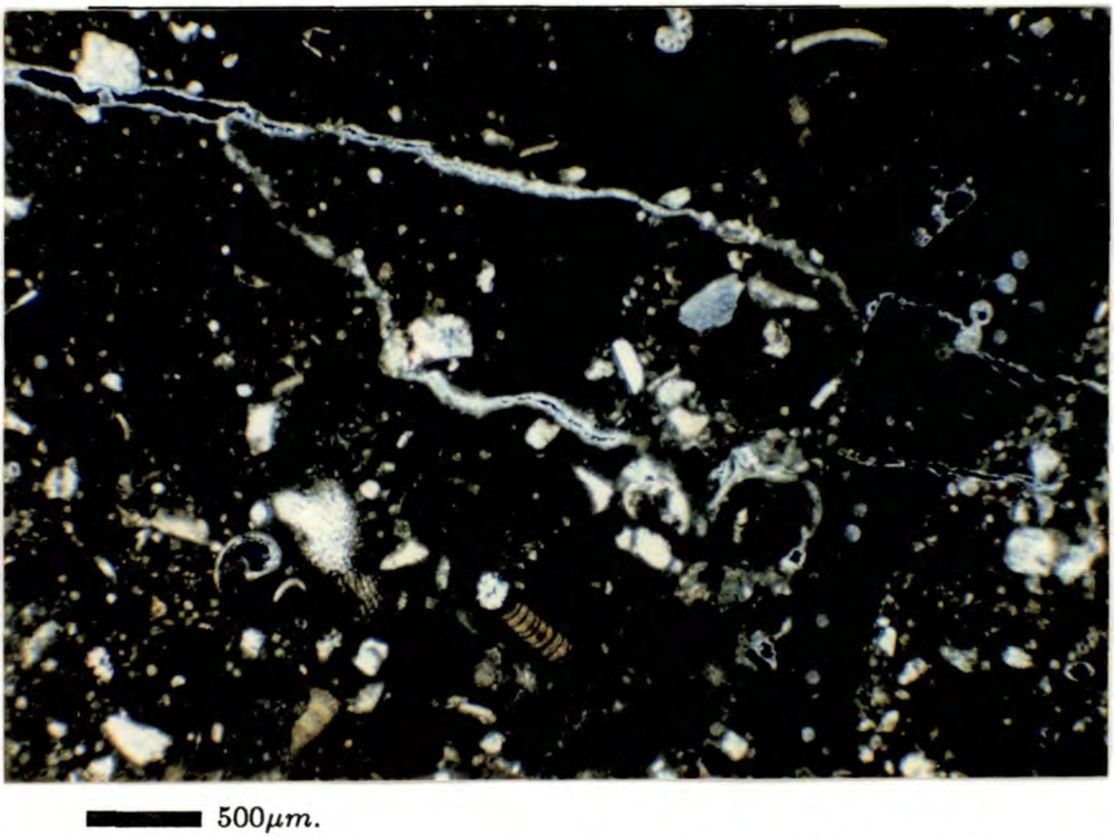

Figure 2.43 Variation in the textures of micrites (= physically deposited material), apparent within individual thin sections. It is not possible to determine the proportion of cement within these internal sediments. (C9L)

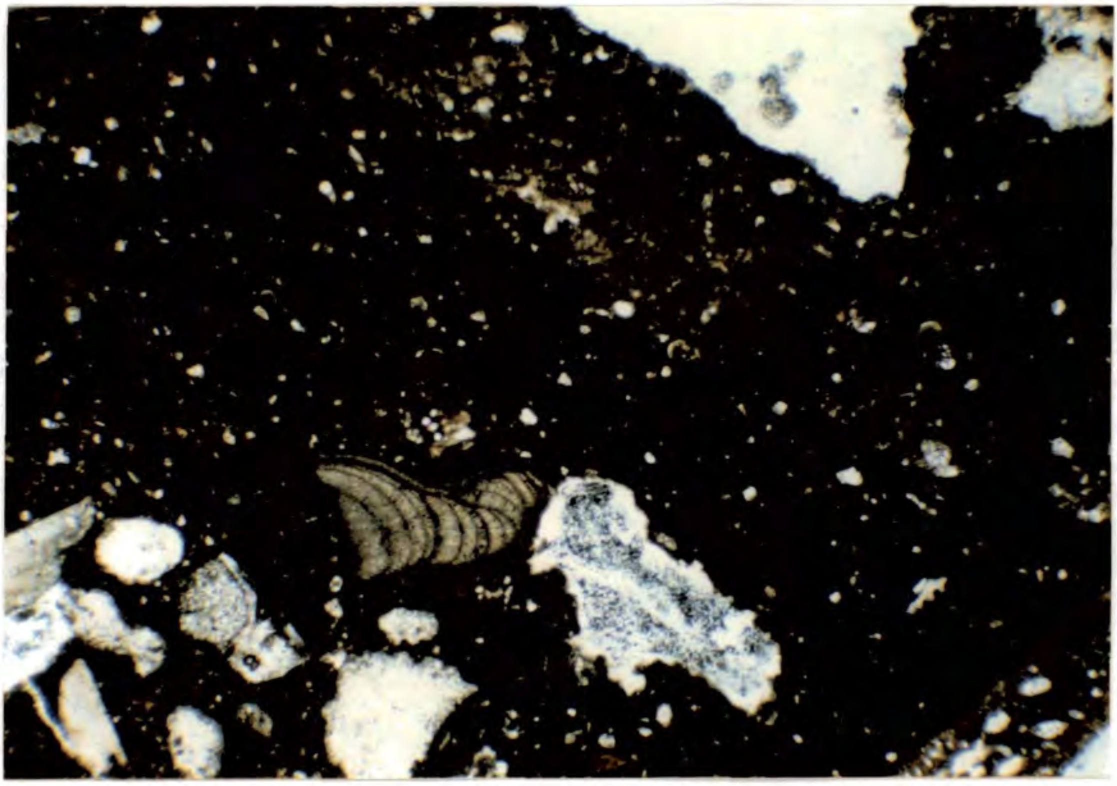

The suggestion is, therefore, at least for the Alligator reef samples, that the majority of the dark pore filling material is indeed physically deposited micrite. Only where lithified, is there a significant proportion of precipitated cement. Under the optical microscope it is impossible to distinguish cement from micrite in such pore fills, although it may be possible under the SEM (Loreau, 1982). This is true throughout the range from packstones to mudstones. However, in the case of lithified grainstones, the dark brown microcrystalline material which can be observed at the grain contacts can safely be assumed (by default) to be a precipitated phase (Figure 2.42). It is interesting to consider whether packstones are physically deposited as such, or whether they were originally deposited as grainstones which were then converted to packstones via the precipitation of pore filling microcrystalline cements!

Hence, in the petrography of this material and in the point counting data presented in Appendix 1, pore filling materials have been defined in separate groups. These are micrite (where most of the material is of clay size), packstone & wackestone (collectively describing material with a significant amount of non clay sized material), and grainstone (by definition, grain supported with no significant matrix content). This description has been based on observation under the optical microscope alone, and is therefore, somewhat subjective. A quantitative description of the amount of cement that may be present has not been attempted.

The conclusion of this discussion on micrite is that the majority of the dark brown pore filling material is truly micrite in its strictest definition and that only a small proportion can be considered to be a precipitated cement. This contrasts with other descriptions of Mg-calcites within reef rocks (James et al., 1976), where the Mg-calcite microcrystalline cements have often been considered to be predominant. This is certainly not the case in the samples from Alligator reef, and it may be that the volumes have been overestimated in other studies.

2.7.5 Peloidal Magnesium calcite.

This is the most abundant form of magnesium calcite cement and is very similar in appearance to the peloidal cements described from many other reefs (Macintyre, 1977; Alexandersson, 1978; Marshall & Davies, 1981). The origin of the peloids, and the question of whether they are a cement under the strict definition of an 'in situ' precipitate, has been debated at length in the literature (Schroeder, 1972b; Land & Moore, 1980; Marshall & Davies, 1981). Macintyre (1985) summarised the five major hypotheses. These are that the peloids are of algal origin, are a replacement texture, are sedimented particles, are produced by pelletising organisms, or are precipitated in situ.

Some peloidal textures observed in thin section are undoubtedly produced by calcifying algal filaments, cut in cross section. However, it is clear from SEM studies of the Florida samples, that the majority of the peloids are individual subspherical entities, and are therefore not calcified algal filaments. The suggestion that the peloids are produced by pelletising organisms is considered to be unlikely as they are monomineralic; microprobe studies show them to be magnesium calcite only. In addition, they are present in far too large quantities (up to 20% of the whole rock) to be produced by pelletising organisms. Their restricted size range (20–60μm.) makes it unlikely that they are aggregated and sedimented from the water column, since if they were, a wider size range would be expected. Finally, SEM examination gives no evidence for replacement textures being present.

Macintyre (1985) concluded that, "whilst some peloidal textures are probably created by the above mechanisms, the most likely origin is through the repeated nucleation around fine grained centres." For the purposes of this study, the peloids are considered to be in situ precipitates. They do, however, occur in geopetal fabrics (Figure 2.44), but this is rare and probably represents suspension and re-sedimentation in the pore spaces or very local derivation and transport under episodic turbulent conditions.

A major point of interest about these peloids is their association with organic matter, as shown under ultra-violet light (Figure 2.45). It is suspected that this organic matter may play a significant role in the precipitation of the cements and this is investigated in Chapter 4.

2.7.6 Description of Peloids.

The magnesium calcite peloids are spherical to subspherical in shape and average about $40\mu m.$ in diameter, with a range of not more than 20–$60\mu m.$. They apparently consist of two phases of precipitation as revealed by study under the SEM (Figure 2.46). The early growth phase is a precipitate of micron or sub-micron sized anhedral crystals of magnesium calcite. It is this phase which is associated with the organic matter, the small crystal size indicating a rapid nucleation rate. This is followed by a slower more ordered precipitate of equant crystals, also of magnesium calcite. These second phase crystals have rhombic terminations and range from 4–$30\mu m.$ in size. These two phases of crystals can be followed by a precipitate of fibrous aragonite (Figure 2.47), but this is considered to be an entirely separate phase of cement and is discussed further in the section on sequences of cements (Section 2.9).

The peloids form in a range of textures reflecting the density of packing, varying from a very open form (Figure 2.48) through a more and more densely packed texture to that which is only distinguishable from a featureless micrite by the presence of faint circular outlines. The latter densest packing means that the peloids are often difficult to distinguish under the SEM, and can only be positively identified in thin section under plane polarised light. This variation in density probably reflects a slightly later stage of precipitation of microcrystalline Mg-calcite rhombs within the interpeloidal spaces. Variation in the amounts of this later stage precipitate leads to the variation in observed fabric. Evidence for this process can be identified under the SEM (Figure 2.46).

2.7.7 Occurrence of the peloids in relation to substrate.

Peloidal cements are ubiquitous within the reefs of Florida. As the great majority of the material studied is coral framestone, it is difficult to deduce any particular substrate specificity. They do, however, occur in greater amounts at the surfaces of coral skeletons and, whilst it is difficult to prove conclusively, there does appear to be an affinity with encrusting organisms. The peloids do not occur in the pores of the encrusters but do appear in concentrations just below the surface of the encrusted coral samples. It may be, therefore, that the peloids are in some way associated with encrusting organisms, but it should be made very clear that this may be just a coincidence. Peloids may occur at the surfaces of coral skeletons simply because the surfaces are nearest the flow of pore water or indeed they may be associated with the death and decomposition of the coral polyps themselves.

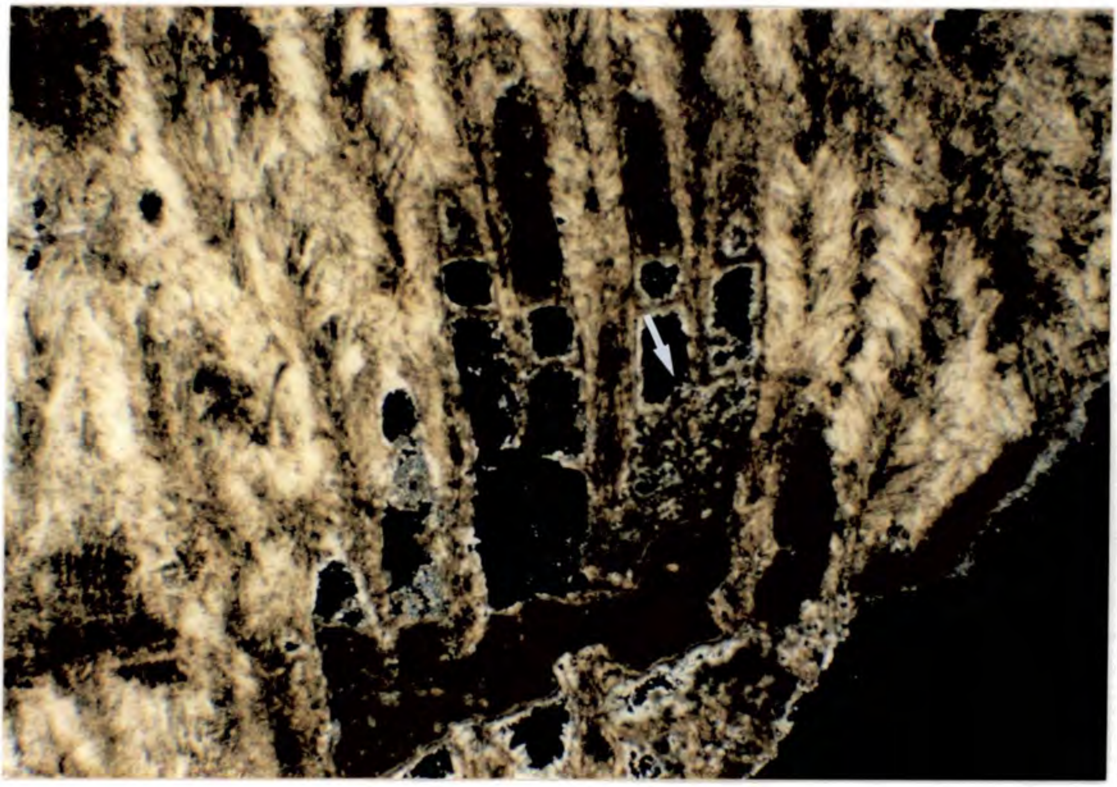

Figure 2.44 Geopetal fabric in peloidal cements, with internal sediments also filling pores geopetally. This suggests that the peloids have been transported, but it is likely that the distances involved are quite small. Resuspension in the same pore could create the same effect. Photomicrograph, xpolars.

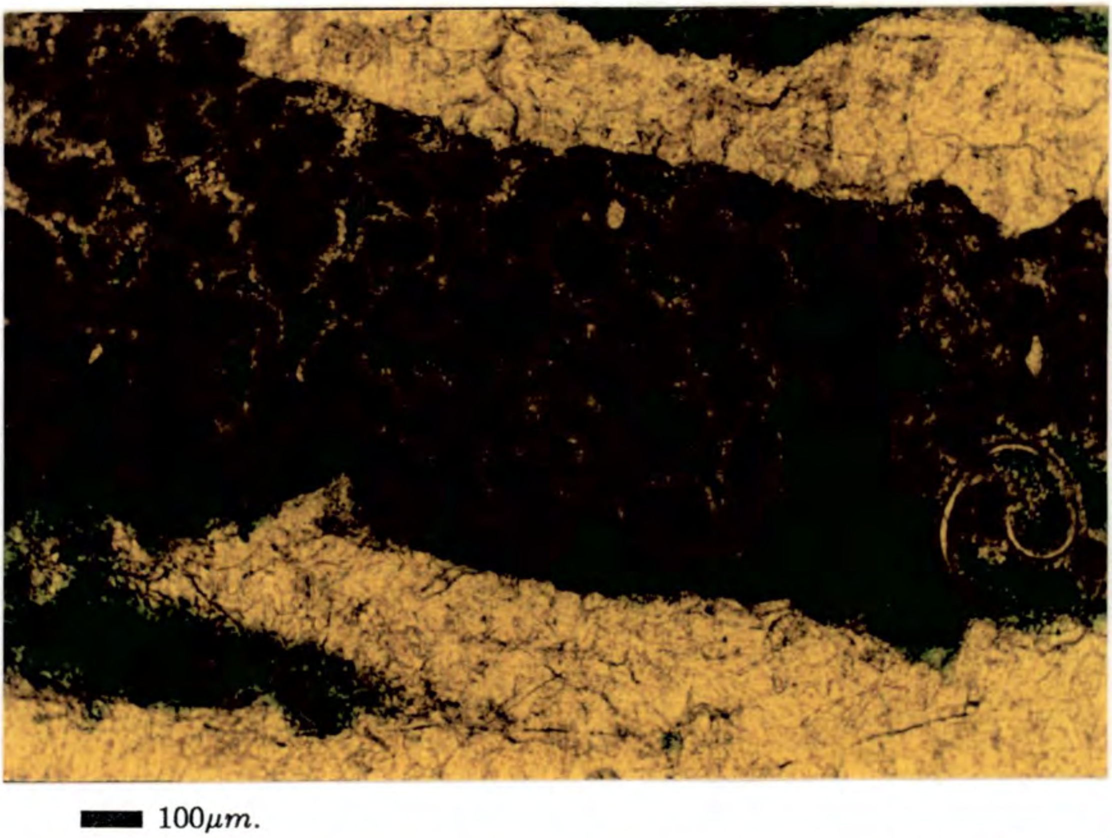

Figure 2.45 Complementary pictures of the peloidal cements, the upper one in plane polarised light, the lower viewed in reflected ultra-violet light. Bright fluorescence of the peloids indicates the presence of organic matter. (H.S. Alligator Reef).

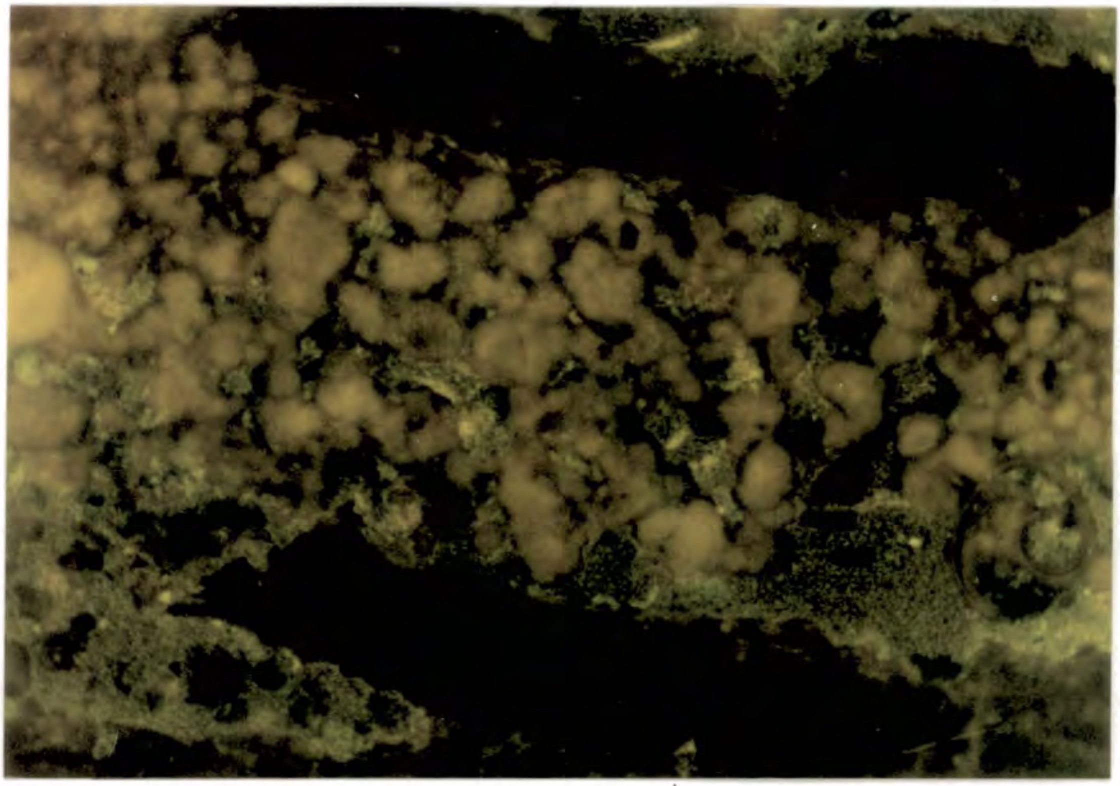

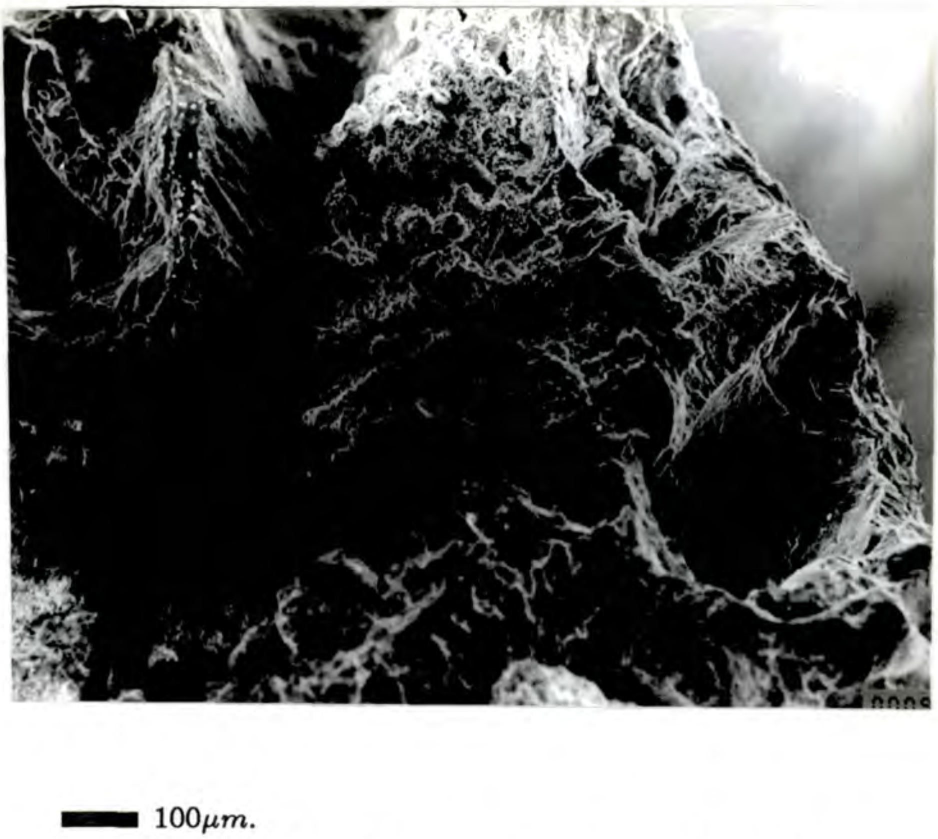

Figure 2.46a SEM photo of peloidal cements, in quite a densely packed texture within a coral pore.

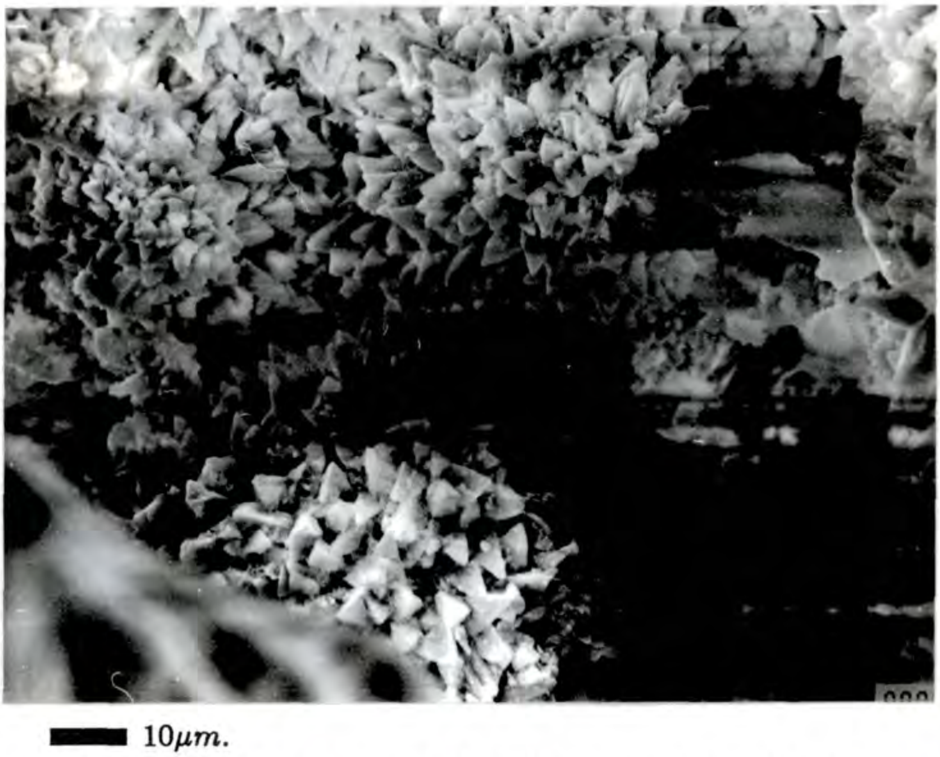

Figure 2.46b Close-up of the above, with the individual peloids somehat clearer, clusters of rhombic Mg-calcite crystals covering the surfaces. (H. S., Alligator Reef)

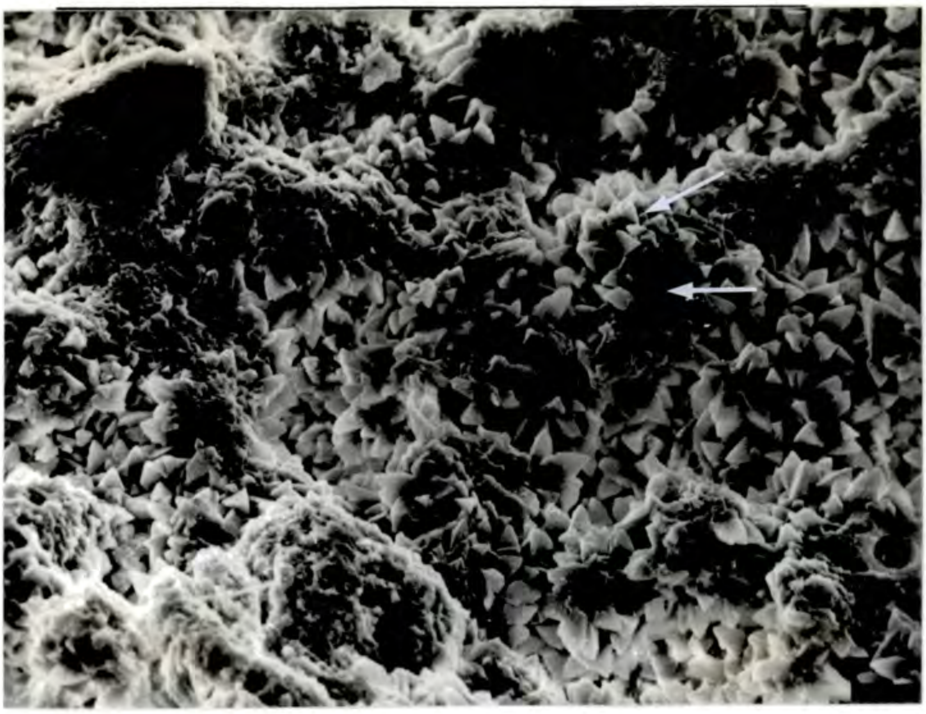

$10\mu m.$

Figure 2.46c Close-up of the peloidal cements, showing the two phase growth (arrows). The first phase precipitate is a fine-grained sub-micron sized anhedral precipitate, which is followed by the euhedral growth of rhombic crystals. (H.S. Alligator Reef)

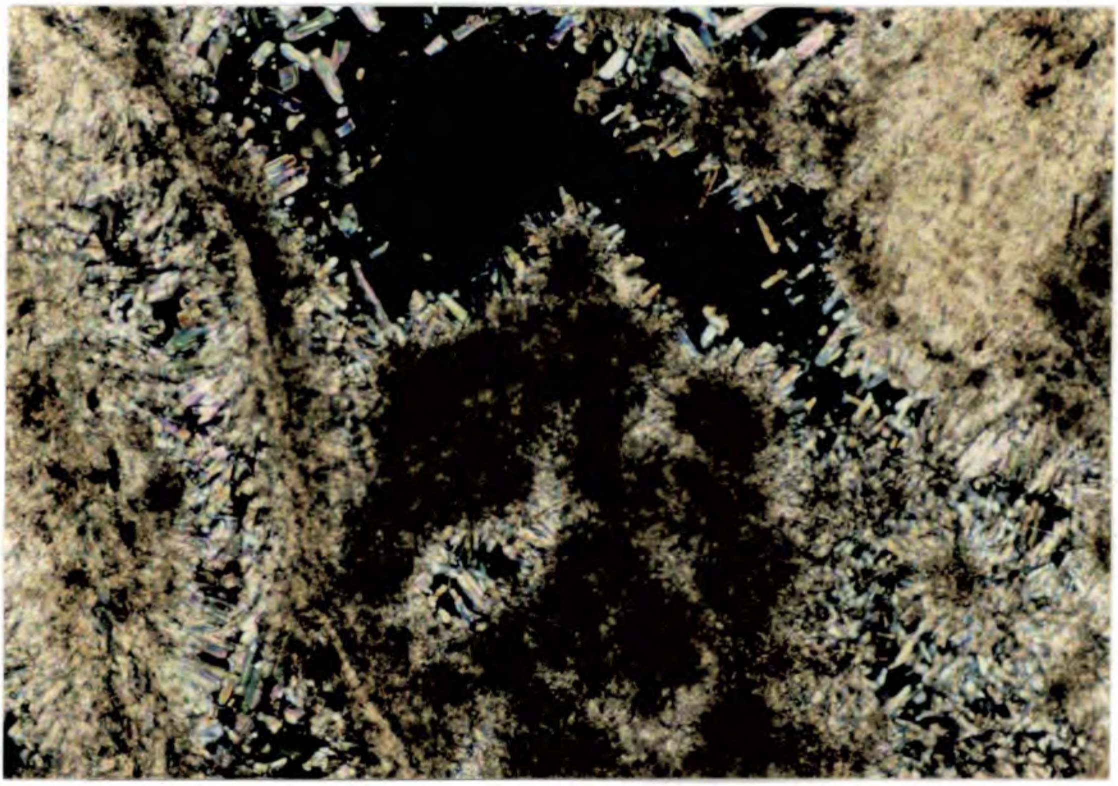

$50\mu m.$

Figure 2.47 Mg-calcite peloids followed by the precipitation of acicular aragonite crystals. Photomicrograph, xpolars. |E9|

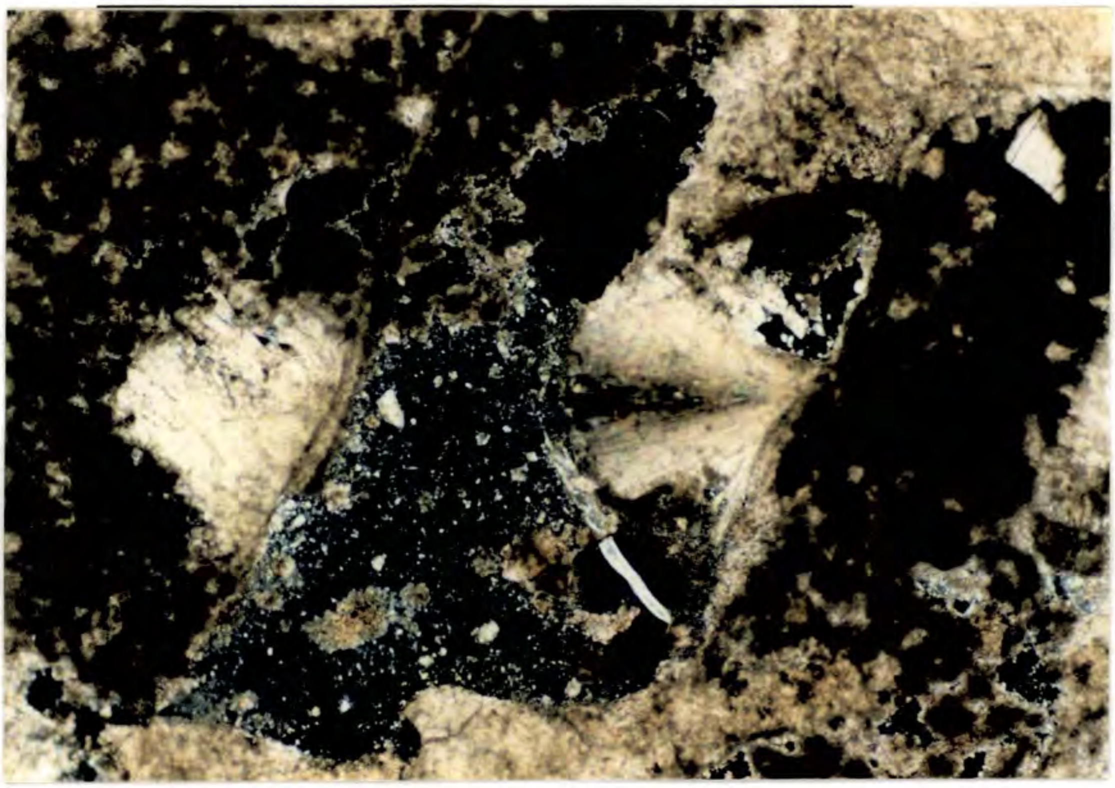

Figure 2.48 The range of 'packing' density is evident in these two photos. There is consdierable variation within the same pores evident at the lower right of the above example. In the lower photo, the peloids have been stained red (due to the Mg-content) by Titan yellow. Photomicrographs, xpolars . (D14)

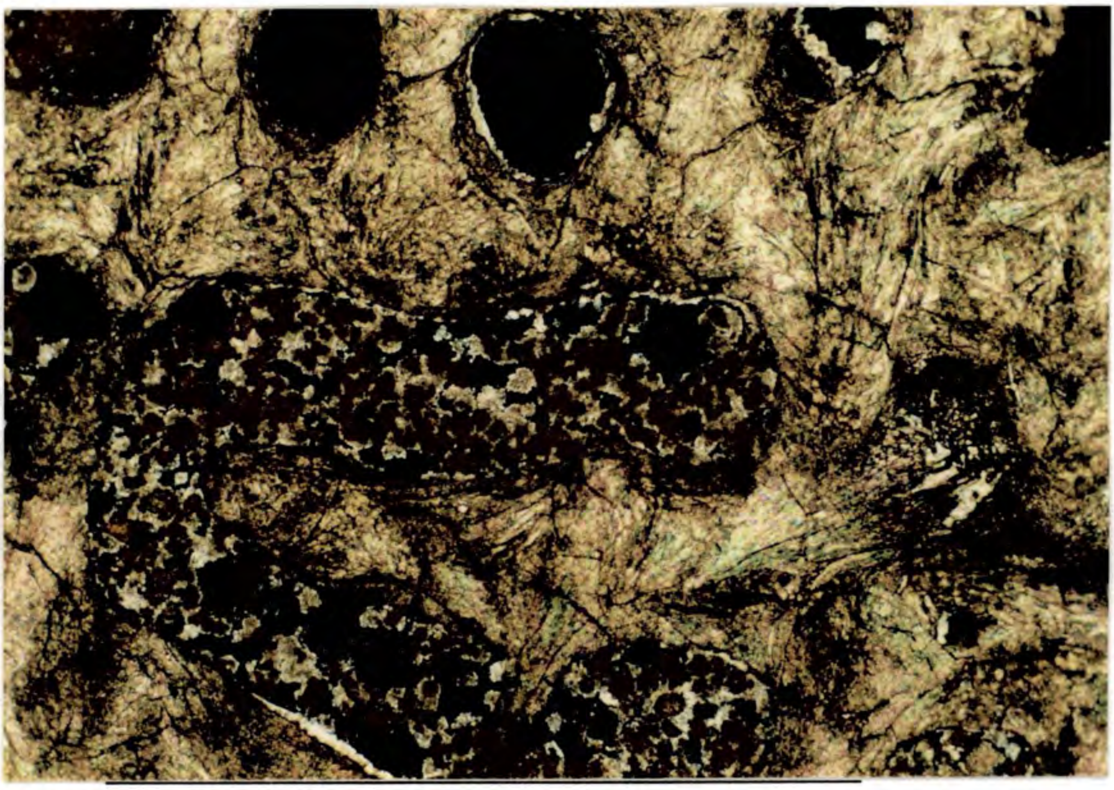

2.8 Cement Distribution.

This section discusses the distribution of cements within Alligator reef in some detail. For most of the description, cement is considered as a collective term to include all the morphologies and mineralogies described in above sections, but some comments are concerned with particular cement phases. The distribution of cements is considered with respect to substrate, species, reef facies, position on the reef, depth in the cores, and on the pore, thin section, hand specimen, core, reef and regional scales. A general observation is that the distribution is extremely inhomogeneous on all levels, down to and including the thin section and pore scales. It is, therefore, difficult to observe any trends in the distribution of the cements. This irregularity reflects the complexity of the interaction between the major processes contributing to reef formation, these in turn affecting the poroperm characteristics in space and time.

This same irregularity has been noted in many other descriptions of the distribution of cements in reefs of all ages (Schroeder, 1972a; Ginsburg & Schroeder, 1973). This problem has led to there being very few thorough descriptions of the relative abundances of cements, and none which consider the distribution with respect to a variety of aspects on a range of scales, which are backed up by analytical data.

2.8.1 Species specificity of cementation.

The observed cements have been studied in relation to their substrates and the species has been recorded during the point counting. No obvious species specificity has been observed with respect to any of the minor species of boring, encrusting or secondary framebuilding organisms. This type of analysis has been restricted to those cements which are common enough to produce a meaningful result and therefore concerns the fibrous and spherulitic aragonites and the peloidal Mg-calcites only. As far as major species are concerned, this was restricted to an analysis of *Acropora palmata*, *Montastrea annularis* and the coralline algae. As a group, there is a potential affinity between the coralline algae and spherulitic aragonite. There is no obvious specificity with respect to any of the aragonite cements in relation to either *Montastrea annularis* or *Acropora palmata*. (See Table in Appendix A1.2)

There is an apparent species specificity for the peloidal cements in that they are much more abundant in the Acropora species than in the Montastrea species. However, this deduction has been made by comparing the abundances of peloids in Alligator reef (principally *Acropora palmata*), with the abundances in the Dry Tortugas reefs (principally *Montastrea annularis*) and so the specificity may be artificial and due to some other regional differences not yet considered.

When considering overall volumes of cements, there might be expected to be a greater degree of cementation in those species with higher porosity and permeablity than others. This is an assumption that can be substantiated on the basis of the mathematical modelling presented in Chapter 5, but it is useful to introduce the concept at this point, in order to be able to emphasize several aspects of the reef system. Table 2.1 gives the porosity and permeability figures for several species; it is obvious from the table that *Diploria sp.* (with the highest permeability), would be expected to be cemented to the greatest extent. Although the total number of *Diploria sp.* specimens studied is rather small, none of them show a particularly high degree of cementation as expressed as a percentage of the porosity. This fact serves to highlight the observed heterogeneity in the cementation patterns, and to suggest that care must be taken to consider the frame of reference of the particular sample under scrutiny. The *Diploria sp.* samples may, for example, have occurred in a position surrounded by low permeability areas and so may not have been in an active flow regime.

The point to be emphasised when considering individual small samples is that although their own environment may appear favourable, the heterogeneity of reef formation may be such that the immediate surroundings are not favourable for cementation to occur. The local environment must be considered as well as all the characteristics of the sample itself.

Sample	Species	Thin Section Porosity	Porosity %	Permeability milliDarcies
1	*Acropora*	-	49.4	-
2H	*Montastrea*	66.5	56.8	24.2
2V *	*Montastrea*	-	58.1	57.9
3 *	Lithified Belize	-	9.2	84.6
4H	*Acropora*	55.6	51.2	8,900
4V *	*Acropora*	57.2	50.5	3,800
5H	*Diploria*	-	54.6	<10,000
5V	*Diploria*	50.8	58.0	<10,000

Table 2.1 Porosity and permeability of several coral species. The 'H' and 'V' refer to cores taken perpendicular to and parallel to the trend of the corallites.

2.8.2 Substrate specificity.

As the great majority of the potential substrates within the material studied are coral framestone, this discussion of substrate specificity is bound to be biased towards precipitation on corals themselves. However, a number of valid observations relating to substrate control on mineralogy and morphology can be described. The most abundant cement type, fibrous aragonite, is best developed in the intra-skeletal porosity of coral framestone, commonly growing in optical continuity with the substrate. It is rare to observe the same development of fibrous aragonite within the intra-skeletal pores of coralline algae or any other encrusters or secondary framebuilders. It should be noted that the pores within the latter groups are generally much smaller than in the corals and so a similar development would not be possible anyway. Nevertheless, it is certainly true that the best development of fibrous aragonites is within coral skeleta, reflecting a certain degree of substrate control.

The spherulitic and botryoidal cements also occur within the intra-skeletal pores of corals, but in addition, they are well developed on coralline algal substrates, where they most commonly occur in bores through the skeletal material. As such, they are the most common type of cement to occur in cavities which are obviously bioerosional in origin, and in fact are almost exclusively the only cements to form in such pores (Figure 2.49). This affinity has been previously noted (Schroeder, 1972b; Marshall, 1983a, 1983b) and can be explained in a number of ways. It is not clear whether the coralline algal substrate is particularly favourable for the development of these spherulites, or whether the increased permeability due to the boring, enhances the rate of growth in relation to the nucleation rate, thereby producing a single spherulite rather than a random arrangement of multi-nucleated fibres.

The more ordered form of aragonite needles is restricted to the surfaces of molluscs and foraminifer shell fragments (Figure 2.31), and may be due to some substrate control of the lattice growth, although no specific relationship has been observed either in transmitted light or under the SEM.

Microcrystalline aragonite appears to be restricted to the pores of *Acropora palmata* and *Montastrea annularis*. The precipitation of this cement may be related to the release of calcium rich fluids from the soft parts of the corals shortly after death; the very fine crystal size suggesting a particularly rapid nucleation rate such as might be expected on the release of fluids associated with skeletal growth sites

The Mg-calcite fibrous cements are so rare as to preclude any meaningful deduction to be made with respect to their substrate specificity. The most common occurrences are as isopachous coatings on the surfaces of cavities in internal sediments. The problems involved in the identification of the microcrystalline Mg-calcite cements make it impossible to observe any substrate control that may be occurring. Mg-calcite peloidal cements are not precipitated onto substrates in the same manner as the other cements and so substrate specificity is not relevant.

The variations noted above are particularly interesting with respect to the precipitation of cements in primary porosity and such secondary porosity as is created by bioerosional effects, specifically in relation to the timing of these events (Section 2.17.3). A general conclusion can be drawn that cements tend to precipitate preferentially on substrates of the same mineralogy.

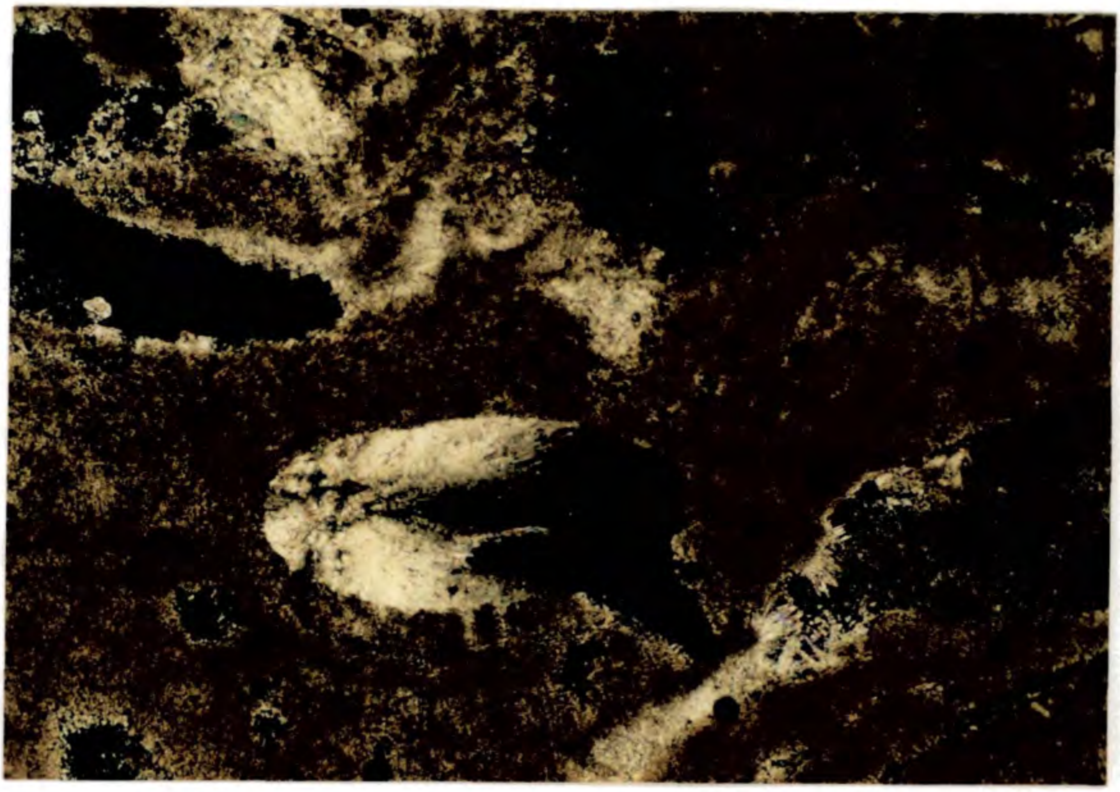

100μm.

Figure 2.49 Spherulitic and Botryoidal aragonites precipitated within bores in coralline algae. Large botryoidal growth in the centre with smaller spherulites to the right. Photomicrograph, xpolars.. (A8)

2.8.3 Facies specificity.

As the material from Alligator reef comes exclusively from reef core material, it is impossible to study the variation of cementation processes with reef facies in a manner such as that published by James et al. (1976). However, there may be a slightly greater degree of cementation in sub-facies which are encrusted, but as with previous mentioned associations of this sort, it is exceedingly difficult to demonstrate a causative relationship.

This relationship can be explained in several ways:

i) The encrusting organisms have some metabolic activity which promotes cementation.

ii) The nature of the encrusted surface affects the flow through the sample. Marshall (1983a) suggested that the encrustation would form a barrier to the flow, thereby directing it through the sample. Although this directional control seems unlikely, it is certainly true that the encrustation would form a barrier to the flow, due to the low permeability of such a surface. It is unlikely that this would direct flow through the sample, but it would reduce the rate of flow through the sample and might therefore have some effect on the morphology of the cement. Given & Wilkinson (1985) suggested that a reduction in the flow rate may enhance the precipitation of Mg-calcite in preference to aragonite, and hence, this effect may also have some control on the cement mineralogy.

iii) The observation reflects a fortuitous relationship that is misinterpreted in i) above. It may be that the increased degree of cementation observed within samples close to encrusted surfaces, simply reflects the closeness to the surface. Being closer to the surface means that the flow of pore waters will be greater; this in itself may lead to the increased cementation.

This situation is again complex and illustrates the difficulty and the dangers of assuming causal relationships from observed spatial relationships, where the temporal sequence is not defined.

A final point with respect to facies specificity can be highlighted with respect to the apparent lack of cementation within the sands in the vugs and caverns within the reef. These sands were only rarely recovered by the coring methods used, indicating a general lack of cementation within these grainstones. The lithification may in fact have been to the same degree as the framestone material, approximately 4% cement (equivalent to that percentage of cement in the framestone that could be expected to play a lithifying role). However, it is not surprising that this small degree of lithification did not contribute to the strength of the grainstones sufficient to enable them to be recovered. The framestone material obviously has a very great strength in itself and the relatively small volumes of cement probably do not contribute significantly to it. The grainstones, however, might be expected to receive a greater volume of cement due to their very high permeability and this is not observed in those samples which were preserved in core (Figure 2.42). The reason for this is probably due to the fact that a stable substrate is necessary for cementation to occur (Section 1.6). At the time when the grainstones were at the surface of the reef, the energy would have been high enough to keep the grains virtually in constant motion and this motion would cause any early crystals to be destroyed by the mechanical abrasion. As will be explained in Section 2.8.6, the cementation rate is probably much slower just below the surface of the reef, and so once the uncemented sands became buried below the surface, the chances of them being further cemented were greatly reduced and they have, therefore, remained unlithified. Another possibility is that the sands have filtered in to cavities which were at some depth in the reef and so have never been in an active cementation zone for long enough periods of time to become lithified.

2.8.4 Thin section scale distribution.

The distribution of cements on the thin section scale is one of the easiest scales on which to illustrate the inhomogeneity of the cementation. There is in fact a whole hierarchy of heterogeneity in the observed cementation patterns and it is most obvious on the thin section scale. This applies both to the overall volumes of cement and the individual distributions of different mineralogies and morphologies. Hence, in any given thin section, even of an otherwise unaltered coral framestone, the cementation is frequently observed to be restricted to small areas, with the remainder of the thin section being totally devoid of cements. This degree of irregularity is easier to illustrate (Figure 2.50) on a sub-thin section scale of just a few pores, this being suitably convenient to see under a low power objective. On this level, it is a very common observation that pores adjacent or within a few mm. of each other, may be either full, partially full or completely devoid of cements. The same variety in cement morphology and mineralogy also occurs; with aragonite fibres, spherulites and Mg-calcite peloids all occurring in close vicinity of one another (Figure 2.51).

It is possible that pore waters in adjacent pores might precipitate different cements, but this implies a very strong control of pore water chemistry on a microenvironmental level. In Section 1.6 it was pointed out that there was a necessity for a very large throughput of water in order to precipitate cements, and this requirement suggests that it is unlikely that closely situated pores could be completely unconnected, as would be necessary in order to maintain different pore water chemistries. It is unlikely, therefore, that the controls on the precipitation of the cements are geochemically based. The necessity for a large water flux indicates that the volume of cements may certainly be affected by the varying flow rates through the individual pore systems; this type of control may also operate on any larger scale and may, therefore, be able to account for the irregular distribution of the cements, at least in terms of their overall volumes. This concept is developed further and is mathematically modelled in Chapter 5. The conclusion of this discussion and the basis of the modelling is that the permeability (as considered from the frame of reference of a single pore) is the major factor controlling the distribution of the cements on the thin section level.

Using this argument it can then be seen that those pores which are devoid of cement at present have probably never received any flow; they are non effective porosity (Figure 2.50). This does not, however, imply that such pores will never become cemented, as they may become interconnected with the flow at some future date through the involvement of bioerosional or other destructive processes.

This concept of a dynamic interaction can be used to explain the variations in the mineralogy of cements precipitated in adjacent areas, in that the temporal aspects of the interaction should be considered. Hence, the various sources of pore waters to which individual pore systems are open may well vary with time. The suggestion is, therefore, that where aragonite and Mg-calcite cements occur in adjacent pores, although there may be no demonstrable temporal sequence, it may be that the two were precipitated at different times. This therefore implies a geochemical control of the distribution of the cement mineralogies over time and not in space, a concept which is much more logically acceptable.

Morphological variations are much more difficult to explain; the reasons why fibres are precipitated in some pores and spherulites in others may be due to subtle differences in the substrates on a very small and unobserved scale. The fact that some crystals are observed to grow in optical and therefore lattice continuity implies that these controls may operate at the unit cell scale. In particular, the morphology of the fine grained spherulites and the botryoids implies that the growth rates are rapid in comparison to the nucleation rates. Hence the initial nucleation of one of these spherulites may occur at a particularly favourable site in an otherwise unfavourable pore. This might occur in such a circumstance that no new nucleation within that pore would occur and so growth of the spherulite could therefore continue unhindered by new nucleation events. This would also explain the observation that when these spherulites are observed, they generally occur as individuals in any given pore. The similarity of the spherulites to those on a much smaller scale ($2\mu m$), which form the coral skeleta leads to the tentative suggestion that, at least for those precipitated within coral skeleta, the spherulites are precipitated at centres of skeletogenesis, with the old biogenic controls on the crystal morphology remaining active.

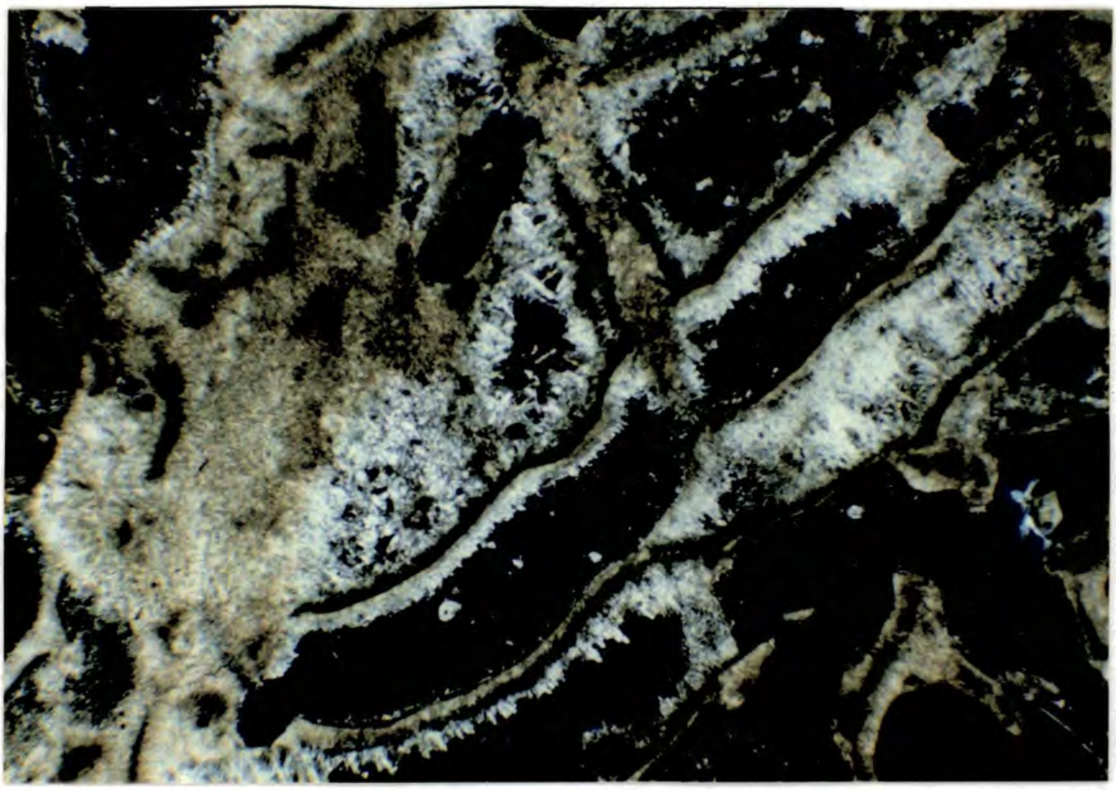

Figure 2.50 Illustration of the pore-scale variation in cementation of coral framestones. Some pores are filled with acicular aragonite crystals, some have just a thin lining and others are completely devoid of cements. These empty pores are probably non-effective porosity. (B3)

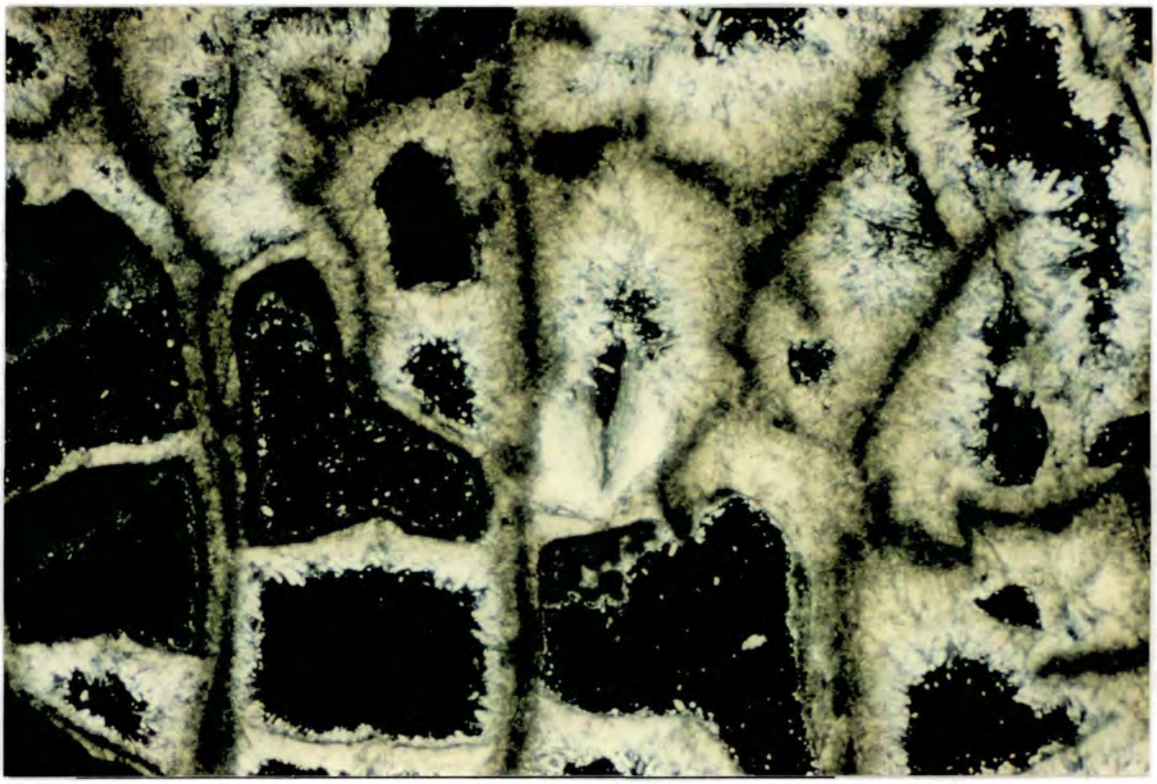

Figure 2.51 Similar small scale variation in morphology and mineralogy. Spherulitic and fibrous aragonite and peloidal Mg-calcite all occurring in pores adjacent to one another. (C8)

2.8.5 Hand specimen scale distribution of cements.

The degree of cementation in hand specimens collected from Alligator reef is generally very low. These samples were all collected from the reef surface, in the most turbulent zone which is continually affected by waves and swell, and even quite large samples are in constant motion. This ought to imply a very large throughput of water and hence high degree of cementation, but this does not occur for several reasons.

Firstly, the hand specimens collected from the reef surface are all heavily encrusted by various organisms, with all available surfaces coated (Figure 2.52). This layer is typically 2–3mm. thick, sufficient to form quite an effective seal over the surface, as the permeability of the laminar encrusting organisms is very low. This seal therefore prevents fluids from flowing into the pores of the samples.

Secondly, the samples are in continuous motion, and in such a situation much of the thrust of the waves and swell is expended as the kinetic energy of the moving material. There is, therefore, much less energy involved in forcing water through the pore systems. In contrast with the core of the reef framework, where the flow has to pass through the pore systems, much of the flow can be deflected around the surfaces of the unstable substrates. Finally, there are large volumes of internal sediments in the outer edges of the hand specimen samples and this further decreases their permeability.

A similar surface sealing effect occurs with the material from an earlier Holocene reef from Florida, described by Lighty (1985). Samples from this reef have been used to study the peloids (Chapter 4) because of their high content of these cements. These samples have been previously studied by Lighty (1985), and he recognised that the magnesium calcite peloids are precipitated in large concentrations at the surfaces of the coral skeletons, forming a seal over the remainder of the sample . This diagenetic seal is observed on the hand specimen and the reef scales.

The general heterogeneity of the cementation on the hand specimen scale can be observed by comparing thin sections taken from adjacent areas of the same samples. Serial thin sections have been studied where the volume of cements varies from 4 to 16 % in successive sections. The same variation can be observed on a scale of a few centimetres, as in samples A3L and A3U (Appendix 1).

Figure 2.52 Surface coating of coralline algae on small head coral, forming quite an effective seal due to the very low permeability of the algal laminae. (H.S. Alligator Reef)

2.8.6 Distribution of cements on the core scale.

The seven cores through Alligator reef all penetrate to a depth of approximately 3 meters. The variation in the degree of cementation with depth has been studied through the use of point counting of 90 thin sections. The full data are given in Appendix 1. In a study of this sort, it is critical to consider quite carefully how to represent the degree of cementation. The most accurate method is to compare values for the progression of the cementation measured as the percentage cements divided by the percentage porosity available at the time of cementation. Due to the complex interaction over time of the various reef forming processes, it is very difficult to assess accurately the volume of porosity available at the time of cementation. The detailed interaction of the processes affecting the porosity (boring, sedimentation and cementation), are discussed in Section 2.17. For the sake of simplicity, the total available porosity is considered in the same way for all thin sections, though three different methods of calculating the porosity are employed:

i) Available porosity = remaining micro or intra-skeletal porosity + the volume now occupied by the cements.

ii) Available porosity = i) + bioerosional or macro-porosity.

iii) Available porosity = ii) + volume occupied by internal sediments.

Hence in case i), bioerosional and sedimentation processes are considered to have occurred after the precipitation of the cements. In case ii) the boring activity is assumed to be pre-cements and the sedimentation post cementation. In the final case, both bioerosion and the deposition of internal sediments are considered to have occurred before the cementation phase. The following discussion is based on the porosity as calculated in ii) above, although all the data are presented in Appendix 1. It is important to consider the porosity available at the time of precipitation of the cements because a major control on the distribution of the cements is the local permeability which is related to the distribution of the porosity. The interaction of these processes in time is one of the most important controls on the system.

The total cement is considered to be the sum of the fibrous, spherulitic and microcrystalline aragonites and the peloidal Mg-calcite, though this definition is later split so as to consider the aragonite and Mg-calcite cements separately. The results of these analyses are presented in graphical form in Figure 2.53.

Similar studies reported in the literature generally consider simply the volume of cements and its variation with depth. No obvious trends in cementation with depth were observed by Marshall (1983a, 1983b) in a study of the Great Barrier Reef, though it was not clear whether his calculations were based on a percentage of the porosity or as simply total volumes. The fact that there was no increase in cementation with depth was thought to imply that most of the precipitation occurs at the surface. The results of the study of the Florida reefs suggest basically the same conclusion.

It can be seen that there is a somewhat greater degree of cementation in the top 0.5m. of the cores (Figure 2.53), and this is consistent for six of the seven cores, as calculated for total cements. This tends to confirm that most of the cementation does occur at the surface of the reef. The effect has been enhanced in this case as there has been no growth over the past 4000 years, but the reef has remained at very nearly the same depth below sea level, due to the levelling off of the sea level rise over the same period. These results also indicate that little cementation occurs once a section of reef has been buried. These observations are broadly comparable with those from reefs of the Great Barrier Reef (Marshall, 1983a, 1983b), and of Panama (Macintyre, 1977).

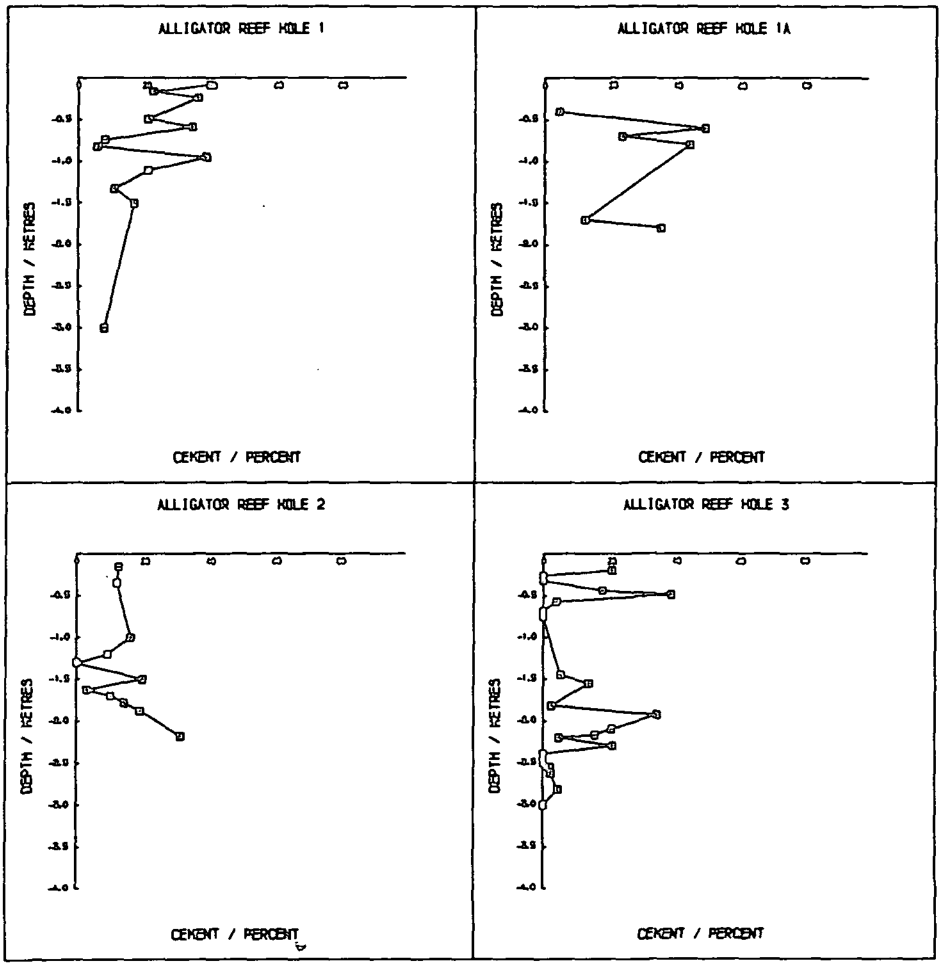

Figure 2.53a Graphs showing the variation in degree of cementation with depth in Alligator Reef cores. The percentage cement is calculated as the point counted percentage of fibrous, spherulitic and microcrystalline aragonite and peloidal Mg-calcite divided by the total porosity available at the time of precipitation. This available porosity is calculated as the sum of the intra-skeletal, bioerosional porosity and the volume of cements. The cementation is very irregular, but there is some evidence that the degree of cementation is higher at the surface.

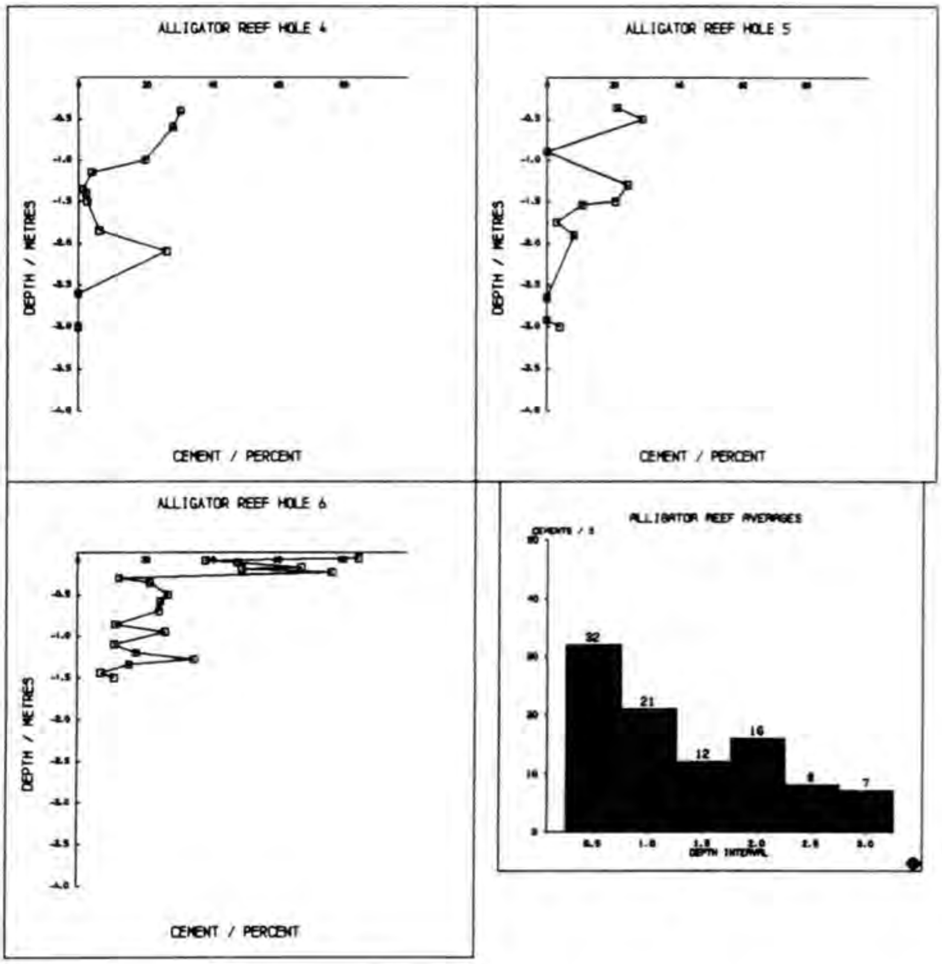

Figure 2.53b Cements vs. depth for the final three cores through Alligator Reef. Also shown is a bar graph which plots the degree of cementation every half meter averaged over all seven cores, further suggesting that cementation is slightly higher at the surface.

2.8.7 Distribution of cements on the reef scale.

Only a handful of studies have been made of the distribution of cements on the reef and regional scales. James et al. (1976) noted that the cementation was concentrated in the seaward facing sides of reefs and in the upper metre or so of the reef pavement. On a larger regional scale, cementation appears to be concentrated along the shallow seaward margins of barrier and atoll reefs and is generally absent from lagoonal patch reefs (James et al., 1976; Marshall, 1985).

Earlier papers emphasised the apparent preference for cements to occur in areas subject to frequent storms and generally cementation has been correlated with high energy environments (Shinn, 1969; Alexandersson, 1972; Ginsburg & Schroeder, 1973). In a study of the Enewetak atoll, Ladd and Schlanger (1960), noted that there was a 1 metre thick cemented pavement below which unconsolidated sediments could be found. Similar observations were made by Marshall (1985) in a study of cross shelf trends in cementation in the Great Barrier Reef. In the latter, extensive cementation of outer reefs was contrasted with lesser lithification in inner reefs. These trends were mimicked by the larger reefs where windward margins are well cemented and leeward margins remain uncemented.

All of these observations can be explained by the same controls as above, principally the rate of fluid flux, simply operating on a larger scale. Whilst the average permeability may not vary across the shelves or across individual reefs, the energy conditions certainly do. The degree of cementation is therefore correlatable with the energy of the environment; where the average energy is higher, the degree of cementation is greater due to the greater flux of water through the pore systems. Whilst Marshall (1985) noted that the variation in degree of cementation cannot be entirely explained on the basis of present energy conditions, he nevertheless acknowledged that the distribution is controlled by some sort of variation in flow characteristics. A further important point is that one should be careful to consider the variation in conditions throughout the history of the reef and not just the present characteristics.

In the case of Alligator reef, although there are variations in the total degree of cementation with position on the reef, there are no consistent trends. The lack of any trend is probably due to the fact that all the holes were drilled through the reef core, and the study is therefore, restricted to the reef core facies. The holes were drilled in two transects (Figure 2.6), perpendicular to the trend of the reef, and one might expect to see a higher degree of cementation in the seaward holes compared to the shoreward ones. Figure 2.54 illustrates the variation in the degree of cementation with position on the reef. The calculations are based on both the average over the whole core, and on the average of the top 0.5m. of the core. The degree of cementation is determined as a percentage of the porosity as calculated by method ii) in Section 2.8.6.

Hole 6 (which is the furthest seaward hole in the northern transect), confirms this expectation as it has the highest degree of cementation of all the seven cores, averaged over the whole core. However, the trend is not the same in the southern transect, with the two shoreward holes showing a higher degree of cementation. The same inhomogeneity is apparent if the average cementation values for the surface 0.5m. are compared.

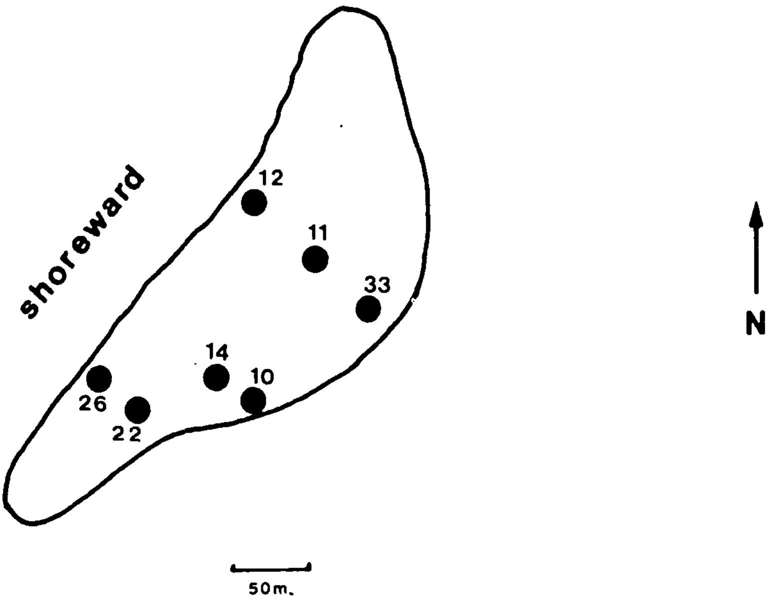

Figure 2.54 The distribution of cements in Alligator Reef. The upper diagram shows the figures for each core averaged over the whole core, whereas the lower diagram shows the averages over the top 0.5 metre. There are no clear trends in the degree of cementation on the reef scale.

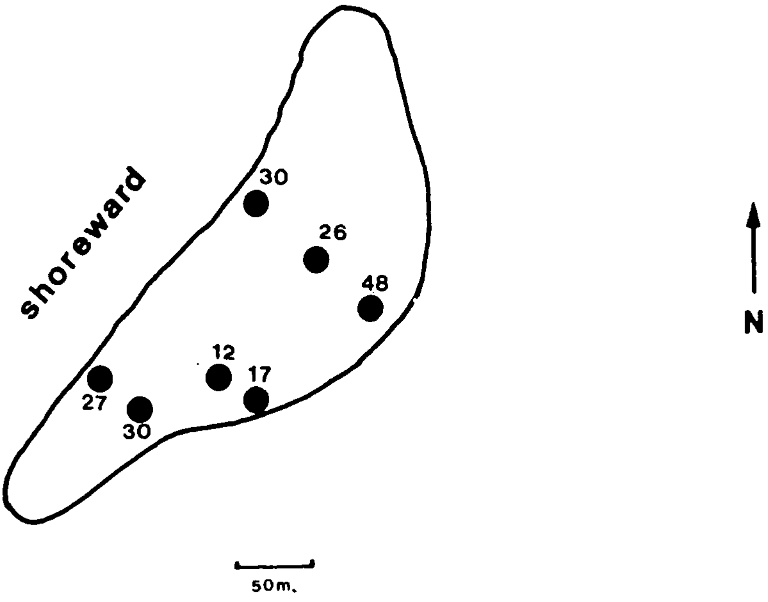

2.9 Cementation sequences.

There are many references in the literature discussing the sequences of submarine cements in various reefs (Schroeder, 1972a; Ginsburg & Schroeder, 1973; Marshall 1983a, 1983b), and most possible permutations have been reported. In the samples from Alligator reef, five major types of cement have to be considered; fibrous, spherulitic and botryoidal aragonite and peloidal and microcrystalline high Mg-calcite.

Fibrous aragonite is usually the first of all the cements to precipitate and this is followed in individual examples by the other morphologies of aragonite (Figure 2.55), and by magnesium calcite (Figure 2.56). There is sometimes evidence of a phase of bioerosion separating the sequences; this process may in fact be responsible for the change in cements due to the alteration of the environment. This alteration could be a direct chemical effect, or could be simply an indirect result of the boring as it changes the pattern of flow through the pores. The opposite sequence of cements does also occur with aragonite fibres clearly postdating both peloids and microcrystalline Mg-calcite (Figure 2.57).The sequences are restricted in all cases to two phases of cements and no interlamination has been observed. It would appear that the phase of aragonite may start prior to the phase of Mg-calcite precipitation, but both then continue simultaneously.

Figure 2.55 Fibrous cements apparently followed by spherulitic and botyroidal aragonite. Photomicrograph, xpolars.. (G13)

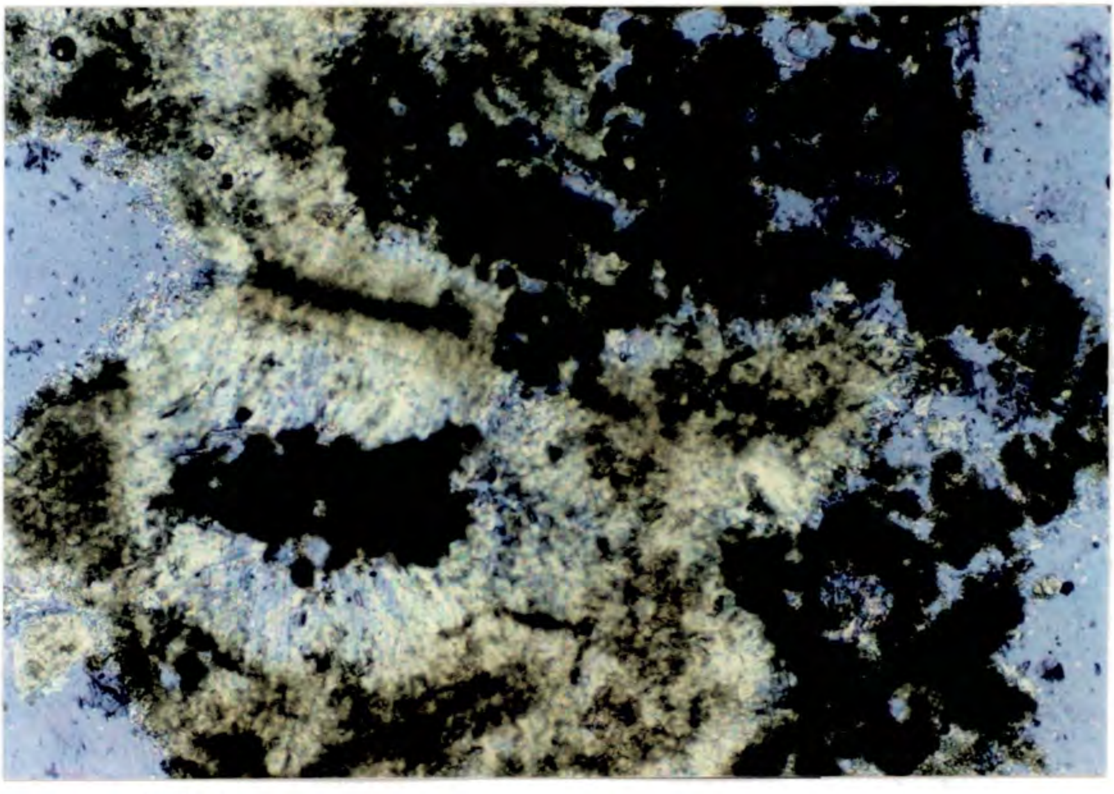

Figure 2.56 Fibrous aragonite followed by Mg-calcite peloidal cements, confirming that the precipitation of one mineralogy does not prevent a different mineralogy from forming subsequently. Photomicrograph, xpolars.. (B5)

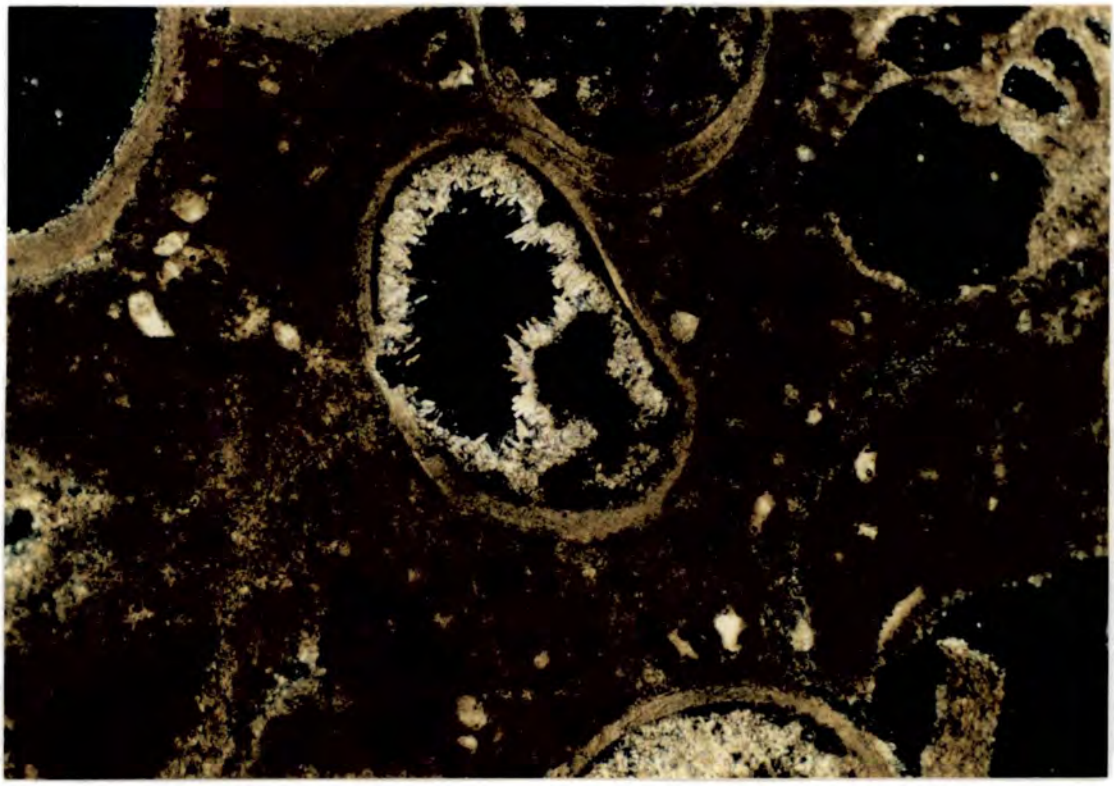

Figure 2.57 Acicular aragonite post dating micrites / microcrystalline Mg-calcite cements. Photomicrograph, xpolars.. (A1)

2.10 Dry Tortugas Reefs.

2.10.1 Core description.

Five holes were drilled through South East Reef Dry Tortugas as shown in (Figure 2.58). All of the holes passed through reef core facies, holes 1 and 2 passing through the thickest Holocene reef section of approximately 15 metres. Hole 3 is a very short section through an individual coral head. Hole 4 is approximately 3 metres deep and Hole 5 was drilled near the toe of the reef and passes through only a short Holocene section followed by a large unit of unrecovered sands and finally penetrates several metres of the Pleistocene substrate. Holes 1 and 2 also recovered some Pleistocene material and this is briefly described in Section 2.18. Full core logs are shown in Figure 2.58, with approximate sampling points and positions of thin sections given in Appendix 1. There is a great deal of reef rubble recovered in all of the cores, indicating that the reef may not have grown in the classical sense, but more probably built up as a mechanical accumulation produced by frequent storms (Shinn et al., 1977).

The total porosity (calculated as the 100−framestone + encrusters) including that presently filled by cements and internal sediments is similar to that of Alligator reef with an average of 53%. The total remaining porosity is 33% on average and this is somewhat more variable than in the Alligator reef cores, varying from 30–40%. This figure is split into 25% intraskeletal porosity and 8% bioerosional or macro porosity, suggesting a slightly greater activity of the boring organisms than was observed in Alligator reef. The 20% cavity filling material is split into 3% marine cements and 14% internal sediments with 3%

meteoric spar cements. There is less apparent encrusting activity in the Dry Tortugas material: of the total rock, an average of 42% is coral framestone and only 5% is encrusting organisms.

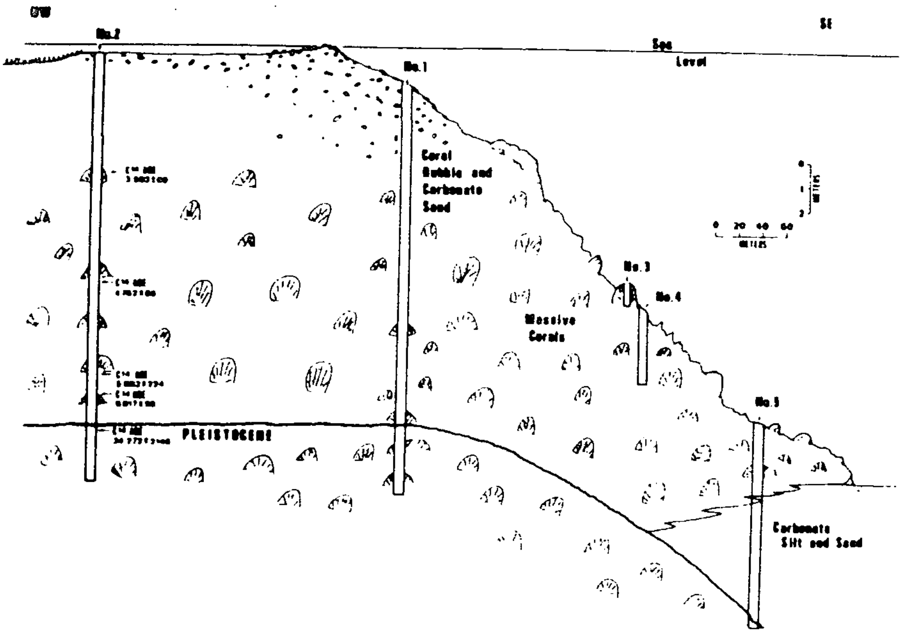

Figure 2.58a Position of cores drilled through South East Reef, Dry Tortugas. (From Shinn et al., 1977).

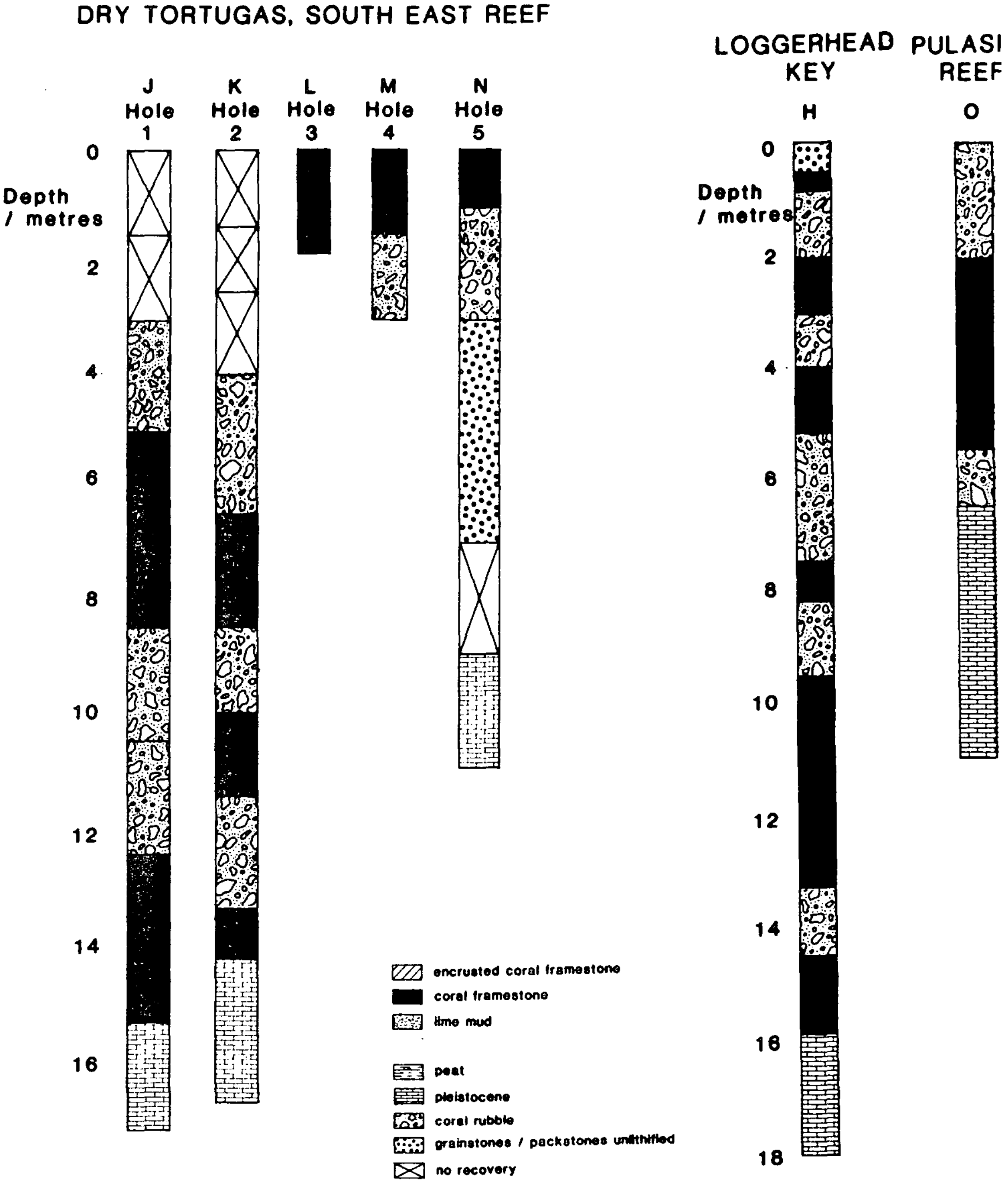

Figure 2.58b Logs for South East Reef, Dry Tortugas cores. Also shown are the logs for Loggerhead and Pulaski reefs (Section 2.15). Repeated from Figure 2.9.

2.11 Detailed components.

This section is analogous to Section 2.5 and will simply highlight the major differences between the material from South East reef and Alligator reef. Where volumes have been quantified, the analogous figure for the Alligator reef is included in parentheses for comparison.

The principal framebuilders are *Montastrea sp.* with rarer *Diploria sp.* and *Siderastrea sp.*. No *Acropora palmata* has been recognised from the reef suggesting that the energy conditions are on average somewhat lower than at Alligator reef as *Acropora palmata* only thrives in the highest energy environments. Secondary framebuilders are present to a lesser degree than for Alligator reef but the same species occur. Encrusting, dwelling and boring organisms are also similar.

Internal sediments are present in a wide variety of textures and abundances in a similar fashion to Alligator reef. Total volumes average 14% (15%), but range up to 25% of individual samples. About half of this figure is true micrite and the remainder is packstone to wackestone with the same characteristics and composition as in Alligator reef.

All the same types of porosity are present, with a possible greater but unquantified contribution by the intergranular porosity due to the large amount of unlithified reef rubble and rudstone material observed in the cores. Intraskeletal porosity was originally 50% on average, but ranges up to 75% in some specimens of *Diploria sp.*

2.12 Cementation.

The abundances of both mineralogies of cement are significantly less in the South East reef than in Alligator reef. Aragonite cements average 2% (4%) and the Mg-calcite peloids represent only 0.5% (3%) of the total rock. A strict comparison should be based on the volumes of cement relative to the porosity; the sum of the aragonite and Mg-calcite cements has a range of 0–27% (0–85%), confirming that the degree of cementation is significantly lower. The reasons for this lower overall cementation are dicussed in Section 2.20.7.

The aragonite cements show the same morphologies with perhaps a relatively more common occurrence of the spherulitic cements, but in all other respects they are the same as observed in Alligator reef. Although the peloidal Mg-calcite cements are much rarer in South East reef, when they do occur, their morphologies and substrates are identical to the previous descriptions. Fibrous Mg-calcites are again restricted to a few occurrences and the same problems in the identification of the microcrystalline cements were encountered.

2.13 Cement Distributions.

The same inhomogeneity is observed on the pore, thin section and hand specimen level and will not be further discussed. The distribution on the core scale cannot be compared with the Alligator reef samples as there was virtually no material recovered from the surface of the Dry Tortugas reefs. Graphical representation of the results is given in Figure 2.59, using the same methods of calculation as in Section 2.8.6.

The reason for the overall lower cementation of this reef may be due to its faster growth or accumulation rate. Shinn (1969) noted that slow sediment accumulation rates are necessary for cementation to occur, and similar requirements for slow reef accretion rates have been suggested by many authors (James et al., 1976; Macintyre, 1977; Marshall & Davies, 1981). Although the rate of precipitation may be the same for both reefs, as South East reef has accumulated at a faster rate than Alligator reef (Section 2.3), then over any fixed period of time the volume of material to be cemented has been larger in the case of South East reef and hence the overall degree of cementation appears to be lower. There are no obvious trends in the cementation on the reef scale.

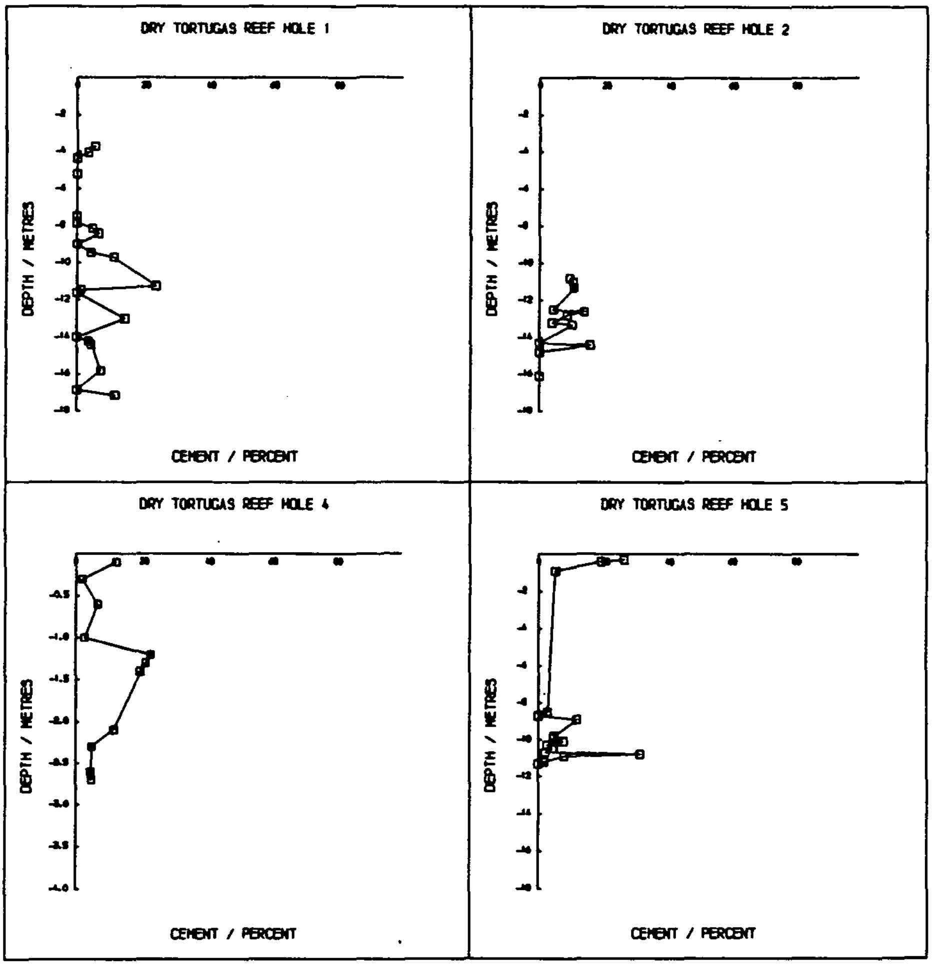

Figure 2.59 Distribution of cements with depth for South East Reef, Dry Tortugas. The calculations are based on the same principles as Figure 2.53. There are no trends obvious, and cementation is generally lower than in Alligator Reef. Hole 3 is not shown as it is very short and contained no cement.

2.14 Cement Sequences.

Observations of sequences of cements are very rare due to the low total cement volumes, but where they do occur, the characteristics are very similar to those described from Alligator reef (Section 2.9).

2.15 Loggerhead & Pulaski Reefs.

Two final cores have been studied, one drilled on Loggerhead reef and the other on Pulaski reef, both in the Dry Tortugas area. The following brief section compares these two cores with the South East reef and Alligator reef material. Core locations and logs are given in Figures 2.7 & 2.58 respectively.

2.15.1 General description.

Both cores reach the Pleistocene substrate after penetrating substantial thicknesses of Holocene reef core, (16 and 11 metres respectively). There appears to be more in place coral framestone than in the South East reef, but there is still a substantial amount of reef debris. The total remaining porosity is remarkably consistent with the other cores through Dry Tortugas reefs at about 37% and this is split in a similar ratio of 30% intraskeletal and 7% bioerosional porosity. The total primary porosity including the volume presently filled is approximately 53% completing a very consistent pattern over the whole of the Florida area. Of the 16% cavity filling material, 12% is internal sediments and 4% is cements, reflecting a very slightly higher degree of cementation in these two cores compared to South East reef. There is a similar volume of encrusting material, of the total framework of 47%, approximately 6% is encrusting growth. Some samples of slightly lithified grainstone material were preserved, in particular at the surface of the Loggerhead core (Figure 2.9).

Framebuilding organisms are again predominantly *Montastrea annularis* with some other coral heads and rare *Acropora palmata* samples. The encrusting organisms are very similar to those previously described. Internal sediments are also similar, with the same relative abundances as in the other reefs (12% of which half is mudstone and the remainder pack- or wackestone). No obvious differences in the contribution of the various porosity types has been identified.

2.15.2 Cementation.

Both previously observed cement mineralogies occur in these two cores, with a slightly higher abundance than in the other Dry Tortugas reef material. The average values over the whole core are 3% aragonite and 0.8% peloidal cements compared to 2% and 0.5% respectively for South East reef. The errors in point counting estimation at these low figures suggest that the differences are probably negligible. The abundances are, however, significantly lower than for the Alligator reef material, particularly with respect to the peloidal Mg-calcite phase. The ranges of cementation in individual thin sections are 0–10% of the rock and 0–40% of the porosity. Cement morphologies and occurrences are exactly as described for the other Dry Tortugas reef samples.

As only one core has been studied from each reef, no observations about the distribution of the cements can be made on that scale. There is no obvious trend in the distribution of the cements on the core scale. The same heterogeneity on the smaller scales is present and similar observations of sequences of cements have been made.

2.16 Regional Variations in the Cementation.

Only a few other studies have discussed the regional variations in cement abundances; those that have suggest that a greater degree of cementation might be expected in the seaward reefs and the seaward edges of reefs, in relation partly, but not entirely to the energy conditions (James et al., 1976; Marshall, 1985). In the Florida area, the cementation is noticeably lower in the Dry Tortugas reefs than in Alligator reef and this may reflect a lower average energy of the former. This may seem initially contradictory with the idea that the Dry Tortugas reef accumulated as a storm product, but nevertheless, the average energy of the Alligator reefs may still be higher over a period of 8000 years as the storm events, though capable of moving large volumes of material are very short lived.

Whilst the volumes of aragonite cements are not greatly different in the two areas, the relative amounts of the peloidal cements most certainly are (3%, 0.8%) and the reasons for this are not immediately apparent. In the South East reef, the low peloidal abundance is coincident with the smaller amount of encrusting material, but this may be simply coincidental. Other explanations for the low volumes of peloids rely on a regional difference in availability of organic matter on which these peloids might nucleate, but this is very tenuous and the problem remains largely unexplained.

In conclusion, two possible reasons for the lower cementation can be suggested, the first relating to the more rapid accumulation rate of the Dry Tortugas reefs and the second being a lower average energy of the environment.

2.17 Process Interactions, Timings and Intensities.

Cementation is but one of several processes which interact in a dynamic fashion during reef formation. This section highlights the complex nature of the interaction of the four major processes, reef growth, sedimentation, destruction and cementation. The sequences of these processes and the relationships between them are described as observed on the thin section and hand specimen scales. The importance of the interaction of the reef growth with the cementation process has been illustrated by the previous section. This section therefore, concentrates on the interaction of the sedimentation, destruction and cementation processes.

A general observation can be made that applies to all the 14 cores and the hand specimens studied from the Florida area. The number of cross-cutting relationships between sedimentation, destruction and cementation is actually quite low, indicating that the intensities of these processes is low relative to reef growth. Where cross cutting relationships are noted, there are no obvious preferences in terms of the timing of processes, hence both cement in bores and bores in cement occur equally often, as do both sediments post cements and cements post sediments. This general point serves to strengthen the concept that the major reef forming processes interact dynamically in both space and time. Specific descriptions of the interactions follow.

2.17.1 Cementation and Sedimentation.

There appear to be fewer occurrences of cements post internal sediments than internal sediments post cements, although the situation is complicated by the problem of distinguishing sediments from microcrystalline cements, as this may lead to an underestimation of the former sequence. In addition, a lack of observed occurrences of cements post internal sediments does not necessarily imply that the cementation process occurs prior to most sedimentation as the precipitation of cements may be inhibited by the sediments themselves.

Nevertheless, it is more common, where cross cutting relationships exist, to observe sediments postdating the growth of aragonite crystals (Figure 2.60). Relationships with the peloidal cements are very difficult to determine (Figure 2.61). Further complexity is introduced in examples where sediments are filling bores which cross cut cements (Figure 2.62). This general sequence of sediments postdating boring activity is extremely common. This might be expected because the bioerosional activity both increases the permeability of the pore network thereby increasing its connectivity with possible sediment sources, and creates substantial volumes of re-sedimented material anyway. The ideal example of this is shown in Figure 2.18, where clionid sponge chippings are filling a clionid excavation. Many of the occurrences of sediments postdating cements are probably created when the initial boring process of the above sequence happens to cross cut a cement phase.

Other observations confirm that the cementation process is likely to start prior to the deposition of sediments. Cementation is known to occur within millimetres of the living surface of coral colonies (Hubbard, 1972) and the polyps are known to be capable of removing even very fine material from their surfaces. Hence in a specimen of coral whose outer edges are living, cementation may be occurring below the surface and internal sediments would be unable to accumulate until after the death of the organism.

The above discussion prompts another important point to be made related to the distribution of cements on the scale of individual colonies, in particular, with respect to the growth of the massive head corals. During the growth of the colony, cementation may be occurring in the inner parts of the skeleton, but the rate of flow of pore fluids is likely to be quite low due to the controls exerted by the living organism, which covers most of the outer surface. On death of the coral, fluid flow through the surfaces of the colony will become increased and so the rate of cementation will increase. As the coral is no longer increasing in size, it might be expected that the surface of the coral will receive a greater volume of cements than the inner parts of the skeleton. Although no conclusive evidence of this has been seen for head corals studied in this thesis, some evidence of this is observed in hand specimens of *Acropora palmata* and the same observation has been reported in the literature (Lighty, 1985). The greater cementation will then also contribute in a type of positive feedback manner to further reduce the permeability through the surface to the inner parts of the skeleton.

This concept explains a commonly observed heterogeneity in the core material. Where continuous pieces of core are recovered, indicating the presence of a single large colony, whilst small areas of the core may be cemented, the majority of the sample is often completely devoid of cements. Hence, the centre of the large coral colonies may be substantially less open to physical exchange of pore fluids than are the outer edges. Only when boring activity has reached a high enough intensity will the inner parts of the colonies become susceptible to the precipitation of cements and the deposition of internal sediments.

The general scarcity of cross cutting relationships may be explained by the fact that much of the sediment observed in thin section is probably deposited after a phase of boring. The size of the intra-skeletal pores into which cements are precipitated is quite small relative to the size of a typical bioerosional cavity, (1–500μm. compared with 1–2cm.). A relationship between this later phase of sediment and the cements will only be created when a boring cross cuts a cemented area, preserving some of the cement. Due to the relatively large size of the boring, the latter event is probably quite rare. The two factors (rare cross cutting of cements by bores and most of the sediment being post boring), lead to a general scarcity of cement/sediment relationships.

Finally, in examples where sediments clearly do bear a post dating relationship with a cement phase, it should be noted that there may well have been an intermediate phase of boring of which no evidence has been preserved in the specific two dimensional plane under study. The conclusion is therefore that the internal sediments probably start to accumulate at some time after the first phase of cementation.

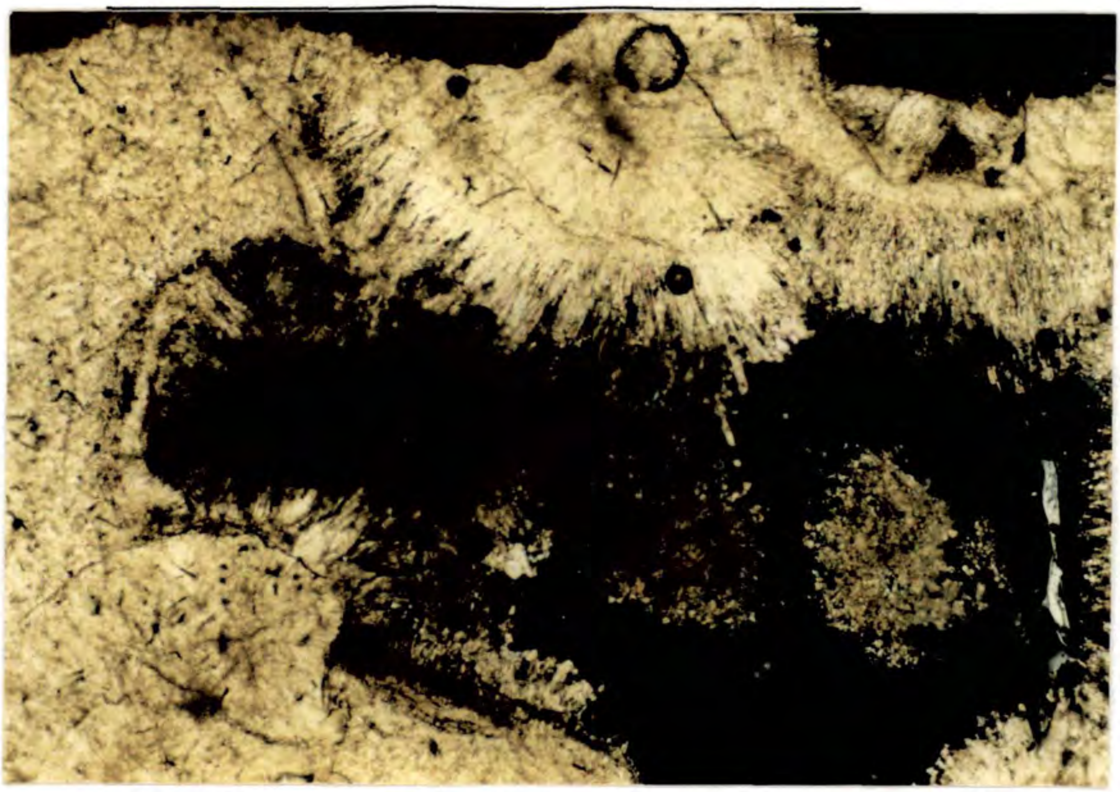

Figure 2.60 Cements postdated by internal sediments (microcrystalline cement ?). Photomicrograph, xpolars. (K14)

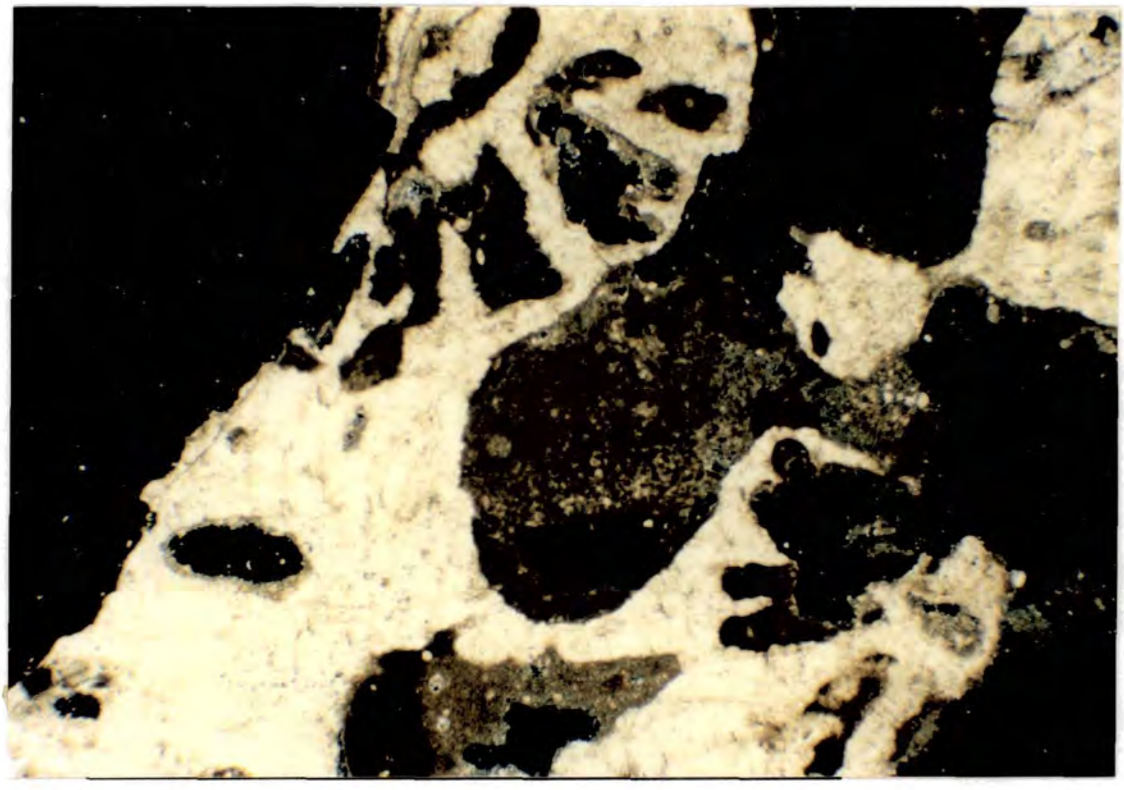

Figure 2.61 Peloidal cements in a complex relationship with internal sediments, all within a bivalve boring. (K14)

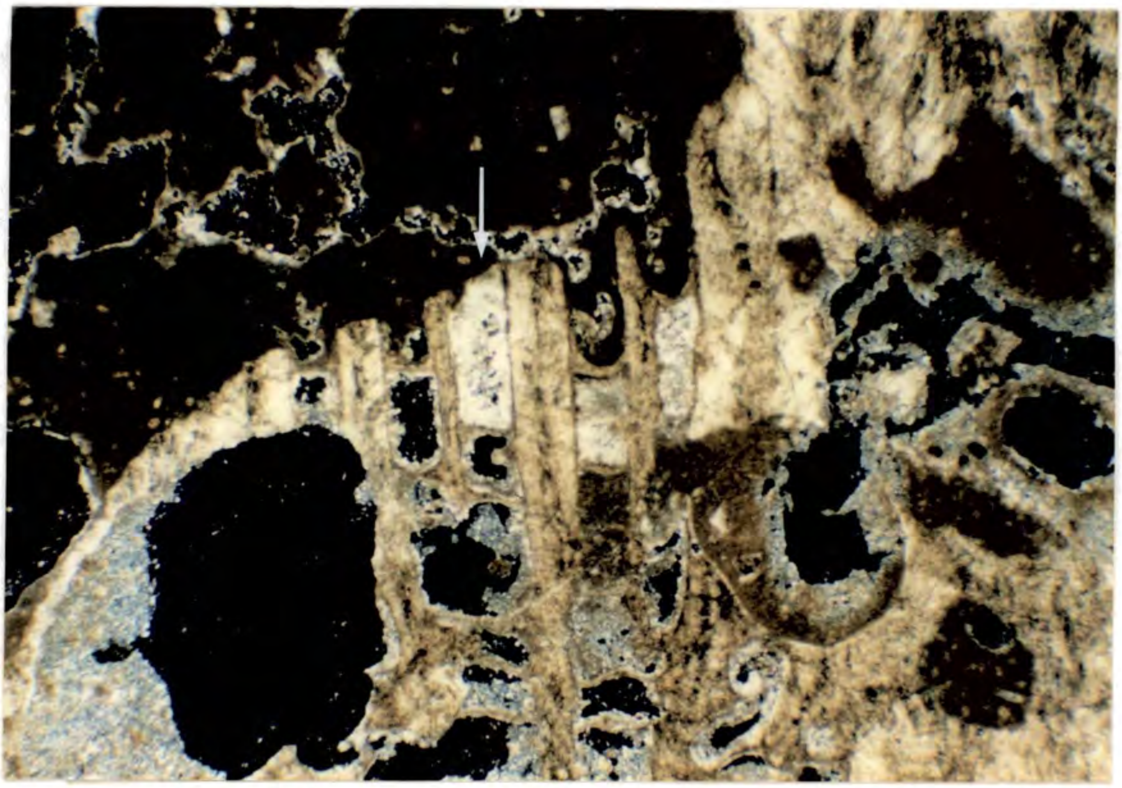

▬ 250μm.

Figure 2.62 Sediments filling a boring which cross cuts fibrous aragonite cements. (N 8)

2.17.2 Cementation and destruction.

The two principal destructive processes are mechanical abrasion and bioerosion. Although the mechanical destruction caused by the energy of the reef environment is extremely important, it is too catastrophic to describe on the thin section and hand specimen scale. Some of the aspects of the interaction of bioerosion and cementation have already been mentioned in relation to the interaction with sedimentation in the previous section. Some further observations are described below.

The temporal interaction of bioerosion and cementation is similarly difficult to interpret as the cross cutting relationships are rare. In addition, many of the pores which are of bioerosional origin may not be recognised as such, so that the occurrence of cements within borings is only rarely identified.

Cements appear to occur more commonly within borings through encrusting organisms than through framestone corals, but this observation may be simply due to the ease of identifying bores through encrusters than through corals. (Figure 2.49). Cements are also observed in bores through internal sediments (Figure 2.62). Both of the above examples (Figures 2.49 & 2.62), show aragonite cements precipitating on Mg-calcite substrates, indicating that the substrate and cement mineralogies are not always the same, and that the presence of one mineralogy does not mutually exclude the precipitation of another.

The other sequence is also observed, that of bores cross cutting cements (Figure 2.64), and although this relationship is less common than that of cements post dating bioerosional porosity, it should not be assumed that boring is the first process to occur.

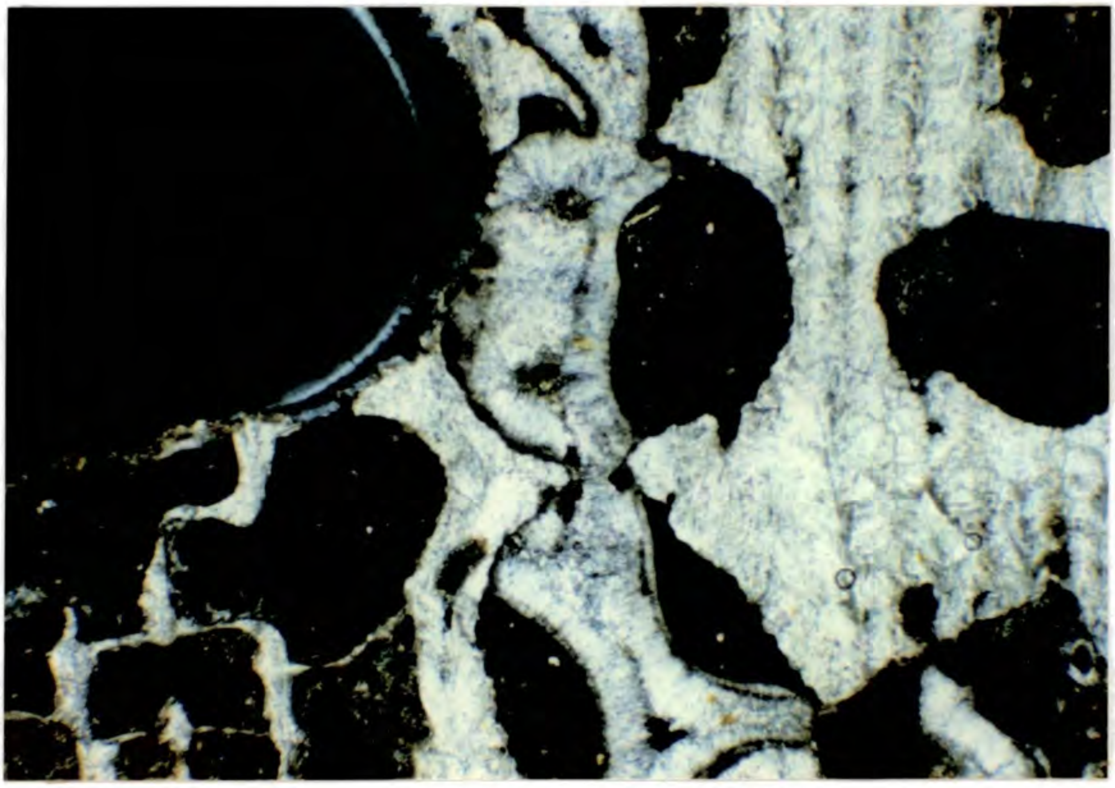

Figure 2.63 Aragonite cements present within bioerosional porosity in a coral skeleton. Cement nucleated both on the aragonitic coral and on the Mg-calcite / aragonite sediment. Some bioerosion post-dated the precipitation. (H 13)

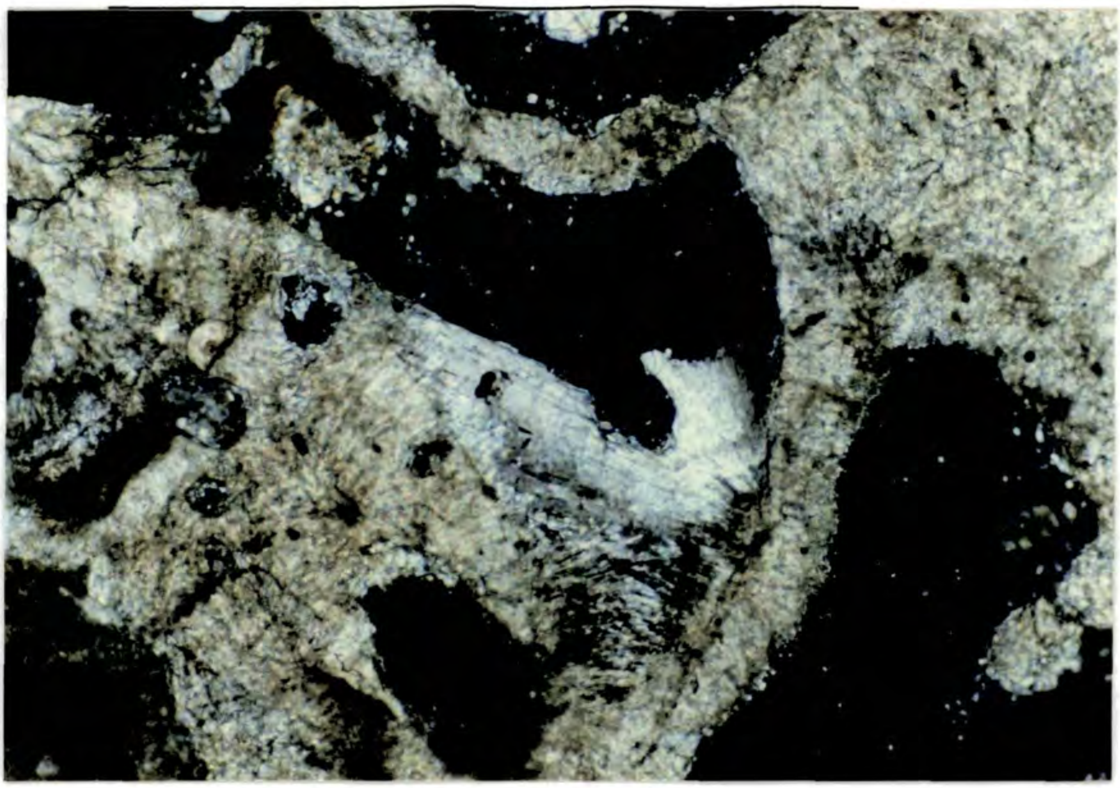

Figure 2.64 Two examples of bores cross-cutting cements, a feature which is much rarer than the cements postdating bores. B5)

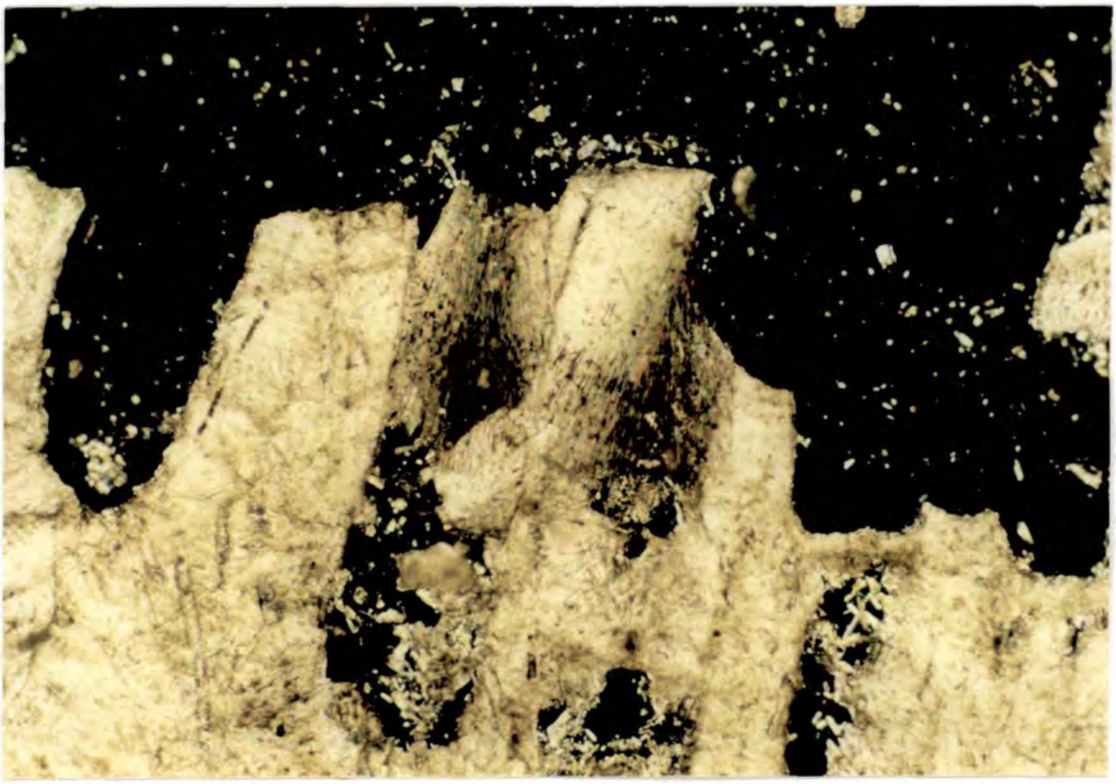

2.17.3 Multiple sedimentation and bioerosional events.

The interaction of multiple generations of internal sediments is intimately related to the multiple generations of bioerosion as it is through the erosional processes that the permeability of pore systems and their connection with sediment supplies is increased. In addition, the major sources of the sediments themselves are the very same bioerosional processes.

Multiple sedimentation events are commonly preserved in the reef rock and can be observed in thin section, the generations of sediments being distinguished by slight changes in the colour and texture of the successive layers (Figure 2.20). The relationship of the successive sediments with multiple generations of boring activity is clearly demonstrated.

The intensity of these two processes can be so great as to obliterate virtually all of the primary fabric of the rock. Hence, in Figure 2.20, so many successive boring and sedimentation events have occurred such as to make it almost impossible to identify the original lithology as being a coral framestone.

2.18 The Pleistocene Reefs of Florida.

2.18.1 Introduction.

Several of the holes cored in the Dry Tortugas Reefs penetrated the Pleistocene reef substrates on which the Holocene growth was initiated. The material is very difficult to distinguish in the core specimens, exhibiting a slightly whiter, chalky texture when compared to the Holocene samples. Only a small number of Pleistocene samples were collected, and there is not enough material to permit a regional or reef scale study to be made. However, the few specimens do show a number of interesting diagenetic features, characteristic of alteration in meteoric pore fluids.

The distribution of the diagenetic products shows the same inhomogeneity as observed in the Holocene samples, again reflecting the variability in the local permeability, and the requirement for the exchange of large volumes of pore water. The variability is evident on both thin section and hand specimen scale, and in the one core which is mostly Pleistocene (Hole 5, Dry Tortugas), point counting highlights the larger scale inhomogeneity (Appendix 1). All the complexity of the marine diagenetic system is involved, with the added factor of the differences in the stability of aragonite and calcite in meteoric water. The major component of the samples is coral framestone, so aragonite is the dominant mineralogy, but some high Mg-calcite components (coralline algae and echinoid fragments) are also present. The difference in degree of alteration is very noticeable, with the neomorphic fabric being developed to a greater extent in the aragonite substrates.

Features characteristic of alteration in both the meteoric phreatic and vadose zones are present, with meteoric spar cements rarely observed in the same pores as fibrous aragonite cements typical of the marine diagenetic zone. The fibrous cements occur in varying degrees of preservation, both as ghosts, and as intact, unaltered aragonite. Similar characteristics of variable preservation have been reported from other Pleistocene reefs (Schroeder, 1968, 1984; Pierson & Shinn, 1985).

2.18.2 The meteoric cements.

Meteoric spar cements are present in many of the samples, precipitated as isopachous rims and as pore filling anhedral crystals, up to 500μm. in size. The cements form in greatest abundance in the intra-skeletal cavities of corals, often leaving the aragonite surfaces unaltered. Spars are observed in pores adjacent to acicular aragonite cements (Figure 2.65) and both cements occur in the same pores in a few examples (Figure 2.66). In some cases the acicular crystals are visible only as 'ghosts' within large unit extinguishing calcite crystals (Figure 2.67), but most are preserved as aragonite as identified by the high strontium content measured by the electron microprobe. Spars have also been rarely observed precipitated within the interstices of marine peloidal cements (Figure 2.68) and as overgrowths on echinoid fragments.

There are a number of examples where spar cements were clearly formed in a vadose environment, exhibiting the characteristic dripstone and meniscus features (Figure 2.69) (Longman, 1980). A particularly interesting fabric is developed in some samples containing large amounts of internal sediments. Spar cements are evident in what appear to be fractures in the micrite (= physically deposited) (Figure 2.70). These may have formed in the vadose zone, as a result of repeated wetting and drying which occurs due to variations in the amount of rainfall and the intensity of evaporation (Longman, 1980). As such these are very similar features to those developed in the intertidal zone (Shinn, 1968), and in some rare cases, spar filled microcavities are very similar to fenestrae or 'birdseyes'.

2.18.3 Neomorphism and dissolution.

The degree of neomorphism is highly variable, although the aragonite substrates are certainly affected to a greater extent than Mg-calcites. The coral skeletons can be completely replaced, with calcite crystals of up to 4 mm. in size forming an interlocking mosaic. However, other corals within a few centimetres are commonly unaltered in any way. This feature is illustrated by the point counting figures (Appendix 1), where the percentage of the skeleton that is now calcite spar was measured. The figures vary in an irregular fashion from 0–35%. In some specimens, a neomorphic replacement front can be seen (Figure 2.71).

Other aragonite bioclasts also show neomorphic fabrics, with some rare biomouldic porosity and some coral specimens also show the development of secondary porosity. The fact that some of the spar cements are slightly corroded (Figure 2.72) suggests that there was some flux of undersaturated water after their precipitation. Peat layers are evident in most of the cores, and it is possible that the meteoric water dissolved CO_2 from the soil zone causing it to become undersaturated. The dissolution may also have been enhanced by the acidic conditions within the peat.

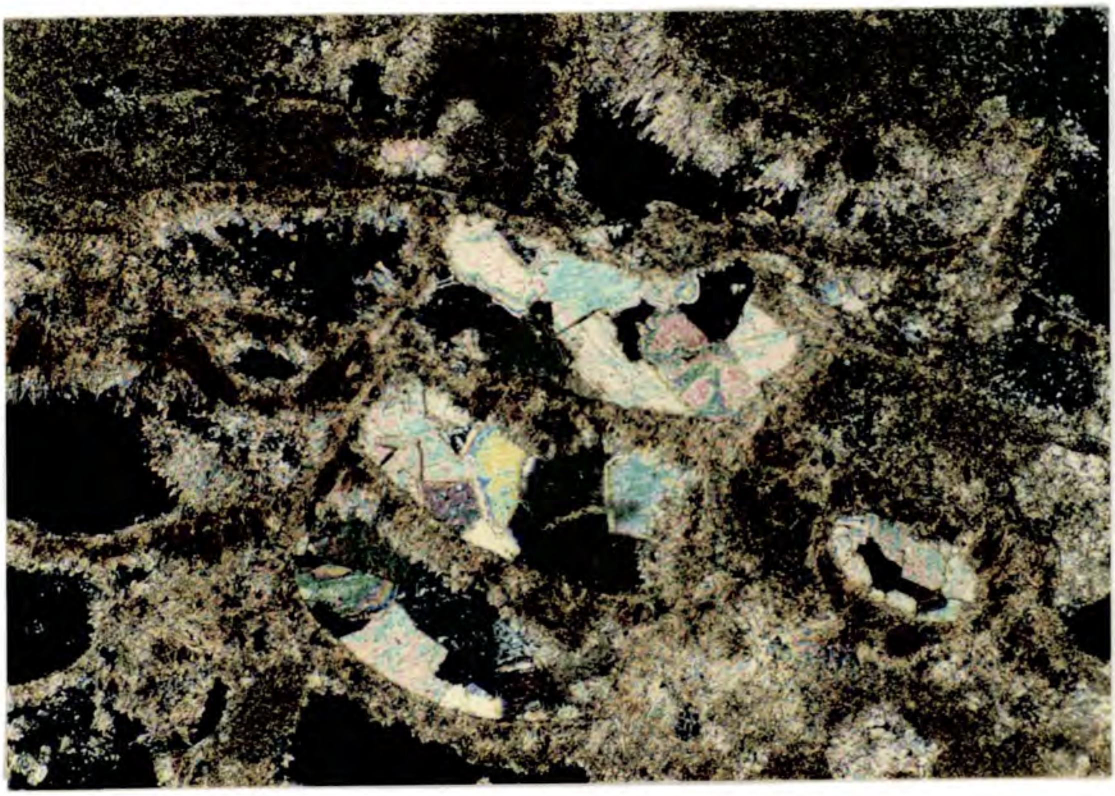

100μm.

Figure 2.65 Thin section photomicrograph of Pleistocene sample from Dry Tortugas. Meteoric spar cements are evident in pores adjacent to marine fibrous aragonite. Photomicrograph, xpolars. (N 10)

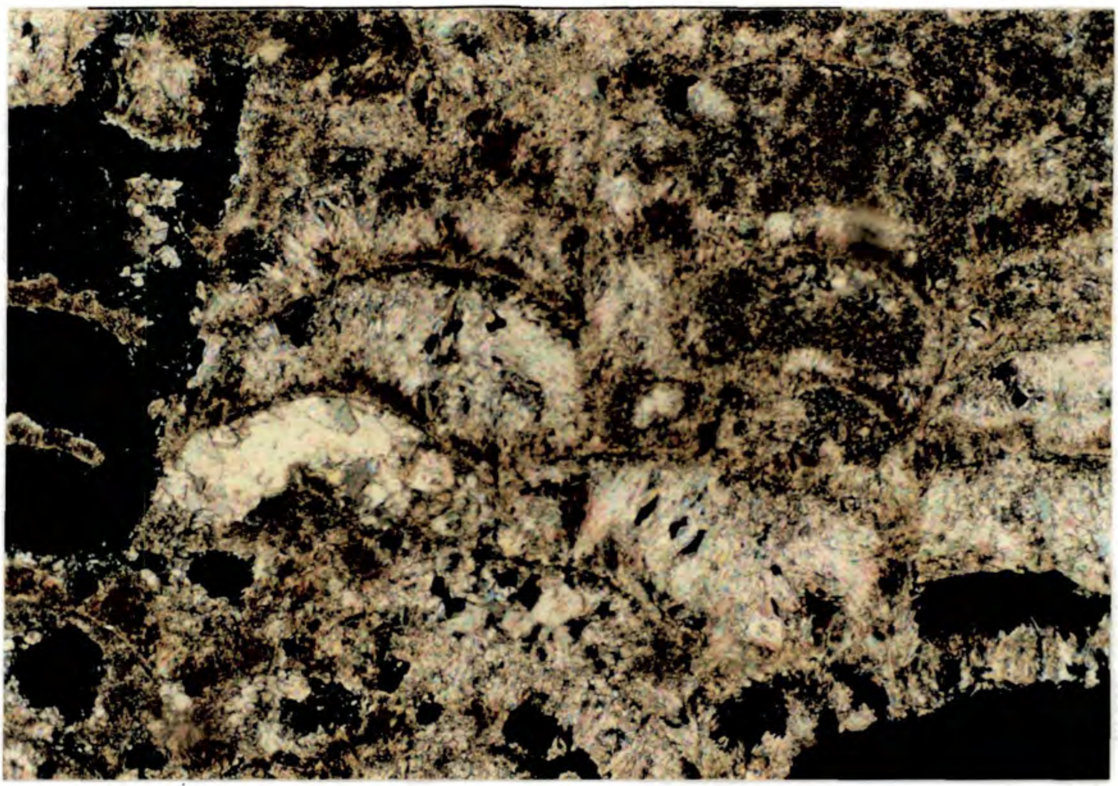

Figure 2.66 Spar cements occurring in the same cavities as fibrous aragonite. The fibres are preserved as aragonite as evident through the detection of 6–8000 p.p.m. Sr (by micro-probe). Photomicrograph, xpolars. (N10)

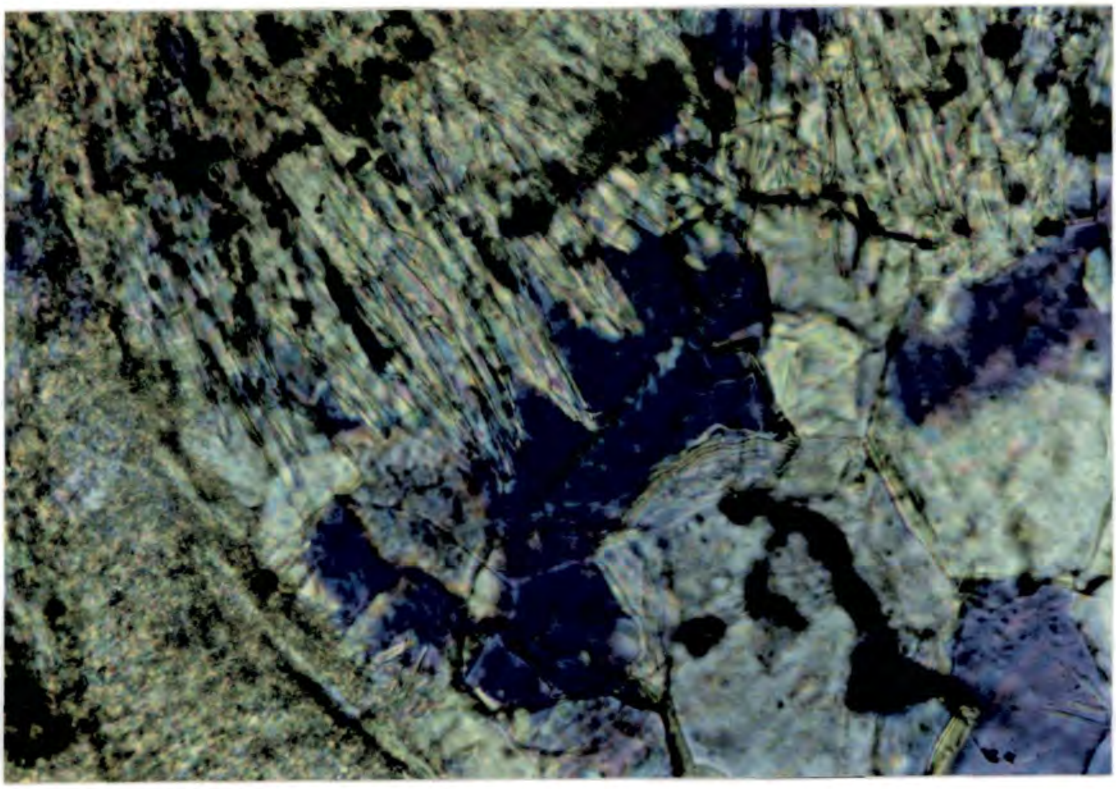

Figure 2.66 Detail of fibres present in same cavity as spar cements. Photomicrograph, xpolars.

(N 10)

$100\mu m$.

Figure 2.67 Fibrous aragonite filling intra-skeletal cavity of a coral. In this example some of the fibres are preseved only as 'ghosts' within unit extinguishing calcite spars (arrows). Lower photo is with the stage rotated so that a different part of the spar is at extinction. Photomicrographs, xpolars. (N 10)

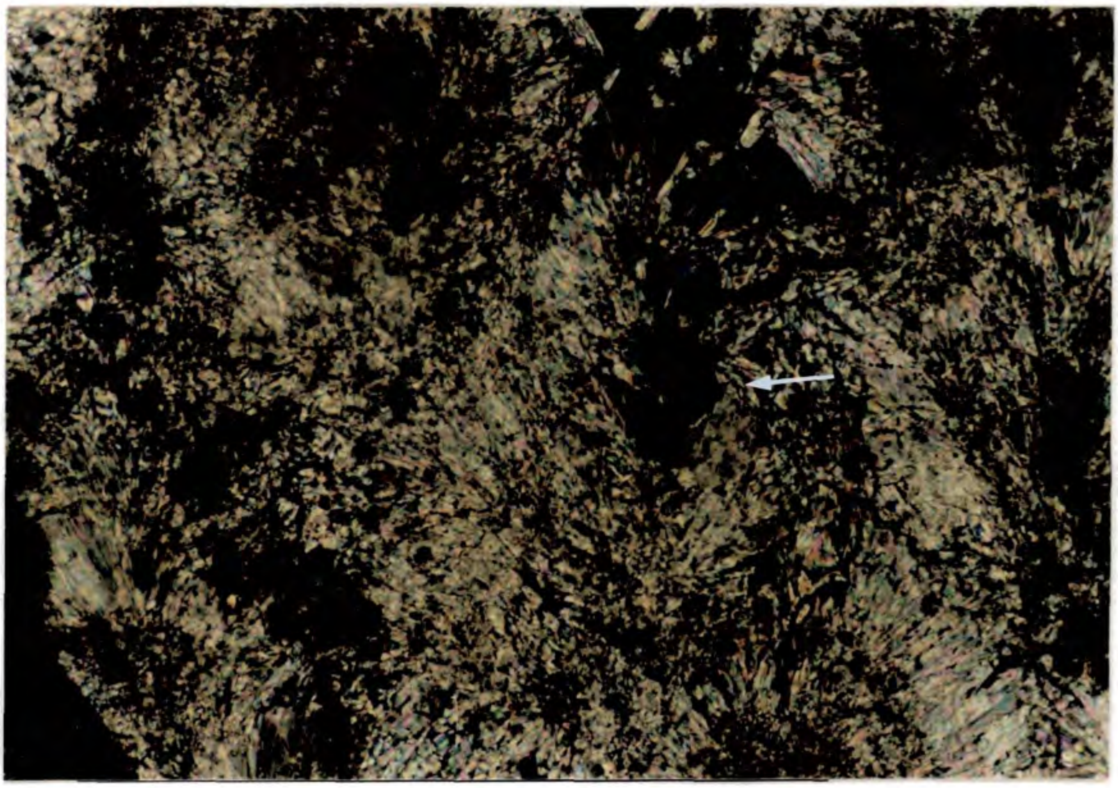

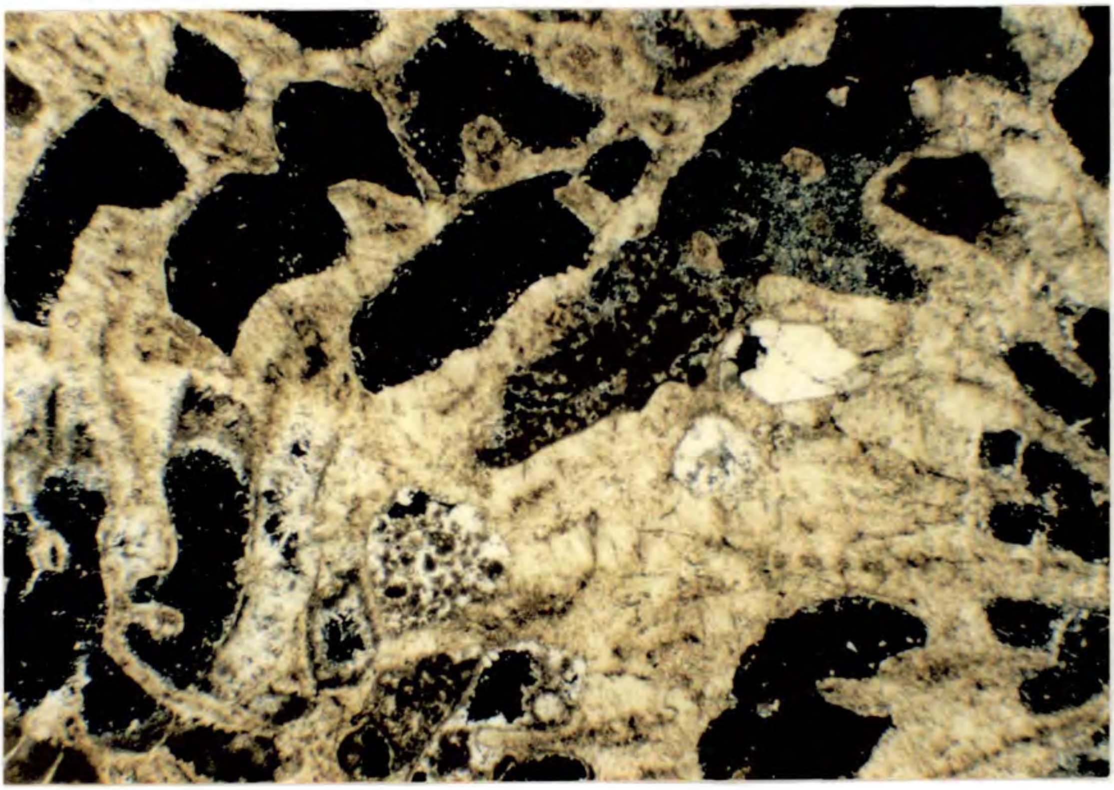

Figure 2.68 Spar cements in pores adjacent peloids, and filling inter-peloidal porosity. Photomicrograph, xpolars. (N 14)

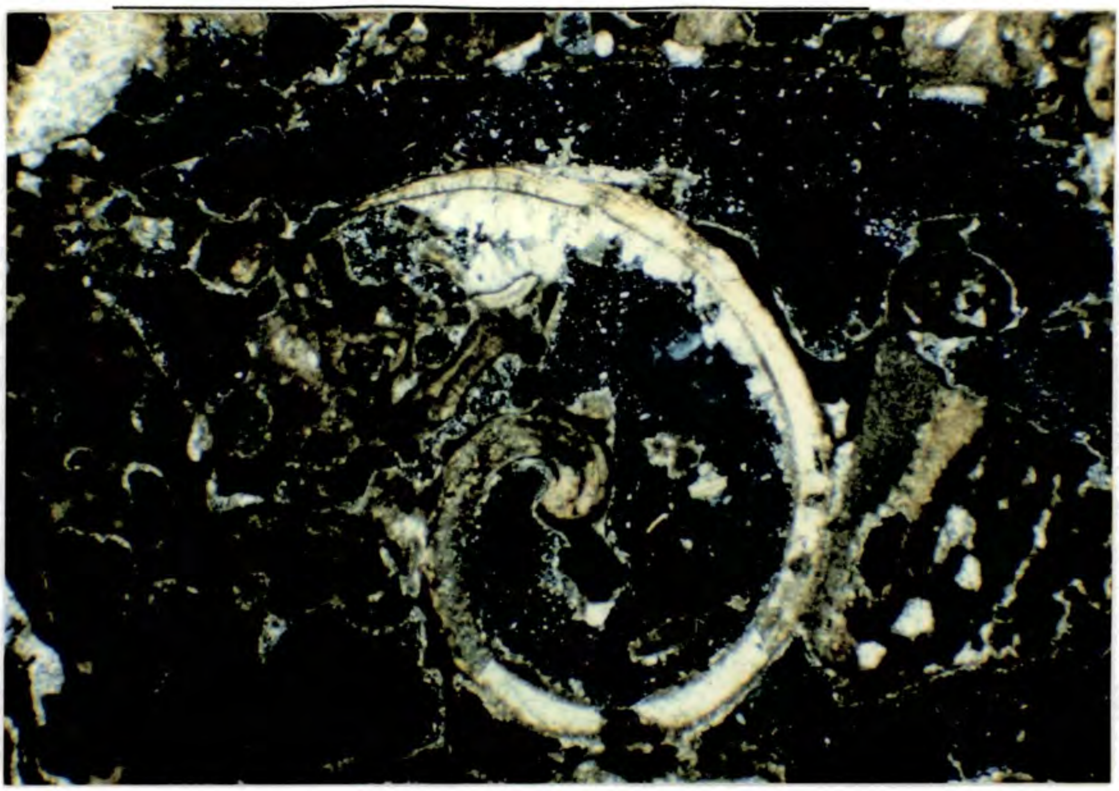

Figure 2.69 Two examples of 'dripstone' fabric of meteoric spars, characteristic of precipitation in the vadose environment. Photomicrographs, xpolars. (N 6)

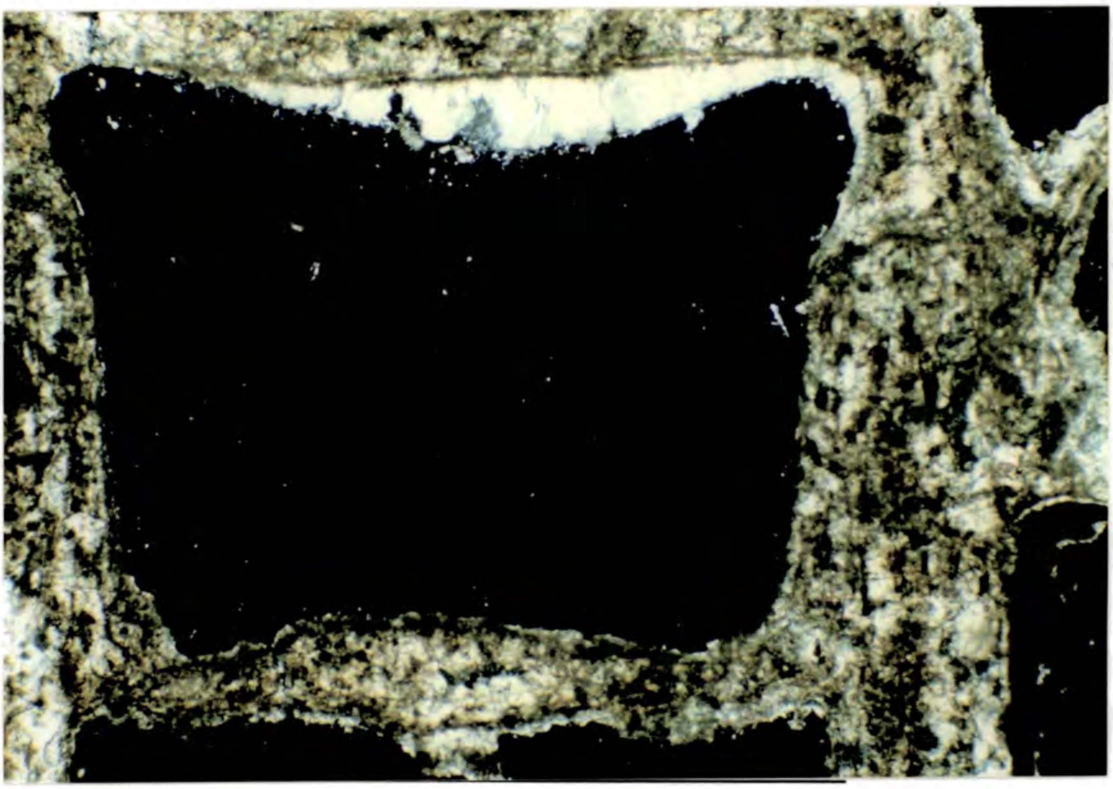

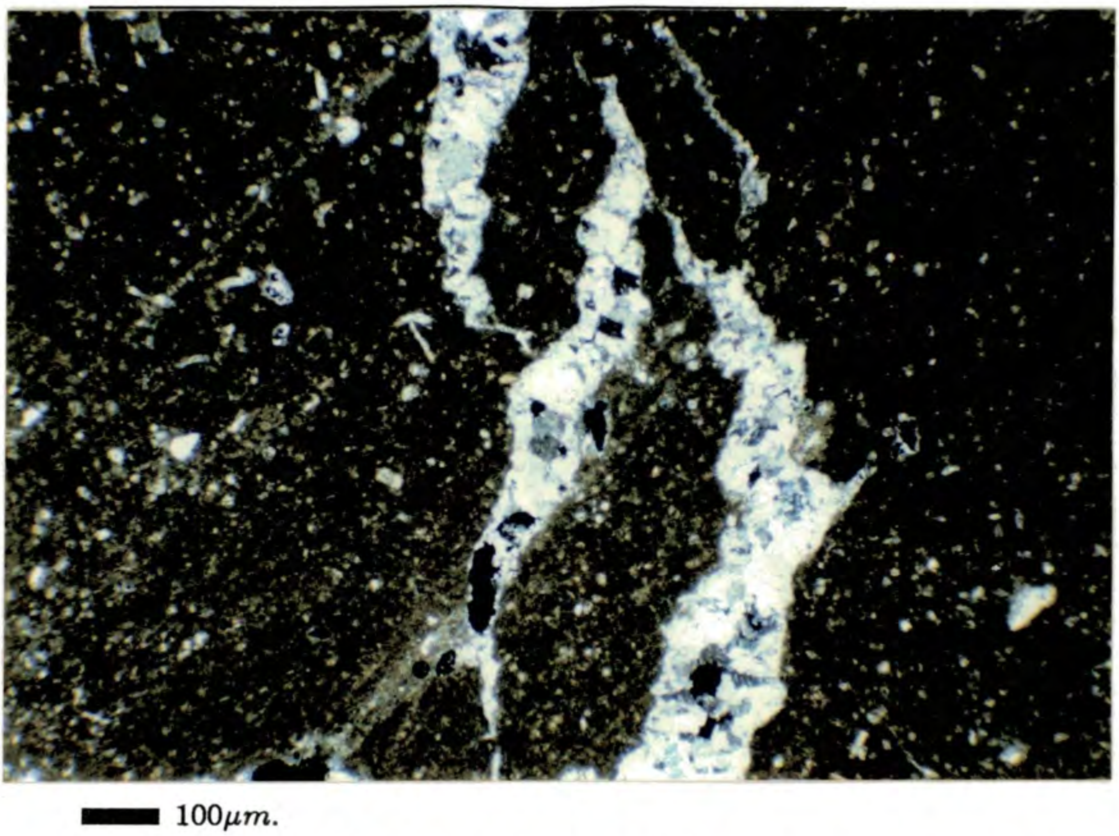

Figure 2.70 Micrites with linear spar filled cavities. These were possibly formed as the result of repeated wetting and drying, also in the vadose environment, and were subsequently filled with meteoric spar. (N10)

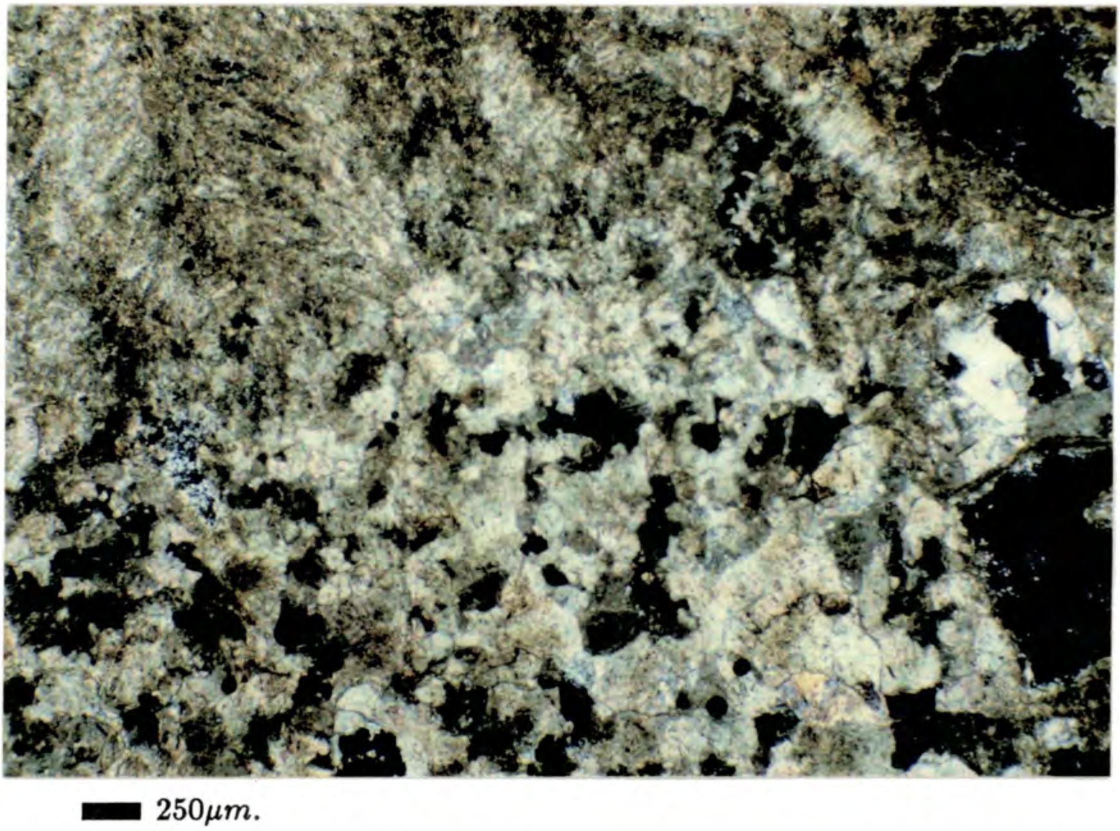

Figure 2.71 Neomorphism of coral skeleton with very clear neomorphic 'front'. Photomicrograph, xpolars. (N94)

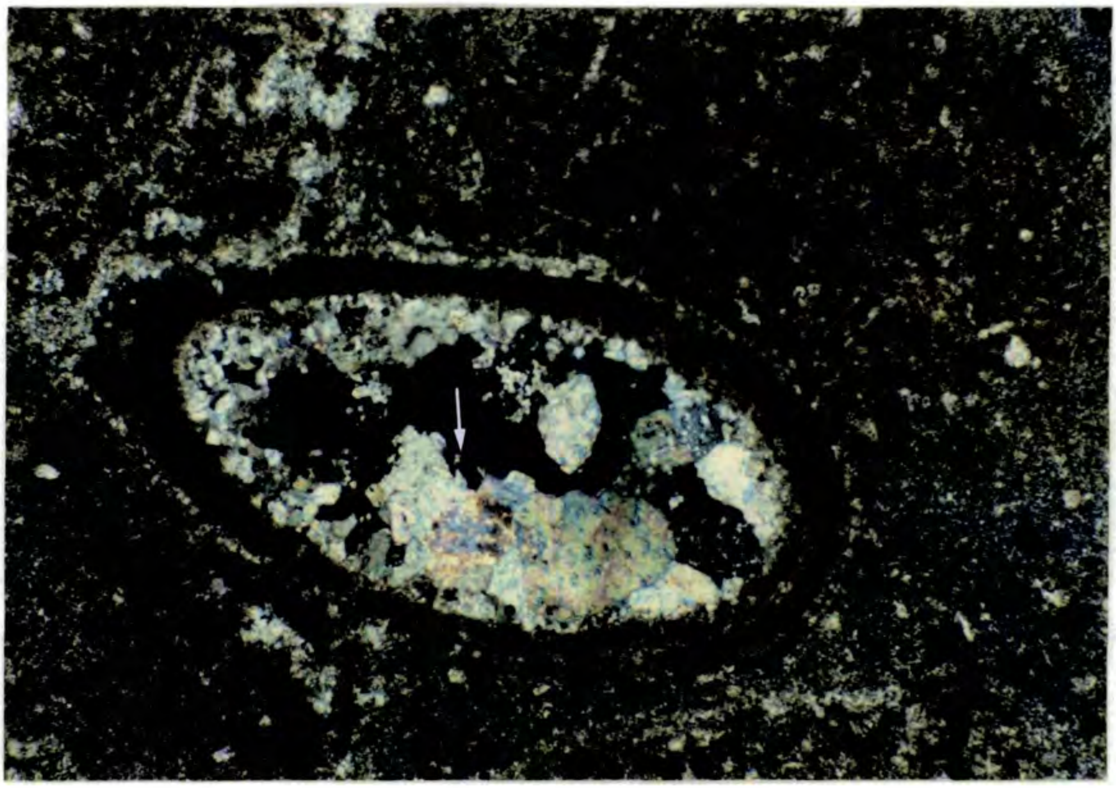

Figure 2.72 Evidence of dissolution of spar cements, indicative of the passage of undersaturated waters, possibly linked to the development of a peat zone during early transgressive phase. (N9L)

2.19 Early Holocene Shelf Edge Reef.

Samples provided by Professor Lighty of Texas A&M University were studied solely for their very high content of Mg-calcite peloidal cements. The cements occur in concentrated bands at the surface of *Acropora palmata* skeletons and these samples were therefore used in the analysis of the organic matter present associated with the peloids. The samples were collected from an Early Holocene relic shelf edge reef situated approximately 40 km. north of Miami (Figure 2.73). This reef has been described in detail (Lighty, 1977, 1985) and apparently forms part of a 100 km. long barrier reef now in 30 metres of water. There has been no growth for the past 6000 years, such that the long exposure of the surface of the reef has resulted in the extensive precipitation of marine cements. The peloids are present in quantities of up to 20% of the whole rock, filling up to 40% of the total porosity. Point counting indicates that they form an average of 60% of the void filling material in the surface of the skeletons, with a further 30% being fibrous aragonite, and the remaining 10% being internal sediments.

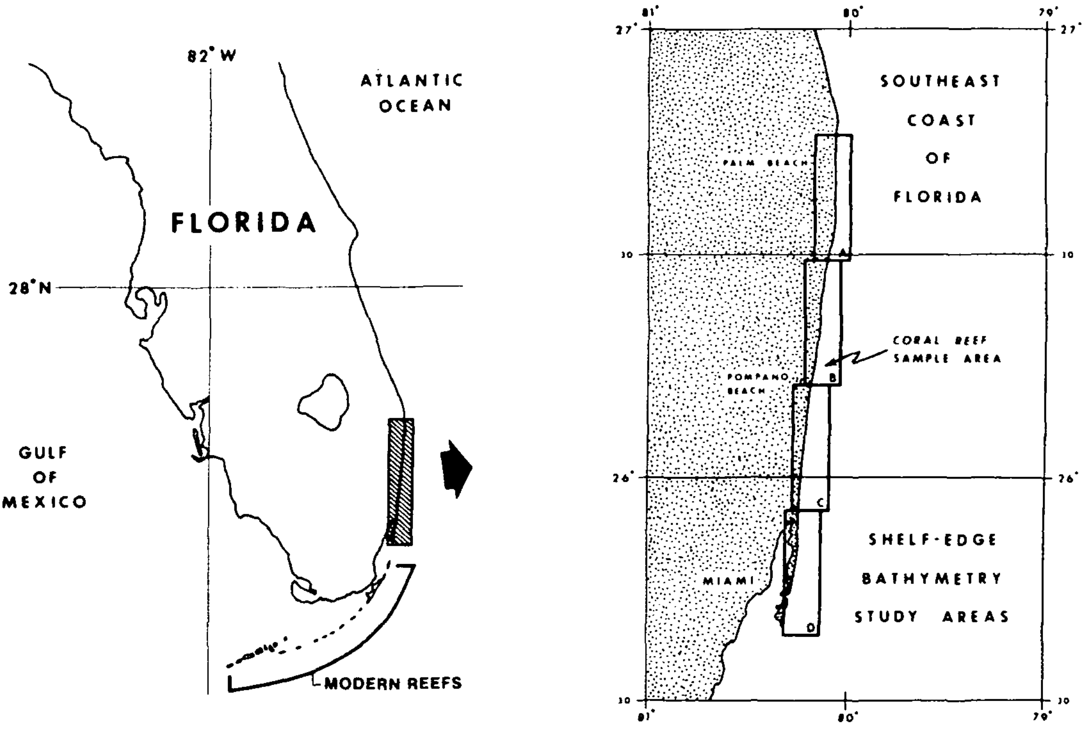

Figure 2.73 Location map showing the position of the Early Holocene relic shelf edge reef from which samples containing abundant peloids were collected. (From Lighty, 1985).

2.20 The Cementation of Holocene reefs of Belize.

2.20.1 Introduction.

The shallow water carbonate producing area of offshore Belize is another example of a rimmed shelf (Ginsburg & James, 1974). The rim consists of a quite continuous barrier reef extending 250 km. in length (Figure 2.74). The samples described in this section were collected and later described by James & Ginsburg (1979). They come from the fore-reef of Glovers reef which is an isolated platform located a few kilometers offshore from the rimmed shelf.

It is not the intention in this section to redescribe the samples, but they serve as an interesting comparison to the samples from the Florida reefs. They provide an opportunity to study both the distribution of cements in the fore-reef facies (which was not studied in Florida), and the interaction of the reef formation processes over a rather longer period. These samples are up to 15,000 years old compared with a maximum of 7,500 years for the Florida reef samples.

2.20.2 Local setting.

Glover's reef is an atoll situated 15km. east of the barrier reef and is approximately 30km. by 10km. in size (Figure 2.75). The seaward edge of the reef is facing the open Caribbean sea and is therefore subject to the highest energy environment present in the Belize area. The surface of this seaward edge consists predominantly of coralline algae, live corals are quite rare. The samples studied come from the reef wall and fore-reef of the atoll at depths of up to 100 metres. The terminology for the reef description and the specific sampling points are illustrated on (Figure 2.76). The samples were collected using a submersible, after the creation of artificial outcrops through the use of explosive charges (James & Ginsburg, 1979).

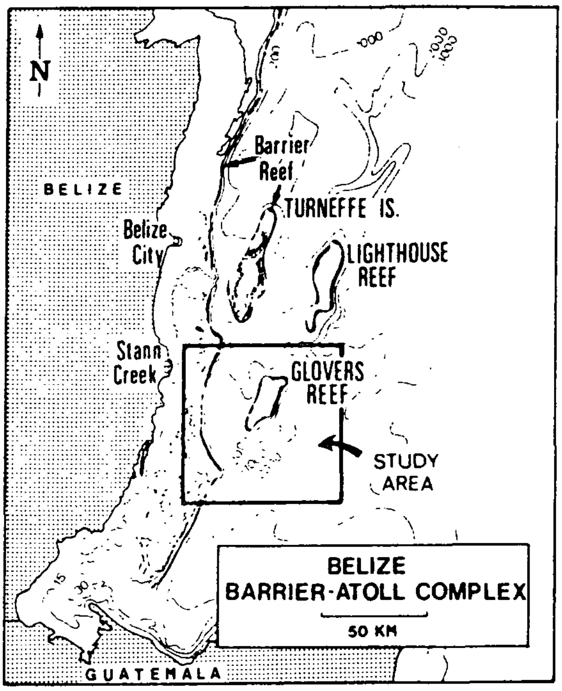

Figure 2.74 The Belize continental margin, showing the main features of the Belize reef tract. (From James & Ginsburg, 1979).

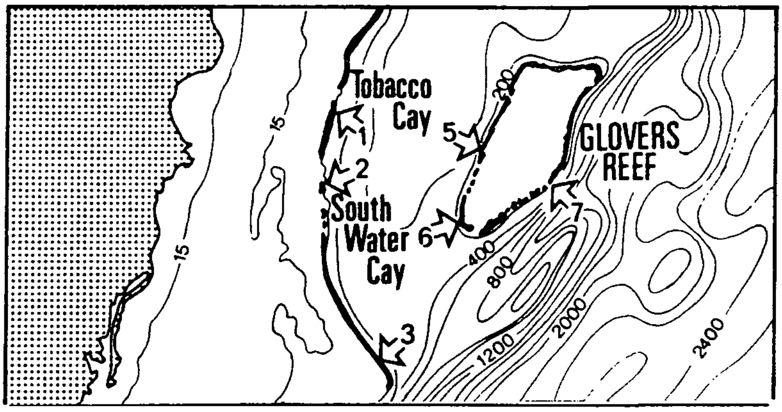

Figure 2.75 Detail of above showing Glovers Reef. Samples studied came from sites on the eastern side of the reef.

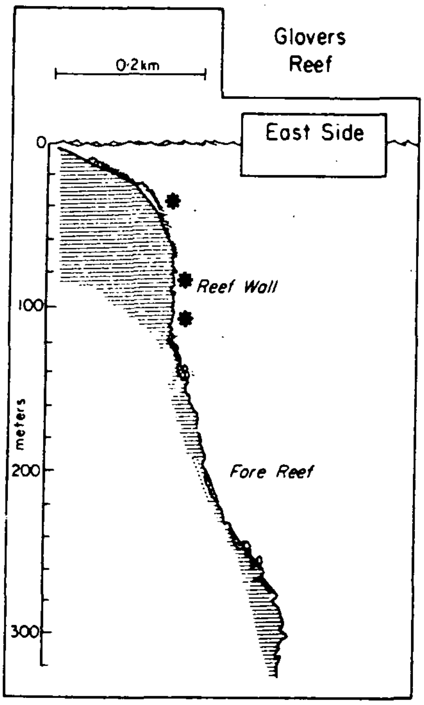

Figure 2.76 Location of sampling points on the eastern edge of Glovers Reef.

2.20.3 Appearance and composition of the samples.

The hand specimens vary in appearance from clean white coral framestones to cream or light brown samples with a mottled fabric indicative of multiple generations of bioerosion, sedimentation and lithification (Figure 2.77). The composition varies from coral framestone to fully lithified grainstone and packstone. The coral species are predominantly *Montastrea annularis*, with lesser amounts of *Montastrea cavernosa* and *Porites sp.*. It is apparent that many of the samples were originally coral framestones which have been extensively altered to produce well lithified pack- and wackestones with so little remaining primary framework that it is very difficult to identify the original framebuilding species. The role of encrusting organisms as secondary framebuilders is highly variable, but in general there is a greater proportion of these organisms than in the material from Florida. In individual hand specimens, more than 80% of the rock can be encrusting material (Figure 2.78). Full details of the framebuilding, encrusting, boring and dwelling organisms can be found in James and Ginsburg (1979), but they are very broadly similar to those observed in the Florida reefs. The major differences between the Belize and Florida samples are the volume of sediments (and/or microcrystalline cement ?) and the degree of cementation.

2.20.4 Internal sediments.

The internal sediments observed in the Belize samples, whilst exhibiting the same broad range of textures as those from Florida, form a much greater proportion of the total rock. The average component of sediments is approximately 40% (Appendix 1), and the range varies up to as high as 65% of the total rock. Of this, the major proportion is the pack- and wackestone material (22%), with lesser amounts of grain- and mudstones. The sediments are clearly deposited in a complex manner as a result of multiple generations of bioerosional and resedimentation events.

2.20.5 Porosity.

The type and overall porosity within these samples is markedly different from that in the Florida material as a result of the much greater intensity of the destructive and sedimentation processes in the Belize fore-reef. Only in the centres of large coral samples is there any identifiable primary intraskeletal porosity and most of this is usually filled by cements or sediments (Figure 2.79). The remaining porosity is on average approximately 10%, half of which is intraskeletal with the remainder being unidentifiable small vugs of multiple origins.

Figure 2.77 Hand specimen sample from Glovers Reef wall. The sample is extremely well lithified, the mottled appearance indicative of multiple bioerosion and sedimentation events.

Figure 2.78 Heavily encrusted sample, originally a coral framestone. Major encrusting and secondary frame-building organisms include coralline algae, serpulids and *Homotrema*. (H.S.)

2.20.6 Cementation.

The morphologies and mineralogies of cement observed in these samples are very similar to those described in Section 2.7 from Florida reefs. The only major differences are in the total abundances of the cements. The volumes of cement vary up to 30% of the whole rock and up to 80% of the porosity which was apparently available at the time of cementation. The average is 11% of the whole rock and 45% of the porosity. The majority of this figure is made up of fibrous and botryoidal aragonite cements (Figures 2.79 & 2.80), with lesser amounts of fibrous Mg-calcite fringes (Figure 2.81). The spherulitic aragonite morphology does also occur, but in much smaller amounts relative to the fibrous cements. Magnesium calcite peloidal cements also occur in large amounts and can fill intra-skeletal and bioerosional cavities (Figure 2.82). The internal sediments are also very well lithified, so there may be a significant contribution to the overall cementation by microcrystalline cements whether of aragonite or Mg-calcite mineralogy. The figures above do not include any such contribution due to the problems of estimating how much of the lithified cavity fill is actually precipitated material.

The same sequences of cements occur as described from the Florida samples with the addition of a common observation of the precipitation of fibrous Mg-calcite after an earlier phase of aragonite (Figure 2.83). The reverse has not been observed, indicating that the controls on this sequence may be related to the relative supply rates of the calcium and carbonate ions, as described by Given & Wilkinson (1985). In addition, the number of cement phases observed can be larger than in the Florida samples, and the relationship between the phases can be very complex. This again reflects the greater intensity of the cementation, bioerosion and sedimentation processes, thus producing the observed complex relationships between the various products.

2.20.7 Comparison with the Florida samples.

The principal differences between the Florida and Belize samples are in the degree of cementation and the volumes of internal sediments. This reflects a much greater intensity of the cementation, sedimentation and bioerosional processes, relative to the fundamental process of reef growth. There are several reasons for the greater intensity of cementation compared to the Florida samples. The first is that the energy of the environment of the fore-reef is much greater than that of the reef core from which all the Florida samples were collected. In addition, the average energy of the entire area around Glovers reef is probably higher than that of the Florida reefs, as the former is situated in the open Caribbean, whereas the latter has the protection of the Bahama Banks. Hence as the energy is higher, the flux of pore fluids through the reef is higher and so (according to the results of the mathematical modelling in Chapter 5), the degree of cementation can be expected to be greater. Secondly, the Belize Holocene reefs have been subject to the marine diagenetic system for a longer period than the Florida reefs: a maximum period of 15,000 years for the former, compared to a maximum of only 7,500 years for the latter.

The longer timescale and the greater energy are also probably the principle reasons behind the observed greater intensity of the boring and sedimentation processes. Finally, it is possible that the greater intensity of the bioerosional processes made a significant contribution to the observed high degree of cementation. Although the porosity of the samples is presently very low, this is due to the fact that most of the final stage bioerosional porosity is filled by internal sediments and of course cements. However, if the evolution of the porosity is considered over the entire period since the initial formation of the primary framework, then it is apparent that due to the high intensity of bioerosional activity, there will have been periods when the porosity was particularly high. The general distribution and nature of bioerosional porosity is such that it can substantially increase the permeability of the primary rock fabric. This increased permeability will then enable a larger rate of flow of pore water through the system and so potentially lead to a greater degree of cementation.

This concept appears particularly attractive when the Belize material is compared to that from Florida. The intensity of the bioerosional processes in the Florida reef material is quite low, and the inherent permeability of the coral framestone is also quite low, particularly when considered on the scale of several metres. In contrast, as an average over its very early diagenetic history, and due to the contribution from the bioerosional processes, the permeability of the Belize fore-reef material was probably much higher. This may therefore account for the much higher degree of cementation observed in the Belize samples.

Figure 2.79 Thin section photo of coral framestone, with very low remaining porosity. Aragonite and Mg-calcite (yellow stain from Titan yellow) cements and internal sediments filling intra-skeletal porosity. Photomicrograph, xpolars. (H.S.)

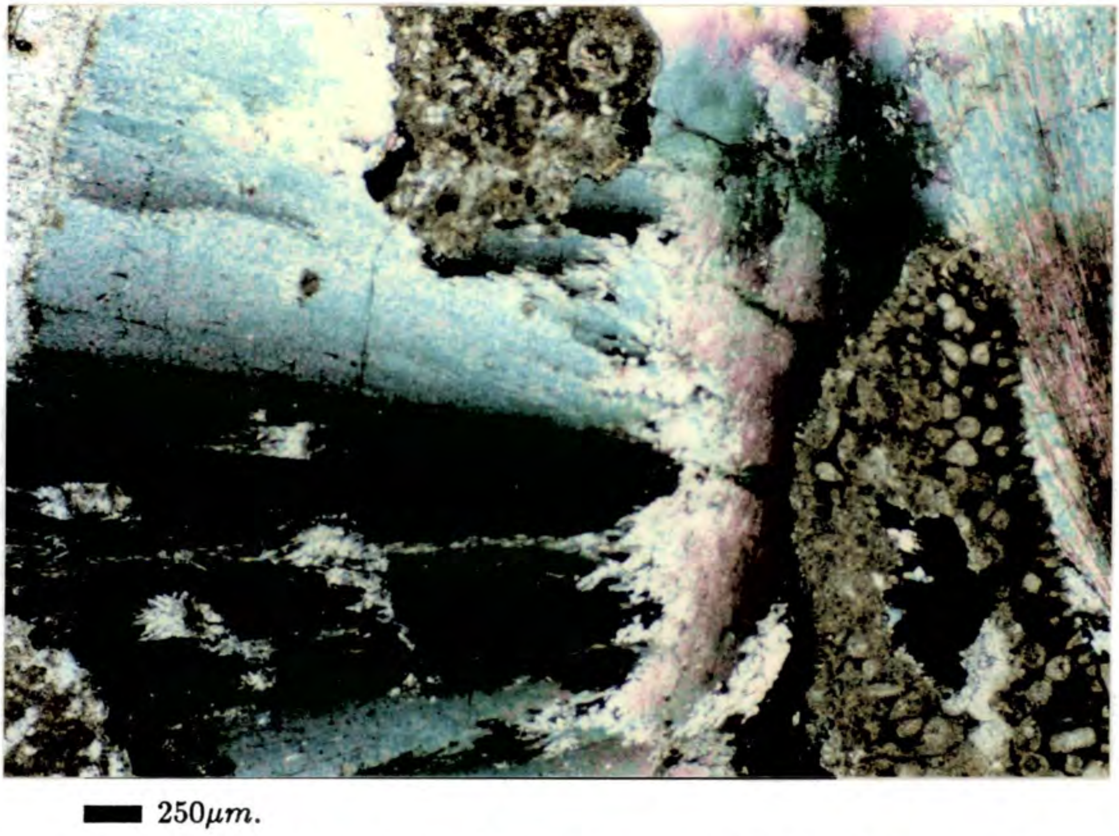

Figure 2.80 Characteristic large botryoidal aragonite cements, maximum size of 4cm. observed. Photomicrograph, xpolars. (H.S.)

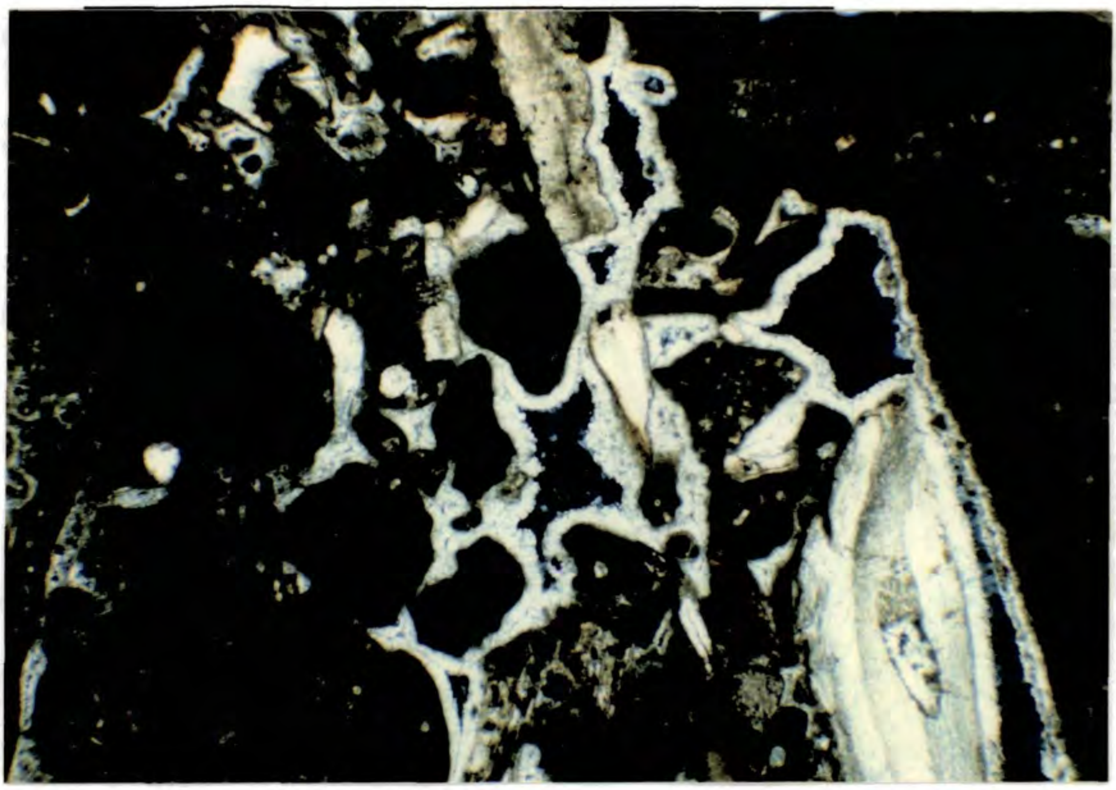

Figure 2.81 Isopachous Mg-calcite fringing cements formed within packstone sediments. Photomicrograph, xpolars. (H.S)

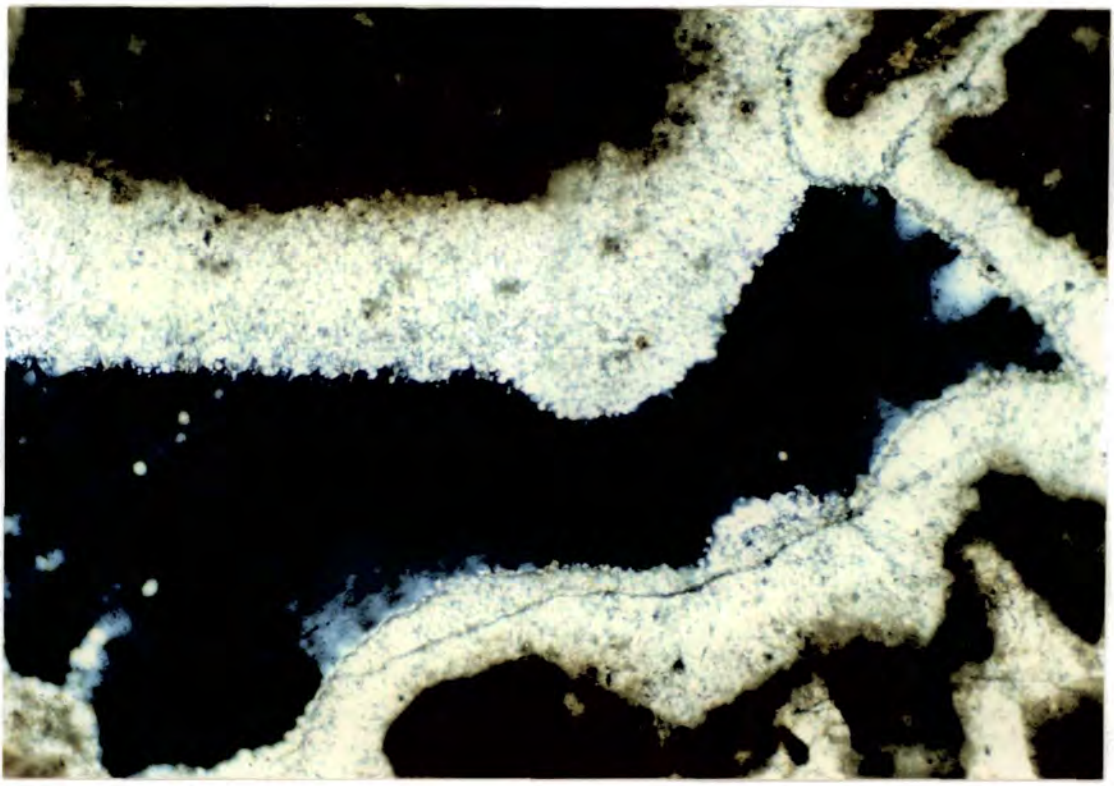

Figure 2.81 Detail of above showing growth zones and compromise boundaries. Photomicrograph, xpolars. (H. S.)

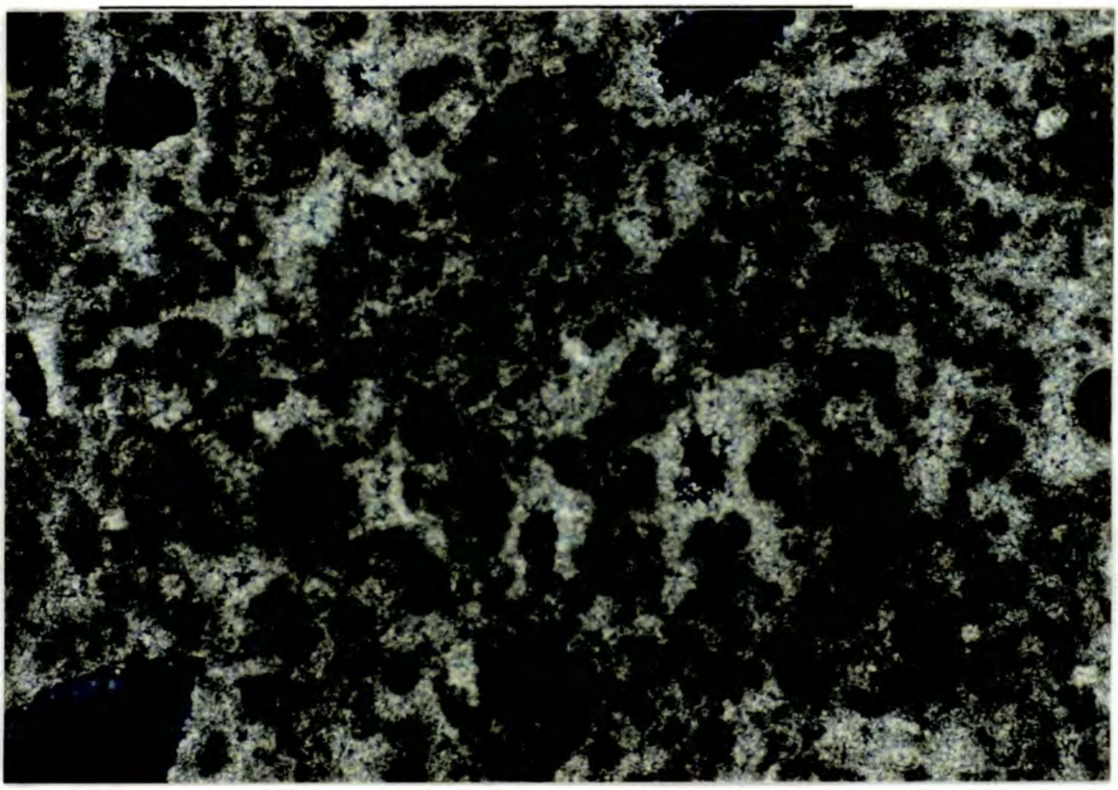

Figure 2.82 Mg-calcite peloidal cements developed in very similar fabrics to those in the Florida reefs. Photomicrograph, xpolars. (H.S)

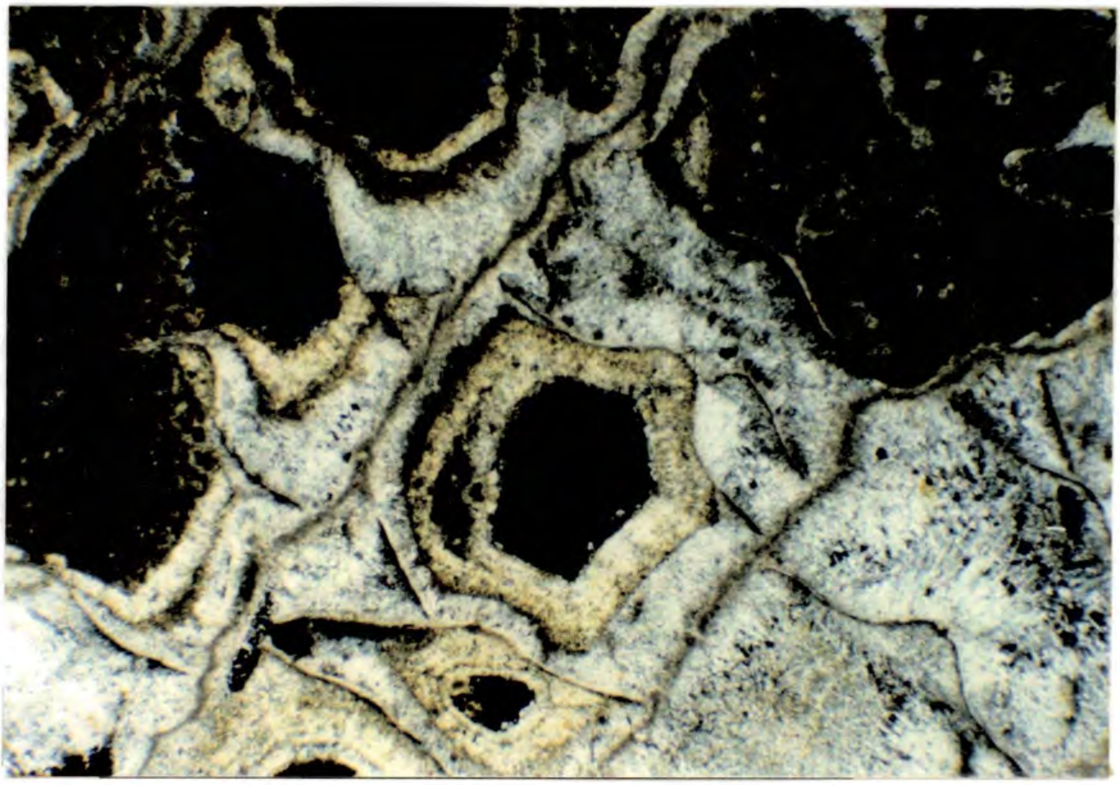

Figure 2.83 Complex interaction of fibrous and peloidal cements, bioerosion and sedimentation. Photomicrograph, xpolars. (H.S)

2.21 Summary and Conclusions.

The Holocene reefs of Florida are cemented by a variety of aragonite and high Mg-calcite precipitates which form approximately 7% of the total rock or 18% of the porosity available prior to cementation. The cement is precipitated within the intra-skeletal porosity of the reef building corals and coralline algae. There is no apparent species specificity for the cementation, with the exception that the spherulitic aragonite is more commonly observed within *Montastrea sp.*. There is some substrate specificity in terms of the cement mineralogy as the aragonite cements are best developed on aragonite substrates. The very small amount of fibrous Mg-calcite is precipitated on both substrate mineralogies, and there is no apparent specificity for the occurrence of the peloidal cements.

One of the very important controls on the process of cementation is the interaction, in both space and time, with the other reef forming processes. The great variety of primary porosity is continually modified by the effects of bioerosion, sedimentation, construction and cementation itself. It is clear that an accurate description of the degree of cementation should be based on the cements as a percentage of the porosity available at the time of precipitation, and not as a percentage of the total rock. Calculations on this basis highlight the heterogeneity of the cementation patterns. The major control on the distribution of cements appears to be the flux of water through the pores, and this control operates on all scales. At the pore to pore level, the variability in cementation is due to variations in the volume of water flowing through the individual pores. On the thin section scale, cementation varies from 0–25% of the total rock or 0–85% of the total porosity. Similar controls operate on the hand specimen and core scale, such that the degree of cementation is dependent on the local permeability. Although there are no trends in the Florida reefs on the whole reef scale, comparison with samples from the fore-reef of Belize indicate that the energy level controls the degree of cementation. The higher energy environments are cemented to a greater degree, again as a direct result of the higher fluid flux.

The fact that Alligator reef is cemented to a slightly greater degree at the surface is also attributable to a greater total flux of pore waters, and this is due to two factors. The first is that the flow rates are high at the surface of the reef and decrease rapidly with depth, suggesting that most of the cementation occurs at the surface. With constant growth / burial rates, this would produce a uniform cementation pattern, but in the case of Alligator reef, there has been no growth for the past 4,000 years, so that the total flux through the surface has been higher than through the rest of the reef.

The mineralogy of the cements appears to be under some substrate control and this is probably a purely inorganic control, although the possible mediation of the precipitation by organisms is investigated in Chapter 3, through a study of the isotopic chemistry of the cements. The peloidal cements are a special case, as they are clearly associated with organic matter; this phase is studied in Chapter 4. The distribution of cements is extremely inhomogeneous on all scales and the primary control on the distribution is the flux of water through the pores. The flux is itself dependent of two major factors, these being the energy level and the permeability. Although the energy level is predictable, the permeability is not, and the great variation in permeability is a result of the spatial and temporal interaction of the processes of construction, bioerosion, sedimentation and cementation itself.

CHAPTER 3

The Role of Biogenic Processes in the Precipitation of Cements.

CHAPTER 3

The Rôle of Biogenic Processes in the Precipitation of Cements.

3.1 Introduction.

The precipitation of marine cements is known to occur within millimetres of the living surfaces of reef building organisms and has been specifically observed within corals and coralline algae (Hubbard, 1972; Bosence, pers.comm.). This close association of the cements and the living parts of the organisms suggests that the precipitation may be mediated to a certain degree by biological processes. It is the intention of this chapter to investigate this possibility and to identify the nature of any involvement.

This section serves to outline the various roles in which biogenic processes may be involved. Section 3.2 describes the potential of several methods in helping to identify such roles, if they exist. Sections 3.3 and 3.4 describe the background necessary for the interpretation of the stable carbon and oxygen isotopic compositions of the cements, as this is the major tool used to study the biogenic mediation. Section 3.5 discusses what it may be possible to deduce from the observed isotopic compositions. The data are presented and interpreted in Section 3.6, with a brief comparison to previous work in Section 3.7. The chapter is concluded in Section 3.8.

There are several ways in which the organisms may be involved in the cementation process:

i) Direct source of $CaCO_3$ from inorganic body fluids.

Calcifying organisms have efficient biogenic systems for transporting, compartmentalising and secreting the ions necessary to nucleate calcium carbonate minerals for the growth of their own skeleta. It is conceivable that catastrophic events, including death of the organisms, may result in the release of both highly reactive nuclei for calcification, and calcium enriched body fluids, thereby causing precipitation.

ii) Direct source of HCO_3^- through decomposition of organic matter.

Decomposition of organic matter by various pathways can lead to the precipitation of calcium carbonate from seawater (Berner, 1968). In such examples, the carbon of the calcium carbonate is sourced directly from the organic matter.

iii) Direct biogenic mediation.

This type of interaction does not actually cause the precipitation of cements, but it may promote it. Although the seawater is still the major source of the calcium and bicarbonate ions, the geochemistry of the pore waters may be modified by the biogenic mediation and the cements produced may then appear to be precipitated out of equilibrium with the oceanic bicarbonate reservoir.

iv) Indirect biogenic mediation.

Many calcifying organisms, and in particular the scleractinian corals, are known to produce complex organic materials which control the precipitation of skeletal material. These 'mineralising matrices' are high molecular weight polymeric molecules with highly efficient Ca^{2+} binding affinities (Degens, 1979).

Although they would be isolated from the marine pore waters whilst the organisms are alive, these components may be released after death, and would then act as initial nucleation centers on which further precipitation of calcium carbonate could occur. In this mode of interaction, the seawater is the sole source of calcium and carbonate, with the biogenic role being simply the promotion or catalysis of the precipitation.

3.2 Investigation of the Biogenic Effects.

3.2.1 Observations.

The observation of the association of cements with particular organisms and with particular aspects of the skeletal organisation suggests that there is some biogenic involvement in the precipitation, but it is very difficult to demonstrate any conclusive genetic relationship. There are no published examples where recognisable cements are seen to be nucleating on intact recognisable organic structures and no such observations have been made in this study. There are, however, several examples in which precipitates are seen to be nucleated on organic matter of unknown origin, such as in ooids (Mitterer, 1968; Davies et al., 1978), and kopara deposits (Défarge & Trichet, 1984, 1985). The latter observations provide strong evidence that a type (iv) mediation, as described above, is occurring.

The magnesium calcite peloidal cements described in Section 2.7.6 are clearly associated with organic matter, although the precise relationship is uncertain. The evidence cited in the past for the presence of organic matter within these peloids has been rather circumstantial, namely the 'brown colouration' . Further evidence that organic matter is present has been provided in this study by the observation of fluorescence under u-v light and by the extreme volatility of the peloids under a defocussed electron beam of the electron microprobe. Organic geochemical techniques have been used to isolate the organic matter and a detailed analysis is presented in Chapter 4. The fine-grained nature of the inorganic phase suggests that precipitation was rapid, thus indicating that the organic matter may be acting to promote the precipitation in the manner described in (iv) above.

The fact that some cements are observed in specific spatial concentrations such as the aragonite spherulites in coralline algae (Section 2.7.2) and the Mg-calcite peloids in the surfaces of coral skeletons (Lighty, 1985) further suggests some involvement with the life cycle of the organism. The former is difficult to interpret as the spherulites most commonly occur in bioerosional cavities in the algae. The bioerosional process may itself be mediating the precipitation of the cement and so it is not necessarily any property of the algae which is involved.

The concentration of peloids at the surfaces of coral skeletons has been noted previously (Macintyre, 1985) and is confirmed in this study. This suggests that the formation of the peloids could be associated with processes occurring at or shortly after the death of the coral.

3.2.2 Analysis of the organic matter.

There are two aspects of the analysis of organic matter which can help to identify its role in the precipitation of cements. Both provide information on the indirect biogenic mediation, type (iv) above. The first and most useful technique relies on the identification of 'biological markers'. These are low molecular weight compounds with specific structures that have been found to be produced only by certain organisms or groups of organisms. Their recognition therefore allows the identification of an input from organisms for which there is no preserved hard fossil evidence. This can lead to an understanding of the origin of the organic matter, but it does not provide any information on the nature of the organic-inorganic interaction. The latter has to be derived from a full characterisation of the higher molecular weight components, and this is the second aspect that has been investigated. (Section 4.6).

3.2.3 The stable carbon and oxygen isotopic composition of the cements.

The stable carbon and oxygen isotopic composition of the cements is a potentially powerful tool with which to investigate the controls on the precipitation of cements, and in particular can provide evidence for the biogenic mediation of types (i), (ii) & (iii) in Section 3.1 above.

The partial separation of the isotopes or isotopic fractionation which leads to the different isotopic compositions of the various phases can be characteristic for particular reactions or processes. Fractionation occurs either through kinetic effects (the different isotopes react at different rates), or due to equilibrium effects (which reflect the second law of thermodynamics), such that the isotopes redistribute themselves to attain a state of minimum free energy in the system.

The isotopic composition of the cements is dependent primarily on the composition of the fluid from which it is precipitated, and it is the variation in this porewater composition which provides clues as to the involvement of biogenic mediation. The fractionation process is, however, sensitive to various other physical parameters such as temperature and rate of reaction, and so the final isotopic composition of the cements can be produced by a combination of effects. It can therefore be difficult to interpret the compositions in terms of individual controls. Prior to discussing the results, it is necessary to consider the various fractionation effects in some detail.

3.3 The Precipitation of $CaCO_3$ and Equilibrium Isotopic Fractionation of Carbon and Oxygen Isotopes.

The notation used for the expression of isotopic compositions can be found in Appendix 3.

3.3.1 Oxygen equilibrium fractionation.

The precipitation of $CaCO_3$ from water involves an equilibrium fractionation of the oxygen isotopes, and this fractionation is temperature dependent. The relationship given below (equation 3.1), was derived by Epstein et al. (1953) and was modified by Craig & Gordon (1965). It was based on the analysis of both calcite and aragonite precipitated by molluscs under controlled conditions.

The data fit an expression as follows:

$$T[^\circ C] = 16.9 - 4.2(\delta_c - \delta_w) + 0.13(\delta_c - \delta_w)^2 \qquad 3.1$$

where δ_c is the $\delta\ ^{18}O$ of CO_2 liberated by reaction with 100% phosphoric acid and δ_w is the $\delta\ ^{18}O$ of CO_2 in equilibrium at 25 °C with the water from which the carbonate was precipitated. All the values are relative to PDB. It is often more convenient to express the relationship so that the water composition is relative to SMOW, such as in equation 3.2:

$$T[^\circ C] = 16.0 - 4.14(\delta_c - \delta_w) + 0.13(\delta_c - \delta_w)^2 \qquad 3.2$$

O'Neil et al. (1969, 1977) also determined the fractionation and its dependence on temperature by inorganically precipitating calcite from water. Both methods agree very well (Figure 3.1), particularly in the temperature range of interest. Other interesting data shown on Figure 3.1 are for the theoretical calcite–water fractionation and for the precipitation of aragonite and Mg-calcite. The latter naturally occurring forms have different fractionation factors from pure calcite. Tarutani et al. (1969) estimated that Mg-calcites precipitated inorganically at 25 °C are enriched in ^{18}O relative to pure calcite by 0.06 ‰ per mole% $MgCO_3$ and that aragonites are enriched by 0.6 ‰ at 25 °C. The aragonite–water fractionation curve is described by equation 3.3, (Grossman and Ku, 1981):

$$T[^\circ C] = 19.00 - 3.52(\delta_c - \delta_w) + 0.03(\delta_c - \delta_w)^2 \qquad 3.3$$

where δ_c is relative to PDB and δ_w is relative to PDB also.

3.3.2 Carbon equilibrium fractionation.

The precipitation of calcium carbonate also involves the fractionation of carbon isotopes, and in this case the situation is a little more complex as there are several species of dissolved carbon which may contribute to the CO_3^{2-} in $CaCO_3$. The fractionations amongst these species is shown in Table 3.1. Although all the species are present in seawater, the dominant species is HCO_3^- and so we are most interested in $\alpha_{CaCO_3-HCO_3^-}$, or $\varepsilon_{CaCO_3-HCO_3^-} = 2.1\,‰$ at $25\,°C$.* This compares with a value of $\varepsilon_{CaCO_3-HCO_3^-} = 1.8\,‰$ as derived by Emrich et al. (1970). There is a temperature dependence for this fractionation as can be seen from Figure 3.2 but this is much smaller than for the oxygen fractionation. The fractionation is different for different mineralogies (Anderson & Arthur, 1983).

These are therefore the carbon and oxygen equilibrium fractionations for the precipitation of calcite, Mg-calcite and aragonite. In addition to kinetic fractionations described in the following section, there is the possibility that the carbonates can be precipitated out of equilibrium with seawater (Section 3.4.3).

* By calculation from Deines et al. (1974).. See Table 3·1.

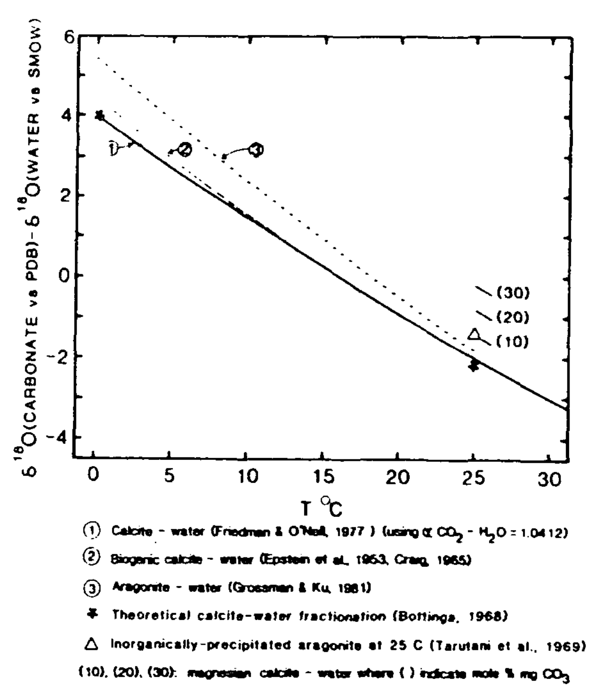

Figure 3.1 The temperature dependence of the oxygen isotopic fractionation between calcium carbonate and water. The curves plotted are for biological and inorganic precipitates. Also shown are the theoretical values for calcite, aragonite and Mg-calcite. (From Arthur & Anderson, 1983).

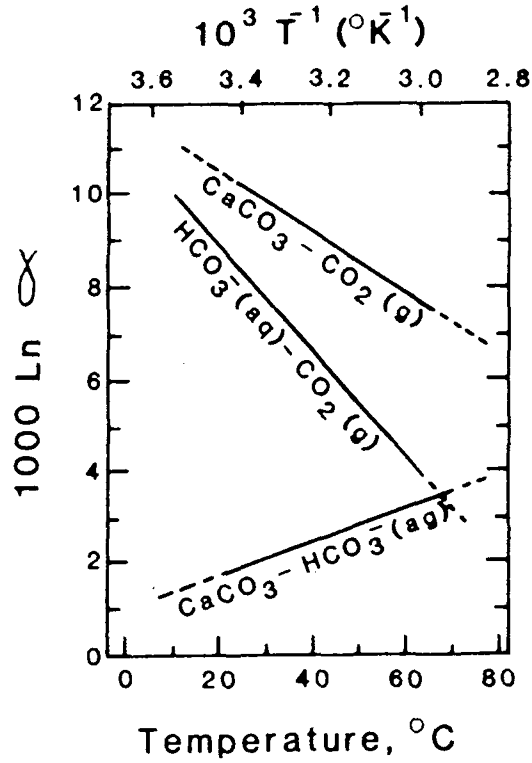

Figure 3.2 The temperature dependence of the carbon isotopic fractionation between calcium carbonate and seawater. (From Arthur & Anderson, 1983).

3.4 Biogenic Kinetic Fractionation.

The above equilibrium fractionations allow derivation of the theoretical composition of carbonates precipitating from seawater at various temperatures. If there is no biogenic mediation then the isotopic compositions of the cements should fall in the ranges described by those fractionations.

In order to be able to understand the effects of the biogenic mediation, the composition of the biogenic skeletal material has to be considered. Many organisms exert physiological controls on the carbon and oxygen isotopic composition of their skeleta and do not precipitate calcium carbonate at equilibrium with the oceanic HCO_3^-. These 'vital effects' are due to the mixing and isotopic exchange of seawater and metabolic CO_3^{2-} at or near to the sites of skeletogenesis. Metabolic CO_3^{2-} is depleted in both ^{13}C and ^{18}O due to a kinetic fractionation which occurs in both photosynthesis and respiration (Weber & Schmalz, 1968; Weber & Woodhead, 1970) and this therefore produces skeletal material lighter than would be expected from theoretical equilibrium calculations.

3.4.1 Oxygen fractionation.

Some calcifying organisms, notably the molluscs and brachiopods appear to produce skeletal material whose composition is equal to that expected for equilibrium fractionation from seawater (Epstein et al. 1953; Lowenstam, 1961). These organisms therefore record the seawater composition and temperature quite accurately. Several organisms are known to exhibit large deviations from predicted oxygen isotopic equilibrium. The corals for example (Weber & Woodhead, 1970, 1972) and the red algae (Keith & Weber, 1965) produce skeletal material up to 2.5 ‰ lighter than the equilibrium values (Figure 3.3).

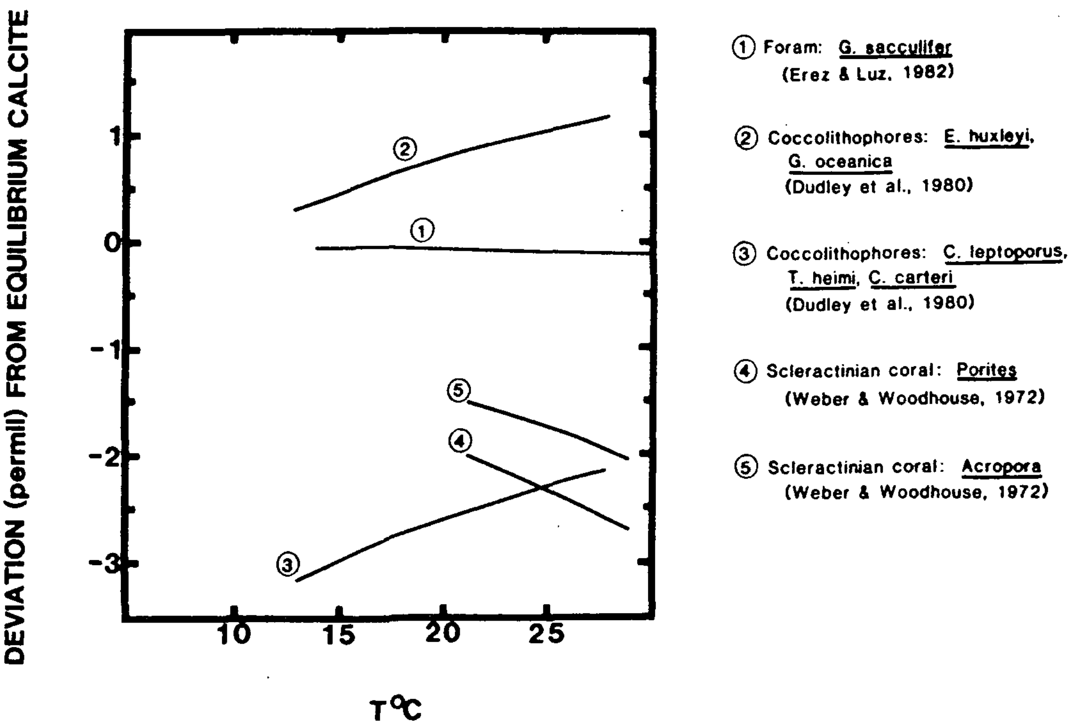

Figure 3.3 The deviation from oxygen isotopic equilibrium with water for some calcareous marine organisms. The curves numbered 4 & 5 are of particular interest as they for the corals *Porites* and *Acropora* respectively. (From Arthur & Anderson, 1983).

3.4.2 Carbon fractionation.

Carbon isotopic equilibrium is very seldom recorded in biogenic precipitation (Anderson & Arthur, 1983). The fractionation of the carbon isotopes takes place in a number of processes that occur in the organisms and these can interact in quite a complex manner. In the case of hermatypic corals, several models have been developed to describe this interaction (Goreau, 1977; Weber & Woodhead, 1970). Goreau's model divides the system into 9 pools (Figure 3.4) and although there is some doubt as to the validity of this system (Swart, 1983), it serves as a useful basis from which to study the possible isotopic compositions of cements precipitating within coral skeleta. The most significant problem with the model is that there is no consideration of the fractionations between the various dissolved carbonate species as shown in Table 3.1. Whilst HCO_3^- is the predominant species in the open oceanic reservoir, other species are certainly important within the skeletogenesis systems of the corals (Swart, 1983). Three areas of the model are of particular interest to this study, namely the seawater bicarbonate pool, the skeletal carbonate pool and the group of pools representing the coral – algal symbiosis. The latter includes the photosynthesis and respiration processes. A knowledge of the composition of these pools allows constraints to be placed on the possible routes for carbon in the system, as mass balance must always be obeyed. The composition of any pool therefore reflects the isotopic composition of the sources from which it was derived and the sinks which it supplies. Of specific interest to the precipitation of cements are the possible effects of the mass balance requirement of the three pools or groups of pools mentioned above on the isotopic composition of the porewater

HCO_3^- . This is shown schematically in Figure 3.5.

Confirmation that these mass balances do operate as described in the model, comes from the observation that the carbon isotopic composition of coral skeletal matter varies with the density of the zooxanthellae, (Cummings & McCarthy, 1982). As the density of zooxanthellae increases, the photosynthetic productivity increases. The carbon for photosynthesis comes from the intra-cellular carbon pool of the corals, and the preferential uptake of ^{12}C by the zooxanthellae (Park & Epstein, 1960) means that the internal pool becomes progressively enriched in ^{13}C. The corals use the same pool to source their skeletal matter and hence as the zooxanthellae density increases, so the isotopic composition of the skeletal material gets heavier. It is interesting to consider whether the same biogenic processes described in the preceeding paragraph may be capable of significantly altering the isotopic composition of the pore waters and furthermore, whether this is recorded in the precipitation of cements (Section 3.6.2).

The above model was developed for corals, but it might be expected that similar overall topologies of the pools may occur in other organisms, particularly the coralline algae. Whilst the pools may be similar, the demands on each will certainly be different from those of the corals, and from these differences comes a potential basis for distinguishing cements precipitated via a coral biogenic mediation from those precipitated via an algal biogenic mediation.

Equilibrium	ε [‰]
$H_2CO_3(aq) \leftarrow CO_2$ (g)	−0.8
$HCO_3^-(aq) \leftarrow CO_2$ (g)	+7.7
$CO_3^{2-}(aq) \leftarrow CO_2$ (g)	+6.4
$CaCO_3(s) \leftarrow CO_2$ (g)	+9.8
$CaCO_3(s) \leftarrow HCO_3^-$ (aq)	+2.1
$CaCO_3(s) \leftarrow HCO_3^-$ (aq) CALCITE	+0.35–3.37
$CaCO_3(s) \leftarrow HCO_3^-$ (aq) ARAGONITE	+1.7–4.8

Table 3.1 Carbon isotope fractionation factors for reactions involving inorganic carbonate species. Upper four are from Deines at al. (1974), lower two from Turner (1982).

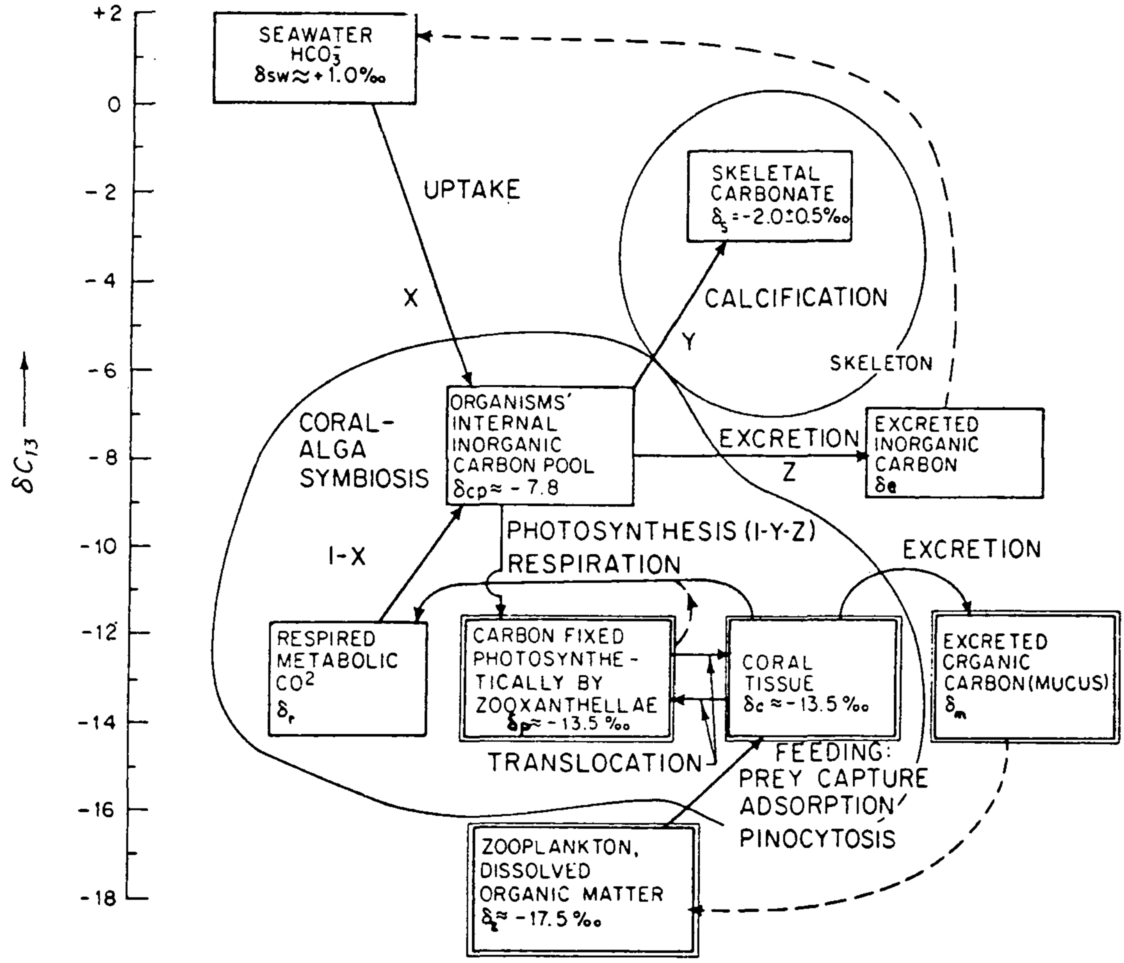

Figure 3.4 Model of carbon metabolism in corals. The inorganic pools are in single lined boxes and the organic pools in double lined boxes. Of paticular interest in this study are the effects of the biogenic cycles on the seawater bicarbonate reservoir. (From Goreau & Hayes, 1977).

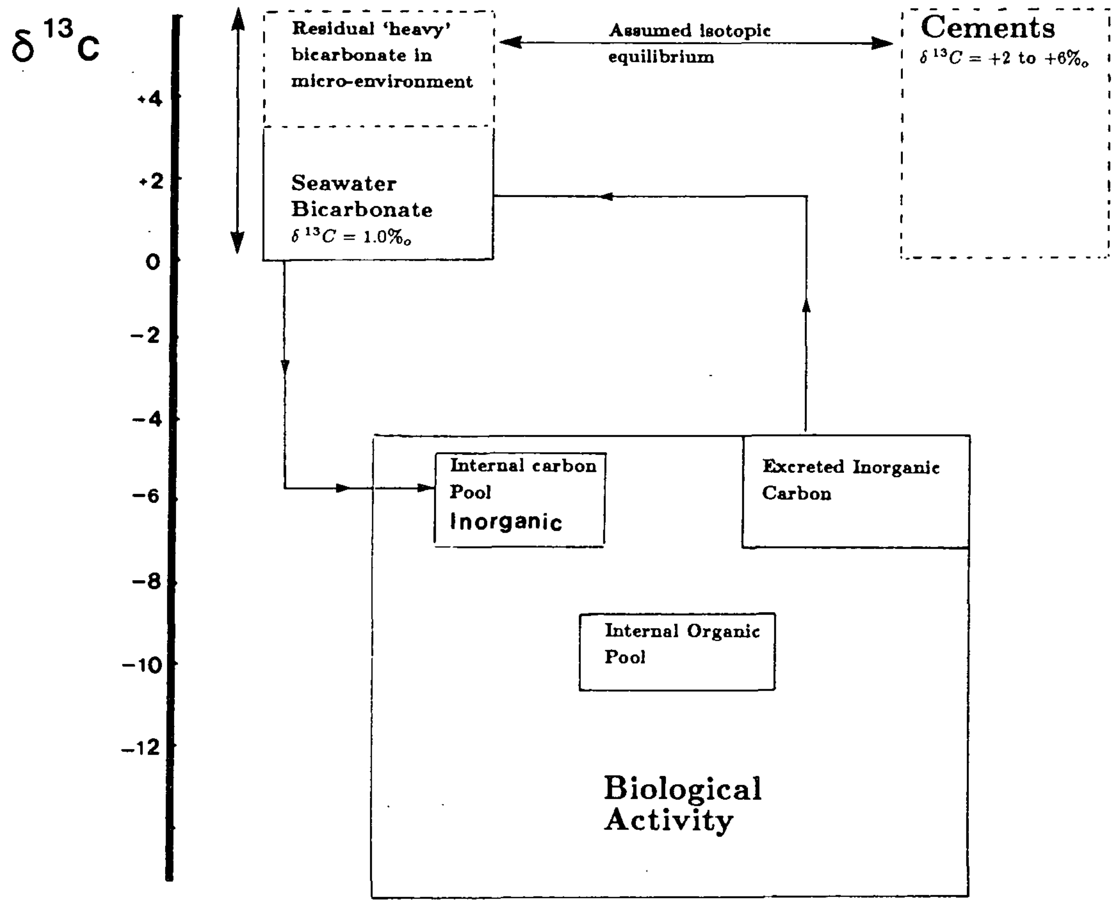

Figure 3.5 Simplified version of Figure 3.4, indicating the possible effects of the biogenic cycle, either enriching or depleting the carbon isotopic composition of the ocean bicarbonate. This could lead to enrichment or depletion of the precipitated cements.

3.4.3 Other kinetic effects.

A major problem with the calculated equilibrium fractionation of carbon isotopes (Section 3.3) is that they are apparently dependent on the rate of precipitation of the carbonate. In a series of rate controlled experiments with precipitation of calcite and aragonite, Turner (1982) discovered that the isotopic fractionation of ^{13}C depended on the precipitation rate, as was first suggested by McCrea (1950), being lower at faster rates. Turner (1982) reported that $\varepsilon_{CaCO_3-HCO_3^-}$ for the precipitation of calcite varies from 0.35 ‰ to 3.37 ‰ at 25 °C. The value of $\varepsilon_{aragonite-calcite}$ was estimated as 1.4 ‰ at slow precipitation rates, diminishing at higher rates.

The suggestion is that an instantaneous precipitate will have a composition identical to that of the reservoir as the isotopes would not have enough time to reach their equilibrium fractionation. Only at slower rates is the true thermodynamic equilibrium reached. These figures are compared in Table 3.1 with those previously derived (Section 3.3).

These additional factors complicate the problem of identifying the controls on the isotopic compositions of cements. Furthermore, before one can start to analyse the data on the cements, it is necessary to know the precise isotopic composition of the oceanic HCO_3^- reservoir, and as described in the following section, this can also vary considerably.

3.4.4 The isotopic composition of seawater.

There is a great scarcity of data for the isotopic composition of seawater in the Florida area. The data used in this discussion comes from studies on the Great Barrier Reef (Swart & Coleman, 1980) and in the North-Atlantic, (Kroopnick et al., 1972). The $\delta^{18}O$ composition of seawater is dependent on the salinity (Lowenstam, 1957) but local variations have generally been considered not to affect the isotopic composition of skeletal material. However, Swart & Coleman (1980), reported that the local variation around Heron Island Reef on the Great Barrier Reef is 0.4–1.7 ‰ (SMOW), which could mask the expected temperature variations. This variation could certainly be recorded in the precipitation of cements and it is important to note that the above range represents $5\,^{\circ}C$ (as calculated from equation 3.2). The predominant species of dissolved carbon is HCO_3^-, whose $\delta^{13}C$ composition is thought to be approximately 1 ‰ (PDB), but this is also known to vary (Weber, 1971).

3.4.5 Other possible sources of variation.

There are two final points which should be noted :

i) The variation in seawater temperature on and around reefs can be up to $12\,^{\circ}C$ daily (Swart & Coleman, 1980) and is up to $9\,^{\circ}C$ in the Florida area on a seasonal basis (Emiliani et al., 1978). Although this will not affect the carbon isotopic composition of the cements by very much, it represents a 2.5 ‰ variation in the $\delta^{18}O$ of precipitated carbonate and could therefore mask any potential biogenic control on the oxygen isotopic composition of the cements.

ii) The $\delta\,^{13}C$ and $\delta\,^{18}O$ composition of the reservoir HCO_3^- is known to vary by up to 1 ‰ depending on whether it is day or night. This variation occurs due to the alternation of the photosynthesis and respiration cycles. Photosynthesis during the day removes light carbon and oxygen from the reservoir, leaving it enriched in the heavier isotopes. The reverse occurs during the night, when respiration returns light isotopes to the reservoir. Although the oceanic reservoir is very large and so might be expected to be buffered against these effects, diurnal variations of this sort have been measured in areas of high productivity such as would be expected on the reef flat (Weber, 1971).

In summary, both carbon and oxygen isotopic fractionations differ markedly from the expected thermodynamic equilibrium values. In addition, the composition of the dissolved carbon and oxygen species varies significantly, due to several interdependent factors. It may be that such uncertainties are sufficient to mask the potential effects of biogenic mediation of the isotopic geochemistry of the cements, and the results should therefore be interpreted with some caution.

3.5 Results.

3.5.1 Sample collection.

Several points need to be made with regard to the philosophy behind the collection of samples. Isotopic data on Recent marine cements are very scarce, presumably reflecting the difficulty of collecting pure samples of large enough size for analysis. Typical problems are illustrated in the early work, when authors have noted that cement samples could have been contaminated with the surrounding skeletal material. When attempting to interpret the data on modern cements in terms of any possible biogenic mediation, it is clearly of the utmost importance to ensure that the cement samples are indeed free of contaminating skeletal material.

The petrography of the modern reef material has indicated that the controlling processes are operating on a variety of scales, and that the microenvironments may differ from pore to pore. In order to ensure that the data collected are representative of processes operating on such small scales, collection of individual samples ought ideally to be from single pores. The minimum sample necessary to provide a reliable result has proven to be between 100 and 200 micrograms, and whilst most of the analysed samples were collected from single pores, a few had to be collected from several pores in order to obtain enough material. In every case, however, all the material came from less than 10 individual pores within 1 or 2mm. of each other.

Sampling was carried out under the binocular microscope under both transmitted and reflected light, from unpolished $60\mu m$. thick thin sections, using dental drills carefully ground down to points of approximately $20\mu m$. in diameter. The sampling was done in a two stage process, first removing all the surrounding non-cement material, thereby making it easy to ensure that the cement samples collected in the second stage were uncontaminated (Figure 3.6). The samples were transferred into micropipettes on the surface of the thin section, these could then be easily sealed for storage and later analysis.

The full data set is presented in Table 3.2 and Figure 3.7.

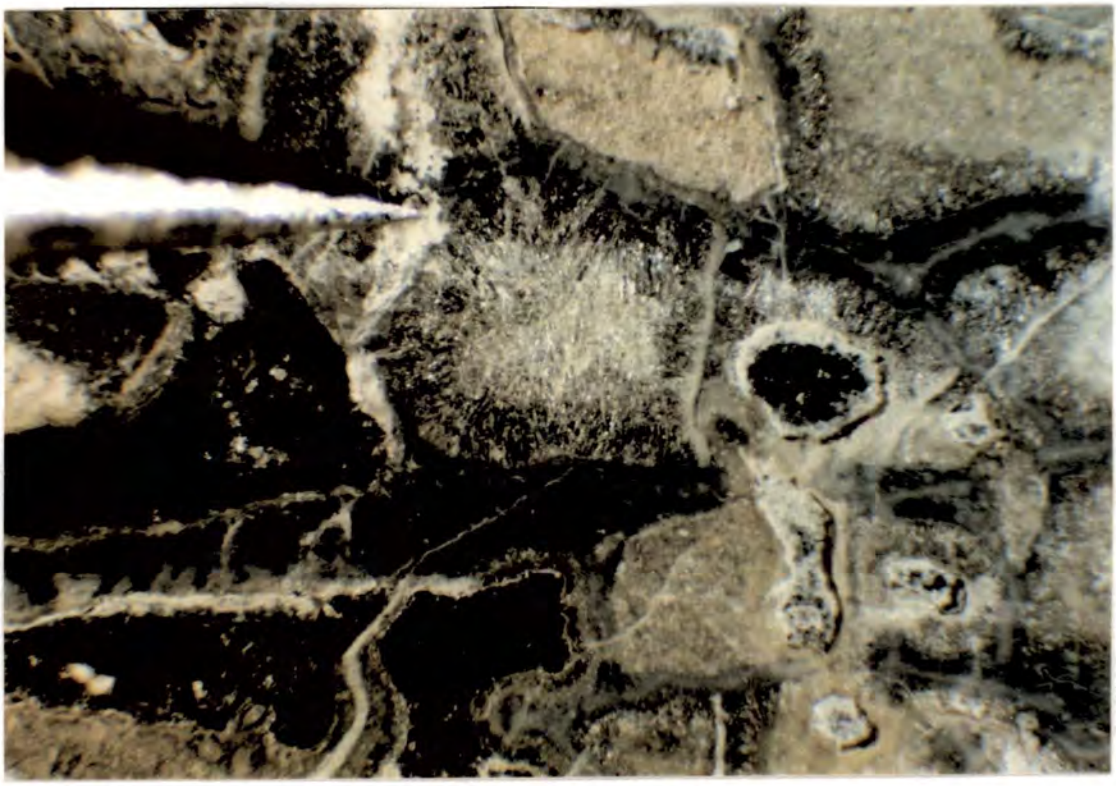

Figure 3.6 Illustration of the collection of cements for isotopic analysis. Extraneous material surrounding the cement is removed in the first stage, which is almost complete in the lower photograph. The cement is then scraped off the thin section with the tool shown above, and then collected and put into a micro-pipette on the surface of the thin section.

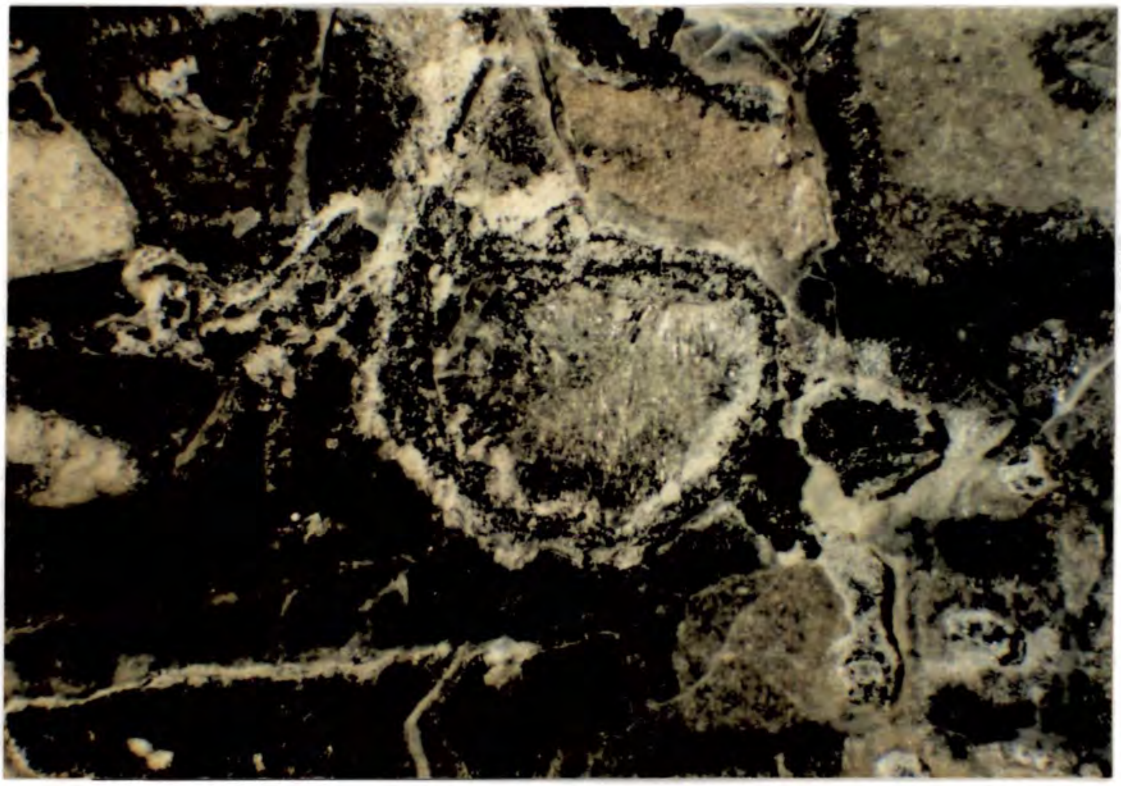

Figure 3.6 .

3.5.2 What can we hope to deduce ?

The discussion in the previous sections indicates that although the isotopic composition of the cements may be a powerful tool to aid the interpretation of their origin, the many possible processes leading to fractionation could mask the effects of the biogenic mediation, if indeed any exists. It is useful therefore to consider which aspects of the possible roles (as listed in Section 3.1), might be expected to be reliably interpreted. Three major possibilities are being considered.

i) Organisms acting as skeletal sources of Ca^{2+} and HCO_3^- ions.

ii) Organisms acting as organic sources of the carbon in HCO_3^- .

iii) Organisms acting in a purely mediatory fashion, with potential modification of the geochemical microenvironment, but not acting as major sources of HCO_3^- .

The first and second processes would be expected to be very easy to recognise as they would lead to light isotopic compositions. The $\delta^{13}C$ composition of the internal inorganic carbon pool of corals is approximately -7.5 ‰ (Figure 3.4). $CaCO_3$ forming from fluids of such composition would then be expected to have $\delta^{13}C$ compositions of -3.5 ‰ to -7.5 ‰ due to the fractionation involved in the precipitation ($\varepsilon_{CaCO_3-HCO_3^-} = 4$ ‰ at maximum). The internal organic pool has a $\delta^{13}C$ of approximately -13 ‰ , and cements precipitated from such fluids would therefore fall in a range of -9 ‰ to -13 ‰ . Decomposition of the organic matter in an anoxic environment could lead to heavy $\delta^{13}C$ compositions, due to the input of methanogenesis (Irwin et al., 1977). Although this process is unlikely to occur in the oxic environment of modern reefs, methane derived cements have been recognised in reefs of the Great Barrier Reef (Sansone, 1985).

The third process may be much more difficult to demonstrate conclusively, as the variations would be expected to be quite small and probably of comparative order to the $\delta^{13}C$ variations in the HCO_3^- reservoir and the $\delta^{18}O$ variations caused by temperature fluctuations. The concept of this direct biogenic mediation is based on the fact that the organisms are not acting as a major source of HCO_3^-, but may be promoting the precipitation within microenvironments by adding to the pore water HCO_3^- content. Although it is not necessary to invoke such contributions from organisms in order for precipitation to occur (as the pore waters are already supersaturated with respect to aragonite and Mg calcite), the input may still be significant. Such input can be either from respiratory CO_2 or from inorganic body fluids normally excreted at skeletogenesis sites. Both of these would be expected to impart a light isotopic composition to the pore fluids. However, the signature will be diluted by the pore waters suggesting that it is unlikely that this input would be reliably identified from either carbon or oxygen isotopic data.

The reverse effect on the isotopic composition can also be argued, although in this instance there would be no biogenic catalysis. In corals with a high density of photosynthesising zooxanthellae, it has already been noted that recognisable enrichment of the inner body fluids occurs. The corals themselves withdraw HCO_3^- of $\delta^{13}C$ about $-7.5\,‰$ and in removing this light carbon may cause enrichment of the reservoir HCO_3^-. This was the process suggested to be occurring in Section 3.4.2 (Weber & Woodhead, 1970). Unfortunately as the dilution effect of the reservoir will still operate, the maximum enrichment would probably be of the order of 2–3 ‰ and this could be masked by the previously described non-equilibrium kinetic effects (Section 3.4.3). Only in the case of a slowly precipitated cement, such that $\varepsilon_{CaCO_3-HCO_3^-}$ was equal to the equilibrium value could such an effect be reliably identified. In such an example, with a normal seawater HCO_3^- $\delta\,^{13}C$ composition of 1 ‰ , locally enriched to perhaps 2–3 ‰ by the biogenic mediation, and $\varepsilon_{CaCO_3-HCO_3^-}$ at a maximum of 4 ‰ , the resulting cement would therefore be expected to have a $\delta\,^{13}C$ of 7–8 ‰ . There are no reported modern reef cements of that $\delta\,^{13}C$ composition.

Holocene Reef Cements - Isotopic Composition.

Sample Number	Locality	Cement Morphology	Mineralogy	$\delta^{13}C$ ‰[PDB]	$\delta^{18}O$ ‰[PDB]	Calculated Temp. [°C]
1	Belize	Botryoid 1	A	4.39	0.78	17.6–22.3
2	Belize	Botryoid 2	A	4.22	0.81	17.6–22.3
3	Beli	Botryoid 3	A	4.32	0.73	17.8–22.5
4	Beli	Botryoid 4	A	4.24	0.28	19.4–24.1
5	Beli	Botryoid	A	4.71	1.29	15.9–20.6
6	Beli	Substrate	A/C	3.79	1.24	—
7	Beli	Fibrous	A	4.30	1.26	15.9–20.6
8	Beli	Spherulite	A	4.76	0.84	17.5–22.2
9	Beli	Substrate	A	0.72	−1.64	—
10	Beli	Peloid	C	3.50	1.58	14.4–19.8
11	Beli	Peloid	C	3.51	1.52	14.5–19.9
12	Beli	Micrite	A/C	2.64	0.82	—
13	Flori	Peloid	C	3.03	−0.27	22.0–28.1
14	Flori	Micrite	A/C	3.07	−0.54	—
15	Flori	Micrite 2	A/C	2.61	−0.31	—
16	Flori	Fibrous	A	4.47	−0.66	22.8–27.5
17	Flori	Substrate	A	−2.31	−4.36	—
18	Flori	Peloid 2	C	2.83	−0.21	22.0–28.1

Table 3.2. ples 1–4 represent a transect across a Botryoid of 3cm in size. The samples w llected at equal spacings, perpendicular to the growth direction, Sample 4 the youngest. 'Substrate' refers to the sample immediately above. A = ar te, C = high Mg-calcite.

Tempera es calculated from $\delta^{18}O_{PDB}$ of sample and water $\delta^{18}O_{SMOW}$ ranging 0.4 to 1.7‰ (see 3.4.4.)

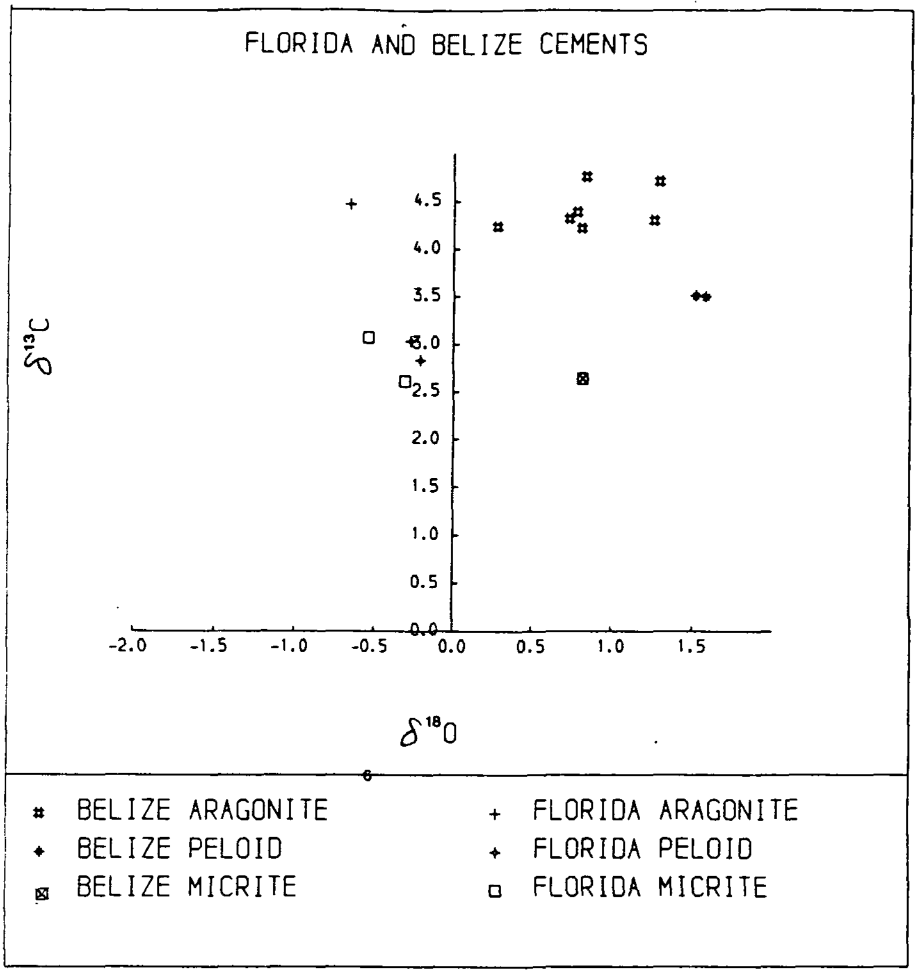

Figure 3.7 Crossplot of the stable carbon and oxygen isotopic compositions of the Florida and Belize cements. Note that the Belize cements have heavier oxygen isotopic compositions than the Florida examples. Further discussion in text.

3.6 Interpretation.

3.6.1 Oxygen isotopes of the Florida samples.

The oxygen isotopic composition can be interpreted in terms of the temperature of the water from which it was precipitated, and as we already know the likely temperature ranges, any deviation from the expected value could indicate either unusual seawater composition or a biogenic effect.

The $\delta\,^{18}O$ of the fibrous cement from Florida (Sample 16) is $-0.66\,‰$. Using equation 3.3 and a seawater composition of $\delta\,^{18}O\ =\ 0.4$–$1.7\,‰$, this implies a temperature of 22.8–27.5 $°C$, which is within the temperature range measured at Hens and Chickens reef, Florida (Emiliani et al., 1978). It is likely therefore that the aragonite is a purely inorganic precipitate at equilibrium with normal seawater.

The $\delta\,^{18}O$ of the peloidal Mg-calcite cements is slightly heavier at $-0.27\,‰$, and this probably reflects the different equilibrium fractionation of the magnesium calcite. Tarutani et al. (1969) suggested that Mg-calcite is 0.06 ‰ per mole% $MgCO_3$ heavier relative to calcite and that aragonite fractionation is 0.6 ‰ greater than calcite at 25 $°C$. The Mg-calcite peloids are approximately 15–17 mole% $MgCO_3$ (Appendix 2), which implies that they ought therefore to be 15–$17\times\ 0.06\ =\ 0.9$–$1.0\,‰$ heavier than calcites or 0.3–0.4 ‰ heavier than aragonites. Within the experimental error, this comparison fits. The Florida cements appear therefore to be precipitated in oxygen isotopic equilibrium with normal seawater.

3.6.2 Oxygen isotopes of the Belize samples.

The botryoidal and fibrous aragonite cements collected from the Belize samples show significantly heavier oxygen isotopic compositions compared to the Florida samples. Using the same range of seawater $\delta^{18}O$, the supposed temperature of precipitation is 15.9–22.5 $^{\circ}C$ for all but Sample 4 which is somewhat higher at 24.1 $^{\circ}C$. These temperatures are markedly lower than calculated for the Florida cements and significantly lower than the measured temperature of the present day Belize surface water (28 $^{\circ}C$), according to James & Ginsburg (1976). Even for the deepest sample analysed, at 100 metres, the measured temperature is 25 $^{\circ}C$, still higher than the range calculated from the $\delta^{18}O$ samples. The salinity variations with depth of approximately 1 ‰ (37 ‰ at 100m c.f. 36 ‰ at the surface), would only alter the $\delta^{18}O$ by 0.2 ‰ (Lowenstam & Epstein, 1957) so this cannot explain the discrepancy either. Similar results have been published for analyses of cements from a variety of areas (Gonzalez & Lohmann, 1985). Assuming that the equilibrium fractionation factors are correct (Section 3.3), two explanations can be suggested to account for the heavy $\delta^{18}O$ composition. Either the seawater $\delta^{18}O$ is significantly heavier than 1.7 ‰ or the cements are precipitated out of equilibrium with the seawater, possibly due to some biogenic mediation. If the latter is true then it would have to be a type (iii) mediation with the organisms removing light oxygen from the reservoir, leaving it enriched in the heavy isotope.

If the cements were precipitated at a glacially related low stand in sea-level, as might have been the case at 15,000 years b.p. (the maximum age of the Belize samples), then the water could be expected to be slightly heavier in

$\delta^{18}O$ composition. An enrichment of approximately 1.2 ‰ has been suggested (Anderson & Arthur, 1983; Saller, 1986). In addition, the temperature of the sea water may have been up to 1.5 °C lower at that time (Broecker, 1982). These two corrections imply an expected minimum sea water temperature of 23.5 °C, and a range as calculated from the $\delta^{18}O$ of the cements of 23.5–28.2 °C, assuming the $\delta^{18}O$ of the water is 3.0 ‰ . Under these conditions, the cements could have been precipitated at equilibrium with the sea water.

It is tempting to try and compare the relative cement–coral substrate compositions of the Belize samples 8 and 9 and the Florida samples 16 and 17, but having illustrated the many problems in the previous sections, any conclusions would be rather tenuous. However, the fact that all of the Belize samples have heavier isotopic compositions than their Florida equivalents tends to suggest that there may be a difference in the seawater composition.

The Belize peloidal cements show a $\delta^{18}O$ enrichment of 0.3–0.4 ‰ relative to the fibrous cements which is very similar to that observed for the Florida samples, again surely a result of the different equilibrium fractionations of the two minerals, as predicted by Tarutani et al. (1969). Sample 12, a non-peloidal micrite, shows an expected lighter oxygen isotopic composition compared to the peloidal cements, due to the input of biogenic material to the micrite.

It is interesting to note the drop of 0.5 ‰ in the youngest sample of the botryoid samples 1 to 4. This corresponds to an increase in temperature of 1.6 °C. However, this may not be significant when the experimental errors and other possible variations are considered.

3.6.3 Carbon isotopes of the Florida samples.

The carbon isotopic composition can be interpreted principally on the basis of the source of the carbon and hence whether precipitation is from seawater of normal composition. Smaller scale variations near to the equilibrium fractionation may be controlled by different rates of precipitation (Turner, 1982).

The fibrous aragonite cement from Florida (Sample 16), has a $\delta\,^{13}C$ of 4.47 ‰ which suggests a fractionation of approximately 3.5 ‰ from the normal seawater $\delta\,^{13}C$ of 1 ‰. The equilibrium fractionation measured for calcite at $25\,^{\circ}C$, $\varepsilon_{CaCO_3-HCO_3^-} = 1.8$ ‰ (Emrich et al., 1970) and Turner (1982) estimated $\varepsilon_{Calcite-Aragonite} = 1.4$ ‰ (1.6 ‰ according to Rubinson & Clayton 1969), so that for aragonite, $\varepsilon_{CaCO_3-HCO_3^-}$ = 3.2–3.4 ‰. The fibrous cement is therefore within the range expected for equilibrium fractionation.

The lighter carbon isotopic composition of the peloids ($\delta\,^{13}C = 3.03$ ‰), is probably indicative of a faster rate of precipitation, although it could be interpreted in terms of a minor input of organically-derived carbon. The former theory is supported by the fine grained nature of the crystals forming the peloids, which is itself indicative of a faster precipitation rate.

The micrite of Sample 15 has a slightly lighter isotopic composition than the peloids, again indicative of the input of light carbon skeletal material, and is similar to the Belize micrite (Sample 12). However, the first Florida micrite (Sample 14) has the same $\delta\,^{13}C$ value as the peloidal cements, suggesting that it may have a significant precipitated component, bringing it to a level between the fibrous aragonite and the other micrites. This further illustrates the difficulty in distinguishing between fine-grained precipitated and mechanically deposited materials.

3.6.4 Carbon isotopes of the Belize samples.

The botryoidal and fibrous aragonite cements have similar $\delta\,^{13}C$ values, both within the Belize samples and when compared to the Florida fibres, all falling in a range of 4.2–4.8 ‰. This almost certainly implies precipitation at equilibrium with unmodified seawater, with no biogenic mediation detectable. The peloids are again approximately 1 ‰ lighter than the fibrous cements, mirroring the trend observed in the Florida samples. The similarity of the Florida and Belize micrites (Samples 12 & 15) has been previously noted, but it is interesting to compare the $\delta^{13}C$ of those with the Sample 6 micrite, which was clearly lithified with a significant recognisable component of cement. This sample shows an expected alteration towards the heavier carbon isotopic composition of the precipitated phases. Finally, there is no significant trend across the botryoidal cement (Samples 1–4).

3.6.5 General conclusions.

i) Oxygen isotopes.

The oxygen isotopic composition of the Florida cements is indicative of precipitation at an equilibrium fractionation from normal seawater at temperatures from 23–28 $^\circ C$, with no detectable biogenic influence. The Belize oxygen composition, in contrast, is somewhat heavier than can be explained for suitably sub-tropical temperatures and normal seawater. Although some biogenic mediation could explain these figures (Section 3.4.1), this is not in any way confirmed by the $\delta\,^{13}C$ composition. The fact that the Belize samples are consistently heavier than the analogous Florida examples suggests that the Belize seawater may have been enriched in ^{18}O relative to the Florida water. In order to bring the Belize calculated temperatures into the reasonable range of 23–28 $°C$, the seawater HCO_3^- would have to have a $\delta\,^{18}O$ composition of 3.0 ‰ , possible if glaciation effects are considered. The consistent differences between the $\delta\,^{18}O$ of aragonite and Mg-calcite cements are in accordance with published estimates of the respective equilibrium fractionation factors.

ii) Carbon isotopes.

All of the cement samples analysed show $\delta\,^{13}C$ compositions within the ranges expected from published equilibrium fractionation estimates. The Mg-calcite peloids show a substantially lighter composition which is thought to be due to a smaller $\varepsilon_{CaCO_3-HCO_3^-}$ due to the faster precipitation rate. It could also be suggested that the lighter composition is due to some input from an organic source, and indeed organic matter is closely associated with the peloid inorganic phase. The $\delta\,^{13}C$ of this organic matter has been measured at approximately −26 ‰, (Appendix 4), and therefore an input of 5% of the carbon from the organic source would be sufficient to produce the observed 1 ‰ difference between the peloidal and fibrous cements.

3.7 Comparison with other Data.

There are a number of published studies which present large amounts of data on the isotopic compositions of carbonate sediments, but very few of these analyses are of pure modern marine cements (Shinn, 1969; Ginsburg et al., 1971; Land, 1971; Milliman, 1974; James & Ginsburg, 1979; Land et al., 1979;

Macintyre, 1982; Botz & von derBorch, 1984; Gonzalez & Lohmann, 1985). The data available are shown in Figure 3.8 together with the samples analysed in this study. The compositions of the cements can be seen to be very similar to the previously reported analyses, the latter including data on ooids, which are also considered to be inorganic precipitates. There are reports of other samples which have extremely depleted carbon isotopic compositions (Hathaway & Degens, 1969; Nelson & Lawrence, 1984); these are supposedly derived from methane and are certainly not precipitated from normal marine waters.

Data shown are for those samples described as cements only, no whole rock values are included.

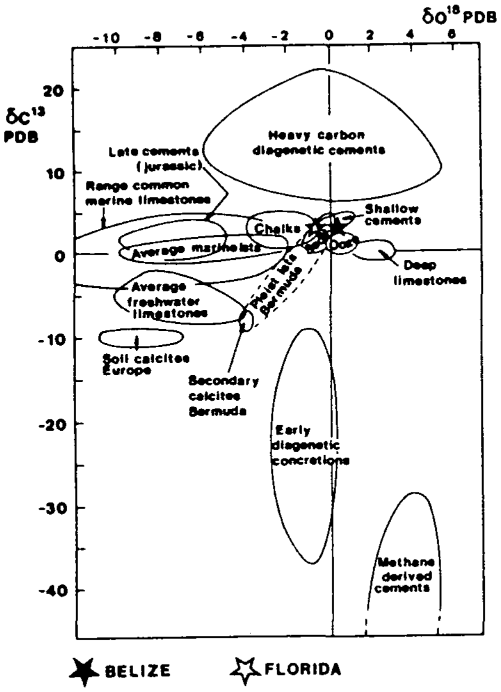

Figure 3.8 Comparison of the data collected in this study with that published. Discussion in text. (From Hudson 1977). Cements analysed in this study are shown by stars above and see key below.

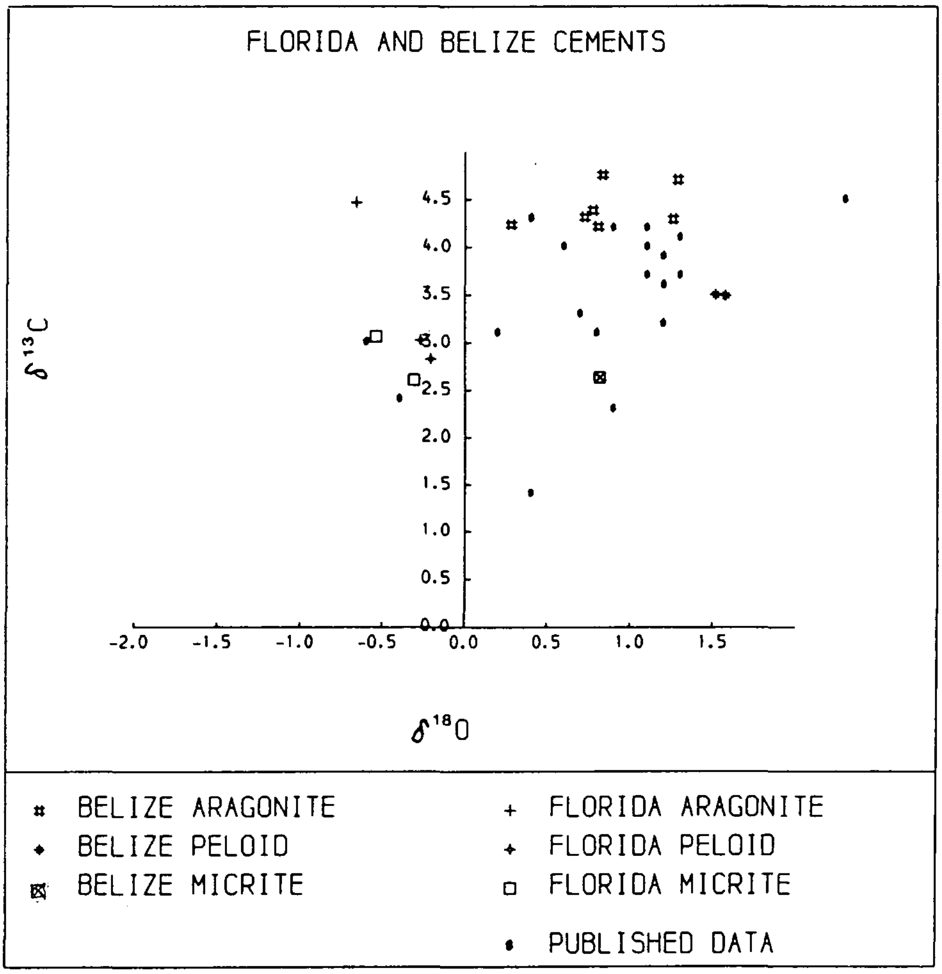

3.8 Conclusions.

The discussion presented in this chapter illustrates the complexities involved in determining the equilibrium fractionations for the precipitation of carbonate cements from seawater. The fine scale variations observed in the carbon and oxygen isotopic compositions of cements collected from the reefs of Florida and Belize can be accounted for by a variety of processes, and in most cases it is impossible to identify the relative inputs of each. Variation in the seawater composition, the temperature of the water, the rates of precipitation and the intensity of the organic productivity can all individually create a spread in the $\delta\,^{13}C$ and $\delta\,^{18}O$ compositions of the cements of several ‰. It is therefore difficult to make a conclusive identification of any biogenic mediation, as the influence of this mediation would be of very similar order of magnitude to the intrinsic variations in the system.

However, with respect to the four originally defined possible roles for biogenic processes in the precipitation of modern marine cements, the following certain conclusions can be made :

i) Direct source of $CaCO_3$ from inorganic body fluids. This would result in cement compositions similar to that of biogenic skeletal material, and is certainly not observed in the Florida and Belize reefs.

ii) Direct source of HCO_3^- from the decomposition of organic material. If this process was occurring, the cement compositions would be expected to show light carbon isotopic signatures. Although there may be a slight input to the peloidal cements, this process is of no general significance.

The above inputs would be expected to occur after death of the organism involved; process (iii) in contrast, would only operate during the living cycle. Process (iv) could occur at any time.

iii) Direct biogenic mediation. This type of mediation is based on the concept that the organisms may be able to control the geochemistry of the cements, by changing the pore water geochemistry. In terms of the isotopic composition of the cements, this mediation could cause either enrichment or depletion in both $\delta\ ^{13}C$ and $\delta\ ^{18}O$, (as argued in Section 3.5.2). The only possible example of this effect is seen in the heavy isotopic composition of the Belize cements. However, the trend is not confirmed by the carbon isotopes of the same samples, and the conclusion has to be that no clear evidence of this type of biogenic mediation has been observed.

iv) Indirect biogenic mediation would not be expected to alter the isotopic composition itself, but if it increases the rate of precipitation, an indirect effect could be observed. The peloidal cements do appear to be precipitated under the influence of some organic matter, which is undoubtedly of biogenic origin (Chapter 4).

The data for the different mineralogies appear to confirm the reported difference in the equilibrium fractionation factors for aragonite and magnesium-enriched calcites. With the exception of the peloidal cements, where some indirect biogenic catalysis is suspected, all of the modern marine cements observed in this study are therefore thought to be precipitated by purely inorganic processes.

CHAPTER 4

The Role of Organic Matter in the Precipitation of Cements.

CHAPTER 4

The Rôle of Organic Matter in the Precipitation of Cements.

4.1 Introduction.

The interaction of organic matter with the inorganic phase in the precipitation of carbonates is a process which has been much studied, but it is nevertheless only poorly understood. Bathurst (1975) reiterated the thoughts of Cayeux (1935) who stated that it was surprising that "so large a body of writing should contain so small a measure of definite achievement". These observations were made specifically relating to the formation of ooids, but a similar feeling was echoed by Degens (1979). In a review of biomineralisation he suggested that the assertion of Urist (1962), that "the nature of the local mechanism of calcification is one of the most important unsolved problems in biochemistry", was still largely correct.

The same mystery surrounds the problems of the interaction of organic matter in the precipitation of cements in modern reefs, as illustrated in several recent publications. Given & Wilkinson (1985) stated that "the role of organic matter is enigmatic", with regard to the composition of the cements and Marshall (1985) acknowledged the fact that the precipitation of cements is not understood with relation to "biological factors". Organic metabolism is recognised to be an important influence on the diagenesis of reefs in a recent review by Schroeder & Purser (1986), but a thorough understanding of the nature of the involvement is still not apparent.

The widely based literature on calcification emanates not only from the geological sciences, but also from the realms of pure chemistry and biochemistry and from the medical profession. The latter deals mainly with the precipitation of calcium phosphates in bones and cartilage, but calcium carbonate is known to precipitate pathologically. In addition, there are significant similarities in the published ideas on phosphate deposition in humans and carbonate deposition in other organisms.

The literature on calcification in the geological sciences presents a rather confused picture of the nature of the organic-inorganic interactions. Suggestions range from inhibition of precipitation to active catalysis of the nucleation process and the confusion arises because there is no general rationale or theory to account for these two opposites. This introduction is not intended to be a review of the literature, as several summaries exist elsewhere, but it is useful to mention some previous work in order to illustrate the different ways in which organic matter has been suggested to be involved in the cementation process.

Early studies on the effects of pure organic compounds on the precipitation of $CaCO_3$ showed that the formation of calcite was encouraged by some compounds, whereas others caused aragonite to precipitate (Kitano & Hood, 1965; Kitano & Kanamori, 1966). Conversely, Chave (1965) discovered that carbonate particles are coated with a thin layer of organic matter which hinders the equilibration with seawater. Several other studies demonstrated that carbonates actually adsorb the organic coatings from the water (Chave & Suess, 1967; Suess, 1970, 1973). The kinetics of the precipitation of aragonite were investigated in some detail by Berner et al. (1978), and the inhibitory effects of both pure and natural organic matter were noted. Whilst the earlier work had suggested that the degree of inhibition was proportional to the number of carboxyl (COO^-) groups, Berner found this to be inconsistent. The inhibition does not follow the binding affinity for Ca^{2+} either, as EDTA (ethylene-di-amine-tetra-acetic acid), which chelates Ca^{2+} ions very strongly, does not appear to affect the kinetics (Berner et al., 1978).

Organic matter is thought to play a more direct role in actively promoting the precipitation of ooids (Mitterer, 1968; Mitterer & Cunningham, 1985). Experimental results support this suggestion as some success has been achieved in producing ooids in the presence of humic materials in the laboratory (Davies et al., 1978; Ferguson et al., 1978).

There is an equally diverse literature on aspects of biomineralisation, recently reviewed by Degens (1979), Lowenstam (1981) and Leadbeater & Riding (1986). Although the results of the previous chapter indicate that there is no major direct biogenic control on the precipitation of cements, a valuable insight into the possible modes of interaction of organic and inorganic phases can be gained by studying the processes of biological mineralisation. Any organic matter that is involved will be ultimately of biogenic origin, and it is likely that the interactions would be similar, particularly on the molecular level at which this study is directed.

The roles and degree of involvement of the organic matter are clearly diverse, being both preventative and promotional in nature. The fact that such diversity exists, illustrates the powerful control that biochemical processes can exert. In exceptional circumstances, as discussed in Section 4.6.2, it is conceivable that the same molecule can play both opposing roles simultaneously, albeit under strict spatial biological control, and it is clear that a thorough understanding of the products of the organic-inorganic interaction can only be derived from the study of the processes at the molecular level. The intention of this chapter is first to outline the mechanisms of this interaction from a chemical point of view, hopefully thereby clarifying the role of organic matter in the precipitation of carbonates, and second to investigate the source and nature of the organic matter associated with the Mg-calcite peloids described earlier (Section 2.7.5).

Section 4.2 briefly outlines the past literature which has directly considered the role of organic matter in cement formation and Section 4.3 formally defines the possible roles in which organic matter could be involved and considers the potential sources of such organic matter. The major part of the chapter is a study of the organic matter associated with the peloidal cements. Section 4.4 discusses the sample preparation and extraction of the organic matter, highlighting the problems of contamination, and the precautions taken to ensure that any such contamination is recognised. The emphasis throughout the chapter is on the necessity for a full characterisation of the organic matter to be made. This characterisation is split into two parts. The first discusses the origin and source of the organic matter through the recognition of molecular biomarkers (Section 4.5), and the second (Sections 4.6 & 4.7), attempts to define the molecular nature of the organic-inorganic interaction. Section 4.8 concludes the chapter. N.B. All molecular structures are presented in Appendix 4. Structures illustrated are referred to through the use of roman numerals given in parentheses after the name of any compound.

4.2 Organic Matter and the Precipitation of Cements.

The fact that organic matter may play a role in the precipitation of cements was recognised shortly after it was first realised that cements are precipitated in the marine environment. In order to explain the prevailing supersaturation state of seawater, several authors have suggested that all carbonate particles are coated with organic matter , thereby actually preventing precipitation from occurring, (Chave & Suess, 1967). The suggestion that organic matter might act as a nucleus for precipitation was first made by Mitterer (1968, 1972), and shortly after this it was realised that organic matter might be affecting the cementation of modern reefs (Schroeder, 1972b). Since then, most studies on the morphology and mineralogy of cements in reefs have invoked a general involvement of organic matter in the cementation process. It is very common to see unusual or otherwise inexplicable geochemical observations to be attributed to "some process, presumably organic in nature ". It is hoped that the study presented in this chapter will enable a more precise definition of this concept to be made.

Earlier sections of this thesis have indicated that there is no biogenic or organic involvement in the formation of most of the cements precipitated in the early marine diagenetic environment. The one important exception to this is the case of the Mg-calcite peloidal cements, which form approximately 50% of the total volume of cement observed in the Florida reefs. These cements are clearly associated with organic matter (Figure 2.45), but its role is not fully understood. The peloids are not just a local phenomenon, as they have been reported from reefs all over the world, and most authors have mentioned the presence of organic matter.

Section 2.7.5 outlines the extensive discussion of the origin and mechanism of formation of the peloids, but of the many publications, none have attempted to investigate the nature of the organic matter. One of the most recent suggestions has been that the peloids are a bacterially induced precipitate (Chafetz, 1986), and some organic chemical data were cited as evidence to support such a conclusion. Previous suggestions as to the origin of the organic matter have included an algal source (Schroeder, 1972b), pelletising organisms (Land & Moore, 1980) and simple aggregation from the water column (James et al., 1976). The analyses presented in Section 4.5 were undertaken to investigate whether there was any molecular evidence for the participation of any particular organism.

Irrespective of any specific conclusions which are drawn at the end of this chapter, the available literature does not present a coherent understanding of the possible roles that organic matter may play in the precipitation of cements, nor of the likely sources of such organic matter . The following section represents an attempt to clarify this situation.

4.3 Theory of the Role of Organic Matter and its Interaction with the Inorganic Phase.

4.3.1 Introduction.

The concept of an indirect mediation of the precipitation of cements by organic matter was first introduced in Section 3.1, in which the role of organisms themselves was discussed. This section expands on that concept, with the emphasis on the nature of the interaction on the molecular level. In addition, this discussion is intended to be relevant to any organic matter, whether it is of direct biological origin or whether it is more accurately described as a geopolymer. In the following discussion, the interaction is considered to be completely divorced from any viable biological control, though the organic matter could be similar to that involved in skeletogenesis.

4.3.2 The possible roles of organic matter.

There are three possible mechanisms by which the organic matter may be interacting with the precipitation of $CaCO_3$:

(i) Direct source of HCO_3^- .
(ii) Prevention or inhibition of precipitation.
(iii) Promotion of precipitation.

(i) The role of organic matter as a direct source of HCO_3^- has already been discussed (Section 3.5.2), and the isotopic evidence presented suggests that this type of input is not important for any of the cements discussed in this thesis.

(ii) Prevention of the precipitation of $CaCO_3$ would result from the adsorption of a layer of organic matter onto the surfaces of potential nuclei. Such a coating would effectively act as a physical barrier to the attachment of Ca^{2+} or HCO_3^- ions to the nucleus. Whilst organic matter is known to be specifically adsorbed onto carbonate surfaces (Chave, 1965; Chave & Suess, 1967; Mitterer, 1972; Mitterer & Cunningham, 1985), it is particularly difficult to demonstrate conclusively that the organic matter is acting in such a preventative manner. Some further discussion of the molecular mechanism of this prevention is given in Section 4.6.2, but this chapter is principally devoted to a study of the promotional activity of organic matter.

(iii) Promotion of precipitation.

The precipitation of crystals was described in Section 1.8.1 as a two stage process, the main growth phase being preceeded by a nucleation event. There is an energy barrier to this nucleation (Figure 1.7), and anything that can reduce this barrier will catalyse the precipitation. This is the effect that the organic matter has in promoting precipitation, by providing an initial nucleation surface which may be highly reactive due to the local chelation of Ca^{2+} ions. Nucleation has been observed to occur on such surfaces in many calcifying organisms (See Section 4.6.3), and in such examples it is strictly controlled by the skeletogenesis process of the organism. The interaction of organic surfaces with cements has not yet been so clearly demonstrated, but whatever the nature of such interaction, on a molecular level, it is likely to be similar to the skeletogenesis process. It should be emphasised that the catalytic activity may operate through two mechanisms: through the provision of a nucleation surface, and through the

Ca^{2+} binding ability of the organic matter which can lead to an increase in the local saturation state with respect to $CaCO_3$. Furthermore, it is conceivable that the mineral deposited could be controlled by the specific orientation of the components of the organic matter . Hence an organic matrix with molecular dimensions similar to that of the aragonite lattice, may be able to preferentially nucleate aragonite, rather than calcite. This possibility is recognised in some models of mollusc skeletogenesis (Section 4.6.3).

From a chemical point of view, there are a fairly limited number of molecular species which would be capable of playing this catalytic activity, having to form a stable two dimensional surface and have some ability to bind onto carbonate substrates. The likely possibilities are molecules with highly reactive functional groups, such as have been developed by organisms to perform specialised biochemical tasks, and include proteins, polysaccharides and phospholipids. These three types of molecule have several basic attributes in common. They all possess some structural rigidity, are capable of forming two and three dimensional stable structures and have reactive functional groups which can interact with ionic species in aqueous solution. The latter comment hints at the reason for the ability of such molecules to play both preventative and promotional roles. Their flexibility in this respect lies in the fact that the molecules possess both hydrophobic and hydrophilic domains. Exposure of the hydrophobic parts of the molecule to the aqueous phase will hinder interaction with ionic species and so prevent precipitation, whereas exposure of the hydrophilic parts will attract ions and promote nucleation thereby facilitating the precipitation of cements.

4.3.3 Sources of the organic matter.

The ultimate origin of the organic matter is of course biological, but at this stage it should not be assumed that the source is necessarily from reef building organisms. High molecular weight acidic material is formed during the early diagenesis of organic matter and this can have marine or terrestrial or mixed origins. This type of geopolymer, described by a variety of terms including humic and fulvic acids and 'Gelbstoffe' (Ehrhardt, 1977), might well be expected to be able to play the preventative role. It seems unlikely, however, that this material would play the more precise role of a nucleating and/or chelating agent for the precipitation of a specific mineralogy of cement. It is more reasonable to suggest that the latter role is played by an organic phase, quite closely related, both in structure and diagenetic state to matrices associated with the biominerals.

The following sections present the results of several analytical techniques which have been employed to help determine the precise origin of this organic matter . At this stage there are several individual possibilities, though of course, the material may be of multiple origin. The corals must be the first possibility as they are the most common group of species and produce the largest amount of skeletal material. Encrusting organisms must also be be considered, in particular the coralline algae, whose association with peloids has already been commented upon (Section 2.7.7). Less obvious sources include other marine pelletising organisms, green algae, and bacteria, all of which have been suggested to be associated with the formation of peloids in the literature (Land & Moore, 1980; Schroeder, 1972b; Chafetz, 1986; respectively). Although the cyanobacteria or blue-green algae have never been directly implicated in the formation of peloidal cements, their common association with the precipitation of carbonates suggests that they also should be considered as a possible source. The only molecular evidence cited to back up these suggestions was that provided by Chafetz (1986), who quoted the discovery by Land (1971), that the long chain 16 carbon fatty acid was present in peloidal samples. At the time that these analyses were carried out the molecule was considered to be of bacterial origin. It is now well established that this biomarker is produced by a wide variety of other organisms other than bacteria (Trichet, 1970; Meyers, 1977; Wakeham et al., 1983), and can therefore no longer be used as a diagnostic indicator of bacterial input. This is discussed at length in Section 4.5.4.7.

This study of the organic matter in the peloids in split into two parts. The first part is presented in Section 4.5 and investigates the possible sources of the organic matter through the identification of biomarkers in the lower molecular weight lipid fraction. Whilst this helps to define the origin of the organic matter, it cannot provide direct information about the nature of the organic-inorganic interaction. There are no reported data on the molecular nature of such interactions in reef cements, but there is some information on aspects of biomineralisation. Information on this interaction has to be derived from a study of the higher molecular weight, more polar fractions of the organic matter. Such a study is presented in Section 4.7.

Prior to discussing the results, the following section describes the preparation of the samples and extraction of the organic matter. The procedures used to ensure recognition of any contamination, and minimise its effects are described.

4.4 Isolation of the Organic Matter.

4.4.1 Introduction.

The emphasis of this study of the organic matter associated with the peloidal cements has been to complete a detailed characterisation of the organic phase. The extraction procedure was therefore employed to maximise the information derived from the study. The procedure is illustrated in Figure 4.1 and it was originally intended to study the organic matter in four parts:

1) The solvent extractable organic matter,
2) The bound lipids of the solvent extractable organic matter,
3) The higher molecular weight polar fraction of the extractable organic matter,
4) The organic matter residue not extracted by organic solvents.

The analyses of first two fractions are described in Section 4.5 and the third in Section 4.7. As carbonates are known to adsorb organic matter quite strongly, it was expected that a significant proportion of the organic matter would remain bound to the $CaCO_3$ after solvent extraction. In order to study this fraction it is therefore necessary to remove the inorganic phase. Whilst the obvious first choice for this procedure is to use dilute hydrochloric acid, it has been reported that significant losses of organic matter occur with this method, particularly in the extraction of modern samples (Robertson et al., 1973), and so a milder reagent is preferable. EDTA (i) also dissolves $CaCO_3$ quite efficiently, and has been used in many studies of carbonate associated organic materials, (Westbroek et al, 1986). Using this method attempts were made to collect the organic matter remaining after the solvent extraction. Although the dissolution of the $CaCO_3$ was effective, the isolation of the organic matter from the resulting aqueous phase proved to require biochemical techniques beyond the resources of this study and no further characterisation of this fraction was carried out. Details of the procedures are given in Appendix 4.

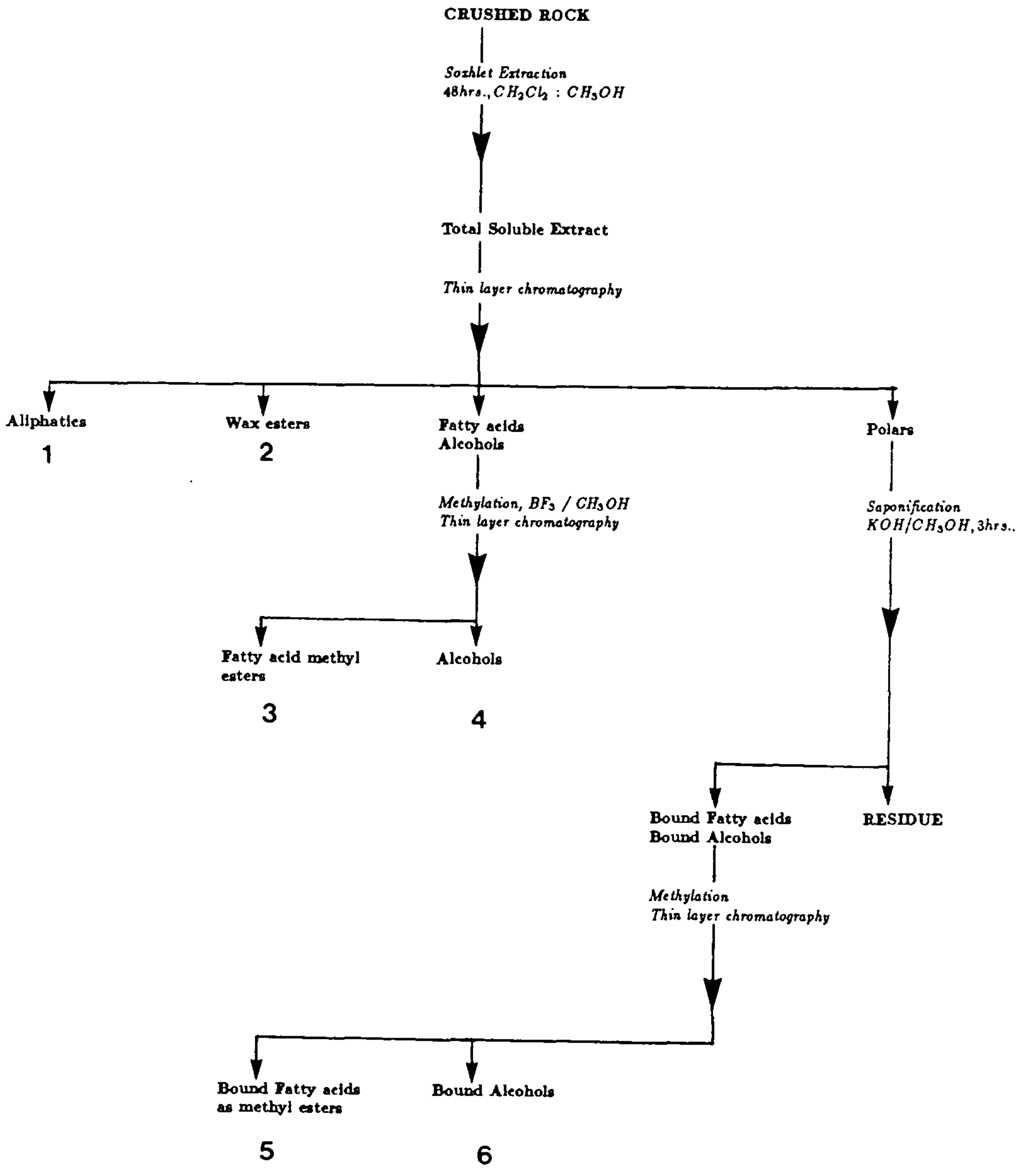

All thin layer chromatography was carried out on preparative SiO_2 plates with Hexane : Ethyl acetate (95 : 15) as the solvent.
Fractions 1–6 were analysed by gc-ms.

Figure 4.1 Extraction diagram showing the techniques used to separate and purify the organic matter within the peloidal cements. The fractions collected were the solvent extractable free and bound lipids, which included aliphatics, wax-esters, alcohols, sterols and fatty acids. Further discussion in the text.

4.4.2 Sample choice and preparation.

The material used in this study comes from an Early Holocene reef described by Lighty (1977, 1985), and the samples were kindly provided by him. They consist entirely of large hand specimens of *Acropora palmata* which contain dark 1–2 cm. thick surficial rims. These rims are reported by Lighty (1985) to consist almost exclusively of the peloidal Mg-calcite cements. Similar observations of this surface concentration have been noted from other reefs by Marshall (1983) and Macintyre, (1985).

Ideally, in a study of the organic matter associated with the peloids, one would wish to separate the cement from the rock matrix. Although this is possible on a small scale, a rough calculation on the weight and probable organic content of the peloids (1–5 % by weight at maximum), and the amount of separated organic matter required for the geochemical study (100 milligrams at minimum), indicates that approximately 4×10^9 individual peloids would be required. As the peloids can only be reliably identified in thin section, this task is clearly impractical.

The extraction and study of the organic matter, therefore, has to be on a bulk sample basis, and this clearly introduces some complications into the interpretation of the results. However, the nature of the spatial distribution of the peloids and careful use of blank or control samples allow a specific study of the peloidal organic matter to be made. Thin section study confirms that the peloids are present in high concentrations at the surface of the coral skeleta and point counting indicates that an average of 20% of the total rock in the surface 2cm. is formed of peloids. This is equivalent to 40% of the total porosity and on average represents 60% of the total infilling material. The other infills are of fibrous aragonite cements (30%) and internal sediments (10%). Although the fibrous cements do not contain any organic matter , the internal sediments probably do, but the small proportion of these is considered to be unimportant. In addition to these internal sediments, there is sometimes (but not always), a surface encrustation of various species. The *Acropora palmata* samples have been ^{14}C-dated at 7,700 years old (Lighty, 1985).

Sample preparation was carried out so as to exclude as much extraneous material as possible. Samples without encrustation were chosen preferentially and macroscale internal sediments were removed, as was any remaining encrusting material. The surface 1–2 cm. dark grey layer was removed with a circular saw and the resulting slices were then washed in distilled water and rinsed with organic solvents to remove any surface contaminants. Whilst samples were handled with prewashed clamps and aluminium foil, it has to be realised that the samples were not originally collected for geochemical work of this sort, so the possibility of previous contamination by handling and storage certainly exists. In order to facilitate recognition of any such contamination, blank samples were also extracted. In the peloid rich slices, the only other major component is the coral skeletal material, and it would be expected that extraction of these samples would lead to some of the organic matter being derived from the corals and not from the peloids themselves. In order to be able to identify material from such a source, the blank sample used was a piece of unaltered *Acropora palmata* from the same hand specimens.

The entire study of the organic matter was therefore carried out on two samples. The first was the peloid-rich material and the second was a control sample, consisting of *Acropora palmata* only. Because the control material was collected from the same samples as the peloid rich surficial layer, this enables the input from the coral and the possible contamination to be identified from a single sample.

Treatment of the two samples was carried out in parallel in identical procedures, thereby also ensuring that any further contamination could be recognised. The obvious differences between the peloidal and control samples are therefore undoubtedly diagnostic of inputs to the peloidal organic matter .

4.4.3 Solvent extraction of the organic matter.

Extraction of the organic matter was achieved by dissolution into organic solvents. A mixture of dichloromethane and methanol was used so as to ensure that both non-polar low molecular weight lipids and polar higher molecular weight material was isolated. Two hundred and fifty grams of both samples were extracted and this produced 225 milligrams of organic matter from the peloidal sample and 50 milligrams from the coral control sample. The former was a green solid material, and the latter was an oily brown viscous liquid. The lipids were separated according to polarity using thin layer chromatography as described in Appendix 4. This produced purified fractions of aliphatic hydrocarbons, wax esters, sterols and fatty alcohols and fatty acids, leaving a highly polar residue. The residue formed approximately half of the total peloidal organic matter (by weight), but only about 20% of the coral sample. This residue was treated with methanolic potassium hydroxide, a reagent that cleaves ester bonds. It is known that a proportion of the potentially informative lipid material is commonly bound to the higher molecular weight polar material in this fashion, and so the treatment is used to release this material into solution. The resulting samples were again purified by t.l.c. to produce further fractions of bound sterols, fatty alcohols and fatty acids.

After this process, there was still a significant proportion of residual highly polar material, from which no biomarker data could be derived. There was a great deal more of this residue in the peloidal sample than in the coral blank, and it is suspected that this fraction is responsible for the interaction with the inorganic phase. The highly polar nature is consistent with the presence of a large number of functional groups which could interact with Ca^{2+} and HCO_3^- ions in the aqueous phase. Some molecular information has been derived from this residue as part of the total sample studied in Section 4.7.

The purified organic fractions are studied in the following section using high resolution capillary gas chromatography-mass spectrometry (gc-ms), a technique capable of separating complex mixtures of comparatively low molecular weight compounds and identifying individual components. Recognition of certain components allows inferences to be drawn about the sources of the organic matter.

4.5 Chemical Fossils in the Peloidal Cements.

4.5.1 Introduction.

A biological marker is any organic compound present in the geosphere whose structure is identical to, or whose carbon skeleton suggests an unambiguous link with a known natural product (Mackenzie et al., 1982). The identification of such compounds present in sediments allows the recognition of an input from particular organisms or groups of organisms without any hard parts being preserved. Whilst we can quite confidently extrapolate from what is known about the chemotaxonomy of organisms to ascertain the major sources of organic matter in sediments, it must be emphasised that the chemotaxonomic database is far from complete. Although some molecules are known to be produced only by a restricted number of species, this high degree of specificity is rare. As a greater volume of information is discovered regarding the distribution of biological markers both in sediments and organisms, it is becoming clear that few biolipids can be assigned to one organism alone.

A particular example of this is the compound 24-ethylcholest-5-en-3 β-ol (ii), which has commonly been considered to indicate organic matter of a terrestrial origin. This sterol has more recently been found to be produced in large quantities by some species of marine phytoplankton and so its reliability as a terrestrial indicator is not certain (Volkman, 1986).

Despite these complications, the overall distribution of lipids in sediments is derived from a variety of organisms, and hence differences in the nature or relative abundance of the organisms will produce recognisable variations in the lipid content of the environment. Studies of a range of lipid classes can therefore allow more certain conclusions to be made regarding the source of the organic matter, than would be realistic from the study of a single set of components.

4.5.2 Quantitative comparison of results.

In order to be able to compare the two samples more accurately and thereby deduce the major inputs to the peloids, the analyses have been carried out in a quantitative manner. Addition of an internal standard of known concentration to the samples immediately prior to their analysis allows a quantitative comparison of the components to be made.

The standard used is a hydrocarbon with a molecular weight of 360, 9-n-dodecyl-perhydro-phenanthrene, as used previously in quantitative studies (Rullkötter, 1984). There are a number of assumptions being made about the performance and behaviour of the instruments which make it difficult to compare the concentrations of components observed in this study with other reports. However, these approximations do not affect the comparison of identical molecules between samples run under similar conditions on the same instrument. In addition, some of the compounds identified are present at levels lower than nannogram per gram of original sample and at this low level, calculation of absolute concentrations is unlikely to be highly accurate. The figures given in the presentation of results are therefore deliberately dimensionless, indicating that the quantitation should be regarded as relative.

4.5.3 Introduction to the biomarker classes.

Five major classes of biomarkers are being investigated in this study; these are aliphatic hydrocarbons, wax esters, fatty alcohols, sterols and fatty acids. This section briefly describes each class in turn and is intended as a simple introduction to the molecular nature of these biomarkers. It serves as a basis from which the individual components of the classes are discussed in Sections 4.5.4.1 to 4.5.4.7.

4.5.3.1 Aliphatic Hydrocarbons.

The hydrocarbons are a class of organic compounds which contain only carbon and hydrogen atoms. They occur in a number of homologous series, the simplest of which has the general formula C_nH_{2n+2} and is known as the normal alkanes. Many other series exist in ever increasing complexity, but the samples studied in this example are dominated by the long chain alkanes. These compounds are ubiquitous amongst sediments and organisms. Some of the most important natural molecules fall into this class also, the acyclic and cyclic isoprenoids, which are biosynthesised from the basic isoprene building block (iii).

4.5.3.2 Wax esters.

Wax esters are simple primary esters of long chain fatty alcohols and long chain fatty acids. The chain length of both acid and alcohol moieties can vary, as can the degree of unsaturation in each. A typical wax ester is palmitoyl oleate (iv), being an ester of the saturated C_{16} alcohol with the C_{18} acid with one double bond. A commonly used notation for this wax ester would be 16:0/18:1, and this can be combined as 34:1, describing a wax ester with 34 carbon atoms and one double bond. As the information regarding the chain lengths of the acid and alcohol parts of the molecule cannot always be deduced from the mass spectrum, the latter notation is used in this study.

4.5.3.3 Fatty alcohols.

The alcohols comprise a wide range of components which are related to the alkanes through the attachment of any number of alcohol (–OH) groups. The simplest organic alcohol is methanol (CH_3OH), which is one of the solvents used to extract the organic matter. This class of lipids is dominated in the two samples studied by the saturated alcohols, exactly analogous to the normal alkanes, with the general formula $C_nH_{2n+2}O$. Another major alcohol group is a series of tetra-cyclic molecules called stérols, described in the next section.

4.5.3.4 Sterols.

The sterols are a important group of biomarkers and all are based on the carbon skeleton shown in Figure 4.2, with the addition of usually one but potentially more alcohol groups. These molecules act as rigidifiers of biological membranes and are therefore ubiquitous, at least in eucaryotic organisms. They are quite stable and so are useful biomarkers because the carbon skeleton can be preserved essentially unaltered over long periods of geological time. The numbering system is also shown in Figure 4.2 and this is particularly important as it is constantly referred to in the names of the sterols, to indicate the precise positions of the functional groups and double bonds. The other major attribute of the sterols is that they possess several structural features which can be very diagnostic for a particular source. These include the patterns of the side chain, the positions of unsaturation and the stereochemistry of the ring substituents. The powerful resolution and sensitivity of the gc-ms technique is illustrated by the fact that it is possible to distinguish, for example, between two sterols whose only difference in structure is the stereochemistry of a single hydrogen atom (either behind or in front of the plane of the ring system).

Some of the side chain patterns are restricted to a few occurrences within organisms, making them particularly useful in identifying sources of organic matter. However, many sterols are widely distributed in biological systems and so individual molecules are of little diagnostic use. Nevertheless, the distribution and relative amounts of a variety of sterols can still be of great informative value. As more information is produced on the occurrence of sterols in biological systems, it is becoming obvious that it is essential to investigate other chemical fossils in order to confirm inputs which may be indicated by the sterol distribution (Volkman, 1986). This is exactly the approach taken in this study.

4.5.3.5 Fatty acids.

The fatty acids are a class of compound analogous to the aliphatic hydrocarbons and alcohols but with a carboxyl (-COOH) group attached in place of the alcohol group. This class is again dominated by the simple straight chain molecules in the two reef samples studied, but in this case there are a large number of unsaturated components present. Identification of the position and geometry of the unsaturation(s) in the alkyl chain can be of great diagnostic value. However, care must be exercised, as in a similar fashion to the other classes, fatty acids are produced in large amounts by a wide variety of organisms.

4.5.3.6 Hopanoids.

The hopanoids are a group of compounds with the basic skeletal structure shown in Figure 4.3. They are, like the sterols, derived from the basic isoprene unit, but are pentacyclic, and are part of a large class of compounds known as the triterpenoids. Many of their structural characteristics indicate that they are phylogenetic precursors of the sterols (Ourisson et al., 1979). They are very useful as biomarkers as they are present in many organisms and are relatively easy to identify. A wide variety of structures are known from both sediments and organisms, but of particular interest are the series of 'extended' hopanes ranging up to C_{36} (v). These molecules are thought to be derived mainly from micro-organisms (Ourisson et al., 1979), in particular the bacteria, which are known to synthesise bacterio-hopane-tetrol (vi).

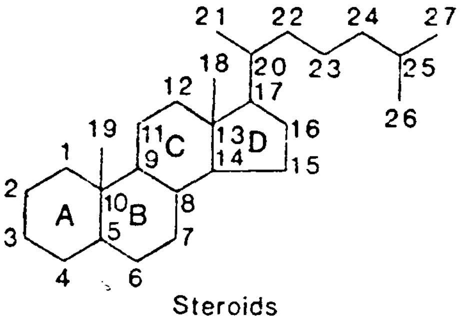

Figure 4.2 The sterol carbon skeleton and numbering system.

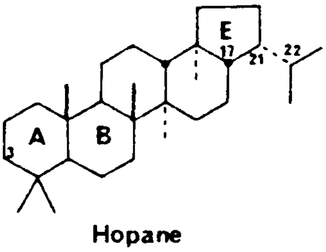

Figure 4.3 The carbon skeleton of the hopanes.

4.5.4 Results.

The results for each lipid class from the analyses of the peloidal and coral blank samples are shown in Figures 4.4 to 4.12.

This section compares the results obtained with a wide literature that is available for both organisms and sediments. However, specific studies on reef sediments are quite rare (Shaw & Johns, 1985), and the few papers discussing coral biomarkers (Meyers, 1977; Sassen, 1977) have concentrated solely on the fatty acid distributions. Comparison with other marine sediments has enabled several interesting conclusions to be drawn regarding the likely sources of the peloidal organic matter.

4.5.4.1 Aliphatics.

Straight chain hydrocarbons have been identified in significant concentrations, but with no major differences between the distributions in the coral and peloidal samples. The n–alkanes are ubiquitous amongst marine organisms and no specific information can be derived simply from the fact that they are present. More details can be deduced by looking at the overall distribution of the entire alkane series. Another important point is that the alkanes can be derived from a plethora of environmental contaminants, and so it is not certain that they are autochthonous. There are however, several interesting points about the distribution as shown in Figures 4.4 & 4.5.

A common observation in extracts of marine sediments is that there is a higher concentration of odd carbon numbered alkanes than even, the so called o/e preference (Schenck, 1969). This is generally considered to imply a higher plant input (Shaw & Johns, 1985; Brooks et al., 1976), due to the fact that they synthesise mainly even numbered fatty acids which are de-carboxylated, losing one carbon atom, to produce the odd numbered alkanes. Whilst the Florida shelf edge has no major terrestrial input, it might be expected that an input from mangroves would be recognisable. The o/e ratio for mangrove leaves is reported to be up to 7:1 (Wannigama et al., 1981).

However, neither coral or peloidal sample show any odd carbon number preference, indicating that there is no input from terrestrial sources or from the mangroves. In fact if anything, there is a slight reversed preference in the coral sample with even alkanes predominating. The lower homologues of the peloidal sample also show a slight e/o preference. This reversed distribution is quite common in carbonates (ten Haven, 1985), apparently due to the formation of the alkanes via reduction of alcohols, without the loss of a carbon atom, rather than the more usual decarboxylation. The reduction process would be expected to occur in carbonate sediments where reducing conditions prevail, and this cannot therefore be a fully adequate explanation for such a distribution to occur within reefs. It should be noted, however, that the e/o ratio is quite small and may not represent a very significant even preference.

Of much greater interest is the very high observed concentration of the n-C_{22} alkane in both samples. This observation has been previously noted and a few species of algae are known to produce excess C_{22} (Schenck, 1969). High concentrations of the alkane have been associated with hypersaline environments (ten Haven, 1985), although no rationale was suggested for this. Whilst the alkane may be of algal origin, most other studies indicate that algae produce alkanes in a range from C_{14} to C_{32} which maximise at C_{15} to C_{17} with no o/e preference (Tissot & Welte, 1984; Volkman et al., 1980). Cyanobacteria are also known to produce large amounts of C_{17} alkanes (Boudou, 1986). Even disregarding the C_{22} alkane, neither sample shows a maximum in the C_{15} to C_{17} region. There is no evidence for the presence of the 7– and 8–Me–C_{17} alkanes thought to be specific to cyanobacteria (Cardoso et al., 1978). However, the abundance of the alkanes in algae is generally quite low (Volkman et al., 1980), and so a possible algal input may be masked by other larger inputs.

The overall picture is clearly one of a number of inputs to the aliphatic fraction, but the sources are certainly autochthonous and not terrestrial in nature. The significance of the very high C_{22} alkane is not fully understood, and the fact that there is little difference between the peloid and coral samples means that no positive identification of organic matter source can be made from the observed aliphatic distributions.

4.5.4.2 Hopanes.

A series of hopanes was observed in both samples in trace amounts. These included 30-norhopane (vii), $17\alpha(H),21\beta(H) - Hopane$, $17\beta(H),21\alpha(H) - Hopane$ and the C_{31} to C_{34} extended hopanes. These molecules, and in particular the extended hopanes, are considered to be degradation products of polyhydroxybacteriohopanes (Brassell & Eglinton, 1983) and these imply a bacterial (Rohmer & Ourisson, 1976), or cyanobacterial (Ourisson et al., 1979) input to the organic matter . These molecules are present in trace amounts only, and occur in both samples, so although bacteria may be present, their input is of minor importance. Their very low concentrations suggests that they may not be genuine, but are present by contamination. This observation contradicts the suggestion that the peloids are the products of bacterial induced precipitation (Chafetz, 1986).

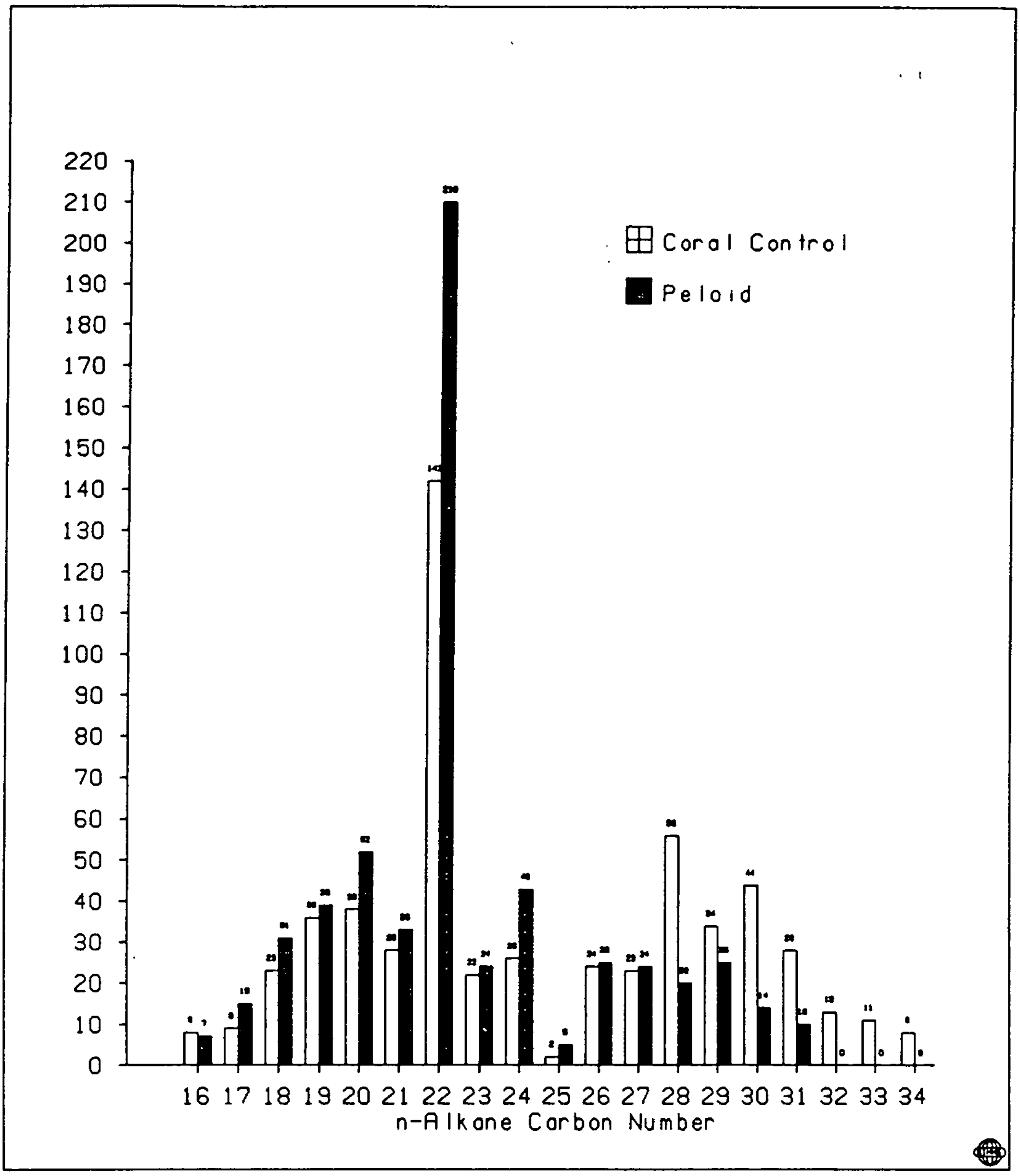

Figure 4.4 Peloidal and coral n-alkane distribution. Note the very high n-C_{22} content. Discussion in text.

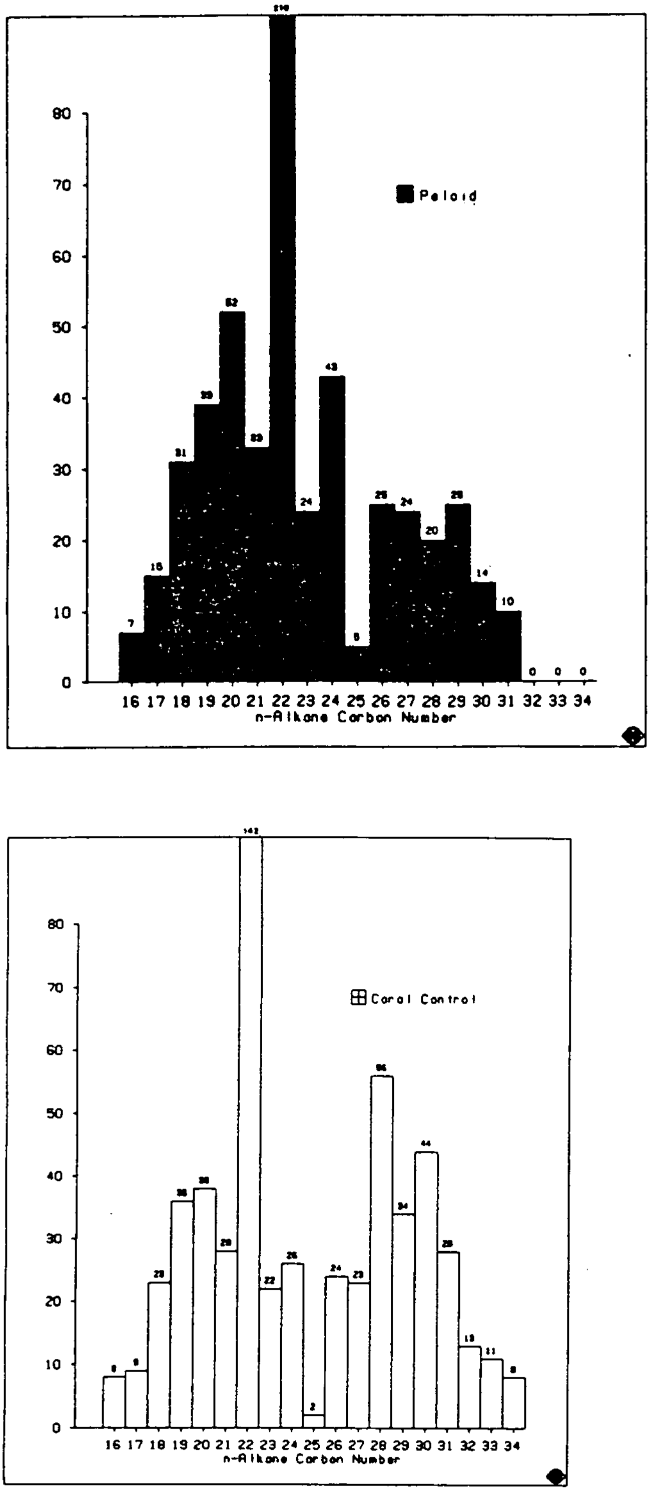

Figure 4.5 Peloid and coral n-alkane distributions separated for comparison. Discussion in text.

4.5.4.3 Wax Esters.

Wax esters are present in large amounts in marine animal phyla (Cranwell & Volkman, 1981), and are generally unknown in other marine organisms (Sargent et al., 1981), although the C_{32}, C_{34}, and C_{36} wax esters have been reported to occur in bacteria (Bryn et al., 1977; Russell & Volkman, 1980). Zooplankton are known to produce large amounts of wax esters, and quite extensive slicks of predominantly wax ester composition have been observed in some areas (Sargent, 1976). Wax esters are known to be produced by Coelenterates (Sargent et al., 1981) suggesting that the most likely source in the reef samples is the corals, in which the C_{32} wax ester is particularly abundant (Weiner et al., 1983). The longer chain wax esters produced by higher plants (C_{40-54}) are not observed in the samples studied.

The distribution of the wax esters in the coral blank includes saturated and unsaturated molecules from C_{30} to C_{36} (Figure 4.6) and it is expected that these are indeed coral inputs. It is interesting, however, that only the C_{32} and C_{34} esters were detected in the peloidal sample and this indicates that the input of organic matter of coral derivation to the peloids is small.

The total concentration of wax esters is itself very low, being less than 20% of the other lipid classes and this may mean that the concentrations were near to the limit of detection. In reality, therefore, there may have been a fuller distribution in the peloidal sample. The low overall concentration further indicates that the coral contribution to the organic matter is minimal.

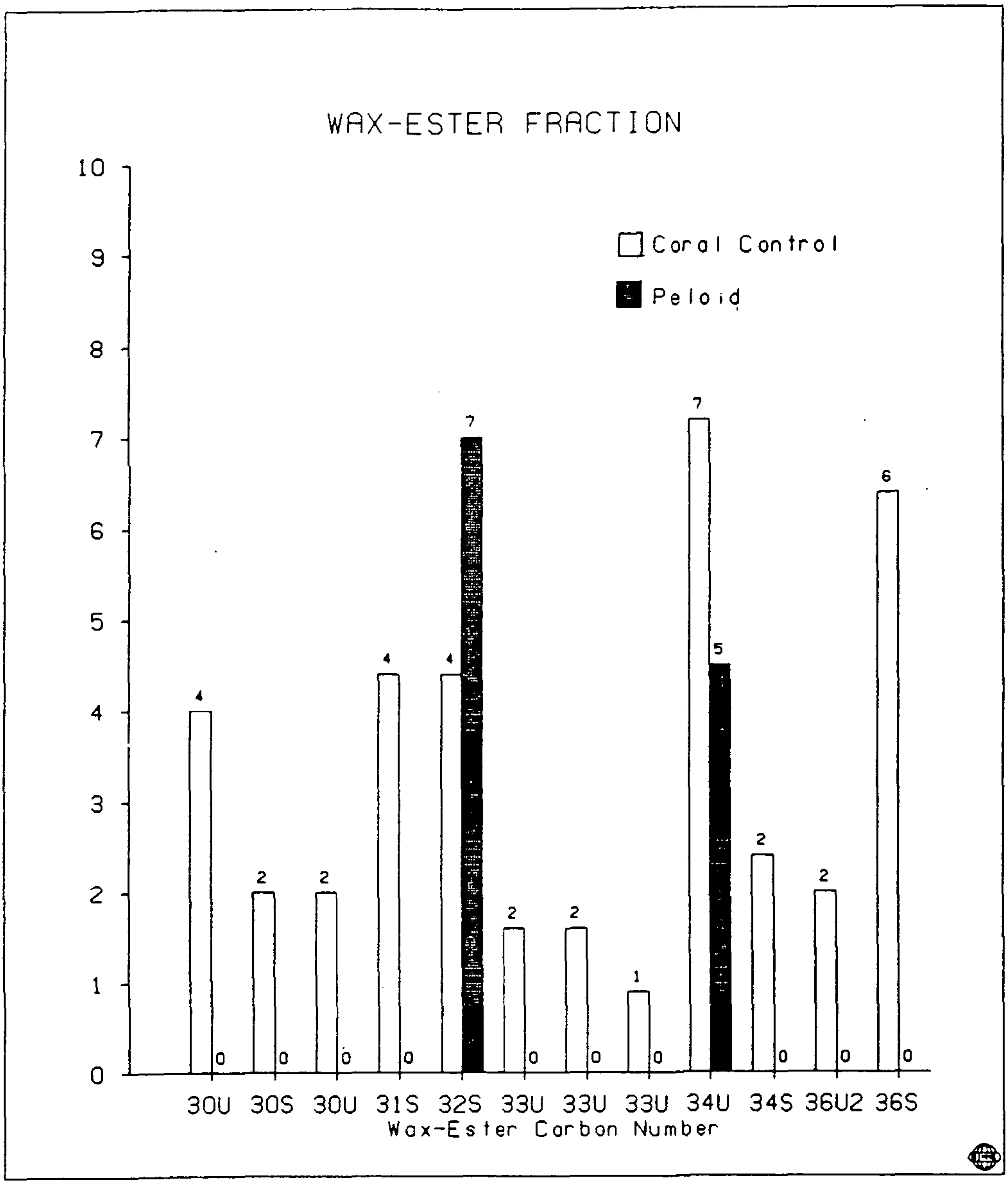

Figure 4.6 Peloidal and coral Wax-ester distribution. Discussion in text..

4.5.4.4 Fatty alcohols.

This group of biomarkers has been identified in two forms; as free alcohols and as bound or esterified moieties. The observed distributions are shown in Figures 4.7 & 4.8. Unfortunately, the n-alcohols are also produced in abundance by a variety of organisms, and their presence is not particularly diagnostic. There is a significantly larger concentration of the shorter chain C_{16} to C_{21} alcohols present in the peloidal sample, with the C_{16} and C_{18} being particularly predominant. This may be reflecting the similar predominance of the C_{16} and C_{18} fatty acids also observed (Figure 4.10). Only the C_{18} alcohol is present in the bound fraction.

Longer chain n-alcohols generally arise from higher plants (Robinson et al., 1986) and the low observed concentration of those above C_{25} provides further evidence that there is no higher plant input.

The presence of a range of n-alcohols in cyanobacteria has been reported (Boon et al., 1983) but no particular interpretation was presented on the distribution. β–OH–acids, thought to be reliable markers for bacteria (Goossens et al., 1986), were not detected in the reef samples.

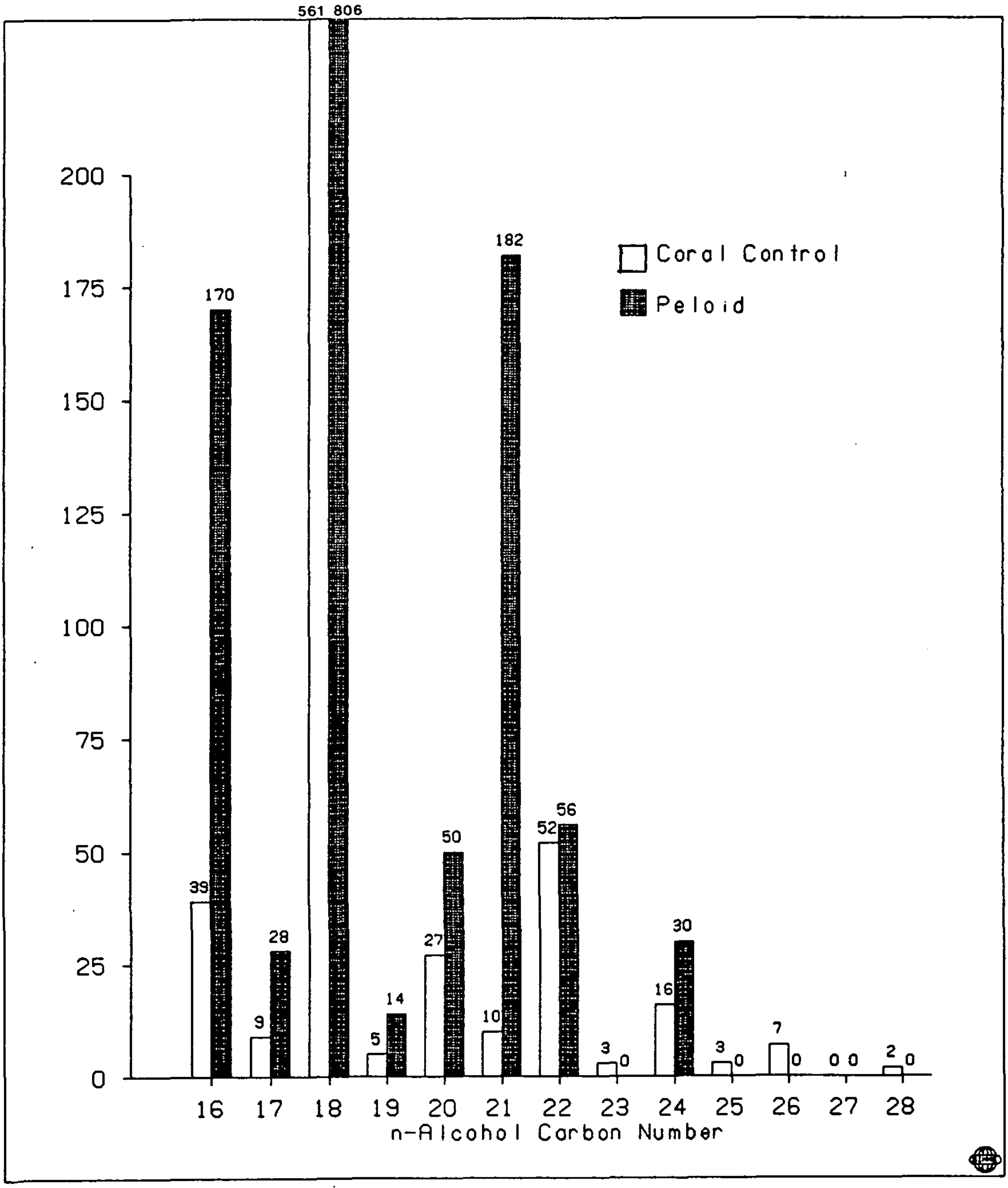

Figure 4.7 Peloidal and coral free fatty alcohol distributions. Only the n-C_{18} alcohol is present in the bound phase and is in large excess in the peloidal sample. Discussion in text..

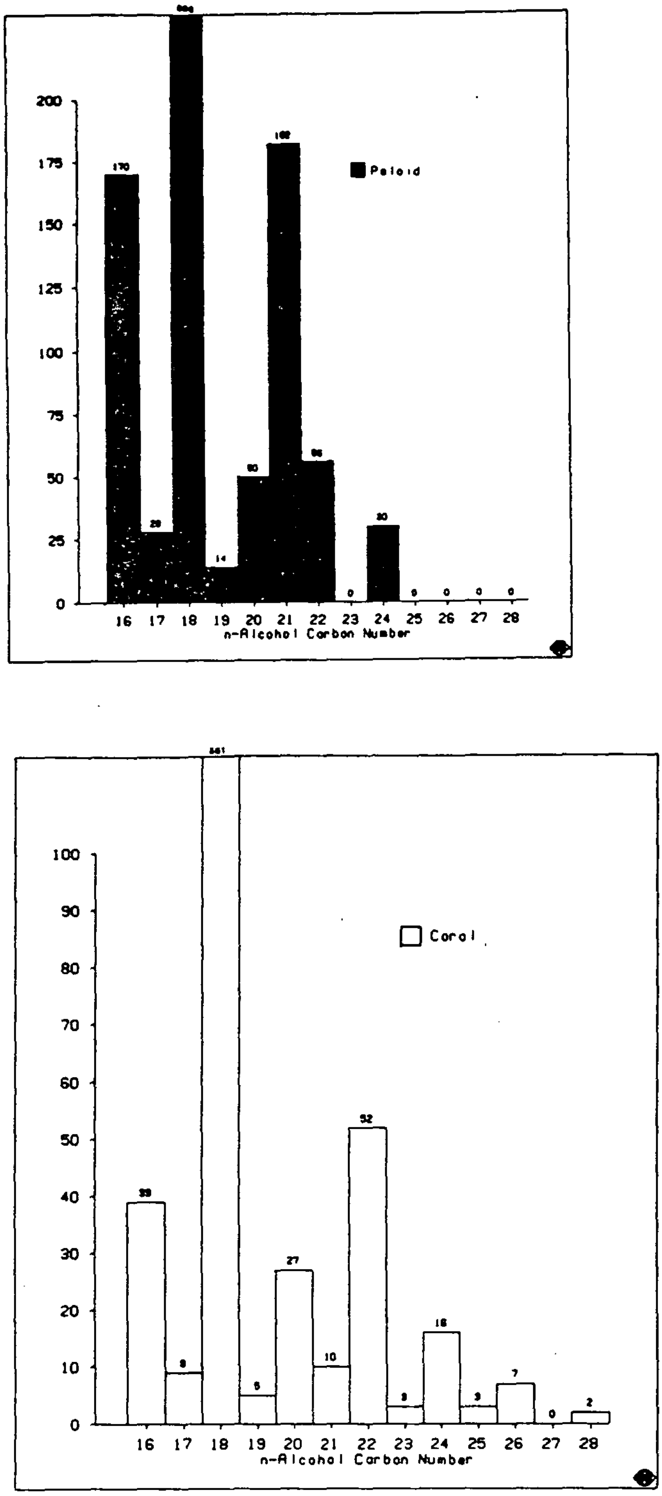

Figure 4.8 Peloidal and coral fatty alcohol distributions separated.

4.5.4.5 Sterols.

The sterols are also present in both free and bound forms and the distributions are shown in Figure 4.9. This group of lipids shows the most significant differences between the two extracts, most components being present in more than ten fold greater concentrations in the peloidal sample.

As noted in the introductory paragraph on this lipid class, sterols are produced by a wide range of organisms and there is still not enough detail known about the distributions within many classes of organism to be able to definitively infer the input of one specific group (Volkman, 1986). There are some general trends within groups however, and these help to identify likely sources.

The major components in the reef samples are the Δ^5 unsaturated series, cholest-5-en-3β-ol, 24-methylcholest-5-en-3β-ol and 24-ethylcholest-5-en-3β-ol (viii, ix, ii), and the first two are considered to be indicative of planktonic organisms (Brassell & Eglinton, 1983). 24-Ethylcholest-5-en-3β-ol is produced by higher plants and it has been used as a marker for terrestrial input (Huang & Meinschein, 1976; Saliot et al., 1982; Gagosian et al., 1983), but recent evidence indicates that a number of marine phytoplankton produce this sterol (Brassell & Eglinton, 1983; Volkman, 1986) and in particular, it can be a major constituent of cyanobacteria (Nes & Mckean, 1977; Boon et al., 1983).

The C_{27} and $C_{28}\Delta^5$ sterols are very common amongst marine organisms and one has to look at their relative concentrations to be able to derive any useful information. Cholest-5-en-3β-ol is known to be the major sterol constituent in seawater (Volkman, 1986), and it is the sole sterol produced by higher organisms (Huang & Meinschein, 1976). It is also frequently the most abundant component synthesised by more primitive organisms.

Whilst marine algae probably contribute to the cholest-5-en-3β-ol input, they are considered to be the major source of the other predominant sterols identified in the reef samples (Boon & Rijpstra, 1977; Mackenzie et al., 1982) 24-Methylcholest-5-en-3β-ol is certainly produced by algae, particularly those which do not synthesise Δ^7 sterols (x). Some cyanobacteria are also known to produce small amounts of the $C_{28}\Delta^5$ sterol, in addition to the $C_{29}\Delta^5$ mentioned above. No Δ^7 sterols were identified in this study.

The $C_{29}\Delta^{5,22}$ (xi) sterol identified in the peloidal and coral sample is commonly considered to be produced by diatoms, but if this were the case, the C_{27} and C_{28} equivalents should be present, and these were not identified. The presence of the 24-ethylcholestan-3β-ol (xii) in the peloidal sample is interesting, and this could be formed by the sedimentary hydrogenation of the corresponding sterol. However, the analogous C_{27} and C_{28} stanols are not observed, as would be expected if this diagenetic process was significant. The C_{29} stanol is probably therefore input directly from some organism and it has been identified from a few marine algae (Nishimura & Koyama, 1977).

Low concentrations of the 4,24-dimethyl5α(H)-cholestan-3β-ol (xiii) have been detected in the bound phase, and this is considered to represent inputs from dinoflagellates (Robinson et al., 1984), but this component is present in both sample in equal amounts and it is therefore unlikely that there is a major dinoflagellate input to the peloidal organic matter.

The interpretation of the sterol distributions is clearly quite complex and in these samples there are certainly several input sources. The major differences between the peloidal and coral samples are the much larger concentration of the C_{27}, C_{28}, and $C_{29}\Delta^5$ sterols in the former, the input of cholest-5-en-3β-ol being by far the highest. In addition, there is a significantly greater concentration of the $C_{29}\Delta^{5,22}$ and of the C_{29} stanol in the peloidal sample. It is useful to compare this observed distribution with those observed in various groups of organisms (See the recent review by Volkman, 1986).

The simplest but important deduction that can be made from the observed distribution is that marine algae are the major source of the organic matter in the peloids. At this stage of the discussion, this includes the blue-green algae.

Many green algae (Chlorophyta) would be expected to produce a range of Δ^7 sterols as well as those observed in the reef samples (Holden & Patterson, 1982; Volkman, 1986), but some species are known to contain mainly the Δ^5 series identified above in the peloidal extract. In those species discussed by Volkman (1986), the $C_{28}\Delta^5$ and $C_{29}\Delta^{5,22}$ tend to predominate, with smaller amounts of the $C_{29}\Delta^5$. Most research has been concentrated on the Chlorophyta, and possible contributions from other classes of algae are not well defined.

Cyanobacteria also appear to produce small amounts of sterols, in which the $C_{27}\Delta^5$ and $C_{29}\Delta^5$ predominate, and they could also be a major source of these sterols in the marine environment (Volkman, 1986).

In summary, the input to the peloidal samples is from several sources. The very large amount of cholest-5-en-3β-ol reflects sources from both marine animals and algae, possibly including the cyanobacteria. Green algae are probably the main source of the 24-methylcholest-5-en-3β-ol, and the somewhat lower amount of 24-ethylcholest-5-en-3β-ol is likely to be input from both green algae and cyanobacteria. Green algae are almost certainly the source of the $C_{29}\Delta^{5,22}$ sterol also. The sterol distribution therefore is consistent with a green algal source for the peloidal organic matter, with a possible contribution from cyanobacteria. It must be emphasised that the lack of data for other classes of algae means that other possible contributions, in particular from the encrusting red algae, may not have been recognised.

4.5.4.6 Bacterio-hopanol.

One final component which has not yet been mentioned in the alcohol class is the molecule 17β(H),21β(H) bishomohopan-32-ol (xiv), which was recognised in small amounts in the peloidal sample and was not identified in the coral control. This is an early diagenetic degradation product of the known bacterial marker, bacteriohopanetetrol (vi) (Rohmer & Ourisson, 1976). The latter species degrades rapidly to produce a series of extended hopanes which were mentioned in Section 4.5.4.2. The low concentration means that the bishomohopan-ol may also have been present in the coral sample but was below the detection limit. Nevertheless, the presence of this compound is a definite indicator of a bacterial input to the organic matter of the peloids. The fact that the concentration is low coupled with the observation that other bacterial biomarkers are not present suggests that the input is fairly minor.

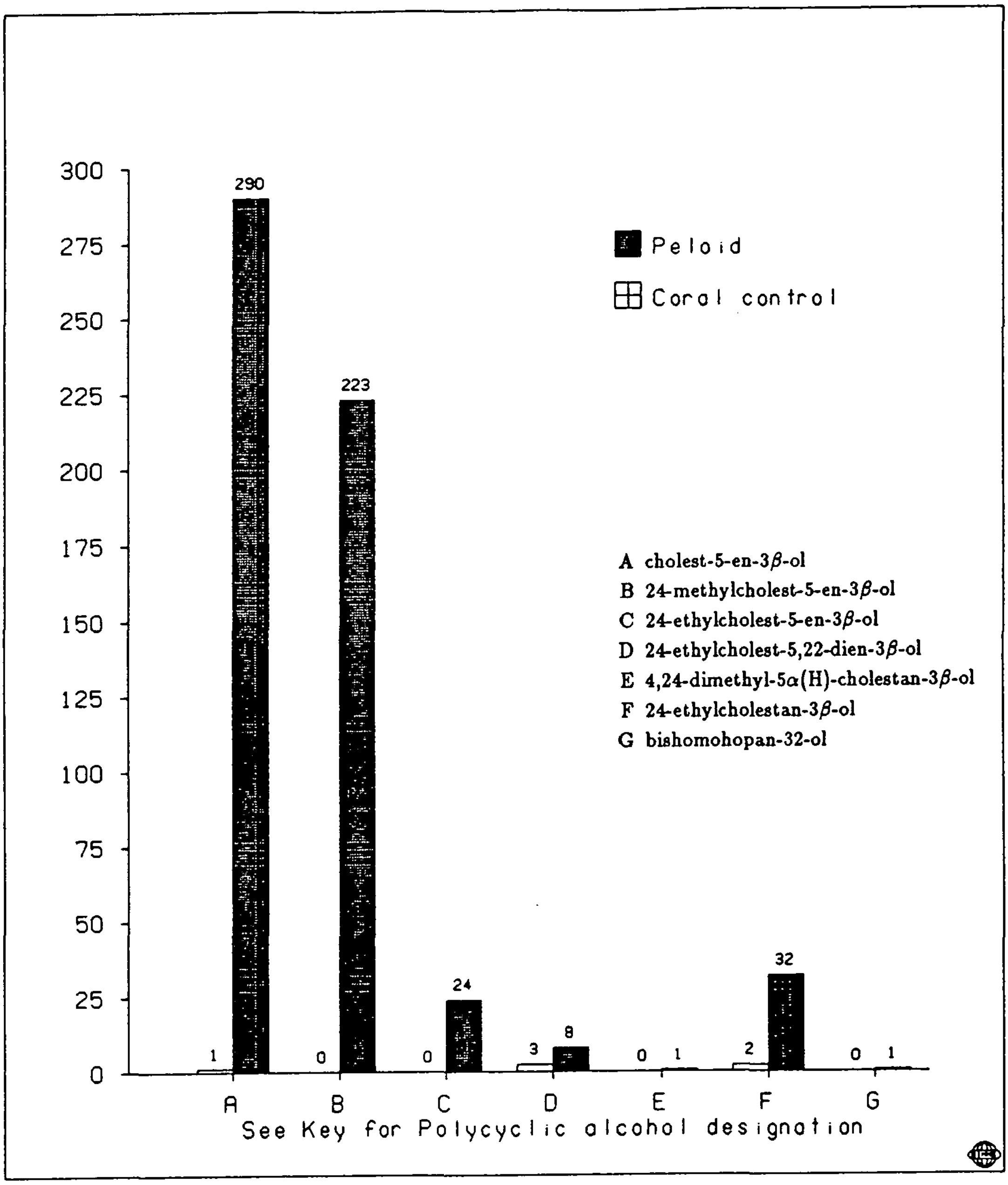

Figure 4.9 Peloidal and coral free sterols distribution. Discussion in text. The bound sterol fraction contained only cholesterol which was in large excess in the peloid sample.

4.5.4.7 Fatty acids.

The distribution of the fatty acids in both free and bound forms for peloid and coral extracts is shown in Figure 4.10. The distributions in all the samples are dominated by the saturated C_{16} and the saturated and unsaturated C_{18} acids, these being present in 5–10 times the concentration of the other components. All of the other acids are saturated, and most are the straight chain normal isomers, though C_{15}, C_{16}, and C_{17} branched chain acids were identified. Some information can be derived from detailed studies of the stereochemistry of the unsaturated acids (Perry et al., 1979; Gillan et al., 1983), but such information was not obtained in this study. However, a number of interesting observations can be made about the distributions of the fatty acids.

Although the occurrence of fatty acids in the biosphere is as complex as for the sterols, there is appreciably more information available on the distributions within particular groups of organisms. In particular, much has been achieved in identifying valid bacterial biomarkers within this class of lipids.

The observation that the major components are the C_{16} and C_{18} acids is in common with several other studies. They are considered to be the most common acids occurring in nature (Schenck, 1969). The C_{16} acid occurs in very large concentrations (second only to cholesterol) in both samples and interestingly, its presence has been noted before in peloidal samples (Land & Goreau, 1970; Land, 1971). These authors considered it to be derived from a bacterial source, and Chafetz (1986) used this assumption to support other circumstantial evidence that the peloids are of bacterially induced origin. It is now clear, however, that although the n-C_{16} acid does undoubtedly occur in bacteria, it also occurs in large amounts in many other organisms. The most relevant identification is that made by Meyers (1977, 1979), who noted that this was the major acid present in *Acropora palmata* specimens. Also recognised in that study was the high concentration of the saturated C_{18} acid as well as significant amounts of the C_{14} and C_{20} acids, all of which have been identified in the coral and peloidal samples. This observation was confirmed by Sassen (1977), who studied a variety of reef samples and again found the C_{16} acid to be predominant in corals, accompanied by large amounts of saturated and unsaturated C_{18}. The latter included the $18:1\,\Delta^9$, $18:1\,\Delta^{11}$ and 18:2 acids which have also been identified in the samples studied in this chapter. Sassen (1977) also identified several poly-unsaturated acids which were not observed in either the peloidal or coral extracts. However, these components would be quite rapidly hydrogenated, oxidised or degraded in the conditions on the Florida shelf, and the 7,700 year age of the peloidal samples would probably be sufficient for these processes to remove them.

The fatty acid distributions and relative concentrations observed previously, are similar to the reef samples studied here, suggesting that contamination problems are minimal, and therefore that the biomarkers observed in the coral control can be considered to be autochthonous.

Further examples of the predominance of the C_{16} acid in coralline sediments can be found in the literature, but it should be noted that this compound and the other members of this class identified above could be sourced from other organisms. Mangroves, for example, also produce a range of fatty acids (Wannigama et al., 1981) though an input from this source has already been discounted (Section 4.5.4.1). The absence of the longer chain components confirms the earlier conclusion that there is no significant terrestrial input (Shaw & Johns, 1985).

There are, however, a number of other organisms which produce fatty acids, and may be contributing to the overall distribution. Zooplankton, for example, are known to contain large amounts of the C_{16}, C_{18}, C_{20} saturated and the $18:1\,\Delta^9$ acids (Wakeham, 1983). Cyanobacteria have also been found to contain the C_{16} acid which predominates over smaller amounts of C_{18} unsaturated and C_{20} acids (Trichet, 1970; Gossens et al., 1986).

The bound fatty acids in the peloidal and coral samples are also dominated by the C_{16} and C_{18} saturated molecules, with lesser, but significant amounts of the C_{18} unsaturates. This observation is similar to previous studies in many organisms (Cranwell & Volkman, 1981). Algae in particular show a predominant C_{16} acid in the bound phase with smaller concentrations of the C_{18} unsaturated compound (Orcutt & Richardson, 1970). However, a similar distribution of bound acids has been observed in fungi and higher plants (Kemp & Mercer, 1968; Mercer & Bartlett, 1974) and so it cannot be considered diagnostic for algae.

The distribution of fatty acids in bacteria has been the subject of many publications, due to the search for bacteria specific biomarkers. In earlier literature the presence of the $18:1\,\Delta^{11}$ acid was considered to be diagnostic, and this molecule is present in both coral and peloidal samples. More recently, however, the latter has also been found to be produced by other organisms (Gillan et al., 1983; Wakeham, 1983). There are a number of other fatty acids which are still considered to be diagnostic for bacteria, most notably the $18{:}1\Delta^7$isomer (Wakeham, 1983; Shaw & Johns, 1985). Whilst this molecule was not identified in this study, it can be difficult to differentiate from other 18:1 isomers, so its presence could have been overlooked.

A number of other bacterial specific acids including several 15:1 isomers, the $17:1\Delta^9$ and the cyclopropyl 17:0and C_{21}acids (Perry et al., 1979), were also not identified in this study, further suggesting that the bacterial input is of limited importance.

In summary, the fatty acid distribution of the peloidal and coral samples is dominated by the C_{16} and C_{18} acids with very little difference between the two. Several groups of organisms, including the corals and possibly cyanobacteria, are known to produce these acids and no absolute conclusions can be made regarding the source. The similarity of the distributions with previous studies of corals, and the similarity of the coral and peloidal samples in this study, tend to suggest that the coral input is the most important although this conclusion is not supported by the wax ester distribution. The only major difference between the peloid and control samples is in the concentration of bound acids, and this could tentatively be attributed to an algal source.

In the free fatty acid fraction, the only significant difference is the higher concentration of the 18:2 isomer, but this is again of little diagnostic value. The conclusion that can be drawn from the fatty acid distribution is that the lack of some bacterial biomarkers, whilst not ruling out the presence of bacteria, certainly indicates that if they are present, their role is of minor importance. The situation cannot be considered to be fully understood, but the suggestion that peloids are of bacterial induced origin, based on the presence of the C_{16} acid (Chafetz, 1986), must be in doubt.

The fatty acid input appears to be from a coral source, with an algal, potentially cyanobacterial contribution.

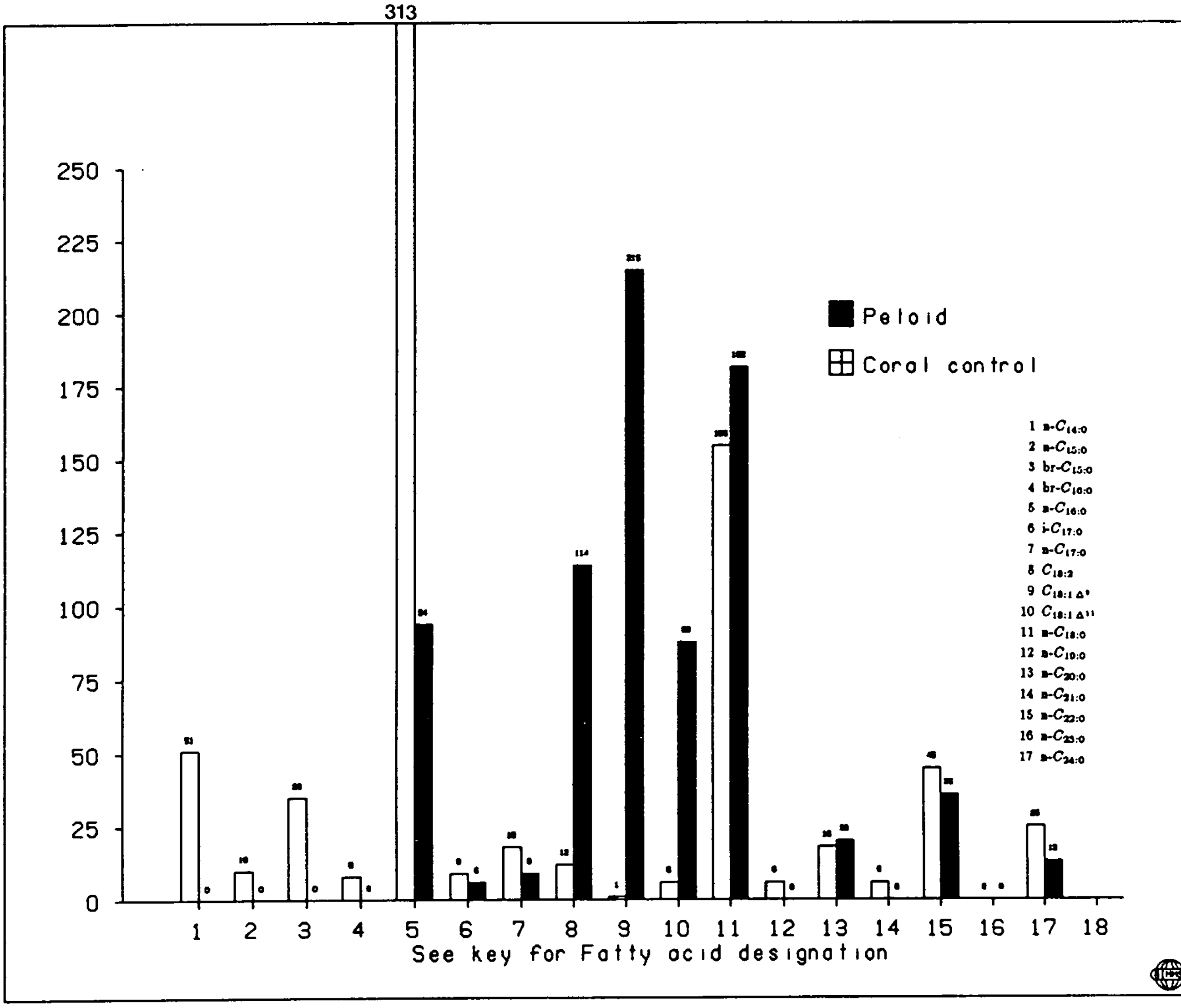

Figure 4.10 Peloidal and coral free fatty acid distributions. Discussion in text.

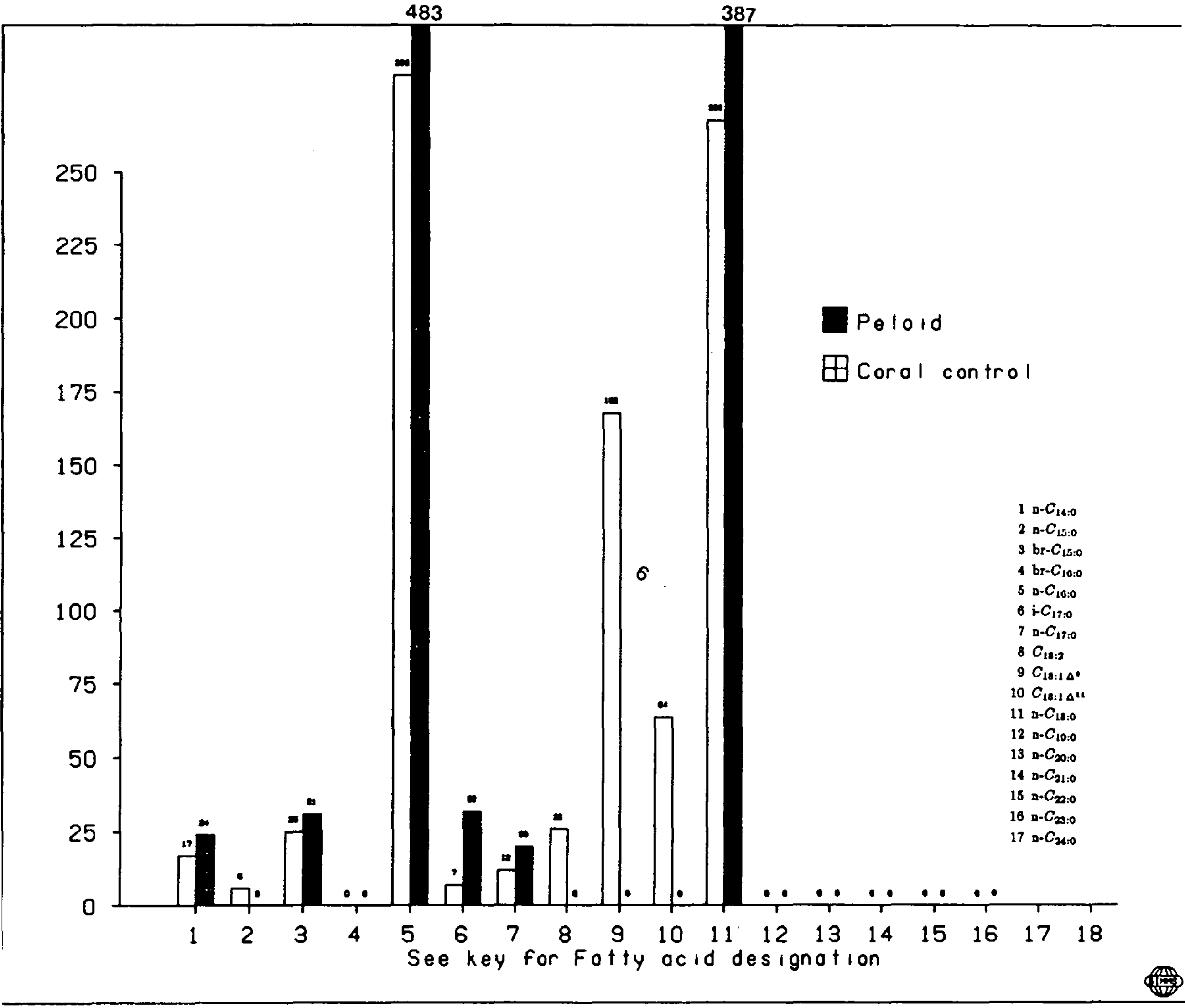

Figure 4.11 Peloidal and coral bound fatty acid distributions. Discussion in text.

4.5.4.8 Polar material and saponification residue.

The polar fractions of the solvent extractable organic matter were saponified (Section 4.4.2) to produce the bound sterols, fatty alcohols and fatty acids already discussed. There was a large amount of the saponified material remaining as a highly polar residue, and this was therefore inaccessible to gc-ms analysis. In addition, there were a large number of components in the bound lipid fractions which were detected by gc-ms but were not identified.

This material has been studied by several other techniques, as part of bulk analyses of the total solvent extractable organic matter and the results and derived information are presented in Section 4.7.

4.5.5 Summary of biomarker data.

The most reliable information on the origin of the peloidal organic matter that can be derived from the biomarker study must come from the major differences between the peloidal and control extracts, and these are summarised in this section.

The distinct lack of a range of wax esters in the peloidal sample tends to suggest that there is a minimal contribution to the organic matter from marine animal fauna, and this includes the corals themselves. This is substantiated by the very low overall concentration of the wax esters in comparison to other lipid classes.

The most important differences between the two samples are in the sterol fraction, where certain components are present in the peloidal sample at up to 10 times the concentration observed in the coral control. Whilst it is acknowledged that many organisms biosynthesise the sterols, the distribution is indicative of a marine algal input, and both green and blue green algae may be involved. There is unfortunately no detailed information of the sterol content of red algae, and so the potential contribution from the encrusting coralline algae (which have been associated with the peloids) cannot be evaluated.

Certain significant differences are also noticeable in the distribution of the fatty alcohols and fatty acids, but the widespread occurrence of these lipids in the biosphere limits their diagnostic value. However, having already discounted the possibility that marine animals, mangroves and other higher plants are providing an input, this leaves the algal or cyanobacterial sources as the most likely source of fatty acids and alcohols.

4.5.6 Evidence for bacterial input to the organic matter.

The only previously reported chemical molecular data for peloidal cements have been the recognition of the C_{16} fatty acid (Land & Goreau, 1970; Land, 1971). Although this has already been discussed and the conclusion drawn that it cannot be considered diagnostic for bacteria (Section 4.5.4.7), it is interesting to consider whether there is any other chemical fossil evidence for the involvement of bacteria in the precipitation of peloids.

Visible remains of bacteria have been observed in some peloids by careful etching (Chafetz, 1986), and they are apparently similar in appearance to travertine deposits which are also considered to be bacterial in origin (Chafetz & Folk, 1984). In addition, it is well recognised that bacteria are capable of altering the pore water carbonate chemistry, and many laboratory based experiments have shown that they do cause the precipitation of $CaCO_3$ (Lalou, 1957; Malone &

Towe, 1970; Krumbein, 1979a, 1979b).

The identification of the series of hopanes in the aliphatic fraction certainly indicates the presence of bacteria, but these compound were present in equal amounts in both peloidal and control samples and the low concentration tends to suggest that they are present as contamination only. The other particularly diagnostic biomarker for bacteria, bishomohopan-32-ol, was only identified in the peloidal sample, and therefore confirms that there is a measurable bacterial input to the organic matter. However, the concentration is very low compared to the other diagnostic lipids, and a number of other biomarkers which might be expected to occur if the bacterial input was significant, were undetected.

4.5.7 Conclusions of the lipid analysis.

The lipid analyses presented above can provide information only on the possible sources of the peloidal organic matter . Due to the fact that the peloids were not separable from the coral framestone, care has to be exercised to consider only the major differences in the lipid content of the peloidal and control samples to be reliable indicators of the organic matter origin. The most obvious differences (in the sterol distributions), coupled with the general lack of evidence for marine animal inputs, are most consistent with an algal source. The organic matter is certainly not sourced by a single species, and the distributions are indicative of both green and blue green algal involvement, although there is no definitive evidence for the latter. There is certainly no evidence for higher plant or mangrove input and surprisingly, the evidence suggests that the input from a coral source is limited. The presence of bacteria is recognised, but their involvement is considered to be minimal.

4.6 Interaction of Organic Matter and the Inorganic Phase.

4.6.1 Introduction.

The biomarker studies do not provide any information on the nature of the interaction of the organic matter with the inorganic phase of the peloidal cements and the relationship of the two is unclear under the microscope. In transmitted light the organic matter appears to be finely disseminated throughout the inorganic phase and no recognisable organic structures can be seen in unetched samples under the scanning electron microscope. This suggests that the inorganic material is coating the organic phase and was precipitated on the surface by a repeated nucleation process. The small crystal size confirms this suggestion as it indicates that the nucleation rate was high compared to the growth rate.

In order to understand fully the involvement of the organic matter, the nature of the interaction must be studied at the molecular level. Section 4.7 illustrates the use of techniques which can give useful information about the molecular nature of the total organic matter. The physical interaction has to be approached from a theoretical point of view, and a good insight into the possibilities can be gained by considering the state of knowledge about biomineralisation (Section 4.6.3).

The organic matter involved in the interaction is unlikely to consist of low molecular weight compounds like the chemical fossils because such simple molecules have little structural rigidity and cannot provide a spatially defined substrate on which the nucleation could occur. Such roles are more likely to be played by the higher molecular weight polar material left as a residue after the separation of the lipid fraction as described in Section 4.5.4.8. The latter would be able to provide a stable substrate, and due to its polarity, it may well have the ability to chelate Ca^{2+} ions.

From a purely chemical point of view, there are a limited number of organic matter types that are likely to be involved. Structural rigidity and the ability to bind and/or control local cation concentrations are essentially limited to those species associated with membranes and cell walls in biochemical systems. The most powerful molecules are the proteins; these are capable of highly precise three dimensional control and can exhibit a high degree of specificity. This group of molecules would certainly have the ability to discriminate between calcite and aragonite (Degens, 1976). Polysaccharides are polymeric molecules formed from many linked sugar units, one of the simplest building blocks being glucose (xv). These polymers also form three dimensional structures and their polar nature facilitates ionic interactions. The phospholipids are another natural product and are the major class of molecules that form membranes. These might also be capable of controlling inorganic phases, although they do not have the same range of properties as the proteins and polysaccharides. It is conceivable that the organic matter involved is a mixture of these types; mucopolysaccharides and glycoproteins are produced by many organisms and are used for specific processes.

These types of molecules might be expected to show a quite refractory nature towards the microbial and oxidation processes (Ehrhardt, 1977), as is essential for the survival of organic matter in the highly oxic reef environment.

4.6.2 The chemical nature of the interaction.

The general confusion in the literature with regard to the fact that organic matter can apparently act in both preventative and promotional roles can be clarified by considering the chemical properties required for interaction with ionic species in solvents of high dielectric constant such as seawater. Simple hydrocarbon type organic matter is hydrophobic in nature and is incompatible with the hydrogen bonded structure of water, so that interactions with species in aqueous solution is impossible. The introduction of polar groups into organic materials creates regions which have a more hydrophilic nature and it is these more reactive domains which can interact with ionic species. It is well established that proteins, polysaccharides and phospholipids commonly have spatially distinct hydrophilic and hydrophobic domains within the same molecule. Phospholipids have perhaps the simplest and most characteristic example of this property, with a hydrophobic hydrocarbon chain attached to a hydrophilic phosphate group. This is illustrated in Figure 4.12.

The preventative role would therefore involve the hydrophobic domains of such molecules, and the promotional role would be played by the hydrophilic part, with which the Ca^{2+} binding sites would be associated. It is interesting to consider how a particular molecule may be able to play both roles simultaneously. This could arise from the presence of two separate Ca^{2+} binding sites, one strong and one weak. The strong binding site would allow the molecule to attach itself securely to a $CaCO_3$ substrate, effectively insulating the substrate from the environment and preventing precipitation by presenting a hydrophobic surface to the aqueous solution. However, in another area of the molecule, the weaker binding site would attract or chelate Ca^{2+} ions, but might allow some exchange with the solution, this hydrophilic interaction being the basis for the catalysis of nucleation. Exactly this type of dual behaviour has been observed in polysaccharides isolated from, and believed to be essential to the formation of, coccoliths (Westbroek et al., 1986). (See Section 4.6.3.)

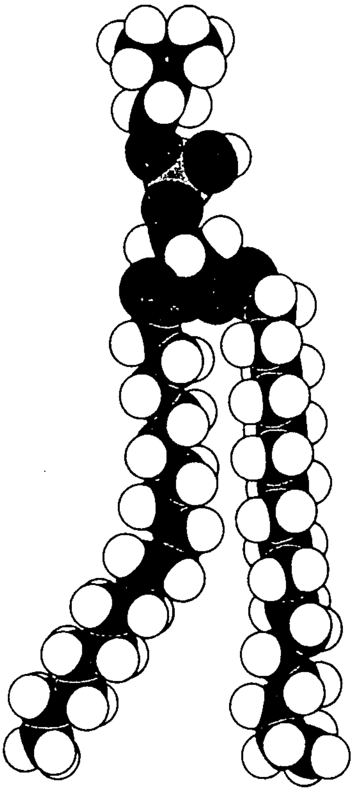

Figure 4.12 Space filling model of a phospholipid (phosphatidyl choline), showing long hydrophobic chain and ionic, hydrophilic head. (From Stryer, 1975).

4.6.3 Biomineralisation and skeletogenesis.

The mode of interaction of organic materials with the precipitation of skeletal material and the degree of control on the morphology and spatial distribution of biominerals varies enormously between organisms. Lowenstam (1981) suggested that two basic types of interaction occur, the first being an "organic matrix mediated" mechanism in which the organism manipulates a matrix on which precipitation occurs, whereas the second "biologically induced" mechanism is such that the organism acts as a causative agent in the precipitation. These are of course two end members, and the reality can often be somewhere in between. Many details are reviewed in Simkiss (1986). The following paragraphs briefly discuss the skeletogenesis mechanisms in a number of organisms in order to illustrate the most important and characteristic molecular interactions.

i) Corals.

The major phase of the skeletogenesis of corals occurs extra-cellularly, although the initial nucleation is an intra-cellular process (Goreau & Hayes, 1977; Hayes & Goreau, 1977). This is a little difficult to define in the above scheme as it is not readily apparent whether any matrix is involved, although large amounts of skeletal protein and polysaccharide are present (Mitterer, 1978; Weiner et al., 1983). The ability of the corals to nucleate only aragonite is not understood, but it may be due to an interaction in a specific manner with a matrix whose molecular dimensions are more similar to the aragonite rather than the calcite lattice.

Analysis of the proteinaceous material has revealed large amounts of aspartic acid to be present (Mitterer, 1978) and the similarity of the carboxyl group of this molecule with the carbonate ion may be responsible for the interaction with the $CaCO_3$(Figure 4.13). Proteinaceous material can apparently form a substantial proportion of the total organic matter of scleractinians but polysaccharide-type material is also known to be present Degens, 1979), and the sugar constituents released by hydrolysis have been used as biological markers for corals (Bõhm et al., 1980). Other studies on corals are reviewed briefly in Weiner et al. (1983), but the information on the molecular level is rather sparse.

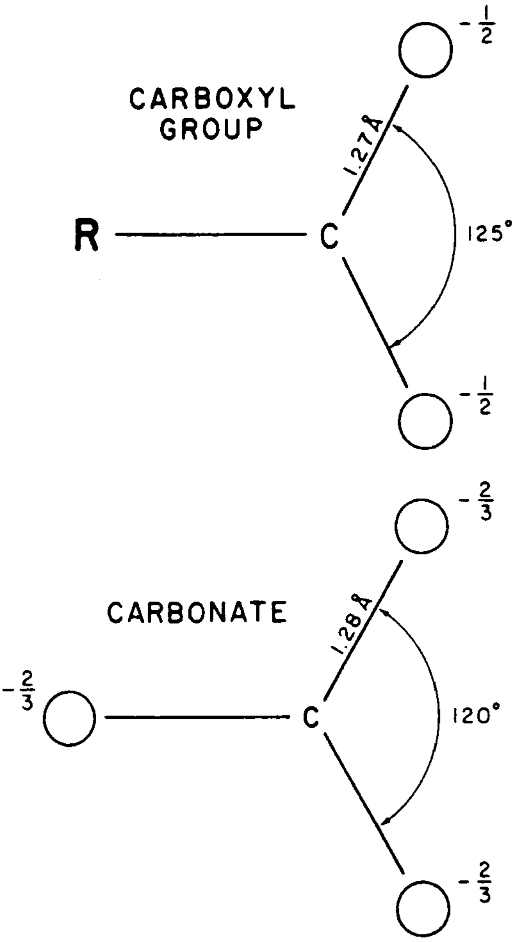

Figure 4.13 Diagram to show the similarity of the inorganic carbonate ion and the carboxylic acid group of some amino-acids. (From Mitterer & Cunningham, 1985).

ii) Mollusc skeletogenesis.

Degens (1976) presented a simple model which described the interaction of the organic and inorganic phases in the production of mollusc skeletal material. The model illustrates the ability of the organic matrix to behave in both the preventative and promotional manners, and this is a classic type of organic matrix mediated skeletogenesis. Whilst the model was developed from studies on molluscs, it has been suggested that the mineralisation process may be quite common and similar in other organisms (Degens, 1979).

The inorganic phase, whether calcite or aragonite, is associated with two major high molecular weight organic molecules. The first, called a carrier protein, is secreted by the organism in the form of sheets which form a thin film over the present skeletal surface. This functions as a binding matrix onto which an acidic polypeptide or glycoprotein fraction is attached. The latter has a high binding efficiency for Ca^{2+} ions.

Mineralisation occurs on the surface of the organic complex, and precipitation of ordered (and perhaps even epitaxial) crystals continues until a new layer of the glycoprotein becomes attached to the inorganic surface. When this occurs, the $CaCO_3$ is sandwiched by organic material which is presenting a hydrophobic surface to the surrounding solution, thereby inhibiting further precipitation. The process is illustrated in Figure 4.14. Continuation of skeletal growth can only occur after the secretion of another layer of carrier protein. The glycoprotein then becomes attached to the carrier protein with its hydrophilic Ca^{2+} binding sites exposed to the aqueous medium, and nucleation can then restart (Figure 4.14).

Degens (1976, 1979) suggested that strict control of the conformation of the carrier protein and variation in the geometry of the Ca^{2+} binding sites of the glycoprotein may result in the ability of the organism to control the stereochemistry of the precipitation. Hence, $Ca^{2+}O_9$ polyhedra would produce an aragonite lattice, whereas $Ca^{2+}O_6$ co-ordination would cause the precipitation of calcite.

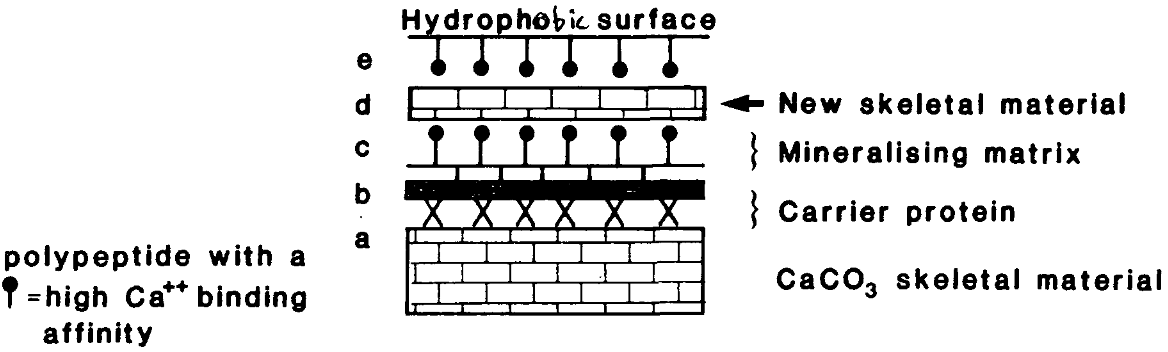

Figure 4.14a Calcification Mechanism of the mollusc matrix. Discussion in text.

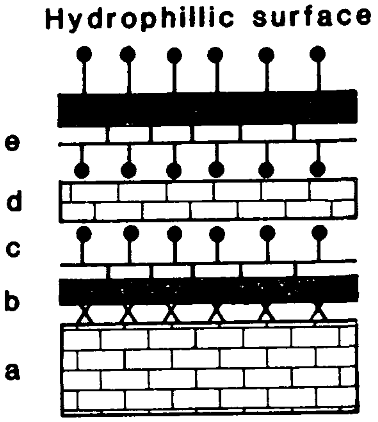

Figure 4.14b Second stage of the same.

iii) Algal calcification.

Calcification in the green alga *Halimeda sp.* begins with the formation of nuclei on the fibrous material in the cell wall (Simkiss, 1986) and a similar form of matrix mediated precipitation was observed in a species of calcareous red algae (Okazaki et al., 1979).

Although there was no information given on the nature of the nucleation surface in those studies, polysaccharides with strong Ca^{2+} binding affinities have been isolated from other red algae (Degens, 1976). A particular structural study of one of these polysaccharides is discussed by Rees (1977), who describes a molecule called carrageenan. This is a polymer of a simple disaccharide unit illustrated in Figure 4.15. It is thought that the sulphate group in this unit is responsible for the binding of Ca^{2+} ions.

iv) Calcification in Cyanobacteria.

Scanning electron microscope studies of the calcification process in kopara deposits on Pacific atolls (Défarge et al., 1985) have revealed that the precipitation of carbonate occurs on the surface of an organic matrix which is considered to be the polysaccharidic cell wall of the cyanobacteria. The polysaccharide sheaths have a distinct three dimensional structure which can apparently control the morphology of the precipitate.

v) Coccolith biosynthesis.

Polysaccharides are known to be associated with the production of coccoliths of the marine alga *Emiliania huxleyi* (van der Wal et al., 1983; Westbroek et al., 1986) and this is also thought to be a matrix mediated precipitation. The polysaccharide has been isolated and purified and is known to have a high binding capacity for Ca^{2+} ions (Kok et al., 1986). The role is thought to be similar to the mineralising matrix in the mollusc skeletogenesis and it is particularly interesting that this water soluble molecule of molecular weight 60,000 has two binding sites for Ca^{2+}. The first strong binding site is located on the main sugar backbone of the polysaccharide and this may provide the ability to bind to the $CaCO_3$ substrate (Borman et al., 1982). The molecule also has a repeating side chain which contains the second weaker binding site. The Ca^{2+} ions can apparently exchange with the medium quite easily at the latter site.

It is clear therefore that fairly simple protein and/or polysaccharide high molecular weight molecules have the capacity both structurally, and in terms of Ca^{2+} binding, to play a controlling role in both the prevention and catalysis of the nucleation of cements. The most intriguing facts are that both roles can be played by the same molecule, and that the three dimensional geometry of these molecules may be able to control both the mineralogy and morphology of the precipitate.

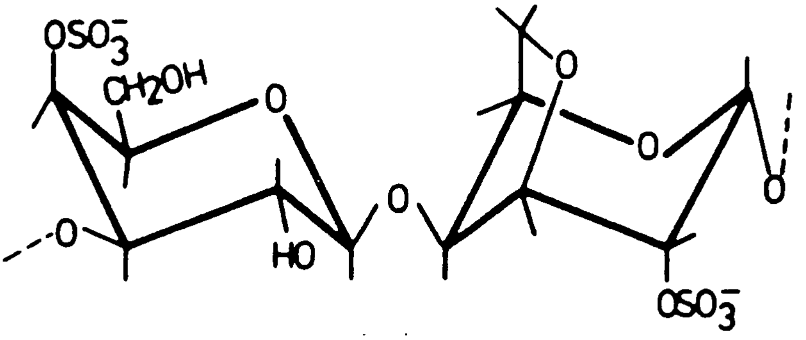

Figure 4.15 Carrageenan, a simple polymer of 3-linked β-D-galactopyranose 4-sulphate and 4-linked 3,6-anhydro-α-D-galactopyranose 2-sulphate, which has a very high Ca^{2+} binding capacity and may be involved in the precipitation of some marine skeletal material.

4.6.4 The formation of ooids.

Whilst there have been no previous studies of the interaction of organic matter in the precipitation of carbonate cements, there have been some interesting studies of the organic matter associated with another inorganically precipitated phase, the ooid.

The association of proteinaceous material with ooids has been recognised by several authors and this organic matter has been studied in some detail (Mitterer, 1968, 1972). The ooids are found to contain similar distributions of amino acids as are observed in some skeletal material, most notably the high concentrations of acidic molecules containing carboxyl groups. Mitterer (1972) noted that approximately 30% of the total organic matter was protein, with a further 25% being "mucopolysaccharide" in nature. The importance of this organic matter has also been noted in terms of its effect on the early diagenesis of the ooids (Ferguson et al., 1984) and in its potential conversion to oil (Ibe et al, 1983).

Attempts to produce ooids in the laboratory have been quite successful, particularly in the presence of a variety of both bio- and geopolymeric organic matter (Ferguson et al., 1978; Davies et al., 1978). These experiments have suggested that ooids may be formed in nature in association with an organic matrix whose properties are similar to the molecules involved in skeletogenesis. Ferguson et al., (1978) suggested that a high molecular weight polymer formed the basic substrate, and attached to this were smaller molecules possessing functional groups capable of interacting in a hydrophilic fashion with Ca^{2+} ions in seawater. Although the presence of both proteins and polysaccharides has been recognised within the organic phase, there is no detailed information on the molecular structure of the matrix. Ferguson et al. (1978), in discussing the type of organic matter that might be involved concluded that, "a group of compounds which appears to deserve special consideration in this respect are protein–mucopolysaccharide complexes".

It is therefore apparent that both skeletogenesis and purely inorganic precipitation can be controlled by protein and polysaccharide type organic matter. The following section describes the use of a number of analytical tools, in an attempt to discover whether these types of molecules are present in the peloidal organic matter.

4.7 Analysis of the High Molecular Weight, Polar Components of the Peloidal Organic Matter.

4.7.1 Introduction.

The fingerprinting techniques described in this section are able to provide evidence for the presence of specific molecules through the characteristic patterns produced when samples are bombarded by a variety of types of radiation. In pure samples or simple mixtures, the use of such analyses can frequently lead to the conclusive identification of compounds present. In complex mixtures such as the peloidal organic matter, which probably contains up to 1000 different molecules, conclusive identification is unlikely to be possible. The results can be used simply to indicate the presence of particular functional groups. Characteristic combinations of such functionality can then strongly suggest the presence of a class of compound such as, for example, polysaccharides. Comparison of the complex results with analyses of pure components can then be used to positively identify the presence of a specific molecule.

Techniques such as nuclear magnetic resonance spectroscopy are rarely used in the analysis of complex natural samples, but they can provide valuable evidence. These techniques as well as pyrolysis gc-ms have been used and the results are described in the following sections. The analyses were performed on the bulk solvent extractable organic matter from both peloidal and coral control samples.

4.7.2 Nuclear Magnetic Resonance Spectroscopy.

4.7.2.1 Introduction.

The nuclei of certain atoms are considered to spin in a manner analogous to electrons. This spinning generates a magnetic moment along the axis of the spin, and so the nuclei act as bar magnets. The most useful atoms for the purposes of studying organic matter are ^{1}H and ^{13}C. If these atoms are placed in a magnetic field, their own magnetic moment can be aligned either with or against the external field, and these two possibilities are manifested in two energy levels in which the nuclei can exist. Alignment with the external field is the lower energy level, and in order to cause the nuclei to jump to the higher level, with the magnetic moment opposed to the external field, some energy must be input to the system. In the analytical technique, this input is achieved by the bombardment of the sample with radiation of suitable energy. The power of nmr spectroscopy is due to the fact that the environment of any particular atom in a molecule is affected by the surrounding atoms. The magnetic field of each nucleus interferes with those of surrounding nuclei, such that the effective magnetic field at any point in the molecule is not equal to the applied magnetic field. The technique detects these variations, albeit in an indirect fashion. The sample is placed in a magnetic field and is bombarded by a certain fixed frequency of radiation. The magnetic field is then varied and at specific positions, energy is absorbed as the nuclei of specific atoms jump to the higher energy level, to produce an absorption spectrum as shown in Figures 4.16 & 4.17. The peaks in the spectrum are therefore diagnostic of particular groupings of atoms within molecules in the sample. The spectrum for the carbon atoms are recorded separately from the hydrogen or proton spectrum. Instrument details and the notation are explained in Appendix 4.

The proton nmr spectra for the peloidal and coral control extracts are discussed first (Figure 4.16).

4.7.2.2 ^{1}H-nmr spectrum of the peloidal organic matter.

There are a number of simple observations that can be made for peaks which occur in characteristic ranges of the spectrum and these are listed below:

i) The sharp peak at 0.0 p.p.m. is the internal standard (tri-methyl-silane, xvi), used to calibrate the spectrum.

ii) The complex peak at 0.85 p.p.m. is from protons of methyl groups, $RC{-}H_3$.

iii) The single peak at 1.25 p.p.m. is also from aliphatic protons, from methylene groups in long chains, $R_2C{-}H_2$.

The peaks in (ii) and (iii) arise from the alkanes, fatty acids and fatty alcohols identified in Section 4.5.4. Some contribution to these peaks may also be due to methyl and methylene protons in the polar residue.

iv) Peaks in the region of 1.5–3.0 p.p.m. include a broad peak at approximately 2.8 p.p.m. which probably arises from carboxylic acid groups of the fatty acids.

v) Large singlet peak at 3.4 p.p.m. is due to the methanol solvent.

Peaks in the region of 3–5 p.p.m. are produced in general by protons attached to electronegative atoms such as oxygen or carbon.

vi) The broad peak at 3.5–3.7 p.p.m. is complex, indicating a number of different environments, perhaps indicative of a higher molecular weight molecule.

Both polysaccharides and polypeptides are reported to show broad resonances in this area of the spectrum (Gillam & Wilson, 1985).

vii) The sharp peak at 3.8 p.p.m. is probably due to protons in alcohol functional groups, RO–H.

viii) The two groups of peaks at 4.0 and 4.3 p.p.m. are particularly interesting as they appear to be coupled together, as the two groups have a mirror image symmetry. Peaks due to a variety of sugars are known to occur in this region (Breitmaier & Voelter, 1984; Gillam & Wilson, 1985) and the fact that the peaks are quite sharp indicates that they may well arise from a small molecule containing only two different sugars. This would be analogous to the structure of carrageenan (Figure 4.15).

ix) The sharp peak at 7.2 p.p.m. is also from solvent, chloroform.

x) A minor group of peaks at 7.4–8.1 p.p.m. are thought to arise from olefinic or aromatic protons. As there is no other evidence for aromatic material, these peaks probably arise from the unsaturated fatty acids identified in Section 4.5.4.

4.7.2.3 ^{1}H-nmr spectrum of the coral control extract.

In order to identify the input to the peloidal material, the differences between the peloid and coral extracts must be identified. Due to the much smaller amount of the coral extract, it was analysed on a more sensitive instrument than the above sample and the calibration has proved to be slightly different, resulting in a slight offset in the p.p.m. range. This spectrum is described below.

i) The peaks at 0.95 and 1.35 p.p.m. are equivalent to the aliphatic protons of i) and ii) above.

ii) The sharp peak at 2.2 p.p.m. is not present in the peloidal extract and is probably due to methylene protons, $RC{=}CHC{-}H_2$.

iii) The complex peak at approximately 2.8 p.p.m. in the peloidal extract is apparently not present in the control sample. This was previously assigned to the carboxylic group of the fatty acids which are known to be present in the control sample also. This suggests that the peloidal sample contains some other carboxylic acid containing molecule not present in the control.

iv) The peak at 3.3 p.p.m. is the methanol solvent.

v) The most notable difference is the lack of the broad peak noted in the peloidal sample at 3.5–3.7 p.p.m. which was suggested to possibly arise from polysaccharides and / or polypeptides.

vi) The sharp peak at 3.6 p.p.m. is equivalent to the alcohol group peak in the peloidal sample.

vii) Another interesting difference is in the region of 4.0–4.5 p.p.m. , where there is a single triplet peak. If these peaks are due to polysaccharides then this might suggest that the control sample contains a molecule with only one sugar type compared to two in the peloidal sample, although this is highly speculative.

viii) The large peak at approximately 4.8 p.p.m. is due to the presence of water, but fortunately this does not interfere with the comparison as no peaks are present in this region in the peloidal spectrum.

ix) There is no peak at about 7 p.p.m. because no chloroform solvent was used.

x) Small peaks in the region of 7.5 p.p.m. are probably also due to olefinic resonances analogous to the peloidal sample.

The absence of the peaks in the region of 2.8, 3.5, and 4.0 p.p.m. in the control sample indicates that the peloidal organic matter might contain polysaccharides not present in the control. This could be of similar structure to the carrageenan previously described, in that it appears to be formed of two sugars. It must be emphasised, however,that this conclusion is only very tentative.

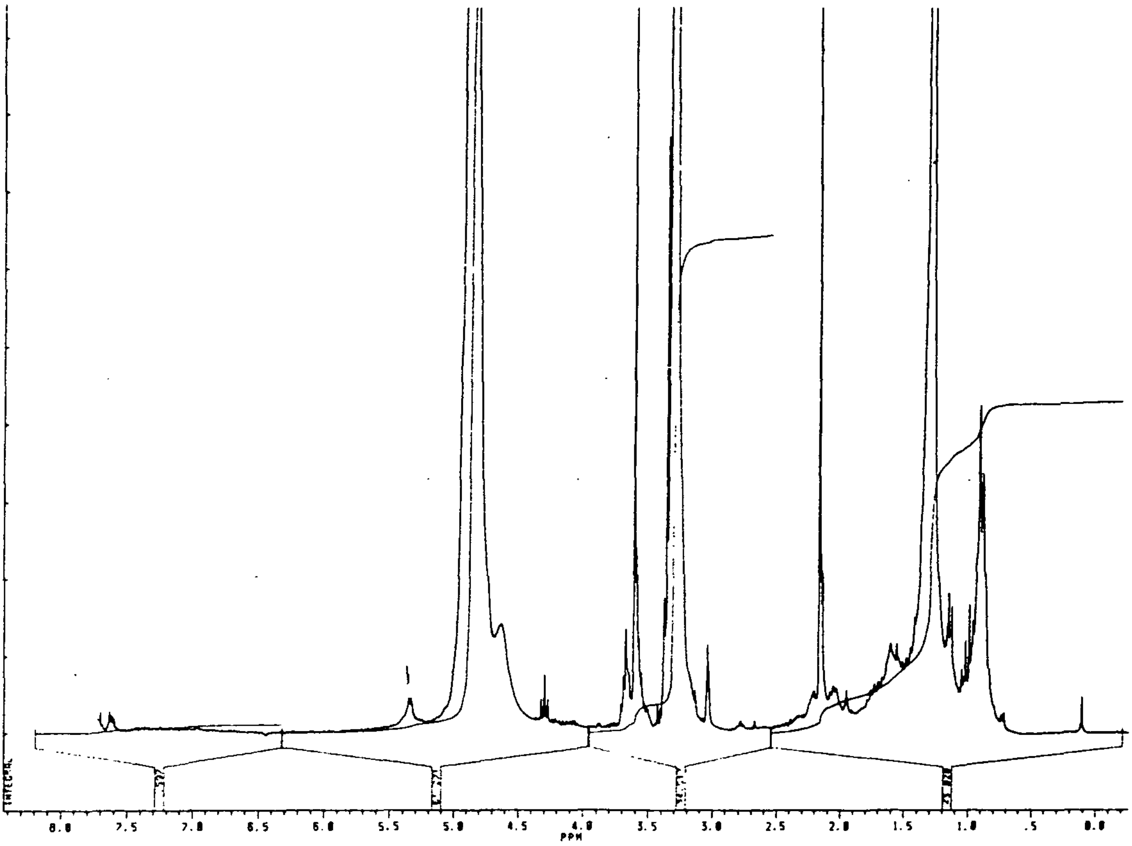

Figure 4.16a ^{1}H-nmr spectrum of coral sample. Discussion in text.

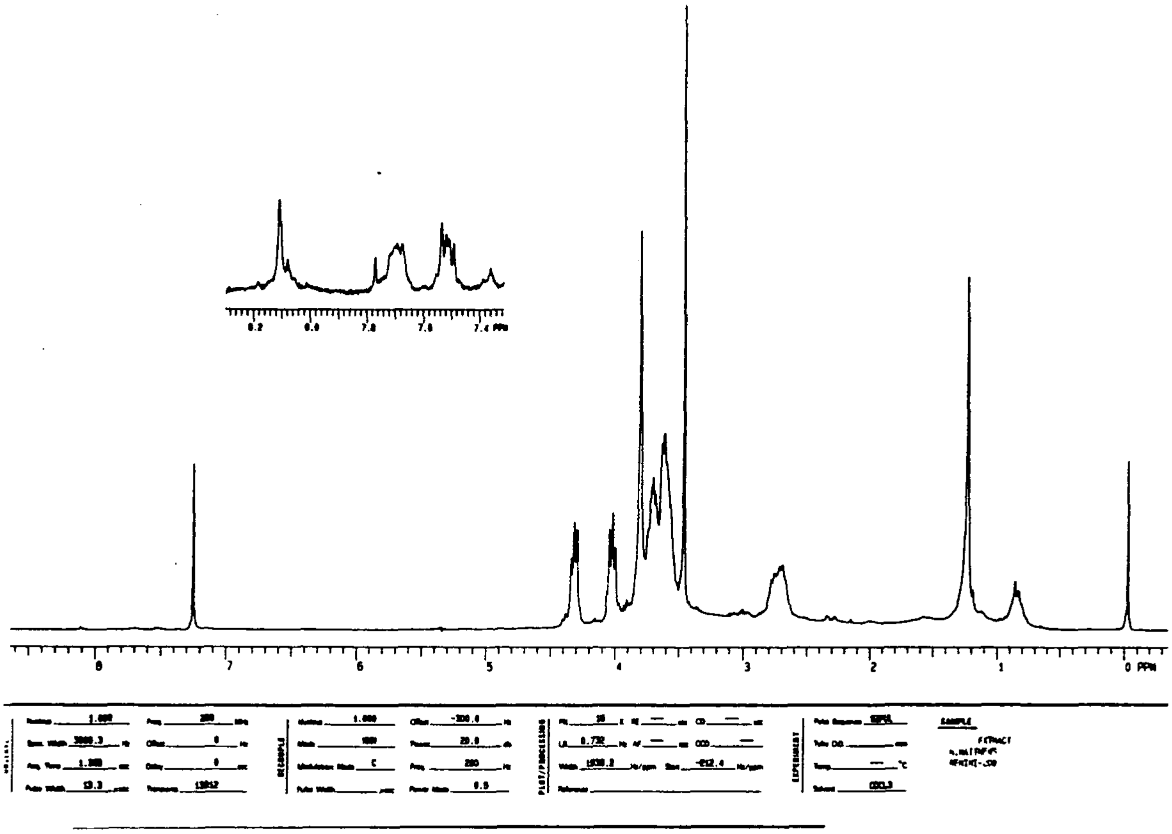

Figure 4.16b ^{1}H-nmr spectrum of peloid sample. Discussion in text.

4.7.2.4 ^{13}C-nmr spectrum of the peloidal organic matter.

The carbon nmr spectra are considerably less sensitive than the proton nmr but some interesting peaks can be seen (Figure 4.17).

i) The peak at 30 p.p.m. is due to methylene carbons, R_2–C–H_2.

ii) The peak at 49 p.p.m. is due to the methanol solvent.

iii) The peak at 50.7 p.p.m. is also of alcohol origin.

iv) The peak at 56.7 p.p.m. is from carbon atoms of methoxy groups, RO–C–H_3. (Gillam & Wilson, 1985).

v) The two peaks at 59 and 61 p.p.m. are also due to carbon bonded to alcohol groups, and could be arising from the same molecule which produces the mirror image triplets in the proton spectrum.

vi) A range of small peaks in the region of 65–75 p.p.m. and in particular at 72.5 p.p.m. has been previously reported to be due to polysaccharides. (Gillam & Wilson, 1985; Breitmaier & Voelter, 1984).

vii) The very large triplet centered at 77 p.p.m. is due to the chloroform solvent.

viii) The small singlet at 86 p.p.m. may also be of carbohydrate origin (Gillam & Wilson, 1985).

It is interesting to note that there are several peaks which suggest polysaccharides are present, confirming the indications fron the proton nmr spectrum. Whilst the evidence in the latter was that some peaks may also be due to polypeptides, such molecules should produce resonances in the carbon nmr in the region of 40–50 p.p.m. and no such peaks are observed.

4.7.2.5 ^{13}C-nmr spectrum of the coral control.

It is difficult to compare the carbon spectra of the two samples as the control was run on a more sensitive instrument and so the peaks are much larger. All of the peaks present in the peloidal sample can be identified in the control with the exception of the peak at 50.7 p.p.m. in the former which is not of very much diagnostic value, as it simply indicates the presence of alcohol groups, with no detailed information.

4.7.2.6 Conclusions from the nmr data.

Although any conclusions must be tentative, it appears that both peloidal and coral control samples may contain polysaccharides . The proton nmr indicates that if such polysaccharides are present, then the molecules present in the peloids are more complex than those present in the control, and it may just possibly be a polymer of two sugars similar to carrageenan. There is little evidence for the presence of any proteinaceous type organic matter .

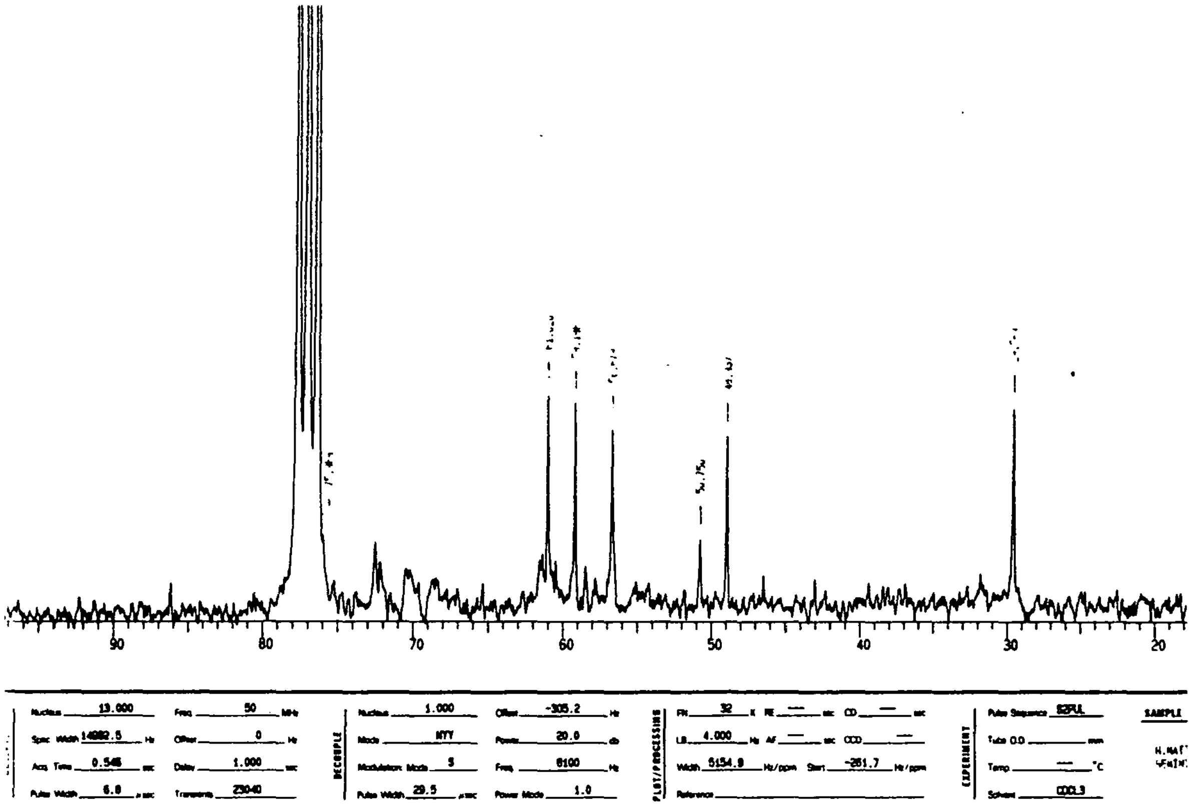

Figure 4.17a ^{13}C-nmr spectrum of the peloid sample.

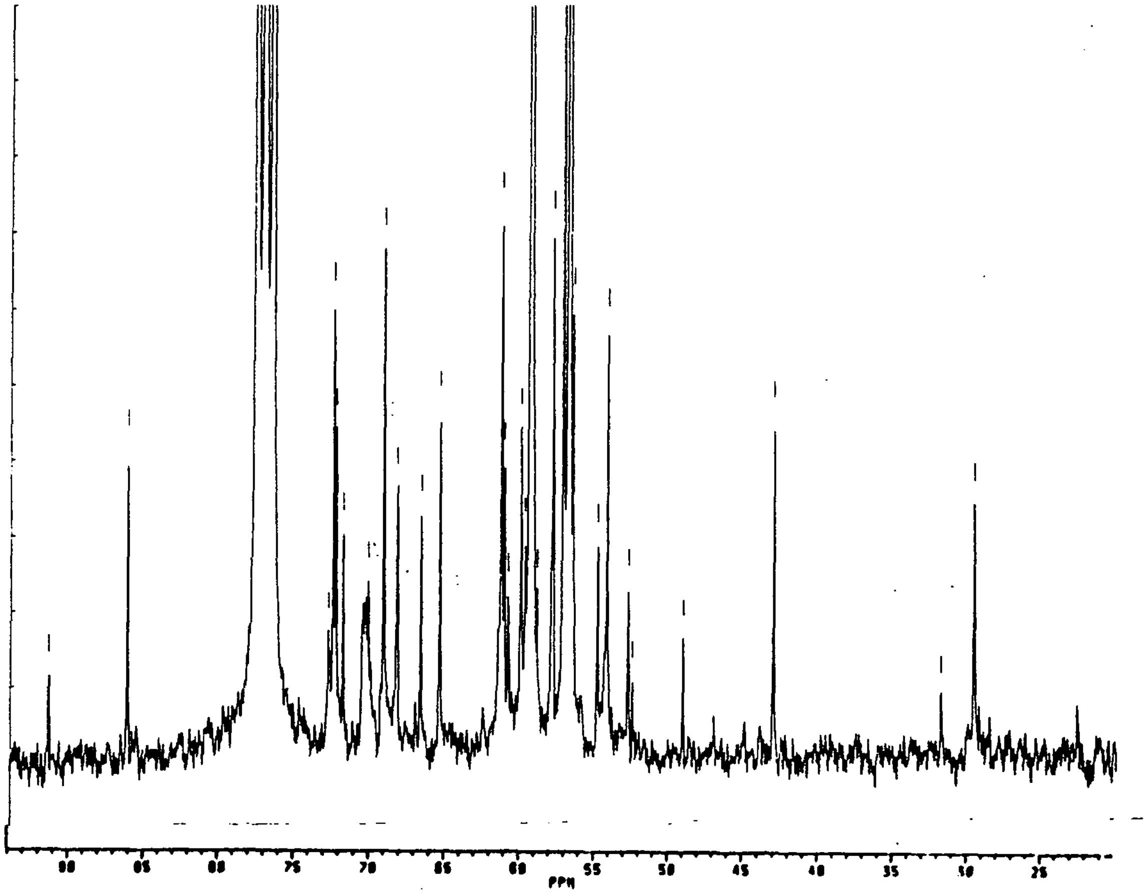

Figure 4.17b ^{13}C-nmr spectrum of the coral sample.

4.7.3 Pyrolysis Gas Chromatography–Mass Spectrometry.

This technique is similar to the gc-ms analyses described in Section 4.5, but the use of pyrolysis enables the study of the higher molecular weight polymeric fraction of the organic matter. The pyrolysis stage cleaves the large molecules in to smaller fragments which can then be readily separated by gas chromatography and identified by mass spectrometry.

The same procedures have been employed to enable recognition of any posible contamination and contribution from the coral substrate. The bulk organic extracts from the peloidal and coral control sample were analysed by the geochemistry unit of the University of Delft, The Netherlands. As a preliminary study the samples were analysed by pyrolysis gas chromatography alone, a standard procedure for these samples. The results of these analyses are presented in Figure 4.18.

The pyrolysis products elute in the first 40 minutes and the remainder of the chromatogram consists of low molecular components present as such in the samples and analysed in full in the previous sections. The very large peak present at an elution time of 50 minutes is probably the n-C_{16} fatty acid identified in Section 4.5.4.7 (van de Leeuw, pers. comm.).

Although the differences in scale on the two traces should be emphasised, there appear to be more pyrolysis products in the peloidal sample, confirming the presence of high molecular weight materials. The next stage in the analysis would be to use py-gc-ms to identify the pyrolysis products, but at the time of completion of this thesis these results have not been received, so no further information regarding the structure of this material can be presented.

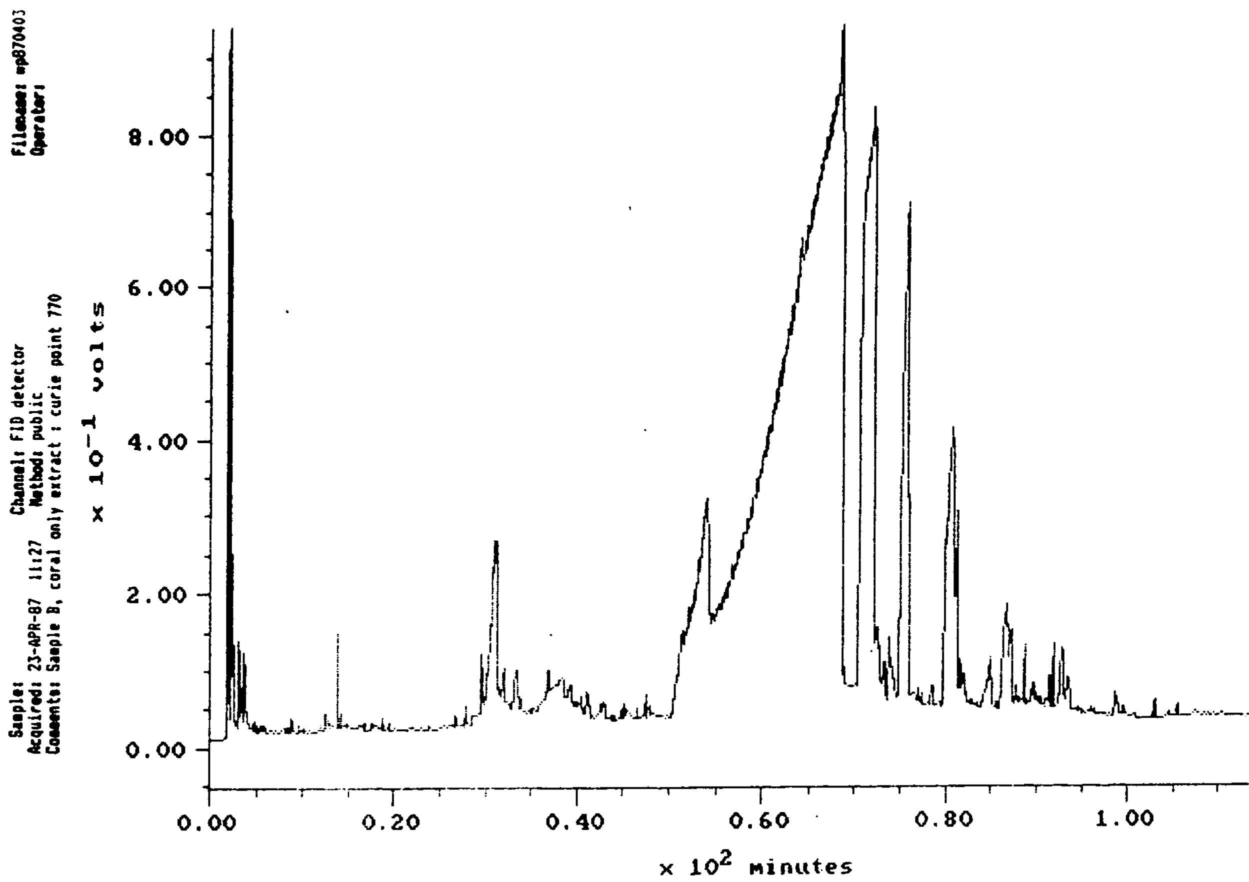

Figure 4.18a Pyrolysis gc trace for the coral sample.

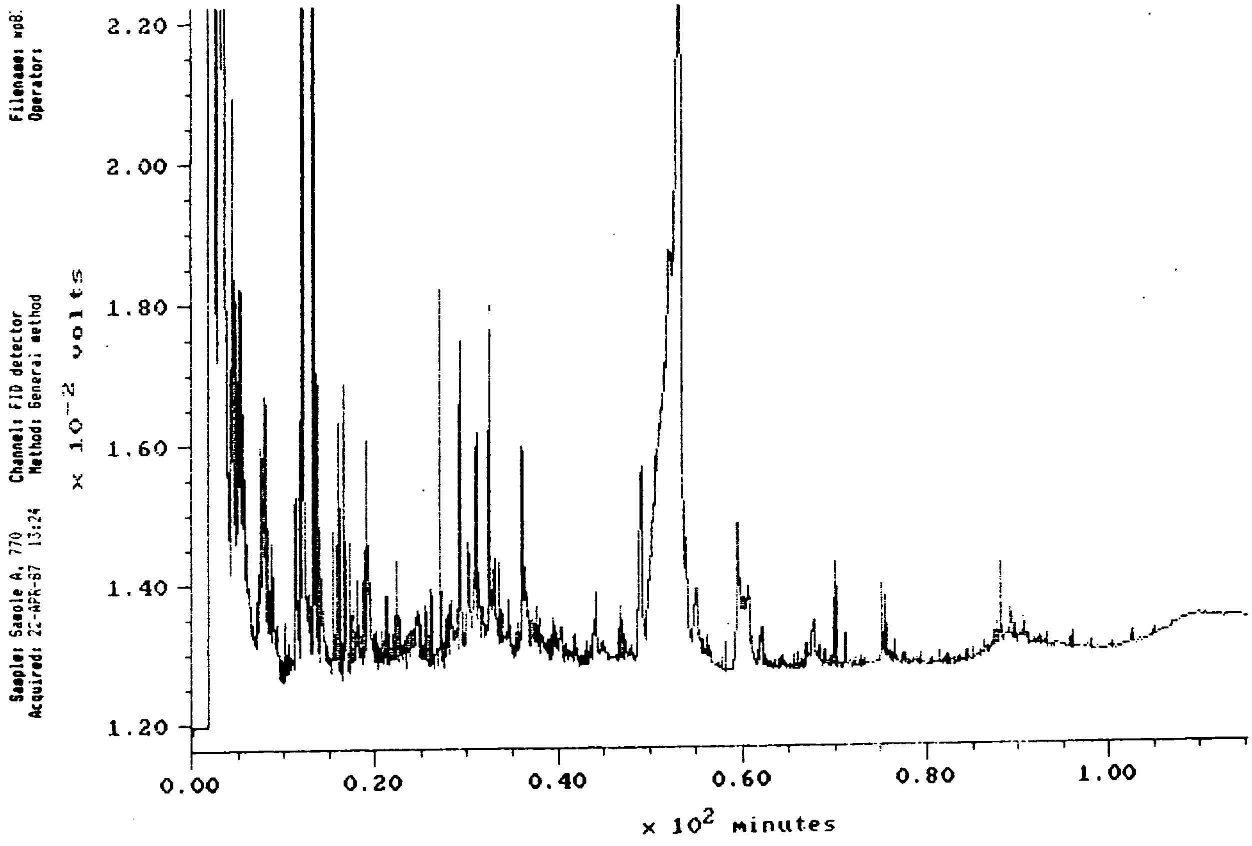

Figure 4.18b Pyrolysis gc trace for the peloid sample.

4.8 Conclusions on the Origin and Role of the Organic Matter in the Peloidal Cements.

Three major roles for organic matter have been identified. These are: a direct source of the bicarbonate for the precipitation, a preventative coating, and a promotional or mediatory phase. No evidence has been identified in this study for the direct source of inorganic bicarbonate from organic matter, and comparison with most other studies of Recent cements confirms that the majority are precipitated at or near to equilibrium with marine waters of normal composition. The isotopic composition of the inorganic phase of the peloidal cements indicates no organic contribution.

The prevention of precipitation by organic matter is a process which is very difficult to prove though is theoretically reasonable to suggest, as there are a wide variety of natural products which would be able to bind to and coat calcium carbonate substrates. It is unlikely that this process is capable of preventing cementation entirely, particularly in the oxic conditions of modern reefs, but it is a contributory factor in the maintenance of a high supersaturation state.

The role of the organic matter in the peloidal cements appears to be a promotional one, and the source of this organic matter and the nature of the organic-inorganic interaction have been discussed above. The results of the biological marker studies are most consistent with an algal source for the organic matter, and no further evidence for the participation of bacteria has been recognised.

From a theoretical chemical point of view, the interaction of the inorganic phase is likely to be with higher molecular weight, polar fractions of the organic matter. The mechanism of this interaction is likely to be similar to that in skeletogenesis processes, and it is poossible that the mineralogy could be controlled by the geometry of the organic phases. Study of these complex materials is exceedingly difficult, and no particular species has been identified. However, of the two most likely classes of molecules (proteins and polysaccharides), the n.m.r. studies suggest that polysaccharides are more important in the peloidal organic matter. Pyrolysis chromatography techiques have confirmed the presence of higher molecular weight material and further pyrolysis mass spectrometry could lead to the conclusive identification of particular classes of molecules.

CHAPTER 5

Hydrodynamic Modelling of Cementation Patterns.

CHAPTER 5

Hydrodynamic Modelling of Cementation Patterns

5.1 Introduction.

Although there have been a very large number of studies of the diagenetic products in reefs of all ages, most concentrate on the the geochemistry of the pore water and the precipitated cements with very little explanation of the observed distribution patterns. The inhomogeneity of the cementation patterns within modern reefs has been illustrated in Chapter 2 and is frequently commented upon in the literature (Marshall, 1985; Schroeder & Purser, 1986). In particular, the extent of the cementation has been observed to vary on a very small scale, down to the individual pore level.

The aim of the mathematical modelling presented in this chapter is to show that the rate of flow of pore water through the rock matrix is the major factor controlling the extent of the cementation and that the permeability therefore controls the cementation patterns. This modelling has been developed on the basis of a representation of the real system on the thin section level, but the principles of the model are applicable on all scales.

On the reef and formation scale, Buddemeier (1986) has presented virtually the only study which discusses the internal hydrology of carbonate formations, reefs in particular. He noted that the fluid fluxes will have a major controlling effect on the nature, rate and extent of diagenesis and emphasised that the poroperm characteristics of reefs are extremely variable on the whole reef scale. This inhomogeneity is a direct result of the small scale variations in structure and texture that typify modern reef growth.

This heterogeneity makes it very difficult to use formation scale poroperm characteristics in any definitive predictive fashion within the reef body itself, where relatively low permeability framestone and bindstone material, higher permeability coarse sands and the highest permeability vugs and caverns are all present in a complex three dimensional distribution. Expansion of the modelling to the reef scale therefore depends on the input of sufficient data to characterise adequately the three dimensional variation.

Section 5.2 outlines the theory behind the concept that the hydrodynamic characteristics control the distribution patterns of the cements, and Section 5.3 illustrates the design of the mathematical model used to represent the poroperm characteristics of carbonate framestones. Section 5.4 describes the simple mathematical basis of the model and describes the various parameters used to tune it to the real system. Section 5.5 illustrates a series of interesting results obtained during the development of the model and presents the final stages of the process which compare most favourably with the real cement distributions. Section 5.6 discusses the limitations of the present model and indicates its future potential on several scales and Section 5.7 presents some data on the poroperm characteristics of a Miocene reef which were collected in an attempt to increase the scale of the modelling to the whole reef level. This Chapter is concluded in Section 5.8.

5.2 Precipitation, Growth and Distribution of Carbonate Cements.

The realisation that the cement distribution can be inhomogeneous even on the thin-section level has led to the development of the concept of the microenvironment (Schroeder, 1972a), and there has been much discussion on the chemical nature of and the geochemical controls on this microenvironment (Schroeder & Purser, 1986). Decomposition of organic matter and other biogenic metabolic effects have generally been considered to be a major factor controlling the microenvironment, variation in the chemistry on this level leading therefore to the different products and the varying extents of cementation in individual pores. Hence the spatial variation in the pore water chemistry has been thought to produce the observed spatial variation in the cementation.

However, the research presented in the previous chapters has provided little evidence for any modification of the seawater chemistry on such spatial scales. In addition, irrespective of the mechanism of precipitation, there is a requirement for a large volume of water to flow through the reef matrix in order to precipitate a substantial volume of cement. Although the water in the Florida area may be several hundred percent supersaturated with respect to both common forms of $CaCO_3$, the total molar concentration of Ca^{2+} and HCO_3^- is still quite low, (10^{-3} to 10^{-2} M), such that the minimum volume of water required to precipitate $1cm^3$ of $CaCO_3$ would be of the order of ten thousand cm^3 (Bathurst, 1975; Berner, 1980). This figure is based on removal of all the $CaCO_3$ from the water which would of course only occur on evaporation. In reality, only that volume of $CaCO_3$ which is above the supersaturation state would be precipitated, and in addition, the process is bound to be inefficient. It seems likely therefore, that up to 100,000 pore volumes of water would have to pass through a pore in order to fill it with cement.

These mass balance calculations indicate that the diagenetic system within modern reefs must be physically 'open' (in the sense defined by Pingitore, 1982) on all scales, so that effective chemical exchange can occur. This fact is difficult to rationalise with the earlier suggestions of chemically varying microenvironments, as the persistence of such chemical differences would require at least a partially closed system. The suggestion to be investigated with the mathematical models is that the major factor controlling the cementation pattern is the microenvironment as determined not by the pore water chemistry but by the flux of such pore fluids, and therefore, by the permeability on the pore to pore scale.

A fundamental understanding of the controls on cementation must be based on the identification of the rate limiting step in the process. Crystal growth in the hydrodynamic regime present in reef sediments is thought to be transport and not surface controlled (Berner, 1980), implying that the rate of growth of $CaCO_3$ cements is limited by the rate at which Ca^{2+} and HCO_3^- ions are supplied to the growing surface. Some authors have suggested that surface diffusion is the rate limiting step in the growth of crystals (Turner, 1982), but these studies are based on a free supply of Ca^{2+} and HCO_3^- ions to the surface on an atomic level. Whatever the control on that scale, the requirement for supply of ions to the pore in which cement is forming is clearly the rate limiting factor, as the precipitation of cement in a pore which is sealed from the environment will cease as soon as the available $CaCO_3$ is removed from solution.

Hence, during a fixed time period, the greater the rate of flow of water through any pore, the greater will be the extent of cementation. These flow rates will vary on a pore to pore scale and will be determined by the local permeability of the rock matrix. The suggestion is therefore that the microenvironments are not chemically controlled in space, but are permeability controlled. This permeability has to be considered at the level at which the variation in the cementation is being observed, and so in this study it is considered from the frame of reference of individual pores. It is debatable whether one can consider permeability as a property of an individual pore, but the above concept can be tested without a specific knowledge of that parameter. In the following model, it is represented simply on the basis of the flow velocity through any given pore.

Although the concept of the microenvironment as determined by the permeability may be able to explain the observed variation in the degree of cementation, the model does not attempt to account for the spatial variation in the morphology or mineralogy of the cement. The observation of sequences of cements and variations in the sequences has to be explained by the variation in the pore water chemistry, but this variation need not be on a spatial level. Temporal modification of the water chemistry coupled with spatial variation in the poroperm characteristics could lead to the observed cement sequences. Whilst the microenvironment is not necessarily chemically controlled in space, there may be a chemical control in time. One could also argue that a permeability control in space is equivalent to a chemical control in time as the former causes a variation in the number of Ca^{2+} and HCO_3^- ions passing through the pores.

The variation in the flow rates through the reef will be dependent on the spatial and temporal variation in the permeability; this is the principle property recreated in the model described in Section 5.3. However, flow rates will also be dependent on the hydraulic gradient, for it is the presence of such a gradient that provides the driving force for flow to occur. This hydraulic gradient is produced by a combination of wind, tide and ocean currents pumping water through the reef, leading to a simple hydraulic head or difference in water level across the reef. The equilibration of these water level differences might be expected to make a major contribution to the total flux through a reef body in an atoll, where the lagoon is effectively sealed by the encircling reef. In the Florida reefs there is no such seal as the shelf edge reef tract is far from continuous. In this case, tidal channels between the reefs are likely to distribute much of the excess water as tides rise and fall. Thus the flow through the reefs by the hydraulic head mechanism may be quite small.

In addition to, and perhaps more important than, the flow induced by hydraulic heads, will be the flow caused by the pumping action of waves passing over the reef flat, particularly when the surface of the reef is within a few metres of sea level. However, wave energy is rapidly attenuated with depth in the water column and with depth into the porous medium, and may therefore only contribute to flow in the surface of the reef. Wave energy has frequently been considered to be an important factor controlling the precipitation of cements (Ginsburg & Schroeder, 1973; James et al., 1976), and this may explain the observation that cements are present in greater concentration at the surface of Alligator reef rather than in the shallow subsurface (Section 2.8.6).

5.3 Modelling of the Permeability Characteristics of Carbonate Framestones.

The design of the model and the philosophy behind the development of the model are illustrated in Figure 5.1 & 5.2, which are described in the following paragraphs. The modelling has been concentrated exclusively on coral framestone material as this is the major component of the Holocene reefs of Florida. A mathematical model of a real system has to be based on a valid conceptual model which describes the principal factors controlling the aspects of the system to be investigated. In this case, the conceptual model is that the distribution of the cements in modern reefs is determined by the permeability characteristics of the rock matrix. Based on this concept, a simple mathematical model was derived which is controlled essentially by just one fluid mechanics relationship which describes the nature of flow through porous media.

The input of some basic data to define the permeability and the rate of cementation allows the calculation of a solution which in this case is presented in a graphical form. This solution must then be compared to the real system in order to evaluate whether the model accurately recreates the aspects of reality. Development and tuning of the model to the real system is then achieved in an iterative process, by altering the basic data input until a sufficiently accurate representation is achieved. If a reasonable solution cannot be produced, then the original conceptual model has to be altered or abandoned. Fortunately in this study, the original concept appears to be valid.

Figure 5.2 describes the original design of the model, some aspects of which have not been incorporated into the mathematical description, but whose potential use is discussed in Section 5.6. Most notably, it has proven difficult to use a spatially valid statistical method to compare the created and real cement distribution. Nevertheless, visual comparison indicates that the model is successful.

MODEL PHILOSOPHY

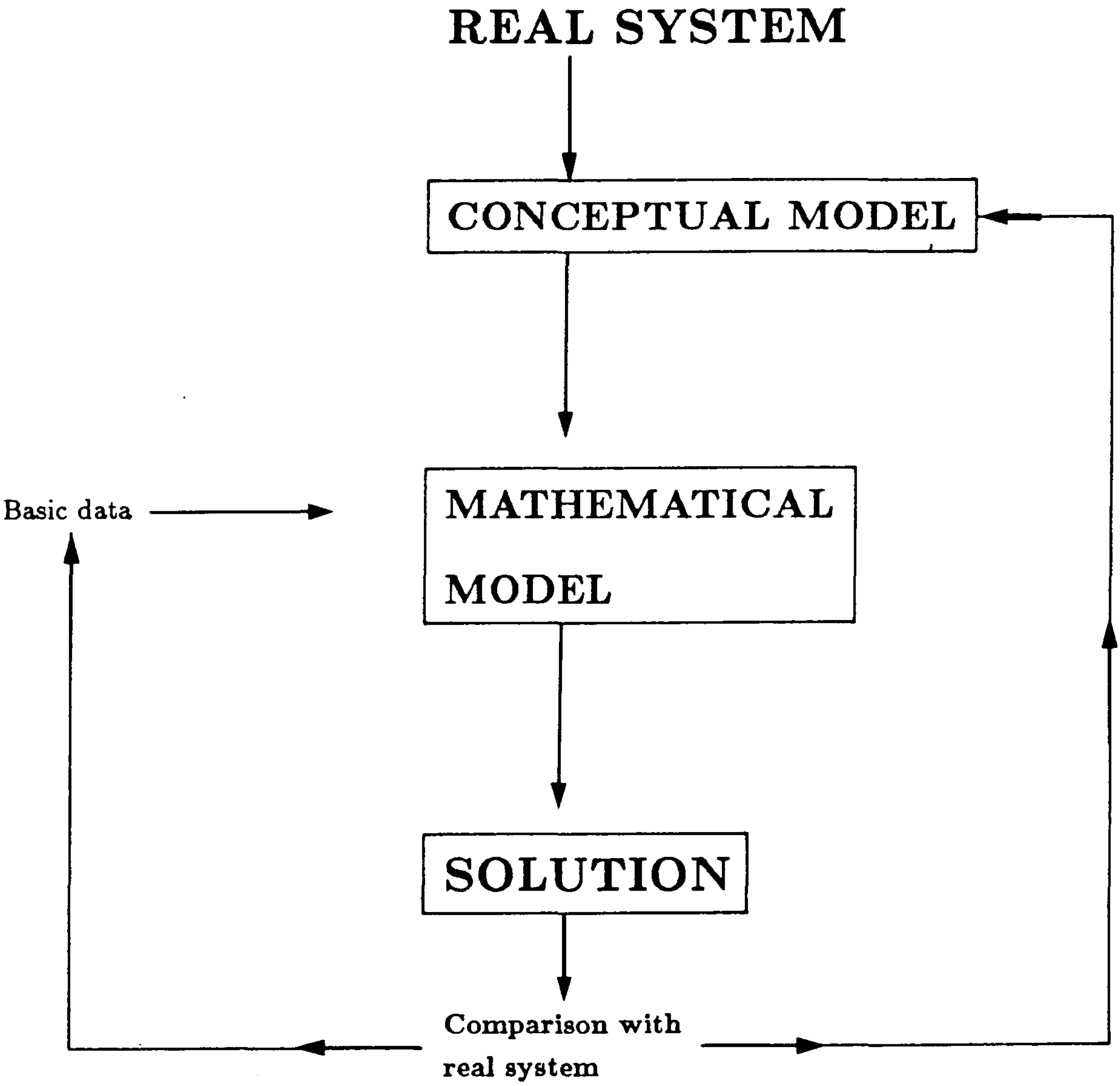

Figure 5.1 The philosophy behind the mathematical modelling of a real system. Discussion in the text.

MODEL DESIGN

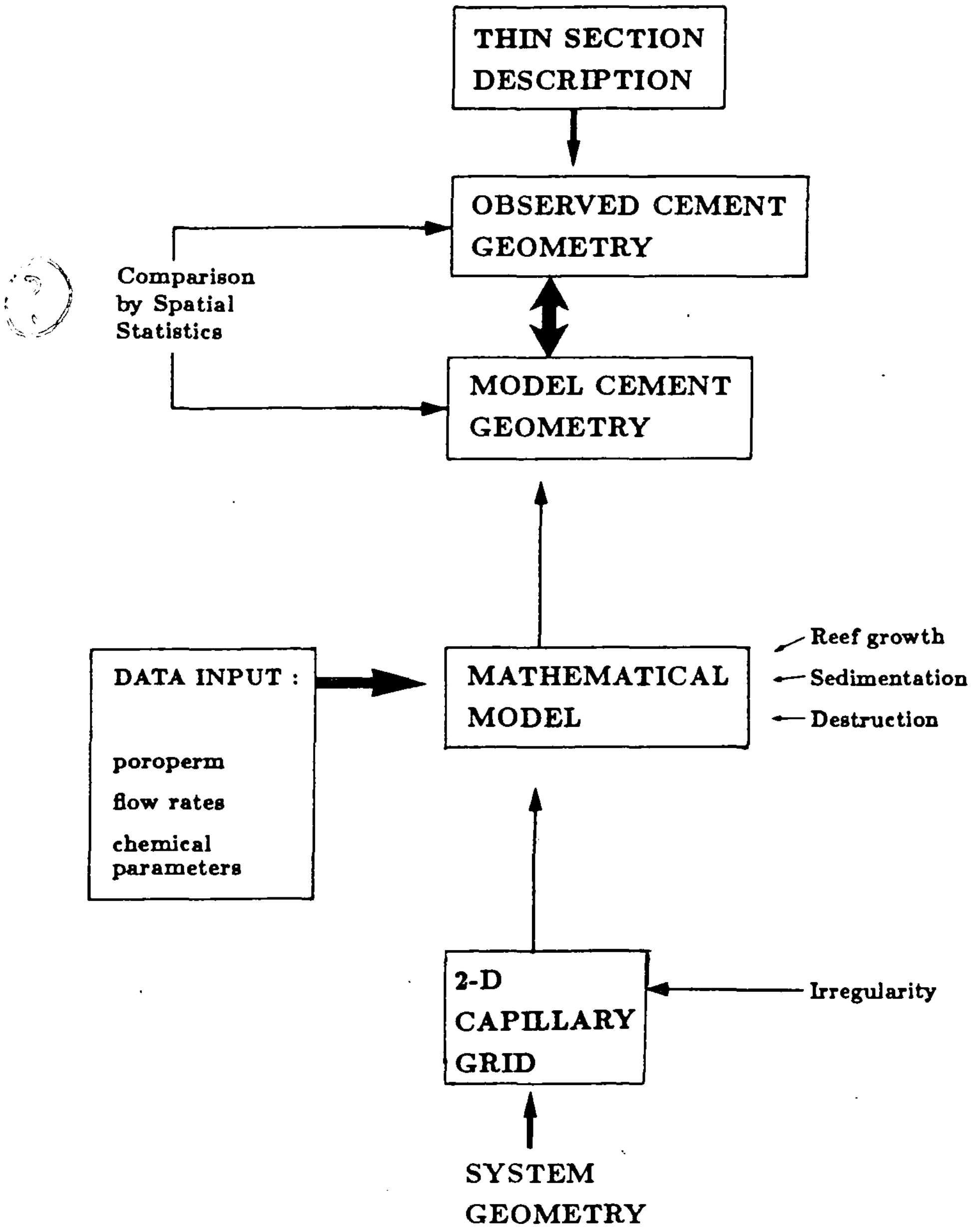

Figure 5.2 Design of the mathematical model to study cementation in coral framestones. Not all of the aspects indicated have been incorporated as discussed in Section 5.6.

The basic system geometry is of a grid of capillary tubes, into which some irregularity can be introduced. This geometry is described mathematically, and input to this are data which define the porosity of the system, the rate of flow and, in an indirect fashion, chemical parameters describing the precipitation of cements. The model then produces a cementation pattern whose geometry can be compared to the real cement distribution as described from the thin-section. A number of assumptions have been made in order to be able to describe the real system in simple terms :

i) The real system is in a laminar flow regime; flow through the pores of the system is non-turbulent. This assumption can be verified by calculating the dimensionless number - the Reynolds number, as follows :

$$N_{Re} = \frac{v.r.\rho}{\mu} \tag{5.1}$$

where v is the fluid velocity in a pore of radius r, ρ is the fluid density and μ is the fluid viscosity. This is a standard fluid mechanical term which can be used to determine the nature of the fluid flow through any system. The flow becomes turbulent at Reynolds numbers between 1200 and 2000. Whilst this range is strictly only valid for flow through a uniform, smooth cylindrical tube, flow in rougher tubes is still laminar up to about $N_{Re} = 1$. Calculation of the Reynolds number using geologically reasonable values for the flow of pore fluids (1 to 10 metres per day), through pores of radius 1 to $1000\mu m.$, and standard data for the viscosity and density of water, reveals a range for N_{Re} of 10^{-1} to 10^{-6}. This clearly indicates that the real system is in a laminar flow regime.

ii) Solute transport is considered to be by bulk flow only; there is no significant ionic diffusion. Another dimensionless number, the Peclet number (Lerman,

1979) can be used to confirm this assumption :

$$N_P = \frac{Q.w}{D} \tag{5.2}$$

where Q is the fluid flux (related to fluid velocity, v), w is a particular length scale and D is the diffusion coefficient for the solutes of interest, in this case Ca^{2+} and HCO_3^- . For Peclet numbers greater than 1, bulk flow is the most important. Using values of the fluid velocity of 1 to 10 metres per day, a length scale (w), of 1 mm to 1 metre and standard data for the diffusion coefficients (both approximately $10^{-5} cm^2 s^{-1}$, Weyl, 1967), the calculated Peclet number has a range of 10 to 10^5 for the real system. Therefore, diffusive mass transport is negligible when compared to bulk mass transport, so no diffusion term is included and transport of solutes is considered to be by bulk flow only.

iii) The model operates in two dimensions only, and this obviously introduces some approximations. The major difference is that the model therefore requires a greater degree of interconnectivity of the pores to have the same permeability as the real system. This realisation highlights the subtle difference between modelling in two dimensions and observing the reality in a two dimensional section through a three dimensional object. Hence the matrix of the model appears to have a greater pore connectivity than is observed in thin-section.

Although it was the original intention to define the model in terms of the geological reality, specifying times, flow rates and permeability figures, the development stages indicated that this might restrict the interpretation of the results to individual examples. The great variety expected in these parameters, probably over several orders of magnitude, makes the choice of a 'typical' case rather futile. It was therefore decided to leave the descriptive parameters as relative values only, allowing the model to be more flexible. The definition of the model parameters according to geological reality would be of much greater value in recreating the flow characteristics on a larger scale in three dimensions. The potential use of this technique is discussed in Section 5.6.3.

It is interesting to study the variations in the porosity and permeability of coral framestone material on a small scale, as measured in thin sections and by core plugs. Some poroperm data for modern corals are presented in Table 5.1. These figures were obtained from unaltered hand specimens of several coral species as indicated on the table. It is interesting to note that the samples have similar porosity, but very different permeability. The *Montastrea annularis* has similar porosity values to the *Acropora palmata* but its permeability is two orders of magnitude smaller. It is also important to note that the permeability is anisotropic, with the core taken parallel to the trend of the corallites having more than twice the permeability of the core perpendicular to it. This latter property is very obvious on the hand specimen scale. Figures for the *Diploria sp.* sample are very high, with the permeability greater than 10,000 mD, being higher than was measurable with the apparatus used.

A final point to notice from Table 5.1 is that the porosity as determined from thin section point counting is commonly higher than that determined by bulk methods. This illustrates the fact that a substantial proportion of the porosity observed in thin section is non-effective; this feature is recreated in the results of the modelling and is discussed in Section 5.3. There is clearly the variability in the poroperm character of coral framestone sufficient to produce a wide range of flow rates and inhomogeneous cementation patterns. It should be emphasised that the above figures are derived from unaltered coral skeletal material. In the formation of reefs, bioerosional and other physical processes (including cementation itself), interact with the primary framebuilding process, and undoubtedly act to increase the range of permeability described above.

Sample	Species	Thin Section Porosity	Porosity %	Permeability milliDarcies
1	*Acropora*	-	49.4	-
2H	*Montastrea*	66.5	56.8	24.2
2V *	*Montastrea*	-	58.1	57.9
3 *	Lithified Belize	-	9.2	84.6
4H	*Acropora*	55.6	51.2	8,900
4V *	*Acropora*	57.2	50.5	3,800
5H	*Diploria*	-	54.6	<10,000
5V	*Diploria*	50.8	58.0	<10,000

Table 5.1 Porosity and permeability data for selected coral framestones.

5.4 The Theoretical Basis of the Model.

5.4.1 The rock matrix.

Network codes describe a regular square grid of capillary tubes (Figure 5.3) which represents the rock matrix (rock in grey, porosity in white). In all of the examples in this paper the grid is 10 by 10 square, though theoretically, any size can be computed.

5.4.2 Fluid flow.

There is considered to be a fixed pressure gradient (ΔP) across the grid; this drives the pore fluid from bottom to top. Laminar flow is controlled by Poiseuille's Law;

$$Q = \frac{\Pi.r.^4\rho.\Delta p}{8.\mu.l} \qquad 5.3$$

where Q is the fluid flux through the capillary, r is the capillary radius, ρ is the pore fluid density, Δp is the pressure difference across the capillary, μ is the viscosity of the fluid and l is the length of the capillary. The model then calculates the fluid velocities in each segment of the grid in the following manner. At each node in the grid, fluid must be conserved, so the sum of the velocities at each node must equal zero. A standard numerical iterative technique is used to calculate the velocities in each segment. An initial guess at the pressure difference between each node is made, and a velocity calculated from that using equation 5.3. The iterative technique is pursued to the point when the sum of all the velocities at every node in the grid is zero. Note that the inlet and outlet boundaries (the top and bottom of the diagrams), are at constant pressure, and that the edges of the cell are connected together as though the diagrams were wrapped around a cylinder.

5.4.3 The cementation process.

It is assumed that the rate controlling step in the growth of the cements is the rate of supply of solutes to the growing surfaces and that the main transport of solutes is by bulk flow. The rate of growth is therefore directly proportional to the flow velocity. The cementation process is described as a decrease in the radius of the capillary tubes. This decrease is calculated to be directly proportional to the flow velocity :

$$\frac{dr_i}{dt} = \beta . v_i \qquad 5.4$$

where r_i is the radius of the ith capillary, v_i is the fluid velocity in the ith capillary and β is a proportionality constant. Note that this constant acts as a time scale and relates the model results to geological reality. In the later examples, this constant is called a cementation factor. In the reef system, as cementation progresses, the pore radii will decrease. From equation 5.3, the fluid flux or velocity will also decrease and so will the rate of precipitation (from equation 5.4). This negative feedback is built into the model by calculating the overall result via a number of stages or time steps (usually 10). After each step new flow velocities are calculated from the capillary radii as modified in the previous step. In the figures described below, the cement precipitated is shown in black.

5.4.4 Matrix geometry.

The simple example in Figure 5.4 is perhaps representative of a supermature sandstone or a carbonate grainstone, but it is obviously not a good description of a coral framework as shown in Figures 5.5 & 5.6. There are several parameters which may be used to alter the matrix geometry so that it is more representative of carbonate framestones. These parameters are input by the user at the start of the computer program and are listed at the edges of the relevant diagrams (Figures 5.8 to 5.15). The parameters are described below;

i) λ_x, λ_y. These are two parameters which control the capillary radius distribution (in the x and y directions respectively) according to the following condition:

The probability of there being a capillary tube of radius r is $\frac{1}{2}\lambda$ for;

$$1 - \lambda < r < 1 + \lambda \qquad 5.5$$

and zero otherwise (Figure 5.7). A value for each parameter is input at the start of the program. This can be any number between 0 and 1.

In the 10 by 10 matrix used throughout this study, there are 100 capillary segments in both the x-and y-axis directions. The use of a probability distribution such as that above allows a non-uniform capillary radii distribution to be created, simply by the input of a single value for the x and y directions. As the value of λ is increased, the variety in the capillary radii also increases. If $\lambda = 0$, from equation 5.5, r varies from $1 - 0$ to $1 + 0$, i.e. all the radii are equal and of unit size. Similarly, if $\lambda = 0.5$, r varies from 0.5 to 1.5 units. Increasing λ to 0.9 produces a wider distribution in the radii, from 0.1 to 1.9 units. The probability distribution (Figure 5.7), shows that for any value of λ, there is an equal probability, $(\frac{1}{2}\lambda)$, that any radius within the range of $1 - \lambda$ to $1 + \lambda$ will occur in the grid.

ii) P_x, P_y. These two parameters represent the fraction of the capillary segments (in the x and y directions respectively) which are non conducting. This therefore introduces a degree of matrix connectivity. The parameters can have any value from 0 to 1. Hence, $P_x = 0.5$ means that half of the capillary segments in the x direction are non conducting. The visible effect on the matrix is that half of the x-axis segments are sealed.

The program calculates the initial and final permeabilities ($K_{init.}$ and K_{final}) of the grid from a simplified version of Poiseuille's Law;

$$Q = \frac{K.\Delta P}{\mu.L} \qquad 5.6$$

where Q = fluid flux out of the top of the grid, ΔP is the pressure difference across the grid, μ is the fluid viscosity and L is the length of the grid. These permeabilities are of course only relative. The initial porosity $\varphi_{init.}$ can also be chosen by the user; the program will then calculate the final porosity (φ_{final}). Variation of these input parameters leads to a wide range of results, some of which are shown in Figures 5.8 to 5.15.

Figure 5.3 The regular square grid of capillary tubes which forms the basis of the model matrix. In these examples the grid is 10 × 10 square, though any size can be computed. The rock is in grey and porosity in white.

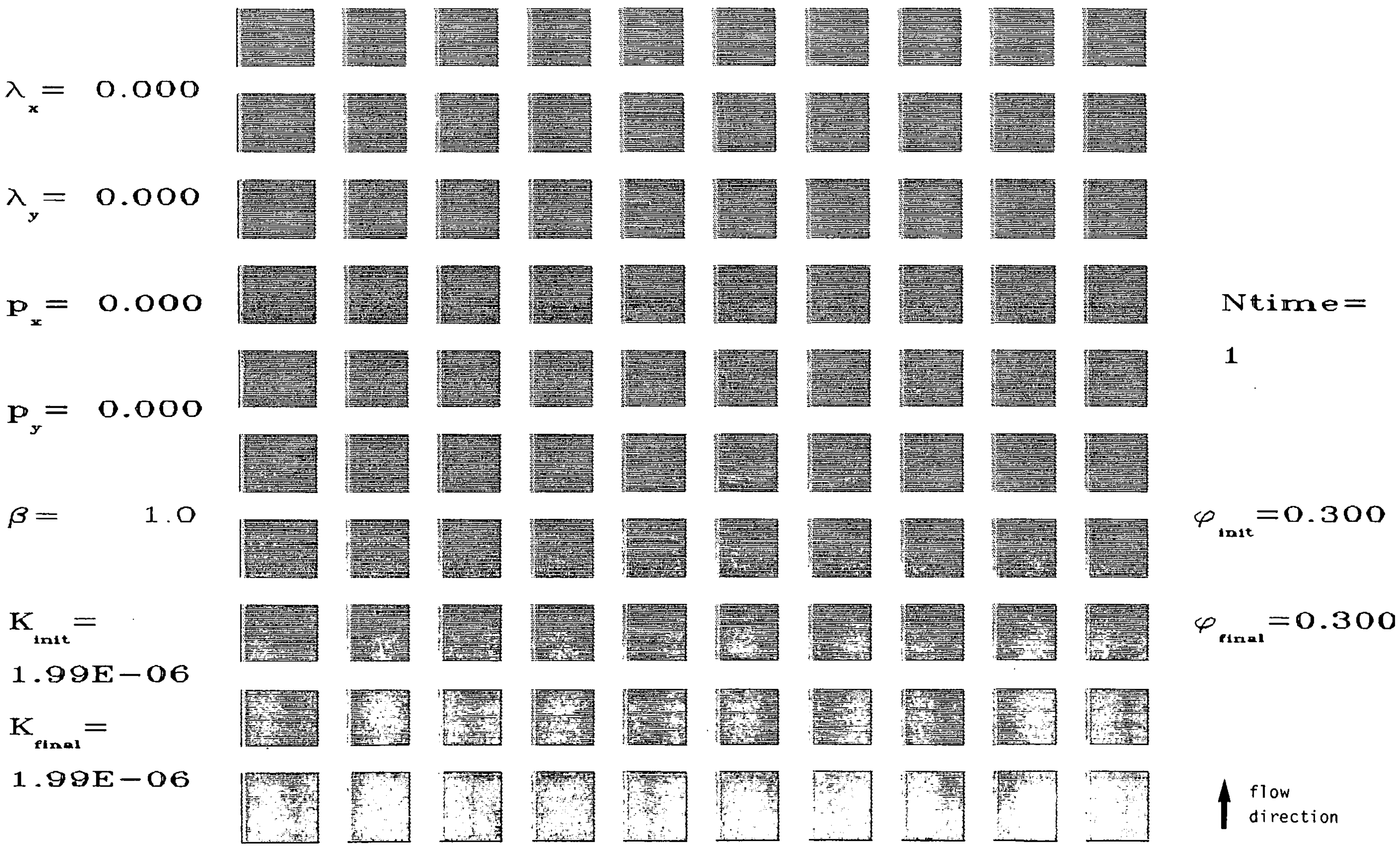
$\lambda_x =$ 0.000
$\lambda_y =$ 0.000
$p_x =$ 0.000
$p_y =$ 0.000
$\beta =$ 1.0
$K_{init} =$
1.99E−06
$K_{final} =$
1.99E−06
Ntime=
1
φ_{init}=0.300
φ_{final}=0.300
flow direction

Figure 3.

Figure 5.4 The regular square grid. Cementation (shown in black) occurs along the y-axes only because flow is in that direction only. This example serves as a standard with which to compare the effects of changing the matrix description.

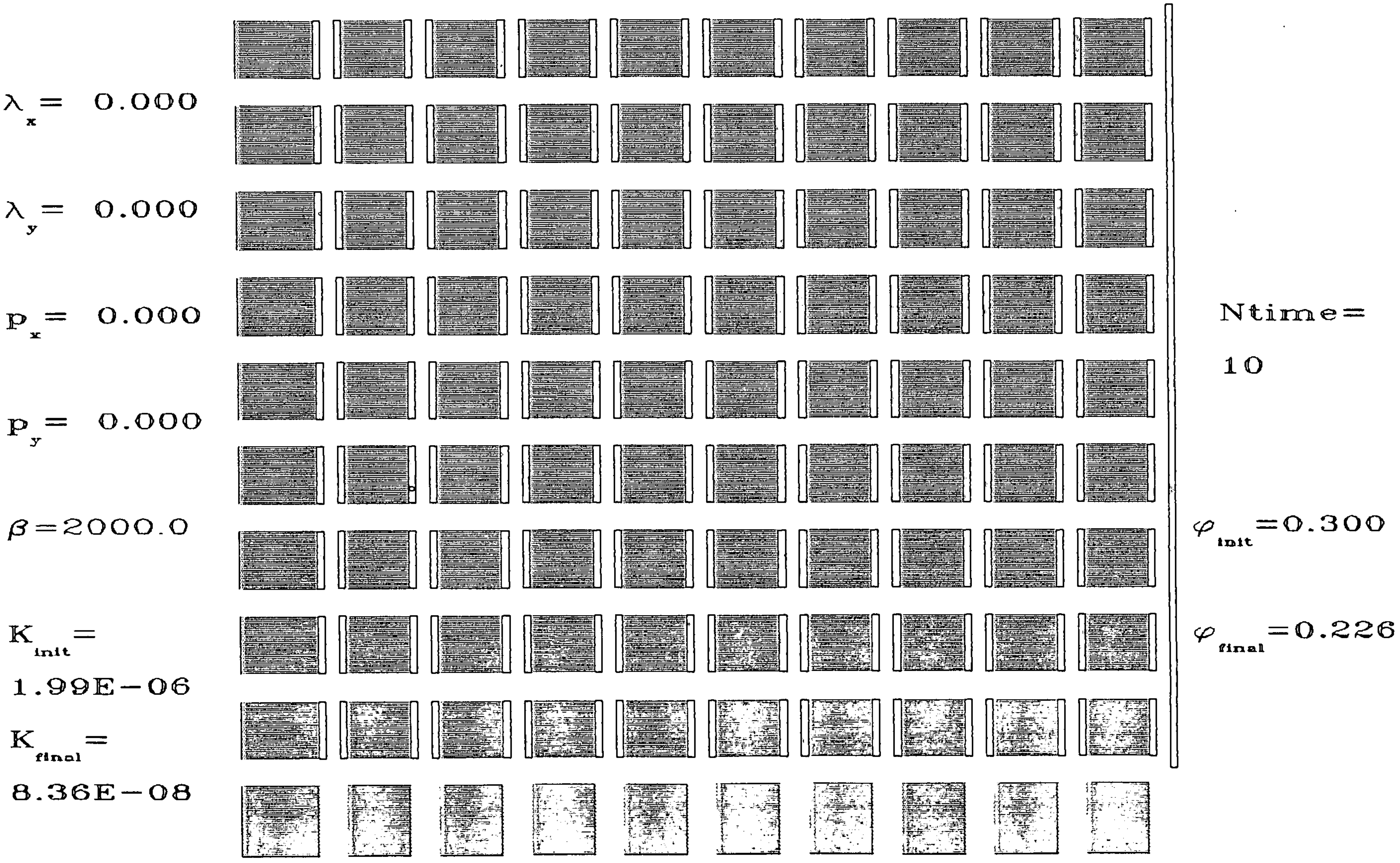
$\lambda_x =$ 0.000
$\lambda_y =$ 0.000
$p_x =$ 0.000
$p_y =$ 0.000
$\beta = 2000.0$
$K_{init} =$
1.99E−06
$K_{final} =$
8.36E−08
Ntime=
10
$\varphi_{init} = 0.300$
$\varphi_{final} = 0.226$

Figure 4.

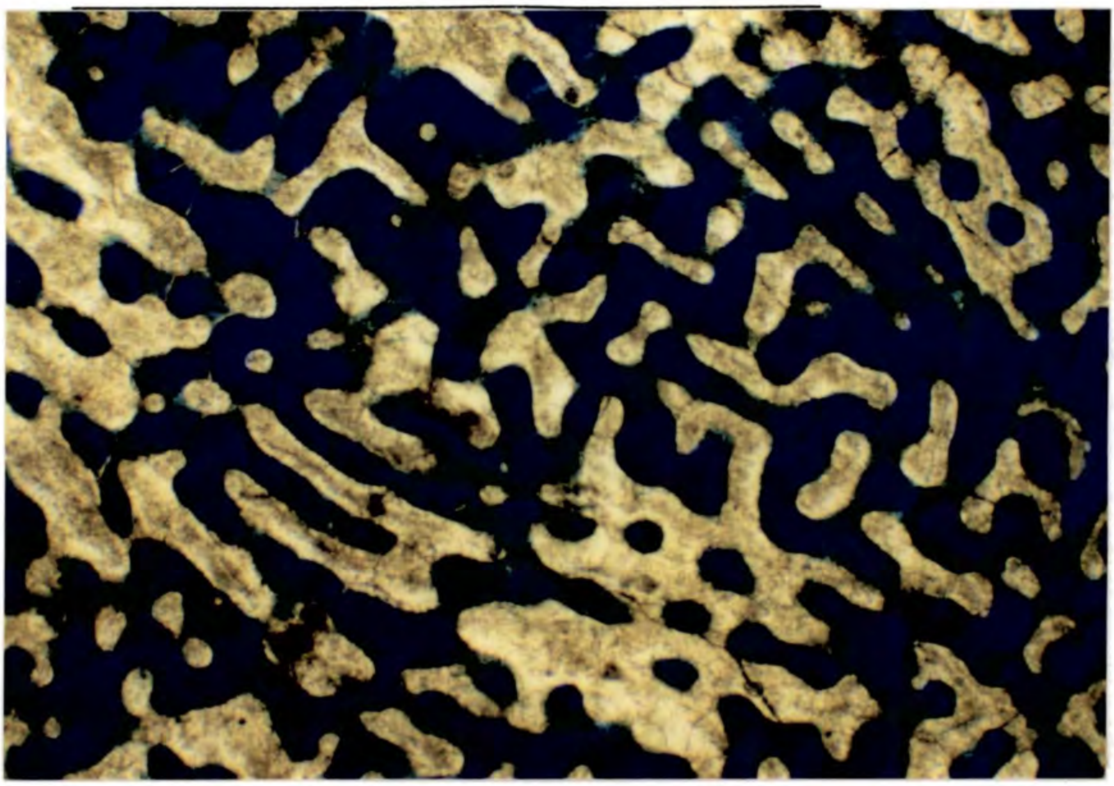

Figure 5.5 Two examples of the unaltered coral framestone matrix. Upper sample is *Acropora palmata* and the lower one is *Montastrea annularis*. Porosity highlighted by resin impregnation. Photomicrograph, ppl..

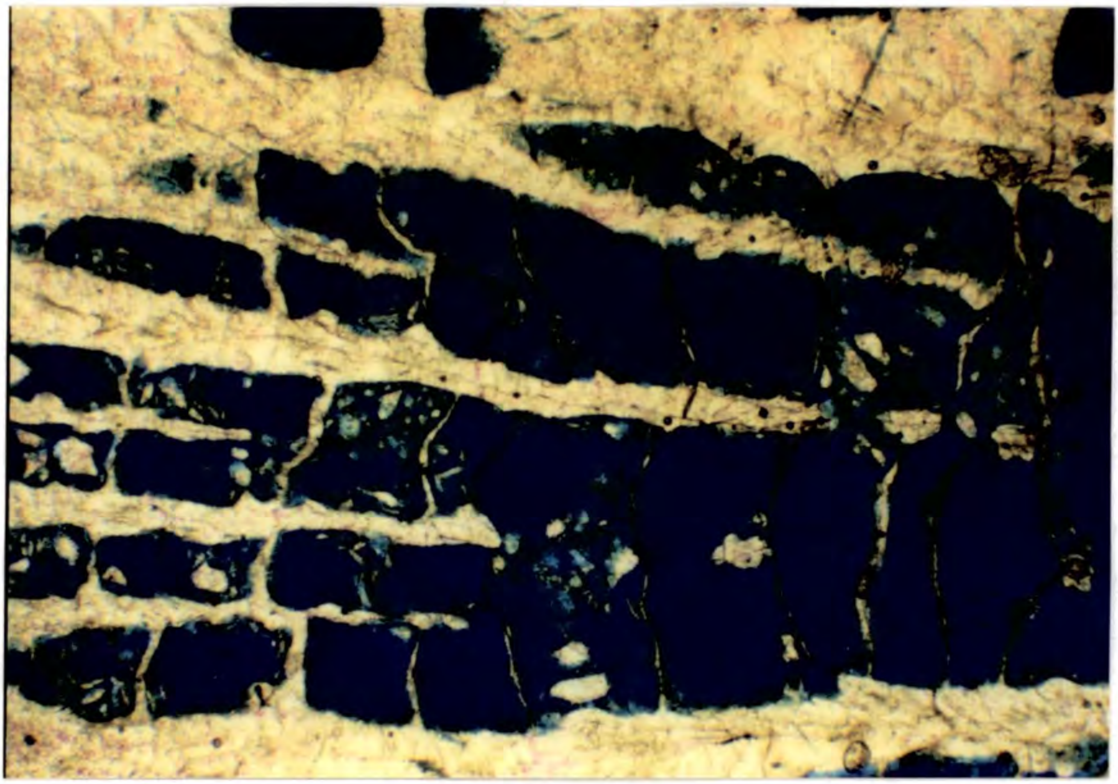

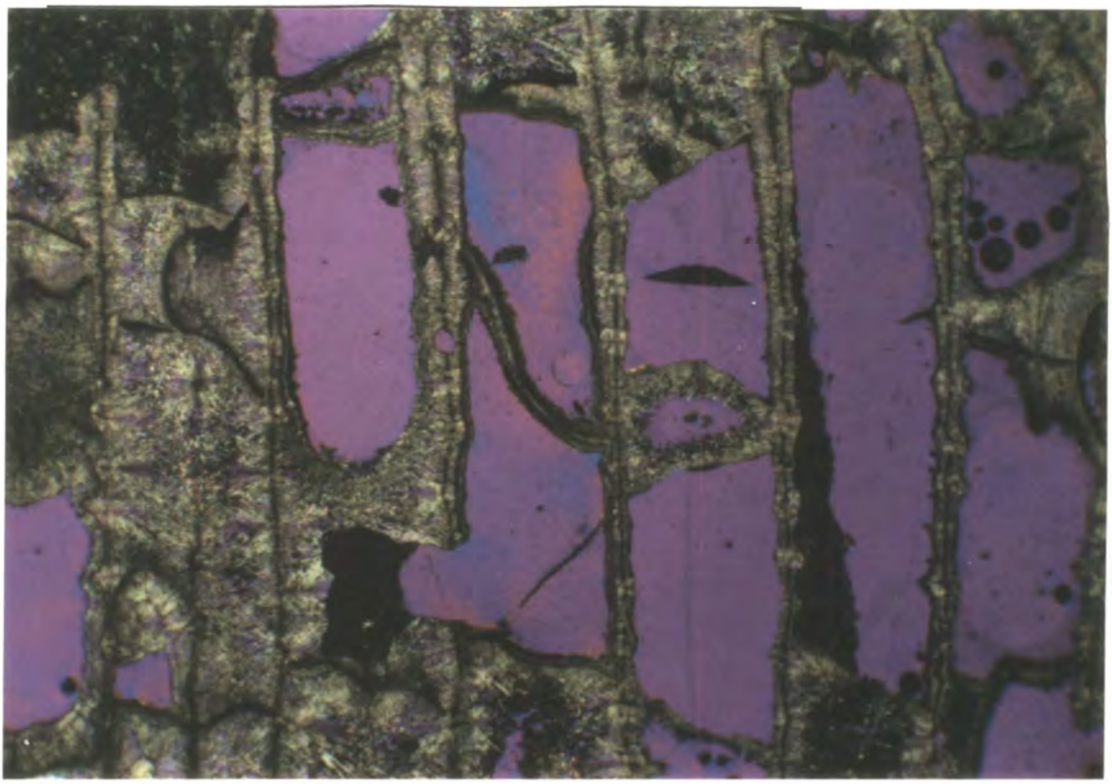

250μm.

Figure 5.6 Examples showing the inhomogeneous nature of the cementation in coral framestones from Florida and Belize. Upper photo is from Belize sample, lower one from Florida. Note that some pores are full of cement, some have a thin isopachous lining and some are devoid of cements altogether. Both Photomicrographs, xpolars.. Both Samples are Montastrea sp.

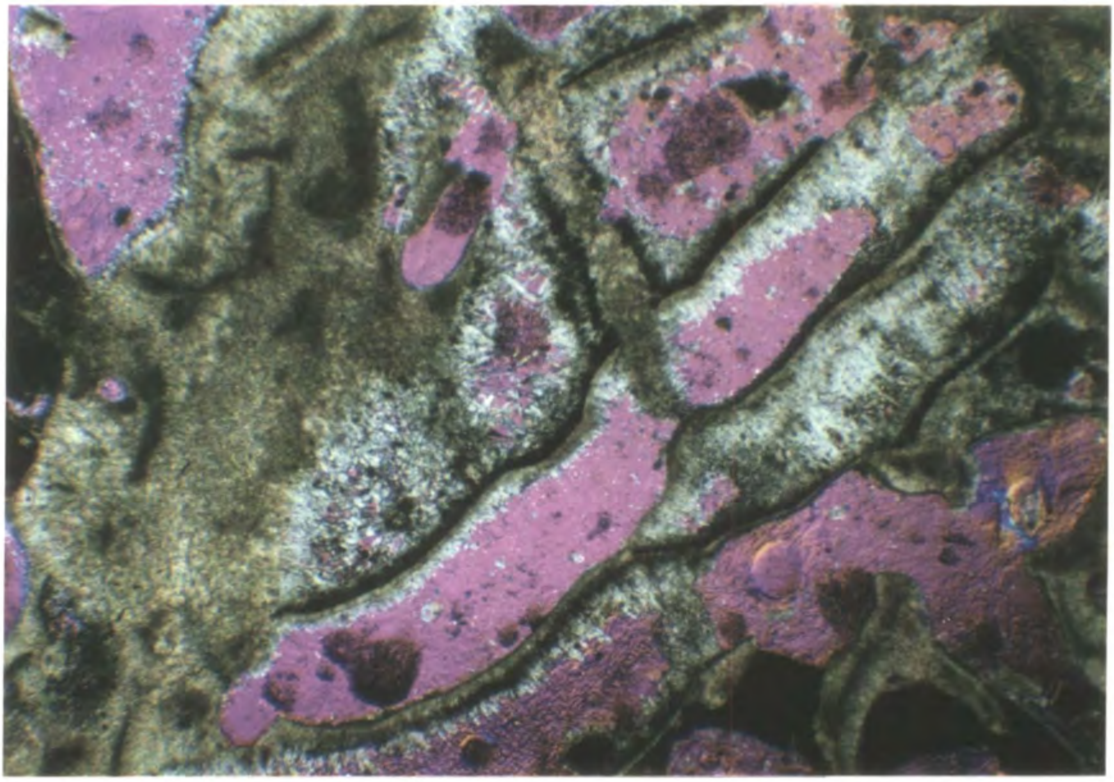

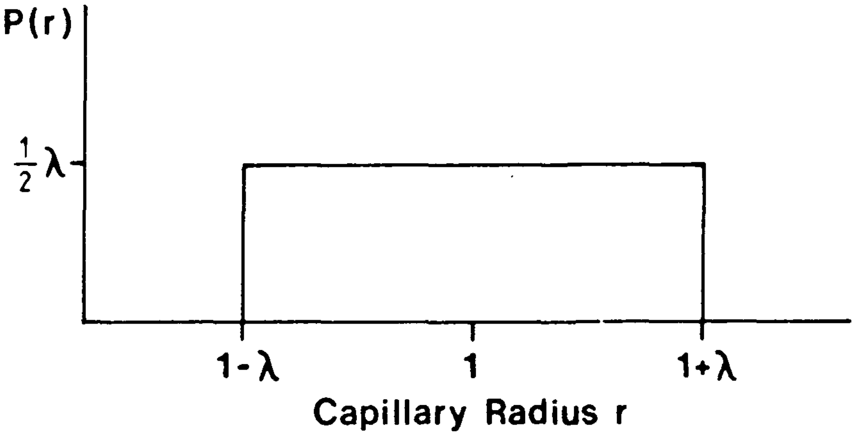

Figure 5.7 The capillary radius probability distribution function. Discussion in the text.

5.5 Results.

5.5.1 Introduction.

The results presented below illustrate various stages in the development of the model as produced by varying the parameters described above. Study of these intermediate results provides a valuable insight into both the nature of the permeability in coral framestones and the control of that permeability on the distribution of cements. A final version of the model which is considered to be a good representation of the real system is given in Figure 5.11 and this is used as a basis from which to observe the effect of varying the porosity and cementation rate. Each example is the result of an individual experiment, created using the parameters listed at the edges of the relevant figure, and the series does not represent a sequential process. Using the final version (Figure 5.11), the model can be run in a sequential fashion, to illustrate the variation in the extent of cementation with time, and several examples of this are shown in Figures 5.12 to 5.15.

Presentation of the results of this modelling is therefore in two parts;

i) The effects of the matrix geometry on the cementation patterns (Section 5.5.2).

ii) The effects of varying β, the cementation factor (Section 5.5.3)

Each example below is the result of an individual experiment created using the parameters listed at the edges of the relevant Figure.

5.5.2 Matrix geometry.

Figure 5.4 shows the cementation pattern created using the regular square grid as in Figure 5.3. The precipitated cement (shown in black) occurs in a uniform pattern along the y-axis surfaces only. This is because there is no pressure difference across the capillaries in the x-direction, and so flow is in the y-direction only. This result is in itself geologically unreasonable, though mathematically valid as we are assuming the system to be in a laminar flow regime. In reality, one would expect to see precipitation on all surfaces irrespective of the main flow direction. Introduction of irregularities into the matrix in the following examples does indeed cause precipitation of cements on the x-axis surfaces. This example serves as a standard with which to compare the effect of changing the matrix parameters. The uncemented 'gap' at the base of all the diagrams is a function of the graphics program and should be ignored.

5.5.2.1 Variation in P_x and P_y.

Figure 5.8 shows the effect of introducing a proportion of pores which are non conducting. Sealing half of the pores in the x-direction has very little effect on the cementation pattern as it does not alter the flow path or the initial permeability ($K_{init.}$ for Figure 5.8 is 1.99×10^{-6}). However, it is interesting to note that sealing half the pores in the y-direction has a marked effect (Figure 5.9). In this case the matrix tortuosity is greatly increased and the flow is forced along capillaries in the x-direction. An appreciable degree of inhomogeneity has been created. Note the concomitant reduction in initial permeability. (K_{init} is 8×10^{-7} in Figure 5.9 compared with 1.99×10^{-6} in Figure 5.7).

Figure 5.8 In this example, half of the pores in the x-direction are non-conducting . The effect on the cementation pattern is minimal and flow is still in the y-direction only.

$\lambda_x = 0.000$

$\lambda_y = 0.000$

$p_x = 0.500$

$p_y = 0.000$

$\beta = 2000.0$

$K_{init} =$
1.99E−06

$K_{final} =$
8.36E−08

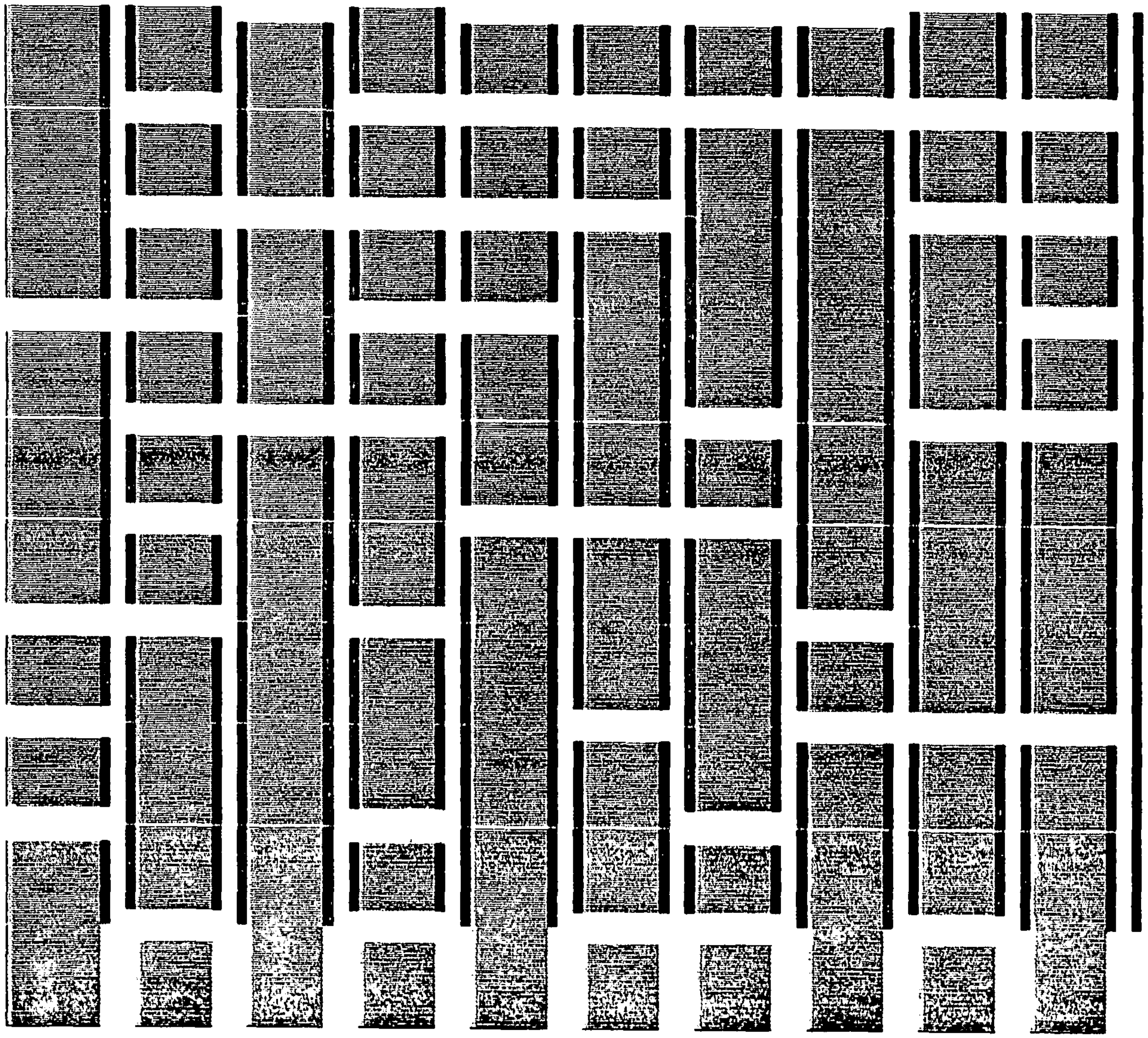

Ntime=
10

$\varphi_{init} = 0.228$

$\varphi_{final} = 0.154$

Figure 5.9 Sealing half of the pores in the y-direction has a much more pronounced effect on the cementation pattern. The matrix tortuosity is increased and flow is forced along capillaries in the x-direction. Note the concomitant reduction in initial permeability compared to Figure 5.8.

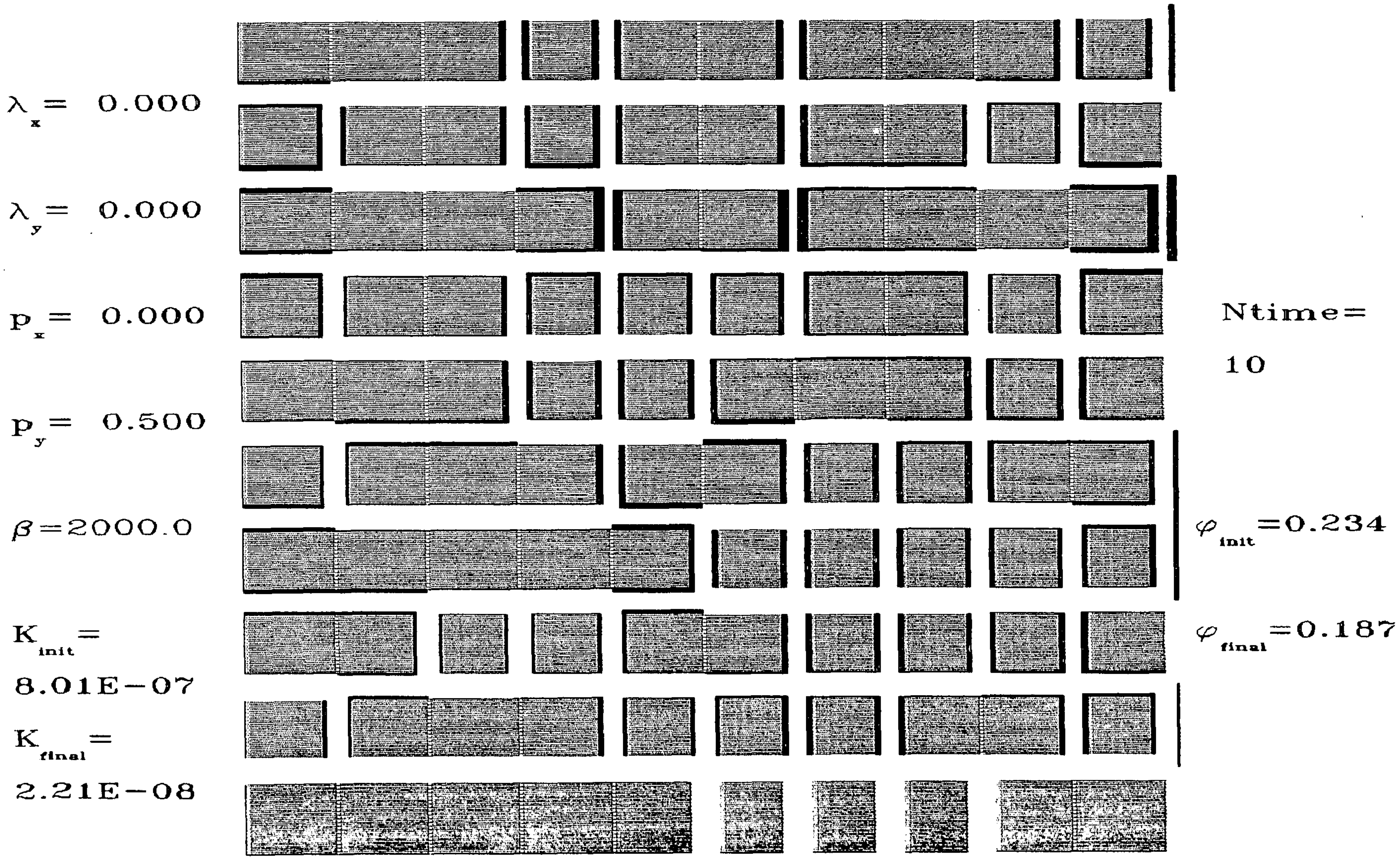
$\lambda_x = 0.000$
$\lambda_y = 0.000$
$p_x = 0.000$
$p_y = 0.500$
$\beta = 2000.0$
$K_{init} =$
8.01E−07
$K_{final} =$
2.21E−08
Ntime=
10
$\varphi_{init} = 0.234$
$\varphi_{final} = 0.187$

Figure 9.

5.5.2.2 Variation in λ_x, λ_y.

In the examples discussed above (Figures 5.3 to 5.9), λ_x and λ_y are both zero, so the capillary radius distribution function (Figure 5.7), reduces to a single value and all the pore radii are equal. Varying λ introduces a distribution of pore radii as shown in Figure 5.10, where $\lambda_x = 0$, $\lambda_y = 0.5$. Note that for the analogous situation, $\lambda_x = 0.5$, $\lambda_y = 0$ there would be very little effect on the cementation pattern (for the same reason as P_x has no effect) as this has no effect on the flow paths. In Figure 5.10 there is, therefore, a distribution of y-axis capillary radii, with all x-axis radii equal and all pores conducting (P_x, $P_y = 0$).

The Poiseuille flow dependence on the capillary radius raised to the fourth power is evident here ($Q \propto r^4$, equation 5.1). A substantial degree of variation in the cement thickness has been created, with the larger pores initially receiving a greater volume of cement.

5.5.2.3 Representation of coral framework.

A combined variation of λ_x, P_x, and P_y, creates a matrix geometry that is a reasonable representation of coral frameworks (Figures 5.11 to 5.15). In Figure 5.11, P_x and P_y are both 0.5, thereby decreasing the matrix connectivity. Many of the features apparent in the real system are now present in the model results. Both dead-end and non-effective porosity are present and a wide variation in the degree of cementation is apparent. The lower left corner of Figure 5.11 has received no cement whatsoever as all the porosity is either non- effective or dead-end. Some of the pores in the upper left side have received small volumes of cement, but the majority of the cement has been 'precipitated' in the centre and right hand side of the grid.

Using this matrix description, the following examples show the effects of varying the porosity and the cementation factor β. In Figure 5.12, the input parameters are the same as for Figure 5.11, but the initial porosity figure has been increased. The capillary radii are therefore increased and again the Poiseuille dependence on r^4 is evident; to produce roughly the same volume of cement as in Figure 5.11, the cementation factor has to be reduced from 2000, to 100.

Figure 5.10 Using λ_y =0.5 creates an irregular distribution of y-axis capillary radii. As the rate of cementation is directly proportional to the flow velocity, which is itself dependent on the fourth power of the radius, the larger pores receive substantially more cement.

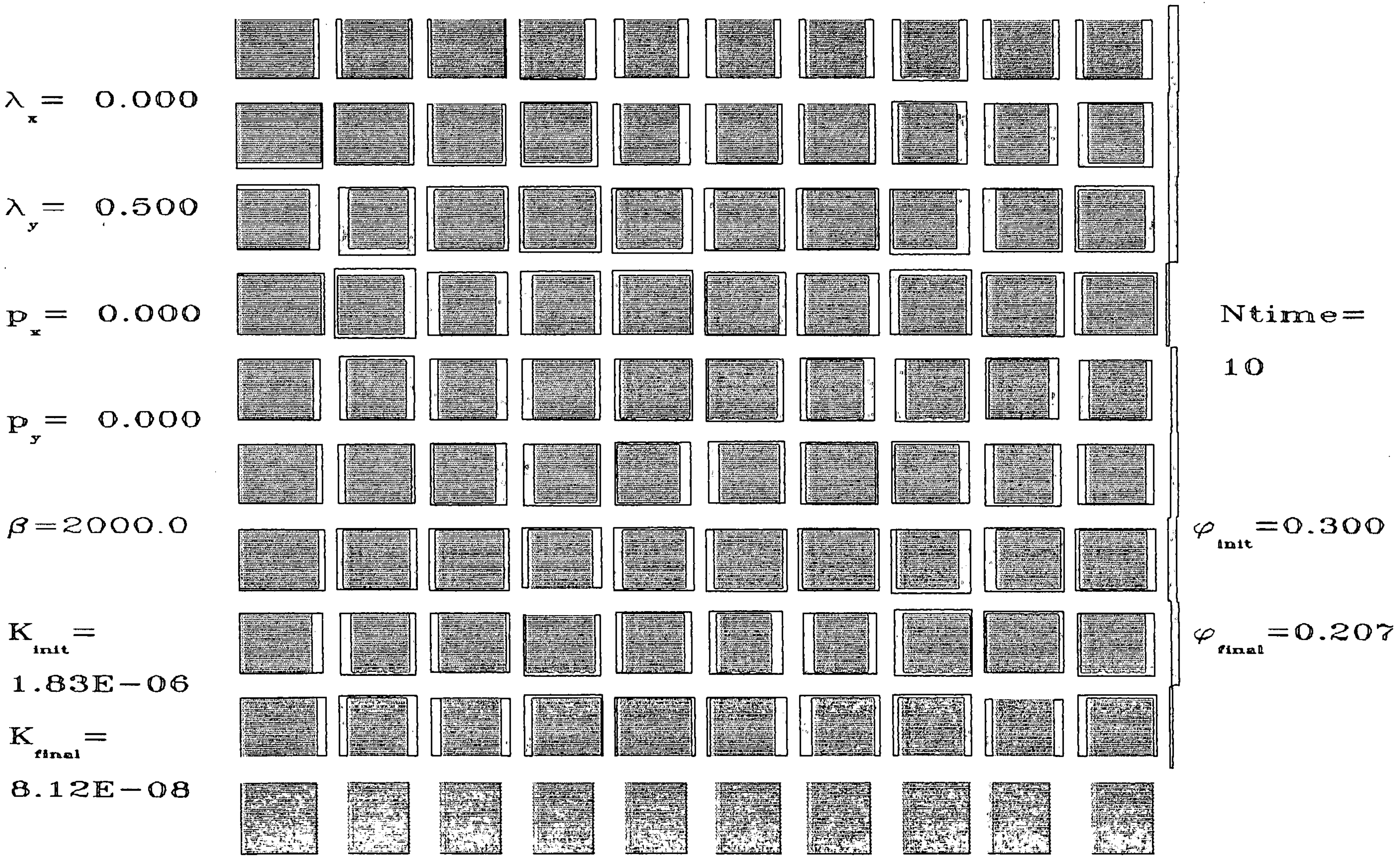
$\lambda_x = 0.000$
$\lambda_y = 0.500$
$p_x = 0.000$
$p_y = 0.000$
$\beta = 2000.0$
$K_{init} =$
1.83E−06
$K_{final} =$
8.12E−08
Ntime=
10
$\varphi_{init} = 0.300$
$\varphi_{final} = 0.207$

Figure 10.

Figure 5.11 Results more representative of the reality can be achieved by increasing the matrix connectivity as in this example (Compare with Figures 5.5 & 5.6). Both 'dead-end' and 'non-effective' porosity are apparent here, and there is a considerable variation in the degree of cementation.

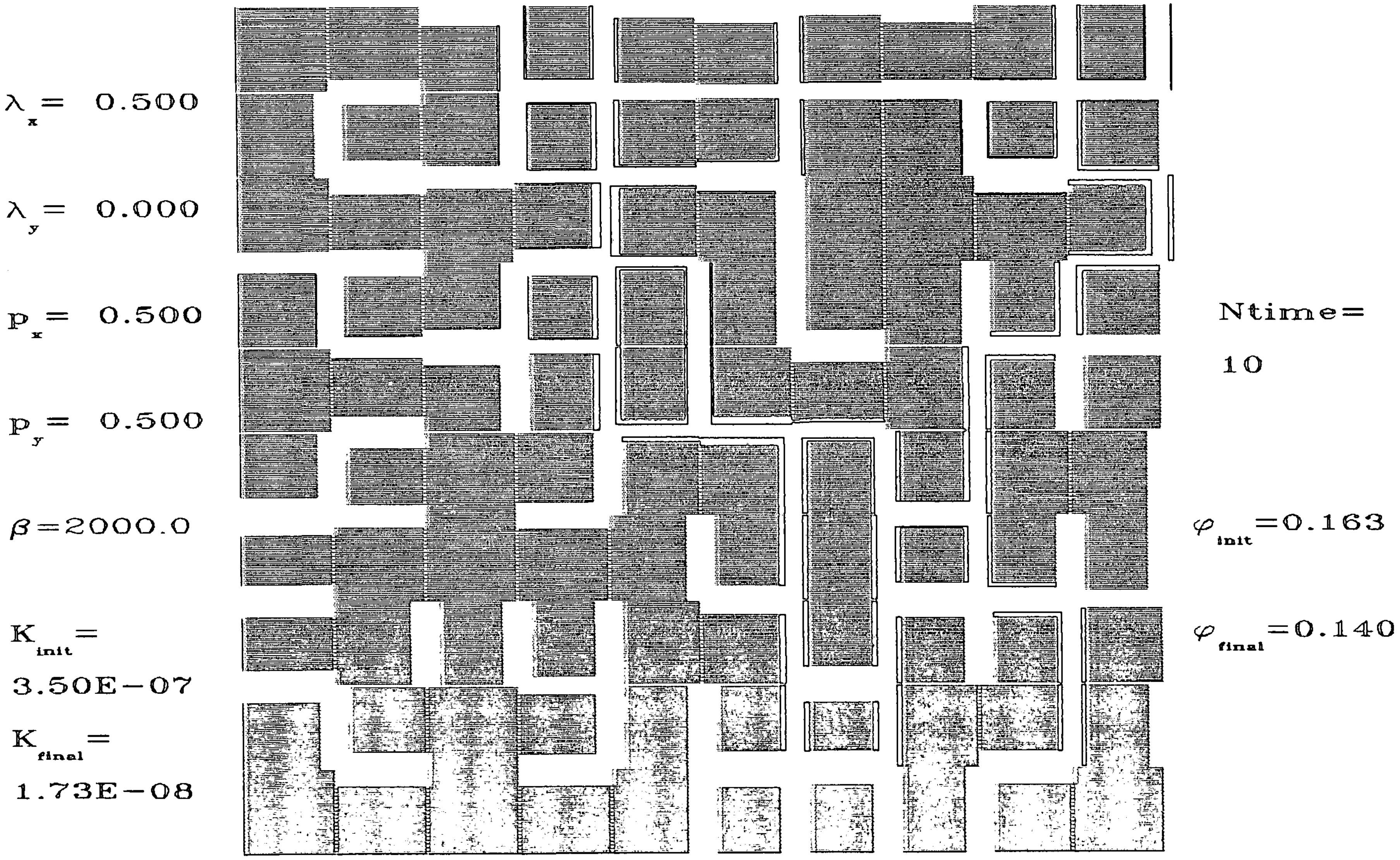
$\lambda_x = 0.500$
$\lambda_y = 0.000$
$p_x = 0.500$
$p_y = 0.500$
$\beta = 2000.0$
$K_{init} =$
3.50E−07
$K_{final} =$
1.73E−08
Ntime=
10
$\varphi_{init} = 0.163$
$\varphi_{final} = 0.140$

Figure 11.

5.5.3 The cementation factor β.

The parameters used in Figure 5.11 produce the most accurate representation of coral framestone geometry as observed in thin section. Using this basis it is interesting to observe the effects of increasing β on the cementation patterns Figures 5.12 to 5.15. The volume of cements increases progressively, until, in Figure 5.15, where β is very large, the grid has been fully cemented. Non-effective* and 'dead-end' porosity have remained unaffected. Comparison of this result with the photomicrographs in Section 2.8.4 and Figures 5.5 & 5.6 suggests that those empty pores adjacent to fully cemented ones are probably non-effective porosity only revealed in the two dimensional section. Such pores have very little or no fluid flow through them. Whilst the last four examples are separate results created by increasing the cementation parameter β , it is possible to use the model in an incremental manner such that successive cement zones are created. Figures 5.3 to 5.15 were created using 10 time steps, with only the final result being displayed. By setting the program to display the results after several time steps, in a sequential fashion, a series of cement zones is produced. The thickness of each zone progressively decreases according to the dependence on the fourth power of the radius. This is illustrated in Figure 5.16, where there are four successive layers, highlighted in different colours. The thickness of each layer is better demonstrated in the expanded version of the same example as shown in Figure 5.17. In an identical manner, Figure 5.18 was produced by arranging for the results to be displayed after each of ten time steps.

* N.B. Non effective porosity, (here and elsewhere), is intended to describe that porosity which is not connected to any flow channels - i.e. is effectively sealed from other pores and cannot therefore contribute to permeability.

This clearly illustrates the reduction in permeability caused by the precipitation of cement as time progresses. Although the figures are not shown in the above examples, it is possible to follow the reduction in permeability with time, as the values are recalculated after each time step.

Figure 5.12 Using the same matrix description as in Figure 5.11, the porosity has been increased in this example. Due to the r^4 dependence, the cementation factor has to be reduced by an order of magnitude.

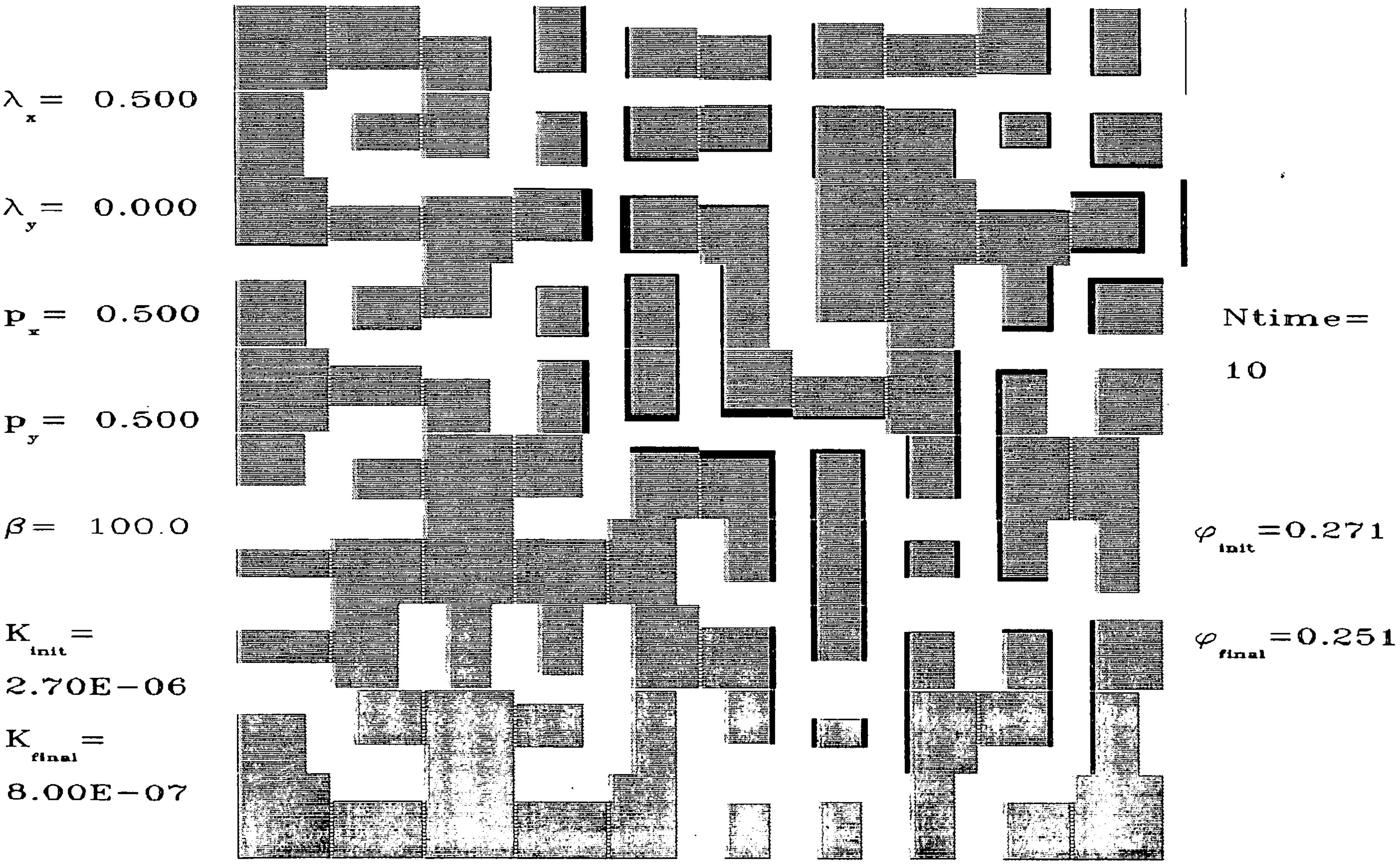
$\lambda_x =$ 0.500
$\lambda_y =$ 0.000
$p_x =$ 0.500
$p_y =$ 0.500
$\beta =$ 100.0
$K_{init} =$
2.70E−06
$K_{final} =$
8.00E−07
Ntime=
10
$\varphi_{init} = 0.271$
$\varphi_{final} = 0.251$

Figure 12.

Figure 5.13 It is interesting to observe the effects of progressively increasing β, the cementation factor. In this example $\beta = 500$ (Compared to Figure 5.12, where $\beta = 100$).

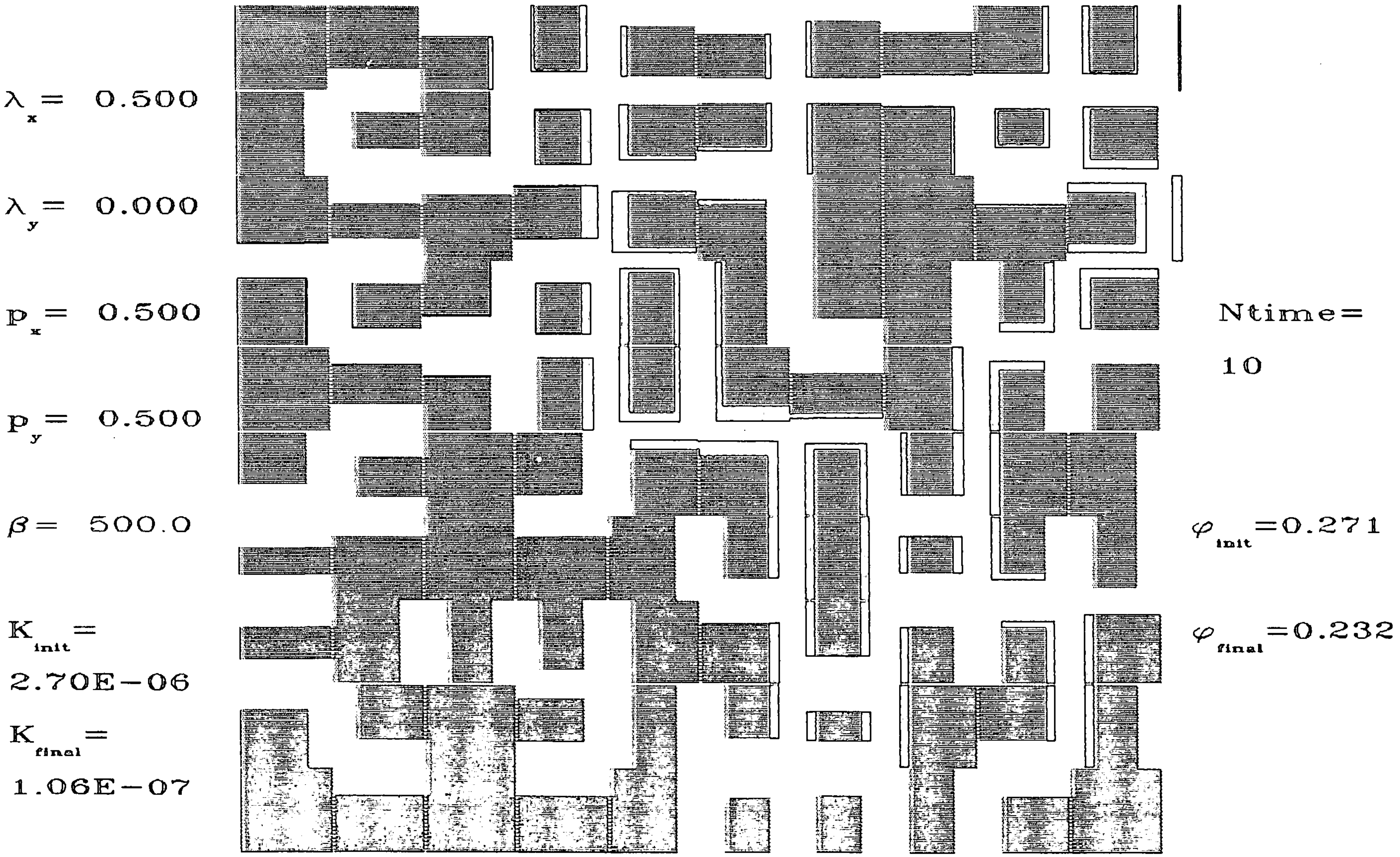
$\lambda_x = 0.500$
$\lambda_y = 0.000$
$p_x = 0.500$
$p_y = 0.500$
$\beta = 500.0$
$K_{init} =$
2.70E-06
$K_{final} =$
1.06E-07
Ntime=
10
$\varphi_{init} = 0.271$
$\varphi_{final} = 0.232$

Figure 13.

Figure 5.14 Here, $\beta = 4000$ and most of the effective porosity has been filled by cement.

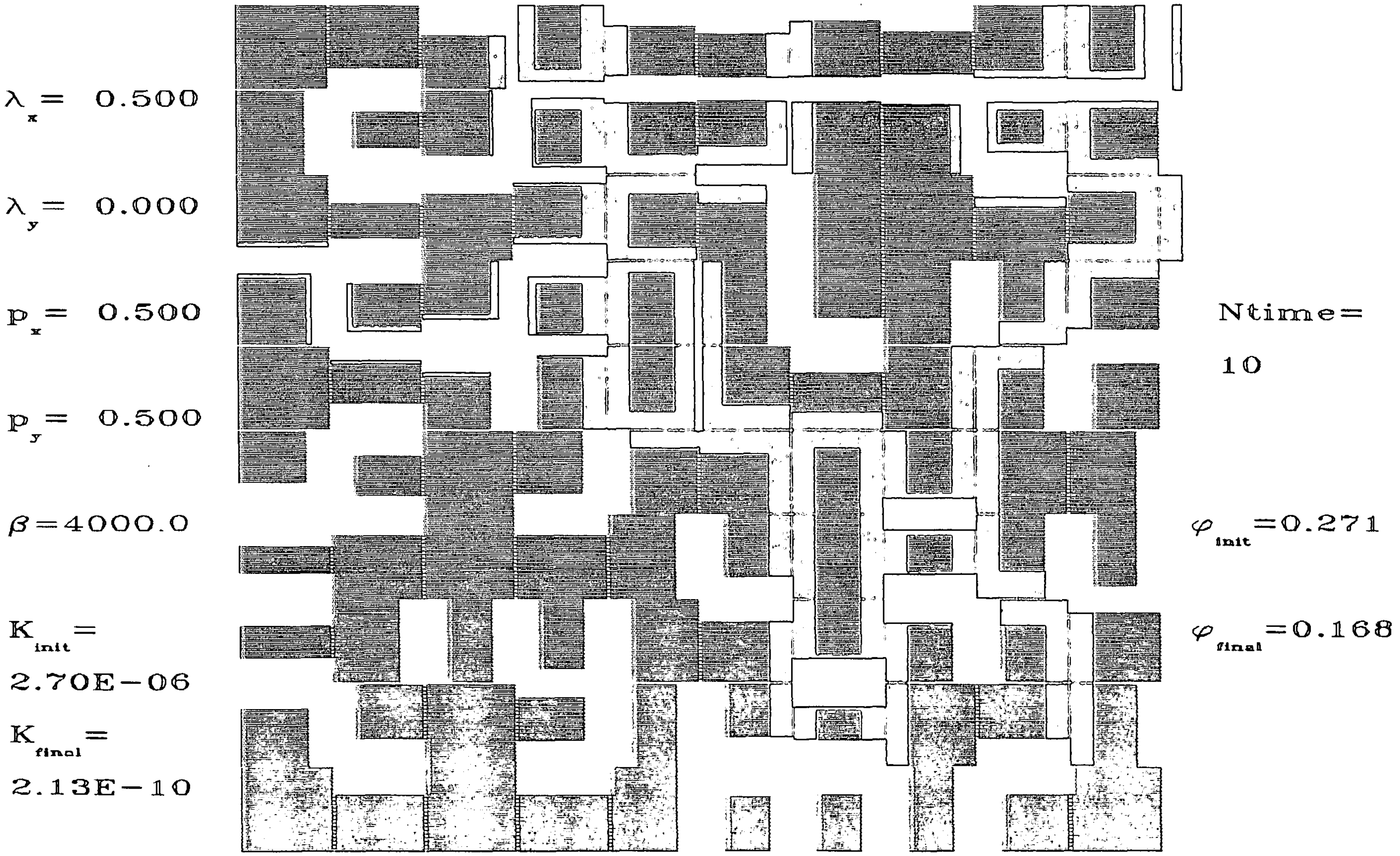
$\lambda_x = 0.500$
$\lambda_y = 0.000$
$p_x = 0.500$
$p_y = 0.500$
$\beta = 4000.0$
$K_{init} =$
2.70E−06
$K_{final} =$
2.13E−10
Ntime=
10
$\varphi_{init} = 0.271$
$\varphi_{final} = 0.168$

Figure 14.

Figure 5.15 In this example, β is very large and the effective porosity has been fully cemented. Note that as the flow is considered to be laminar, the 'dead-end' porosity remains unaffected. Non-effective porosity receives no flow and is, therefore, also unaltered.

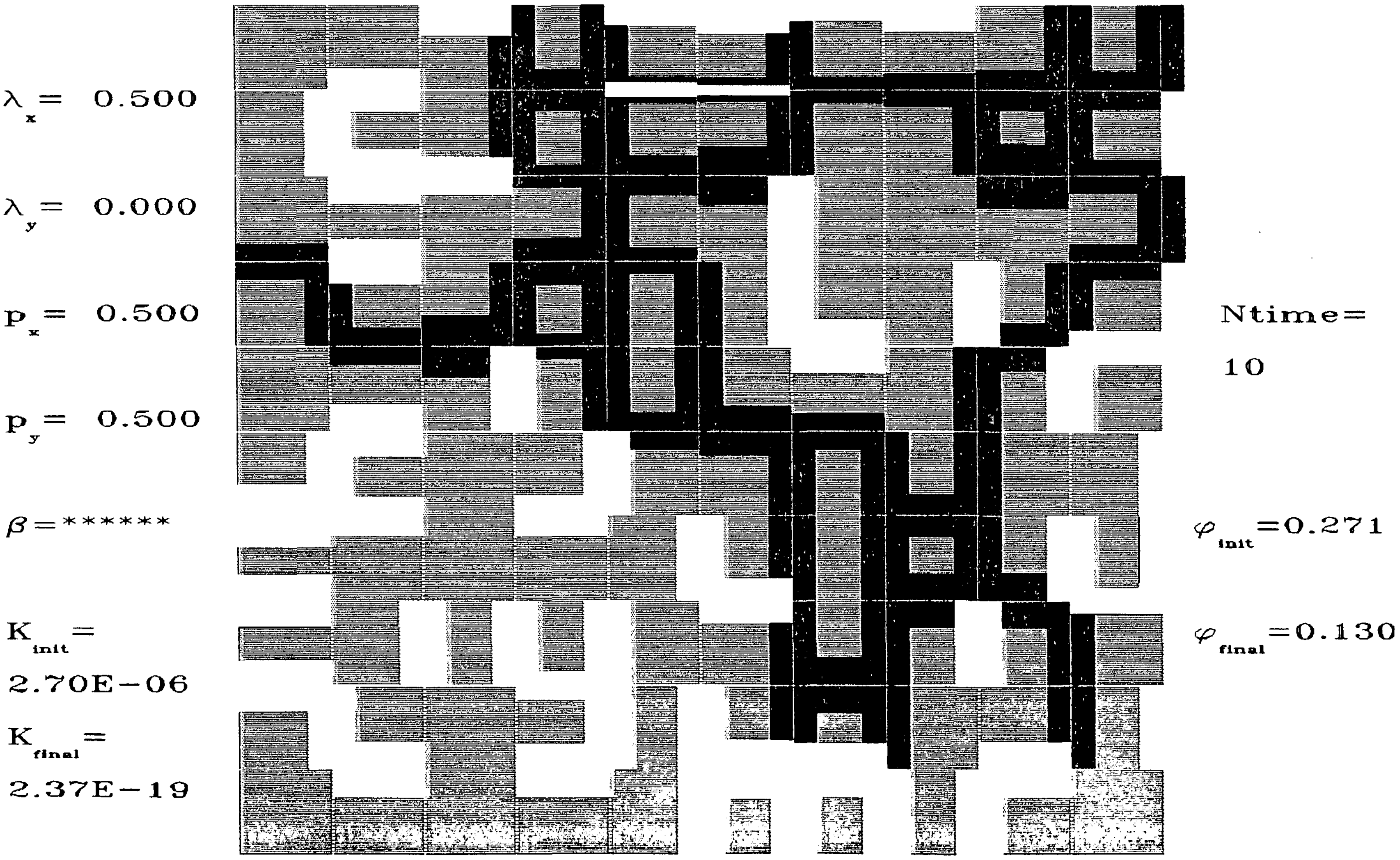
$\lambda_x = 0.500$
$\lambda_y = 0.000$
$p_x = 0.500$
$p_y = 0.500$
$\beta = ******$
$K_{init} =$
2.70E−06
$K_{final} =$
2.37E−19
Ntime=
10
$\varphi_{init} = 0.271$
$\varphi_{final} = 0.130$

Figure 15.

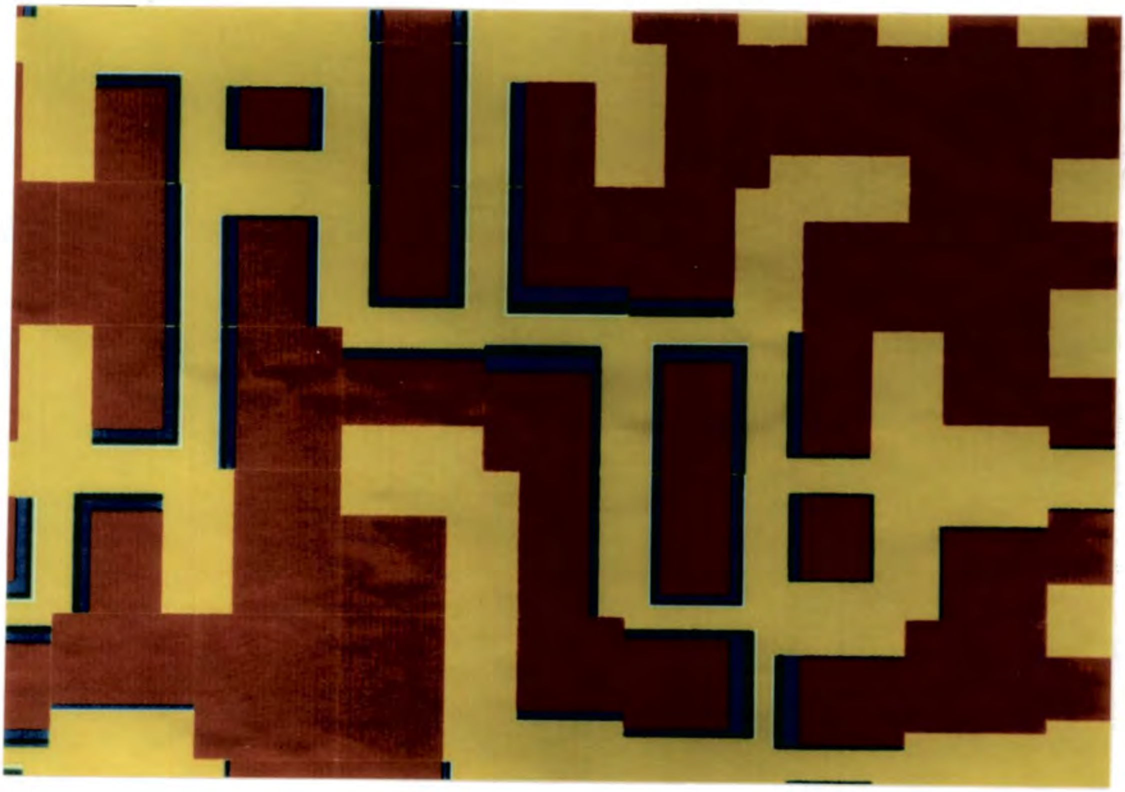

Figure 5.16 The model can also be set to run in a sequential fashion and this produces a series of cement zones. The thickness of each zone decreases progressively according to the dependence on the fourth power of the radius. Although the layers are not clear in this picture, they are enlarged below.

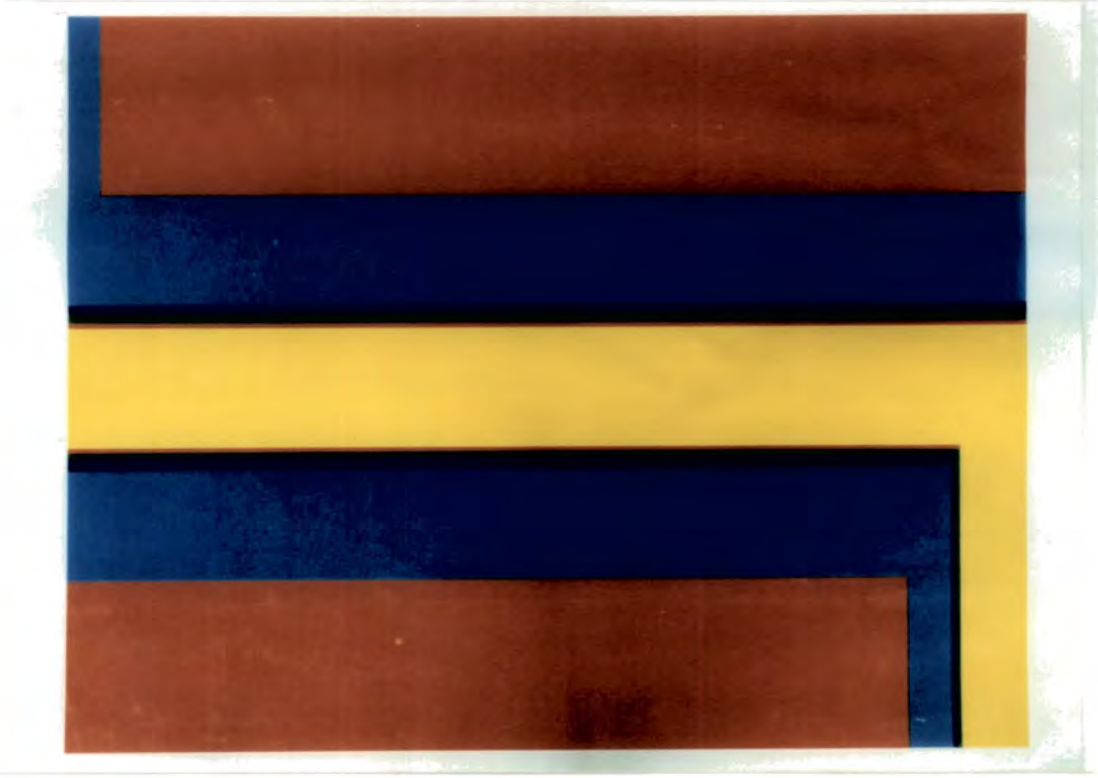

Figure 5.17 Expanded version of the above example, here with four very clear cement zones of progressively decreasing thickness. Each zone is equivalent to an equal time period.

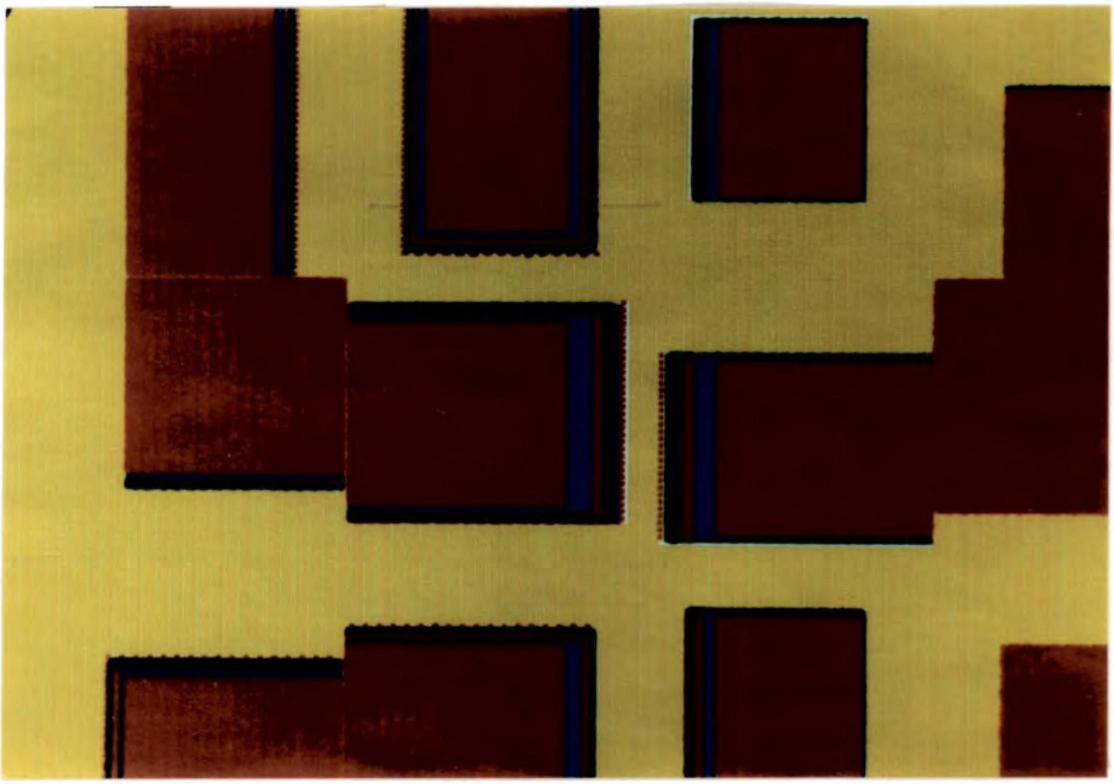

Figure 5.18 Similar example to Figure 5.16, but in this case ten cement zones have been produced. Enlarged photograph is shown below.

Whilst all of the above examples have been on a 10 × 10 grid, any grid size can be used, limited only by the resolution of the graphics and the central processor time required to compute the result. Figure 5.19 is an example of a 25×25 grid, and it is in the use of these larger grids that the possibility of modelling flow patterns on a larger, geologically relevant scale can be seen. Although this particular example is of little predictive value, it could be considered as a first approximation to the cementation patterns of a reef core unit. Whilst the majority of the unit is cemented fully, areas at the left hand upper edge are of lower permeability relative to the rest and have received less cement. Dead end cavities or areas which are isolated from the flow have received no cement whatsoever.

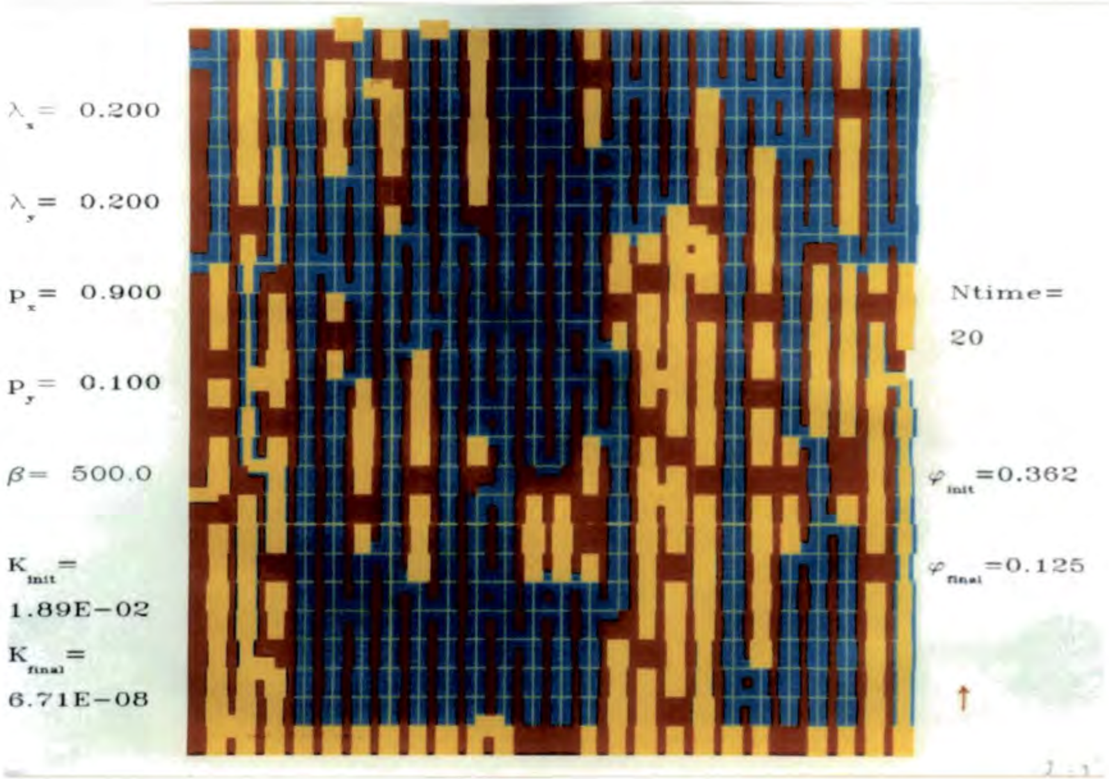

Figure 5.19 This photograph shows the results of a model calculation with a 25 × 25 grid. The increase in size indicates the possibility of modelling the flow patterns on the reef and formation scale. Although this example shows a suggested cement distribution, the model could be easily altered to produce flow contours. Whilst a large proportion of the unit has high flow rates, certain parts have no flow whatsoever. This type of model could be accurately calibrated to geological reality through the use of capillary pressure curves shown in Figure 5.20.

5.6 Limitations and Future Potential of this type of Modelling.

5.6.1 Limitations of this model.

The modelling described above has been limited to the thin section level, and in order to be able to model the poroperm characteristics of large rock units effectively, it would be necessary to make a number of modifications to the present method of describing the matrix.

i) The use of a regular square grid restricts the variation in capillary radii to essentially one order of magnitude. The network codes should be modified so that actual measured values are used to describe the poroperm characteristics of the rock, rather than the rather arbitrary $\lambda_{x,y}$ and $P_{x,y}$ factors used above. An example of the pore throat radius distribution of a Holocene coral framestone is given in Figure 5.20, and use of this distribution to define the capillary radii distribution in the model would result in an extremely accurate representation of the poroperm characteristics of such a rock. This modification would therefore permit the modelling of the flow characteristics of any rock, given its pore throat radius distribution as derived from capillary pressure curves similar to Figure 5.20.

ii) Expansion of the network codes to three dimensions would be advantageous, although the visualisation of the results would be more difficult. The results could be viewed as two dimensional sections through the three dimensional shape, either using the same type of graphical output as presented in the above diagrams or by producing contour diagrams of either flow rate or extent of cementation. Another possibility would be to produce a graphical output illustrating the pore throat radius distribution after cementation had occurred. This would be of similar appearance to Figure 5.20 The evolution of the poroperm characteristics of the rock could then be observed.

iii) The early cementation processes described in this thesis interact in a dynamic fashion with numerous other processes including reef growth, sedimentation and bioerosion and these processes could be included in the program codes. In particular, reef growth appears to have a significant effect on the cementation pattern as observed on the reef scale (Section 2.8.6), and this process could be modelled in an interactive fashion, by mathematically describing the burial of a fixed unit of reef at a given rate.

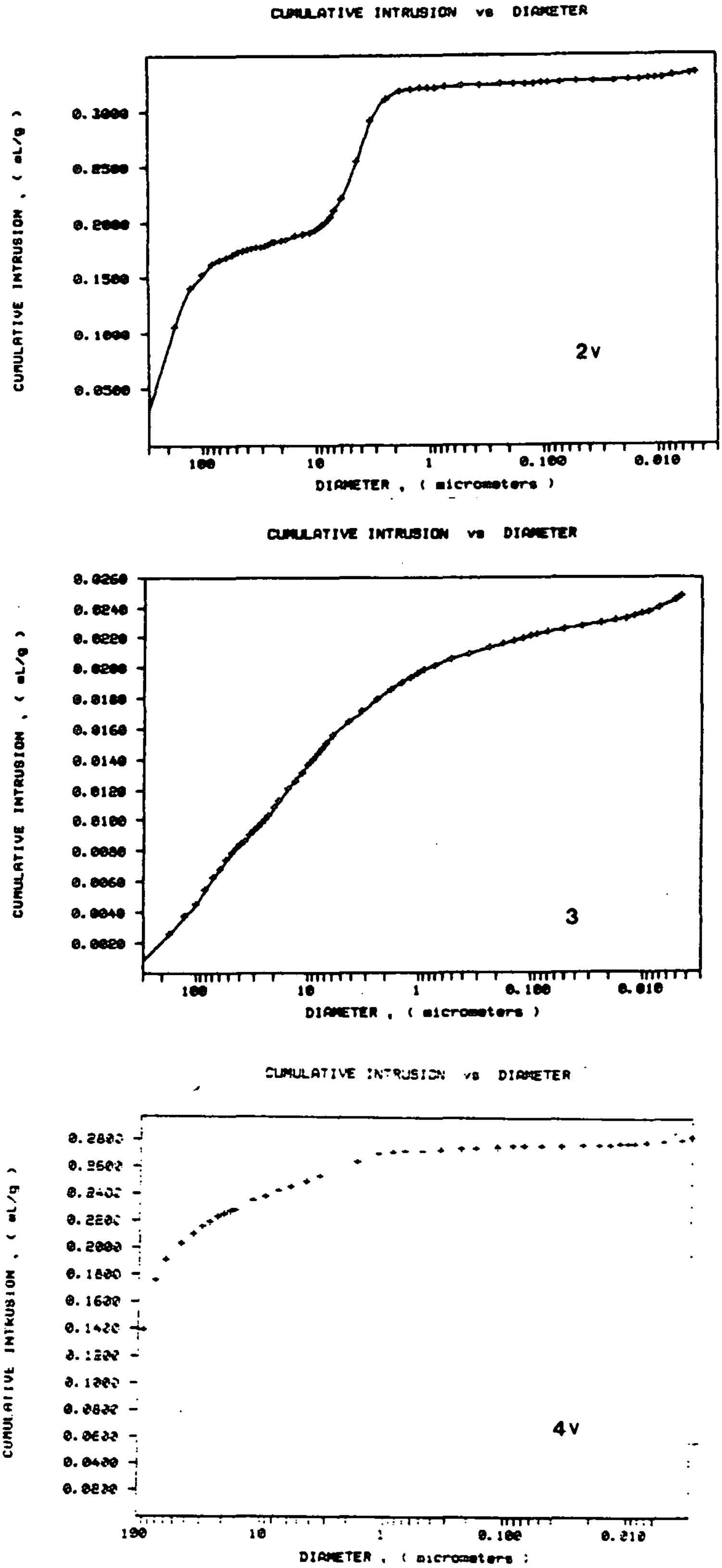

Figure 5.20 The pore throat radius distribution for several Holocene corals as measured by mercury injection poreassymetry. This type of capillary pressure curve could be used to tie the model to geological formations. Discussion in the text.

5.6.2 The nature of flow on different scales.

The theoretical basis of the modelling as presented above is that laminar flow is occurring. This is certainly the case in the main body of the reef at the thin section level, but it may not be true for the surface of the reef which is in a very turbulent zone. This turbulence would not alter the distribution of the cements, but may affect the overall extent of the cementation, due to the fact that a greater volume of water would be forced through the pores.

A related problem is that of the creation of eddies and vortices around the irregularities in the rock matrix. The above model does not take account of this possibility, and it would be difficult to do so. One could argue that the lack of cements in dead end porosity, as shown in the examples above, is geologically unreasonable as these eddies would cause the circulation of pore water even in such restricted cavities. However, the surface tension and capillary force effects may be strong enough to prevent circulation in such porosity on the micro-scale, even in the presence of turbulent effects. On the whole reef scale, however, it is clear that such eddies would be able to cause some circulation of pore fluids.

This discussion serves to highlight that the flow rates through pores may be much higher at the surface of the reef than in the interior, due to the rapid attenuation of the wave energy. It is possible that two very different flow regimes exist on the reef scale, the surface metre or so being in a rapid flow regime of perhaps 10–500 metres per day, with the reef core being in a zone of much slower flow, perhaps of the order of 10 cm. or less per day. Water in restricted pores (on all scales) would therefore exchange with the oceanic reservoir at only a very slow rate. This distinction between rates may not be just at the surface, as there will be high permeability conduits throughout the main body of a reef, formed by coarse reef rubble and large cavities, and these will also receive large flow rates.

5.6.3 Modelling on a larger scale.

Expansion of the scale of the modelling could be achieved in two different ways. The first would be by completely altering the mathematical description of the matrix of the model such that it was representative of the permeability characteristics of the whole reef rather than of the rock type. This would require a good characterisation of such properties on the three dimensional level at that scale. It is difficult to see how the distribution of the permeability on that scale could be accurately ascertained. The second method would be to use the same mathematical descriptions as used on the thin-section level, with the modifications as suggested in Section 5.6. The model could then be progressively enlarged in scale using the three-dimensional capillary grids as building blocks. Capillary pressure curves for the different lithologies present and for variations in the poroperm properties of the individual lithologies could be quite easily obtained. This would lead to an accurate representation of the flow characteristics of the sub-units that comprise the reef as a whole. The only remaining problem would be that of describing the three dimensional geometry of the distribution of the sub-units. It is debatable whether this approach could ever usefully predict the cementation pattern on the reef scale, as the amount of data needed to do so would probably be prohibitive. However, the modelling of general flow characteristics on this scale could certainly be achieved with some accuracy. It is this general aim which is discussed in Section 5.7.

The problem of the inhomogeneity within particular lithologies which form the reef is even greater when the original depositional porosity is masked by the effects of diagenesis. This is clearly the case in the Miocene reef samples briefly described in the following section. Samples were collected from a small patch reef which exhibits very well defined facies changes on a scale that could easily be modelled given suitable poroperm data. Porosity and permeability figures were measured for the different facies and the variations within facies was also examined. The intention was to build up a model of the whole reef by considering the facies as sub-units and using the poroperm characteristics of each as building blocks as outlined above. The data reflect the diagenetic texture of the reef and as can be seen from Figure 5.29, there is as great a variation within facies as between them. This is primarily due to the fact that the present porosity is a diagenetic product which bears very little resemblance to the primary depositional fabric.

The following is not intended to be a full petrographic description of the reef, but as a summary of the major characteristics, it is useful to illustrate the problems in modelling the poroperm characteristics of ancient reefs.

5.7 The Miocene Reef of Sant Pau D'Ordal, Barcelona, Spain.

5.7.1 Introduction.

The Sant Pau D'Ordal Reef occurs in the Penedès Basin, near Barcelona, N.E. Spain and occurs in Middle Miocene strata, of Vindobonian age. The reef has been previously described (Permanyer & Esteban, 1973; Alvarez, et al., 1977) and is interpreted as being situated behind a major barrier in a lagoonal environment of fairly low energy. This patch reef forms an ideal example for this study of the porosity and permeability characteristics on the whole reef scale, as it is very well exposed, exhibits a clear zonation and is of suitable size (100-150 metres in cross section.) Samples were collected in a gridded format from each of five major subfacies as indicated in Figure 5.21. These sub-facies represent stages in the growth of the reef and are described in the following section.

5.7.2 Description of the reef and the diagenetic features.

The reef exhibits the classical stages of formation as identified by James (1979), notably stabilisation, colonisation, diversification and domination. An accumulation of skeletal fragments, forming grainstones and packstones, with an abundant fauna of molluscs, foraminifera, echinoids and digitate coralline algae represents the stabilisation stage. The effects of meteoric diagenesis are very apparent, with most of the porosity in the samples being mouldic, the outlines of the bioclasts preserved by the lithified interstitial sediments (Figure 5.22). The dissolution of most aragonite clasts is complete, but the Mg-calcite organisms are quite well preserved. Some dissolution cavities within coralline algal fragments are filled or partly filled by a meteoric spar cement, the crystals increasing in size towards the centre of the pores (Figure 5.23). The intra-skeletal cavities of some encrusting serpulids are also filled by this phreatic cement. The average porosity is approximately 15%.

The upper surface of this unit contains more encrusting organisms, with some development of rhodoliths (Figure 5.24), and this passes gradually upwards into a bindstone and bafflestone colonisation stage. In this unit the crustose coralline algae are the major organisms, with a diverse fauna present in the interstices. The samples are in some cases quite extensively altered by the meteoric fluids, both neomorphic fabrics and spar cements being developed. Some small coral skeletons are present, and these are typically pervasively replaced by crystals of calcite spar up to $200\mu m.$ in size (Figure 5.25). This spar also fills most of the primary porosity and is precipitated in continuity with the neomorphic spar of the coral substrate. The presence of the original skeletal material is only recognised by the remaining outlines, possibly formed by the organic matrix of the coral. Some specimens are extensively neomorphosed with very little primary fabric visible in thin section (Figure 5.26)

The diversification stage contains numerous coral skeletons, with *Montastrea* and *Tarbellastrea* being the dominant species. The coral colonies are generally less than 30 cm. in diameter, and the cavities between colonies are filled by large volumes of sediments. These sediments have a very clear biomouldic porosity (Figure 5.27), and much of the remaining material is formed of a neomorphic calcite mosaic.

The major reef building unit of up to 6 metres in thickness is of massive appearance, formed almost entirely of large coral colonies (up to 1.5 metres in diameter), with very little sediment. This framestone unit might be described within the diversification stage in the model suggested by James (1979), as it forms the bulk of the reef mass. However, Alvarez et al. (1977) described this unit as the domination phase, and it is certainly very clearly distinguishable from the early diversification. The reef does not appear to have developed the characteristic encrusting features as described by James (1979) in his domination phase, probably due to the fact that it grew in the calmer lagoonal environment and was never exposed to the high energy conditions of the surf zone. Substantial development of dissolution porosity is evident at outcrop, though this may be a result of relatively recent weathering. In thin section, the effects of extensive meteoric diagenesis are evident, with the coral skeletons being completely calcitised, and most of the primary porosity occluded by further calcite spar (Figure 5.28).

5.7.3 Summary of the diagenesis.

There is very little evidence of marine diagenesis in this patch reef, a fact that is likely, due to the low energy of the environment. The entire reef is characterised by extensive dissolution and neomorphism caused by meteoric waters. There is no evidence of any vadose cements, and the high degree of alteration of many samples suggests that the diagenesis occurred in a phreatic environment, probably in an active zone with pore fluids saturated with respect to calcite (Longman, 1980). The greatest majority of the porosity is biomouldic in origin with most of the aragonite grains dissolved or replaced. Bioclasts which were originally high Mg-calcite are well preserved, although the present Mg content was not measured. The porosity is highest in the packstones and grainstones of the stabilisation and colonisation stages. Porosity is also high in the sediments between corals in the diversification stage. The domination stage has a much lower porosity due to the widespread occlusion of intra-skeletal cavities by calcite spar. This probably reflects the high amount of aragonite in this facies which is more than 80% coral framestone. The pore fluids passing through this unit would have rapidly become saturated with respect to $CaCO_3$ due to the dissolution of large amounts of aragonite. This resulted in the local reprecipitation of the stable calcite, both as a neomorphic spar, and as a further pore occluding phase.

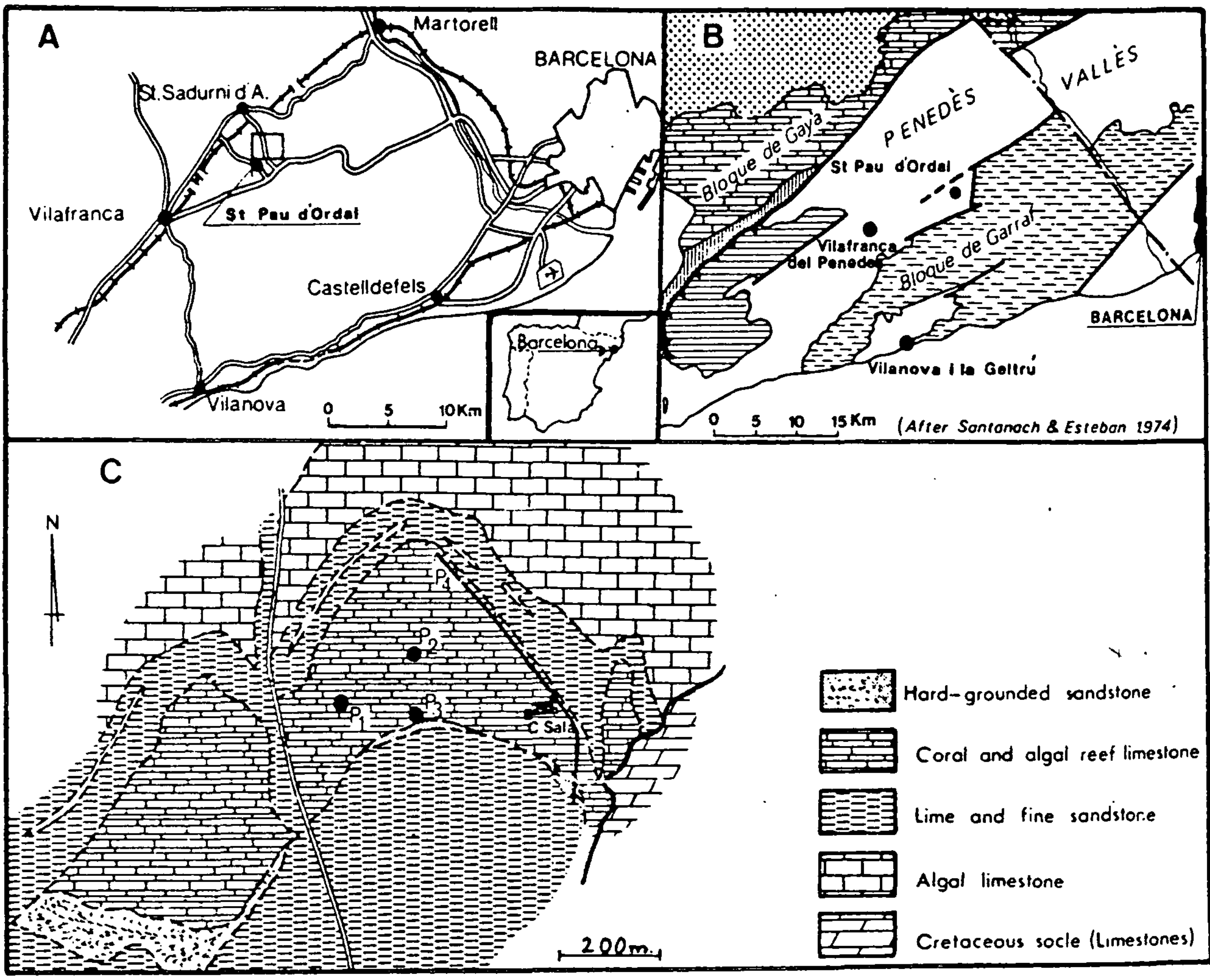

Figure 5.21a Location Map showing the position of the Sant Pau D'Ordal Reef to the west of Barcelona, Spain. (From Alvarez et. al. 1977)

Figure 5.21b Outcrop photograph and sketch detailing sampling points.

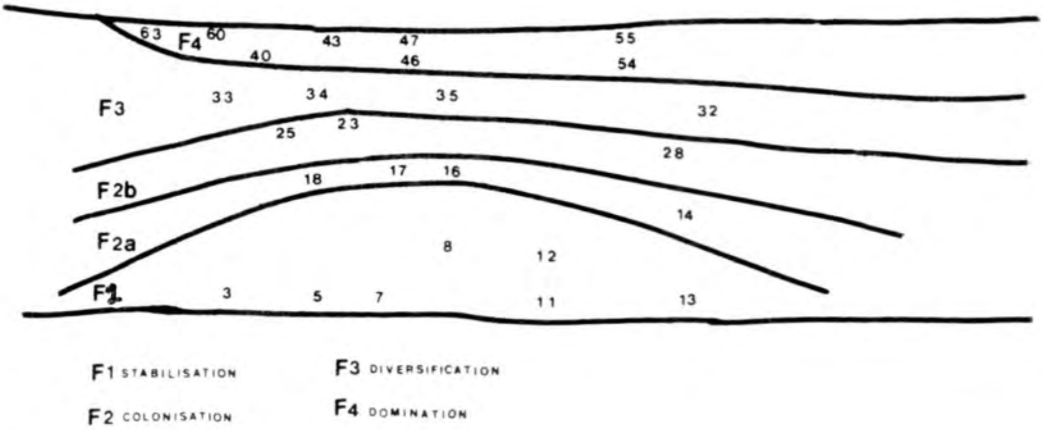

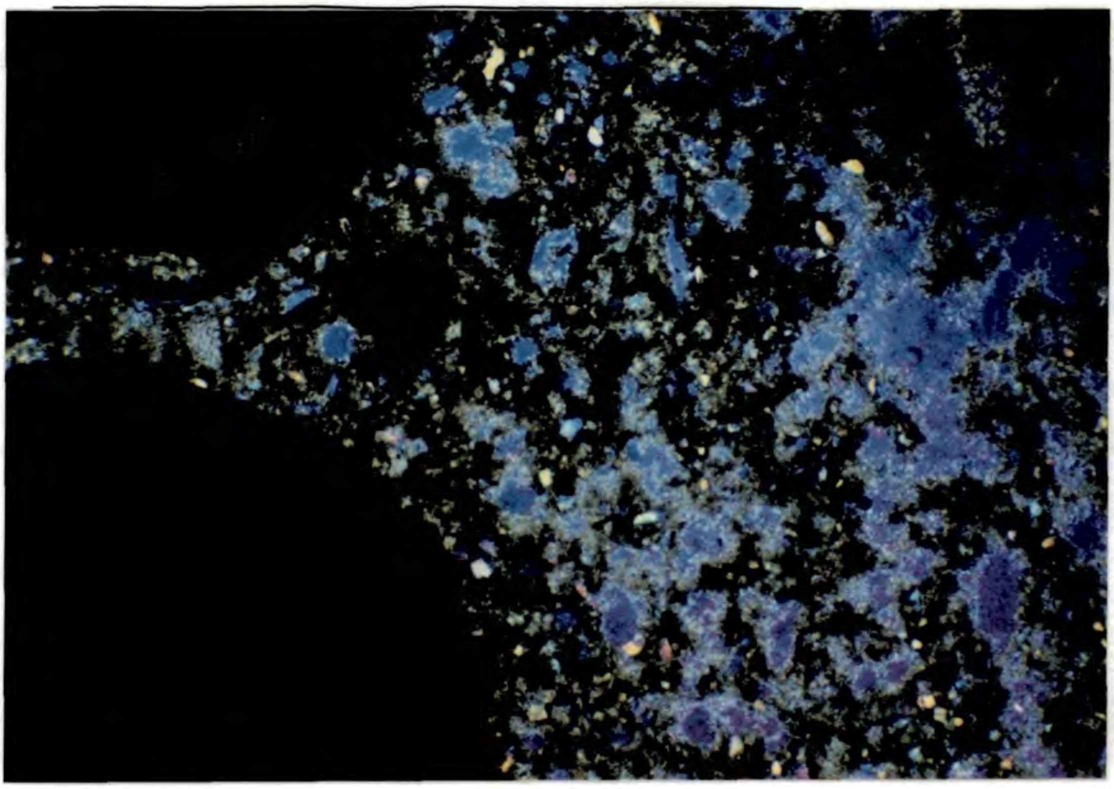

Figure 5.22 Biomouldic porosity of samples from the stabilisation stage of the reef. Dissolution of aragonite clasts is complete. Photomicrograph, xpolars.

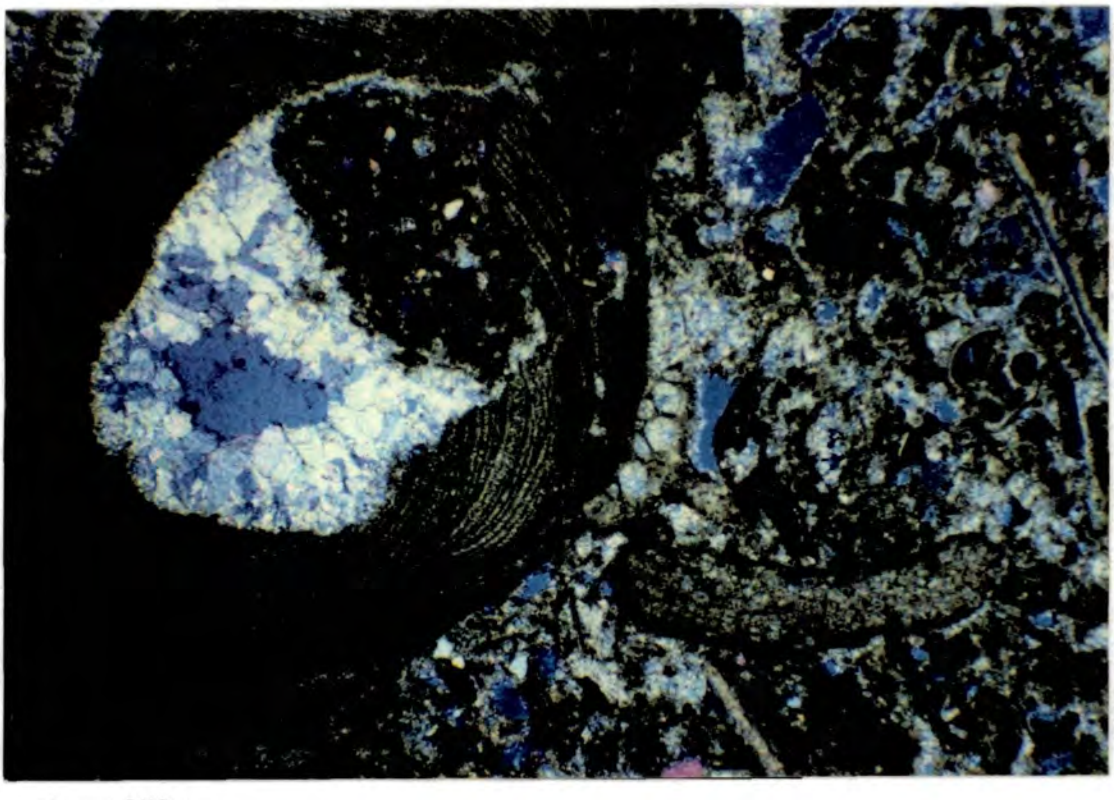

Figure 5.23 Some of the Mg-calcite fragments also show evidence of dissolution, and meteoric spar cements are occluding the secondary porosity. Photomicrograph, xpolars.

Figure 5.24 Photograph of a core sample taken from the colonisation stage, showing the development of rhodoliths.

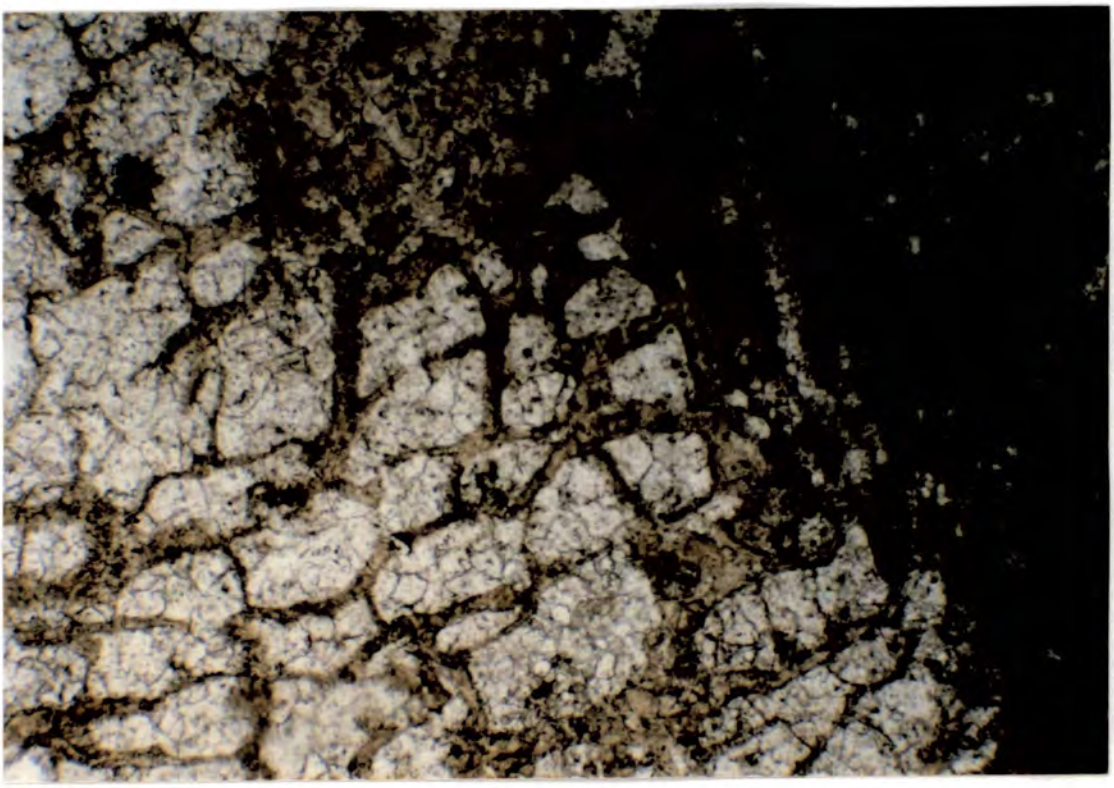

Figure 5.25 Coral from the colonisation stage. All of the primary intra-skeletal porosity has been filled by spar cements. Photomicrograph, ppl..

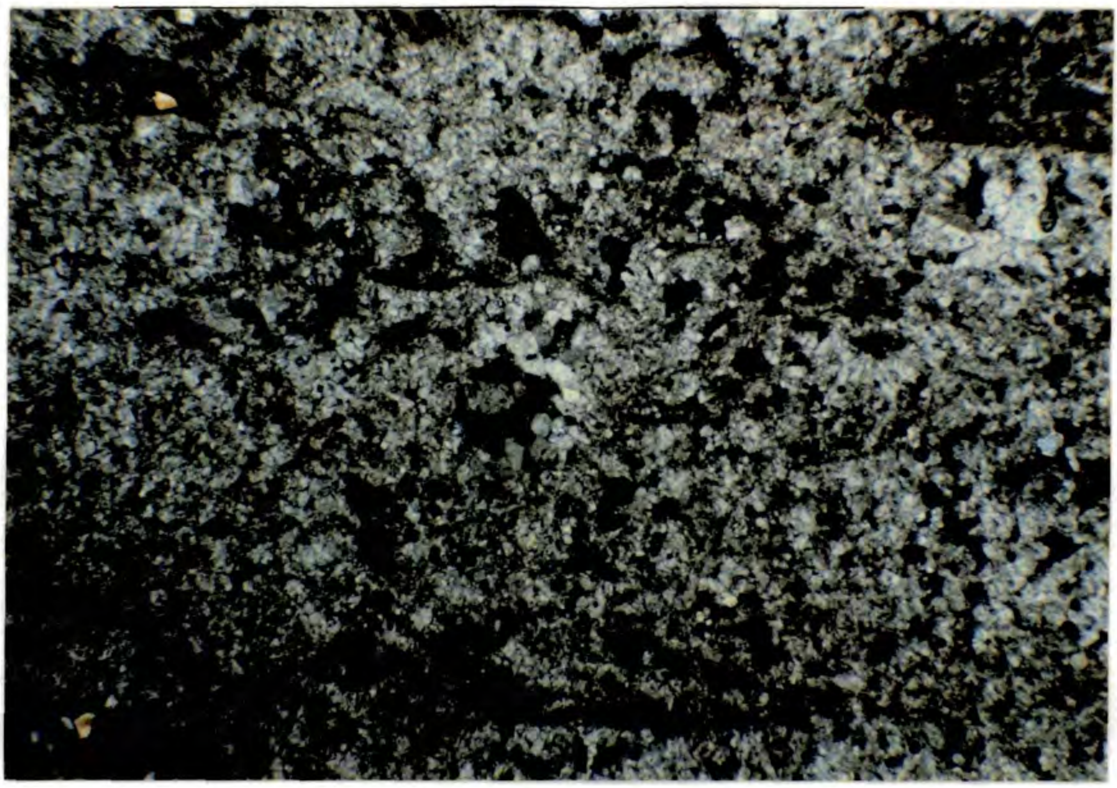

Figure 5.26 Sample from a similar area to that shown in Figure 5.25, here extensively altered with some secondary porosity and little recognisable primary fabric. Photomicrograph, xpolars.

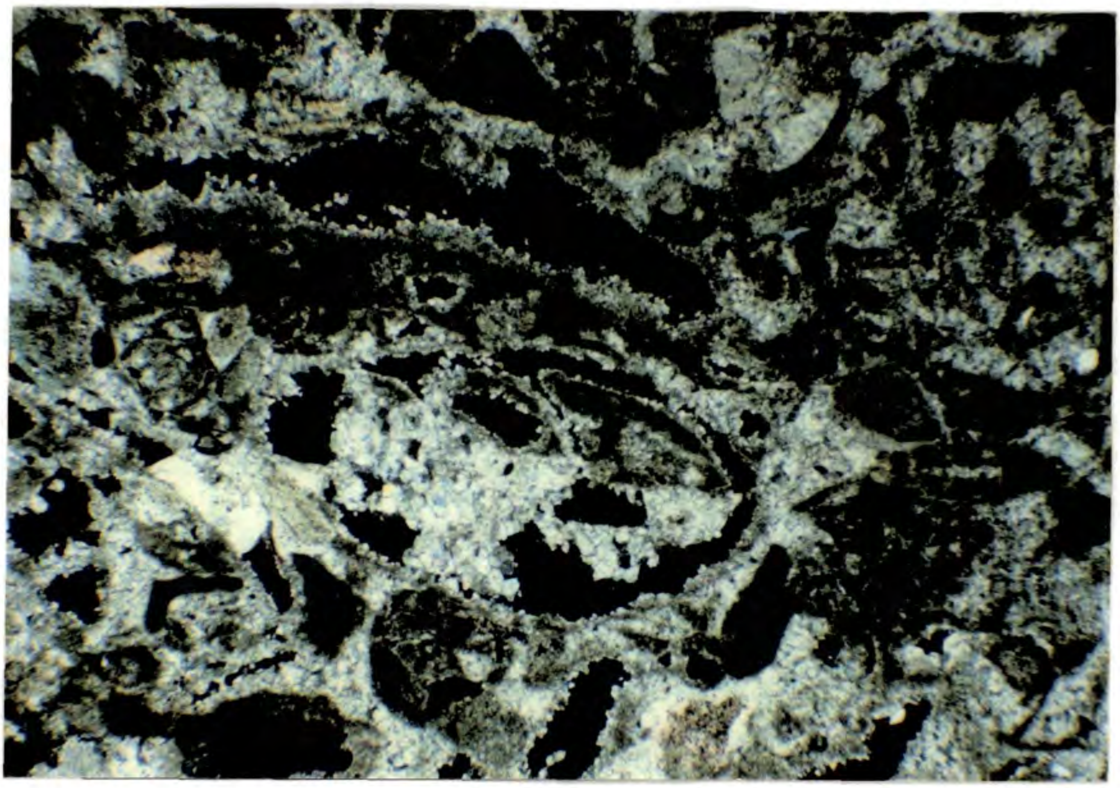

Figure 5.27 Sediments filling cavities between corals in the diversification stage. These samples have well developed biomouldic porosity. Photomicrograph, xpolars.

Figure 5.28 These samples are from the major reef building coral dominated stage. The corals are completely calcitised, with large spar cement crystals occluding most of the primary intra-skeletal porosity. Upper Photomicrograph, ppl., lower Photomicrograph, xpolars.

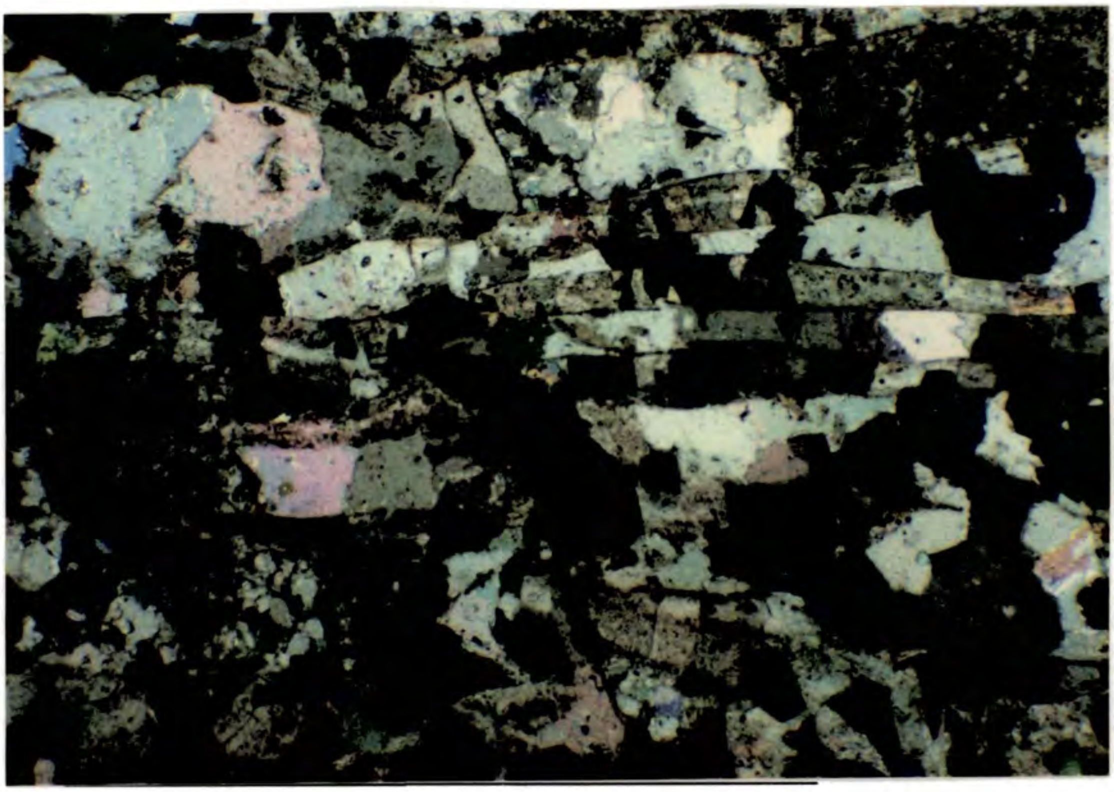

5.7.4 Porosity and permeability characteristics.

The porosity and permeability of the reef samples was measured using 1 inch diameter core plugs and the results are presented in Figure 5.29 and in Appendix 5. The effect of the meteoric diagenesis has been to reverse the porosity distribution as expected from the primary depositional characteristics of the different reef facies. Hence the coral framestone facies which would have had up to 50% primary porosity is now the least porous unit. The grainstones and packstones of the stabilisation and colonisation stages which might be expected to have had an original porosity range of 45–70% (Enos & Sawatsky, 1981) have a porosity of up to 20% which is not related to the primary characteristics.

The permeability values are very inhomogeneous, varying from zero to several hundred mD in the same hand specimens. The two highest figures are due to fractures in the small cores. The one clear result is that the coral framestone facies has a consistently low permeability, a fact directly attibutable to the extensive precipitation of meteoric spar cements (Figure 5.28). Some samples from the diversification phase have substantial permeability, these tend to consist of the sediments filling the interstices of the small coral heads. Samples of the corals themselves again have very low or zero permeability due to the occlusion of pore space by meteoric cements (Figure 5.25).

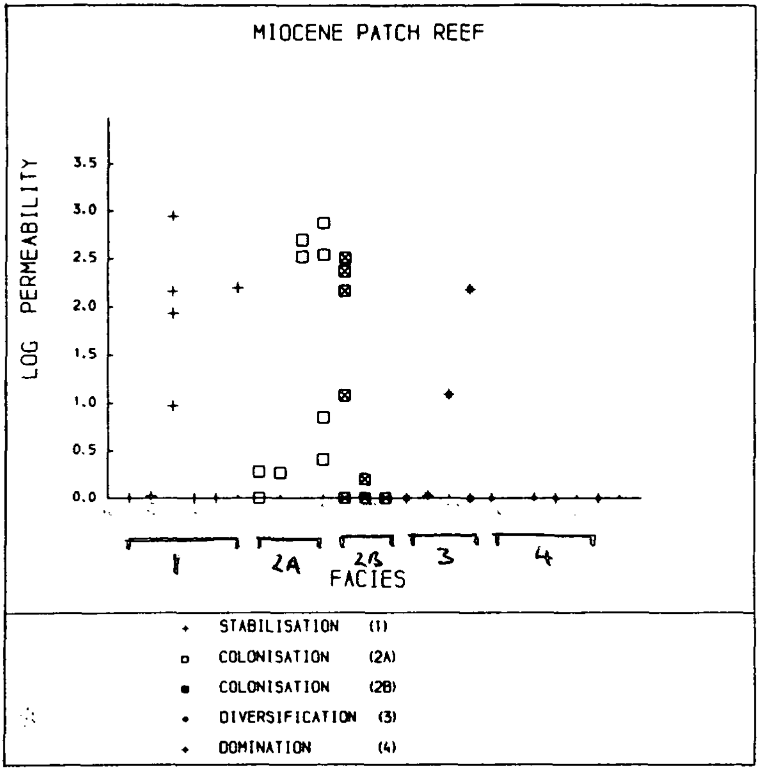

Figure 5.29 Porosity and permeability of the Miocene Reef samples. The upper graph shows the log of the permeability plotted against the samples divided into facies. The lower graph is a plot of the porosity. The x - axes are simply a list of samples. Several samples were taken from each hand specimen. These repeat measurements are plotted vertically above one-another, in order to emphasis the variability within individual hand specimens.

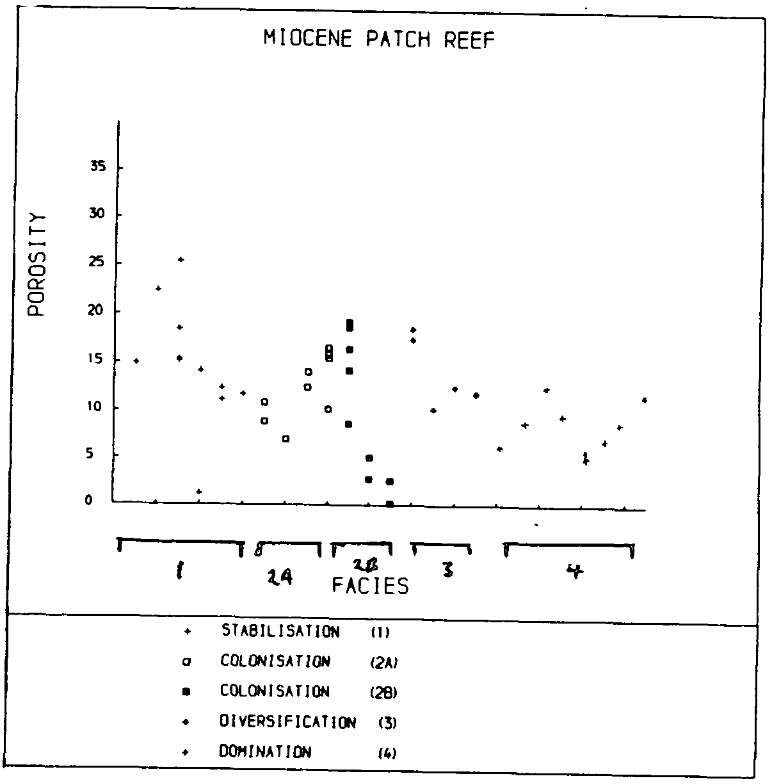

5.7.5 Summary and Conclusions of the Miocene Reef Study.

The great variation in porosity and permeability of the samples from this Miocene reef make the study of the hydrologic characteristics on the reef scale very difficult. Although the reef exhibits well defined facies changes, the diagenetic imprint has masked the depositional characteristics. The fact that variations are as large within hand specimens as across facies means that the development of a model system on the basis of data from 1 inch cores would be unreliable. Realistic representation would require extensive study of the porosity and permeability using larger core samples, and the measurement of pore-throat radii distributions. Only with this data and a thorough analysis of the distribution of the diagenetic products would it be possible to develop an effective modelling system. Modification of the codes used in this study so that the model geometry was controlled by measured characteristics, would enable modelling to be carried out on the whole reef scale.

5.8 Conclusions.

The development of mathematical models to investigate the hydrologic characteristics of carbonate framestones has proven to be successful. Using simple mathematical descriptions of the distribution of porosity and the nature of the cementation process, a number of the features of the real system have been reproduced. This success supports the suggestion that the major control on the distribution of precipitated cements is the rate of flow, or the total fluid flux through a pore or pore system. This control operates on all scales, though the modelling has been concentrated at the thin section level. The results indicate that a substantial amount of the porosity as observed in thin section is 'non-effective', and confirms that if laminar flow occurs, 'dead end' porosity will not receive any cement. Simple modifications of the network codes would enable effective modelling of the hydrological characteristics on the reef and formation levels. The essential requirement is for permeability and pore-geometry data which are representative of the material at the scale at which the study is considered. The problem of obtaining such representative data is particularly acute for carbonates in which the diagenetic imprint is commonly important and the poroperm characteristics can be unrelated to depositional fabrics. In order to develop model systems in these cases, there is a necessity for the acquisition of a large amount of data. Measurement of pore throat radii distributions may result in the clarification of trends with respect to the spatial distribution of the diagenetic effects.

CHAPTER 6

Cementation in Ancient Reefs. The Hafelekar Reef Complex, Middle Triassic, Northern Alps.

CHAPTER 6

Cementation in Ancient Reefs —
The Hafelekar Reef Complex
Middle Triassic, Northern Alps.

6.1 Introduction.

The emphasis of previous chapters has been on the investigation of cementation in modern reefs, with a view to gaining an understanding of the controls on the geochemistry and distribution of the observed cements. The distribution has been considered on a broad range of spatial scales, but the temporal scale is, at least geologically speaking, very short.

Many petroleum reserves have been discovered within reefs and associated facies, and with particular reference to the investigation of reservoir quality, it is essential to consider the temporal evolution of the porosity of the formation. The timing and spatial extent of various diagenetic events has to be evaluated in order to characterise fully the nature of the present porosity and permeability. The precipitation of early cements can have a controlling effect on the evolution of the porosity and it is this aspect of the diagenesis of ancient reefs which is studied in this chapter.

The emphasis of the study has been to describe the marine cements and their distribution on the reef scale, highlighting any variations observed within the reef proper and between the reef and associated facies. A qualitative understanding of the effect of various cement phases on the porosity and permeability of the reef and therefore on subsequent diagenetic events has been achieved.

The identification of marine cements and the comparison of such cements throughout the reef complex have been based primarily on petrographic criteria. The effects of post-depositional diagenetic events have also been studied petrographically, with the backing of stable carbon and oxygen isotopic and trace element data. The geochemical data have highlighted the fact that many of the cements have not retained their marine compositions, but have been uniformly altered by diagenetic fluids whose origins are discussed in some detail. This alteration makes it difficult to correlate cements across reef facies on the basis of geochemical evidence alone. A thorough understanding of the diagenetic overprint on the depositional characteristics is also useful in interpreting the porosity evolution in reefs. The geochemical evidence helps to describe this overprint, and a brief description of the full diagenetic history and the relative timing of various events is presented in the concluding section. The nature of the diagenetic products depends on the initial mineralogy, the diagenetic environment and the geochemical characteristics of the pore fluids, and hence the following discussion concentrates on evaluating these three factors.

The material studied comes from the Middle Triassic of the Northern Limestone Alps, near Innsbruck, Austria. More specifically, the area is known as the Hafelekar Reef Complex, a buildup which forms a prominent part of the Wetterstein limestone, the location and stratigraphy of which are given in Figure 6.1). The palaeoecology of the reef has been described previously (Bradner &

Resch, 1981) and will not therefore be repeated here.

In order to interpret ancient sedimentary sequences, and to construct models to account for the principal features thereof, there tends to be a great dependence on the observations made in the modern environment. It is, however, quite difficult to compare modern and ancient reefs, as the major organisms contributing to the growth have changed with time. The appearance of many ancient reefs is therefore very different from most modern examples (James & Macintyre, 1985).

The Middle Triassic represents a particularly interesting phase in the geological history of fossil reefs, as there had been a hiatus in reef formation since the end of the Permian. During this interval there appears to be no record of reefs at all and a great scarcity of reef building organisms worldwide. Reefs of Triassic age occur principally on the margins of the widening Tethys and along the west coast of North America (Heckel, 1974), and are best studied in the Alps where they occur on the margins of large carbonate platforms.

The late Middle Triassic, in which the Hafelekar Reef occurs, sees the first development of the scleractinian corals, in particular *Thecosmilia* and *Montlivaltia*, but the most important reef building biota are typically calcisponges, stromatoporoids and the blue-green alga *Tubiphytes*, the latter commonly being dominant. Classical Middle Triassic buildups in the Dolomites of the Southern Alps have been the subject of much previous study (Bosellini & Rossi, 1974), but less has been published on the reefs of the Northern Limestone Alps. The latter usually show much better preservation of primary structure due to the lesser degree of dolomitisation.

The following section (6.2) introduces and briefly describes the Hafelekar Reef Complex and serves as a basis for the petrographic description of the cementation patterns and other diagenetic products which is presented in Section 6.3. Section 6.4 discusses the results of the stable carbon and oxygen isotopic analyses within the constraints of the petrographic descriptions, and further geochemical evidence is produced from trace element data, described in Section 6.5. Section 6.6 concludes the chapter with a description of the diagenetic history as determined from all the available data.

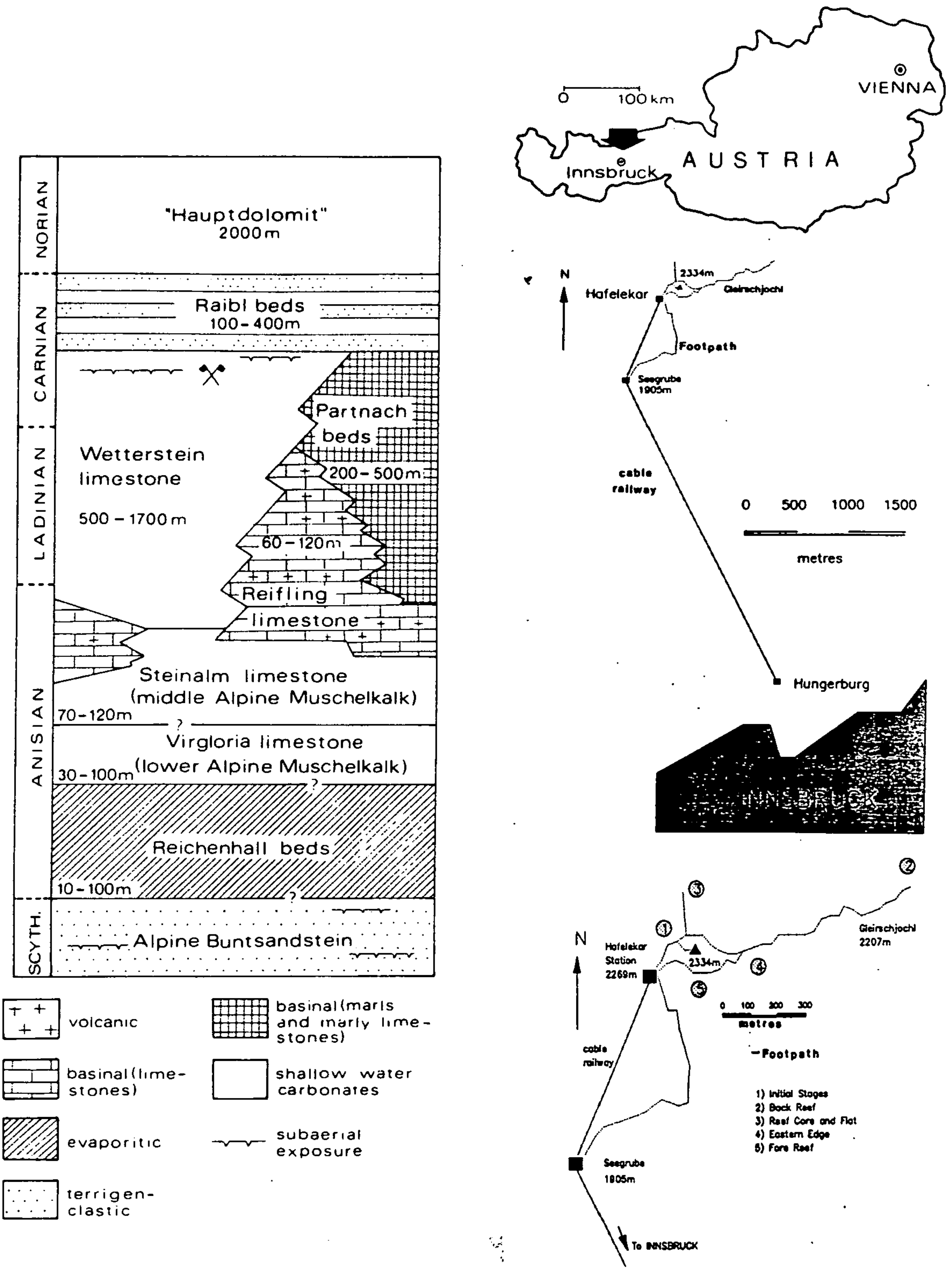

Figure 6.1 Location and stratigraphic position of the Wetterstein Limestone. The Hafelekar Reef Complex is situated in the Nordkette Range to the north of Innsbruck.

6.2 The Hafelekar Reef Complex.

6.2.1 Introduction and Regional Setting.

The Hafelekar Reef Complex is a prominent feature of the Wetterstein limestone exposed in the Innsbruck Nordkette Range. This mountain range forms part of the Northern Limestone Alps, the latter being one of the major structural units of the Eastern Alps. The entire platform margin occurs within a single tectonic unit of the Inn Valley Nappe (Bradner & Resch, 1981), and so this study is not affected by the interpretation of the nappe tectonics of the area. The limestones now exposed in the Northern Limestone Alps were formed on the north-west border of the newly created Tethys oceanic zone. This region of mobile rifting affected the relatively unstable shelf and sedimentation on the platform was influenced by varying subsidence, sea level changes and block faulting.

The stratigraphy of the area is given in Figure 6.1, from which it is apparent that the development of the Northern Limestone Alps took place in three regressive cycles. Three carbonate platforms were slowly built up, each being terminated rather abruptly, producing the Anisian Steinalm limestone, the Ladinian–Carnian Wetterstein limestone and the Upper Triassic Hauptdolomit. The presence of the pelagic Reifling limestone and Partnach limestones and marls on top of the Steinalm limestone indicate a gradual subsidence and suggest that the Steinalm platform was never subaerially exposed. In contrast, the top of the Wetterstein limestone shows some evidence of erosion (Bradner & Resch, 1981) and although very little indication of subaerial exposure is suggested in the Hafelekar reef outcrops, meteoric diagenesis is recognised in other Wetterstein reefs to the east (Heinrich & Zankl, 1986). The latter study asserts that the transgressive, terrigenous Raibl beds were deposited after several episodes of karst development which interrupted sedimentation in the uppermost Wetterstein limestone.

The Hafelekar Reef Complex is the final stage of reef development in the Nordkette Range, and it originated in patch reefs in the lower parts of the sequence. The total thickness of the Wetterstein limestone is in excess of 1700 metres (Flügel, 1981).

6.2.2 Reef Development.

The Hafelekar Reef Complex developed on the shallow slope of the platform margin, in two major phases, being repeatedly affected by sea level changes and syn-sedimentary tectonic activity. This is illustrated in Figure 6.2. The first stage was the growth of the Goetheweg reef which was subsequently affected by block faulting during the Cordevolian. Bradner & Resch (1981) emphasise that there is no steeply sloping reef talus as has been recognised in reefs of the Dolomites (Bosellini & Rossi, 1974), and suggest that the fore-reef slope is a feature of quite limited extent, with a shallow gradient. However, the slope was artificially steepened due to the effects of block faulting (Figure 6.2), and some considerable collapse of the Goetheweg reef body was recognised (Bradner & Resch, 1981). This collapse created a megabreccia, with blocks of several metres in diameter, and the cavities of this breccia were later filled by layers of fibrous cement. This was followed by a second phase of reef growth, forming the Hafelekar reef itself.

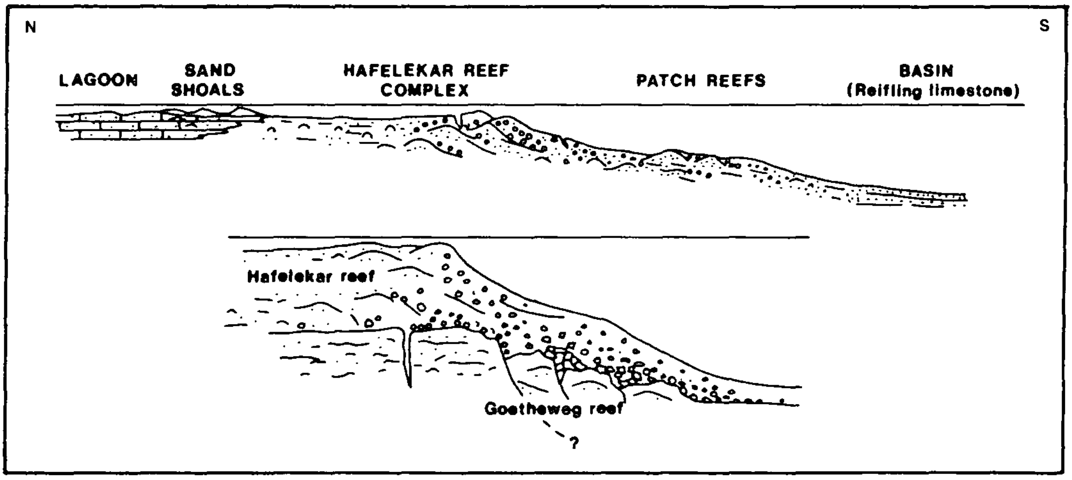

Figure 6.2 Diagram to show the development of the Hafelekar Reef Complex. The Goetheweg reef was the first massive reef development, and was affected by some tectonic activity during the Cordevolian. Block faulting occurred and the steep fault walls collapsed to produce the breccia shown. Further reef development created the Hafelekar reef from which all the samples were collected.

6.2.3 The reef framework.

The Wetterstein reefs, in common with many ancient reefs, lack extensive wave resistant structures. The growth of the Hafelekar Reef Complex was controlled by the stabilisation and encrustation of debris, with most of the organisms playing a sediment binding and baffling role. The most important primary framebuilders were the blue green algae, *Tubiphytes*, and the coral, *Thecosmilia*. The latter are considered by Bradner & Resch (1981) to be more important than had been previously recognised. *Tubiphytes* plays a framebuilding role in quieter water areas, but more of an encrusting role in more agitated environments. Many other encrusting organisms are also involved, including various hydrozoans, calcisponges and calcareous algae. Reef dwelling organisms include foraminifera, ostracods and molluscs.

There is an obvious zonation from the fore-reef to the reef flat and central reef area, reflected in the distribution of organisms, probably as a result of varying turbulence and energy conditions. The central reef area is typified by in situ organisms with interstitial grainstones, which contrasts with the fore-reef where most of the organisms are not in life positions and a larger amount of reef debris is present.

High energy conditions resulted in the winnowing out of muddy sediments leaving a high initial porosity of up to 50%, and very high permeability. These cavities were then filled by submarine cements. This extensive cementation is a characteristic that is recognisable throughout the reef.

6.2.4 Sample Collection.

Samples were collected from areas of the Hafelekar reef itself and the breccia of the Goetheweg reef on which it was founded, but the Goetheweg reef body was not studied. Location of the collection points is shown in Figure 6.3 and a description of each area follows.

i) Initial Stages. The Hafelekar reef growth was initiated on top of a block rubble sequence, consisting of mostly reef debris with scattered corals. Cavities between the debris are filled by layers of fibrous cement, and both substrate and cements are dolomitised to a variable extent.

ii) Back-Reef. This shows a bedded sequence of grainstones and packstones with prominent sheet cracks. The latter were also filled by fibrous cements.

iii) Reef Core and Reef Flat. This is characterised by a diverse frame building fauna, and the presence of layered fibrous cements precipitated within growth framework and secondary dissolution cavities. Fine skeletal sand is entrapped by *Tubiphytes* and other baffling organisms. Encrustation of the surfaces provided the substrate on which reef growth continued, areas of *Tubiphytes* and *Thecosmilia* framework interspersed by accumulations of grainstones. A variety of biocoenoses were recognised and described by Bradner & Resch (1981).

iv) Eastern Edge. The reef wedges out to the east and samples were collected in an area where Hafelekar reef growth interfingers with reef rubble. Extensive cementation is again evident, with the development of botryoidal masses of layered fibrous cements.

v) Fore-Reef Megabreccia. The fore-reef facies is characterised by the presence of a megabreccia, with blocks of several metres in diameter, the cavities of which are filled by 10–20 cm. thick layers of fibrous cements similar to those observed in the reef core. The cement layers are now replaced to varying degrees by dolomite.

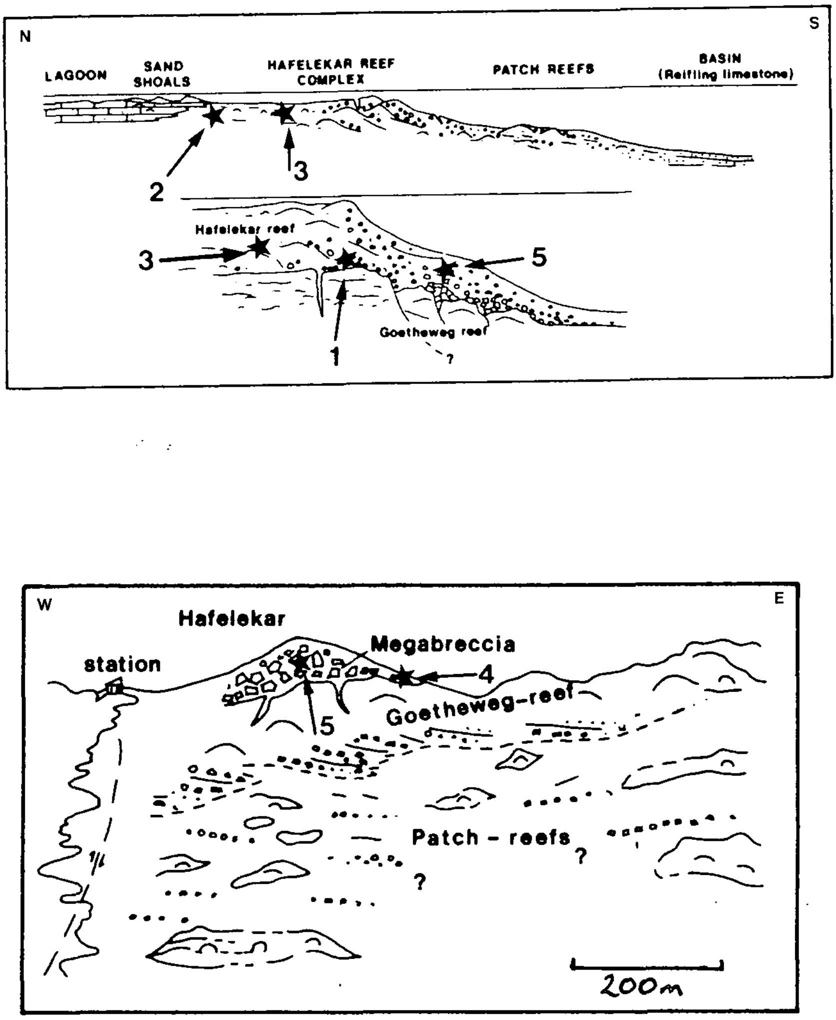

Figure 6.3 The Hafelekar Reef Complex, showing the collection points described in the text.

1) Initial stages.
2) Back-reef.
3) Reef core and Reef flat.
4) Eastern edge.
5) Fore-reef.

6.2.5 Burial History.

The Wetterstein limestone platforms were separated by small basins containing thin layers of marls, notably the Partnach beds and the Reifling limestones. Prevailing relief of the Wetterstein limestones was levelled during the late Carnian by a supply of terrigenous sediments of 100–400 metres in thickness, and above this level surface were deposited the initial dolomites of the Upper Triassic. This Hauptdolomit Limestone is very continuous over large areas, being up to 2000 m. thick (Bradner & Resch, 1981; Flügel, 1981; Piller, 1981), though generally thinner in the north, the variation being due to differential subsidence (Piller, 1981). During the late Triassic there was some differentiation of the platforms into basinal areas with a terrigenous influence, the Kössen beds, and this phase was followed by some further reef development (400 m. maximum) in the Rhaetic. The latter concluded the development of the Northern Alpine shelf which broke up during the lower Jurassic. Carbonate blocks subsided and were displaced, giving rise to a pronounced relief, with the thin nodular red limestones of the Ammonitico Rosso being deposited on palaeohighs and manganese-rich shales and marls in the deep basins. The climax of the subsidence was reached at the end of the Middle Jurassic with the deposition of some thin siliceous sediments (Zankl, 1971). The maximum sediment overburden appears therefore to be of the order of 3 km. and as the Northern Limestone Alps are in one of the highest nappes (Bradner & Resch, 1981), this is also likely to be the maximum burial depth, in agreement with figures previously quoted (Germann, 1968; Zankl, 1971).

6.3 Petrography and Diagenesis.

6.3.1 Introduction.

Bradner and Resch (1981), noted that the major feature of the diagenesis of the Hafelekar Reef Complex was the extensive cementation and early dolomitisation, and their observations have been confirmed in this study. The intention of this section is to describe the early diagenetic products and to analyse their spatial distribution, both within facies and in the reef as a whole. The application of cement stratigraphy has been successful in many past studies, allowing correlation of diagenetic events over large distances (Meyers & Lohmann, 1985). Similar techniques, using petrographic and geochemical studies, have been employed here to investigate the spatial extent of various diagenetic events. The results of the geochemical analyses are presented in the following two Sections (6.4 & 6.5). It is apparent, as is very commonly the case with fossil reefs, that the geochemical characteristics do not represent solely the original depositional environment of the cements, but also record some diagenetic overprint. The petrography presented in this section illustrates the diagenetic events, most notably several phases of dolomitisation.

The characteristics of samples from the five areas previously mentioned are first described separately, from which some concept of the distribution of the early cements will become apparent. This is followed by a summary of the diagenetic history on the reef scale, paying particular attention to the spatial extent of individual events, and the effects of such events on subsequent diagenesis.

Although petrographic description can often provide definitive proof of the nature, environment and relative timing of diagenetic events, some textures are difficult to interpret in a conclusive fashion. Hence a final description of the diagenetic history is left until Section 6.6, after the discussion of the chemical evidence.

6.3.2 The fore-reef megabreccia.

The cementation of the fore-reef breccia is the most spectacular diagenetic event in the history of the Hafelekar Reef Complex, and is therefore described first. The breccia blocks are themselves lithified by early marine fibrous cements, which are observed as isopachous linings within inter- and intra-particle pores (Figure 6.4). The cavities in the megabreccia can be several metres long and up to 30cm. wide and are filled by alternating layers of fibrous cements (Figure 6.5), the 'Großoolith' described by Bradner & Resch (1981). Similar development of the Großoolith cements has been recognised from other areas of the reef, but nowhere is the development so extensive. In the fore-reef they form up to 50% of the rock at outcrop, effectively sealing the cavities within the block framework, leaving little remaining primary porosity.

These 'Großoolith' cements have been described as alternating calcite and dolomite layers, interpreted as possibly being originally layered aragonite and high-Mg calcite (Bradner & Resch, 1981). However, careful petrographic observation indicates that all layers contain some dolomite which forms equant euhedral rhombs, typically 10–30 μm. in size (Figure 6.6), often only evident in the fibrous matrix after some etching. The fabric of the cement is quite variable, being mostly radial fibrous. However, some samples exhibit the characteristic convergent optic-axes, divergent sub-crystals and curved twin planes that define the radiaxial fibrous fabric (Bathurst, 1975). In some cases, the cement has the appearance of interfering clusters of fibres (Figure 6.7), very similar to the 'coconut meat' fabric described by Folk & Assereto (1976). Particularly noticeable is that the 'Großoolith' cements are nucleated on a layer of the substrate that is quite pervasively dolomitised. The latter dolomite has an anhedral to subhedral form, is coarser than the equant dolomite described above (40–200μm.) and is fabric destructive, although some vague ghosts of bioclasts can be recognised (Figure 6.8). This pervasively dolomitised layer varies in thickness (0.5–1.5 mm.) but is quite continuous throughout the fore-reef material. The rest of the substrate is also dolomitised but by a much finer grained dolomite mosaic, exhibiting some selectivity for grains rather than cement and some selectivity between grains. This distribution could reflect both original mineralogy and texture. The fabric preservation in the substrate below the surface layer is quite good, and this could indicate two phases of dolomitisation.

An important point is that the first precipitated layer of the fibrous cement is predominantly calcite, containing less dolomite than any other layers. The dolomite that is present in this zone and occurs in later zones in much larger amounts, is similar in appearance to the dolomite in the core of the substrate. This observation suggests that the fibrous cement was precipitated after the event that dolomitised the surface of the substrate, and there was a second dolomitisation phase which affected both substrate and cement.

It is interesting to note that the degree of dolomitisation in the core of the substrates has some dependence on the gross fabric. Those parts of the fore-reef debris which consist of grainstone type materials tend to be dolomitised to a greater extent than samples which appear to contain more of a reef framework type texture. This may be due to the higher initial permeability of the grainstones to the dolomitising fluids.

The substrate-parallel lamination of the 'Großoolith' evident in hand specimen, particularly clear in weathered samples (Figure 6.9) reflects the varying dolomite content, lighter layers containing more dolomite. These layers (up to 12 have been recognised), can be traced and correlated throughout the fore-reef, over distances of several hundred metres, with the thicknesses of the layers being identical (Figure 6.10). The high permeability of the cavities within the block framework was probably the major control on the precipitation, a suggestion supported by the results of the modelling presented in Chapter 5. The similarity of the thicknesses of individual layers suggests that the permeability of the fore-reef was quite uniform. It is interesting to compare this layered pattern with the results of Chapter 5, though it must be borne in mind that the layers within a particular sample do not necessarily represent equal time periods.

A late phase of coarse dolomite is quite commonly recognised within the substrate, and in general it appears to be a cement phase, although some crystals are replacive. The crystals are invariably euhedral, with very well developed rhombic faces and some show inclusion-rich centres with limpid outer edges (Figure 6.11). This fabric is usually interpreted as the result of the solution of local $CaCO_3$ during dolomitisation with the subsequent growth of the dolomite into the void-space thus created (Schofield & Adams, 1986). These dolomites are characterised by their sweeping extinction, with curved crystal faces being recognised in some examples. This is a characteristic of 'baroque' dolomite as described by many authors and interpreted as forming at elevated temperatures of perhaps 60–150 °C (Radke & Mathis, 1980).

The diagenetic history of the fore-reef material is apparently quite complex, particularly with respect to the dolomitisation events. There is evidence that some dolomitisation occurred prior to the precipitation of the 'Großoolith' cements, most notably the pervasively dolomitised surface of the substrates. The similarity of the finer euhedral dolomite in the core of the substrates with that in the cements themselves perhaps suggests that they are contemporaneous, but the relationship cannot be easily proven. Both of these dolomitisation events appear to be quite early, however, occurring in the very shallow subsurface. There is an additional, much later precipitation of baroque dolomite, indicative of formation after some burial.

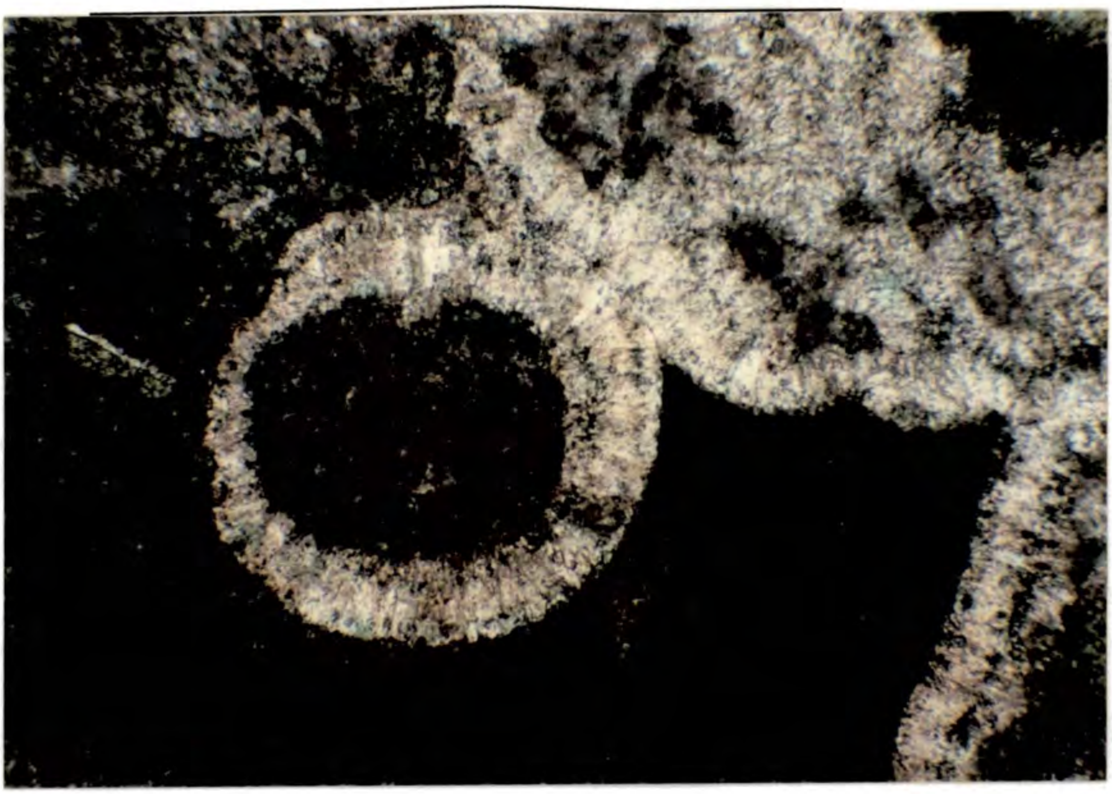

250μm.

Figure 6.4 Reef material from the fore-reef. The substrate is dolomitised, with the porosity filled by predominantly calcite isopachous fibrous cements. Stained with Alizarin Red S (ARS). Photomicrograph ppl..

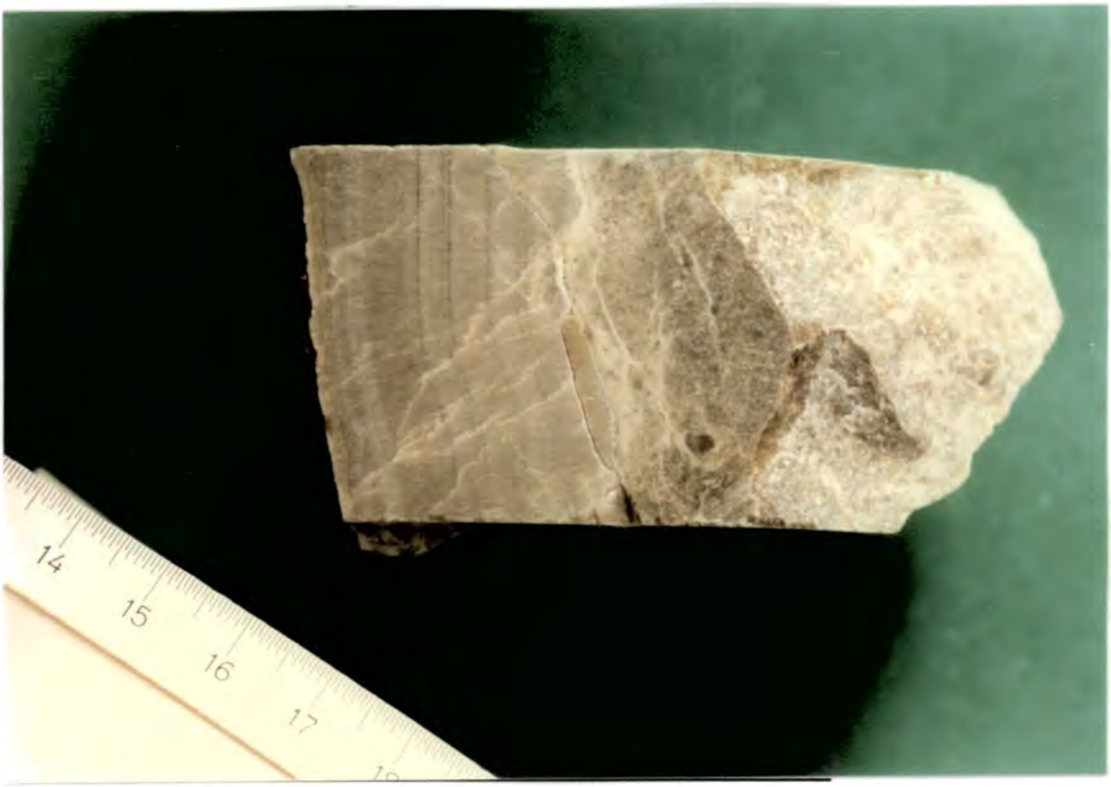

1cm.

Figure 6.5 Fore-reef sample. At the left is the zoned 'Großoolith' cement. Zones can be correlated throughout the fore-reef facies. Substrate to the right is shown in Figure 6.4 above.

Figure 6.6 Subhedral to euhedral dolomite within zoned fore-reef 'Großoolith' cement. Photomicrograph ppl..

Figure 6.7a Fibrous fabric of the 'Großoolith' cements, some of which is radiaxial fibrous in nature (above), particularly close to the substrate. Much of the cement is, however, reminiscent of the 'coconut-meat' fabric (below), described by Folk & Assereto (1976). Photomicrograph xpolars.

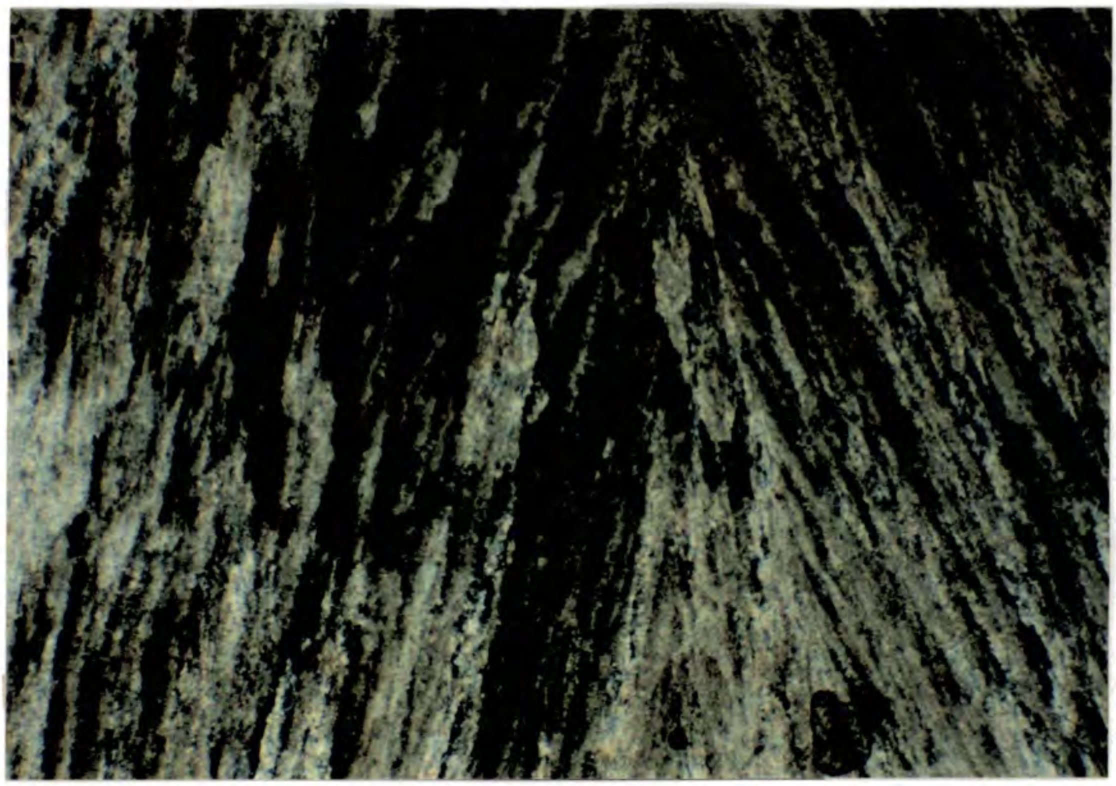

Figure 6.7b .

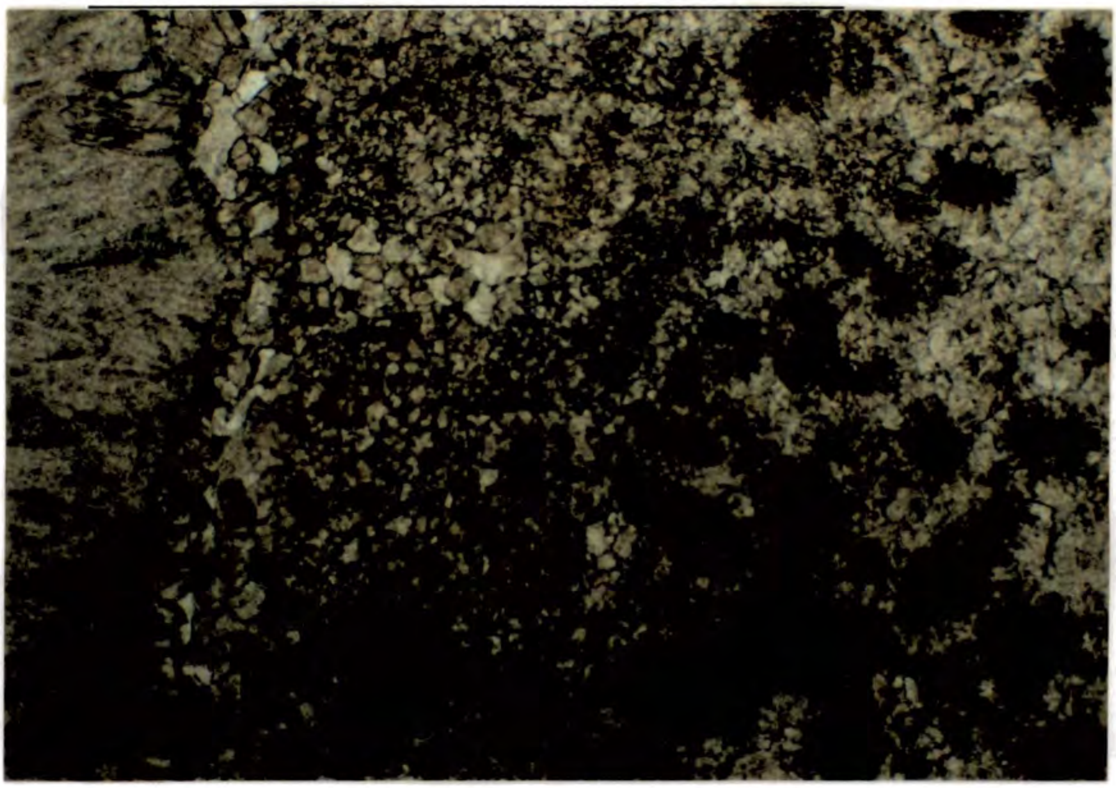

Figure 6.8 Fore-reef sample showing the junction of the substrate and the 'Großoolith' cement. The surface of the substrate is pervasively dolomitised, some ghost bioclasts can be seen.

Figure 6.9 Weathered surface of the 'Großoolith' cement. The zones (up to twelve) are clearly recognisable. Lighter zones contain more dolomite.

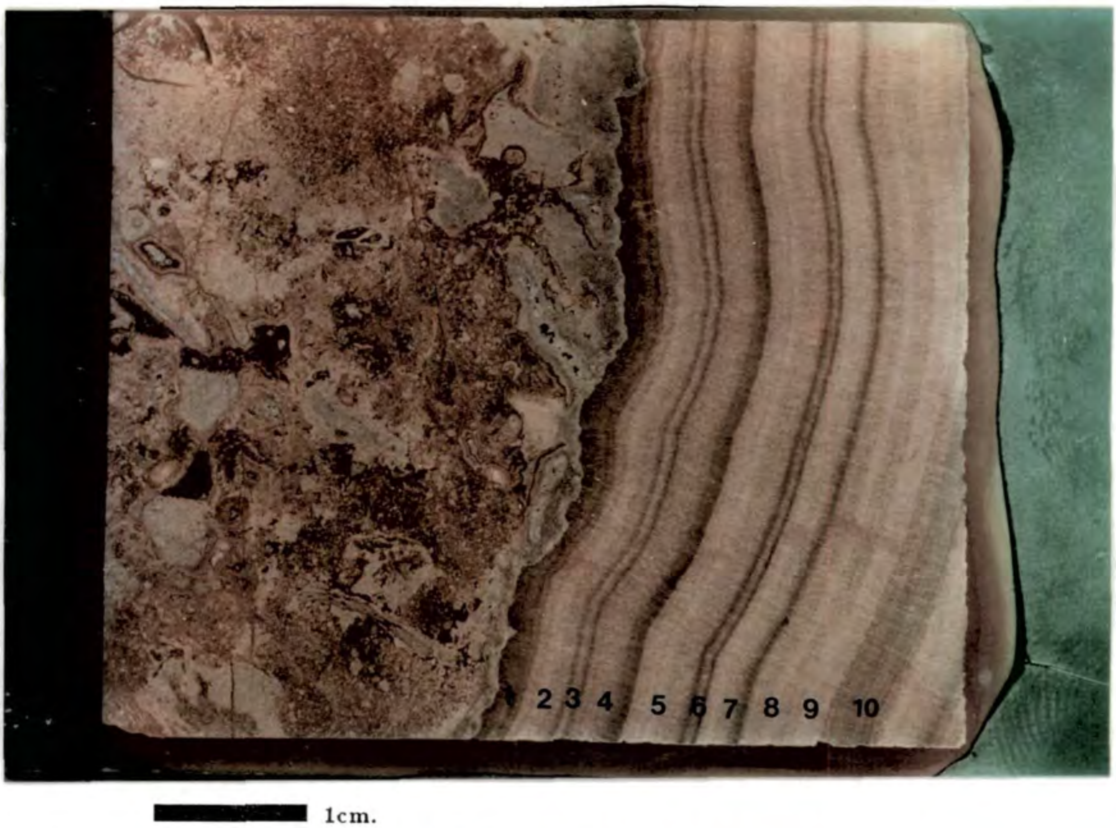

Figure 6.10a Layers numbered for comparison with lower photo.

Figure 6.10b Both samples are from the fore-reef, separated by several hundred metres. The upper photo shows a large ARS stained thin section. The zones are easily correlated between the two samples.

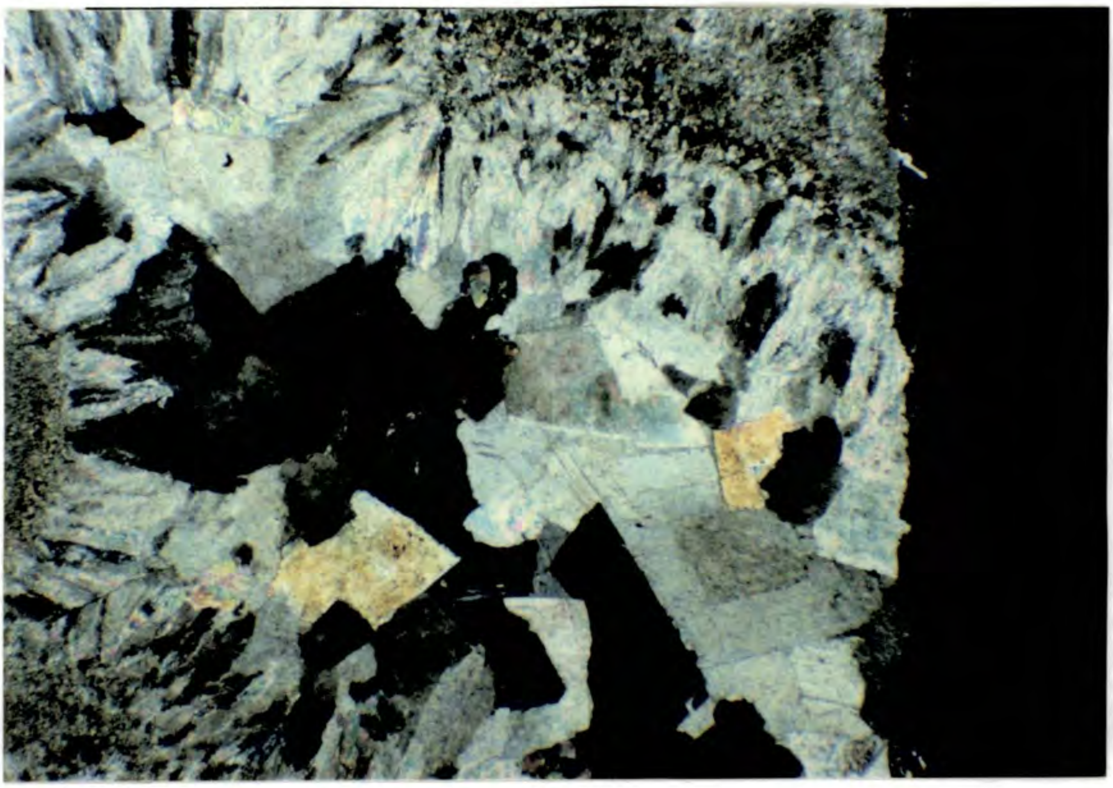

Figure 6.11a Dolospar filling cavity within the fore-reef material. Some crystals of dolomite exhibit curved edges and sweeping extinction characteristic of baroque dolomite. Photomicrograph xpolars.

Figure 6.11b Close-up of above showing euhedral dolomite crystal with inclusion rich centre and limpid rim. Photomicrograph ppl..

250μm.

Figure 6.11c Further example of late baroque dolomite from the fore-reef, sweeping extinction evident, and at least partly replacive in growth. ARS stain. Upper Photomicrograph ppl. , lower Photomicrograph xpolars.

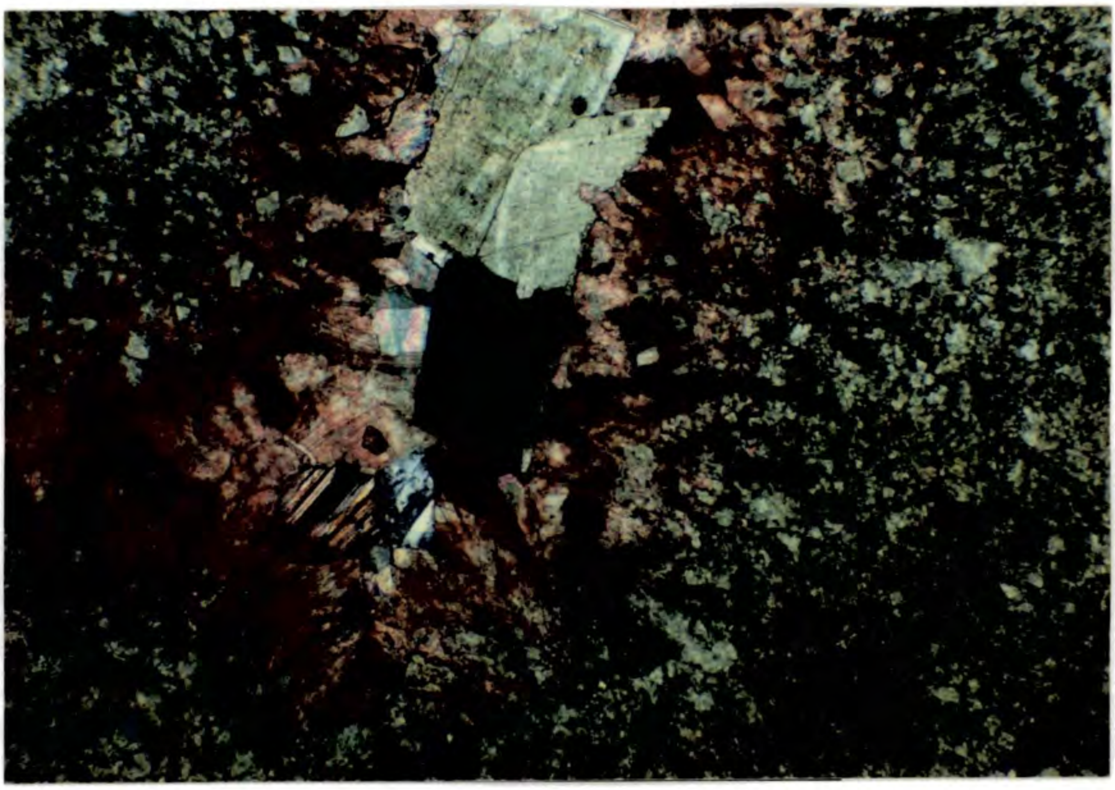

6.3.3 The initial stage of the Hafelekar reef.

The initial stage of the Hafelekar reef occurs on top of a block rubble sequence which is similar to the fore-reef material in derivation. The samples consist mainly of poorly sorted reef debris, the most characteristic diagenetic feature of which is the presence of layered fibrous cements similar to those observed in the fore-reef material (Figure 6.12). The fabric of the cements is also very similar; etching and staining reveals a variable content of dolomite in the layers in analogous fashion to the 'Großoolith' cements. The layers are not so clearly identifiable in thin section (Figure 6.13), but they are very apparent on the weathered surface of the rock. Individual zones are not identical in thickness to the fore-reef examples, such that they can only be broadly correlated. Up to 10 separate zones are present and these can be more accurately correlated between samples within the initial stages of the reef. The maximum thickness of the cements is 10–15 cm. The substrate is also dolomitised, again exhibiting the coarse surface replacement. The extent of dolomitisation in the core of the substrate is quite variable, possibly being related to initial permeability, with no particular selectivity being apparent.

The first zone of fibrous cement is again predominantly calcite, confirming that the layered cements present in the initial stages of the reef are the same phase as the 'Großoolith' cements. Another feature of the cementation observed in these samples is that some small cavities, which may have been primary growth framework in origin, are also cemented by a fibrous cement (Figure 6.12). This cement is petrographically identical to the 'Großoolith' cements, forming isopachous linings around the voids, with a maximum thickness of 1 cm. There is very little dolomite present in this phase, suggesting that it may have precipitated contemporaneously with the first layer of 'Großoolith' cement. Remaining primary porosity is commonly filled by an equant calcite spar cement, but no development of baroque dolomite has been observed in these samples.

There is clearly a close similarity in the diagenetic products present within the fore-reef and initial stages of the Hafelekar Reef. The differences in the thicknesses of cement zones can be explained on the basis of different permeabilities, the fore-reef having extremely high permeability, with fluids being delivered to the initial stages of the reef through the cavities of the block rubble on which it was initiated (Figure 6.2).

Figure 6.12a Sample from the initial stages of the Hafelekar reef showing the characteristic development of zoned fibrous cements.

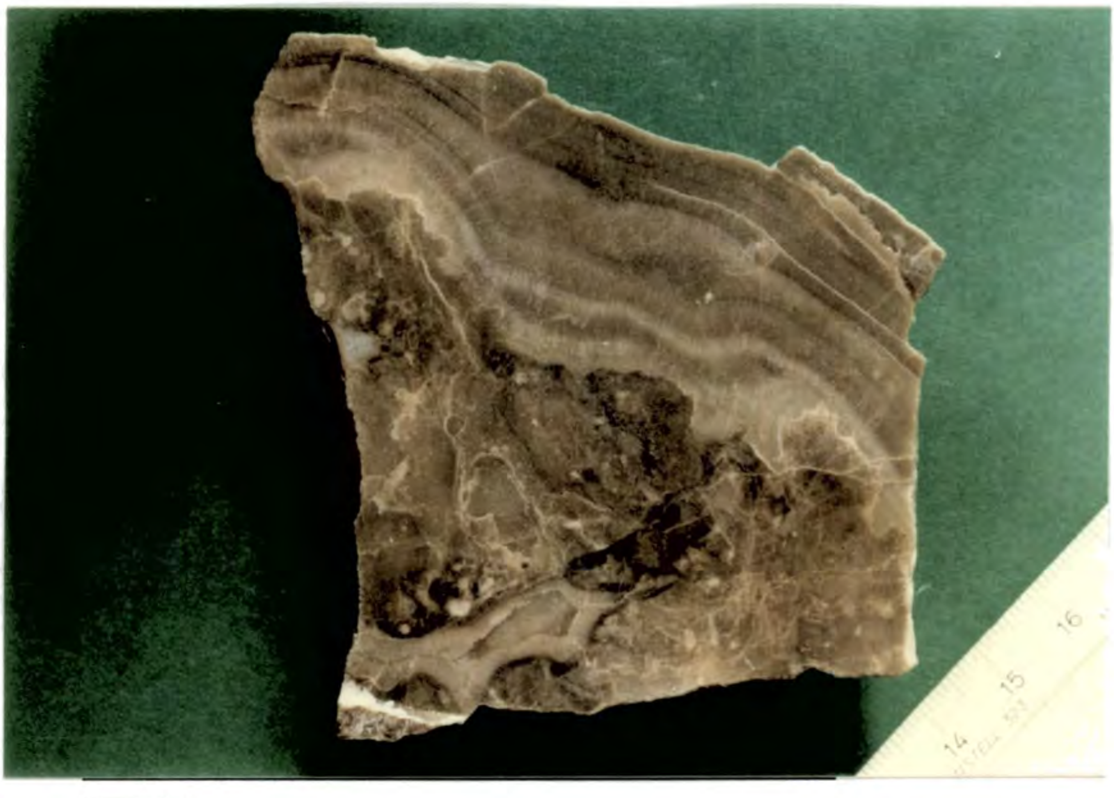

Figure 6.12b Sample from the same area, polished surface. Zoned cements evident at the top, with further thinner development of fibrous cement with framework growth (?) cavity.

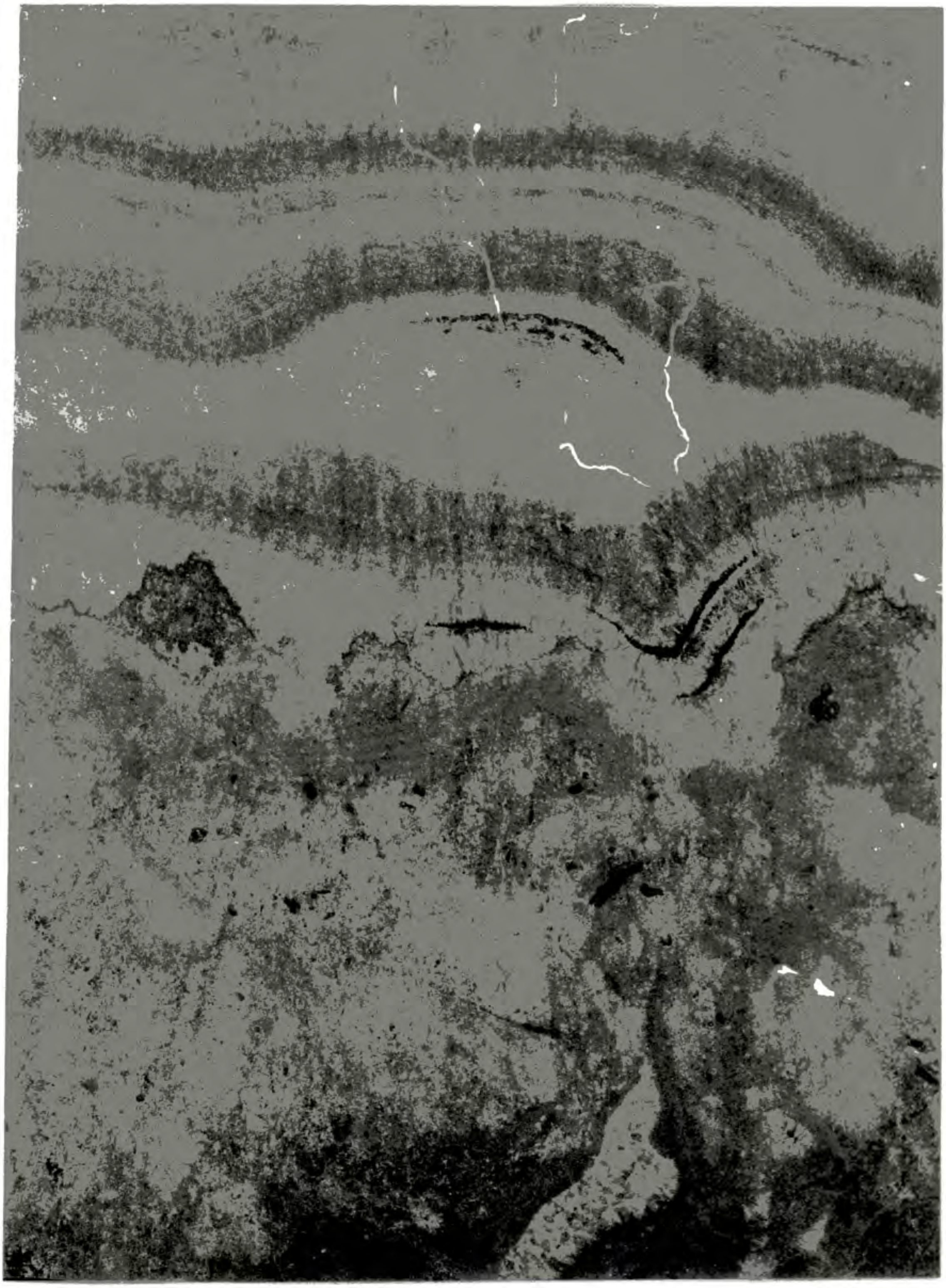

Figure 6.13 Negative print of thin section of the sample shown in Figure 6.12b. Surface of substrate shows lighter areas which are pervasively dolomitised. Further phase of fibrous cement within substrate at centre bottom of photo.

6.3.4 Back-reef.

The back-reef samples consist of well cemented grainstones and packstones, the cements being fibrous and again forming isopachous coatings indicative of early marine origins. A very characteristic diagenetic feature is the presence of extended thin linear cavity fills of fibrous cement, the original cavities interpreted as sheet cracks (Figure 6.14). Somewhat later fractures, cross cutting the fibrous cement are also present, these being filled with a clear sparry calcite indicative of a later burial origin (Figure 6.15).

The sheet crack fibrous cements are typically 1cm. in thickness, reaching 4–5 cm. in some cases (Figure 6.16). Although the fibrous fabric itself is similar to the other cements from the fore-reef, the sheet crack cements are noticeably different in their appearance in thin section (Figure 6.15). The latter contain a high density of dark solid inclusions which form distinctly zoned layers, a feature that is apparently absent, or at least much more poorly developed in the 'Großoolith' cements of other facies. Staining and atomic absorption analyses (Appendix 6), indicate that there is very little dolomite in these cements, a fact which is of considerable significance. The substrate is also unaffected by dolomitisation.

The presence of the inclusions in these sheet crack cements which otherwise appear to be precipitated at the same time as the 'Großoolith', together with the fact that there is no dolomitisation, suggest that the former are marine cements which have escaped any major dissolution-reprecipitation events. Other fibrous cements described earlier might have been originally coeval, but suffered some dissolution process, possibly related to the dolomitisation, during which the inclusion density was decreased.

6.3.5 Reef flat.

The bedded grainstone and packstone facies of the back-reef passes laterally into more reef framework dominated material (Figure 6.17), and as some primary growth cavities appear, so does the partly dolomitised fibrous cement. The diagenetic texture appears to change quite abruptly; samples collected less than 30 metres from the sheet cracked material exhibit the pervasively dolomitised surface layer characteristic of the facies described in the two previous sections.

It would appear, therefore, that the dolomitisation events affected the reef core and fore-reef facies, leaving the back-reef sands essentially unaffected. This could have been due to the fact that the back-reef sands were very well cemented prior to the influx of dolomitising fluids. Thick isopachous fringes are evident around the bioclasts (Figure 6.18), and this extensive cementation would have substantially reduced the permeability of the grainstones, effectively sealing them from later dolomitising fluids. Although the same extent of cementation might have occurred in the reef core facies, the growth framework porosity may not have been totally occluded, such that the permeability of the reef core may have remained at a higher level than that of the back-reef.

Figure 6.14 Back-reef grainstone packstone sample, with fibrous cement developed at the top in what have been interpreted to be sheet cracks. The dark layer contains some algal (?) laminae close to the surface of the sediment, but is otherwise a cement phase. Later fractures cross cutting substrate and cement.

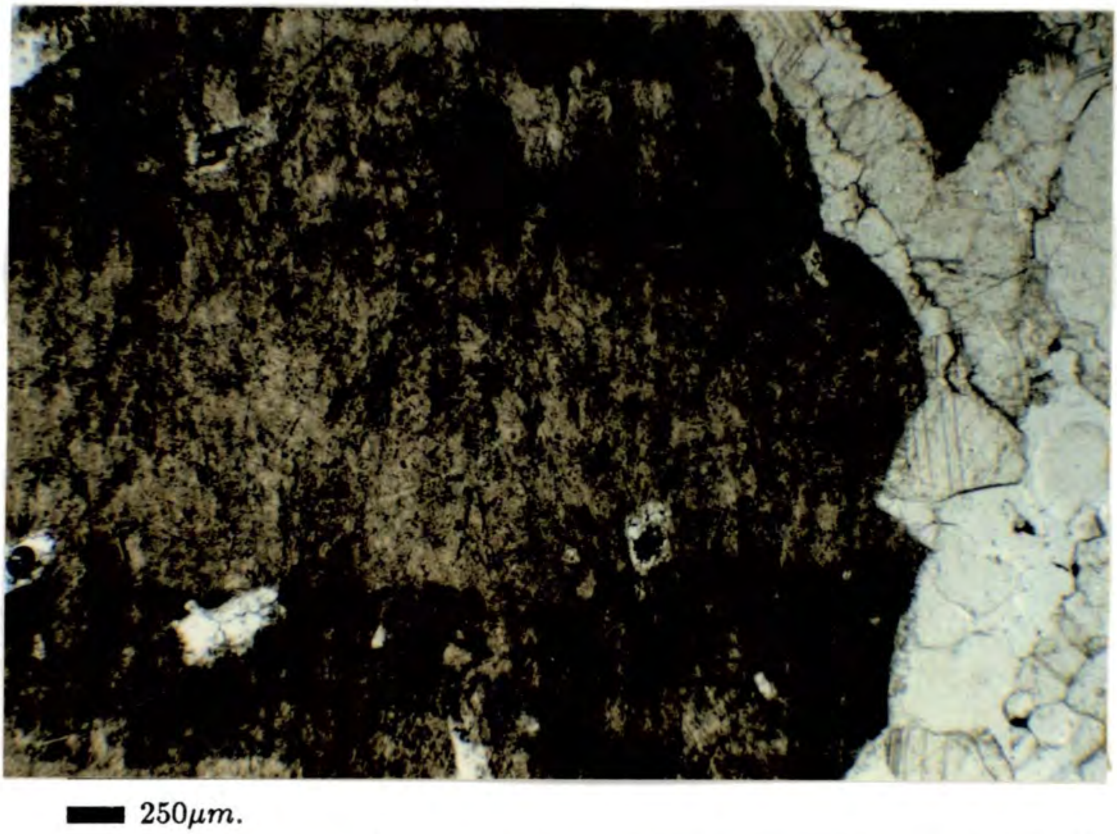

Figure 6.15 Thin section photo of above sample. The fibrous calcite contains a much higher density of inclusions than the fore-reef fibrous cements. Clear fracture filling spar with no sediment clasts indicative of later burial origin.

Figure 6.15 Negative print of a thin section of the back-reef sample shown in Figures 6.14 & 6.15. Substrate clearly very well lithified, with a variety of algal and mollusc fauna.

1cm.

Figure 6.16 Sample showing thick development of fibrous cement in a sheet crack. Characteristic dark layer also evident.

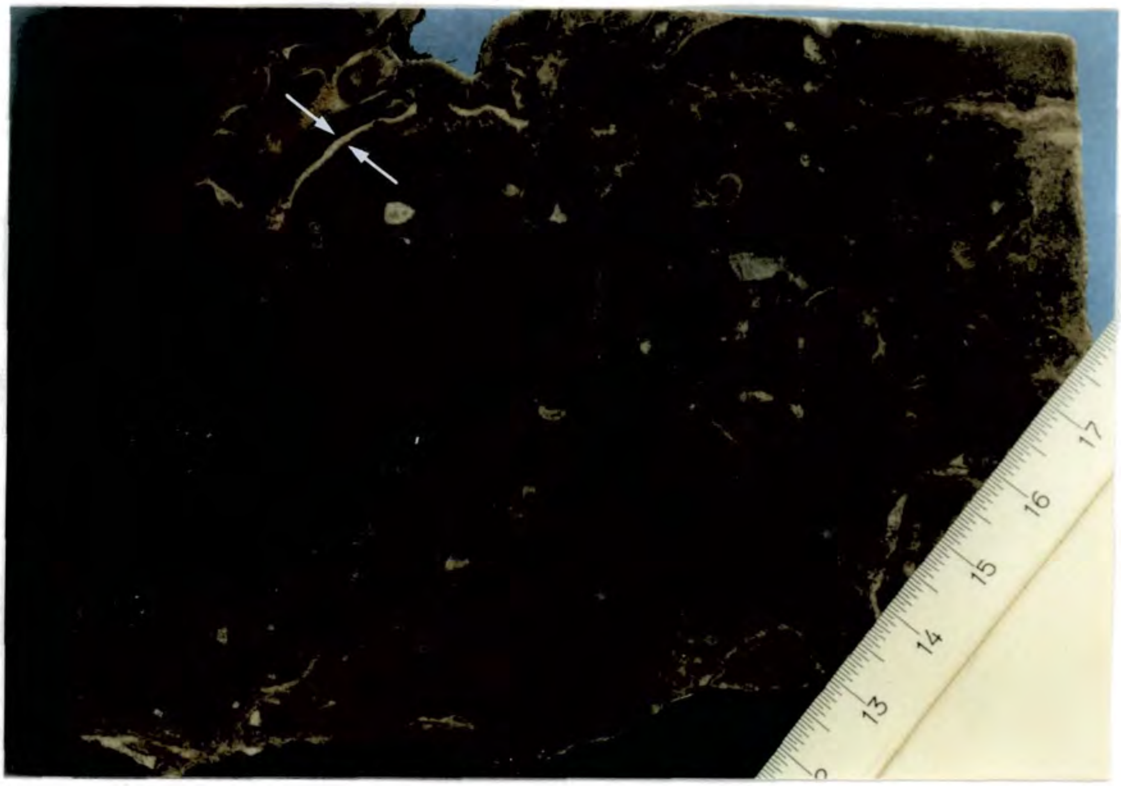

1cm.

Figure 6.17 Sample from the reef flat area. Some primary or possibly secondary dissolution porosity infilled by a fibrous cement. Pervasively dolomitised surface layer also evident.

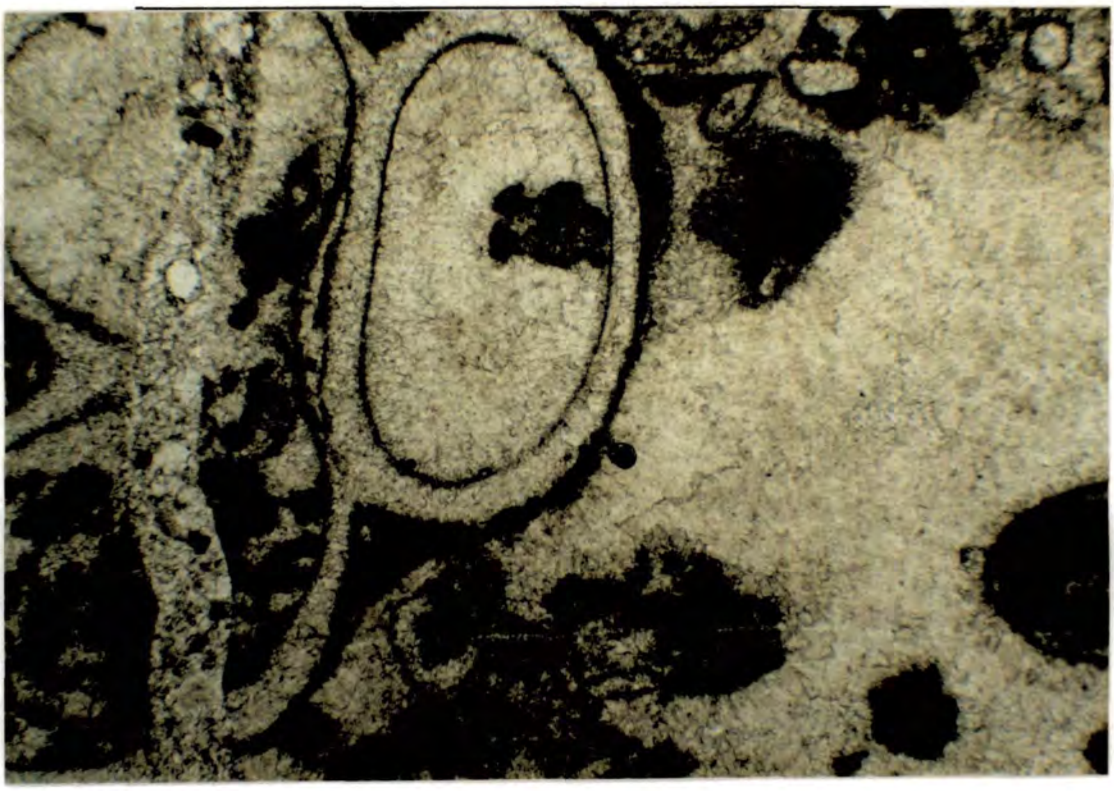

250μm.

Figure 6.18 Back-reef sample shown both in ppl. and under xpolars. Extensive lithification by isopachous fibrous marine cements. Mollusc fragment cut by later fracture.

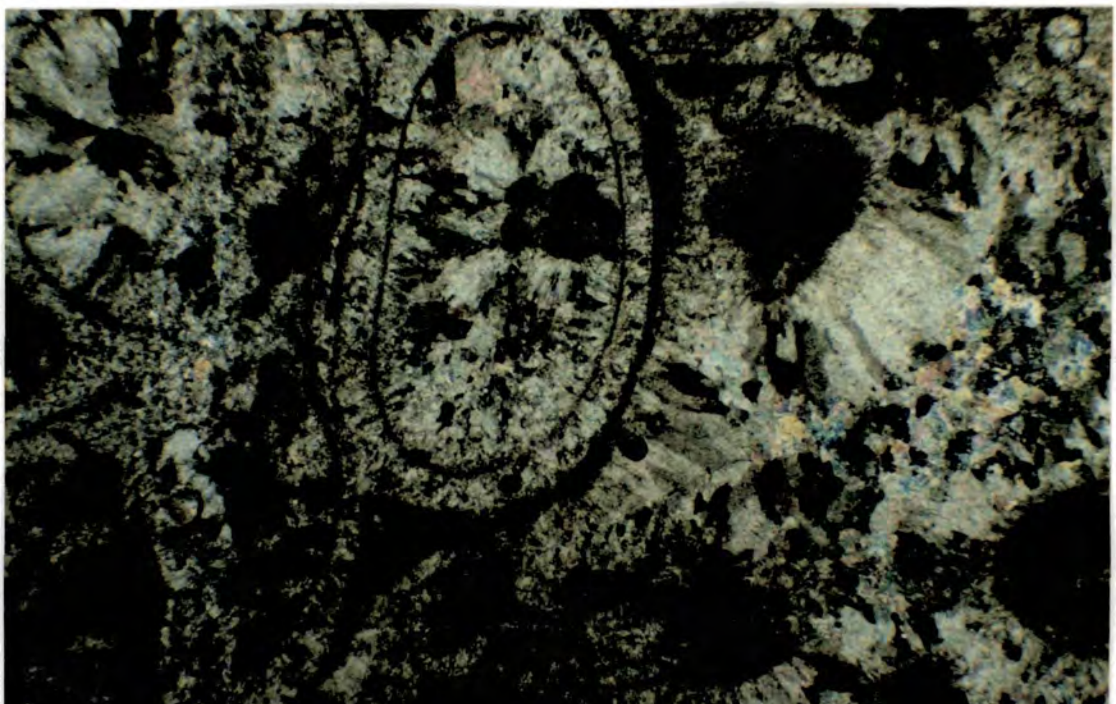

6.3.6 Reef core.

The major diagenetic feature of the reef core is again the precipitation of a single zone of fibrous cement whose petrographic characteristics are identical to similar cements in the reef flat described above and to those in the initial stages of the reef. This cement is commonly pore filling and the development of compromise boundaries is apparent (Figure 6.19). Some slight zonation is apparent due to a low content of euhedral dolomite and the cements are relatively inclusion free. The thickness of the cements can be up to 2 cm. in larger reef framework cavities or in voids between reef debris. The reef debris is predominantly formed of grainstones and packstones which were clearly lithified at an extremely early stage, as the major phase of cement cross-cuts earlier isopachous inter-particle marine cements (Figure 6.19). Remaining primary porosity is commonly filled by a late calcite spar (Figure 6.20).

Further evidence for the occurrence of a dolomitisation event prior to the precipitation of the fibrous cement is provided by the observation that the latter cross-cut dolomitised bioclasts (Figure 6.21), albeit only rarely. In addition, in some patchy areas of the reef core, the substrate can be seen to be pervasively dolomitised, with coarse anhedral dolomite preserving very little primary fabric. Within the cavities of this are fibrous cements which are predominantly calcite. Irrespective of the differences in original mineralogy and the possibility of selective dolomitisation, it is difficult to conceive of a mechanism which could entirely replace the substrate leaving the cement relatively unaffected. One possibility might be due to differences in the texture, with the very coarse grained nature of the fibrous cement making it less susceptible to dolomitisation compared with the fine-grained texture of the sediments.

Some samples show evidence of a phase of dissolution, presumably by meteoric water, which may be linked with the dolomitisation event described above. Although the evidence is not abundantly clear, there are examples of cross cutting fabrics which do not seem likely to have been created by a simple reworking of lithified material (Figure 6.22). In addition, there are some bioclasts whose outline is preserved by micritic rims, but which appear to have been replaced by a neomorphic spar (Figure 6.23). These were probably originally aragonite skeletal fragments, and although the texture is typical of alteration in a meteoric fluid, it is possible that the dissolution could have occurred at depth in water of marine origin (Tucker, 1985; Saller, 1986). Other areas of the reef core are dominated by frame building but rather delicate branching corals, the interstices of which are filled by medium to well sorted grainstones (Figure 6.24). The primary cavities are again filled by the fibrous calcite cements (Figure 6.25) and dolomitisation of the corals and grainstones is also apparent. The timing of the dolomitisation is particularly difficult to determine in these samples, being very inhomogeneous in distribution. There is no internal structure apparent in the corals, and the degree of alteration to dolomite varies from being virtually non-existent to total replacement by a coarse dolospar (Figure 6.26). In some sections, the outer rim of the corallite remains predominantly calcite, with euhedral dolomite filling the rest of the intra-skeletal cavity. Some presumably later baroque dolomite is also present in the centre of the cavities. There is evidence for the original presence of fibrous cement fringes in the intra-skeletal cavities (Figure 6.26).

Larger cavities show some development of the layered fibrous cements similar to the fore-reef 'Großoolith' (Figure 6.27). These layers cannot be correlated between the two facies, but are similar within the central reef area. These are petrographically identical to the previously described 'Großoolith' cements.

Figure 6.19 Fibrous cements in the reef core facies. Some of the cavities may be primary growth framework in origin, but the apparent weathering out of some clasts (arrow); the shape of the debris pieces and some cross cutting of clasts suggests that some porosity may be of secondary dissolution origin.

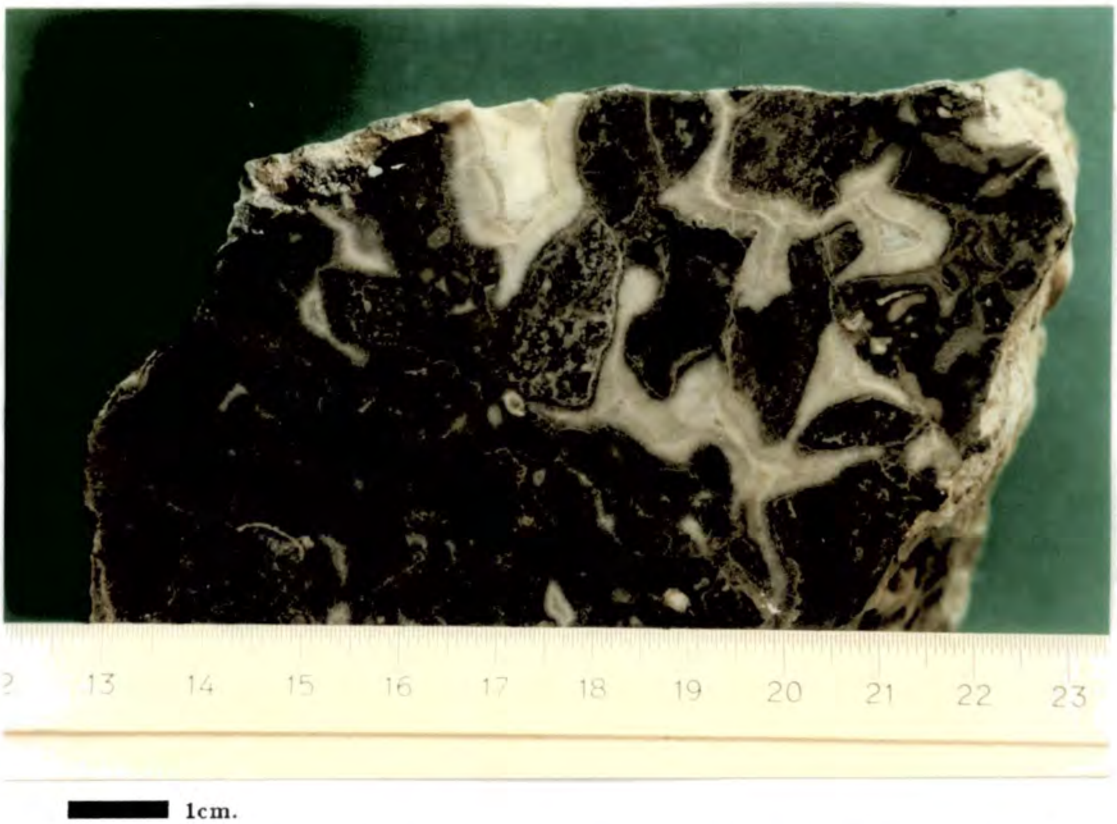

Figure 6.20 Reef core facies, with fibrous cements showing some compromise boundaries. Later pore-filling spar evident at the top of the photograph.

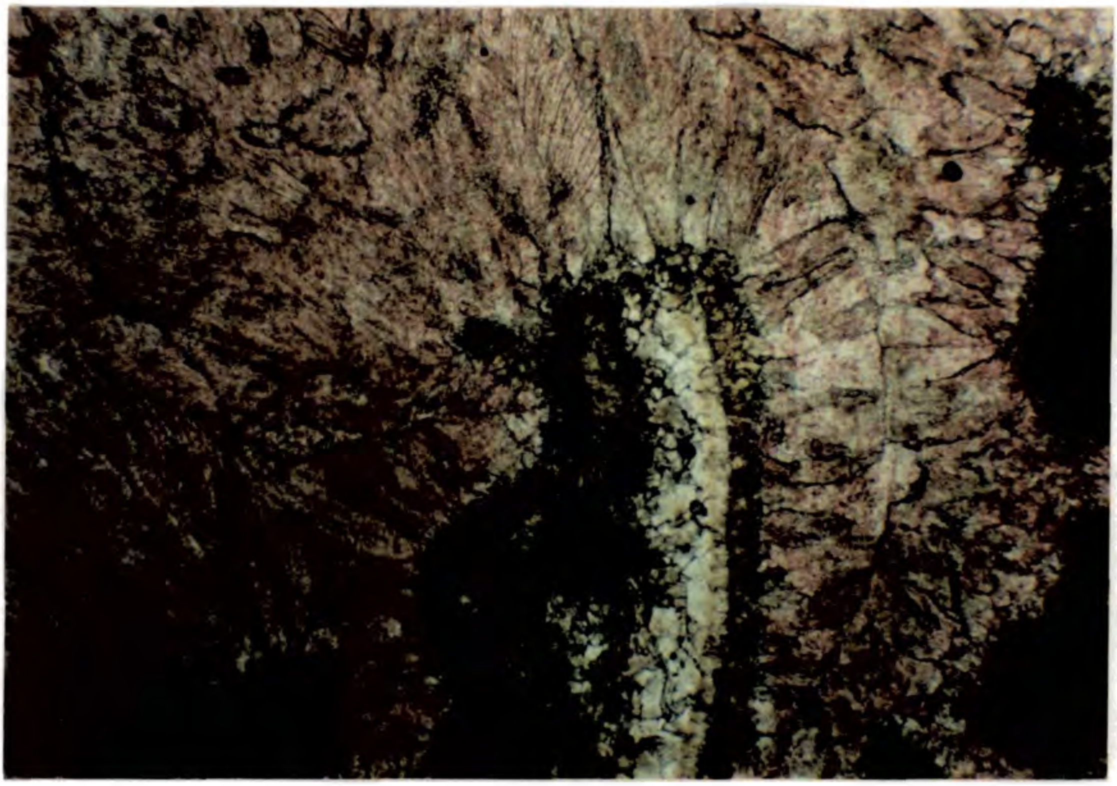

Figure 6.21 Sample again from the reef core showing evidence of a dolomitisation event prior to the precipitation of the fibrous calcite spar (stained red). The dolomitised bioclast is clearly cross cut by the cement which is predominantly calcite. Photomicrograph ppl..

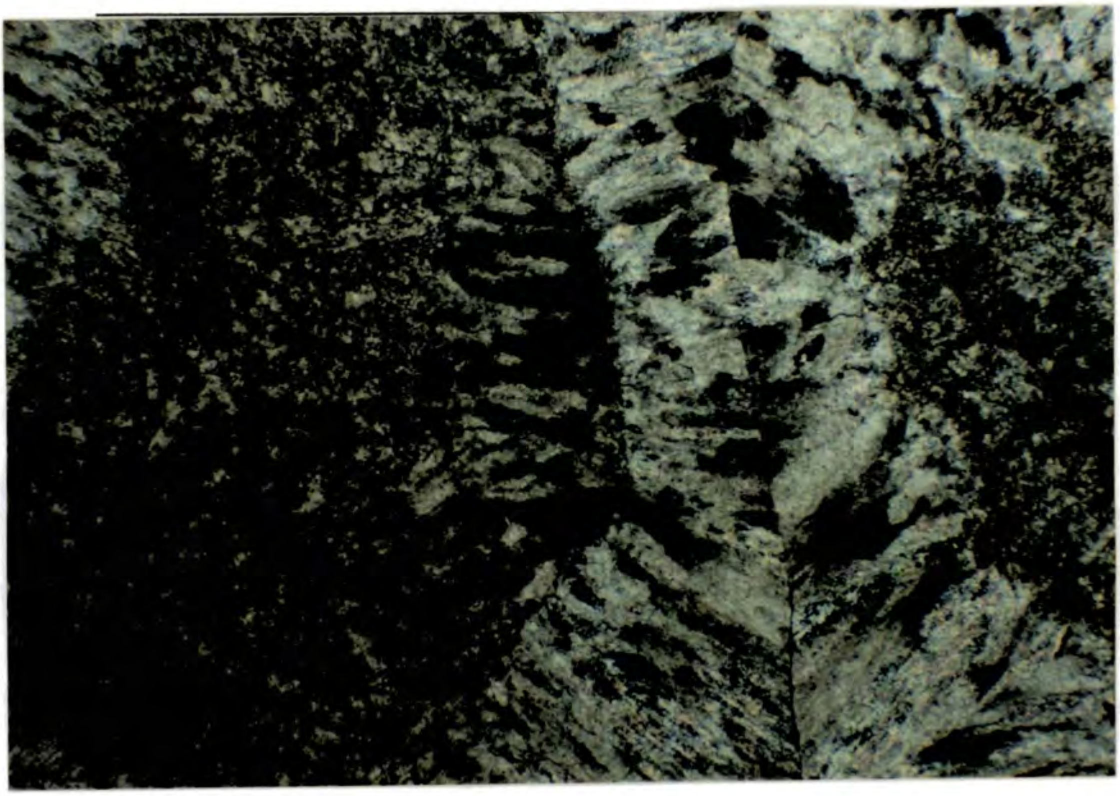

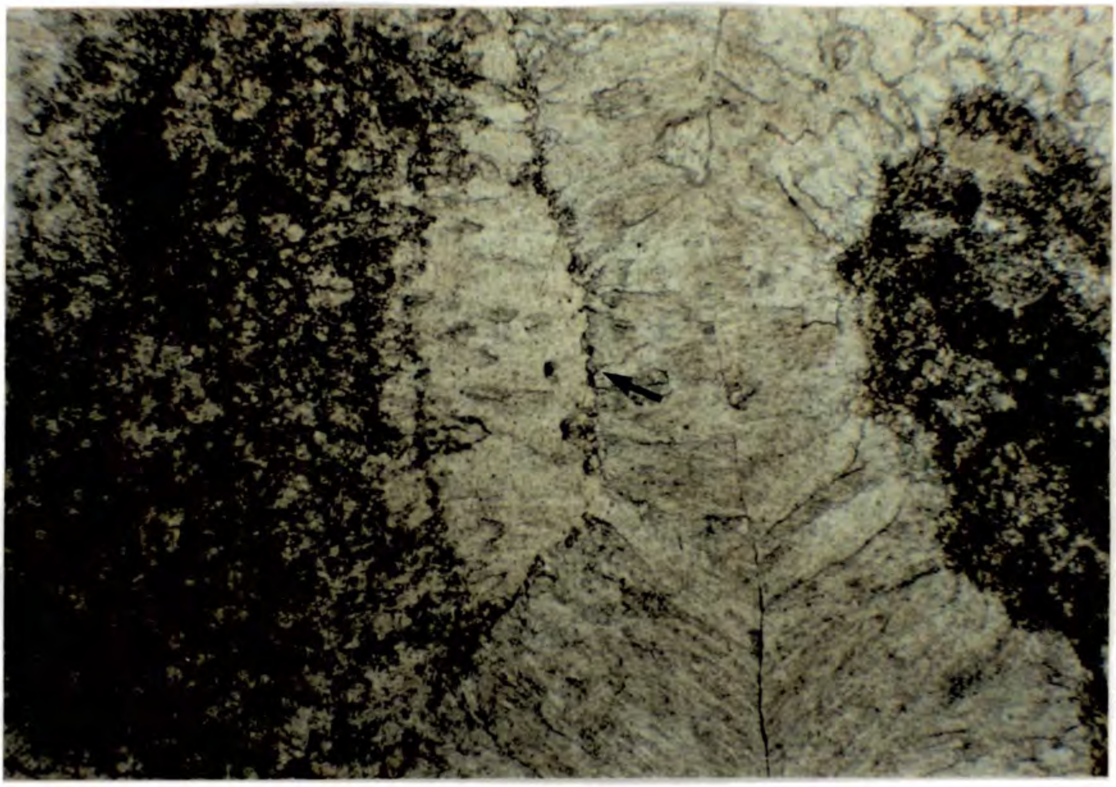

250μm.

Figure 6.22 Evidence in these photomicrographs for some dissolution porosity infilled by later fibrous cement. The substrate at the edges of the photographs are well cemented and a 300μm. layer of early fibrous calcite is evident (arrow). This appears to be cross-cut by a later cement, slightly lighter in colour in the upper photo. The surface of the earlier cement has features suggestive of dissolution.

Figure 6.23 Spar filled bioclast, reef core, the shape preserved by micrite rims. Probably originally aragonite, neomorphosed to calcite by meteoric fluids. Photomicrograph xpolars.

Figure 6.24 Reef core coral sample, exhibiting variation in the replacement textures. Some branches are predominantly calcite, with others replaced by a coarse white dolospar.

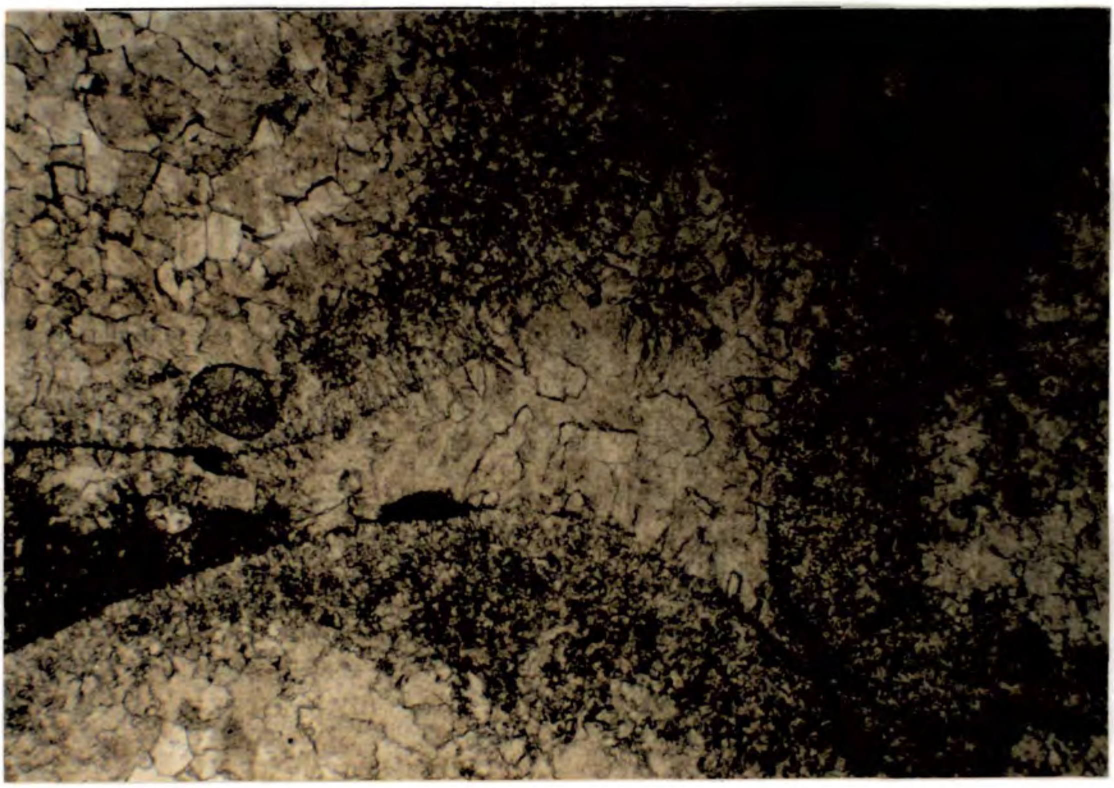

Figure 6.25 Reef core coral sample with fibrous cement in inter-skeletal porosity.

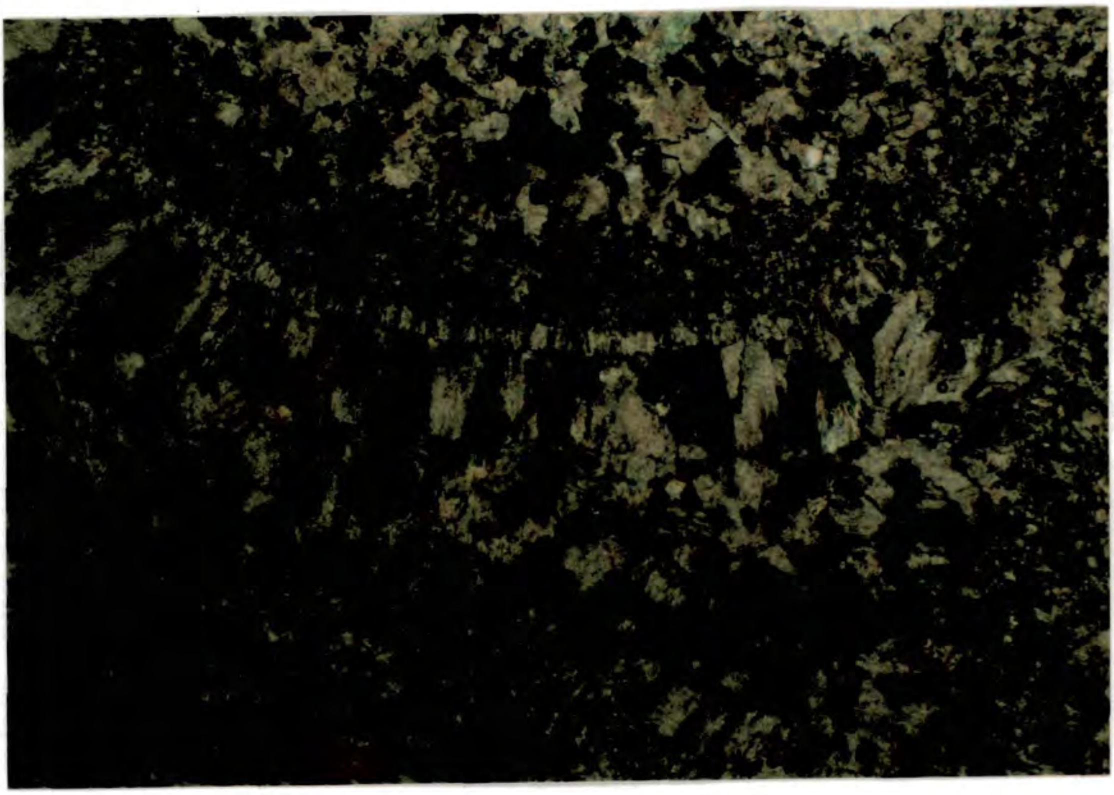

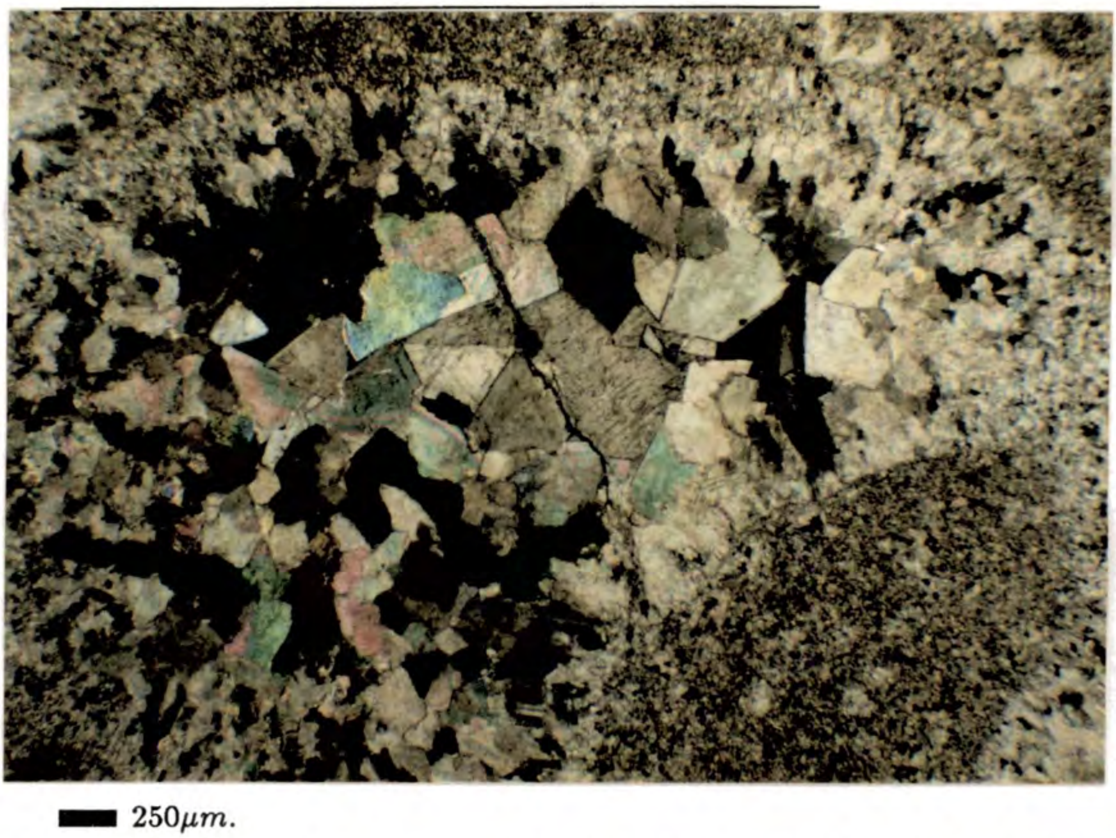

Figure 6.26 Reef core coral, same specimen as in Figure 6.25. Here the intra-skeletal cavity is now formed of a coarse dolospar, with some possibly later calcite in the centre of the cavity. The upper photograph shows evidence of an early fibrous isopachous fringe cement. Upper Photomicrograph xpolars , lower Photomicrograph ppl. , stained with ARS.

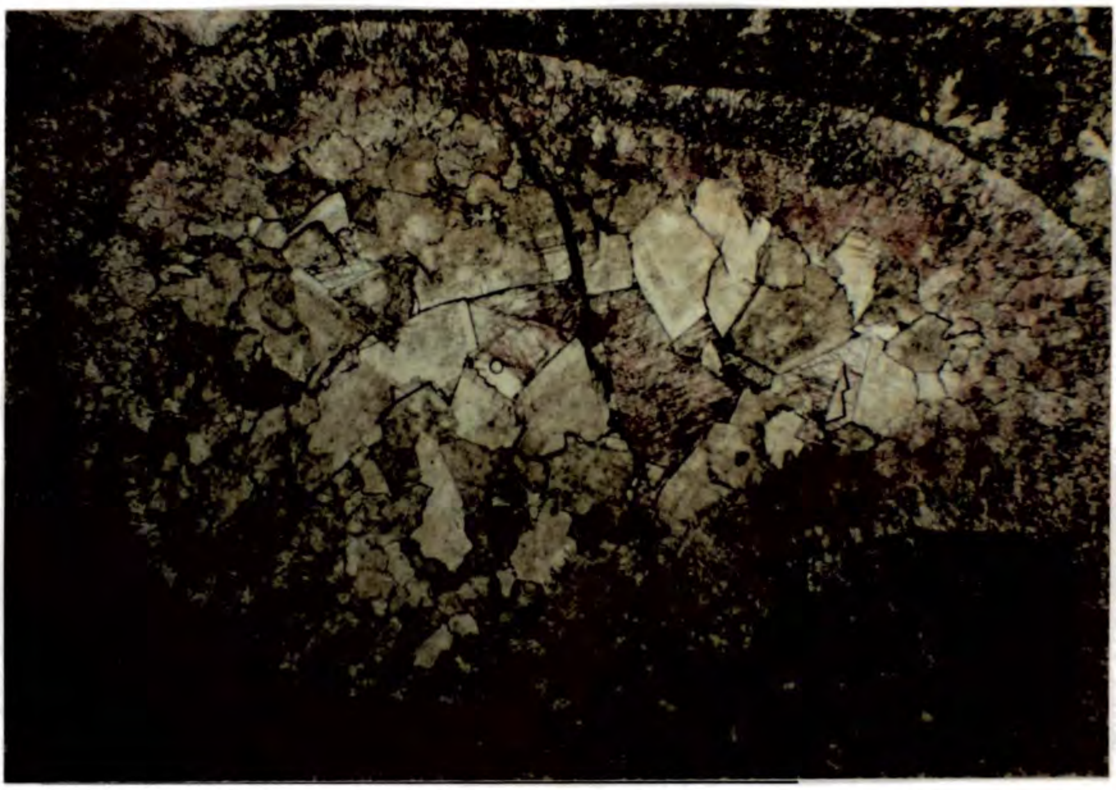

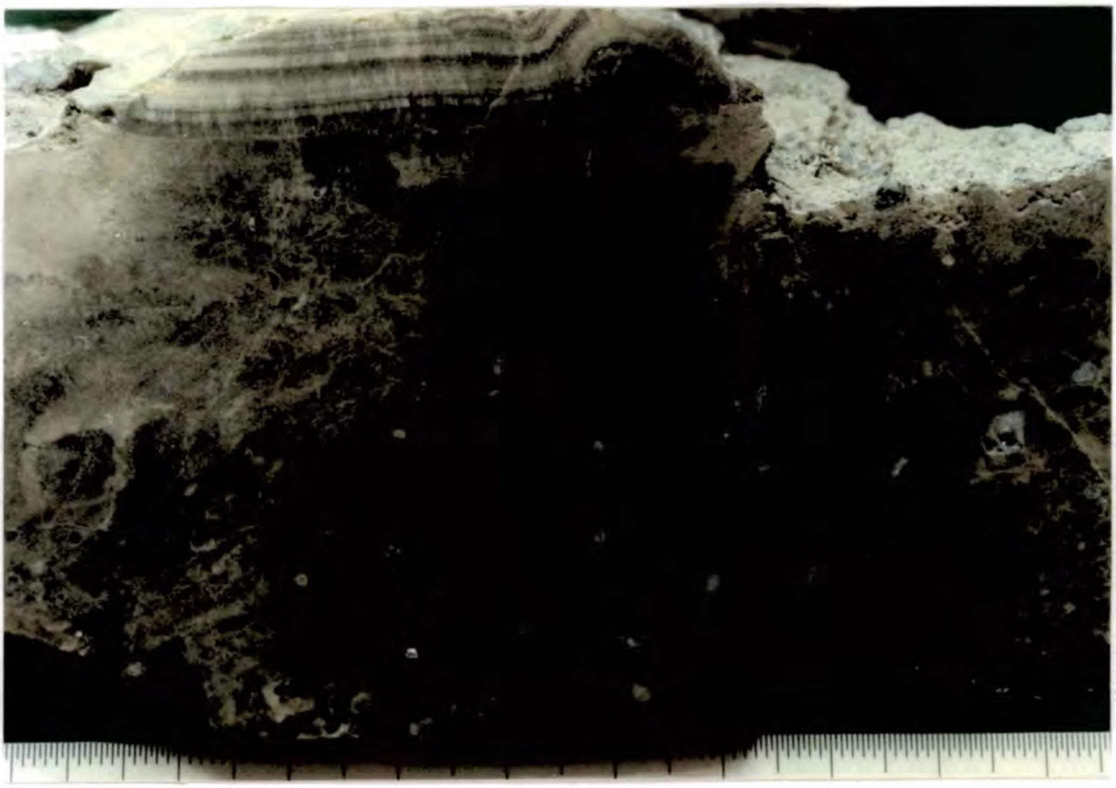

1cm.

Figure 6.27 Reef core sample in hand specimen. Zoned fibrous cements similar to the 'Großoolith' are developed (at the top of the photograph).

6.3.7 Eastern edge.

The reef complex wedges out to the east, where it interfingers with the reef rubble of the underlying Goetheweg reef. The development of marine cements in these samples is very similar to that previously described, some samples containing pore lining and pore filling 1–2 cm. thick fibrous calcite (Figure 6.28), with others showing the characteristic development of 'Großoolith' cements up to 15 cm. in thickness (Figure 6.29). The latter show dolomitisation fabrics similar to those observed in the fore-reef, with dolomite percentages being more uniform, averaging 45%. The former non-layered fibrous cement generally contains somewhat more dolomite than similar examples from other areas, up to 15%. The substrates are also typically quite extensively dolomitised, particularly at the surfaces, the latter being a similar characteristic to that previously identified in the fore-reef and initial stage samples.

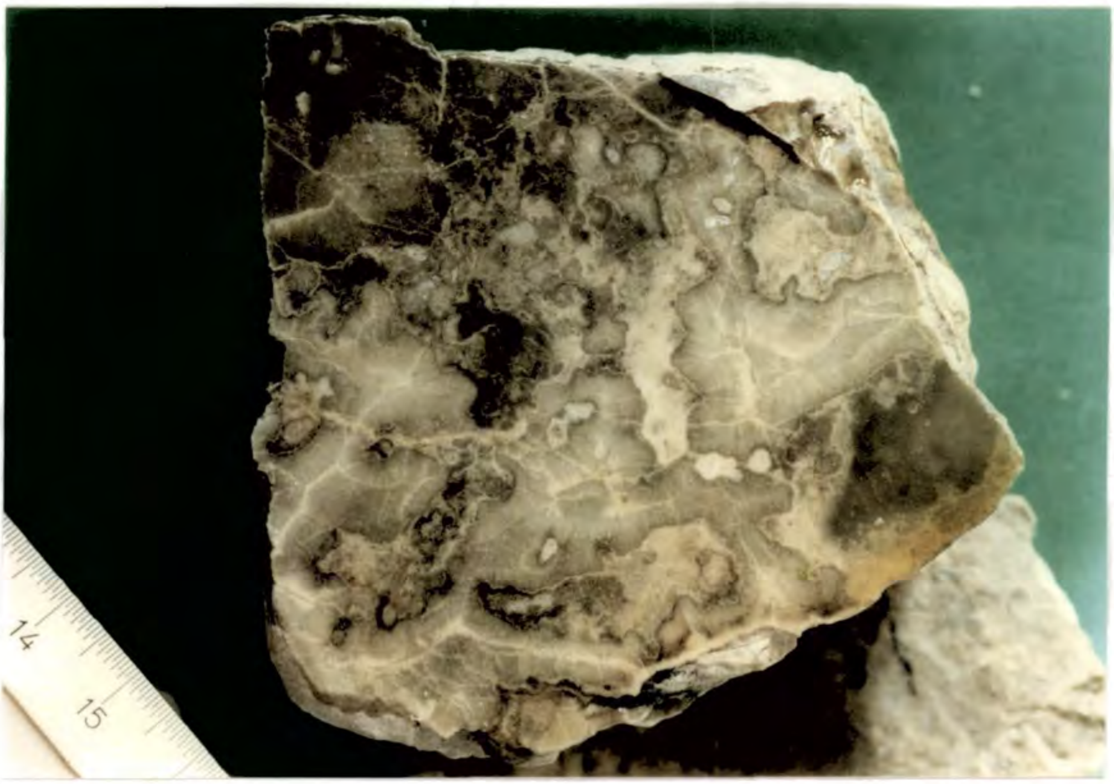

1cm.

Figure 6.28 Sample from the eastern edge of the reef complex, with well developed single zoned fibrous cements similar to those recognised from the reef core, reef flat and initial stages.

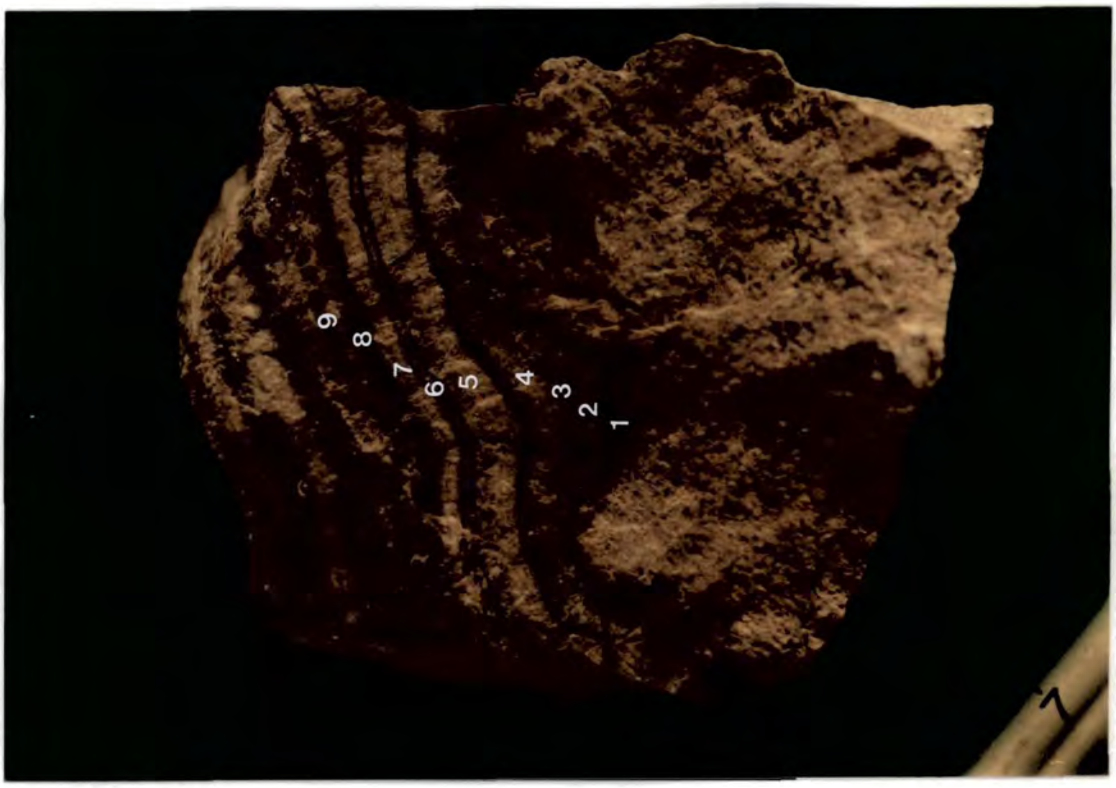

1cm.

Figure 6.29 Sample again from the eastern edge of the reef, with thick development of 'Großoolith' -type cements. Some zones can be correlated with zones from the fore-reef (Compare the numbers with Figure 6.10).

6.3.8 Spatial distribution of the cementation.

The major volumetric feature of the marine cementation is the precipitation of the decimetre thick 'Großoolith' cements. These are most important in the fore-reef breccia, throughout which the individual layers can be closely correlated. The whole sequence of up to 12 separate zones forms up to 50% of the total rock at even the outcrop scale, clearly effecting a massive reduction in porosity and permeability of the fore-reef material. This 'Großoolith' cement is present in other reef facies, recognisable by the thick development and the variation in the dolomite content of the layers. The observed zonation cannot usually be correlated exactly with the material in the fore-reef, the thicknesses of the individual layers being quite variable. This variability is likely to have been caused by variations in the permeability of the substrates, the latter hypothesis being suggested from the results of the modelling presented in the previous chapter. The layers can usually be correlated rather well within particular reef facies, individual zones typically being recognisable over several tens of metres.

Großoolith cements are present in the initial stages of the reef and in the block rubble on which it was founded, suggesting that the circulation of the fluids through the Goetheweg reef debris was quite extensive. The same cements are also developed in the reef flat and the reef core, though generally to a lesser extent than in the higher permeability coarse reef rubble. No such development is observed in the back-reef facies, principally due to the lack of large voids and cavities in which it could have formed.

It is apparent, therefore, that the 'Großoolith' type fibrous cements are distributed quite extensively throughout the reef framework, wherever there were large primary growth cavities, fractures or rudstone debris. The lateral distribution is also quite high, thick similarly zoned fibrous cements being recognised at the eastern edge of the reef complex. The latter can be directly correlated to the zones in the fore-reef deposits (Figures 6.10 & 6.29).

The other major early cement is also a fibrous calcite, which is generally of one zone only and characteristically is predominantly calcite. Thickness of the cement is usually 0.5–2 cm. and it forms an isopachous lining of primary cavities. This cement phase has been recognised throughout the Hafelekar Reef, being identified in samples from the initial stages, the reef core and the reef flat, as well as in samples from the eastern extremities of the complex.

The low dolomite content and the otherwise identical petrographic features, suggest that this phase may be contemporaneous with the first layer of the 'Großoolith' cement, although this relationship cannot be proven from the petrography alone. Both phases appear to be precipitated after a dolomitisation event. This fibrous cement accounts for at least 90% of the porosity that would have been present before its precipitation and as such represents by far the most significant porosity reducing event.

The back-reef facies appears to be differentiated from the rest of the reef in that it has not been dolomitised to any significant extent. The development of a fibrous cement in cavities that have been interpreted as sheet cracks, is similar to the other fibrous cements in the reef itself, but has a noticeably higher density of inclusions. It may be that this cement was in fact of similar origin to the reef cements, but has suffered less later diagenetic alteration, such that the texture appears slightly differentiated. This inclusion-rich fibrous calcite is restricted to the back-reef facies only.

The final phase of cementation is represented by the presence of a late spar which is of minimal volumetric significance, but tends to seal any remaining interconnected primary porosity. The spar is most frequently observed in cavities left open after the precipitation of the single zoned fibrous calcite, but also occurs within the substrate itself. It is quite widely distributed, however, being present in all facies described above. This is commonly followed or perhaps replaced by euhedral crystals of baroque dolomite, the latter often exhibiting inclusion rich cores and limpid edges. In some samples, it appears that there may have been a further pore occluding precipitate of calcite spar which is characteristically clear and may be related to the fracture filling spar observed in the back-reef grainstones. This final precipitate is of insignificant volume, having been identified in only one or two instances.

6.3.9 Summary and sequence of events.

The timing of the various diagenetic events, in particular the dolomitisation, is particularly difficult to demonstrate conclusively due to the general lack of obvious cross cutting relationships. The following is a suggested sequence of events which is by no means definitive; the problems are discussed further after the geochemical evidence has been examined.

It is clear that the majority of the reef material, particularly the interstitial sands were well lithified prior to the precipitation of the major fibrous cements described in detail above. Much of the material in the reef core consists of clasts of reef debris formed of medium to well sorted sands. These grainstones are cemented by an isopachous marine cement which is cross cut by the single zoned fibrous calcite. The size of the intra-particle pores in the carbonate sands is too small to allow identification of the fabric of the cement, and it is not certain that all of the interparticle pore space was occluded prior to the precipitation of the major phases of fibrous cements.

The fibrous calcite rarely cross-cuts dolomitised bioclasts (Figure 6.21), but the several occurrences suggest that there was a prior dolomitisation event. There is some evidence to suggest that this was linked to a period of exposure to meteoric fluids. Some areas of the reef core and samples from the eastern edge of the reef complex exhibit pervasively dolomitised substrates with fibrous cements preserved as more than 90% calcite, a fact which would be very difficult to explain if the dolomitisation occurred after the precipitation of the cement. Many samples have been studied in which the fibrous single zone cement and / or the first zone of the 'Großoolith' cement are nucleated on a substrate whose surface is pervasively dolomitised to a depth of 1–2 mm. In these examples, the dolomite in the surface is formed of anhedral crystals which all but destroy the primary fabric of the substrate. Below this surface the substrate may still contain a substantial amount of dolomite, but the latter is commonly fabric retentive. The fact that the substrate is dolomitised, leaving the fibrous cement immediately adjacent virtually unaffected, suggests that the cement was precipitated after dolomitisation. The later zones of the fibrous 'Großoolith' cements are commonly dolomitised also, but this dolomite has a quite different form from that described above. The euhedral crystals are smaller than the former dolomite, with well developed rhombic faces. This phase is similar to the dolomite in the core of the substrates, the latter exhibiting some fabric selectivity possibly dependent on the original mineralogy of the clast being replaced. This selectivity on the basis of mineralogy may also explain the zoning in the 'Großoolith' cements, dolomitisation occurring preferentially in the Mg-rich layers.

At some time after the precipitation of the fibrous cements, there was a phase of calcite spar precipitation, forming less than 10% of the total volume of cements. A minor phase of precipitation of baroque dolomite then occurred, indicative of temperatures above 60 °C (Radke & Mathis, 1980). The latter appears to occur both as a replacive feature and as a cement, and may be followed by a final pore filling calcite spar. This final phase of cement could be that which fills late fractures in the back-reef grainstones, but it is limited to so few occurrences that interpretation is extremely tenuous.

6.4 Stable Carbon and Oxygen Isotopic Composition of the Cements.

6.4.1 Introduction.

The isotopic compositions of a variety of cements from the Hafelekar Reef Complex were measured in the hope that the data would help to evaluate both the spatial distribution of individual cement phases and the effects of other diagenetic events. It was expected that the data might provide some further information on the likely sequence of events and the relative time scales over which these events operated. The data are presented in Appendix 6 and are represented in a graphical form on Figure 6.30. Preparation methods and correction procedures are also given in Appendix 6.

Many of the cements are mixtures of calcite and dolomite, and although the collection was carried out with great care, using tools developed for the isotopic studies discussed in Chapter 3, it was not possible to separate all of the samples into the constituent minerals. Previous experience with attempts to separate calcite and dolomite by heavy liquid techniques suggested that this method was unsuitable, and so it was decided to analyse the mixtures as they were collected. Some correction for the differing phosphoric acid fractionation factors was then applied on the basis of the dolomite content. A discussion of the likely errors is left to the Section dealing with the results (Section 6.4.4). The next Section discusses the problems involved in the interpretation of isotopic data from ancient limestones, and this is followed by a description of the samples analysed (Section 6.4.3). The results are interpreted in Sections 6.4.5 & 6.4.6.

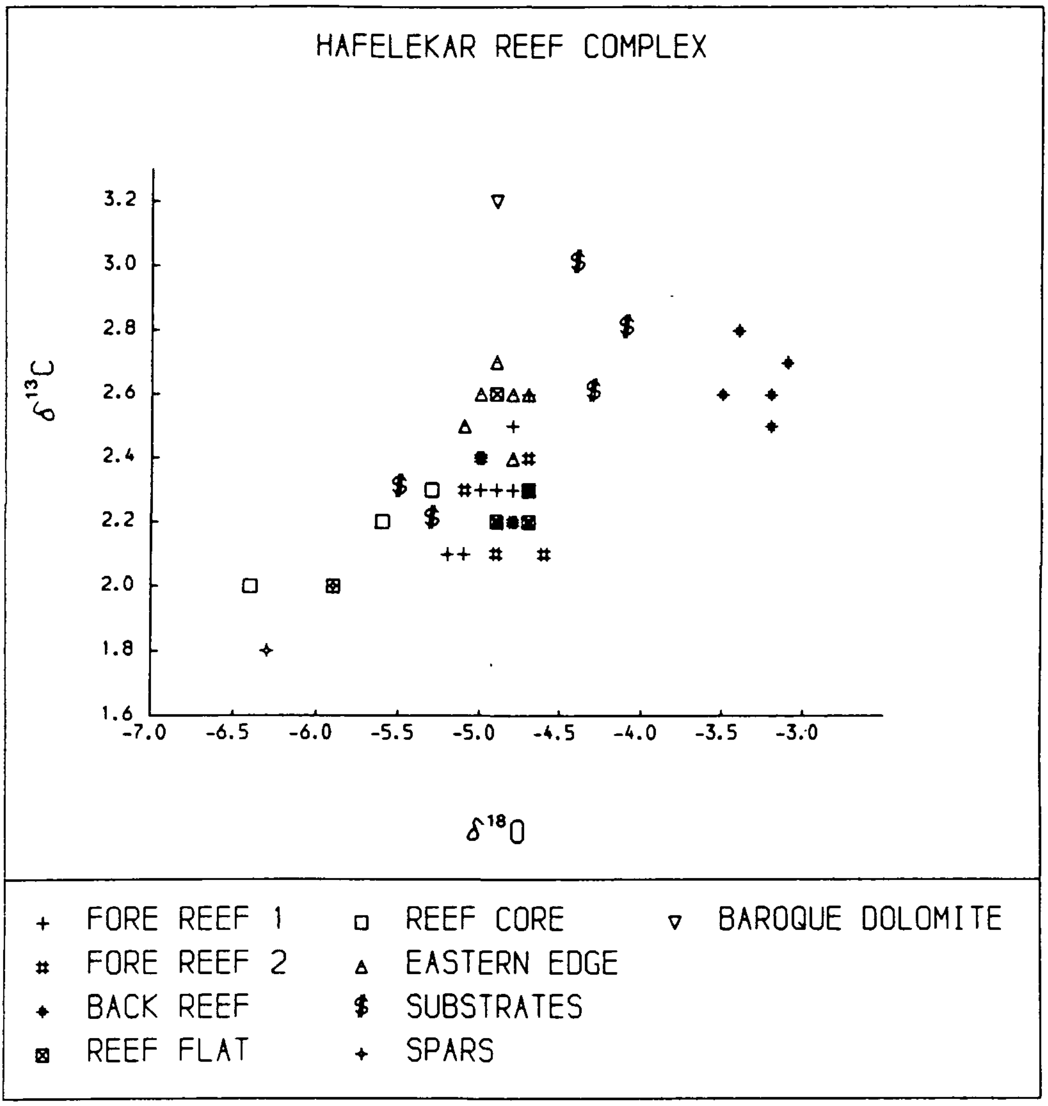

Figure 6.30 Crossplot of stable carbon and oxygen isotopic compositions of the Hafelekar Reef Complex cements. All data refer to samples collected in this study. Full list appears in Appendix 6.4 and sample numbers in the Appendix refer to Figure numbers in the text.

6.4.2 Theoretical Considerations.

There are a number of major problems that hinder the interpretation of the isotopic composition of ancient carbonates, particularly when the mineral dolomite is involved. The subject has been discussed at length by various authors (Land, 1980, 1985; Anderson & Arthur, 1983), and it is not the intention to repeat the discussion in detail here. The following presents a brief summary of the relevant points under which constraints the data have been interpreted. Most of the problems are pertinent to the consideration of the oxygen isotopic composition.

The temperature dependence of the fractionation of $\delta\,^{18}O$ between water and calcite is well known, both from laboratory controls and natural but carefully monitored processes (Anderson & Arthur, 1983). However, the inability to precipitate ordered dolomite at low temperatures has precluded the direct observation of the dolomite–water fractionation. Figures that are used have had to be extrapolated from high temperature studies (Northrop & Clayton, 1966; O'Neil & Epstein, 1966; O'Neil et al., 1969), or interpreted from natural examples which are demonstrably coeval with calcite (Land, 1980). A figure that appears to be generally accepted is that the $\Delta^{18}O_{Dolomite--Calcite}$ is 3 ± 1 ‰ (Land, 1985) although values of +1 to +7 "can be used as alternative working hypotheses" (Land, 1980).

The carbon isotopic composition of ancient carbonates is often dominated by the composition of the precursor sediments, irrespective of the diagenetic processes which may have occurred. This is because the reservoir of carbon in the rock is vastly larger than that in the diagenetic fluids, such that the latter very rapidly reach an equilibrium state with the rock. The carbon isotopic composition of diagenetic phases is commonly, therefore, of typical marine signature, and provides little useful information on the diagenetic environment. The exception to this is in settings where a substantial degree of oxidation or fermentation of organic matter occurs, in which case the carbon signature can be significantly modified. The range of carbon isotopic composition in massively dolomitised rocks has been noted to be quite small (Land, 1985).

Secular variations in the oxygen isotopic composition of the oceans is another still unresolved problem. Many authors have documented a decrease in the $\delta^{18}O$ signature in marine carbonates with increasing age (Anderson & Arthur, 1983), and several explanations for this variation have been proposed (Veizer et al., 1986). The most favoured reason is that the $\delta^{18}O$ of ocean water was lower in the past; studies on brachiopods, chosen for their high stability, have indicated that sea water may have been up to 6 $‰_0$ lighter during some periods. The major variations appear to be in the Palaeozoic, however, and although estimates of Triassic sea water composition are rare, it appears from recent papers that a range of 0 to -2 $‰_0$ would be a reasonable estimate (Veizer et al., 1986). The carbon isotopic composition was apparently similar to modern sea water.

A further aspect which has to be taken into consideration in interpreting the results of isotopic analyses, is the nature of the diagenetic system, as to whether it is 'closed' or 'open'. This concept can be described in a semi-quantitative fashion using the term solute index (Veizer, 1983). A solute index (SI) of 100 implies that the entire solute content of a fluid is provided by the fluid itself (a high water/rock ratio or open system), whereas a SI of 0 means that the entire solute content is provided by a dissolving phase, a low water/rock ratio or closed system. Hence the composition of a diagenetic phase will only be in equilibrium with the bulk pore fluid if the SI is 100. In addition, even for a fixed water/rock ratio, the solute index will vary depending on the concentration of the particular solute in the rock and in the fluid (Pingitore, 1978; Veizer, 1983).

In the case of the oxygen isotopes, there is a very much larger concentration of oxygen in the water than in the rock, and so the SI will be relatively high even when water/rock ratios are low, such that the isotopic composition of the water will not be greatly affected by any dissolution of the rock. The opposite situation applies to the carbon isotopes, as has been alluded to above.

The oxygen isotopic composition is, therefore, likely to provide the most useful information regarding the formation and distribution of the cements in the Hafelekar Reef Complex. The figures will reflect both the composition of the precipitating fluid and the temperature dependent fractionation factor. Finally, there remains the perennial problem of whether the present composition truly reflects the characteristics of the primary depostional environment, or whether it has been altered by some later diagenetic re-equilibration event(s).

There are clearly, therefore, a number of complicating factors which have to be considered in the process of interpreting the geochemical data presented in Figure 6.30. Nevertheless, the isotopic composition of the cements can act as a useful corollary to the petrographic studies.

6.4.3 Sample choice.

Samples for geochemistry were chosen so as to enable the evaluation of variations in the compositions of the diagenetic phases across the reef facies. The final phases of baroque dolomite and late spar were not present in large enough quantities to enable collection from all facies, and so the spatial distribution of these two minor phases was not studied. Full details of samples is given in Appendix 6.

i) Fore-reef megabreccia. Samples were collected from the zoned 'Großoolith' cements identified in the petrographic descriptions. In order to confirm the widespread extent of these cements, 10 correlated zones were collected from two samples separated at outcrop by several hundred metres. Negative prints of the specific thin sections from which the samples were removed can be seen in Figures 6.31 & 6.32. Substrates from both samples and the spar evident in the substrate of Figure 6.31 were also collected.

ii) Back-reef. The sheet crack fibrous cement was sub-sampled in layers parallel to the inclusion zones, from two separate specimens. The very dark black layer shown in Figure 6.16 was also collected.

iii) Reef flat. The zoned fibrous cement described from specimens relatively close to the back-reef sands was collected from the thin section shown in Figure 6.33. Four separate layers were sampled.

iv) Reef core . The fibrous cements were again sampled from several separate specimens, illustrated in Figures 6.34 & 6.35. The actual thin section from which some of the cements were collected is shown in Figure 6.36. Spar cements nucleated on the fibrous phase as well as filling remaining substrate porosity were sampled as indicated in Figure 6.36. Bulk substrates from both specimens were also analysed.

v) Eastern Edge. Zoned cements similar to the 'Großoolith' were collected from the thin section illustrated in Figure 6.37. In this example it was possible to compare equivalent zones from opposite sides of the cavity. Three sub samples of each were separated. The single zoned fibrous cement was also analysed, this being collected from a different specimen shown in Figure 6.38. Bulk substrates were also analysed.

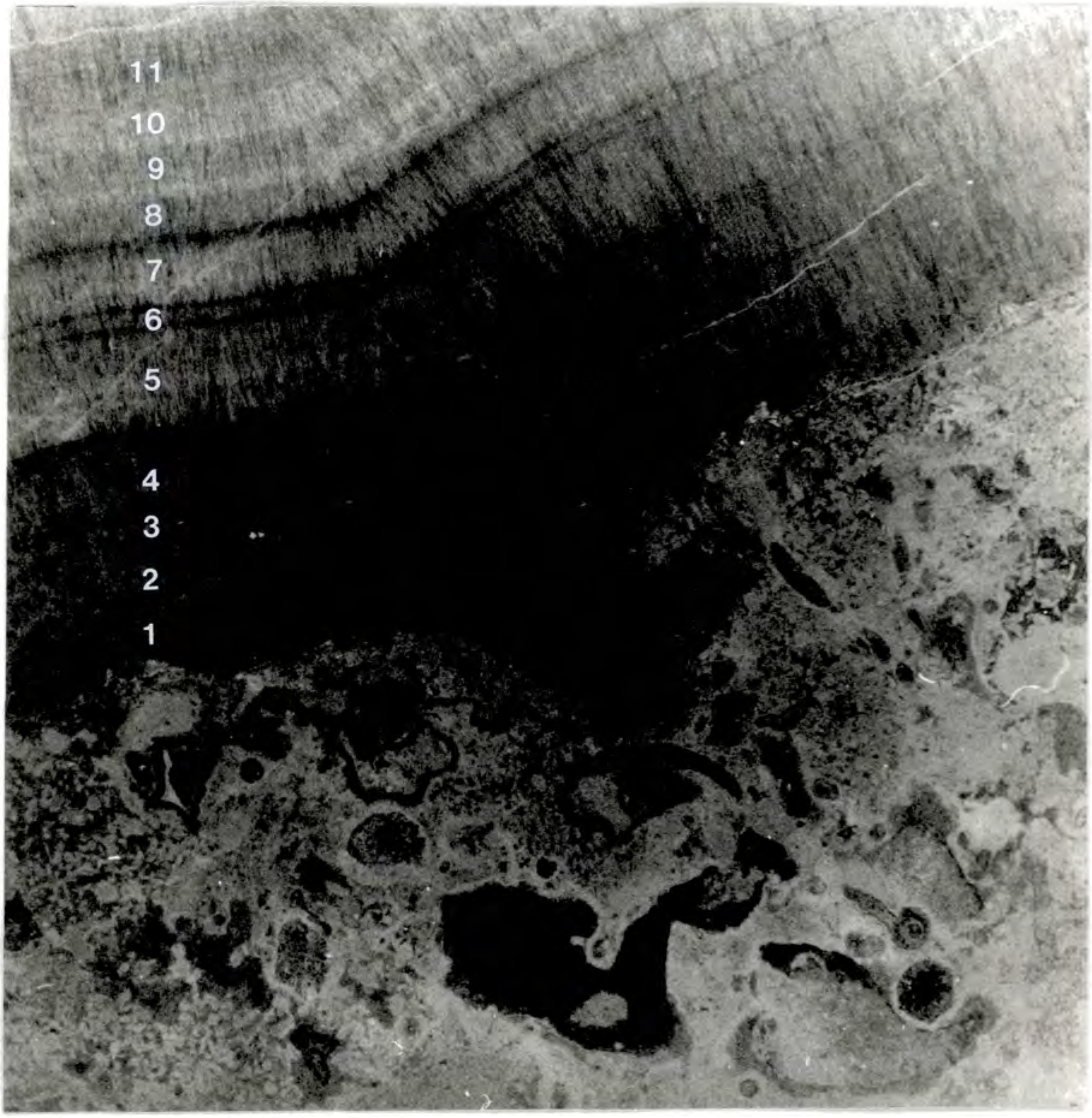

Figure 6.31 Fore-reef sample negative print of thin section. Samples collected as illustrated with numbers.

Figure 6.32 Second fore-reef sample separated by several hundred metres fom that in Figure 6.31 Individual zones correlated.

Figure 6.33 Zoned fibrous cement from which four subsamples were analysed. The specimen comes from the reef flat area.

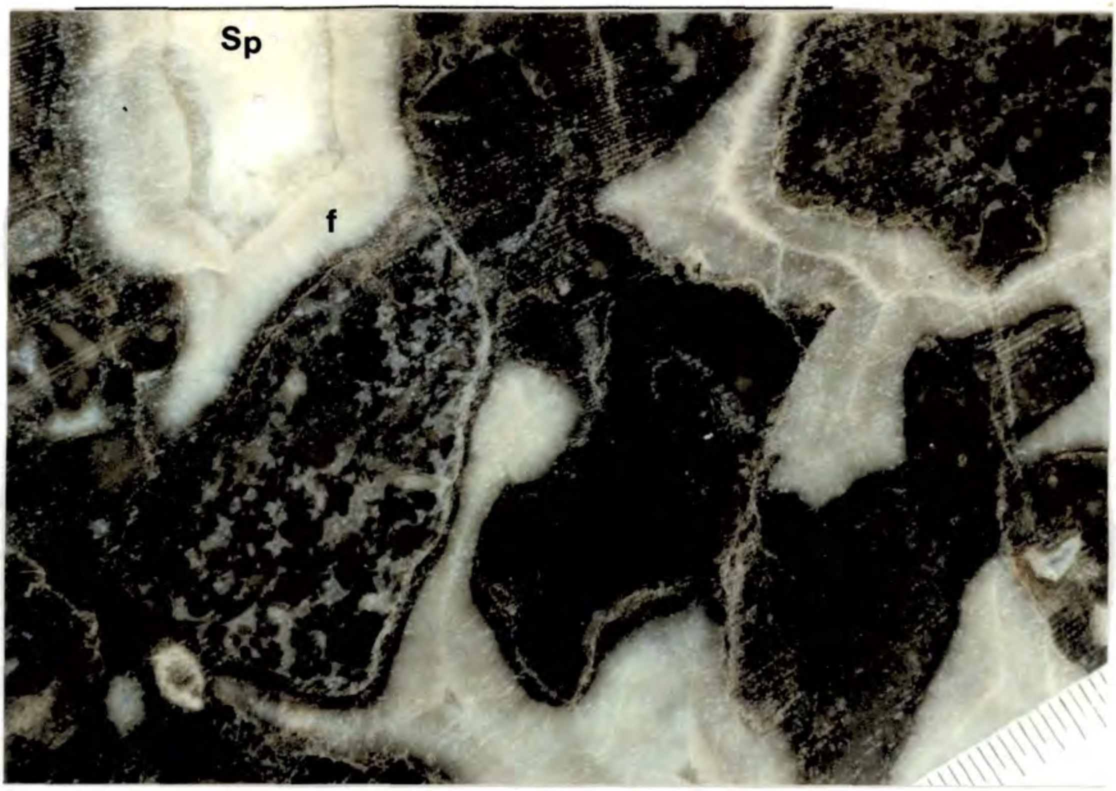

0.5cm.

Figure 6.34 Reef-core fibrous cement and calcite spars collected for isotopic analysis as indicated.

1cm.

Figure 6.35 Second reef core specimen. Fibrous cements sampled as indicated with letters

Figure 6.36 Thin section from which reef core cement samples were collected. Negative print.

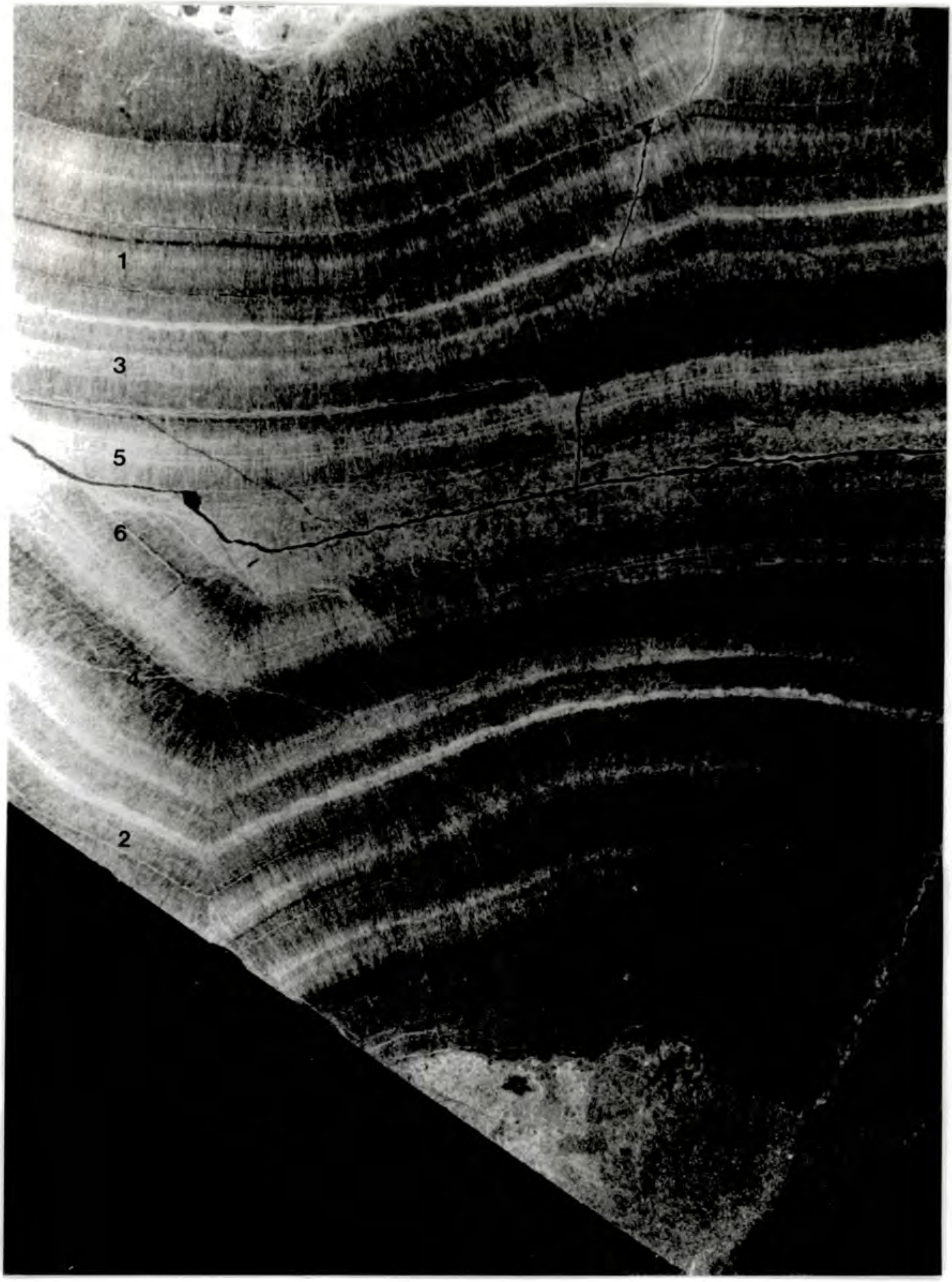

Figure 6.37 Negative print of thin section from the eastern edge of the reef complex. Cements were collected from this thin section as indicated.

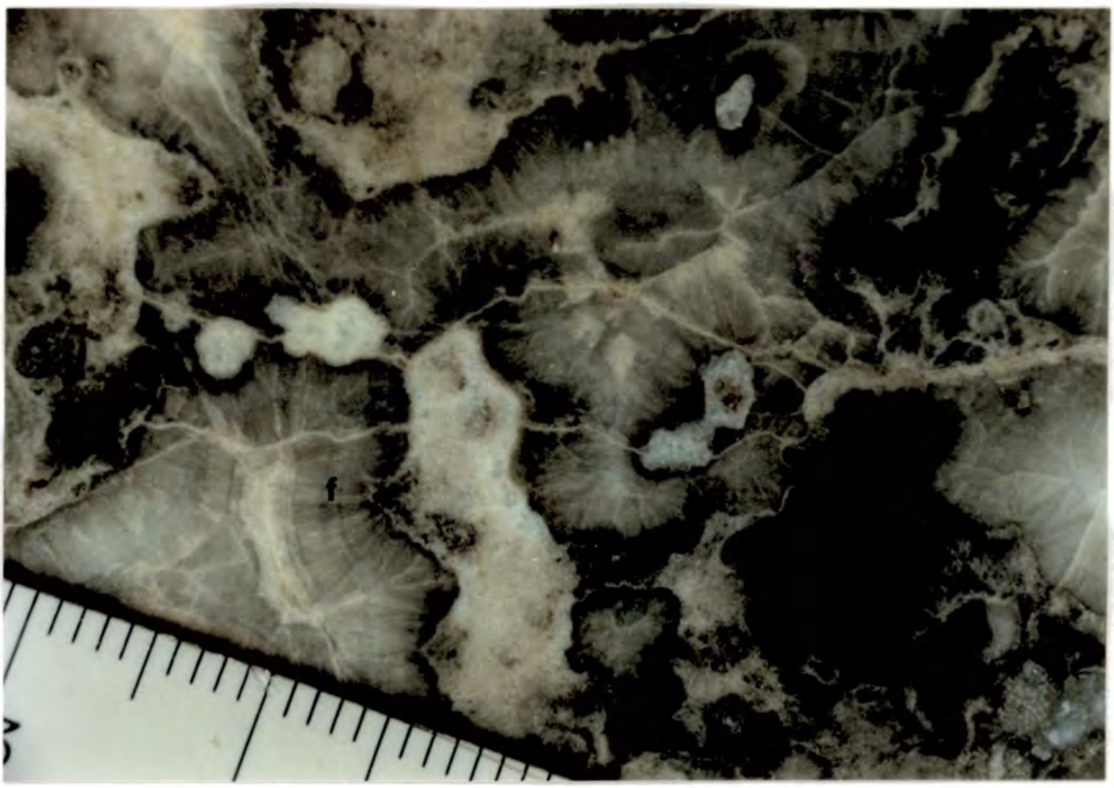

Figure 6.38 Sample from the eastern edge of the reef showing thinly developed fibrous cement collected for isotopic analysis as shown.

6.4.4 Introduction to the results.

The full data set is presented in Figure 6.30 and in Appendix 6. Reproducibility was measured as better than 0.1 ‰ for carbon and 0.2 ‰ for oxygen, based on the repetition of 15% of the samples and the analysis of laboratory standards. Values are quoted as measured against the PDB scale.

Some correction was applied to the mixtures of dolomite and calcite. This was made on the basis of the 0.84 ‰ difference in the oxygen isotope fractionation for the two minerals in their reaction with phosphoric acid (Land 1980, 1985). Carbon isotope fractionation is the same for both and so no correction is necessary. Dolomite levels were estimated from the Mg concentration in the acid solutions after the collection of the carbon dioxide gas (by ICP spectroscopy). This involves some approximations concerning the stoichiometry of the dolomite and an assumption that all the Mg is present in the dolomite and none in the calcite. However, XRD analyses of the zones in the fore-reef 'Großoolith' cement, indicate that the errors are not too large. Calcite peaks occur precisely as expected for pure calcite with no offset towards the high-Mg calcite diffraction angle. Dolomite peaks are sharp, indicative of good ordering, and measurements of the dolomite content from the peak areas agree quite well with the ICP analyses. XRD data are given in Appendix 6. The maximum error in the calculation of the dolomite content is probably about 10%, equivalent to a variation in isotopic composition of 0.08 ‰ . As this is significantly less than the many other uncertainties described above, the corrected results can be confidently interpreted. This error has to be considered as addititive to the analytical error mentioned above, making total uncertainties for $\delta^{18}O$ of 0.3 ‰.

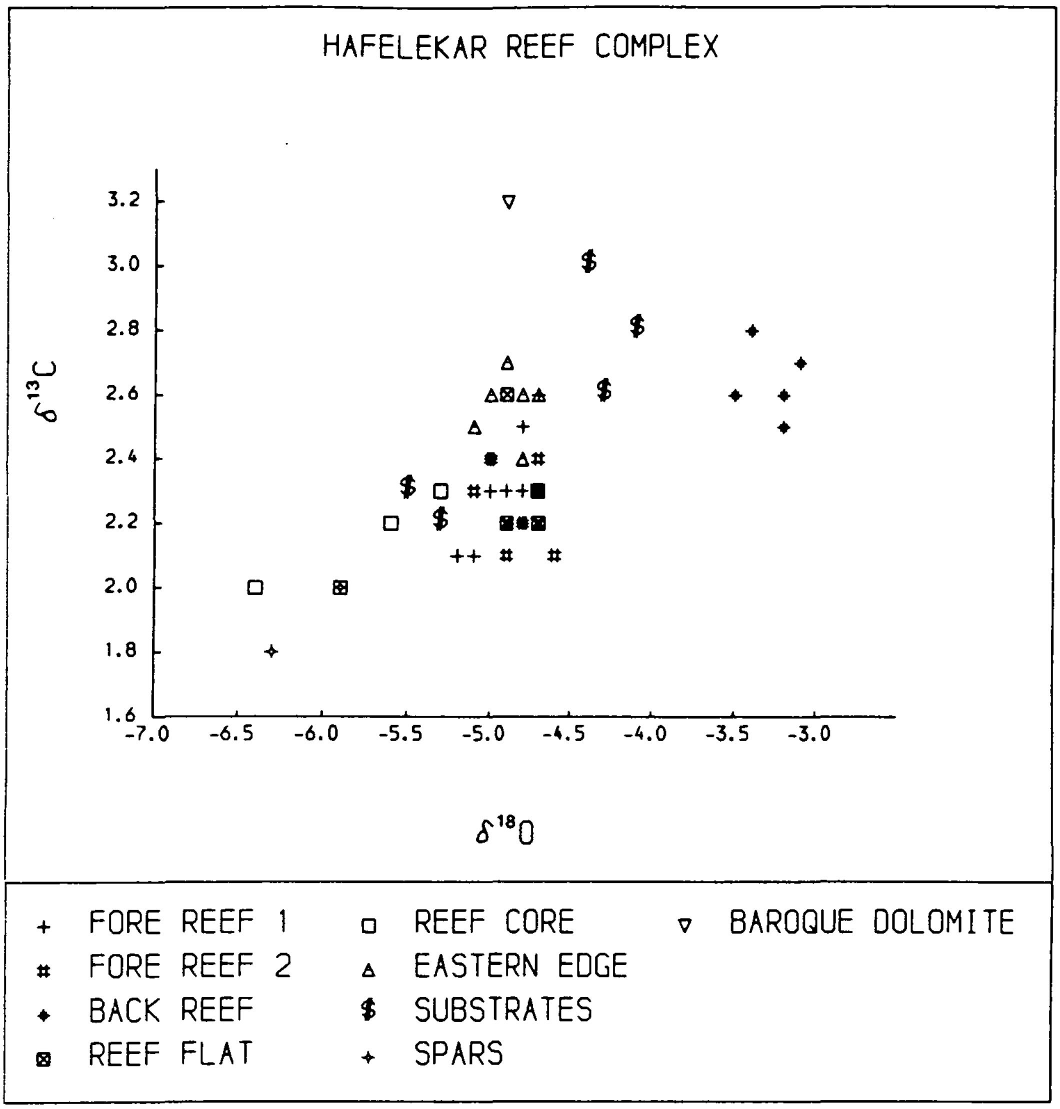

Figure 6.30 Carbon and oxygen isotopic data for Hafelekar reef cements repeated. Discussion in the text.

6.4.5 The carbon isotopic composition.

The $\delta^{13}C$ composition of the fibrous cements is remarkably consistent throughout the samples, being in a range of 2.4±0.4 ‰. The very narrow range precludes any meaningful comparison between samples, and there are no significant trends across any cement zones or reef facies. The value of 2.4 ‰ is a typical marine figure, but cannot be used to imply that the cements are unaltered from their marine origin as it may simply reflect the bulk limestone composition imparted to the cements by a later diagenetic re-equilibration event. The very low value for the fore-reef substrate, an unidentified bioclast, is probably indicative of some vital effect and may be a primary composition. Other substrates and spars fall within a range of 2.4±0.8 ‰, and are therefore of little diagnostic value. The least positive value is +1.8, from a late burial calcite spar, and this may indicate some slight carbon isotopic difference between seawater and the burial pore waters.

6.4.6 The oxygen isotopic composition of the cements.

The oxygen isotopic compositions of the cements can provide more information about the precipitational environment. The extensive development of the fibrous cements suggests that the flux rates were high, a fact confirmed by the general lack of muddy sediments, indicative of high energy. The water/rock ratio was therefore high and so the composition of the cements ought to reflect accurately the nature of the pore fluids from which they were precipitated. This is only true if there has been no subsequent dissolution-reprecipitation event.

In the light of these problems, it seems most logical to consider the composition of the least altered cements first. The petrography indicates that the back-reef sheet crack fibrous cements are purely calcite and have the least altered textural appearance. The lack of dolomite in the substrate and the generally good preservation of the texture confirms that these samples are the ones most likely to retain a primary signature.

The fibrous cement from two separate samples has a composition of -3.3 ± 0.2 ‰ , a range smaller than the analytical error. This figure is on average 1.5 ‰ heavier than all the other fibrous cements. The low Mg concentration confirms the lack of dolomite (<4%). The value of -3.3 ‰ can be used to calculate a possible range of precipitation temperatures, from the known temperature dependence of the fractionation factor for the precipitation of calcite from water (Equation 3.2). A near surface temperature would confirm that precipitation occurred from seawater or from very shallow subsurface pore fluids.

Unfortunately, it was not possible to estimate the Triassic sea water composition directly. Brachiopods are considered to be the most reliable indicators of marine water composition as they do not exert any vital effects, and their low Mg-calcite mineralogy makes them most resistant to stabilisation in diagenetic waters. However, none were found during the course of this study. Other substrate bioclasts and bulk samples analysed clearly do not preserve a wholly primary signature. The oxygen isotopic composition has therefore to be estimated from published studies. The value is considered here to have a likely range of 0 to -2 ‰. Using this range and a $\delta^{18}O$ composition for the fibrous cement of -3.3 ‰ , the temperature calculated from equation 3.2 is 22–32 °C, which is within a reasonable range for seawater. It would appear therefore that the sheet crack cements reflect a primary marine composition.

The fore-reef Großoolith cements fall in a range of -4.9± 0.3%, and, given a range of water $\delta^{18}O$ of 0 to -2%, this is indicative of precipitation or re-equilibration within a temperature range of 28-40 °C. Assuming an average geothermal gradient of 3 °C per 100 metres, this temperature range implies that the cements were formed or re-equilibrated at a depth of between zero and 500 metres. A further possibility is that some re-equilibration has occurred with a meteoric groundwater at surface temperatures.

Bradner & Resch (1981) have observed meteoric diagenetic products in the lagoonal sediments, and other authors have emphasised that the sedimentation of the upper Wetterstein was interrupted by several episodes of karst formation (Heinrich & Zankl, 1986). There does not appear to be much evidence in the Hafelekar reef for the involvement of meteoric water over long periods, as no major dissolution is evident and no vadose spars have been identified. However, the reef core samples do show some fabrics indicative of dissolution (Figure 6.22) and it may be that some secondary dissolution porosity has been mis-interpreted as primary.

Zoned cements recognised from the eastern edge of the complex (Figure 6.37), and from the reef flat (Figure 6.33), have an identical range of composition to the 'Großoolith' cements, providing further evidence that they were formed from the same fluids at similar times.

The other single zoned fibrous cements of the reef core are slightly lighter than the above multiple zoned examples, and again several possible explanations can be suggested. The simplest involves either alteration at slightly greater depth, or a greater degree of interaction with a meteorically derived water. A further interesting suggestion, albeit rather speculative, is that the differences are linked with the formation of the euhedral dolomite phase. The dolomite content of the single zoned fibrous cements has been noted to be low, a fact confirmed by the chemical analyses, showing values for the four samples of 8,8,14, and 14%. This is compared to a content for the 'Großoolith' -type cements of 25–50%. A plot of the oxygen isotopic composition for these two groups against dolomite content (Figure 6.39), illustrates the point, although there does not appear to be a concise relationship. The fact that the lower dolomite content coincides with the lighter isotopic composition can be explained by the fact that dolomite is known to form with a heavier $\delta^{18}O$ than cogenetic calcite. Whilst it certainly cannot be suggested that the dolomite is coeval with the fibrous calcite, it may be that the dolomitisation event occurred simultaneously with the re-equilibration that left the calcites with their present composition. In other words, the dolomitising fluids pervasively altered the $\delta^{18}O$ composition, such that the precipitation of dolomite was indeed coeval with the diagenetic stabilisation of the marine cement to fibrous calcite. This could have involved Mg loss, as the marine high Mg-calcite was altered to a diagenetic low Mg-calcite, with little fabric destruction other than crystallite coalescence. Hence the higher the content of the dolomite, the heavier the isotopic composition of the diagenetic product.

The only remaining samples to be considered are the spar cements. The purely calcite spar precipitated in the reef core has a $\delta^{18}O$ composition of −6.3 ‰, which as a calcite is indicative of temperatures of 38–49 °C (assuming a water composition of 0 to −2 ‰), or a burial depth of 400–800 metres. The situation is not certain, however, as a similar composition could be derived from a meteoric water. The other reef core spar which is also low in dolomite, has a 0.4 ‰ heavier composition, but this may not be significant bearing in mind the maximum 0.3 ‰ error.

The later spars present in the substrates are partly baroque dolomite, a fact confirmed by the chemical analysis of the sample from the reef core which shows a 80% dolomite content. The $\delta^{18}O$ composition is 4.9 ‰, which as a dolomite is indicative of a temperature range of 43–60 °C. The upper end of this range is in agreement with the lower estimate for the precipitation temperature made by Radke & Mathis (1980), and implies a burial depth of at least 1km. These figures were estimated using a seawater $\delta^{18}O$ of 0 to −2 ‰, but it must be emphasised that this figure may not be a true representation of the burial fluids.

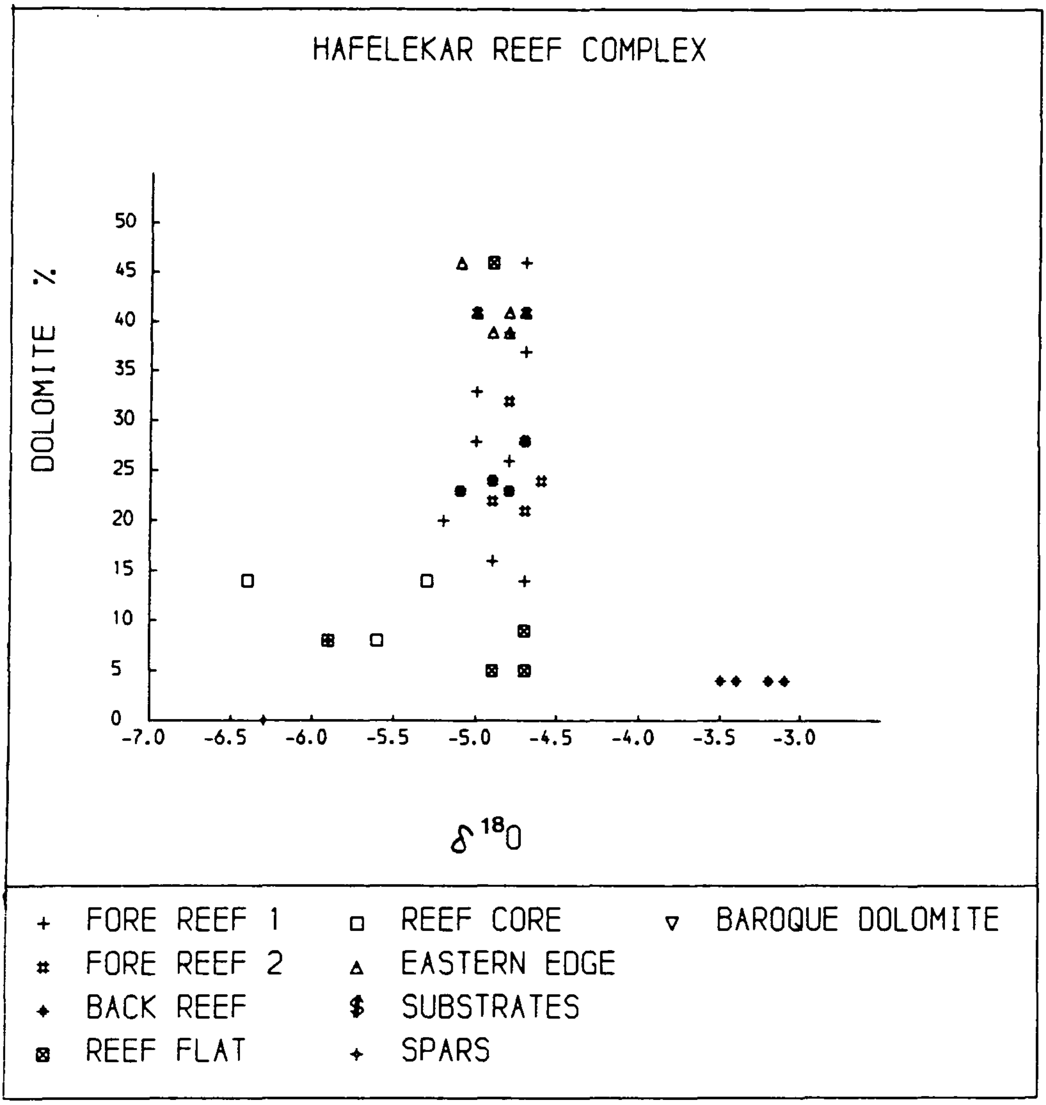

Figure 6.39 Plot of oxygen isotopic composition vs. dolomite content for the cements of the Hafelekar reef. See text for discussion.

6.4.7 Conclusions from the stable isotope data.

The isotopic composition of the cements falls within a narrow range for both carbon and oxygen. The carbon composition is typically marine, but the relative sizes of the carbon pool in the rock and the fluids is such that any non-marine pore fluids would be unlikely to leave a recognisable impression, so the data do not preclude the input of, for example, a later diagenetic fluid of meteoric origin.

The oxygen isotopic composition is also rather difficult to interpret and the narrow range does not help in determining the timing of events. Whether the burial waters were marine, meteoric or of mixed origin, a fact that is certain is that all the diagenetic events were complete within approximately 1km. of burial, implying a date well before the end of the Triassic. The detailed interpretation of the variations between phases which was presented above has to be considered rather speculative. It has, however, been based on petrographic observation, and this approach should improve the credibility of the suggestions. It is apparent that the back-reef samples have not been affected by dolomitisation or other major dissolution-reprecipitation reactions, and the composition of the sheet crack cements is consistent with precipitation from surface marine waters. The discussion above with regards dolomitisation is concerned only with the second phase as identified by the petrography, as samples of the proposed early dolomite were not analysed.

All of the fibrous cements identified in the reef itself have oxygen isotopic compositions significantly lighter than those of the back-reef. If only on the basis of choosing the simplest option, it is likely that they are all contemporaneous, with the former being re-equilibrated after some burial in a fluid of essentially marine origin. The fact that the $\delta^{18}O$ of the cements appears to be correlated with dolomite content, at least forming two separate groups (Figure 6.39), could be tentatively used to suggest that the re-equilibration occurred in the dolomitising fluids in a shallow burial environment. The slightly increased temperature would certainly favour dolomitisation, and it is reasonably well accepted that purely marine fluids can precipitate dolomite (Land, 1985) The euhedral dolomite crystals will have been nucleated preferentially in areas of higher Mg concentration, hence the observed zonation in the 'Großoolith' cements can be explained by primary variations in the Mg content of the marine precipitate. There may not have been enough Mg present in the reef itself to account for all the dolomite, but a net influx from compacting basinal sediments could have provided the necessary excess. This scenario has been suggested in similar models of burial dolomitisation (Mattes & Mountjoy, 1980) and in the case of the Hafelekar reef, the magnesium could have been derived from the Partnach and Reifling basinal sediments.

The composition of the late spars is again complicated by the content of dolomite, but at least broadly speaking, it is consistent with an origin at depth. The petrographic recognition of baroque dolomite suggests a possible third phase of dolomite precipitation, partly as a cement phase. The fact that the isotopic compositions of most of the cements described above do not reflect a primary origin, makes it difficult to interpret the data in terms of the time scale of the original marine precipitation. If the narrow range was primary, it would suggest precipitation over a very short time in an open system where no evolution of the pore water occurred, a theory supported by the petrography. It is possible, however, that an originally broader range has been reduced by the later diagenetic events.

6.5 Trace Element Compositions.

6.5.1 Introduction.

Trace element compositions can be used to help elucidate the diagenetic history of carbonate sediments, and whilst the applications were first discussed almost twenty years ago (Kinsman, 1969), the theory has been recently reviewed in the light of new experimental observations (Veizer, 1983, 1983; Land, 1985). The technique is useful in certain circumstances as a complementary tool to isotope analysis and many of the recent publications discussing reef diagenesis and problems of dolomitisation include both types of data (Moore, 1985; Aïssaoui, 1986; Heinrich & Zankl, 1986; Xun & Fairchild, 1987). Despite these many years of study, there remain some quite fundamental problems which hinder the interpretation of such data, and the most important factors are briefly discussed below. The principle of the technique is that the trace element composition of a growing crystal is proportional to the concentration in the solution, according to a simple relationship:

$$\left(\frac{{}^{m}Me}{{}^{m}Ca}\right)_{CaCO_3} = D.\left(\frac{{}^{m}Me}{{}^{m}Ca}\right)_{Water}$$

where the superscript 'm' indicates molar concentrations and 'Me' stands for the trace element of interest. Hence the molar ratio of the trace element to calcium in the carbonate is directly proportional to the same ratio in the solution. The proportionality constant 'D' is known as the distribution coefficient. This relationship is only valid when the system is at chemical equilibrium and the distribution of the trace elements in both solid and liquid are homogeneous.

The first major problem is that there are several modes in which the trace elements can be incorporated into the carbonate precipitates:

i) By substitution for major cations in the carbonate lattice.
ii) In interstitial sites between lattice planes.
iii) In lattice positions free due to defects.
iv) By adsorption due to remnant charges.
v) As non-carbonate fluid and solid inclusions.

Measurement of the distribution coefficients by laboratory experiments produces values which represent incorporation in all of the above sites, and although the first item above is a systematic process, the others are purely random and non-quantifiable. This therefore implies that the distribution coefficients are approximations only.

Other problems are also linked to the accurate measurement of distribution coefficients. In particular, they are known to be dependent on temperature and the rate of crystallisation, the latter being a similar problem to that discussed for isotopic fractionation discussed in Section 3.4.3. When the mineral dolomite is involved, the situation is more complex due to the preferential incorporation of ions into either calcium or magnesium layers, this in turn being affected by the ordering and stoichiometry of the dolomite.

A final problem is regarding the nature of any replacement reactions, and the relative solute indices, a factor discussed in Section 6.4.2. Veizer (1983) has suggested a bulk solution dis-equilibrium model for the replacement and stabilisation reactions, such that the fluid at the surface of a reaction zone is not necessarily in equilibrium with the bulk solution, making the accurate assignment of a distribution coefficient quite difficult. The various problems are discussed in detail in several publications (Morrow & Mayers, 1978; Veizer, 1983; Land, 1985). It seems sufficient to conclude that the published distribution coefficients should only be used as indications of the trends expected in various diagenetic environments.

In summary, the trace element composition of calcite and dolomite is dependent on three major factors, these being the composition of the precipitating or replacing fluid, the value of the distribution coefficient and the solute index or degree of openness of the diagenetic system. In spite of the problems described above, some useful information can be derived from the analysis of trace element data, particularly relating to the nature of diagenetic fluids. Three trace elements have been analysed in this study, namely strontium, iron and manganese. The range of distribution coefficients is given in Table 6.1 and the molar ratios of the elements in a range of natural waters is shown in Figure 6.40. It should be noted that it is not absolute concentrations of the trace elements which is important for the partitioning into diagenetic products, but the ratio relative to calcium. It is apparent from Figure 6.40 that the Fe and Mn levels in marine fluids are quite low, and hence the levels would be expected to be low in marine precipitates. The shallow subsurface fluids have a significantly higher ratio and Veizer (1983) suggested that meteoric waters may have similar levels. The case is essentially reversed for strontium, with the molar ratio to calcium being significantly higher in marine fluids than in meteoric ground waters.

A similar pattern of properties is apparent for the distribution coefficients (Table 6.1), with the behaviour of Sr being opposite to that of Fe and Mn. This fact is particularly useful in assessing the degree of alteration by diagenetic fluids. The distribution coefficient for Sr is less than one, so that the Sr content of the carbonate will tend to decrease with increasing diagenesis. The opposite is true for both Mn and Fe, for which distribution coefficients are substantially greater than one and hence the content in a carbonate will increase with diagenetic maturity.

Element	Process	Calcite	Dolomite
Sr	Direct	0.13	0.025–0.060
Sr	A-dLMC	0.05	
Sr	LMC-dLMC	0.03	
Mn	Direct	6	
Mn	A-dLMC	15	
Mn	HMC-dLMC	30	
Mn	LMC-dLMC	30	
Fe		1-20	
Mg		0.013–0.06	

Table 6.1 Trace element distribution coefficients. (From Veizer, 1983).

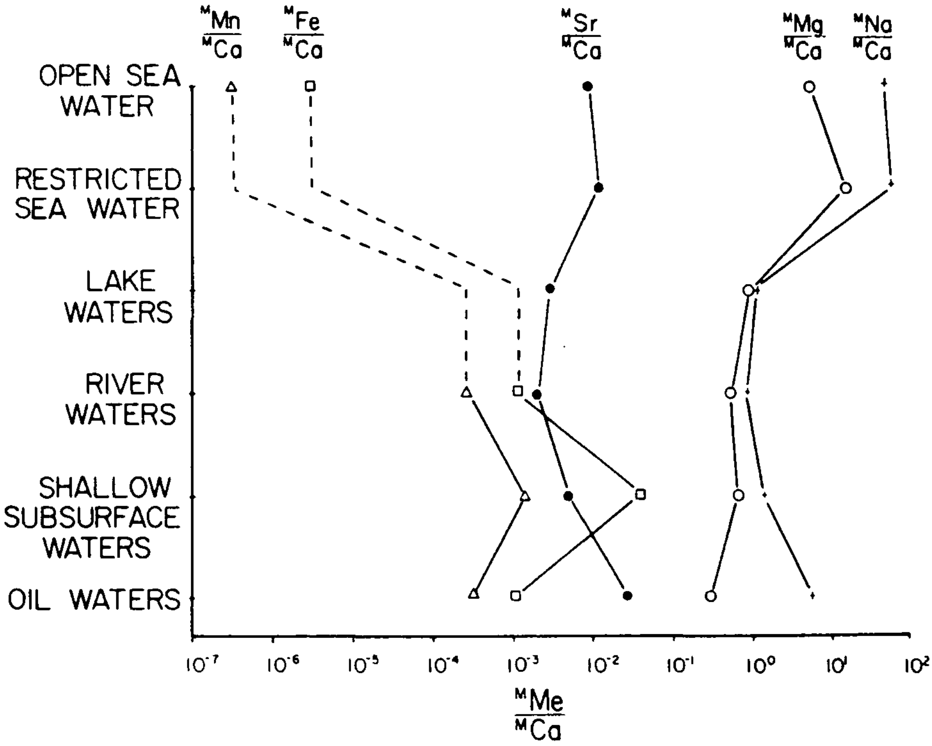

Figure 6.40 Molar ratios of several trace elements in a variety of natural waters. (From Veizer, 1983).

6.5.2 Results.

The full data are listed in Appendix 6, and selected figures are shown in Figure 6.41. Magnesium concentrations have been discussed in Section 6.4 as they have been used to estimate the dolomite content of the cements. The other three measured trace elements are discussed individually below. All the figures have been normalised to mole%.

i) Strontium.

Values for strontium are uniformly low throughout the samples from all facies and all cement phases, being less than 0.04 mole% ($SrCO_3$). The figures for samples from the back reef are slightly higher than other facies, but the differences may not be significantly higher than the analytical uncertainty. Low values could have developed for a number of reasons, and it is difficult to determine which is correct. Aragonite phases would have originally contained approximately 1mole% (8000ppm) strontium ($SrCO_3$), and the reduction of this value to the above low levels would involve a large number of dissolution-reprecipitation reactions (Morrow & Mayers, 1978), a suggestion which is incompatible with the observed textural preservation. However, if one accepts the bulk solution dis-equilibrium model (Veizer, 1983), then a smaller number of bulk recrystallisations would be necessary. A more likely possibility is that the cements were originally calcite, as the initial concentration of strontium would have been lower, at approximately 1300 p.p.m. (Morrow & Mayers, 1978).

ii) Iron.

Concentrations of iron in the cements are extremely variable and have been found to be irreproducible, suggesting that the iron is present as contamination.

Although tests were carried out on the acid used for the digestion of samples, no iron was detected, and the reasons for the poor reproducibility have not been ascertained. Values range widely from zero to 0.4 mole% and there is no facies dependence apparent from the figures. The higher concentrations should have been detected by staining with potassium ferricyanide, but no iron staining was observed, further suggesting that the iron content arises from contamination.

iii) Manganese.

Manganese levels are also variable, though less so than the iron concentrations. Values tend to be somewhat higher in the fore-reef samples than in the reef core and back reef. It might be possible to interpret the higher Mn levels in the 'Großoolith' cements on the basis of the influx of Mn from basinal fluids during the later dolomitisation events, but the results are not consistent. The 'Großoolith' cements in samples from the eastern edge of the reef are high in dolomite content, and yet the Mn content is very low (Appendix 6).

6.5.3 Conclusions from the trace element data.

The trace element data provide little further information on the depositional environment or the diagenetic history of the cements. The problems involved in assigning accurate distribution coefficients, coupled with the question of whether the present compositions represent depositional chemistries or simply the nature of the latest diagenetic fluids, make it difficult to interpret the data with any confidence. Although iron and manganese concentrations are unreliable, the uniformly low strontium concentrations are consistent with the precipitation of calcite cements in the marine environment, followed by some diagenetic re-equilibration.

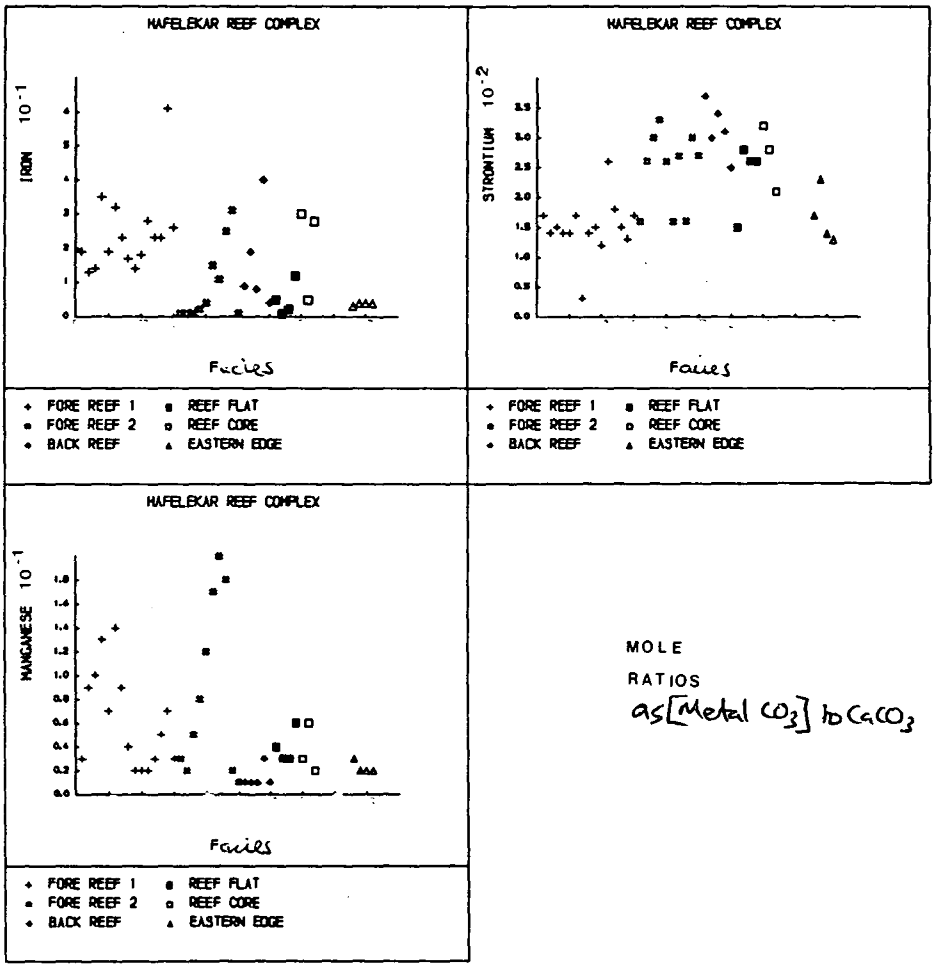

MOLE
RATIOS
as [Metal CO_3] to $CaCO_3$

Figure 6.41 Selected figures for the trace element distributions within cements of the Hafelekar Reef Complex. See text for discussion. Horizontal axis simply represents a list of samples divided into facies as described in the key. Samples plotting immediately above each other are repeat measurements from the same sample.

6.6 Conclusions.

The emphasis of this study has been to describe the distribution of the marine cements both within and between the reef facies. The distribution is in fact, rather simple, with a maximum of three phases of fibrous cements being precipitated throughout most of the reef. The development of the cements is quite homogeneous, particularly within the fore-reef where individual zones can be traced over large distances. The primary control on the distribution of the cements appears to be the permeability of the substrates at the time of precipitation, such that thicker developments of cement occur in the higher permeability areas. The spatial extent of later diagenetic events may also have been influenced by permeability, hence the lack of dolomite in the back-reef facies may have been due to the fact that an early rapid lithification sealed the grainstones and packstones from the later fluids.

The time scale of the marine precipitation appears to be quite rapid, occurring in an open system, as there is no conclusive evidence of any evolution in the pore water chemistry. It must be re-emphasised that the geochemical evidence which would suggest such evolution, may well have been masked by later diagenetic events, a phenomenon often recognised in studies of ancient reefs.

On a superficial level, the long term diagenetic history is also simple. The vast majority of the porosity was occluded by the marine cements, the remainder being progressively filled with spar cements precipitating at burial depths of up to 1km. The precise details of the diagenetic history are, however, somewhat more complex, the relative timing of the dolomitisation being particularly difficult to determine conclusively. Petrographic evidence for the timing of some events, in terms of cross cutting fabrics, is relatively lacking. This fact in itself indicates that individual events were quite rapid on a geological time scale.

Geochemical evidence must always be interpreted cautiously, both for reasons of uncertainty in the theoretical principles, and because the measured compositions may be the result of several chemical equilibrations, rather than one simple concisely definable event. In this respect, chemical data must be considered as complementary to the petrographic evidence and not as isolated information.

A description of the development and the diagenetic history of the Hafelekar Reef Complex follows. This description is not unequivocal, but it is based on a synthesis of the field and petrographic evidence, supported by geochemical data. The diagenesis is summarised in Figure 6.42.

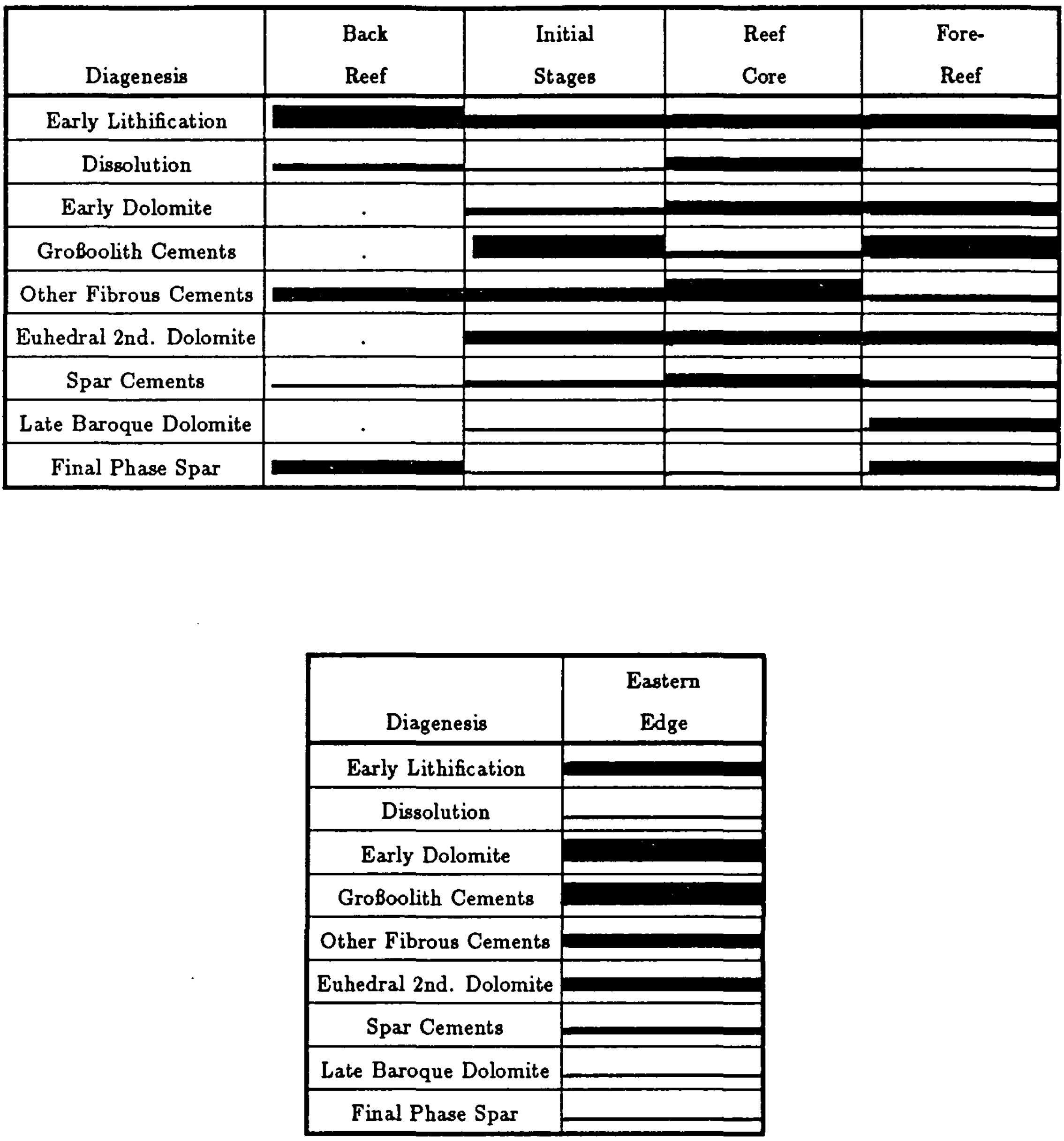

Figure 6.42 Summary of the diagenesis of the Hafelekar Reef Complex.

The initial stages of the Hafelekar reef were founded on top of a block rubble sequence which was created by the demise of the earlier Goetheweg reef (Figure 6.2). The Hafelekar reef grew as the sediment binding and baffling fauna diversified, creating a buildup which consisted of fairly small framework organisms interspersed with a large volume of medium to well sorted sandy sediment. The general lack of muddy sediment is significant, indicative of prolonged high energy conditions.

The reef accumulation was lithified by the precipitation of isopachous linings of fibrous marine cements. The coarse back-reef sands had the highest permeability and were therefore lithified to the greatest extent. Fluctuations in sea level and/or local tectonic activity may have caused a temporary exposure of the reef at this early stage in its history. Whilst the evidence for meteoric diagenesis is not common in this particular reef, other studies have emphasised that subaerial exposure did occur in Wetterstein reefs to the east (Heinrich & Zankl, 1986). In addition, Bradner & Resch (1981) document the presence of meteoric vadose diagenetic products in the lagoonal sediments. Some petrographic evidence for a dissolution event has been recognised in the reef core (Figure 6.22) and the geometry of the porosity prior to the major phase of fibrous cement precipitation is perhaps indicative of a minor karst development (Figure 6.19). The petrographic description suggested that an early phase of dolomitisation occurred (Figure 6.8), with some evidence that this event was partly controlled by permeability. The interstitial grainstone material may well have had a very low permeability at this stage due to the rapid syn-sedimentary cementation. This would explain the observation that the dolomite commonly occurs as only a surface alteration. Some areas, presumably of higher original permeability, appear to have been completely dolomitised at this stage.

The setting and characteristics of this dolomite appear to fit the mixed water or 'Dorag' dolomitisation model (Badiozamani, 1973), a much favoured choice of recent years (Land, 1985). However, there is some doubt about the basic chemical principles upon which this model was formulated (Machel & Mountjoy, 1986; Hardie, 1987) and it may no longer be a viable suggestion. However, the fabric destructive texture of the dolomite indicates that the dolomitising fluid had an aggressive nature. A pore fluid of marine origin with a significant meteoric content seems to be a likely candidate.

An increase in sea level or a general subsidence of the reef complex then restored more normal marine conditions to the reef, at which point the fibrous cements were precipitated into remaining primary porosity and perhaps substantial secondary dissolution porosity. The cavities of the fore-reef megabreccia, which had remained open to this stage, were rapidly cemented by a thick sequence of fibrous cements. The magnesium content of these cements appears to have varied, and this variation may have controlled the later dolomitisation. This phase of cementation was by far the most important porosity reducing event in the diagenetic history of the reef complex. The original porosity of up to 50% was reduced in a relatively short period of time to a figure of less than 5%. The greatest development of cements occurred in the highest energy areas, most notably in the fore-reef, a pattern very similar to that noted in the modern reefs of Belize (Section 2.20; James et al., 1976). The single zoned fibrous cements were also precipitated at this time, and were distributed throughout the reef facies and into sheet cracks of the back-reef. At this stage the porosity of the back-reef sands was negligible.

The next major diagenetic event was a second phase of dolomitisation, probably caused by fluids of essentially marine origin, circulating at depths of up to 800 metres, with the increased temperatures reducing the kinetic barriers to the formation of dolomite. This dolomitisation shows some selectivity, nucleating preferentially on Mg-rich substrates. The dolomite continued to replace the high Mg-calcite zones in the fibrous cements and some influx of magnesium rich pore fluids may have occurred from the compacting basinal limestones and marls. The generally low porosity at the onset of the dolomitisation tends to suggest that this diagenetic phase occurred over a relatively long period of time and this slow replacement explains the observation that the textural preservation is quite good. The geochemical evidence suggests that the dolomitising fluids caused a re-equilibration of the oxygen isotopes of both cements and substrates, in what was the last major pervasive dissolution-reprecipitation event.

The final diagenetic phase was the occlusion of remaining porosity by spar cements. There appear to have been at least three stages in this process, but the occurrences are quite rare and the exact relationships therefore difficult to interpret. A first phase of calcite spar is followed by a baroque dolomite. The latter is at least in part a cement phase though appears to replace the spar in some instances. The precipitation of this dolomite is considered to indicate temperatures above 60 °C, or a burial depth of approximately one km. Further burial up to a maximum of 3–4 km. caused some fracturing, particularly in the back-reef facies, and these fractures were then sealed by a characteristically clear calcite spar. It would appear that the processes described above were complete before the end of the Triassic, over a maximum time scale of 25 million years.

Much of the above has to be considered somewhat speculative, particularly with respect to the diagenetic history and precise timing of some events. However, the primary intention of this study was to investigate the distribution and timing of the early diagenetic products within the reef complex. In summary, the early marine cementation occurred in two major phases, interrupted by a dolomitisation event which may have involved subaerial exposure. The most significant event in the diagenetic history was the precipitation of the fibrous 'Großoolith' cements in both fore-reef and reef core facies. The cements were precipitated in a fairly short period of time, being best developed in areas of highest permeability. This phase of cementation was also laterally extensive, reducing the porosity of the reef complex by up to 90%.

CHAPTER 7

Summary, and Implications for Reservoir Potential.

CHAPTER 7

Summary, and Implications for Reservoir Potential.

7.1 Summary – Cementation in Modern and Ancient Reefs

7.1.1 Introduction.

The aim of this research has been to provide a model to account for the geochemistry and distribution of cements in modern and ancient reefs. Several specific research objectives were identified, concerned with particular aspects of the subject which were not adequately explained in the literature. The study of the controls on the precipitation of cements, together with the knowledge in the literature, has enabled the development of a conceptual model whose major points are briefly described below (Section 7.1.8)

7.1.2 The literature.

The literature review in Chapter 1 highlighted several basic questions which define the problems in the understanding of cementation in modern reefs. The first is a question of what is preventing the precipitation of cements from solutions which are supersaturated with respect to calcium carbonate. The other problems relate to aspects of the precipitation, when it occurs, namely what controls the morphology, mineralogy, spatial and temporal distribution of the cements.

A number of very important principles and controlling factors are understood in detail. There are a number of pre-requisites for the formation of cements; the presence of a stable substrate, lack of mechanical abrasion, supersaturated seawater and a mechanism to cause the exchange of pore fluids. As a direct result of the last requirement, it is important to realise that time is an essential factor, as the cementation process is slow. The realisation that the process of cementation is not isolated but interacts in a dynamic fashion with other reef formation processes is a very important aspect of the literature.

There are several factors which inhibit the precipitation of cement, if not actually preventing it. These include the nucleation energy barrier, the presence of organic coatings (whether simply adsorbed from solution or as a biogenic product), and the kinetic inhibition by inorganic magnesium and phosphate ions.

The principal control on mineralogy is the rather delicately balanced thermodynamics of the system, as the stabilities of aragonite and Mg-calcite are very similar in seawater. However, other controls may be exerted by organic molecules synthesised in skeletogenesis processes. There is evidence for a degree of substrate control, in that cements of one mineralogy tend to nucleate on substrates of the same mineralogy, though there are many exceptions to the rule. Morphological variation is either due to surface charge effects, or to poisoning of growth on certain faces. Irrespective of the exact nature of the control, the morphology is dependent on the relative rates of nucleation and growth, and the relative rates of growth of the different crystal faces.

Spatial distribution of the cements is a particularly difficult aspect to explain from a study of the present literature, due to the great inhomogeneity observed, but in general terms, there appears to be a link between higher energy environments and greater degrees of cementation. Most of the observed facies specificity can also be explained on the basis of relative energies.

The literature review allowed the formulation of several research objectives, based on areas of the topic which were least well understood. There are four main aspects: the possibility of biogenic control, the involvement and role of organic matter, the distribution of cements (on all scales) and the timing of cementation and its effect on the porosity of reef facies. These four aspects provided the topics for Chapters 3–6, which were preceded by a detailed petrographic study of cementation in modern reefs.

7.1.3 Petrographic observations as the basis of the research.

Study of Holocene reefs of Florida and Belize highlighted the fact that the cementation patterns are inhomogeneous on a range of scales. This was identified as being the result of the complex interaction of cementation with the other reef forming processes in a dynamic fashion in both space and time. An important point realised from the petrography was the need to quantify the cementation as a function not of the total rock, but as a percentage of the total porosity available at the time of cementation. A further point was that it is very difficult to distinguish lime mud from microcrystalline cement, and it may be that the amount of cement has been overestimated in past studies. In this particular study, the total volume of Mg-calcite cements, including peloids, was found to be similar to that of aragonite. There is some substrate control on mineralogy, in that the aragonite cements are best developed on aragonite skeletons, but the two mineralogies are certainly not mutually exclusive. No conclusive species specificity was observed. The facies variations cannot be directly compared, as a range of facies was not collected from any one specific reef, but a comparison of the Belize fore-reef with Florida reef core samples supports the suggestion that cementation is dependent on the energy of the environment.

Variation in the degree of cementation on the thin section scale is considered to be due to variations in the rate of flow through each pore, dependent on the very local permeability. It is clear that a substantial amount of the porosity observed in thin section is actually non-effective. Differences in the mineralogy of the cements on a pore to pore scale are a little more difficult to explain, but can be rationalised if the temporal variations in the controls on the mineralogy are considered to occur in parallel with variations in the permeability.

There was very little that could be deduced regarding the distribution of the cements on the core scale, as the cementation in cores was generally fairly low and extremely variable. Some evidence for a higher degree of cementation at the surface was obtained from point counting, and this was attributed to the increased total fluid flux through the surface of the reefs. Variation in the total degree of cementation on a regional scale was considered to be due to variations in the accumulation rate of the reefs.

7.1.4 Biogenic mediation.

Geochemical analyses of the cements have been used to investigate the possible roles of biogenic mediation in the precipitation of cements, concluding that there was no direct biogenic source of Ca^{2+} and/or HCO_3^- ions, nor was there any significant input from the oxidation or any other decomposition of organic matter. Although the slightly heavy oxygen isotopic composition of the Belize cements could be indicative of mediation by organisms, it was considered more likely to be due to a difference in seawater chemistry during the Early Holocene. Some differences were observed between the aragonite cements and the peloidal Mg-calcite cements. Although these could be considered to be due to an input from organic matter to the latter, the differences in the fractionation factors for the precipitation of the different mineralogies were considered to be a more reasonable explanation. The cements within the modern reef samples studied were therefore considered to be precipitated in equilibrium with seawater of normal marine composition.

7.1.5 The role of organic matter.

Probably the most confusing area of the literature is that concerned with the role of organic matter in the precipitation of cements. The study of the peloidal cements, and the full characterisation of the organic matter associated within them, represents a starting point for the clarification of the situation. A review of the problems involved from a basic chemical standpoint identified the principal roles and mechanisms involved. Detailed study at the molecular level can provide a great deal of useful information, but there are many potential sources of contamination, so great care needs to be taken in the interpretation of the results, and in the adequate provision of control samples. The organic matter can play both preventative and promotional roles in the cementation processes and the mechanisms for both have been discussed. It is clear that both roles could be played by the same molecule, though some biogenic control would probably be necessary for this to occur in an ordered fashion. Prevention of precipitation is very difficult to demonstrate conclusively, and was not investigated in any detail in this study. The characterisation of the peloidal organic matter provided some information on its source. This was considered to be of multiple origin, but primarily algal, with no real substantiation of previous suggestions that the peloids are a result of bacterially mediated precipitation. In addition, the evidence indicated that there was no major input from the corals in which peloids are found in large quantities.

The higher molecular weight fractions of the organic matter were also studied, in an attempt to discover the mechanism of the involvement with the inorganic phase. Although there is no literature that specifically discusses organic matter in the peloidal cements, other molecular oriented studies of organic-inorganic interactions have consistently indicated that proteins or polypeptides are involved. The fingerprinting type techniques employed in this study have not confirmed the presence of polypeptides, and have rather tended to suggest that polysaccharide type molecules are involved. However, the studies cannot be considered to prove that polysaccharides are the active components.

The study emphasises the need to characterise fully the organic matter and not to concentrate on particular fractions. A full study of both low and high molecular weight fractions can provide a great deal of valuable information regarding the nature of organic-inorganic interactions. Although the organic matter that is preserved in the Holocene reefs appears to be of algal type and therefore of high oil generation potential, the total organic content is extremely low (of the order of 0.05%), so that reefs are not likely to be significant sources of hydrocarbons.

7.1.6 Modelling of the distribution of cements.

The ability to model accurately the hydrological aspects of diagenesis is a technique that has only very recently been considered as important (Schroeder & Purser, 1986). It is difficult to conceive of a useful mathematical description of a reef due to the heterogeneity of the structure. In this study the approach has been to create a model based on a judicious simplification of the geometry of coral framestones on the thin section scale. The results of the modelling substantiate the hypothesis that the distribution of cements is dependent primarily on the relative flux of pore fluids and further that the flux is itself dependent on the permeability of the microenvironment.

The study of the poro-perm characteristics of the Miocene reef indicates the importance of the meteoric diagenetic environment in the evolution of porosity of reefs and associated facies. Although the reef studied exhibited very well defined stages in the development, whose original porosity and permeability would be expected to be broadly predictable, the effect of the meteoric diagenesis has been to alter completely the depositional characteristics.

Whilst the prediction of cementation patterns on the reef scale will always be extremely difficult, due to the heterogeneity of the structure of reefs, the models described could be applied to the prediction of general flow characteristics on a range of scales. It is clear that effective modelling at any scale has to be based on an accurate description of the rock matrix at that scale. The potential of this type of modelling is very high, particularly if more precise descriptions of the poro-perm characteristics, in the form of capillary pressure curves, could be used to describe the geometry of the model itself. Similar model designs could be used to model the poro-perm characteristics on a larger scale, right up to reservoir or migration pathway levels, if a suitable characterisation of the properties at that level can be made.

7.1.7 Cementation in ancient reefs.

Marine cementation has been shown to be the primary porosity reducing process in the diagenetic history of a Triassic reef complex. The study highlights the important differences between reefs which are formed by the massive growth of framebuilding organisms and those which form by the simple accumulation of material through trapping and binding activities. The latter generally have a much lower primary porosity, although not necessarily lower permeability. The large amount of reef rubble in the latter reefs tends to have particularly high permeability and is therefore particularly rapidly cemented. The fore-reef clearly had the highest original porosity and permeability and so the development of the submarine cements is greatest in that facies. The other facies in which the cementation appears to have been particularly extensive is the back reef sands, again probably due to high permeability. It is interesting to note that the facies with the initially highest reservoir potential are also those that are most likely to be sealed at an early stage. It is also notable that the dolomitisation events do not appear to have significantly enhanced the porosity of the reef.

7.1.8 The conceptual model of cementation in reefs.

The main results of the study, in combination with the literature, can be combined into a succinct conceptual model to account for the geochemistry and distribution of cements in modern and ancient reefs. Whilst the following clearly does not address all the aspects, the major controls are highlighted.

The geochemistry of the cements precipitated in the marine environment is controlled by a delicate thermodynamic balance which may be affected by physical, organic and inorganic processes. Although there appears to be no direct contribution to the cements from organic sources, there is an indirect involvement of organic matter in some phases. This organic matter catalyses the precipitation of the inorganic phase and is probably of algal origin. The distribution and the extent of cementation are controlled primarily by the local permeability of the system. The observed heterogeneity of the cementation sequences is a result of the spatial and temporal interaction of cementation with other reef forming processes of construction, destruction and sedimentation.

7.2 Implications for Reservoir Development in Reefs and Associated Facies.

7.2.1 Introduction.

The poro-perm characteristics of carbonate reservoirs evolve as a function of both depositional and diagenetic characteristics. The depositional porosity and permeability vary with reef facies, and are dependent on the structure of the reef core. The structure of the reef is in turn dependent on the major framebuilding organisms, the nature of which have evolved with time. The depositional characteristics are discussed first, followed by a description of the effects of diagenesis in both marine and other important environments.

7.2.2 Facies variation of initial porosity and permeability.

The depositional porosity and permeability of modern reefs varies with facies in a manner which is fairly simple to characterise. Although the reef core has a particularly high initial porosity, typically 50–70%, the permeability may not be as high as in other facies. This is primarily due to the geometry of the porosity in biogenically produced skeletal material. A substantial proportion of the porosity in coral skeletons has been shown to be non-effective, and the permeability is very markedly anisotropic. The activity of other secondary framebuilding organisms can reduce the permeability substantially due to their lamellar encrusting habit. Nevertheless, the areas within the reef core which are formed of framebuilding material are interspersed with coarse accumulated sediments, and if the volume of these is sufficiently high such that some 3-D interconnection of the rudstone and grainstone pockets occurs, then the reef core as a whole may have good permeability.

The coarse proximal reef talus and the reef flat rudstone and back reef grainstones are likely to have the best and most homogeneous permeability characteristics, because the majority of the porosity is intergranular and not intra skeletal. Lagoonal or more distal back reef sediments are likely to have worse permeability due to the admixture of fine grained sediments in the lower energy environments.

It is essential to describe the primary depositional porosity, but the proportion of this which is preserved is generally quite small, as a result of a variety of diagenetic processes. The evolution of the primary characteristics depends on the degree of involvement of three major aspects; cementation, dissolution and dolomitisation. Early diagenesis can preserve, occlude or enhance initial porosity, and the interaction of the various events depends on the primary porosity and permeability as well as the nature of the organisms. The mineralogy of the components is particularly important also, because of their differing stability in fluids of different compositions. Although the porosity is commonly modified during diagenesis, many reservoirs produce from preserved primary porosity (Roehl & Choquette, 1985).

7.2.3 Reef building organisms.

As the major reef building organisms have evolved, so has the nature of the porosity within reef accumulations. During periods when massive framebuilding organisms were abundant, the primary reef core porosity will have been particularly high. In contrast, some periods of reef formation were dominated by reef mounds lacking major wave resistant frameworks. These were formed by trapping, baffling and binding organisms, and the primary porosity would have been low. The latter reefs can form substantial accumulations, with very large amounts of reef debris, such as is evident in the Triassic example studied in Chapter 6, and although the permeability of the debris itself would be high, the overall permeability would be substantially reduced by the geometry of the binding and baffling organisms. Reef talus and back reef sediments would be similar in poro-perm characteristics, irrespective of the nature of the reef building organisms. In summary, the greater the input of massive reef framework biota, the greater the likely primary porosity in the reef core.

Ordovician reefs were largely reef mounds, formed by cyanobacteria and calcifying algae with a considerable skeletal input but no major framebuilding organisms, but during the Middle to late Ordovician, and through to the end of the Devonian, a major evolution of massive coral and stromatoporoids occurred. A widespread extinction event at the end of the Devonian removed many of the framebuilding organisms, such that Carboniferous buildups are mainly reef mounds. This trend continued into the Permian with the phylloid algal dominated mud mounds. After the end Permian extinction event, there was very little or no reef formation until the Middle to Late Triassic. Some corals existed during this early recovery of reef building biota, but they did not form massive frameworks until Norian and Rhaetian times. The Jurassic was a period when both types of reef were common. The reef mounds generally formed in deeper water, with the framework dominated coral and stromatoporoid reefs growing on the shelf margins. The Cretaceous reefs were dominated by the rudist bivalves and the Cenozoic reefs are broadly similar to modern examples, the major framebuilders being scleractinian corals.

7.2.4 The effects of early marine cementation on reservoir potential.

The development of early marine cements is widespread within modern reefs, and appears to be equally widespread in geological time, with most studies of ancient reefs recognising early marine precipitates (James, 1985; Schroeder & Purser, 1986). In the majority of circumstances and in most facies, the precipitation of marine cements has a detrimental effect on porosity and permeability. In reefs exposed to marine fluids for long periods of time, the porosity is typically reduced from the primary value of 20–50 % to less than 5%. Rapid burial and the concomitant removal from the high energy, high flow-rate environments will prevent such drastic reduction in the porosity. The variation in cementation across facies depends primarily on the permeability, hence it is an unfortunate fact that the facies with highest initial permeability will be most likely to lose that through the precipitation of pore occluding cements. The fore reef will be most rapidly cemented as it is in the highest energy environment, and the cementation rate will reduce as the energy level decreases. Although the reef flat rubble and the coarse back reef sediments have probably the highest permeability, the lack of a stable substrate can significantly retard the cementation at the surface. If accumulation rates are very high, then as in the Dry Tortugas reefs described in Chapter 2, large volumes of reef debris can be buried with much of the primary porosity preserved. The preservation potential is, therefore, controlled by the interaction between accumulation rates, flux of marine pore fluids and the length of time that the formation remains in the shallow marine environment. Hence the back reef sands of the Triassic Hafelekar reef accumulated slowly, were in the marine environment for long periods and were extensively cemented, with very little primary porosity preserved.

It is interesting to note that some slight cementation of grainstone sediments can be advantageous in terms of porosity preservation. Even slight lithification can increase the strength of the sediments substantially, reducing later compaction. Loss of porosity can be minimal, but the contribution to the preservation of porosity and permeability can be substantial (Purser, 1978).

In terms of the overall reef setting, the best potential reservoirs will be in reefs formed in lower energy areas, such as lagoonal patch reefs or the deeper water pinnacle reefs formed on carbonate ramps. This is simply due to the lower energy of these environments such that the extent of cementation will be reduced compared to shelf edge reefs. Rapid accumulation with rising sea level, followed either by drowning and burial by deeper water sediments, or by a rapid regression and burial by lagoonal sediments and evaporites are the ideal sequences for the development of reservoirs in reef facies.

7.2.5 The meteoric diagenetic environment.

Diagenesis in the meteoric environment can have probably the most substantial effects on the evolution of the porosity within reefs and associated facies. In areas of high rainfall, the discharge through groundwater aquifers can be high, and the diagenetic processes can therefore occur in relatively short periods of time. Meteoric fluids can both enhance and occlude primary porosity, with the balance dependent on the saturation state of the fluids, the mineralogy of the substrate and the rate of flux through the formation. Enhancement of porosity occurs by the dissolution of the substrate, a process which tends to follow the primary permeability, leading to the formation of solution enlarged porosity. The higher the amount of unstable components, such as aragonite bioclasts, the greater will be the increase in porosity. Over long periods of time, massive karst features can be developed, producing vuggy and cavernous porosity and exceedingly high permeability.

Creation of secondary dissolution porosity may be facies dependent, tending to occur preferentially in areas of greatest initial permeability. Hence in settings where the back reef sands have been only lightly cemented, the effects of meteoric water can increase the porosity through the dissolution of the aragonite bioclasts. This type of biomouldic porosity is very commonly recognised in hydrocarbon reservoirs (Roehl & Choquette, 1985).

However, the dissolution is dependent on the water being undersaturated at least with respect to aragonite, a situation which will persist only if there is a substantial exchange of fluids. In areas where the flow rates are lower, the meteoric water will rapidly become saturated with respect to calcium carbonate, and net precipitation will occur. Although dissolution may continue close to the recharge area, there may be a considerable volume of meteoric cement precipitated in the downflow direction. The Miocene reef samples studied in Chapter 5 illustrate the effects of meteoric diagenesis. They show very little evidence of cementation in the marine environment, but there is clearly a significant formation of secondary porosity. The relevance of the initial mineralogy is also evident in these samples, with much of the porosity being biomouldic in origin. However, the original porosity of up to 50%, which may have been increased by the dissolution event, was later reduced by the precipitation of large volumes of meteoric spar. Nevertheless, porosity values are still very good in terms of reservoir potential, ranging from 5–20%. The distribution of the porosity and permeability is, however, unpredictable and inhomogeneous, and certainly not related to the primary facies. Permeability values vary from zero to several hundred mD even in small hand specimens.

In a recent compilation by Roehl & Choquette (1985), the effects of meteoric fluids are recognised in the majority of reservoirs producing from reefs or associated facies. In many examples, the greatest amount of porosity is mouldic in origin, and in some reservoirs, production is entirely dependent on the secondary porosity. Porosity can be further enhanced by the fluids rich in organic acids which precede and accompany oil migration. Dissolution processes are very important in the Cretaceous of the Middle East (Harris & Frost, 1984), creating much of the porosity in oolitic and bioclastic grainstone reservoirs.

7.2.6 Dolomitisation.

The generally accepted view that dolomitisation enhances porosity, leading to improved reservoir properties may be an over-estimation. A compilation of data on limestone reservoirs in the United States (Schmoker et al., 1985) indicated that dolomite reservoirs are better quality due to the increased fracturing and not necessarily due to improved poro-perm characteristics of the formation.

The study of dolomitisation in this thesis has been rather limited, but there does not appear to have been any significant increase in the permeability of the Triassic Hafelekar reef (Chapter 6) due to the dolomitisation events. Early dolomite is commonly associated with dissolution, such that the improved porosity is mainly due to that dissolution. Later pervasive dolomitisation occurring during burial can improve the porosity and permeability due to the overall decrease in volume, but this intercrystalline porosity can be reduced by the later burial precipitation of pore filling dolomite cements. Nevertheless, late dolomitisation can improve the reservoir potential of an otherwise 'tight' limestone.

7.2.7 Fractures.

Fracturing can have a very important effect on the reservoir properties of reef carbonates. The reef core may be more prone to fracturing due to its rigidity, compared to the reef sediments which behave in a more plastic manner to the tectonic stresses (Wilson, 1977). Fracturing is more common in dolomitised reservoirs (Schmoker et al., 1985), a fact attributed to the greater ultimate strength of dolomite, leading to a more brittle behaviour than limestones.

The importance of fractures is evident in the results of the permeability measurements made on the Miocene reef material, where the highest permeability figures correspond to the core-plugs in which fracturing is evident. It is difficult to ascertain whether fractures are important on the whole reef scale in the Miocene, but they clearly only improve the general properties. These observations provide further evidence that the measurement of permeability using small core plugs is not a reliable technique for carbonates.

Fracture permeability is commonly referred to in studies of carbonate reservoirs (Roehl & Choquette, 1985), as it can significantly improve the production rate, both by the simple increase in permeability, and by the fact that fractures can interconnect areas of high permeability which were otherwise isolated. This is particularly important in reservoirs where cemented horizons act as barriers to bed normal flow.

Deeper burial can also reduce porosity drastically through the process of pressure solution, whereby large sequences of limestone can be compacted and dissolved, with the additional effect that the dissolved carbonate is commonly precipitated as pore occluding cements in the close vicinity. Further precipitation of burial spars can reduce the porosity of a reef formation to essentially zero, as is evident in the study of the Triassic reef, where even late fractures are sealed.

7.2.8 Summary of the development of reservoir potential in reef carbonates.

The primary porosity and permeability is highest in framework dominated reefs, in particular in the coarse reef flat rubble and both fore-reef talus and back-reef facies. Marine diagenesis reduces the porosity through the precipitation of pore occluding cements, and the precipitation occurs at a faster rate in areas of higher energy and higher initial permeability. Extended exposure to marine pore fluids can reduce the porosity to less than 5%. Reefs formed in lower energy environments which are then rapidly buried are likely to have the highest preserved primary porosity.

Meteoric diagenesis can enhance the porosity and permeability of a reef formation, but can also reduce the reservoir potential significantly due to the precipitation of large volumes of spar cements. There is therefore a balance between net porosity gain and loss, net gain being highest in areas where the largest flux of meteoric water occurs in an open diagenetic system. The initial mineralogical composition of the formation is very important, as the greater the amount of aragonite, the higher is the potential gain in porosity.

Dolomitisation can increase the porosity and permeability of otherwise tight limestones, but the enhancement is not perhaps as great as has been commonly considered. Precipitation of dolomite cement occurs at depth and can significantly reduce porosity. Fracturing is an important process that increases the permeability of carbonate reservoirs of all types.

CHAPTER 8

Conclusions.

CHAPTER 8

Conclusions.

The emphasis in this thesis has been to study the topic of cementation in modern and ancient reefs on a variety of scales, through the use of a range of analytical techniques. The intention has been to clarify the understanding of the controls on the geochemistry and distribution of cements precipitated within reefs and associated facies. Several specific research objectives were identified in Section 1.14, concerned with aspects which were not clearly understood in the literature. These were as follows:

i) The degree of biogenic control in the precipitation of cements.

ii) The role of organic matter in the prevention and promotion of the precipitation of cements.

iii) The factors controlling the distribution of cements on a variety of scales.

iv) The timing of cementation and its effect on the evolution of the porosity of ancient reefs.

With regard to these aspects, a number of general conclusions can be drawn from the research presented in this thesis:

[1] Cementation patterns within modern reefs are extremely inhomogeneous on all levels from the whole reef down to the pore to pore scale.

[2] A major control on the distribution of cements is the interaction of the cementation process, in both space and time, with reef construction, destruction and sedimentation.

[3] Quantification of cementation as a function of the porosity available at the time of precipitation, aids the understanding of the diagenetic history and has highlighted the fact that most of the cementation occurs at the surface of reefs.

[4] A significant amount of the porosity of carbonate framestones, as observed in thin section, is 'non-effective'. It is for this reason that some pores in otherwise well cemented samples are devoid of cement.

[5] The geochemical composition of cements from the modern reefs of Florida and Belize reflect precipitation at or near to equilibrium with seawater of normal marine composition. There is no direct input of organically derived carbon and the reef building organisms do not appear to exert any significant effect on the precipitation of the cements. However, the interaction of the biogenic cycles with the ocean reservoir of bicarbonate could result in recognisable modification of the isotopic composition in closed systems.

[6] Organic matter is definitely associated with the peloidal cements, and does not originate from a single source. The results of biological marker studies are most consistent with an algal source, probably green algal, with a possible contribution from cyanobacteria. There is no support for a bacterial mediation of the precipitation.

[7] Detailed studies of the high molecular weight components of the organic matter may help to determine the nature of the organic-inorganic interaction. From a theoretical point of view, the interaction is likely to be with highly organised molecules such as proteins and polysaccharides, similar to those involved in skeletogenesis processes. The investigation of this type

of material is exceedingly difficult, However, there is more evidence for the presence of polysaccharides in the organic phase of the peloids than there is for proteins.

[8] Simple mathematical models have aided the understanding of hydrologic processes within reef frameworks. The results of this modelling support the suggestion that the distribution of cements within carbonate framestones is controlled primarily by the fluid flux. This in turn is dependent on the permeability of the pore network. Hence, any process which affects the permeability or directly alters flow rates will have an effect on cementation.

[9] Accurate modelling of hydrological characteristics depends on the acquisition of permeability data that are representative of the scale at which the modelling is operative. Diagenetic events can completely mask the primary depositional characteristics, particularly in the case of reef core facies.

[10] In a study of the distribution of cements within one specific Triassic reef, the major reduction in porosity was found to have occurred in the marine environment. Precipitation of fibrous cements was pervasive and occurred under uniform conditions throughout the reef. The porosity was reduced from primary levels of up to 50% to less than 5% at a geologically rapid rate. Remaining porosity was occluded by the precipitation of burial spar cements.

APPENDICES 1–6

Appendix 1

A1.1 Point Counting Data.

The following point counting data are based on 250 points per thin section. Figures are presented for all of the cores through Alligator Reef, the four major cores through South East Reef Dry Tortugas, and the two cores through Pulaski Reef and Loggerhead Key. Depths given in metres are approximate due to some uncertainty in the exact position of the recovered core sections, although the depth order is correct. Some figures for samples of Glovers Reef from Belize are also quoted. Average figures for each core and for the whole of Alligator and South East Reef are also presented below.

The second set of tables give the calculations of the percentage of cements as a function of the total porosity available at the time of precipitation. Three different methods of calculation were employed as described in Section 2.8.6. Values given in columns 'S' below were quoted in the discussion in Chapter 2.

An extra column 'U' is given for Hole 5, Dry Tortugas. In this column the volume of meteoric spar was considered to be porosity. This is assuming that the marine cements were precipitated prior to the precipitation of the spars. The figures in the other columns are based on the assumption that the marine cements were precipitated after the meteoric spars in the present marine conditions.

Alligator Reef Hole 1

Core Code	Depth metres	Framestone %	Porosity %	Bioerosional Porosity	Fibrous %	Peloids %	Micrite %	Encrusters %	Grainstones %	Packstone Wackestone	Microcryst Aragonite	Spar Cement	Neomorphic Calcite	Total %
A10	0.08	20.0	28.5	0.0	5.5	13.5	5.0	27.5	0.0	0.0	0.0	0.0	0.0	100.0
A9	0.16	52.4	26.0	0.0	6.4	1.2	4.0	10.0	0.0	0.0	0.0	0.0	0.0	100.0
A8	0.24	29.4	24.6	0.0	10.4	3.6	8.0	24.0	0.0	0.0	0.0	0.0	0.0	100.0
A7	0.49	17.2	36.0	0.0	6.4	3.2	25.2	12.0	0.0	0.0	0.0	0.0	0.0	100.0
A6	0.59	65.6	20.4	0.0	8.8	2.0	3.2	0.0	0.0	0.0	0.0	0.0	0.0	100.0
A5	0.74	50.8	37.2	0.0	2.4	0.8	8.8	0.0	0.0	0.0	0.0	0.0	0.0	100.0
A4	0.82	54.0	40.0	0.0	2.4	0.0	3.2	0.4	0.0	0.0	0.0	0.0	0.0	100.0
A3U	0.95	52.0	22.0	0.0	10.4	3.4	6.4	5.6	0.0	0.0	0.0	0.0	0.0	100.0
A3L	1.10	33.2	28.4	0.0	2.0	5.6	26.0	4.8	0.0	0.0	0.0	0.0	0.0	100.0
A2	1.33	16.0	41.5	0.0	5.0	0.0	14.0	23.5	0.0	0.0	0.0	0.0	0.0	100.0
A1	1.50	27.2	23.6	0.0	4.8	0.0	20.8	23.6	0.0	0.0	0.0	0.0	0.0	100.0
A1A	3.00	48.0	48.0	0.0	4.0	0.0	0.0	0.0	0.0	0.0	0.0	0.0	0.0	100.0
	mean	38.8	31.4	0.0	5.7	2.8	10.4	11.0	0.0	0.0	0.0	0.0	0.0	

Alligator Reef Hole 1A

Core Code	Depth metres	Framestone %	Porosity %	Bioerosional Porosity	Fibrous %	Peloids %	Micrite %	Encrusters %	Grainstones %	Packstone Wackestone	Microcryst Aragonite	Spar Cement	Neomorphic Calcite	Total %
B6	0.40	12.4	43.6	0.0	1.2	0.8	36.0	6.0	0.0	0.0	0.0	0.0	0.0	100.0
B5	0.60	31.6	27.2	0.0	7.6	18.8	12.4	2.4	0.0	0.0	0.0	0.0	0.0	100.0
B4	0.70	69.2	15.6	0.0	2.8	0.4	8.4	2.0	0.0	0.0	1.6	0.0	0.0	100.0
B3	0.80	46.4	20.0	0.0	9.2	6.8	16.8	0.8	0.0	0.0	0.0	0.0	0.0	100.0
B2	1.70	68.8	25.6	0.0	3.2	0.4	0.8	1.2	0.0	0.0	0.0	0.0	0.0	100.0
B1	1.80	44.8	24.8	0.0	2.4	7.6	4.8	12.0	0.0	0.0	3.6	0.0	0.0	100.0
	mean	45.5	26.1	0.0	4.4	5.8	13.2	4.1	0.0	0.0	0.9	0.0	0.0	

Alligator Reef Hole 2

Core Code	Depth metres	Framestone %	Porosity %	Bioerosional Porosity	Fibrous %	Peloids %	Micrite %	Encrusters %	Grainstones %	Packstone Wackestone	Microcryst Aragonite	Spar Cement	Neomorphic Calcite	Total %
C9U	0.15	12.8	30.4	0.0	2.4	2.0	5.6	24.8	0.0	22.0	0.0	0.0	0.0	100.0
C9L	0.35	36.0	22.8	3.6	1.2	2.4	10.8	20.8	0.0	2.4	0.0	0.0	0.0	100.0
C8	1.00	56.4	20.0	13.2	4.8	1.6	2.4	1.6	0.0	0.0	0.0	0.0	0.0	100.0
C7U	1.20	48.8	12.4	26.8	2.0	1.6	4.8	3.2	0.0	0.0	0.4	0.0	0.0	100.0
C7L	1.30	63.2	34.0	0.0	0.0	0.0	1.6	1.2	0.0	0.0	0.0	0.0	0.0	100.0
C6	1.50	36.0	38.4	0.0	1.2	8.4	10.0	6.0	0.0	0.0	0.0	0.0	0.0	100.0
C5	1.62	0.00	62.4	0.0	2.0	0.0	1.2	34.4	0.0	0.0	0.0	0.0	0.0	100.0
C4	1.70	15.0	39.0	0.0	1.0	3.5	9.0	30.0	0.0	2.5	0.0	0.0	0.0	100.0
C3	1.78	46.0	40.8	0.0	3.6	1.6	4.4	2.0	0.0	0.0	1.6	0.0	0.0	100.0
C2	1.88	32.0	15.2	0.0	0.8	2.0	12.4	28.0	0.0	8.8	0.8	0.0	0.0	100.0
C1	2.18	45.5	37.0	0.0	3.5	5.5	0.5	0.0	0.0	0.0	8.0	0.0	0.0	100.0
	mean	35.6	32.0	4.0	2.0	2.6	5.7	13.8	0.0	3.2	1.0	0.0	0.0	

Alligator Reef Hole 3

Core Code	Depth metres	Framestone %	Porosity %	Bioerosional Porosity	Fibrous %	Peloids %	Micrite %	Encrusters %	Grainstones %	Packstone Wackestone	Microcryst Aragonite	Spar Cement	Neomorphic Calcite	Total %
D17	0.20	34.4	26.4	14.4	5.6	5.2	5.6	0.0	3.6	4.8	0.0	0.0	0.0	100.0
D16	0.26	49.5	20.0	0.0	6.4	1.2	10.5	11.0	0.0	9.0	0.0	0.0	0.0	100.0
D15	0.32	61.0	12.5	0.0	0.0	0.0	0.0	1.0	4.5	21.0	0.0	0.0	0.0	100.0
D14	0.44	54.0	22.0	0.0	3.2	1.6	8.8	0.0	0.0	10.4	0.0	0.0	0.0	100.0
D14	0.49	49.2	20.0	0.0	6.0	6.8	4.8	0.4	1.2	11.6	0.0	0.0	0.0	100.0
D13	0.57	34.0	36.0	0.0	1.5	0.0	4.5	8.5	4.0	11.5	0.0	0.0	0.0	100.0
D12	0.75	60.5	38.0	0.0	0.0	0.0	0.0	0.0	1.5	0.0	0.0	0.0	0.0	100.0
D11	1.45	48.0	36.0	0.0	2.0	0.0	0.4	0.0	10.4	2.8	0.4	0.0	0.0	100.0
D11	1.55	56.0	32.8	0.0	3.2	2.0	4.4	0.0	0.8	0.8	0.0	0.0	0.0	100.0
D9	1.82	33.6	22.8	8.8	0.0	0.0	10.4	0.8	6.4	16.4	0.0	0.0	0.0	100.0
D8	1.93	47.6	24.0	0.0	10.8	2.0	2.8	0.0	4.4	8.0	0.4	0.0	0.0	100.0
D7U	2.10	43.2	30.4	0.0	6.4	1.6	4.8	0.4	12.8	0.0	0.4	0.0	0.0	100.0
D7M	2.17	56.4	30.0	0.0	4.0	1.6	0.8	0.0	4.0	3.2	0.0	0.0	0.0	100.0
D7L	2.20	47.6	31.6	0.0	1.6	0.0	5.2	4.0	8.8	0.0	1.2	0.0	0.0	100.0
D6	2.30	26.0	26.8	0.0	6.0	1.2	7.6	8.0	22.4	2.0	0.0	0.0	0.0	100.0
D5	2.39	0.0	35.6	0.0	0.0	0.0	2.8	58.8	0.0	2.8	0.0	0.0	0.0	100.0
D4U	2.45	0.0	36.0	0.0	0.0	0.0	15.0	49.0	0.0	0.0	0.0	0.0	0.0	100.0
D4M	2.50	0.0	29.6	0.0	0.0	0.0	0.0	68.0	0.0	2.4	0.0	0.0	0.0	100.0
D4L	2.55	2.4	38.4	0.0	0.8	0.0	7.6	35.6	0.0	15.2	0.0	0.0	0.0	100.0
D3	2.62	10.8	32.8	0.0	0.4	0.4	8.0	38.4	0.0	9.2	0.0	0.0	0.0	100.0
D2	2.82	26.0	50.4	0.0	2.4	0.0	5.6	13.2	0.0	2.4	0.0	0.0	0.0	100.0
D1	3.00	14.0	15.2	16.0	0.0	0.0	28.0	19.2	0.0	7.6	0.0	0.0	0.0	100.0
	mean	32.8	30.2	1.7	2.4	1.0	6.5	13.8	4.9	6.2	0.1	0.5	0.0	

Alligator Reef Hole 4

Core Code	Depth metres	Framestone %	Porosity %	Bioerosional Porosity	Fibrous %	Peloids %	Micrite %	Encrusters %	Grainstones %	Packstone Wackestone	Microcryst Aragonite	Spar Cement	Neomorphic Calcite	Total %
E10	0.40	62.0	24.8	0.0	10.0	1.2	2.0	0.0	0.0	0.0	0.0	0.0	0.0	100.0
E9	0.60	33.6	27.6	5.2	3.2	10.0	5.2	3.2	12.0	0.0	0.0	0.0	0.0	100.0
E8	1.00	54.4	36.0	0.0	6.8	2.4	0.4	0.0	0.0	0.0	0.0	0.0	0.0	100.0
E7	1.15	32.0	36.0	2.0	0.8	0.8	3.6	5.2	2.4	17.2	0.0	0.0	0.0	100.0
E6U	1.35	65.6	22.8	5.2	0.4	0.0	6.0	0.0	0.0	0.0	0.0	0.0	0.0	100.0
E6L	1.40	44.8	42.8	0.0	1.0	0.0	11.4	0.0	0.0	0.0	0.0	0.0	0.0	100.0
E5	1.50	37.6	39.2	21.2	0.8	0.8	0.4	0.0	0.0	0.0	0.0	0.0	0.0	100.0
E4	1.85	80.8	18.0	0.0	0.4	0.0	0.0	0.0	0.0	0.0	0.8	0.0	0.0	100.0
E3	2.10	68.4	20.0	2.8	7.2	0.0	0.0	0.0	0.4	0.0	1.2	0.0	0.0	100.0
E2	2.60	61.0	27.0	12.0	0.0	0.0	0.0	0.0	0.0	0.0	0.0	0.0	0.0	100.0
	mean	54.0	29.4	4.8	3.1	1.5	2.9	0.8	1.5	1.7	0.2	0.0	0.0	

Alligator Reef Hole 5

Core Code	Depth metres	Framestone %	Porosity %	Bioerosional Porosity	Fibrous %	Peloids %	Micrite %	Encrusters %	Grainstones %	Packstone Wackestone	Microcryst Aragonite	Spar Cement	Neomorphic Calcite	Total %
F18	0.36	53.0	24.5	4.5	7.0	1.0	6.0	4.0	0.0	0.0	0.0	0.0	0.0	100.0
F18	0.50	20.5	16.5	5.0	7.0	2.0	22.0	17.0	8.0	2.0	0.0	0.0	0.0	100.0
F16	0.90	23.5	29.0	5.5	0.0	0.0	7.5	22.5	12.0	0.0	0.0	0.0	0.0	100.0
F15	1.30	46.0	29.5	3.5	8.5	2.5	8.5	0.0	1.5	0.0	0.0	0.0	0.0	100.0
F14	1.50	57.2	32.0	8.0	0.8	1.2	0.0	0.0	0.0	0.0	0.0	0.0	0.0	100.0
F13	1.54	32.0	28.0	4.5	1.0	3.0	19.5	5.5	6.5	0.0	0.0	0.0	0.0	100.0
F12	1.75	42.5	49.5	0.5	1.5	0.0	4.0	1.0	1.0	0.0	0.0	0.0	0.0	100.0
F11	1.90	36.0	33.0	0.0	1.0	2.0	12.5	15.5	0.0	0.0	0.0	0.0	0.0	100.0
F6	2.65	66.0	13.0	0.0	0.0	0.0	8.0	6.0	7.0	0.0	0.0	0.0	0.0	100.0
F4	2.92	66.2	26.3	0.0	0.0	0.0	2.6	4.9	0.0	0.0	0.0	0.0	0.0	100.0
F3L	3.00	14.5	21.0	3.0	1.0	0.0	5.0	20.0	35.5	0.0	0.0	0.0	0.0	100.0
	mean	41.6	27.5	2.5	3.2	1.0	8.8	8.8	6.5	0.2	0.0	0.0	0.0	

Alligator Reef Hole 6

Core Code	Depth metres	Framestone %	Porosity %	Bioerosional Porosity	Fibrous %	Peloids %	Micrite %	Encrusters %	Grainstones %	Packstone Wackestone	Microcryst Aragonite	Spar Cement	Neomorphic Calcite	Total %
G15	0.07	35.2	5.0	0.0	9.0	20.6	9.4	1.8	19.0	0.0	0.0	0.0	0.0	100.0
G15	0.10	62.5	20.5	0.0	3.0	10.0	3.5	0.0	0.0	0.5	0.0	0.0	0.0	100.0
G14	0.12	44.0	17.5	1.5	11.5	6.5	13.5	5.0	0.0	0.5	0.0	0.0	0.0	100.0
G13	0.18	39.5	11.5	0.0	9.5	15.0	8.5	8.0	0.0	8.0	0.0	0.0	0.0	100.0
G13	0.20	49.0	21.5	0.0	13.0	8.5	5.5	0.0	0.0	2.5	0.0	0.0	0.0	100.0
G13	0.24	35.0	8.0	0.0	14.6	12.8	20.8	0.4	8.4	0.0	0.0	0.0	0.0	100.0
G12	0.31	20.4	45.8	0.0	6.2	0.4	22.2	1.0	4.0	0.0	0.0	0.0	0.0	100.0
G11	0.36	45.2	15.2	3.2	3.2	2.0	7.6	0.0	0.0	23.6	0.0	0.0	0.0	100.0
G10	0.50	65.6	13.2	1.6	5.6	0.0	2.0	0.0	0.0	12.0	0.0	0.0	0.0	100.0
G9	0.58	49.2	21.2	6.0	6.4	0.0	5.2	0.0	0.8	8.4	2.8	0.0	0.0	100.0
G8	0.70	30.4	22.8	16.0	7.6	5.2	5.2	6.8	0.4	5.6	0.0	0.0	0.0	100.0
G7	0.86	1.6	25.2	5.6	0.0	4.0	8.4	52.0	1.6	1.6	0.0	0.0	0.0	100.0
G6	0.95	71.2	8.8	0.0	0.4	2.8	10.4	4.4	0.8	1.2	0.0	0.0	0.0	100.0
G5	1.10	67.2	15.6	3.6	1.6	0.8	2.8	4.4	0.4	3.6	0.0	0.0	0.0	100.0
G4	1.20	85.6	9.2	0.0	1.2	0.8	2.8	0.0	0.4	0.0	0.0	0.0	0.0	100.0
G3U	1.28	64.4	19.2	0.4	8.0	2.8	2.4	2.4	0.4	0.0	0.0	0.0	0.0	100.0
G3L	1.34	3.8	35.4	0.0	6.6	0.0	0.8	6.8	46.6	0.0	0.0	0.0	0.0	100.0
G2	1.44	83.2	15.6	0.0	1.2	0.0	0.0	0.0	0.0	0.0	0.0	0.0	0.0	100.0
G1	1.50	80.0	12.8	0.0	1.2	0.4	3.2	0.0	2.4	0.0	0.0	0.0	0.0	100.0
	mean	49.1	18.1	2.0	5.8	4.9	7.1	4.9	4.5	3.6	0.1	0.0	0.0	

Dry Tortugas Reef Hole 1

Core Code	Depth metres	Framestone %	Porosity %	Bioerosional Porosity	Fibrous %	Peloids %	Micrite %	Encrusters %	Grainstones %	Packstone Wackestone	Microcryst Aragonite	Spar Cement	Neomorphic Calcite	Total %
J29	3.72	16.5	14.5	3.0	1.0	0.0	7.0	47.5	10.5	0.0	0.0	0.0	0.0	100.0
J28	4.04	33.5	16.5	12.0	1.0	0.0	0.0	12.0	1.5	23.5	0.0	0.0	0.0	100.0
J27	4.36	10.5	10.5	6.0	0.0	0.0	0.0	28.0	0.5	44.5	0.0	0.0	0.0	100.0
J25	5.20	65.0	35.0	0.0	0.0	0.0	0.0	0.0	0.0	0.0	0.0	0.0	0.0	100.0
J24	7.50	70.0	30.0	0.0	0.0	0.0	0.0	0.0	0.0	0.0	0.0	0.0	0.0	100.0
J23	7.86	64.0	15.6	0.0	0.0	0.0	2.4	13.2	0.8	4.0	0.0	0.0	0.0	100.0
J22	8.14	2.0	20.6	11.8	1.6	0.0	3.6	49.2	0.0	11.2	0.0	0.0	0.0	100.0
J21	8.42	43.0	49.0	0.0	3.5	0.0	4.0	0.0	0.5	0.0	0.0	0.0	0.0	100.0
J20	9.00	59.5	37.0	0.0	0.0	0.0	2.0	0.0	0.0	1.5	0.0	0.0	0.0	100.0
J19	9.45	52.5	35.5	0.0	1.5	0.0	4.0	3.5	1.0	2.0	0.0	0.0	0.0	100.0
J18	9.70	66.4	23.6	2.0	2.8	0.4	2.8	1.2	0.0	0.8	0.0	0.0	0.0	100.0
J17	11.25	40.4	28.0	0.0	6.0	2.8	13.2	8.8	0.0	0.8	0.0	0.0	0.0	100.0
J16	11.45	60.5	33.0	6.0	0.5	0.0	0.0	0.0	0.0	0.0	0.0	0.0	0.0	100.0
J15	11.60	84.5	15.5	0.0	0.0	0.0	0.0	0.0	0.0	0.0	0.0	0.0	0.0	100.0
J14	13.00	51.6	28.4	0.0	4.8	0.0	12.4	1.2	1.2	0.4	0.0	0.0	0.0	100.0
J13	14.00	35.6	21.2	22.8	0.0	0.0	10.4	0.0	2.8	7.2	0.0	0.0	0.0	100.0
J12	14.20	58.5	37.5	2.5	0.5	1.0	0.0	0.0	0.0	0.0	0.0	0.0	0.0	100.0
J11	14.44	68.2	30.4	0.0	1.4	0.0	0.0	0.0	0.0	0.0	0.0	0.0	0.0	100.0
J7	15.80	10.4	36.0	0.0	0.0	2.8	10.4	5.2	0.0	0.0	0.0	6.8	28.4	100.0
J3	16.85	28.8	33.6	0.0	0.0	0.0	2.0	0.0	0.4	0.0	0.0	4.8	30.4	100.0
J2	17.15	41.2	24.4	0.0	0.8	2.4	9.2	0.0	0.0	0.0	0.0	1.6	20.4	100.0
	mean	45.8	27.4	3.1	1.2	0.4	4.0	8.1	0.9	4.6	0.0	0.6	3.9	

Dry Tortugas Hole 2

Core Code	Depth metres	Framestone %	Porosity %	Bioerosional Porosity	Fibrous %	Peloids %	Micrite %	Encrusters %	Grainstones %	Packstone Wackestone	Microcryst Aragonite	Spar Cement	Neomorphic Calcite	Total %
K15	10.8	38.8	23.6	8.0	2.8	0.4	14.4	3.6	1.2	7.2	0.0	0.0	0.0	100.0
K14	11.0	15.2	18.0	13.2	3.2	0.4	3.6	23.2	5.2	18.0	0.0	0.0	0.0	100.0
K13	11.3	43.2	28.4	12.0	4.8	0.0	6.4	4.0	0.0	1.2	0.0	0.0	0.0	100.0
K12	12.5	61.6	35.2	0.0	1.6	0.0	1.6	0.0	0.0	0.0	0.0	0.0	0.0	100.0
K12	12.6	30.0	25.2	16.8	4.8	2.0	3.2	0.0	4.4	13.6	0.0	0.0	0.0	100.0
K12	12.8	46.0	30.4	16.8	2.0	0.4	0.8	0.0	1.2	0.4	2.0	0.0	0.0	100.0
K11	13.2	36.0	34.5	13.0	1.0	1.0	4.5	1.5	0.0	8.5	0.0	0.0	0.0	100.0
K11	13.3	50.0	32.0	3.6	1.6	2.4	3.2	0.0	0.8	6.4	0.0	0.0	0.0	100.0
K9	14.3	0.0	12.0	0.0	0.0	0.0	7.2	43.6	6.0	17.2	0.0	7.6	6.4	100.0
K9	14.4	25.6	19.2	10.8	5.6	0.0	1.4	7.6	1.6	10.8	0.0	0.8	4.0	100.0
K8	14.8	44.4	14.8	10.8	0.0	0.0	4.4	0.0	2.4	10.8	0.0	2.8	9.6	100.0
K6	16.1	0.0	11.0	33.5	0.0	0.0	17.0	31.5	1.0	5.0	0.0	1.0	0.0	100.0
	mean	32.6	23.7	11.5	2.3	0.6	6.7	9.6	2.0	8.3	0.2	1.0	1.7	100.0

Dry Tortugas Hole 8

Core Code	Depth metres	Framestone %	Porosity %	Bioerosional Porosity	Fibrous %	Peloids %	Micrite %	Encrusters %	Grainstones %	Packstone Wackestone	Microcryst Aragonite	Spar Cement	Neomorphic Calcite	Total %
M11	0.1	61.6	26.4	2.0	4.0	0.0	2.8	1.2	0.0	2.0	0.0	0.0	0.0	100.0
M10	0.3	54.8	36.8	5.2	0.8	0.0	2.4	0.0	0.0	0.0	0.0	0.0	0.0	100.0
M9	0.6	46.0	31.2	8.4	2.4	0.4	4.8	0.8	0.4	5.6	0.0	0.0	0.0	100.0
M7	1.0	48.0	28.8	14.8	1.2	0.0	0.8	0.0	4.4	2.0	0.0	0.0	0.0	100.0
M6	1.2	64.0	23.2	0.0	6.8	0.0	2.4	0.0	0.4	3.2	0.0	0.0	0.0	100.0
M6	1.3	68.0	20.8	0.0	5.6	0.0	3.6	0.0	0.0	2.0	0.0	0.0	0.0	100.0
M5	1.4	51.6	26.4	0.0	5.6	0.8	4.8	0.0	0.0	10.8	0.0	0.0	0.0	100.0
M3	2.1	75.6	21.6	0.0	2.8	0.0	0.0	0.0	0.0	0.0	0.0	0.0	0.0	100.0
M2	2.3	46.0	20.0	19.2	2.0	0.0	0.8	8.8	0.4	2.8	0.0	0.0	0.0	100.0
M1	2.6	73.2	20.0	4.8	1.2	0.0	0.0	0.0	0.8	0.0	0.0	0.0	0.0	100.0
M1	2.7	82.8	15.6	0.0	0.8	0.0	0.8	0.0	0.0	0.0	0.0	0.0	0.0	100.0
	mean	61.1	24.6	4.9	3.0	0.1	2.1	1.0	0.6	2.6	0.0	0.0	0.0	100.0

Dry Tortugas Hole 4

Core Code	Depth metres	Framestone %	Porosity %	Bioerosional Porosity	Fibrous %	Peloids %	Micrite %	Encrusters %	Grainstones %	Packstone Wackestone	Microcryst Aragonite	Spar Cement	Neomorphic Calcite	Total %
N1	0.30	63.6	20.0	0.0	2.0	5.2	4.0	0.0	0.0	5.2	0.0	0.0	0.0	100.0
N2	0.40	64.8	24.8	2.0	4.0	2.4	1.2	0.0	0.0	0.8	0.0	0.0	0.0	100.0
N3	0.90	48.0	14.0	5.0	0.0	1.0	1.0	26.5	4.0	0.5	0.0	0.0	0.0	100.0
N5	8.50	36.8	15.6	12.0	0.8	0.0	4.0	6.0	6.8	3.6	0.0	3.6	10.8	100.0
N6	8.70	54.4	26.0	8.0	0.0	0.0	5.2	0.0	0.0	0.0	0.0	2.4	4.0	100.0
N8	8.90	36.8	23.2	6.8	4.0	0.0	9.2	0.0	3.2	16.4	0.0	0.4	0.0	100.0
N9U	9.80	16.8	19.6	4.0	1.2	0.0	2.0	0.0	0.4	0.0	0.0	21.2	34.8	100.0
N9L	9.90	45.4	22.0	23.2	2.2	0.0	5.6	0.0	0.0	0.8	0.0	0.8	0.0	100.0
N10	10.1	28.8	21.2	18.0	3.2	0.0	24.0	0.0	0.0	2.0	0.0	2.4	0.4	100.0
N12	10.3	3.7	26.2	18.5	1.2	0.0	36.8	0.0	1.2	3.1	0.0	7.5	1.8	100.0
N13	10.5	5.4	17.2	21.3	1.8	0.0	44.5	0.0	2.2	0.0	0.0	3.6	4.0	100.0
N14	10.7	24.4	28.4	27.6	0.8	0.4	16.8	0.0	0.0	0.0	0.0	1.6	0.0	100.0
N14	10.8	30.4	23.6	7.6	7.2	7.2	19.2	0.0	0.0	1.2	0.0	1.2	2.4	100.0
N15	10.9	10.4	19.6	13.2	1.2	1.6	34.8	0.0	1.2	0.0	0.0	2.4	15.6	100.0
N16	11.2	0.0	18.5	10.5	0.5	0.0	58.5	0.0	2.5	4.5	0.0	5.0	0.0	100.0
N16	11.3	0.0	22.5	23.0	0.0	0.0	48.0	0.5	0.5	0.0	0.0	5.5	0.0	100.0
	mean	29.4	21.4	12.5	1.9	1.1	19.7	2.1	1.4	2.4	0.0	3.6	4.6	100.0

Alligator Reef and South East Reef Averages

Reef	No. of Thin Sections	Framestone %	Porosity %	Bioerosional Porosity	Fibrous %	Peloids %	Micrite %	Encrusters %	Grainstones %	Packstone Wackestone	Microcryst Aragonite	Spar Cement	Neomorphic Calcite	Total %
Alligator	92	41.9	27.2	2.2	3.8	2.6	7.3	2.8	2.9	0.3	0.0	0.0	9.0	100.0
South East	60	41.6	24.6	7.7	1.9	0.6	8.4	1.2	4.4	0.0	1.4	2.9	5.4	100.0

Loggerhead Reef

Core Code	Depth metres	Framestone %	Porosity %	Bioerosional Porosity	Fibrous %	Peloids %	Micrite %	Encrusters %	Grainstones %	Packstone Wackestone	Microcryst Aragonite	Spar Cement	Neomorphic Calcite	Total %
H34	0.50	52.8	30.4	8.0	2.8	0.0	3.2	0.0	0.4	0.0	2.4	0.0	0.0	100.0
H33	0.70	42.0	55.2	0.0	2.8	0.0	0.0	0.0	0.0	0.0	0.0	0.0	0.0	100.0
H32	4.50	81.6	18.4	0.0	0.0	0.0	0.0	0.0	0.0	0.0	0.0	0.0	0.0	100.0
H31	4.60	56.4	38.8	0.0	2.0	2.4	0.4	0.0	0.0	0.0	0.0	0.0	0.0	100.0
H30	6.60	46.4	34.0	6.8	4.0	2.2	2.0	0.0	0.4	2.0	1.2	0.0	0.0	100.0
H29	7.20	45.2	34.4	6.4	2.4	4.4	4.4	1.6	0.8	0.4	0.0	0.0	0.0	100.0
H28	7.30	38.4	36.8	7.6	3.6	2.0	4.4	0.0	0.0	7.2	0.0	0.0	0.0	100.0
H27	7.40	35.6	20.4	14.0	6.8	0.0	10.8	0.4	0.0	12.0	0.0	0.0	0.0	100.0
H26	7.60	46.0	40.4	2.0	4.8	2.0	4.0	0.0	0.0	0.8	0.0	0.0	0.0	100.0
H24	8.90	50.0	50.0	0.0	0.0	0.0	0.0	0.0	0.0	0.0	0.0	0.0	0.0	100.0
H23	9.10	58.8	40.4	0.0	0.8	0.0	0.0	0.0	0.0	0.0	0.0	0.0	0.0	100.0
H22	10.4	47.2	27.6	8.4	1.2	0.8	6.4	2.8	0.8	4.8	0.0	0.0	0.0	100.0
H21	10.7	58.8	33.2	0.0	1.2	0.0	4.0	0.4	0.0	0.8	1.6	0.0	0.0	100.0
H20	10.9	46.8	36.8	7.2	2.8	0.0	2.0	1.2	2.4	0.8	0.0	0.0	0.0	100.0
H19	12.2	12.0	22.5	25.0	0.0	0.0	4.5	4.5	0.0	31.5	0.0	0.0	0.0	100.0
H18	12.4	14.8	15.6	26.8	2.4	0.0	16.0	8.0	4.0	12.4	0.0	0.0	0.0	100.0
H17	12.8	38.0	28.0	7.6	3.2	1.2	12.4	0.0	0.0	9.6	0.0	0.0	0.0	100.0
H16	12.9	14.0	17.2	13.2	6.8	0.0	8.0	29.2	1.2	10.4	0.0	0.0	0.0	100.0
H15	13.4	54.0	33.2	8.8	0.8	0.0	3.2	0.0	0.0	0.0	0.0	0.0	0.0	100.0
H14	13.5	22.4	14.8	22.4	3.6	0.4	9.6	14.4	2.4	10.0	0.0	0.0	0.0	100.0
H13	13.6	25.6	16.8	15.2	5.6	0.4	13.2	20.4	0.8	2.0	0.0	0.0	0.0	100.0
H12	13.7	31.6	21.6	12.8	2.8	0.4	2.8	10.8	3.6	13.6	0.0	0.0	0.0	100.0
H11	13.8	50.8	26.0	11.6	2.4	0.0	1.6	3.6	0.0	0.4	0.0	0.0	0.0	100.0
H10	14.2	7.2	19.2	12.8	2.8	0.0	16.0	15.6	2.4	24.0	0.0	0.0	0.0	100.0
H10	14.3	6.8	10.8	6.8	2.0	0.0	10.8	36.4	6.8	19.2	0.0	0.4	0.0	100.0
H8	14.6	18.0	6.4	8.8	8.4	1.6	3.2	12.0	5.2	7.6	0.0	0.0	0.0	100.0
H7	14.7	13.2	14.4	6.8	2.4	1.6	24.0	16.4	4.4	16.8	0.0	0.0	0.0	100.0
H7	14.8	46.0	50.0	1.6	0.4	0.0	2.0	0.0	0.0	0.0	0.0	0.0	0.0	100.0
H6	15.4	6.4	9.6	12.4	7.2	0.0	20.4	29.6	2.4	12.0	0.0	0.0	0.0	100.0
H5	15.7	51.2	23.6	2.0	6.4	3.2	12.4	0.0	1.2	0.0	0.0	0.0	0.0	100.0
H5	15.8	17.2	17.2	10.8	2.8	0.4	10.4	31.2	4.0	6.0	0.0	0.0	0.0	100.0
	mean	36.6	27.2	8.6	3.1	0.8	7.8	7.7	1.4	6.7	0.2	0.0	0.0	100.0

Pulaski Reef

Core Code	Depth metres	Framestone %	Porosity %	Bioerosional Porosity	Fibrous %	Peloids %	Micrite %	Encrusters %	Grainstones %	Packstone Wackestone	Microcryst Aragonite	Spar Cement	Neomorphic Calcite	Total %
O29	0.27	53.0	47.0	0.0	0.0	0.0	0.0	0.0	0.0	0.0	0.0	0.0	0.0	100.0
O28	0.33	57.5	41.0	0.0	1.5	0.0	0.0	0.0	0.0	0.0	0.0	0.0	0.0	100.0
O24	1.05	62.0	38.0	0.0	0.0	0.0	0.0	0.0	0.0	0.0	0.0	0.0	0.0	100.0
O23	1.30	57.0	40.0	0.0	2.0	0.0	1.0	0.0	0.0	0.0	0.0	0.0	0.0	100.0
O21	3.41	51.5	48.5	0.0	0.0	0.0	0.0	0.0	0.0	0.0	0.0	0.0	0.0	100.0
O20	3.51	60.8	34.8	0 0	4.0	0.0	0.4	0.0	0.0	0.0	0.0	0.0	0.0	100.0
O19	3.84	40.0	36.5	4.5	10.5	1.0	7.0	0.0	0.0	0.5	0.0	0.0	0.0	100.0
O17	4.10	40.5	30.0	25.0	2.5	0.5	1.5	0.0	0.0	0.0	0.0	0.0	0.0	100.0
O15	4.30	55.5	41.5	0.0	2.0	0.0	1.0	0.0	0.0	0.0	0.0	0.0	0.0	100.0
O14	4.70	59.0	41.0	0.0	0.0	0.0	0.0	0.0	0.0	0.0	0.0	0.0	0.0	100.0
013	5.60	33.0	32.5	5.5	1.4	5.0	7.5	1.5	0.5	0.5	0.0	0.0	0.0	100.0
O12	5.80	68.5	26.5	0.0	2.0	0.0	1.5	0.0	0.0	1.5	0.0	0.0	0.0	100.0
O12	5.90	38.5	28.0	1.7	2.0	0.0	2.5	0.0	0.0	1.2	0.0	0.0	0.0	100.0
O11	6.10	68.5	31.0	0.0	0.5	0.0	0.0	0.0	0.0	0.0	0.0	0.0	0.0	100.0
	mean	53.2	36.9	3.7	2.9	0.5	1.6	0.1	0.0	1.0	0.0	0.0	0.0	100.0

Glovers Reef, Belize

Core Code	Depth metres	Framestone %	Porosity %	Bioerosional Porosity	Fibrous %	Peloids %	Micrite %	Encrusters %	Grainstones %	Packstone Wackestone	Microcryst Aragonite	Spar Cement	Neomorphic Calcite	Total %
292	-	0.0	7.6	0.0	30.4	0.0	6.8	1.2	52.8	1.2	0.0	0.0	0.0	100.0
294	-	78.8	12.4	1.6	3.6	0.8	0.8	0.0	2.0	0.0	0.0	0.0	0.0	100.0
297	-	89.2	5.2	0.0	2.4	0.8	2.4	0.0	0.0	0.0	0.0	0.0	0.0	100.0
299	-	22.0	9.6	6.4	2.8	9.6	1.8	0.0	2.4	29.2	0.0	0.0	0.0	100.0
299	-	0.0	10.8	0.0	0.0	0.0	3.6	0.0	33.2	52.4	0.0	0.0	0.0	100.0
306	-	2.4	5.6	0.0	22.0	0.0	4.4	0.0	2.0	63.6	0.0	0.0	0.0	100.0
307	-	0.0	4.0	0.0	15.2	0.0	1.2	61.2	15.6	2.8	0.0	0.0	0.0	100.0
309	-	34.0	18.4	2.0	7.2	0.0	10.0	14.8	0.0	13.6	0.0	0.0	0.0	100.0
316	-	49.0	2.5	0.0	1.5	0.0	15.5	0.0	4.0	27.5	0.0	0.0	0.0	100.0
	mean	30.6	8.5	1.1	9.5	1.2	7.0	8.6	12.4	21.1	0.0	0.0	0.0	100.0

Alligator Reef Hole 1

Core Code	Depth metres	Q %	R %	S %	T %
A10	0.08	40.0	40.0	40.0	36.2
A9	0.16	22.6	22.6	22.6	20.2
A8	0.24	36.3	36.3	36.3	30.0
A7	0.49	21.1	21.1	21.1	13.6
A6	0.59	34.6	34.6	34.6	31.4
A5	0.74	7.9	7.9	7.9	6.5
A4	0.82	5.7	5.7	5.7	5.3
A3U	0.95	38.9	38.9	38.9	33.0
A3L	1.10	21.1	21.1	21.1	12.3
A2	1.33	10.8	10.8	10.8	8.3
A1	1.50	16.9	16.9	16.9	9.8
A1A	3.00	7.7	7.7	7.7	7.7
	mean	22.0	22.0	22.0	17.8

Alligator Reef Hole 1A

Core Code	Depth metres	Q %	R %	S %	T %
B6	0.40	4.4	4.4	4.4	2.5
B5	0.60	49.3	49.3	49.3	40.0
B4	0.70	17.0	23.5	23.5	16.7
B3	0.80	44.4	44.4	44.4	30.3
B2	1.70	12.3	12.3	12.3	12.0
B1	1.80	28.7	35.4	35.4	31.5
	mean	26.0	28.2	28.2	22.2

Alligator Reef Hole 2

Core Code	Depth metres	Q %	R %	S %	T %
C9U	0.15	12.6	12.6	12.6	7.1
C9L	0.35	12.0	13.6	12.0	8.3
C8	1.00	16.2	24.2	16.2	15.2
C7U	1.20	8.4	24.4	9.3	8.3
C7L	1.30	0.0	0.0	0.0	0.0
C6	1.50	20.0	20.0	20.0	16.6
C5	1.62	3.1	3.1	3.1	3.0
C4	1.70	10.3	10.3	10.3	8.2
C3	1.78	11.3	14.3	14.3	13.1
C2	1.88	15.6	19.1	19.1	9.0
C1	2.18	19.6	31.5	31.5	31.2
	mean	11.7	15.8	13.5	10.9

Alligator Reef Hole 3

Core Code	Depth metres	Q %	R %	S %	T %
D17	0.20	20.9	29.0	20.9	17.4
D16	0.26	0.0	0.0	0.0	0.0
D15	0.32	0.0	0.0	0.0	0.0
D14	0.44	17.9	17.9	17.9	10.4
D14	0.49	39.0	39.0	39.0	26.0
D13	0.57	4.0	4.0	4.0	2.8
D12	0.75	0.0	0.0	0.0	0.0
D11	1.45	5.3	6.3	6.3	5.8
D11	1.55	13.7	13.7	13.7	12.0
D9	1.82	2.5	3.4	2.5	1.4
D8	1.93	34.8	35.5	35.5	27.5
D7U	2.10	20.8	21.6	21.6	19.3
D7M	2.17	15.7	15.7	15.7	14.1
D7L	2.20	4.8	8.1	8.1	7.1
D6	2.30	21.2	21.2	21.2	16.5
D5	2.39	0.0	0.0	0.0	0.0
D4U	2.45	0.0	0.0	0.0	0.0
D4M	2.50	0.0	0.0	0.0	0.0
D4L	2.55	2.0	2.0	2.0	1.3
D3	2.62	2.4	2.4	2.4	1.6
D2	2.82	4.5	4.5	4.5	3.9
D1	3.00	0.0	0.0	0.0	0.0
	mean	9.5	10.2	9.8	7.6

Alligator Reef Hole 4

Core Code	Depth metres	Q %	R %	S %	T %
E10	0.40	31.1	31.1	31.1	29.5
E9	0.60	28.7	32.4	28.7	25.8
E8	1.00	20.4	20.4	20.4	20.2
E7	1.15	4.0	4.3	4.0	2.6
E6U	1.35	1.4	1.7	1.4	1.2
E6L	1.40	2.3	2.3	2.3	1.8
E5	1.50	2.6	3.9	2.6	2.6
E4	1.85	2.2	6.3	6.3	6.3
E3	2.10	24.0	29.6	26.9	26.9
E2	2.60	0.0	0.0	0.0	0.0
	mean	11.7	13.2	12.4	11.7

Alligator Reef Hole 5

Core Code	Depth metres	Q %	R %	S %	T %
F18	0.36	21.6	24.6	21.6	18.6
F18	0.50	29.5	35.3	29.5	16.5
F16	0.90	0.0	0.0	0.0	0.0
F15	1.30	25.0	27.2	25.0	21.0
F14	1.50	21.2	21.6	21.2	20.6
F13	1.54	11.0	12.5	11.0	7.1
F12	1.75	2.9	2.9	2.9	2.7
F11	1.90	8.3	8.3	8.3	6.2
F6	2.65	0.0	0.0	0.0	0.0
F4	2.92	0.0	0.0	0.0	0.0
F3L	3.00	4.0	4.5	4.0	3.3
	mean	11.2	12.5	11.2	8.7

Alligator Reef Hole 6

Core Code	Depth metres	Q %	R %	S %	T %
G15	0.07	85.5	85.5	85.5	67.3
G15	0.10	38.8	38.8	38.8	34.7
G14	0.12	48.6	50.7	48.6	35.3
G13	0.18	68.1	68.1	68.1	46.7
G13	0.20	50.0	50.0	50.0	42.2
G13	0.24	77.4	77.4	77.4	48.8
G12	0.31	12.6	12.6	12.6	8.8
G11	0.36	22.0	25.5	22.0	9.5
G10	0.50	27.5	29.8	27.5	16.3
G9	0.58	19.0	30.3	25.3	18.4
G8	0.70	24.8	36.0	24.8	20.5
G7	0.86	11.5	13.7	11.5	8.9
G6	0.95	26.7	26.7	26.7	13.6
G5	1.10	11.1	13.3	11.1	8.6
G4	1.20	17.9	17.9	17.9	14.3
G3U	1.28	35.5	36.0	35.5	32.9
G3L	1.34	15.7	15.7	15.7	15.4
G2	1.44	7.1	7.1	7.1	7.1
G1	1.50	11.1	11.1	11.1	9.1
	mean	32.2	34.0	32.5	24.1

Dry Tortugas Hole 1

Core Code	Depth metres	Q %	R %	S %	T %
J29	3.72	3.4	5.7	3.4	1.9
J28	4.04	0.0	0.0	0.0	0.0
J27	4.36	0.0	0.0	0.0	0.0
J25	5.20	0.0	0.0	0.0	0.0
J24	7.50	0.0	0.0	0.0	0.0
J23	7.86	4.7	7.2	4.7	3.3
J22	8.14	6.7	6.7	6.7	6.2
J21	8.42	0.0	0.0	0.0	0.0
J20	9.00	4.1	4.1	4.1	3.5
J19	9.45	11.1	11.9	11.1	9.9
J18	9.70	23.9	23.9	23.9	17.3
J17	11.25	1.3	1.5	1.3	1.3
J16	11.45	0.0	0.0	0.0	0.0
J15	11.60	14.5	14.5	14.5	10.4
J14	13.00	0.0	0.0	0.0	0.0
J13	14.00	3.6	3.8	3.6	3.6
J12	14.20	4.4	4.4	4.4	4.4
J11	14.44	7.2	7.2	7.2	5.7
J7	15.80	0.0	0.0	0.0	0.0
J3	16.85	11.6	11.6	11.6	8.7
J2	17.15				
		4.8	5.2	4.8	3.8
	mean				

Dry Tortugas Hole 2

Core Code	Depth metres	Q %	R %	S %	T %
K15	10.8	9.2	11.9	9.2	5.7
K14	11.0	10.3	16.7	10.3	6.4
K13	11.3	10.6	14.5	10.6	9.1
K12	12.5	4.3	4.3	4.3	4.2
K12	12.6	13.9	21.3	13.9	10.4
K12	12.8	4.8	12.6	8.5	8.3
K11	13.2	4.0	5.5	4.0	3.2
K11	13.3	10.1	11.1	10.1	8.1
K9	14.3	0.0	0.0	0.0	0.0
K9	14.4	15.7	22.6	15.7	9.3
K8	14.8	0.0	0.0	0.0	0.0
K6	16.1	0.0	0.0	0.0	0.0
	mean	6.9	10.0	7.2	5.4

Dry Tortugas Hole 4

Core Code	Depth metres	Q %	R %	S %	T %
M11	0.1	12.3	13.2	12.3	10.8
M10	0.3	1.9	2.1	1.9	1.8
M9	0.6	6.6	8.2	6.6	5.3
M7	1.0	2.7	4.0	2.7	2.5
M6	1.2	22.7	22.7	22.7	19.1
M6	1.3	21.2	21.2	21.2	17.5
M5	1.4	19.5	19.5	19.5	13.2
M3	2.1	11.5	11.5	11.5	11.5
M2	2.3	4.9	9.1	4.9	4.5
M1	2.6	4.6	5.7	4.6	4.6
M1	2.7	4.9	4.9	4.9	4.7
	mean	10.2	11.1	10.2	8.7

Dry Tortugas Hole 5

Core Code	Depth metres	Q %	R %	S %	T %	U %
N1	0.30	26.5	26.5	26.5	19.8	26.5
N2	0.40	19.3	20.5	19.3	18.2	19.3
N3	0.90	5.0	6.7	5.0	4.7	5.0
N5	8.50	2.8	4.9	2.8	2.2	2.5
N6	8.70	0.0	0.0	0.0	0.0	2.0
N8	8.90	11.8	14.7	11.8	6.7	11.6
N9U	9.80	4.8	5.8	4.8	4.5	2.6
N9L	9.90	4.6	9.1	4.6	4.1	4.6
N10	10.1	7.5	13.1	7.5	4.7	7.1
N12	10.3	2.6	4.4	2.6	1.4	2.2
N13	10.5	4.5	9.5	4.5	2.1	4.1
N14	10.7	2.1	4.1	2.1	1.6	2.0
N14	10.8	31.6	37.9	31.6	21.8	30.8
N15	10.9	7.9	12.5	7.9	4.0	7.4
N16	11.2	1.7	2.6	1.7	0.5	1.4
N16	11.3	0.0	0.0	0.0	0.0	0.0
	mean	8.3	10.8	8.3	6.0	7.9

Alligator Reef and South East Reef Averages

Reef	No. of Thin Sections	Q %	R %	S %	T %
Alligator	92	17.7	19.2	18.3	14.3
South East	60	7.2	8.7	7.2	5.6

Loggerhead Key

Core Code	Depth metres	Q %	R %	S %	T %
H34	0.50	6.8	14.6	11.9	11.9
H33	0.70	4.8	4.8	4.8	4.8
H32	4.50	0.0	0.0	0.0	0.0
H31	4.60	10.2	10.2	10.2	10.1
H30	6.60	15.0	19.8	17.1	15.8
H29	7.20	14.3	16.5	14.3	13.0
H28	7.30	11.2	13.2	11.2	9.1
H27	7.40	16.5	25.0	16.5	10.6
H26	7.60	13.8	14.4	13.8	12.6
H24	8.90	0.0	0.0	0.0	0.0
H23	9.10	1.9	1.9	1.9	1.9
H22	10.4	5.3	6.8	5.3	4.1
H21	10.7	3.5	7.8	7.8	6.9
H20	10.9	6.0	7.1	6.0	5.6
H19	12.2	0.0	0.0	0.0	0.0
H18	12.4	5.4	13.3	5.4	3.3
H17	12.8	11.0	13.6	11.0	7.1
H16	12.9	18.3	28.3	18.3	12.2
H15	13.4	1.9	2.4	1.9	1.7
H14	13.5	9.7	21.3	9.7	6.6
H13	13.6	15.8	26.3	15.8	11.3
H12	13.7	11.7	15.0	11.7	11.0
H11	13.8	6.0	8.5	6.0	5.3
H10	14.2	8.0	12.7	8.0	3.7
H10	14.3	10.2	15.6	10.2	4.0
H8	14.6	39.7	61.0	39.7	15.4
H7	14.7	15.9	21.7	15.9	6.1
H7	14.8	0.8	0.8	0.8	0.7
H6	15.4	24.7	42.9	24.7	11.7
H5	15.7	27.3	28.9	27.3	20.2
H5	15.8	10.3	15.7	10.3	6.7
	mean	10.4	15.1	10.8	7.2

Pulaski Reef

Core Code	Depth metres	Q %	R %	S %	T %
O29	0.27	0.0	0.0	0.0	0.0
O28	0.33	3.5	3.5	3.5	3.5
O24	1.05	0.0	0.0	0.0	0.0
O23	1.30	4.8	4.8	4.8	4.7
O21	3.41	0.0	0.0	0.0	0.0
O20	3.51	10.3	10.3	10.3	10.2
O19	3.84	21.9	24.0	21.9	19.2
O17	4.10	5.2	9.1	5.2	5.0
O15	4.30	4.6	4.6	4.6	4.5
O14	4.70	0.0	0.0	0.0	0.0
O13	5.60	33.3	36.9	33.3	29.2
O12	5.80	7.0	7.0	7.0	6.3
O12	5.90	4.3	6.7	4.3	3.3
O11	6.10	1.6	1.6	1.6	1.6
	mean	6.9			

Glovers Reef, Belise

Core Code	Depth metres	Q %	R %	S %	T %
292	-	23.9	26.2	23.9	22.9
294	-	80.0	80.0	80.0	66.1
297	-	38.1	38.1	38.1	29.6
299	-	43.7	56.4	43.7	16.4
299	-	0.0	0.0	0.0	0.0
306	-	79.7	79.7	79.7	23.0
307	-	79.2	79.2	79.2	65.5
309	-	26.1	28.1	26.1	14.1
316	-	37.5	37.5	37.5	3.2
	mean	45.3	47.2	45.3	26.8

$$Q = \frac{FibrousAragonite + Peloids}{Intraskeletal + BioerosionalPorosity + FibrousAragonite + Peloids}$$

$$R = \frac{FibrousAragonite + Peloids + MicrocrystallineAragonite}{IntraskeletalPorosity + FibrousAragonite + Peloids + MicrocrystallineAragonite}$$

$$S = \frac{FibrousAragonite + Peloids + MicrocrystallineAragonite}{Intraskeletal + BioerosionalPorosity + FibrousAragonite + Peloids + MicrocrystallineAragonite}$$

$$T = \frac{FibrousAragonite + Peloids + MicrocrystallineAragonite}{Intraskeletal + BioerosionalPorosity + FibrousAragonite + Peloids + MicrocrystallineAragonite + InternalSediments}$$

A1.2 Species Specificity.

In an investigation of the species specificity of the cementation, the presence or absence of particular cement morphologies and mineralogies were noted. The figures below include only those thin sections in which some recognisable cement was present. The infrequent occurrences of the botyroidal and microcrystalline aragonite and fibrous Mg-calcites meant that these were excluded from the study. As the predominant framebuilding organisms in all the Florida reefs were the corals, the study was restricted to *Acropora palmata* and *Montastrea annularis* only. The 62 thin sections included below come from all the Florida reefs described in Chapter 2. The presence of the cements was noted once and only once from each thin section, irrespective of the total volume present.

Whilst the technique is naturally somewhat speculative, the figures suggest that spherulitic aragonites occur more commonly in *Montastrea annularis*.

Species	No. of thin sections	Spherulites	Peloids	Fibrous only
Montastrea	22	6	9	7
Acropora	40	6	21	13

Appendix 2.

A2.1 X-ray Diffraction Data for Holocene Reef Samples.

Powder XRD was carried out in order to determine the mineralogy of micrites from Holocene reef samples of Florida and to investigate the peloid rich samples from the Early Holocene relic shelf edge reef described in Section 2.19. In most cases the samples were collected from thin section and further ground if necessary. Samples were generally very small and had to be analysed using the Debye Scherrer camera technique. The peloid and coral samples from the Early Holocene reef were sampled in bulk and were smear mounted with acetone onto glass slides. Analyses were carried out by Mr. R. Hardy of the University of Durham, on a Phillips PW 1130 generator / diffractometer assembly using Fe-filtered Co K-α or Ni-filtered Cu K-α radiation. Operating conditions were: 40 kV; 20 mA; range 2–4$\times10^{-2}$ c.p.s.; divergence and scatter slits 1°; recovery slit width 0.1 mm; scan speed 1° of $2\theta min.^{-1}$.

Thin Section No.	Aragonite	High Mg-Calcite	Proportion
1	3.40Å	3.00Å	HMC>A
2	3.40Å	3.00Å	HMC>A
3	3.40Å	3.00Å	A>HMC
4	3.40Å	3.00Å	HMC>A

The sample with aragonite predominant contained shell fragments visible but not identifiable in transmitted light. The traces for the two samples from the Early Holocene reef are shown below. Sample A is the coral blank and B is the coral and peloidal sample. Rough calculation from the relative areas of the 2.99Å(HMC) and 3.40Å(A) peaks indicates the presence of approximately 30% HMC. This assumes the response to both minerals is equal, which is not necessarily correct. Comparison of the two samples, and assuming that the 3.40Åpeak of Sample A represents 100%, leads to an estimation of approximately 85% aragonite and 15% high Mg-calcite in Sample B. Both samples were collected after the extraction of the organic matter as described in Chapter 4.

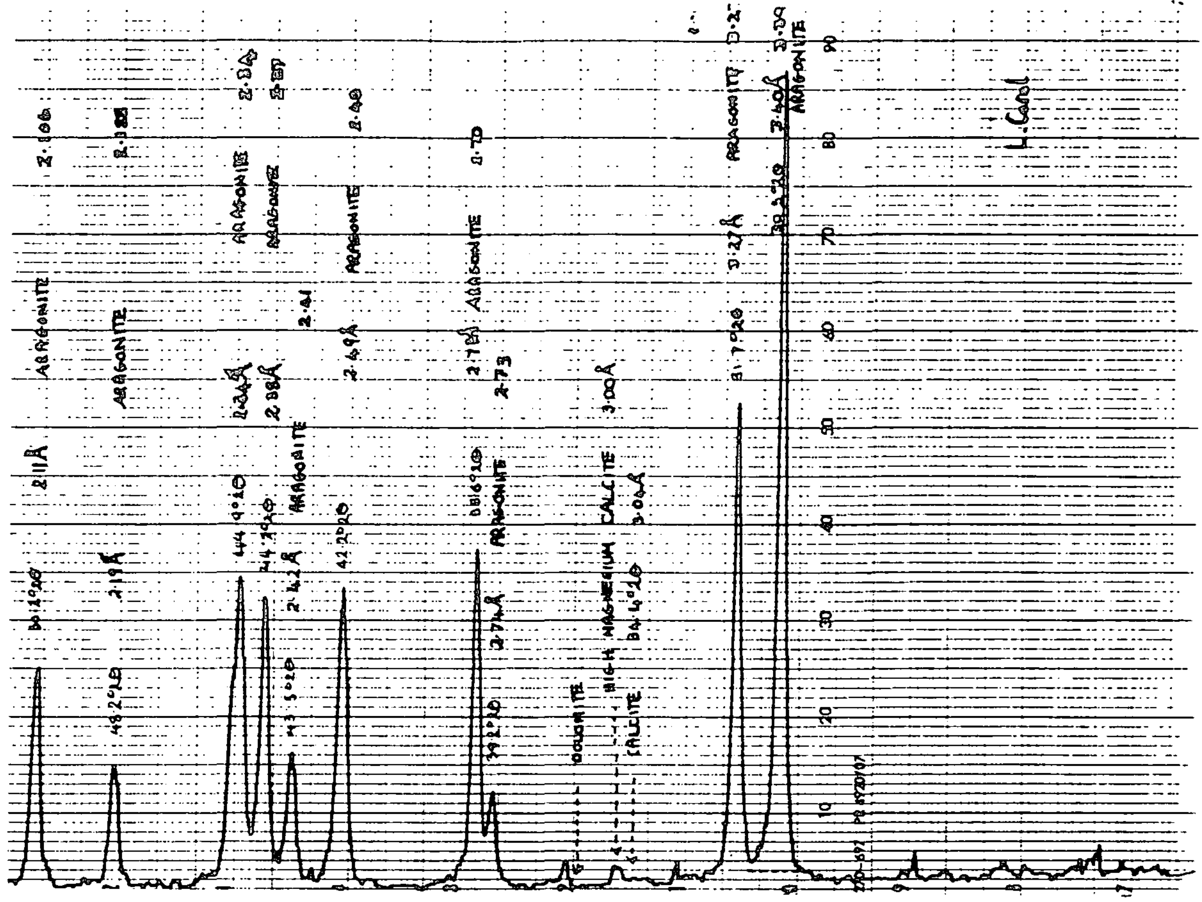

Figure A.2.1.1 XRD trace for the coral blank (above), and the peloidal sample (below).

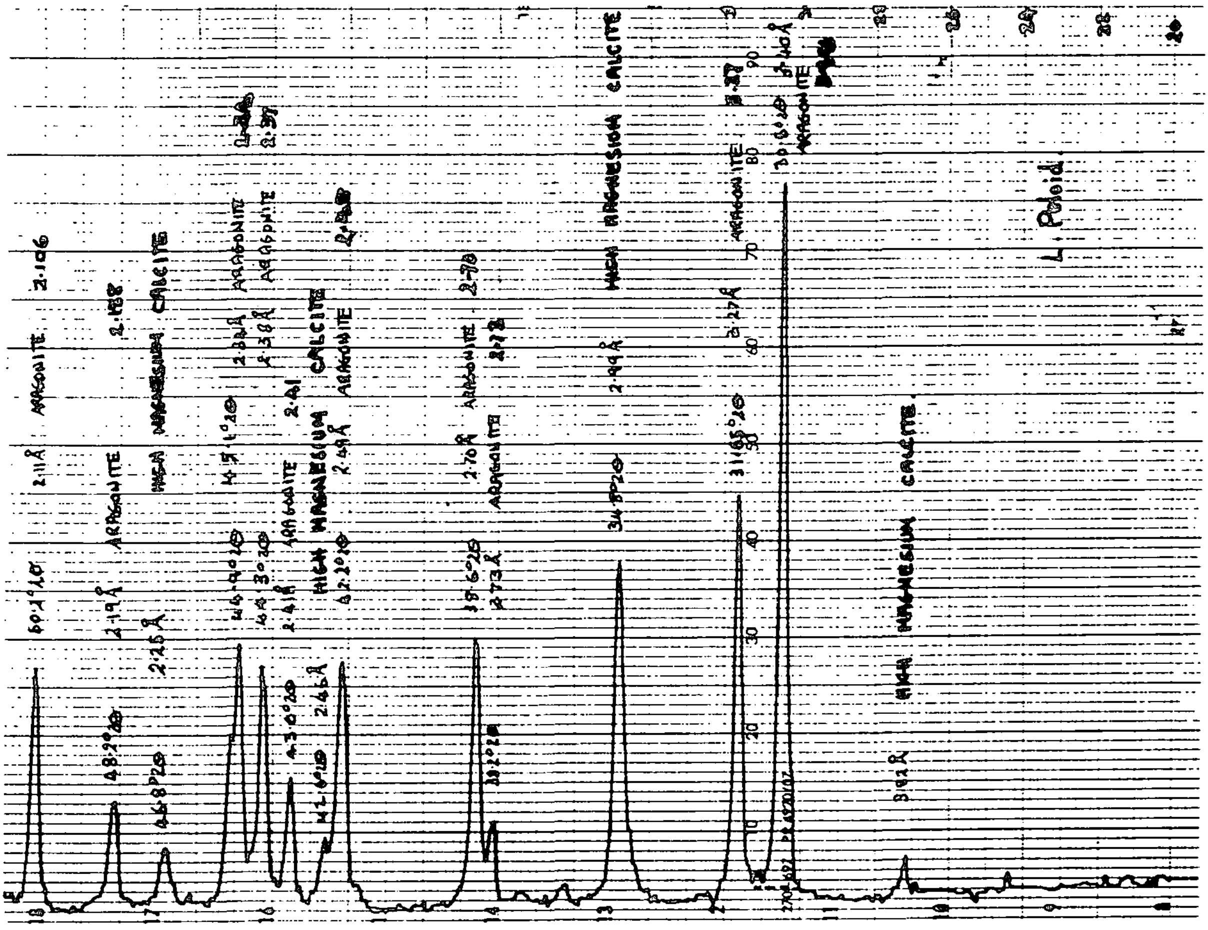

A2.2 Electron Microprobe Analyses.

Electron microprobe analyses were employed to identify the minor and trace element composition of several Holocene and Pleistocene cement samples from the Florida reefs. Mineralogy of the samples was inferred as aragonite where high strontium values were detected, and Mg-calcite where high Mg concentrations were detected. Carbon coated polished slides were prepared and analyses were carried out by Dr. A. Peckett of the University of Durham on a Cambridge Instruments Geoscan electron microprobe. The probe was operated at an accelerating voltage of 20kV and a probe current of 50nA. Analysis totals calculated by an on-line computer were low (85–95%) due to decomposition of the carbonate samples even under a defocussed beam. Standards used for calibration were periclase (Mg) and celestine (Sr). Errors are difficult to estimate due to the significant decomposition problems, but are expected to be $\pm 0.5 mole\%$ for Mg and$\pm 1000 p.p.m.$ for Sr. The decomposition was noted to be particularly high in the analysis of the peloidal cements, indicative of the presence of organic matter.

Sample Code	Description	mole% Mg ($MgCO_3$)	p.p.m Sr
N14 Figure 2.65	Spar	0	0
N14 Figure 2.65	Acicular	0	7,800
N14 Figure 2.66	Acicular in spar	0	1,500
N14 Figure 2.36	Botryoid	0	8,000
N14 Figure 2.70	Micrite	2.0	2,000
N14 Figure 2.71	Neomorphosed Coral	0	2,000
101 Figure 2.30	Acicular	0	8,500
101 Figure 2.47	Peloids	16.5	<400

A2.3 Staining Methods.

Stains used to confirm mineralogy of cements included Feigl's solution (aragonite) and Titan yellow (high Mg-calcite). Preparation and staining procedures published by Friedman (1959) and Choquette & Trusell (1977).

A2.4 Scanning Electron Microscopy.

SEM analyses were carried out at several institutions, including the Universities of Durham and Newcastle, and the British Petroleum Research Centre, Sunbury. All samples were prepared as fracture surfaces, with no etching and were all gold coated by evaporation. Many of the photographs presented in the thesis were taken at the University of Newcastle on a JEOL JSMT 20 instrument, operating at 20kV.

Appendix 3.

A3.1 Stable Carbon and Oxygen Isotopic Composition of Holocene Cements from Florida and Belize.

Notation.

Isotopic compositions are reported here in the δ notation:

$$\delta_{(x)} = \left[\frac{R_{(x)} - R_{(std.)}}{R_{(std.)}}\right] \times 10^3$$

where $R_{(x)}$ is the isotopic ratio $\left({}^{13}C/{}^{12}C,\ {}^{18}O/{}^{16}O\right)$ of the sample and $R_{(std.)}$ is the corresponding ratio in a standard.

Isotopic fractionation between two substances A and B, which occurs during any process is expressed as a fractionation factor:

$$\alpha_{(A-B)} = \frac{R_{(A)}}{R_{(B)}} = \frac{1000 + \delta_{(A)}}{1000 + \delta_{(B)}}$$

A further definition used to express the fractionation in permil is:

$$\varepsilon_{(A-B)} = \ln\left(\alpha_{(A-B)}\right) \times 1000$$

All sample values are reported in permil (‰) relative to the internationally accepted standard, PDB. Some references to water compositions in the text are relative to SMOW, as is standard practice. These figures are used for the purposes of palaeo-temperature calculations, which were all made using equation 3.2. The difference in the two scales is incorporated into that equation. A detailed description of the two scales and the relationships between them can be found in Land (1980).

Methods.

The method of sample preparation and analysis of carbon and oxygen isotopic composition of carbonates is based on McCrea (1950) and Craig (1957). This Appendix refers to samples which were analysed by Dr. M. Hall of the University of Cambridge, Department of Quaternary Sciences. Samples were collected from thin section and stored in sealed micro-pipettes, and were between 0.1 and 0.2 milligrammes in weight. Preparation of samples involved roasting in an oven (425 ° C 30min., in vacuo), to remove organic matter. Carbon dioxide gas was prepared by reacting the samples with 100% phosphoric acid at 50 ° C . The CO_2 was collected on-line and the isotopic composition was measured on a VG-Isogas Micromass 903 triple collection mass spectrometer. Raw data (as δ^{45} and δ^{46} ratios) were corrected for isobaric, crosstalk and other instrument factors, by standard procedures (Craig, 1957; Deines, 1970).

Correction for the temperature dependent fractionation of the oxygen isotopes which occurs between sample and evolved gas was made using the following fractionation factor $\alpha = 1.01025$, corrected to 50 ° C . Analytical precision was measured by duplicate analyses of laboratory standards at values of $\sigma = \pm 0.02$ ($\delta\,^{13}C$), $\sigma = \pm 0.03$ ($\delta\,^{18}O$).

Sample Number	Locality	Cement Morphology	Mineralogy	$\delta^{13}C$ ‰[PDB]	$\delta^{18}O$ ‰[PDB]	Calculated Temp. [°C]
1	Belize	Botryoid 1	A	4.39	0.78	17.6–22.3
2	Belize	Botryoid 2	A	4.22	0.81	17.6–22.3
3	Belize	Botryoid 3	A	4.32	0.73	17.8-22.5
4	Belize	Botryoid 4	A	4.24	0.28	19.4-24.1
5	Belize	Botryoid	A	4.71	1.29	15.9–20.6
6	Belize	Substrate	A/C	3.79	1.24	—
7	Belize	Fibrous	A	4.30	1.26	15.9–20.6
8	Belize	Spherulite	A	4.76	0.84	17.5-22.2
9	Belize	Substrate	A	0.72	−1.64	—
10	Belize	Peloid	C	3.50	1.58	14.4-19.8
11	Belize	Peloid	C	3.51	1.52	14.5-19.9
12	Belize	Micrite	A/C	2.64	0.82	—
13	Florida	Peloid	C	3.03	−0.27	22.0–28.1
14	Florida	Micrite	A/C	3.07	−0.54	—
15	Florida	Micrite 2	A/C	2.61	−0.31	—
16	Florida	Fibrous	A	4.47	−0.66	22.8-27.5
17	Florida	Substrate	A	−2.31	−4.36	—
18	Florida	Peloid 2	C	2.83	−0.21	22.0–28.1

Table 3.2. Samples 1–4 represent a transect across a Botryoid of 3cm in size. The samples were collected at equal spacings, perpendicular to the growth direction, Sample 4 being the youngest. 'Substrate' refers to the sample immediately above. A = aragonite, C = high Mg-calcite.

Appendix 4.

4.1 Extraction and Purification of the Peloidal Organic Matter.

In all of the procedures described below, it must be emphasised that great care was taken to avoid contamination. The coral blank sample and the peloid rich sample were treated in parallel and all procedures were carried out simultaneously for sample and control, where possible. Two hundred and fifty grammes of each sample were prepared. The samples were washed in distilled water, rinsed with dichloromethane to remove surface contamination, and dried in an oven at 50 ° C . Using pre-washed clamps and chisels, any extraneous encrusting material was removed. The samples were then crushed to pass throgh a 180 mesh sieve, in a rotary grinding mill.

All glass-ware was thoroughly washed in detergent (Decon 90), distilled water, and acetone, being finally rinsed in dichloromethane and methanol. Samples were extracted exhaustively (48 hours) in a Soxhlet apparatus which was previously washed by refluxing (again for 48 hours), in dichloromethane and methanol. The extraction solvent was dichloromethane : methanol (1:1). After extraction, all solvent was removed by rotary evaporation to produce 225 mg. of a green waxy substance from the peloidal sample and 50 mg. of a brown oily liquid from the coral control.

These total extracts were separated and purified by preparative thin layer chromatography (t.l.c.) (Silica Gel G, with Hexane : Ethyl Acetate (85:15) as the eluent. Separation of aliphatic hydrocarbons, wax esters, alcohols and fatty acids was achieved by the comparison of retention indices, using n-C_{20} alkane, palmitoyl oleate, stigmasterol and lanosterol as standards. The fatty acids were separated from the alcohols by methylation (BF_3/MeOH; 1 hour, 40 ° C) of the acids and further purification by t.l.c. . The polar material remaining at the origin in the first chromatogram was collected and saponified (5% KOH/MeOH; 3 hours, 80 ° C) to release the bound fractions. Repeating the above separation procedure on the saponified material yielded a further fraction of bound fatty acids and bound alcohols. The alcohol fractions were derivatised with bis-trimethylsilyl tri-fluoro acetamide (BSTFA), to form the trimethylsilyl (TMSi) ethers, in preparation for gas chromatography.

4.2 Low Molecular Weight Biomarker Analyses.

GC analyses were made using a Carlo-Erba Science 4160 instrument fitted with an on-column injector and an open tubular ('Flexsil' 25m., 0.3mm. i.d.) column, wall coated with OV-1 liquid phase. Computerised GC-MS was performed on a Finnigan 4000 mass spectrometer, linked to a Carlo Erba Science Mega gas chromatograph with an on-line Incos 2000 data system. GC conditions were 50–280 ° C @ 4 ° C min^{-1}, held isothermally at 280 ° C for 30 min. with a similar OV-1 column. Spectra were recorded in the mass range 50–550 at one per second, acquisition srarting at 70 ° C .

Quantitation was achieved through the addition of a fixed, known concentration of an internal standard to the sample immediately prior to injection. The standard used was 9-n dodecylperhydrophenanthrene (structure xvii). Quantitation was performed on the basis of relative peak areas calculated from the total reconstructed ion current. Figures presented below are corrected for the different concentrations of each separated compound class as prepared for gc-ms. Correction was also made for the difference in total weight of extract from each original sample. Although the quantitation on the basis of total ion current can be inaccurate due to problems of co-elution, this is considered preferable to quantitation on the basis of base peak mass fragmentography, as the latter assumes that the response of the instrument is uniform throughout the mass range, which it certainly is not. Nevertheless, some of the inaccuracies are nullified as long as samples run at similar times on the same instrument, and for this reason the samples were run in pairs, sequentially. Whilst accurate comparison between two samples is then possible, and although true quantitation of components is also possible (ng. g^{-1}), the generally low concentrations of many components in the reef samples make such quantitation of dubious use. Therefore, figures quoted below are simply as percentages of the internal standard. The values for the separate classes are directly comparable.

Identification of components was made on the basis of mass spectral interpretation, comparison with standard mass spectra and from relative retention times. The comparison of the two samples was aided by the calculation of Kovat's indices. This is achieved through the measurement of the retention times of the n-alkanes, which were co-injected with all samples (except the aliphatic hydrocarbon fraction, which contains them anyway) in small concentrations recognisable in the $m/z = 85$ fragmentogram. The retention times of the n-alkanes are very reproducible, and hence normalisation of the retention times of the 'unknown' components to the n-alkane scale results in reproducible relative retention times, on the Kovat's scale.

Aliphatic Hydrocarbons

n- Alkane	Coral Blank	Peloid
n-C_{16}	8	7
n-C_{17}	9	16
n-C_{18}	23	31
n-C_{19}	36	39
n-C_{20}	38	52
n-C_{21}	28	33
n-C_{22}	142	210
n-C_{23}	22	24
n-C_{24}	26	43
n-C_{25}	2	5
n-C_{26}	24	25
n-C_{27}	23	24
n-C_{28}	56	20
n-C_{29}	34	25
n-C_{30}	44	14
n-C_{31}	28	10
n-C_{32}	13	0
n-C_{33}	11	0
n-C_{34}	8	0

Wax Esters

Wax Ester	Coral Blank	Peloid
C_{30}U	4	0
C_{30}S	2	0
C_{30}U	2	0
C_{31}S	4	0
C_{32}S	4	7
C_{33}U	2	0
C_{33}U	2	0
C_{33}U	1	0
C_{34}U	7	5
C_{34}S	2	0
$C_{36:2}$U	2	0
C_{36}18:18	6	0

Alcohols

n-Alcohol number	Coral Blank Free	Coral Blank Bound	Peloid Free	Peloid Bound
n-C_{16}	39	0	170	0
n-C_{17}	9	0	28	0
n-C_{18}	561	65	806	235
n-C_{19}	5	0	14	0
n-C_{20}	27	0	50	0
n-C_{21}	10	0	182	0
n-C_{22}	52	0	56	0
n-C_{23}	3	0	0	0
n-C_{24}	16	0	30	0
n-C_{25}	3	0	0	0
n-C_{26}	7	0	0	0
n-C_{27}	0	0	0	0
n-C_{28}	2	0	0	0

Polycyclic Alcohols

Alcohol	Coral Free	Coral Bound	Peloid Free	Peloid Bound
cholest-5-en-3β-ol	1	36	290	108
24-methylcholest-5-en-3β-ol	0	11	223	0
24-ethylcholest-5-en-3β-ol	0	0	24	0
$C_{29}\Delta^{5,22}$ sterol	3	0	8	0
4,24 di-methyl5α(H)-cholestan-3β-ol	0	0	1	0
C_{29} stanol	2	7	32	0
bis-homohopanol	0	0	1	0

Fatty Acids

Acid	Coral Free	Coral Bound	Peloid Free	Peloid Bound
n-C_{14}	51	17	0	24
C_{15}br	10	6	0	0
n-C_{15}	35	25	0	31
C_{16}br	8	0	0	0
n-C_{16}	313	283	94	483
C_{17}i	9	7	6	32
n-C_{17}	18	12	9	20
$C_{18:2}$	12	26	114	0
$C_{18:1}\Delta 9$	1	168	215	0
$C_{18:1}\Delta 11$	6	64	88	0
n-C_{18}	155	268	182	387
n-C_{19}	6	0	0	0
n-C_{20}	18	0	20	0
n-C_{21}	6	0	0	0
n-C_{22}	45	0	36	0
n-C_{23}	0	0	0	0
n-C_{24}	25	0	13	0

4.3 High Molecular Weight and Spectroscopic Analyses.

Bulk organic matter from the extraction described above, for both coral control and peloidal samples was analysed by the following techniques.

N.M.R.

^{1}H and ^{13}C nmr spectra were recorded on a variety of instruments, including a Brüker AC 250 (250 MHz) at the University of Durham, Department of Chemistry, and a similar but more sensitive (400 MHz) instrument at the British Petroleum Research Centre, Sunbury. A 200 MHz Varian Gemini instrument at the University of Durham Industrial Research Laboratories was also used. Both deuterated methanol (CD_3OD) and deuterated chloroform ($CDCl_3$) were used as solvents. The resulting spectral positions (chemical shifts) are reported in the δ notation in p.p.m.:

$$\delta_i = \left[\frac{\nu_i - \nu_{(TMS)}}{\nu_0}\right] \times 10^6$$

where δ_i is the chemical shift of the nucleus of interest, $\nu_{(TMS)}$ is the resonance frequency of the internal standard and ν_0 is the operational frequency of the instrument.

Pyrolysis GC.

The samples were analysed in the laboratories of Professor J. van de Leeuw, of the University of Delft. Analyses were performede by curie point pyrolysis on Ni wires (358 ° C) and Fe wires (770 ° C). Volatilised and fragmented products were then analysed by similar on-line gas chromatographic techniques as described above.

The analyses at 358 ° C are considered to be thermo-evaporation, and those at 770 ° C are pyrolysis and thermo-evaporation.

Organic Carbon Isotopes.

The carbon isotopic analyses were performed by Mrs. M. Cox of the British Petroleum Research Centre. Carbon dioxide gas was prepared on a standard organic oxidation rig, and the gas analysed on the spectrometer described in Appendix 6. Both peloidal and coral control samples have very similar isotopic compositions of 26.6 and 26.7 ‰ respectively.

4.4 Molecular Structures.

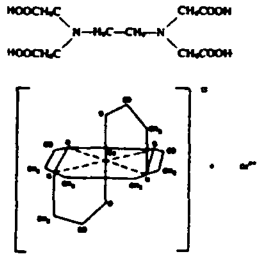

I

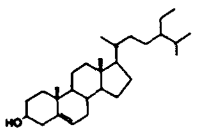

II

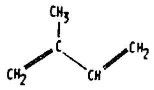

III

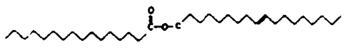

iv

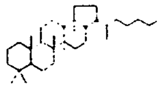

v

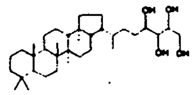

vi

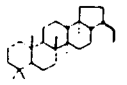

vii

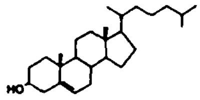

viii

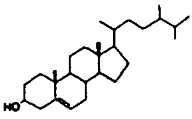

ix

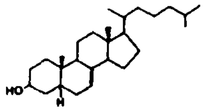

x

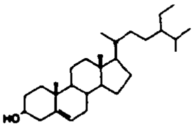

xi

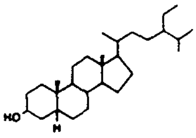

xii

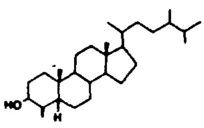

XIII

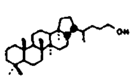

XIV

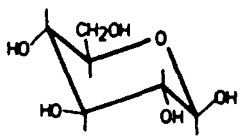

XV

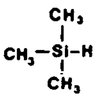

$$CH_3-\overset{\displaystyle CH_3}{\underset{\displaystyle CH_3}{Si}}-H$$

XVI

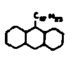

XVII

(i) ethylene-diamine tetra-acetic acid
(ii) 24-ethylcholest-5-en-3β-ol
(iii) isoprene
(iv) palmitoyl-oleate
(v) extended hopane (C_{34})
(vi) bacteriohopane-tetrol
(vii) 30-norhopane
(viii) cholest-5-en-3β-ol
(ix) 24-methylcholest-5-en-3β-ol
(x) Δ^7-sterols
(xi) 24-ethylcholest-5-en-3β-ol
(xii) 24-ethylcholestan-3β-ol
(xiii) 4,24-dimethyl-5α(H)-cholestan-3β-ol
(xiv) bishomohopan-32-ol
(xv) glucose
(xvi) trimethyl-silane
(xvii) 9n-dodecyl-perhydro-phenanthrene

Appendix 5.

5.1 Poroperm data for Holocene corals.

The compilation of data given in the table below has been obtained through the combination of mercury injection porosity and constant head permeability measurements. Analyses were performed by technicians at the British Petroleum Research Centre, Sunbury. Further data for three coral specimens was obtained through the measurement of pore-throat radii on a B.P. Autopore 9220 penetrometer, also at B.P. Sunbury. The distribution of the pore-throat radii for samples marked with an '*' in the table below, were presented in Figure 5.20. Some additional data for these samples is also given below.

Sample	Species	Thin Section Porosity	Porosity %	Permeability milliDarcies
1	*Acropora*	-	49.4	-
2H	*Montastrea*	66.5	56.8	24.2
2V *	*Montastrea*	-	58.1	57.9
3 *	Lithified Belize	-	9.2	84.6
4H	*Acropora*	55.6	51.2	8,900
4V *	*Acropora*	57.2	50.5	3,800
5H	*Diploria*	-	54.6	<10,000
5V	*Diploria*	50.8	58.0	<10,000

	2V	3	4V
Pore area m^2g^{-1}	4.035	1.027	5.428
Median Pore Diameter μm.	64.48	13.74	88.73
Average Pore Diameter μm.	0.33	0.10	0.21

5.2 Poroperm data for Miocene reef samples.

Porosity and permeability of the Miocene reef samples were measured by the Department of Engineering Geology, Durham University. All measurements were made on 1 inch diameter cores. Several repeat samples from each hand specimen were analysed.

Permeability was measured by the constant head method using oxygen free nitrogen on a Ruska gas permeameter. Permeability is calculated from the following relationship:

$$K = \frac{\mu.Q.L}{A.P}$$

where μ is the viscosity (in centipoise) of the gas used at ambient temperature; Q is the average rate of flow through the sample (cm^3s^{-1}); L is the length of the sample; P is the pressure gradient (atm) and K is the permeability (Darcies). The flow rate is calculated from the instrument flow-meter readings by reference to calibration curves.

Porosity was measured as a ratio of pore volume to bulk volume, both of which were determined by mercury injection techniques on a Ruska porosimeter.

Facies	Sample Number	Porosity %	Permeability milliDarcies
1	3	14.9	0.0
1	5	22.5	1.1
1	7	16.4	-
1	8.1	15.2	9.3
1	8.2	15.4	108.5
1	8.3	18.5	86.1
1	8.4	25.5	144.2
1	11.1	1.2	0.0
1	11.2	14.2	0.0
1	12.1	12.4	0.0
1	12.2	11.2	0.0
1	13	11.8	157.8

F1 STABILISATION

F2 COLONISATION

F3 DIVERSIFICATION

F4 DOMINATION

Facies	Sample Number	Porosity %	Permeability milliDarcies
2	14.1	8.9	0.0
2	14.2	10.9	1.9
2	16.1	7.0	1.9
2	*18.1	12.5	492.2
2	18.2	14.1	333.1
2	17.1	15.9	7.1
2	*17.2	15.5	742
2	17.3	16.6	349
2	17.4	10.2	2.6
2a	23.1	16.5	11.9
2a	23.2	18.8	237.7
2a	23.3	14.3	148.3
2a	23.4	8.7	0.0
2a	23.5	19.3	322.9
2a	25.1	2.8	1.6
2a	25.2	5.1	0.0
2a	28.1	0.2	0.0
2a	28.2	2.6	0.0

* = fractured core.

Facies	Sample Number	Porosity %	Permeability milliDarcies
3	32.1	17.5	0.0
3	32.2	18.6	0.0
3	33	10.3	1.1
3	34	12.6	12.2
3	35.1	11.9	155.9
3	35.2	12.0	0.0
4	40	6.2	0.0
4	43	9.0	0.0
4	46	13.7	0.0
4	47	9.8	1.3
4	54.1	5.8	0.0
4	54.2	5.3	0.0
4	55	7.3	0.1
4	60	8.9	0.0
4	63	12.8	1.3

Appendix 6.

A6.1 Stable Carbon and Oxygen Isotopic composition of Triassic Hafelekar Reef Cements.

The technique used for the determination of stable carbon and oxygen isotopic compositions is identical to that described in Appendix 3. Removal of organic matter was achieved using a plasma oxidation apparatus (2 hours). Samples were reacted with 100% phosphoric acid at 25±0.1 ° C (calcites) and 60±0.01 ° C (dolomites). All samples containing dolomite, as determined by staining, were reacted at 60 ° C and corrected as dolomites with the on-line computer. Mixtures were then manually corrected for the percentage calcite as described in Section 6.4.4. Reaction times were 24 hours, or until reaction was complete. Laboratory standards (MCS) calibrated to PDB were prepared in a similar way and included in each batch of samples so that analytical precision could be monitored. Following extraction of the carbon dioxide, analyses were performed on a VG Isogas Sira 12 triple collector mass spectrometer. Raw data was corrected as described in Appendix 3. Dolomites were corrected for the fractionation of oxygen isotopes that occurs on the evolution of the gas, according to the fractionation factor calculated from the following equation:
(Source: B.P. Sunbury Isotopic Analysis Laboratory).

$$\alpha = mT + C$$

$$m = -3.91429 \times 10^{-5}$$

$$C = 1.012069$$

Hence for the reaction at 60 ° C ,

$$\alpha_{(60)} = 1.00972$$

All figures quoted in the tables below are relative to PDB. Precision, as determined by measurement of laboratory standards (45 samples), was as follows:

	n	x	σ
$\delta\,^{13}C$	45	-0.708	0.10
$\delta\,^{18}O$	45	-9.216	0.17

The errors in the instrumental measurement ($\delta\,^{13}C$, $\delta\,^{18}O$, $\sigma = 0.02$ should be added to the above to give error ranges of 0.12 for $\delta\,^{13}C$ and 0.19 for $\delta\,^{18}O$.

A6.2 X-ray diffraction analyses of dolomites.

The percentages of dolomite present in a suite of samples from the 'Großoolith' cements of the fore-reef were measured by X-ray diffraction. Preparation of samples and instrumental conditions were similar to those described in Appendix 2. Areas were calculated as the ratios of the 3.04Å and 2.89Å peaks. There was no sample available with 100% dolomite on which to calibrate the results, so the figures given in the table below are suject to ± 10% error. More quantitative work was carried out on one sample to determine the stoichiometry and ordering of the dolomite. Peaks were located relative to an internal standard (cerium oxide) at scan speeds of $\frac{1}{2}^{o}$ of $2\theta min^{-1}$. The [104] diffraction peak, used to determine mole% $CaCO_3$ in dolomite was located at a d-space of 2.889Å, calculated from the Bragg equation ($\lambda = 2dsin\theta$). Mole% $CaCO_3$ was calculated according to the equation of Lumsden (1979), based on Goldsmith & Graf (1958):

$$N_{CaCO_3} = 333.33 \times d_{[104]} - 911.99$$

The result was that the sample (6.31.5 below) contained 51% $CaCO_3$.

The degree of ordering was calculated from the normalised (to internal standard) areas of the [110] and [015] peaks:

$$\frac{[015]}{[110]} = 0.9$$

A6.3 Staining.

Staining procedures, using Alizarin Red S and Potassium Ferricyanide ($K_3Fe[CN]_6$) were after Dickson (1966).

A6.4 Minor and Trace Element Determination.

Concentrations of magnesium, strontium, iron and manganese were determined by inductively coupled plasma source spectrometry (ICP). Analyses were performed by technicians at the British Petroleum Research Centre, Sunbury, using a Rank Hilgar E100 simultaneous ICP spectrometer. Aliquots were taken from the phosphoric acid digests of the samples after collection of the gas for isotopic measurements. Acid concentrations were adjusted to 7% (v/v). Commercially available standards were prepared to similar viscosity as the samples. Strontium and manganese levels were commonly close to the detection limits of the instrument (0.01 p.p.m. in the final solutions). There was generally not enough sample to permit duplicate analyses. Where the samples were duplicated, the iron analyses were found to be particularly irreproducible for reasons which were not determined. Values below are given in mole ratios. Errors in strontium and manganese levels are of the order of 0.02 mole%. Mg levels were used to give the dolomite percentage, assuming all magnesium was present in the dolomite.

Sample Number re Fig.	$\delta^{13}C$ [‰] PDB	$\delta^{18}O$ [‰] PDB	Dolomite by XRD %	Dolomite by ICP %	Sr mole.R $\times 10^{-2}$	Fe mole R $\times 10^{-1}$	Mn mole R $\times 10^{-1}$
6.31.1	2.3	−4.7	13	14	1.7	1.9	<0.3
6.31.2	2.4	−5.0	32	33	1.4	1.3	0.9
6.31.3	2.1	−5.2	21	20	1.5	1.4	1.0
6.31.4	2.1	−5.1	18	23	1.4	3.5	1.3
6.31.5	2.5	−4.8	30	39	<1.4	1.9	0.7
6.31.6	2.3	−4.9	13	16	<1.7	3.2	1.4
6.31.7	2.6	−4.7	33	37	<1.3	2.3	0.9
6.31.8	1.8	−6.2	32	37	<1.4	1.7	0.4
6.31.9	2.6	−4.7	43	46	<1.5	1.4	<0.2
6.31.10	2.3	−5.0	23	28	1.2	1.8	<0.2
6.31.11	2.6	−4.7	30	37	2.6	2.8	0.2
6.31.5	2.3	−4.9		24	<1.8	2.3	<0.3
6.31.5	2.3	−4.7		28	1.5	2.3	0.5
6.31.5	2.3	−4.8		26	<1.3	6.1	0.7
6.31.5	2.2	−4.8		23	1.7	2.6	<0.3
6.31.Su	−1.1	−6.9					
6.31.Sp	2.0	−5.7					
6.32.1	2.2	−4.8		23	1.6	<0.1	0.3
6.32.2	2.2	−4.7		28	2.6	<0.1	0.2
6.32.3	2.3	−4.7		21	3.0	<0.1	0.5
6.32.4	2.2	−4.9		22	3.3	0.2	0.8
6.32.5	2.2	−4.8		32	2.6	0.4	1.2
6.32.6	2.1	−4.6		24	1.6	1.5	1.7
6.32.7	2.1	−4.9		24	2.7	1.1	2.0
6.32.8	2.4	−5.0		41	1.6	2.5	1.8
6.32.9	2.4	−4.7		41	3.0	3.1	0.2
6.32.10	2.3	−5.1		23	2.7	0.1	<0.1
6.32.Su	2.3	−5.5		32			

Sample Number re Fig.	$\delta^{13}C$ [‰] PDB	$\delta^{18}O$ [‰] PDB	Dolomite by XRD %	Dolomite by ICP %	Sr mole R $\times 10^{-2}$	Fe mole.R $\times 10^{-1}$	Mn mole R $\times 10^{-1}$
6.15.1	2.5	−3.2		4	3.7	0.9	<0.1
6.15.2	2.6	−3.5		4	3.0	1.9	<0.1
6.15.3	2.8	−3.4		4	3.4	0.8	<0.1
6.16.1	2.7	−3.1		4	3.1	4.0	0.3
6.16.B	2.6	−3.2		4	2.5	0.4	0.1
6.33.1	2.6	−4.9		46	1.5	0.5	0.4
6.33.2	2.3	−4.7		9	2.8	0.1	0.3
6.33.3	2.2	−4.7		5	2.6	0.2	0.3
6.33.4	2.2	−4.9		5	2.6	1.2	0.6
6.20.F	2.0	−5.9		8	3.2	3.0	0.3
6.20.Sp	2.0	−5.9		8	<3.3	<0.5	1.1
6.20.Su	2.2	−5.3		3	3.2	0.5	0.5
6.35.F	2.0	−6.4		14	1.2	0.5	0.2
6.35.Su	3.0	−4.4		81	<1.9	0.9	0.3
6.36.F	2.2	−5.6		8	2.8	<0.5	<0.6
6.36.Sp	1.8	−6.3		0	<3.3	<0.2	<0.2
6.36.Su	2.8	−4.1		46	1.2	0.4	<0.2
6.36.SuSp	3.2	−4.9		81			
6.37.1	2.6	−5.0		41	<1.7	<0.3	<0.3
6.37.2	2.7	−4.9		39	2.3	0.4	<0.2
6.37.3	2.6	−4.7		41	1.4	0.4	<0.2
6.37.4	2.6	−4.8		41	1.3	0.4	<0.2
6.37.5	2.5	−5.1		46	1.2	0.4	<0.2
6.37.6	2.4	−4.8		39	1.3	0.4	<0.2
6.38.F	2.3	−5.3		14	2.1	2.8	0.2
6.38.Su	2.6	−4.3		37	1.6	<0.3	<0.2

REFERENCES

REFERENCES.

AÏSSAOUI, D.M., BUIGES, D., & PURSER, B.H., 1986, Model of reef diagenesis: Mururoa Atoll, French Polynesia. In: Reef Diagenesis, Schroeder, J.H., & Purser, B.H., (eds.), p. 27–52.

ALEXANDERSSON, E.T., 1972, Intra-granular growth of marine aragonite and Mg-calcite: evidence of precipitation from supersaturated seawater. Journal of Sedimentary Petrology, v. 42, p. 441–461.

ALEXANDERSSON, E.T., 1978, Discussion: Distribution of submarine cements in a modern Caribbean fringing reef, Galeta Point, Panama. Journal of Sedimentary Petrology, v. 48, p. 665–668.

ALVAREZ, G., BUSQUETS, P., PERMANYER, A., & VILAPLANA, M., 1977, Growth dynamic and stratigraphy of Sant-Pau d'Ordal Miocene patch-reef (Province of Barcelona). Mémoires du Bureau de Recherches Geologiques et Minières, No. 89, p. 367–377.

AMIEL, A.J., FRIEDMAN, G.M., & MILLER, D.S., 1971, Lithification of modern Red Sea reefs. (Abstract). VIII th. International Sedimentological Congress. Program with Abstracts, p. 3.

ANDERSON, T.F., & ARTHUR, M.A., 1983, Stable isotopes of oxygen and carbon and their application to sedimentologic and paleo-environmental problems. In: Stable Isotopes in Sedimentary Geology, Society of Economic Paleontologists and Mineralogists, Short Course No.10, Chapter 1.

APPLIN, P.L., 1951, Preliminary report on buried pre-Mesozoic rocks in Florida and adjacent states. United States Geological Survey Circular, v. 91, 28p.

APPLIN, P.L., & APPLIN, E.R., 1944, Regional subsurface stratigraphy and structure of Florida and Southern Georgia. Bulletin of the American Association of Petroleum Geologists, v. 28, p. 1673–1753.

BADIOZAMANI, K., 1973, The 'dorag' dolomitization model:application to the Middle Ordovician of Wisconsin. Journal of Sedimentary Petrology, v. 43, p. 965–984.

BALL, M.M., 1967, Tectonic control of the configuration of the Bahama Banks. Gulf Coast Association Geological Society Transactions, v. 17, p. 265–267.

BATHURST, R.G.C., 1975, Carbonate Sediments and Their Diagenesis [2nd Edition] Developments in Sedimentology, v. 12, Elsevier Scientific Publishing Company, Amsterdam, 658p.

BATHURST, R.G.C., 1980, Lithification of carbonate sediments. Scientific Progress at Oxford, v. 66, p. 451–471.

BERNER, R.A., 1968, Calcium carbonate concretions formed by the decomposition of organic matter. Science, v. 159, p. 195–197.

BERNER, R.A., 1975, The role of magnesium in the crystal growth of calcite and aragonite from seawater. Geochimica et Cosmochimica Acta, v. 39, p. 489–504.

BERNER, R.A., 1980, Early diagenesis - a theoretical approach. Princeton University Press, 241 p.

BERNER, R.A., WESTRICH, J.T., GRABER, J., SMITH, J., & MARTENS, C.S., 1978, Inhibition of aragonite precipitation from supersaturated seawater: a laboratory and field study. American Journal of Science, v. 278, p. 816–837.

BERNER, R.A., & MORSE, J.W., 1974, Dissolution kinetics of calcium carbonate in sea water (IV): theory of calcite dissolution. American Journal of Science, v. 274, p. 108–134.

BÖHM, L., DAWSON, R., LIEBEZEIT, G., & WEFER, G., 1980, Suitability of monosaccharides as markers for particle identification in carbonate sediments. Sedimentology, v. 5, p. 167–177.

BOON, J.J., HINES, H., BURLINGAME, A.L., KLOK, J., RIJPSTRA, W.I.C., de LEEUW, J.W., EDMUNDS, K.E., & EGLINTON, G., 1983, Organic geochemical studies of solar lake laminated cyanobacterial mats. Advances in Organic Geochemistry 1981, Bjøroy, M., et al., (eds.), John Wiley, p. 207–227.

BOON, J.J., RIJPSTRA, W.I.C., DELANGE, F., de LEEUW, J.W., YOSHIOKA, M. & SHIMIZU, Y., 1977, Black Sea sterol - a molecular fossil of dinoflagellate blooms. Nature, v. 277, p. 125–126.

BORMAN, A.H., De JONG, E.W., HUIZINGA, M., KOK, D.J., WESTBROEK, P., & BOSCH, L., 1982, The role in $CaCO_3$ crystallization of an acid Ca^{2+} -binding polysaccharide associated with coccoliths of *Emiliania huxleyi*. European Journal of Biochemistry, v. 129, p. 179–183.

BOSELLINI, A., & ROSSI, D., 1974, Triassic Carbonate buildups of the Dolomites, Northern Italy. In: Reefs in Time and Space, Laporte, L.F., (ed.), Society of Economic Paleontologists and Mineralogists, Special Publication No. 18, p. 209–233.

BOTZ, R.W., & von der BORCH, C.C., 1984, Stable isotope study of carbonate sediments from the Coorong area South Australia. Sedimentology, v. 4, p. 837–850.

BOUDOU, J.P., TRICHET, J., ROBINSON, N., & BRASSELL, S.C., 1986, Lipid composition of recent Polynesian microbial mat sequence. Organic Geochemistry, v. 9, p. 705–710.

BRADNER, R., & RESCH, W., 1981, Reef development in the Middle Triassic (Ladinian & Cordevolian) of the Northern Limestone Alps near Innsbruck, Austria. In: European Fossil Reef Models, Müller, G., & Freidman, G.M., (eds.), Society of Economic Paleontologists and Mineralogists, Special Publication No. 30., p. 203–231.

BRASSELL, S.C., EGLINTON, G., 1983, Steriods and triterpenoids in deep sea sediments and environmental and diagenetic indicators. In: Advances in Organic Geochemistry 1981, Bjørroy, M., et al., (eds.), John Wiley, p. 648–697.

BREITMAIER, E., & VOELTER, W., 1984, ^{13}C-NMR spectroscopy - methods and applications. In: Monographs in Modern Chemistry, Ebel, H. F., (Series ed.), Weinheim, 303p.

BRICKER, O.P., (ed.), 1971, Carbonate Cements. The Johns Hopkins University Studies in Geology No. 19, 376p.

BROECKER, W.S., 1982, Ocean chemistry during glacial time. Geochimica et Cosmochimica Acta, v. 46, p. 1689–1795.

BROECKNER, W.S., & TAKAHASHI, T., 1966, Calcium carbonate precipitation on the Bahama Banks. Journal of Geophysical Research, v. 71, p. 1575–1602.

BROOKS, P.W., EGLINTON, G., GASKELL, S.J., McHUGH, D.J., MAXWELL, J.R., & PHILIP, R.P., 1976, Lipids of recent sediments–(1). Straight chain hydrocarbons and carboxylic acids of some temperate lacustrine and sub-tropical lagoonal/tidal flat sediments. Chemical Geology, v. 18, p. 21–38.

BRYN, K., JANTZEN, E. & BOVRE, K., 1977, Occurrence and patterns of waxes in *Neisseriaceae*. Journal of General Microbiology, v. 102, p. 33–43.

BUDDEMEIER, R.W., & OBERDORFER, J.A., 1986, Internal hydrology and geochemistry of coral reefs and atoll islands: key to diagenetic variations. In: Reef Diagenesis, Schroeder, J.H., & Purser, B.H., (eds.), Springer Verlag, p. 91–111.

CARDOSO, J., WATTS, C., GOODFELLOW, R., EGLINGTON, G., & GLONBIC, S., 1978, A biogeochemical study of the Abu Dhabi algal mats: a simplified ecosystem. Chemical Geology, v. 23, p. 273–291.

CARTER, P.W., & MITTERER, R.M., 1978, Amino acid composition of organic matter associated with carbonate and non–carbonate sediments.Geochimica et Cosmochimica Acta, v. 42, p. 1231–1238.

CAYEUX, L., 1935, Les roches sedimentaires de France: roches carbonates. Masson, Paris.

CHAFETZ, H.S., 1986, Marine peloids: a product of bacterially induced precipitation of calcite. Journal of Sedimentary Petrology, v. 56, p. 812–817.

CHAFETZ, H.S., & FOLK, R.L., 1984, Travertines: depositional morphology and the bacterially constructed constituents. Journal of Sedimentary Petrology, v. 54, p. 289–316.

CHAVE, K.E., 1965, Calcium carbonate: association with organic matter in surface sea water. Science, v. 29, p. 1723–1724.

CHAVE, K.E., DEFFEYES, K.S., WEYL, P.K., GARRELS, R.M., & THOMPSON, M.E., 1962, Observations on the solubility of skeletal carbonates in aqueous solution. Science, v. 137, p. 33–34.

CHAVE, K.E., & SUESS, E., 1967, Suspended minerals in seawater. Transaction of The New York Academy of Science, v. 29, p. 991–1000.

CHOQUETTE, P.W., & PRAY, L.C., 1970, Geologic nomenclature and classification of porosity in sedimentary carbonates. Bulletin of the American Association of Petroleum Geologists, v. 54, p. 207–250.

CHOQUETTE, P.W., & TRUSELL, F.C., 1978, A procedure for making the Titan-yellow stain for Mg-calcite permanent. Journal of Sedimentary Petrology, v. 48, p. 639–641.

CONSTANTZ, B.R., 1986, The primary surface area of corals and variations in their susceptibility to diagenesis. In: Reef Diagenesis, Schroeder, J.H. & Purser, B.H. (eds.), Springer Verlag, p. 53–76.

CRAIG, H., 1957, Isotopic standards for carbon and oxygen and correction factors for mass spectrometric analyses of carbon dioxide. Geochimica et Cosmochimica Acta, v. 12, p. 133–149.

CRAIG, H., 1965, The measurement of oxygen isotope paleotemperatures. In: Stable isotopes in oceanographic studies and paleotemperatures, Tongiorgi, E., (ed.), Consiglio Nazionale delle Richerche Laboritorio de Geologia Nucleare, Pisa, p. 161–182.

CRAIG, H., & GORDON, L.I., 1965, Deuterium and ^{18}O variations in the ocean and marine atmosphere. In: Symposium on Marine Geochemistry, Schink, D.R., & Corless, J.T., (eds.), University of Rhode Island, Graduate School of Oceanography, Occasional Publications 13, p. 272–374.

CRANWELL, P.A., & VOLKMAN, J.K., 1981, Alkyl and steryl esters in a recent lacustrine sediment. Chemical Geology, v. 32, p. 29–43.

CUFFEY, R.J., & KISSLING, D.L., 1973, Ecologic roles and Paleoecologic implications of Bryozoans on modern coral reefs in the Florida Keys. Geological Society of America, Abstacts with Programs, v. 5, no. 2, p. 152–153.

CUMMINGS, C.E., & MCCARTHY, H.B., 1982, Stable carbon isotopic ratios in *Astrangia danae*: evidence for algal modification of carbon pools used in calcification. Geochimica et Cosmochimica Acta, v. 46, p. 1125–1129.

DAVIES, P.J., BUBELA, B., & FERGUSON, J., 1978, The formation of ooids. Sedimentology, v. 25, p. 703–730.

DAVIES, P.J., & HOPLEY, D., 1983, Growth facies and growth rates of Holocene reefs in the Great Barrier Reef. Bureau of Mineral Resources, Journal of Australian Geology and Geophysics, v. 8, p. 237–252.

DAVIES, P.J., & MONTAGGIONI, L., 1985, Reef growth and sea level change: the environmental signature. In: Proceedings of the Fifth International Coral Reef Congress, Tahiti, v. 3, p. 477–511.

DÉFARGE, C., et TRICHET, J., 1984, Microstructure de sédiments d'origine cyanobactérienne au sein desquels précipitent des carbonates de calcium: application à la compréhension des méchanismes de la biominéralisation. C.R. Academie des Sciences, Paris, t.299, serie II, no. 11, p. 711-716.

DÉFARGE, C., TRICHET, J., & SIU, P., 1985, First data on the biogeochemistry of kopara deposits from Rangiroa Atoll. In: Proceedings of the Fifth International Coral

Reef Congress, Tahiti, v. 3, p. 365–370.

DEGENS, E.T., 1976, Molecular mechanisms in carbonate, phosphate and silica deposition in the living cell. In: Topics in Current Chemistry v. 64, p. 1–112, Springer Verlag Berlin.

DEGENS, E.T., 1979, Why do organisms calcify? Chemical Geology, v. 8, p. 257–269.

DEINES, P., 1970, Mass spectrometer correction factors for the determination of small isotopic composition variations of carbon and oxygen. International Journal of Mass Spectrometry and Ionisation Physics, v. 4, p. 283.

DEINES, P., LANGMUIR,D., & HARMON, R.S., 1974, Stable carbon isotope ratios and the existence of a gas phase in the evaluation of carbonate groundwaters. Geochimica et Cosmochimica Acta, v. , 38, p. 1147–1154.

DICKSON, J.A.D., 1966, Carbonate identification and genesis as revealed by staining. Journal of Sedimentary Petrology, v. 36, p. 491–505.

DICKSON, J.A.D., & COLEMAN, M.L., 1980, Changes in carbon and oxygen isotopic composition during limestone diagenesis. Sedimentology, v. 27, p. 107–118.

DOREMUS, R.H., 1958, Precipitation kinetics of ionic salts from solution. Journal of Physical Chemistry, v. 62, p. 1025–1068.

DRAVIS, J., 1979, Rapid and widespread generation of recent oolitic hard grounds on a high energy Bahamian platform, Eleuthera Bank, Bahamas. Journal of Sedimentary Petrology, v. 49, p. 195–207.

DREVER, J.I., 1982, The geochemistry of natural waters. Prentice Hall, 388p.

DUNHAM, R.J., 1962, Classification of carbonate rocks according to depositional texture. American Association of Petroleum Geologists, Memoir 1, p. 108–121.

EHRHARDT, M., 1977, Organic substances in seawater. Marine Chemistry, v. 5, p. 307–316.

EMBRY, A.F., & KLOVAN, J.E., 1971, A late Devonian reef tract on northeastern Banks Island, N.W.T.. Bulletin of Canadian Petroleum Geology, v. 19, p. 730–781.

EMILIANI, C., HUDSON, J.H., SHINN, E.A., GEORGE, R.Y., & LIDZ, B., 1978, Oxygen and carbon isotopic growth record in a reef coral from the Florida Keys and deep sea coral from Blake Plateau. Science, v. 202, p. 627–629.

EMRICH, K., ERHATT, D.H., & VOGEL, J.C., 1970, Carbon fractionation during the precipitation of calcium carbonate. Earth and Planetary Science Letters, v. 8, p. 363–371.

ENOS, P., & PERKINS, R.D., 1977, Quaternary sedimentation in South Florida. The Geological Society of America, Memoir No. 147, 198p.

ENOS, P., & SAWATSKY, L.H., 1981, Pore networks in Holocene carbonate sediments. Journal of Sedimentary Petrology, v. 51, p. 961–985.

EPSTEIN, S., BUCHSBAUM, R., LOWENSTAM, H.A., & UREY, H., 1953, Revised carbonate water isotopic temperature scale. Bulletin of the Geological Society of America, v. 64, p. 1315–1326.

FERGUSON, J., BUBELA, B., & DAVIES, P.J., 1978, Synthesis and possible mechanism of formation of radial carbonate ooids. Chemical Geology, v. 22, p. 285–308.

FERGUSON, J., BUSH, P.R., & CLARKE, B.A., 1984, The role of organic matter in the early carbonate diagenesis of carbonate ooids - an experimental study. Journal of Petroleum Geology, v. 7, p. 245–266.

FLÜGEL, E., 1981, Paleoecology and facies of Upper Triassic reefs in the northern Calcareous Alps. In: European Fossil Reef Models, Müller, G., & Freidman, G.M., (eds.), Society of Economic Paleontologists and Mineralogists, Special Publication No. 30, p. 291–361.

FOLK, R.L., 1959, Practical petrographical classification of limestones. Bulletin of the American Association of Petroleum Geologists, v. 43, p. 1–38.

FOLK, R.L., 1962, Spectral subdivision of limestone types. In: Classification of Carbonate Rocks, Ham, N.E. (ed.), American Association of Petroleum Geologists, Memoir 1, p. 62–84.

FOLK, R.L., 1974, The natural history of crystalline calcium carbonate: effect of magnesium content and salinity. Journal of Sedimentary Petrology, v. 44, p. 40–53.

FOLK, R.L., & ASSERETO, R., 1976, Comparative fabrics of length-slow and length-fast calcite and calcitized aragonite in a Holocene speleothem, Carlsbad Caverns, New Mexico. Journal of Sedimentary Petrology, v. 21, p. 118–158.

FRIEDMAN, G.M., 1959, Identification of carbonate minerals by staining methods. Journal of Sedimentary Petrology, v. 29, p. 87–97.

FRIEDMAN, G.M., 1985, The problem of submarine cement in classifying reef rock: an experience in frustration. In: Carbonate Cements, Schneidermann, N., and Harris, P.M. (eds.), Society of Economic Paleontologists and Mineralogists, Special Publication No. 36, p. 117–122.

FRIEDMAN, G.M., AMIEL, A.J., & SCHNEIDERMANN, N., 1974, Submarine cementation in reefs - example from the Red Sea. Journal of Sedimentary Petrology, v. 44, p. 816–825.

FRIEDMAN, G.M., & SANDERS, J.E., 1978, Principles of sedimentology. John Wiley, 792p.

FRIEDMAN, I., & O'NEIL, J.R., 1977, Compilation of stable isotope fractionation factors of geochemical interest. In: Data of Geochemistry (Sixth edition), Fleischer, M. (ed.), United States Geological Survey Professional Paper 440-kk, 110p.

GAGOSIAN, R.B., VOLKMAN, J.K., & NIGRELLI, G.E., 1983, The use of sediment traps to determine sterol sources in coastal sediments off Peru. In: Advances in Organic Geochemistry 1981 Bjøroy, M. et al., (eds.), John Wiley, p. 369–379.

GELPI, E., SCHNEIDER, H., MANN, J., & ORO, J., 1970, Hydrocarbons of geochemical significance in microscopic algae. Phytochemistry, v. 9, p. 603–612.

GERMANN, K., 1968, Diagenetic patterns in the Wettersteinkalk (Ladinian Middle Trias), Northern Limestone Alps, Bavaria and Tyrol. Journal of Sedimentary Petrology, v. 38, p. 490–500.

GILLAM, A.H., & WILSON, M.A., 1985, Pyrolysis-GC-MS and NMR studies of dissolved seawater humic substances and isolates of a marine diatom. Organic Geochemistry v. 8, p. 15–25.

GILLAN, F.T., JOHNS, R.B., VERHEYEN, T.V., NICHOLS, P.D., ESDAILE, R.J., & BAVOR, H.J., 1983, Mono-unsaturated fatty acids as specific bacterial markers in marine sediments. In: Advances in Organic Chemistry 1981, Bjøroy, M., et al., (eds.), John Wiley, p. 198–206.

GINSBURG, R.N., & JAMES, N.P., 1974, Holocene carbonate sediments of continental shelves. In: Continental margins, Burke, C.A. & Drake, C.L. (eds.), Springer Verlag, p. 137–154.

GINSBURG, R.N., MARSZALEK, D.S., & SCHNEIDERMANN, N., 1971, Ultrastructure of carbonate cements in a Holocene algal reef of Bermuda. Journal of Sedimentary Petrology, v. 41, p. 472–482.

GINSBURG, R.N., & SCHROEDER, J.H., 1973, Growth and submarine fossilisation of algal cup reefs, Bermuda. Sedimentology, v. 20, p. 575–614.

GINSBURG, R.N., & SCHROEDER, J.H., 1969, Recent syn-sedimentary cementation in subtidal Bermuda reefs. In: Bricker, O.P., (ed.), Carbonate Cements - Bermuda Biological Station for Research, Special Publication, v. 3, p. 31–34.

GINSBURG, R.N., SCHROEDER, J.H., & SHINN, E.A., 1971, Recent synsedimentary cementation in subtidal Bermuda reefs. In: Carbonate Cements, Bricker, O.P., (ed.), Johns Hopkins University Studies in Geology, No. 19, p. 54–58.

GINSBURG, R.N., SHINN, E.A., & SCHROEDER, J.H., 1967, Submarine cementation and internal sedimentation within Bermuda reefs. (Abstract). Geological Society of America, Special Paper 115, p. 78–79.

GIVEN, R.K., & WILKINSON, B.H., 1985, Kinetic control of morphology, composition and mineralogy of abiotic sedimentary carbonates. Journal of Sedimentary Petrology, v. 55, p. 109–119.

GIVEN, R.K., & WILKINSON, B.H., 1985, Kinetic control of morphology, composition and mineralogy of abiotic sedimentary carbonates - reply to discussion. Journal of Sedimentary Petrology, v. 55, p. 921–926.

GOLDSMITH, J.R., & GRAF, D.L., 1958, Relations between lattice constants and composition of Ca-Mg carbonates. American Mineralogist, v. 43, p. 84–101.

GONZALEZ, L.A., & LOHMANN, K.C., 1985, Carbon and oxygen isotopic composition in Holocene reefal carbonates. Geology, v. 13, p. 811–814.

GOREAU, N.I., & HAYES, R.L., 1977, Nucleation catalysis in coral skeletogenesis. In: Proceedings of the Third International Coral Reef Symposium, Miami, v. 2, p. 439–446.

GOREAU, T.J., 1977, Carbon metabolism in calcifying and photosynthetic organisms: theoretical models based on stable isotope data. Proceedings of the Third International Coral Reef Symposium, Miami, v. 2, p. 395–401.

GOSSENS, H., IRENE, W., RIJPSTRA, C., DUREN, R.R., de LEEUW, J.W., &

SCHENCK, P.A., 1986, Bacterial contribution to sedimentary organic matter: a comparative study of lipid moieties in bacteria and recent sediments. Organic Geochemistry, v. 10, p. 683–696.

GROSSMAN, E.L., & KU, T., 1981, Aragonite water isotopic temperature scale based on the benthic foraminifer, *Hoeglundina eleagans*. Geological Society of America Abstracts with Programs, v. 13, p. 464.

HALLEY, R.B., & EVANS, C.C., 1983, The Miami limestone: a guide to selected outcrops and their interpretation, (with a discussion of diagenesis in the formation). Miami Geological Society, 67p.

HARDIE, L.A., 1987, Perspectives on dolomitization: a critical review of some current views. Journal of Sedimentary Petrology, v. 57, p. 166–183.

HARRIS, P.M., & FROST, S.H., 1984, Middle Cretaceous carbonate reservoirs, Fahud Field and northwest Oman. Bulletin of the American Association of Petroleum Geologists, v. 68, p. 649–658.

HATHAWAY, J.C., & DEGENS, E.T., 1969, Methane-derived marine carbonates of Pleistocene age. Science, v. 165, p. 690–692.

ten HAVEN, H.L., de LEEUW, J.W., & SCHENCK, P.A., 1985, Organic geochemical studies of a Messinian evaporitic basin, Northern Apennines (Italy) I: hydrocarbon biological markers for a hypersaline environment. Geochimica et Cosmochimica Acta, v. 49, p. 2181–2192.

HAYES, R.L., & GOREAU, N.I., 1977, Cytodynamics of coral calcification. In: Proceedings of the Third International Coral Reef Symposium, Miami, v. 2, p. 433–438.

HECKEL, P.H., 1974, Carbonate buildups in the geological record: a review. In: Reefs in Time and Space, Laporte, L.F., (ed.), Society of Economic Paleontologists and Mineralogists, Special Publication No. 18, p. 90–154.

HEINRICH, R., & ZANKL, H., 1986, Diagenesis of Upper Triassic Wetterstein Reefs of the Bavarian Alps. In: Reef Diagenesis, Schroeder, J.H., & Purser, B.H., (eds.), p. 245–269.

HOLDEN, M.J., & PATTERSON, G.W., 1982, Taxonomic implication of sterol composition in the genus *Chlorella*. Lipids, v. 17, p. 215–219.

HOSKIN, C.M., 1971, Aragonite crystals in algal biolithite: Alacran Reef, Mexico. In:

Carbonate Cements, Bricker, O.P., (ed.), Johns Hopkins University Studies in Geology, No. 19, p. 66-67.

HUANG, W.Y., & MEINSCHEIN, W.G., 1978, Sterols in sediments from Baffin Bay, Texas. Geochimica et Cosmochimica Acta, v. 42, p. 1391–1396.

HUBBARD, D.K., BURKE, R.B., & GILL, I.P., 1986, Styles of reef accretion along a steep, shelf-edge reef, St. Croix, U.S. Virgin Islands. Journal of Sedimentary Petrology, v. 56, p. 848–861.

HUBBARD, J.A.E.B., 1972, Cavity formation in living scleractinian corals and fossil analogues. Geologisches Rundschau, v. 61, p. 551–564.

IBE, A.C., FERGUSON, J., KINGHORN, R.R.F., & RAHMAN, M., 1983, Organic matter content in carbonate sediment in relation to petroleum occurrence. Journal of Petroleum Geology, v. 6, p. 55–70.

ILLING, L.V., 1954, Bahaman calcareous sands. Bulletin of the American Association of Petroleum Geologists, v. 38, p. 1–95.

IRWIN, H., CURTIS, C., & COLEMAN, M., 1977, Isotopic evidence for source of diagenetic carbonates formed during burial of organic-rich sediments. Nature, v. 269, p. 209–213.

JAMES, N.P., 1979, Facies models 11. Reefs. In: Facies models, Walker, R.G., (ed). Geoscience Canada Reprint Series 1, p. 121–132.

JAMES, N.P., & CHOQUETTE, P.W., 1983, Diagenesis 6. Limestones - the sea floor diagenetic environment. Geoscience Canada, v. 10, p. 162–179.

JAMES, N.P., & GINSBURG, R.N., 1979, The seaward margin of Belize barrier and atoll reefs. International Association of Sedimentologists, Special Publication No. 3, 191p.

JAMES, N.P., GINSBURG, R.N., MARSZALEK, D.S., & CHOQUETTE, P.W., 1976, Facies and fabric specificity of early subsea cements in shallow Belize (British Honduras) reefs, Journal of Sedimentary Petrology, v. 46, p. 523–544.

JAMES, N.P., & MACINTYRE, I.G., 1985, Carbonate depositional environments, modern and ancient. Part 1: reefs, zonation, depositional facies, diagenesis. Colorado School of Mines, Quarterly v. 80, No. 3, 70p.

JINDRICH, V., 1983, Structure and diagenesis of recent algal foraminifer reefs, Fernando de Norohna, Brazil. Journal of Sedimentary Petrology, v. 53, p. 449–459.

KEITH, M.L., & WEBER, J.N., 1965, Vital effect on the carbonate isotopic composition of reef communities. In: Proceedings of the Spoleto Conference on stable isotopes in oceanographic studies and paleotemperatures, p. 267–283.

KEMP, R.J., & MERCER, E.I., 1968, Studies on the sterols and sterol esters of the intracellular organelles of maize shoots. Biochemistry Journal, v. 110, p. 119–125.

KINSMAN, D.J.J., 1969, Interpretation of Sr^{2+} concentrations in carbonate minerals and rocks. Journal of Sedimentary Petrology, v. 39, p. 486–508.

KITANO, Y., & HOOD, D.W., 1965, The influence of organic material on the polymorphic crystallization of calcium carbonate. Geochimica et Cosmochimica Acta, v. 29, p. 29–41.

KITANO, Y., & KANAMORI, N., 1966, Synthesis of magnesian calcite at low temperatures and pressures. Geochemistry Journal, v. 1, p. 1–10.

KOK, D.J., BLOMEN, L.J.M.J., WESTBROEK, P., & BIJVOET, O.L.M., 1986, Polysaccharide from coccoliths ($CaCO_3$ biomineral): influence on crystallization of calcium oxalate monohydrate. European Journal of Biochemistry, v. 158, p. 167–172.

KROOPNICK, P., WEISS, R.F., & CRAIG, H., 1972, Total CO_2 and dissolved oxygen at Geosecs II in the North Atlantic. Earth and Planetary Science Letters, v. 16, p. 103–110.

KRUMBEIN, W.E., 1979a, Calcification by bacteria and algae. In: Biogeochemical Cycling of Mineral-Forming Elements: Studies in Environmental Science, Trudinger, P.A., & Swaine, D.J., (eds.), p. 47–68.

KRUMBEIN, W.E., 1979b, Photolithotropic and chemo-organotrophic activity of bacteria and algae as related to beachrock formation and degradation. Geomicrobiology Journal, v. 1, p. 139–203.

LADD, H.S., & SCHLANGER, S.O., 1960, Drilling operations on Enewetak Atoll. U.S. Geological Survey Professional Paper 260–Y, p. 863–905.

LAHANN, R.W., 1978, A chemical model for calcite crystal growth and morphology control. Journal of Sedimentary Petrology, v. 48, p. 337–344.

LALOU, C., 1957, Studies on bacterial precipitation of carbonates in seawater. Journal of Sedimentary Petrology, v. 27, p. 190–195.

LAND, L.S., 1971, Submarine lithification of Jamaican reefs. In: Bricker, O.P., (ed.), Carbonate Cements. Johns Hopkins University Studies in Geology, No. 19, p. 59–62.

LAND, L.S., 1980, The isotopic and trace element geochemistry of dolomite: the state of the art. In: Concepts and Models of Dolomitization, Zenger, D.H., et al., (eds.), Society of Economic Paleontologists and Mineralogists, Special Publication No. 28, p. 87–110.

LAND, L.S., 1983, The application of stable isotopes to studies of the origin of dolomite and to problems of diagenesis of clastic sediments. In: Stable Isotopes in Sedimentary Geology. Society of Economic Paleontologists and Mineralogists, Short Course No. 10. Chapter 4 (Eds) ARTHUR, M.A., ANDERSON, P.F., KAPLAN, I.R., VEIZER, J., LAND, L.S.

LAND, L.S., 1985, The origin of massive dolomite, Journal of Geological Education, v. 33, p. 112–125.

LAND, L.S., BEHRENS, E.W., & FRISHMAN, S.A., 1979, The ooids of Baffin Bay, Texas. Journal of Sedimentary Petrology, v. 49, p. 1269–1278.

LAND, L.S., & GOREAU, T.F., 1970, Submarine lithification of Jamaican reefs, Journal of Sedimentary Petrology, v. 40, p. 457–462.

LAND, L.S., & MOORE, C.H., 1980, Lithification, micritisation and syndepositional diagenesis of biolithites on the Jamaican Island slope. Journal of Sedimentary Petrology, v. 50, p. 357–370.

LEADBEATER, B.S.C., & RIDING, R., (eds.), 1986, Biomineralisation in lower plants and animals. The Systematics Association Special Volume No. 30. 401p.

LEO, R.F., & PARKER, P.L., 1966, Branched chain fatty acids in sediments. Science, v. 152, p. 649–650.

LERMAN, A., 1979, Geochemical processes, water and sediment. John Wiley & Sons, New York, p. 64–65.

LIGHTY, R.G., 1977, Relict shelf-edge Holocene coral reef: southeast coast of Florida. In: Proceedings of the Third International Coral Reef Symposium. v. 2 p. 215–221.

LIGHTY, R.G., 1985, Preservation of internal reef porosity and diagenetic sealing of submerged Early Holocene Barrier Reef South East Florida Shelf. In: Carbonate Cements, Schneidermann, N., and Harris, P.M. (eds.), Society of Economic Paleontologists and Mineralogists, Special Publication No. 36, p. 123–151.

LONGMAN, M.W., 1980, Carbonate diagenetic textures from near-surface diagenetic environments. Bulletin of the American Association of Petroleum Geologists, v. 64, p. 461–487.

LOREAU, J.P., 1982, Sediments aragonitiques et leur genèse. Mémoirs du Museum d'Histoire Naturelle, Serie C, v. 47, Paris p312.

LOWENSTAM, H.A., 1961, Mineralogy, $^{18}O/^{16}O$ ratios, and strontium and magnesium contents of recent and fossil brachiopods and their bearing on the history of the oceans. Journal of Geology, v. 69, p. 241–260.

LOWENSTAM, H.A., 1981, Minerals formed by organisms. Science, v. 211, p. 1126–1131.

LOWENSTAM, H.A., 1986, Mineralisation processes in monerans and protoctists. In: Biomineralisation in Lower Plants and Animals. Leadbeater B.S.C., Riding R., (eds.) p1-18.

LOWENSTAM, H.A., & EPSTEIN, S.J., 1957, On the origin of sedimentary aragonite needles of the Great Bahama Bank. Geology, v. 65, p. 364.

LUMSDEN, D.N., 1979, Discrepancy between thin section and x-ray estimates of dolomite in limestone. Journal of Sedimentary Petrology, v. 49, p. 429–436.

MACHEL, H.G., & MOUNTJOY, E.R., 1986, Chemistry and environments of dolomitization - a reappraisal. Earth Science Reviews, v. 23, p. 175–222.

MACKENZIE, A.S., BRASSELL, S.C., & MAXWELL, J.R., 1982, Chemical fossils: the geological fate of steroids. Science, v. 217, p. 491–504.

MACINTYRE, I.G., 1977, Distribution of submarine cements in a modern Caribbean fringing reef, Galeta Point, Panama. Journal of Sedimentary Petrology, v. 47, p. 503–516.

MACINTYRE, I.G., 1984, Extensive submarine lithification in a cave in the Belize barrier reef platform. Journal of Sedimentary Petrology, v. 54, p. 221–235.

MACINTYRE, I.G., 1985, Submarine cements: the peloidal question. In: Carbonate Cements, Schneidermann, N., and Harris, P.M. (eds.), Society of Economic Paleontologists and Mineralogists, Special Publication No. 36, p. 109–116.

MACINTYRE, I.G., MOUNTJOY, E.W., & D'ANGELEJAN, B.F., 1968, An occurrence of submarine cementation of carbonate sediments off the West Coast of Barbados, West Indies. Journal of Sedimentary Petrology, v. 38, p. 660–664.

MALONE, P.G., & TOWE, K.M., 1970, Microbial carbonate and phosphate precipitates from sea water cultures. Marine Geology, v. 9, p. 301–309.

MARSHALL, J.F., 1983a, Submarine cementation in a high energy platform reef, One Tree Reef, Southern Great Barrier Reef. Journal of Sedimentary Petrology, v. 53, p. 113–1149.

MARSHALL, J.F., 1983b, Lithology and diagenesis of the carbonate foundations of modern reefs in the Southern Great Barrier Reef. Bureau of Mineral Resources, Journal of Australian Geology and Geophysics, v. 8, p. 253–265.

MARSHALL, J.F., 1985, Cross-shelf and facies related variations in submarine cementation in the central Great Barrier Reef. In: Proceedings of the Fifth Coral Reef Congress, Tahiti, v. 3, p. 221–226.

MARSHALL, J.F., & DAVIES, P.J., 1981, Submarine lithification on windward reef slopes - Capricorn Bunker group, Southern Great Barrier Reef. Journal of Sedimentary Petrology, v. 51, p. 953–960.

MATTES, B.W., & MOUNTJOY, E.W., 1980, Burial dolomitisation of the Upper Devonian Miette buildup, Jasper National Park, Alberta, U.S.A. In: Concepts and Models of Dolomitization, Zenger, et al., (eds.), Society of Economic Paleontologists and Mineralogists, Special Publication No. 28, p. 259–297.

MCCREA, J.M., 1950, On the isotopic chemistry of carbonates and a paleotemperature scale. Journal of Chemical Physics, v. 18, p. 849–857.

MERCER, E.I., & BARTLETT, K., 1974, Sterol esters of *Phycomyces blakesleeanus*. Phytochemistry, v. 13, p. 1099–1105.

MEYERS, P.A., 1977, Fatty acids and hydrocarbons of Caribbean corals. In: Proceedings of the Third International Coral Reef Symposium, Miami. v. 1, p. 529–536.

MEYERS, P.A., 1979, Polyunsaturated fatty acids in corals: indicators of nutritional sources. Marine Biology Letters, p. 69–75.

MEYERS, W.J., & LOHMANN, K.C., 1985, Isotope geochemistry of regionally extensive calcite cement zones and marine components in Mississippian limestones, New Mexico. In: Carbonate Cements, Schneidermann, N., & Harris, P.M., (eds.) Society of Economic Paleontologists and Mineralogists, Special Publication No. 36, p. 223–239.

MILLIMAN, J.D., 1974, Marine Carbonates: Recent Sedimentary Carbonates, Part I. Berlin, Springer Verlag, 375p.

MITTERER, R.M., 1968, Amino-acid composition of organic matrix in calcareous oolites, Science, v. 162, p. 1498–1499.

MITTERER, R.M., 1972, Biogeochemistry of aragonite mud and oolites. Geochimica et Cosmochimica Acta, v. 36, p. 1407–1422.

MITTERER, R.M., 1978, Amino acid composition and metal binding capability of the skeletal protein of corals. Bulletin of Marine Science, v. 28, p. 173–180.

MITTERER, R.M., & CARTER, P.W., 1977, Some analytical and experimental data on organic-inorganic interaction. In: Proceedings of the Third International Coral Reef Symposium, Miami. v. 1. p. 541–547.

MITTERER, R.M., & CUNNINGHAM, R. Jr., 1985, The interaction of natural organic matter with grain surfaces: implications for calcium carbonate precipitation. In: Carbonate Cements, Schneidermann, N., and Harris, P.M. (eds.), Society of Economic Paleontologists and Mineralogists, Special Publication No. 36, p. 17–31.

MOORE, C.H., 1985, Upper Jurassic subsurface cements: a case history. In: Carbonate Cements, Schneidermann, N., and Harris, P.M. (eds.), Society of Economic Paleontologists and Mineralogists, Special Publication No. 36, p. 291–308.

MOORE, C.H., & DRUCKMAN, Y., 1981, Burial diagenesis and porosity evolution, Upper Jurassic Smackover, Arkansas and Louisiana. American Association of Petroleum Geologists Bulletin, v. 65, p. 597–628.

MORROW, D.W., 1982a. Diagenesis 1, Dolomite part 1: The chemistry of dolomitization and dolomite precipitation. Geoscience Canada, v. 9, p. 5–13.

MORROW, D.W., 1982b. Diagenesis 2, Dolomite part 2: Dolomitization models and ancient dolostones. Geoscience Canada, v. 9, p. 95–107.

MORROW, D.W., & MAYERS, I.R., 1977, Simulation of limestone diagenesis - a model based on strontium depletion. Canadian Journal of Earth Sciences, v. 15, p. 376–396.

MORSE, J.W., 1974, Dissolution kinetics of calcium carbonate in seawater (III). A new method for the study of carbonate reaction kinetics. American Journal of Science, v. 274, p. 97–107.

MORSE, J.W., MUCCI, A., & MILLERO, F.J., 1980, The solubility of calcite and aragonite in seawater of 35% salinity at 25°C and atmospheric pressure. Geochimica et Cosmochimica Acta, v. 44, p. 85–94.

MORSE, J.W., ZULLIG, J.J., BERNSTEIN, L.D., MILLERO, F.J., MILNE, P., MUCCI, A., & CHOPPIN, G.R., 1985, Chemistry of calcium carbonate rich shallow water sediments in the Bahamas. American Journal of Science, v. 285, p. 147–185.

MULTER, H.G., 1977, A field guide to some carbonate rock environments: Florida Keys and Western Bahamas. Kendal Hunt, 415p.

NELSON, C.S., & LAWRENCE, M.F., 1984, Methane derived high Mg calcite submarine cement in Holocene nodules from the Fraser Delta, British Columbia, Canada. Sedimentology, v. 31, p. 645–654.

NES, W.R., & MCKEAN, M.L., 1977, Biochemistry of steroids and other isoprenoids. University Park Press, Baltimore.

NISHIMURA, N., & KOYAMA, T., 1977, The occurrence of stanols in various living organisms and the behaviour of sterols in contemporary sediments. Geochimica et Cosmochimica Acta, v. 41, p. 379–385.

NORTHROP, D.A., & CLAYTON, R.N., 1966, Oxygen isotope fractionation in systems containing dolomite. Journal of Geology, v. 74, p. 174–196.

OKAZAKI, M., MISONOU, T., & FURUYA, K., 1979, Particular Ca^{2+} binding substances in marine macro-algae (III). The influence of acid insoluble residues on crystal form of $CaCO_3$ precipitated *in vitro*. Bulletin of Tokyo Gakugei University, Series 4, v. 31, p. 215–221.

O'NEIL, J.R., 1977, Stable isotopes in mineralogy. Physics & Chemistry of Minerals, v. 2, p. 105–123.

O'NEIL, J.R., CLAYTON, R.N., & MAYEDA, T.K., 1969, Oxygen isotope fractionation factors in divalent metal carbonates. Journal of Chemical Physics, v. 51, p. 5547–5558.

O'NEIL, J.R., & EPSTEIN, S., 1966, Oxygen isotope factionation in the system dolomite-calcite-carbon dioxide. Science, v. 152, p. 198–201.

ORCUTT, D.M., & RICHARDSON, B., 1970, Sterols of *Oocystis polymorpa*, a green alga. Steroids, v. 16, p. 429–446.

OURISSON, G., ALBRECHT, P., & ROHMER, M., 1979, The hopanoids: paleochemistry and biochemistry of a group of natural products. Pure and Applied Chemistry, v. 51, p. 709–729.

PARK, R. & EPSTEIN, S., 1960, Carbon isotope fractionation during photosynthesis. Geochimica et Cosmochimica Acta, v. 21, p. 110–126.

PERMANYER, A., & ESTEBAN, M., 1973, El Arrecife Mioceno de Sant-Pau d'Ordal. (Provincia de Barcelona). Instituto de Investigaciones Geológicas, Universidad de Barcelona. v. XXVIII, p. 45–72.

PERRY, G.J., VOLKMAN, J.K., & JOHNS, R.B., 1979, Fatty acids of bacterial orgin in contemporary marine sediments. Geochimica et Cosmochimica Acta, v. 43, p. 1715–1725.

PIERSON, B.J., & SHINN, E.A., 1985, Cement distribution and carbonate mineral stabilization in Pleistocene limestones of Hogsty Reef, Bahamas. In: Carbonate Cements, Schneidermann, N., and Harris, P.M. (eds.), Society of Economic Paleontologists and Mineralogists, Special Publication No. 36, p. 153–168.

PILLER, W.E., 1981, The Steinplatte reef complex, part of an Upper Triassic carbonate platform near Salzburg, Austria. In: European Fossil Reef Models, Müller, G., & Friedman, G.M., (eds.), Society of Economic Paleontologists and Mineralogists, Special Publication No. 31, p. 261–290.

PINGITORE, N.E., 1978, The behavior of Zn^{2+} and Mn^{2+} during carbonate diagenesis: theory and applications. Journal of Sedimentary Petrology, v. 48, p. 799–814.

PINGITORE, N.E., 1982, The role of diffusion during carbonate diagenesis. Journal of Sedimentary Petrology, v. 52, p. 27–39.

PLUMMER, L.N., & MACKENZIE, F.T., 1974, Predicting mineral solubility from rate data: application to the magnesian calcites. American Journal of Science, v. 274, p. 61–83.

PURSER, B.H., 1978, Early diagenesis and the preservation of porosity in Jurassic limestones. Journal of Petroleum Geology, v. 1 p. 83–94.

PYTKOWICZ, R.M., 1965, Calcium carbonate saturation in the ocean. Limnology and Oceanography, v. 10, p. 220–225.

RADKE, B.M., & MATHIS, R.L., 1980, On the formation and occurrence of saddle dolomite. Journal of Sedimentary Petrology, v. 50, p. 1149–1168.

REDDY, M.M., 1977, Crystallization of calcium carbonate in the presence of trace concentrations of phosphorus containing anions. I. inhibition of phosphate and glycerophosphate ions at pH 8.8 and 25°C. Journal of Crystal Growth, v. 41, p. 166–172.

REEDER, R.J.(ed), 1983, Carbonates: Mineralogy & Chemistry. Mineralogical Society of America, Reviews in mineralogy, v. 11, 394p.

REES, D.A., 1977, Polysaccharide shapes. In: Outline Studies in Biology, Chapman Hall. 80p.

ROBBIN, D.M., 1981, Subaerial $CaCO_3$ crust: a tool for timing reef initiation and defining sea level change. In: Proceedings of the Fourth International Coral Reef Symposium, Manila, v. 1, p. 575–579.

ROBBIN, D.M., 1984, A new Holocene sea-level curve for the Upper Florida Keys and Florida reef tract. Bulletin of the American Association of Petroleum Geologists, v. 68, p. 522.

ROBERTSON, A.A., PALACAS, J.G., & FROST, I.C., 1973, Determination of organic carbon in modern carbonate sediments. Journal of Sedimentary Petrology, v. 43, p. 1157–1159.

ROBINSON, N., CRANWELL, P.A., EGLINTON, G., BRASSELL, S.C., SHARP, C.L., GOPHEN, M., & POLLINGHER, U., 1986, Lipid geochemistry of Lake Kinneret. Organic Geochemistry, v. 10, p. 733–742.

ROBINSON, N., CRANWELL, P.A., FINLAY, B.J., & EGLINTON, G., 1984, Lipids of aquatic organisms as potential contributors to lacustrine sediments. In: Advances in Organic Geochemistry, 1983, Organic Geochemistry, v. 6, p. 143–152.

ROBINSON, N., EGLINTON, G., BRASSELL, S.C., & CRANWELL, P.A., 1984, Dinoflagellate origin for sedimentary 4α-methylsteroids and 5α(H)-stanols. Nature, v. 308, p. 439–441.

ROEHL, P.O., & CHOQUETTE, P.W., (eds.), 1985, Carbonate Petroleum Reservoirs, Springer, 622p.

ROHMER, M. & OURISSON, G., 1976, Structure des bactériohopanetetrols d'*Acetobacter xylinium*. Tetrahedron Letters, p. 3633–3636.

RUBINSON, M., & CLAYTON, R.M., 1969, ^{13}C fractionation between aragonite and calcite. Geochimica et Cosmochimica Acta, v. 33, p. 997–1002.

RULLKÖTTER, A.S., MACKENZIE, A.S., WELTE, D.H., LEYTHAEUSER, D., & RADKE, M., 1984, Quantitative gas chromatography-mass spectrometry analysis of geological samples. Organic Geochemistry, v. 6, p. 817–827.

RUSSELL, N.J., & VOLKMAN, J.K., 1980, The effect of growth temperature on wax ester composition in the psychrophilic bacterium *Micrococcus cryphilus* ATCC 15174. Journal of General Biology, v. 118, p. 131–141.

SAIZ-JIMENEZ, C., HAWKINS, B.L., & MACIEL, G.E., 1986, Cross polarizastion, magic-angle spinning ^{13}C nuclear magnetic resonance spectroscopy of soil humic fractions. Organic Geochemistry, v. 9, p. 277–284.

SALIOT, A., GOUTX, M., FEVRIER, A., TUSSEAU, D., & ANDRIE, C., 1982, Organic sedimentation in the water column in the Arabian Sea: relationship between the lipid composition of small and large size, surface and deep particles. Marine Chemistry, v. 11, p. 257–278.

SALLER, A.H., 1986, Radiaxial calcite in Lower Miocene strata, subsurface Enewetak Atoll. Journal of Sedimentary Petrology, v. 56, p. 743–762.

SANDBERG. P.A., 1983, Aragonite cements and their occurrence in ancient limestones. In: Carbonate Cements, Schneidermann, N., and Harris, P.M. (eds.), Society of Economic Paleontologists and Mineralogists, Special Publication No. 36, p. 33–57.

SANDBERG, P.A., 1983, An oscillating trend in Phanerozoic non-skeletal carbonate mineralogy. Nature, v. 305, p. 19–22.

SANSONE, F.J., 1985, Methane in the reef flat porewaters of Davies Reef, Great Barrier Reef, Australia. In: Proceedings of the Fifth International Symposium Congress, Tahiti, v. 3, p. 415–420.

SARGENT, J.R., 1976, Milky water in the North Sea: a rare event? Scottish Fishing Bulletin, v. 43, p. 46–48.

SARGENT, J.R., GATTEN, R.R., & HENDERSON, R.J., 1981, Marine wax esters. Pure and Applied Chemistry, v. 53, p. 867–871.

SASSEN, R., 1977, The fate of fatty acids from corals and mangroves in Holocene sediments of St. Croix: significance with respect to petroleum genesis. In: Proceedings of the Third International Coral Reef Symposium, Miami. v. 2, p. 135–142.

SCHENCK, P.A., 1969, The predominance of the C_{22} n-alkane in rock extracts. In: Schenck, P.A., & Havenaar, I., (eds.), Advances in Organic Geochemistry, 1968. p. 261–268.

SCHLAGER, W., & THE LEG 101 SHIPBOARD SCIENTIFIC PARTY, 1985, Rise and fall of carbonate platforms in the Bahamas. Nature, v. 315, p. 632–633.

SCHMOKER, J.W., KRYSTINIK, K.B., & HALLEY, R.B., 1985, Selected characteristics of limestone and dolomite reservoirs in the United States. Bulletin of the American Association of Petroleum Geologists, v. 69, p. 733–741.

SCHOFIELD, K., & ADAMS, A.E., 1986, Burial Dolomitisation of the Woo Dale Limestone Formation (Lower Carboniferous), Derbyshire, England. Sedimentology v. 33, p. 707–720.

SCHROEDER, J.H., 1972a, Fabrics and sequences of submarine carbonate cements on Holocene Bermuda cup reefs. Geologisches Rundschau, v. 61, p. 708–730.

SCHROEDER, J.H., 1972b, Calcified filaments of an endolithic alga in recent Bermuda reefs. Neues Jahrbuch für Geologie ünd Paleontologie. Monatshefte, p. 16–33.

SCHROEDER, J.H., 1979, Carbonate diagenesis in Quaternary beachrock of Uyombo, Kenya: sequences of processes and coexistence of heterogenic products. Geologisches Rundschau, v. 68, p. 894–919.

SCHROEDER, J.H., 1984, The petrogenetogram of corals: spatial variations in diagenetic sequences. Paleontographica Americana, No. 54, p. 261–271.

SCHROEDER, J.H., & PURSER, B.H., (eds.), 1986, Reef diagenesis. Springer Verlag, 455p.

SCHROEDER, J.H., & ZANKL, H., 1974, Dynamic reef formation: a sedimentological concept based on studies of Recent Bermuda and Bahama Reefs. In: Proceedings of the Second International Symposium on Coral Reefs, v. 2, p. 413–428.

SHAW, P.M., & JOHNS, R.B., 1985, Organic geochemical studies of a recent Inner Great Barrier Reef sediment–1. Assessment of input sources. Organic Geochemistry, v. 8, p. 147–156.

SHERIDAN, R.E., CROSBY, J.T., BRYAN, G.M., & STOFFA, P.L., 1981, Stratigraphy and structure of Southern Blake Plateau, Northern Florida Straits, and Northern Bahama Platform from multichannel seismic reflection data. Bulletin of the American Association of Petroleum Geologists, v. 65, p. 2571–2603.

SHINN, E.A., 1968, Practical significance of birdseye structures in carbonate rocks. Journal of Sedimentary Petrology, v. 38, p. 215–223.

SHINN, E.A., 1969, Submarine lithification of Holocene carbonate sediments in the Persian Gulf. Sedimentology, v. 12, p. 109–144.

SHINN, E.A., HUDSON, J.H., HALLEY, R.B., & LIDZ, B., 1977, Topographic control and accumulation rate of some Holocene coral reefs: South Florida and Dry Tortugas. In: Proceedings of the Third International Coral Reef Symposium, v. 2, p. 1–8.

SIMKISS, K., 1986, The process of biomineralisation in lower plants and animals: an overview. In: Biomineralisation in Lower Plants and Animals. Leadbeater, B.S.C, & Riding, R. (eds.), The Systematics Association Special Volume No. 30, p. 19–38.

SOMASUNDARAN, P., & AGAR, G.E., 1967, The zero point of charge. Journal of Colloid and Interface Science, v. 36, p. 166–172.

STRYER, L., 1975, Biochemistry, W.H. Freeman & Company, 877p.

STUMM, W., & MORGAN, J.J., 1970, Aquatic chemistry: an introduction emphasizing chemical equilibria in natural waters. John Wiley, 583p.

SUESS, E., 1970, Interaction of organic compounds with calcium carbonate (I). Association phenomena and geochemical implications. Geochimica et Cosmochimica Acta, v. 34, p. 157–168.

SUESS, E., 1973, Interaction of organic compounds with calcium carbonate (II). Organic–carbonate association in recent sediments. Geochimica et Cosmochimica Acta, v. 37, p. 2435–2448.

SWART, P.K., 1980, The environmental geochemistry of scleractinian coral skeletons. Unpublished PhD. Thesis, University of London.

SWART, P.K., 1983, Carbon and oxygen isotope fractionation in scleractinian corals: a review. Earth Science Reviews, v. 19, p. 51–80.

SWART, P.K., & COLEMAN, M.L., 1980, Isotopic data for scleractinian corals explain their paleotemperature uncertainties. Nature, v. 283, p. 557–559.

TARUTANI, T., CLAYTON, R.N., & MAYEDA, A.T., 1969, The effect of polymorphism and magnesium substitution on oxygen isotope fractionation between calcium carbonate and water. Geochimica et Cosmochimica Acta, v. 33, p. 987–996.

TISSOT, B.P., & WELTE, D.H., 1984, Petroleum formation and occurrence. Springer Verlag, 700p.

TRICHET, J., 1970, Études des premiers stades d'évolution de la matière organique dans des mares en milieu récifal (Polynésie Française). In: Advances in Organic Geochemistry, 1968, Hobson, G.D., (ed.), p. 265–284.

TUCKER, M.E., 1985, Calcified aragonite ooids and cements from the Late Precambrian of Southern Norway. Sedimentary Geology, v. 43, p. 67–84.

TUREKIAN, K.K., 1969, The oceans, streams and atmosphere. In: Handbook of Geochemistry, Wedepohl, K.H. (ed.), Springer-Verlag, New York.

TURNER, J.V., 1982, Kinetic fractionation of ^{13}C during calcium carbonate precipitation. Geochimica et Cosmochimica Acta, v. 46, p. 1183–1191.

URIST, M.R., 1962, Induced systemic hypersensitivity: Selye's theory. Science, v. 137, p. 120–121.

VEIZER, J., 1983, Chemical diagenesis of carbonates, theory and application of trace element technique. In: Stable Isotopes in Sedimentary Geology, Society of Economic Paleontologists and Mineralogists, Short Course No. 10, Chapter 3. (Eds): ARTHUR, M.A., ANDERSON, P.F., KAPLAN, I.R., VEIZER, J., LAND, L.S.

VEIZER, J., FRITZ, P., & JONES, B., 1986, Geochemistry of brachiopods: oxygen and carbon isotopic records of Paleozoic oceans. Geochimica et Cosmochimica Acta, v. 50, p. 1679–1696.

VOLKMAN, J., 1986, A review of sterol markers for marine and terrigenous organic matter. Organic Geochemistry, v. 9, p. 83–99.

VOLKMAN, J.K., JOHNS, R.B., GILLAN, F.T., PERRY, G.J., & BAVOR, H.J., 1980, Microbial lipids of an intertidal sediment (I). Fatty acids and hydrocarbons. Geochimica et Cosmochimica Acta, v. 44, p. 1133–1143.

van der WAL, P., de BRUIJN, W.C., WESTBROEK, P., de JONG, L., MULDER-STAPEL, A.A., 1983, Polysaccharide localization, coccolith formation, and Golgi dynamics in the coccolithophorid *Hymenomonas carterae*. Journal of Ultrastuctural Research, v. 85, p. 139–158.

WAKEHAM, S.G., FARRINGTON, J.W., & VOLKMAN, J.K., 1983, Fatty acids, waxesters, triacylglycerols and alkyldiacylglycerols associated with particles collected in sediment traps in the Peru upwelling. In: Advances in Organic Geochemistry 1981, Bjøroy, M., et al., (eds.), John Wiley, p. 185–197.

WALTER, L.M., 1983, The dissolution kinetics of shallow water carbonate grain types: effects of mineralogy, microstructure and solution chemistry. Unpublished PhD. dissertation, University of Miami, 320p.

WALTER, L.M., & MORSE, J.W., 1984a, Magnesium calcite stabilities: a reevaluation. Geochimica et Cosmochimica Acta, v. 48, p. 1059–1069.

WALTER, L.M., & MORSE, J.W., 1984b, Reactive surface area of skeletal carbonates during dissolution: effect of grainsize. Journal of Sedimentary Petrology, v. 54, p. 1081–1090.

WANNIGAMA, G.P., VOLKMAN, J.K., GILLAN, F.T., NICHOLS, P.D., & JOHNS, R.B., 1981, A comparison of lipid components of the fresh and dead leaves and pneumatophores of the mangrove *Avicennia marina*. Phytochemistry, v. 20, p. 659–666.

WEBER, J.N., 1971, Diurnal variations in the isotopic composition of dissolved inorganic carbon in seawater from coral reef environments. Geochimica et Cosmochimica Acta, v. 35, p. 891–902.

WEBER, J.N., & SCHMALZ, R.F., 1968, Factors affecting the carbon and oxygen isotopic composition of marine carbonate sediments, (III) Eniwetok Atoll. Journal of Sedimentary Petrology, v. 38, p. 1270–1279.

WEBER, J.N., & WOODHEAD, P.M.J., 1970, Carbon and oxygen isotope fractionation in the skeletal carbonate of reef building corals. Chemical Geology, v. 6, p. 93–123.

WEBER, J.N., & WOODHEAD, P.M.J., 1972, Temperature dependence of ^{18}O concentration in reef coral carbonates. Journal of Geophysical Research, v. 77, p. 463–473.

WEINER, S., TRAUB, W., & LOWENSTAM, H.A., 1983, Organic matrix in calcified exoskeletons. In: Biomineralisation and Biological Metal Accumulation, Westbroek, P., & de Jong, E.W., (eds.), p. 205–224.

WESTBROEK, P., van der WAL, P., van EMBURG, P.R., de VRIND–de JONG, E.W., & de BRUIJN, W.C., 1986, Calcification in the coccolithophorids *Emiliania huxleyi* and *Pleurochrysis carterae.* 1. Ultrastructural aspects. Biomineralisation in Lower Plants and Animals, Leadbeater, B.S.C., & Riding, R., (eds.), The Systematics Association Special Volume No. 30. p. 89–203.

WEYL, P.K., 1967, The solution behaviour of carbonate materials in seawater. International Conference on Tropical Oceanography, University of Miami, Miami, Florida, p. 178–228.

WILSON, J.L., 1977, Limestone and dolomite reservoirs. In: Developments in Petroleum Geology, Hobson, G.D., (ed.), v. 2, p. 1–52.

WOLLAST, R., 1971, Kinetic aspects of the nucleation and growth of calcite from aqueous solutions. In: Carbonate Cements, Bricker, O.P., (ed.), Johns Hopkins University Studies in Geology, No. 19, p. 264–273.

ZHAO, Z., & FAIRCHILD, I., 1987, Mixing zone dolomitization of Devonian carbonates, Guangxi, South China. In: Marshall, J.D., (ed.), Special Publication of the Geological Society of London. (In press).

ZANKL, H., 1971, Upper Triassic carbonate facies in the Northern Limestone Alps. In: Sedimentology of parts of Central Europe, guidebook to excursions. Müller,G., (ed.), VIII International Sedimentological Congress, Heidelberg, Germany, p. 147–186.

ZANKL, H., & MÜLTER, H.G., 1977, Origin of some internal fabrics in Holocene reef rocks, St. Croix, U.S. Virgin Islands. In: Proceedings of the Third International Coral Reef Symposium, v. 2, p. 127–134.